AD721959

FTD-HC-23-242-70

FOREIGN TECHNOLOGY DIVISION



UNSTEADY FLOW AROUND AND AEROELASTIC VIBRATION IN TURBOMACHINE CASCADES

By

G. S. Samoylovich



DDC
RECEIVED
APR 28 1971
C

Distribution of this document is unlimited. It may be released to the Clearinghouse, Department of Commerce, for sale to the general public.

Reproduced by
NATIONAL TECHNICAL
INFORMATION SERVICE
Springfield, Va. 22151

537

EDITED TRANSLATION

UNSTEADY FLOW AROUND AND AEROELASTIC VIBRATION IN TURBOMACHINE CASCADES

By: G. S. Samoylovich

English pages: 526

Source: Nestatsionarnoye obtekaniye i aerouprugiye kolebaniya reshetok turbomashin 1969, Moscow, Izd-Vo Nauka, pp 1-444

Translated under: F33657-70-D-0607-P004

UR/0000-69-000-000

THIS TRANSLATION IS A RENDITION OF THE ORIGINAL FOREIGN TEXT WITHOUT ANY ANALYTICAL OR EDITORIAL COMMENT. STATEMENTS OR THEORIES ADVOCATED OR IMPLIED ARE THOSE OF THE SOURCE AND DO NOT NECESSARILY REFLECT THE POSITION OR OPINION OF THE FOREIGN TECHNOLOGY DIVISION.

PREPARED BY:

TRANSLATION DIVISION
FOREIGN TECHNOLOGY DIVISION
WP-AFB, OHIO.

TABLE OF CONTENTS

	PAGE
INTRODUCTION	
PART I: GENERAL PROPERTIES OF UNSTEADY MOTION OF A FLUID THROUGH CASCADES	
CHAPTER 1. BASIC UNSTEADY AERODYNAMIC AND AEROELASTIC PHENOMENA IN TURBOMACHINES	1
§ 1.1. Classification of Phenomena	1
§ 1.2. Features of Unsteady and Aeroelastic Phenomena in Turbomachines	4
CHAPTER 2. THE BASIC EQUATIONS AND ELEMENTARY (FUNDAMENTAL) SOLUTIONS OF THE UNSTEADY MOTION OF A FLUID	32
§ 2.1. Basic Equations and Galileo and Lorentz Transformations	32
§ 2.2. The Velocity Potential and the Acceleration Potential	39
§ 2.3. Green's Theorem and the Kirchoff Formula	42
§ 2.4. Elementary Solutions for an Incompressible Fluid	43
§ 2.5. Elementary Solutions for Subsonic Flow	51
§ 2.6. Elementary Solutions for Supersonic Flow	59
§ 2.7. Energetic Interaction Between Stream and Body	65
CHAPTER 3. GENERAL PROPERTIES OF UNSTEADY FLOW IN A CASCADE	70
§ 3.1. Preliminary Remarks	70
§ 3.2. The Singularity Cascade in an Incompressible Fluid	70
§ 3.3. A Singularity Cascade in a Subsonic Stream	76
§ 3.4. A Singularity Cascade in a Supersonic Stream	82

PAGE

§ 3.5. A Cascade as a Singular Line 86

§ 3.6. A Dense Cascade in a Nonuniform Vortex Stream 98

§ 3.7. Singularities of Three-Dimensional Flow About a Cascade 112

PART II: UNSTEADY FLOW ABOUT CASCADES

CHAPTER 4. A TWO-DIMENSIONAL CASCADE OF THIN SLIGHTLY BENT PROFILES IN AN UNSTEADY STREAM OF INCOMPRESSIBLE FLUID 122

§ 4.1. Preliminary Remarks 122

§ 4.2. Use of the Acceleration Potential Method 123

§ 4.3. Attached Cascade Masses 138

§ 4.4. A Cascade in an Unsteady Vortex Stream 146

§ 4.5. Flow About a Cascade of Thin Vibrating Profiles 161

§ 4.6. Solution of the Problem of Unsteady Flow About a Cascade by the Vortex Method 185

CHAPTER 5. TOTAL CHARACTERISTICS OF CASCADES IN THE CASE OF UNSTEADY STREAMLINE FLOW 196

§ 5.1. Basic Problems and Total Characteristics 196

§ 5.2. Influence Coefficients 200

§ 5.3. Unsteady Motion for an Arbitrary Relationship to Time 219

§ 5.4. The Influence of a Shift of Profiles in a Cascade 225

§ 5.5. Determination of the Total Quasi-Steady Characteristics of Cascades by Means of an Electrohydrodynamic Analogy 230

CHAPTER 6. A CASCADE OF VIBRATING PROFILES IN A SUBSONIC STREAM 239

§ 6.1. Formulation of the Problem 239

§ 6.2. A Single Vibrating Profile in a Subsonic Stream 243

§ 6.3. A Cascade of Vibrating Profiles in a Subsonic Stream 254

CHAPTER 7. FLOW ABOUT A CASCADE OF ARBITRARY PROFILES, OSCILLATING WITH AN ARBITRARY PHASE SHIFT 269

§ 7.1. Preliminary Remarks 269

§ 7.2. Formulation of the Quasi-Steady Problem of Flow About a Cascade of Arbitrary Profiles With Account Taken of Their Displacement 271

PAGE

§ 7.3. Derivation of the Basic Formulas 277

§ 7.4. A Circle in a Nonstabilized Stream 283

§ 7.5. Purely Circulatory Flow About a Cascade of Circles With a Phse Shift 290

§ 7.6. The Problem of Flow Around a Cascade With Arbitrary Profiles, Oscillating With a Phase Shift, in a Quasi-steady Formulation 294

§ 7.7. Solution of the Problem of the Oscillation of Arbitrary Profiles in a Cascade, With a Phase Shift, by the Method of Integral Equations 303

CHAPTER 8. INTERFERENCE OF TWO CASCADES MOVING IN RELATION TO EACH OTHER IN A POTENTIAL STREAM (QUASI-STEADY PROBLEM) 325

§ 8.1. Calculation of Flow About Two Moving Cascades by the Method of Conformal Transformation 325

§ 8.2. Calculation of Flow About Two Moving Cascades by the Method of Integral Equations 332

§ 8.3. Calculation of Flow About Two Moving Cascades by the Method of Successive Approximations 341

PART III. OSCILLATIONS OF TURBOMACHINE BLADES

CHAPTER 9. FORCED BLADE OSCILLATIONS IN A NONUNIFORM FLOW 346

§ 9.1. Trailing Wake and its Characteristics 346

§ 9.2. Dynamic Stresses in Blades, Produced by Nonuniformity in the Flow 367

§ 9.3. Dynamic Stresses in Blades With Partial Input 378

CHAPTER 10. OSCILLATION OF A COUPLED SYSTEM OF BLADES 392

§ 10.1. The Blade Ring as a Coupled System of Blades 392

§ 10.2. Quasi-steady Influence Coefficients 397

§ 10.3. Energy Exchange During the Oscillation of a Blade System 407

§ 10.4. Free Oscillation of a Blade Ring 415

§ 10.5. Forced Oscillation of a Connected Blade System 423

§ 10.6. The Self-Oscillations of a Connected System of Blades 430

PAGE

CHAPTER 11. INVESTIGATION OF THE AERODYNAMIC CAMPING AND AERODYNAMIC EXCITATION OF TURBOMACHINE BLADES 439

11.1. A Device for the Investigation of Aeroelastic Processes in Turbomachinss 439

11.2. Determination of Aerodynamic Damping 453

11.3. Investigation of Forced Oscillation 470

11.4. Investigation of Dynamic Stresses in the Case of Partial Supply 493

SUPPLEMENTS AFTER PROOF READING 505

REFERENCES 511

NOTATIONS 523

SYMBOL LIST 526

Methods of calculating, and experimental results of research on, unsteady flow in aerodynamic cascades of turbomachines are set forth. The conditions of excitation and damping of blade vibration in compressible and incompressible fluid flow are considered. The theoretical methods are based upon a model of an ideal fluid. The incoming stream may be inhomogeneous and have vortices due to the influence of a preceding cascade. The experimental results pertain to determination of the dynamic stresses brought about by stream inhomogeneity in the turbomachine, as well as to determination of the unsteady aerodynamic forces which excite and damp blade vibrations. Consideration is given to the origination of cascade flutter and the effect of inhomogeneity of an aerodynamic cascade. The experimental research methods are described.

Tables - 32. Illustrations - 72. Bibliography - 152 Titles.

FOREWORD

The theory of steady flow in aerodynamic cascades has been worked out in detail and is finding extensive practical application. It is known that the use of this theory and corresponding experimental research permitted the efficiency of turbomachines to be substantially increased.

Considerable interest has recently been manifested in problems of unsteady flows in turbomachines and, in particular, in aerodynamic cascades. This has been brought about by the fact that unsteady aerodynamic and aeroelastic phenomena affect the limit strength, the reliability, and the operating efficiency and weight of turbomachines. A number of phenomena originating in turbines, compressors, and pumps may be explained only with the study of unsteady flows. Such processes include: air damping, separation due to rotation, various forms of flutter, excitation of blade vibration by moving wakes, surging, etc.

The book considers some problems dealing with non-separating flows in turbomachine cascades. This sufficiently delimits the area of research. With regard to other problems, the book contains only a classification and a brief survey, with references to basic works or to works with a detailed survey and a bibliography.

Problems dealing with unsteady flow around vibrating turbomachine cascades, flow around cascades by an eddy current, and various forms of flutter differ substantially from analogous problems for a single wing. This is explained by the fact that new phenomena are observed in cascades: aerodynamic resonance, cascade flutter, etc.

Another essential feature is the fact that the profiles of turbomachine cascades can be thick and have large curvatures.

It must, however, be emphasized that without the achievements of wing theory it would be impossible to hope for success in the study of flow about a cascade. Basic problems in the theory of unsteady

flow about a wing have been studied by S. A. Chaplygin, M. V. Keldysh, N. Ye. Kochin, M. A. Lavrent'yev, L. I. Sedov, A. I. Nekrasov, M. D. Haskind, L. Prandtl, V. Birnbaum, G. Wagner, G. Kuessner, G. Glauert, T. Karman, W. Sears, C. Possio, D. Miles, etc. Equally essential is utilization of the hydrodynamic theory of steady flow around cascades, at the basis of which lie the works of N. Ye. Zhulovskiy, S. A. Chaplygin, N. Ye. Kochin, L. I. Sedov. This theory was further developed in a number of works, principally by Soviet authors.

In setting forth the problems, the author has attempted to emphasize the physical essence of the phenomena under consideration, which is important in engineering applications.

Also set forth in the book are some experimental results concerning the determination of dynamic stresses in turbomachine blades.

The book is intended for mechanical engineers and staff members of aerodynamic and strength laboratories of plants, scientific research institutes, and design offices working in the field of turbomachines. The book is of interest for teachers, graduate students, and university students in the appropriate fields.

The author thanks his collaborators: I. Neruda, I. N. Pis'min, V. V. Mitusov, B. E. Kapelovich, V. I. Kovalenko, F. Ruben and E. V. Yurkov, who participated in the study of unsteady and aeroelastic phenomena in turbomachines.

The author is sincerely grateful to L. G. Loytsyanskiy for attention and support, to A. S. Zil'berman for helpful discussions of the problems. The author is grateful to G. Yu. Stepanov for valuable remarks made when reading the manuscript.

G. S. Samoylovich

Moscow, March, 1968

PART I

GENERAL PROPERTIES OF UNSTEADY MOTION OF A FLUID THROUGH CASCADES

Chapter 1

BASIC UNSTEADY AERODYNAMIC AND AEROELASTIC PHENOMENA IN TURBOMACHINES

§ 1.1. Classification of Phenomena

In turbomachines (steam and gas turbines, air or gas compressors, hydraulic turbines and pumps), a gas or an imcompressible fluid move through a system of stationary and rotating aerodynamic cascades.

The working process in a turbomachine consists of the exchange of energy between flowing gas and moving cascades. Consequently, the essential feature is the interaction of forces between the flow of fluid and elastic blades.

The process taking place in a turbomachine may, on the average, be regarded as steady (if transient regimes are excluded) in the sense that it must be cyclically repeated at least with every other turn of the rotor. However, this basic cycle is accompanied by a series of unsteady phemomena, which take place in the aerodynamic cascades and in entire turbomachines as a whole.

Unsteady phenomena may be divided into two groups. Purely aerodynamic unsteady phenomena belong to the first group, i.e., phenomena in which the coupling between the aerodynamic and the elastic characteristics of the system is not essential. These phenomena can take place even when the blades of the aerodynamic cascade are absolutely rigid. Obviously, the corresponding problems can be described by aerodynamic equations alone. Such phenomena include:

(1) Flow about aerodynamic cascades by a nonuniform and periodically unsteady flow. In a turbomachine there is a number of reasons for which the absolute flow motion is inhomogeneous in the circumferential direction. Such inhomogeneity is brought about, for example, by viscous trailing wakes propagating beyond the blades of a stationary cascade, the supply of gas along only part of the circumference (partial supply), turning of the stream in the supply system, etc. Inhomogeneity of absolute flow motion brings about nonuniformity in terms of relative motion (and vice versa).

(2) Flow in aerodynamic cascades by a stream with considerable turbulence, formed after the disintegration of vortex wakes. Typical here are influences of a random nature, subject to statistical laws.

(3) Rotation separation originating in a cascade of the turbomachine. The self-exciting unsteady flow asymmetry originating in an aerodynamic cascade when a certain critical entry angle is exceeded is called separation due to rotation.

(4) Surging or self-excited vibration of the gas flowing through the compressor and the feed lines. In such a case instability typically originates not in an individual cascade or stage, but in the entire turbomachine and network.

Phenomena for which the coupling between the aerodynamic and mechanical characteristics is essential belong to the second group. Obviously, these problems can be studied only with simultaneous study of the equations of aerodynamics and elasticity theory.

This class of phenomena may be observed only when the mechanical system can become deformed in the stream. If the stream possesses elasticity, vibrations can originate, and the possibility arises of energy exchange between the mechanical system and the stream. When the vibrating system transmits energy to the stream, aerodynamic damping is observed, and the vibrations, if they are not sustained by some external energy source, will attenuate. The vibrating system may also obtain energy from a uniform stream, and in such a case non-damping vibrations may be maintained. This phenomenon is called self-excited vibration, and in application to aerodynamic cascades and wings it is called flutter.

The phemomena of the second group include:

(1) Aerodynamic damping of the vibration of elastic blades in an aerodynamic cascade around which flows a stream of fluid.

(2) Flexural-torsional flutter of blades in an aerodynamic cascade. The presence of elastic coupling between the flexural and torsional vibrations of an elastic body when the center of mass and the center of torsion do not coincide is essential.

(3) Cascade flutter, which may be excited only in a system of elastic bodies immersed in a stream. Cascade flutter originates in the case of purely flexural or purely torsional blade vibration. The possibility of the existence of this type of flutter depends upon the aerodynamic and mechanical connection of the cascade.

(4) Separation flutter, which originates under specific conditions with the appearance of separation on the cascade profiles. This form of flutter may also originate in a single wing, although the coupling between the blades in a cascade exerts a substantial influence.

(5) Wave flutter, which may appear only in a supersonic stream in the presence of shock waves which interact with the boundary layer.

In essence, all the basic problems pertain to the study of vibration, either of a gas stream or of a system of elastic bodies in a stream. Therefore, classifying the phenomena from the point of view of vibration theory, they may be divided into forced vibration and self-excited vibration. Blade vibration in a nonuniform flow belongs to the first category. All other forms of flutter, rotation separation and surging belong to the second category. Such a classification is based upon the method of energy supply to the vibrating system. In the case of forced vibration, the energy is supplied in portions, since the energy source is periodic (or intermittent). In the case of self-excited vibration, the energy is extracted from a constant source in portions which are regulated by the vibrating system itself.

§ 1.2. Features of Unsteady and Aeroelastic Phenomena in Turbomachines

Let us consider two two-dimensional cascades formed by developing the cylindrical surface intersecting a stage of an axial turbine onto a plane (Figure 1.1). Let us assume that this cross section has been made in cylindrical or almost cylindrical stage, so that the surface may be regarded as the averaged current surface as is done in the theory of axial turbomachines when studying steady flow. The first aerodynamic cascade, which is stationary with respect to the turbine housing, is called the directional or the nozzle cascade. The second aerodynamic cascade, which moves with respect to the first one with a circumferencial velocity of u, is called the impulse cascade. In the majority of cases, modern turbomachines are made with several stages, so that there are adjoining stages before and after the stage under consideration. However, in order to isolate the basic features, we shall simplify the picture and shall regard the stage under consideration as being isolated.

A stream of viscous compressible fluid moves through the cascades. The relationships between the stream velocity, the characteristic dimensions of the blades, and the viscosity of the fluid in turbomachines usually correspond to large Reynolds numbers, and

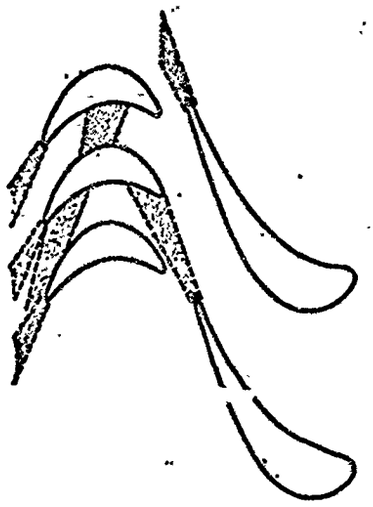


Figure 1.1. Cylindrical section of the aerodynamic cascades of a turbine.

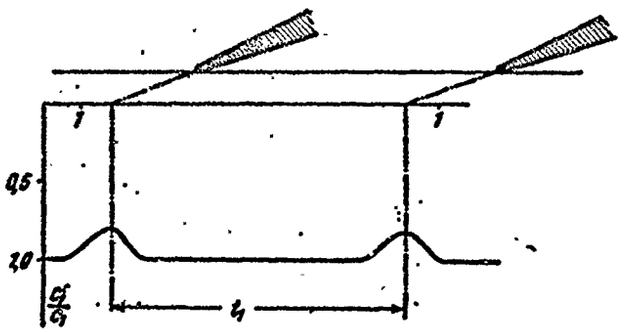


Figure 1.2. Distribution of absolute velocities after the directional cascade.

therefore the methods of boundary-layer theory may be used.

In the nozzle cascade it is possible to distinguish the flow core, in which there is potential flow, and a thin boundary layer, situated on the blade surface. The turbulent streams propagate beyond the trailing edges of the nozzle blades. Thus, the stream emerging from a nozzle cascade is inhomogeneous. At a small distance from the cascade, at the so-called initial portion, there is considerable inhomogeneity of the velocity field, the static-pressure field and direction-angle field of the stream. Somewhat further downstream there is a relatively rapid smoothing out of the static pressure field, and the directional angle field, although the velocity field has considerable inhomogeneity. Figure 1.2 shows the velocity distribution in a control cross section 1 - 1 beyond the directional cascade. The ratio of the local flow velocity to the constant velocity in the potential core is plotted along the ordinate. The pattern is periodically repeated at every step t_1 of the directional cascade.

Let us now consider flow about a moving impulse cascade. Let us sketch velocity triangles for the flow core. The flow proceeds from the nozzle cascade with the absolute velocity c_1 (absolute

velocities are called those which are measured with respect to a stationary cascade) at a constant angle α_1 and enters the impulse cascade with a relative velocity of w_1^0, directed at an angle β_1. We measure the angles with respect to the straight line (cascade axis) connecting similar points of the profiles in the manner shown in Figure 1.3. At the moment when the working blade passes through the zone of the edge wake, the absolute velocity alters its value and, in accordance with this, the relative velocity changes both with respect to magnitude and direction. This brings about a periodic change in the flow regime in the impulse cascade, which is manifested in a change of the pressure distribution with respect to profile and a reformation of the boundary layer.

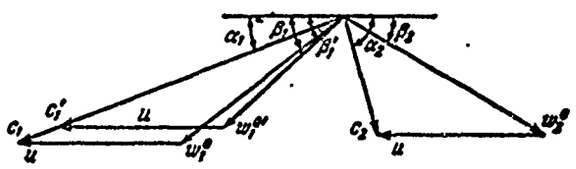


Figure 1.3. Velocity triangles of a compressor stage.

The eddy fluid from the boundary layer is carried away by the stream with a relative velocity of w_2^0 and forms vortex wakes behind the impulse blades. These vortex wakes exist simultaneously with the vortex wakes which originate in steady flow. Steady vortex wakes are neutral in the sense that the intensity of the vortices in a strip laid out across the wake is equal to zero. Unsteady vortex wakes in this case are distinguished by the fact that they are not neutral and induce a velocity field in the ambient fluid, i.e., they change the flow regime in the cascades. With periodic change of the stream pattern, the intensity of the unsteady vortex wakes also changes periodically, and the total vortex intensity carried away by the stream during the period is equal to zero.

The influence of an unsteady vortex wake upon the regime of flow in the cascade constitutes a basic distinctive feature of unsteady flow. In view of the fact that an influence is exerted by all the vortexes previously carried away, the flow regime depends upon the history of the motion.

Vortex wakes trailing from the directing cascade are intersected by the working cascade. Large-scale turbulence originates at first. Then the large vortexes are broken up into smaller ones. Passing along the channel of the working cascade, the turbulent wakes turn, since the main stream in the channels is inhomogeneous. On the back of the blades, the speed of the main stream is greater than on the concave side. At the moment of intersection of the trailing wake by the turbine blade, the angle of attack becomes negative, the pressure on the convex side of the profile increases, and decreases on the concave side. The pressure oscillations along the entire profile occur almost in phase, since the propagation time of the perturbation, which runs along the profile with the velocity of sound plus the stream velocity, is usually an order of magnitude smaller than the period of the oscillations.

Let us note one more important feature of nonsteady streamline flow.

For steady streamline flow, the pressure gradient must be equal to zero, at the sharp trailing edge, which causes the velocities at the outer edge of the boundary layer to be equal on both sides of the edge. For a nonviscous fluid this is postulated by the Zhukovskiy -Chaplygin rule. In non-steady flow the pressure is equal, but the pulsation components of the velocities will not be equal, this being explained by the trailing of the eddy layer of fluid which we have mentioned above.

Let us now consider the motion of gas in the stage of an axial compressor. The aerodynamic cascades are shown in Figure 1.4. In general terms, the phenomena will be the same as in the case of a turbine stage, but there are some special features. The first working aerodynamic cascade moves at a rate of u; the second one — the directing cascade — is motionless. The velocity triangles of this stage are given in Figure 1.5. In the vortex wakes formed by the working cascade, the relative velocity w° will be smaller than in the core of the flow. By virtue of this, the motionless cascade will be

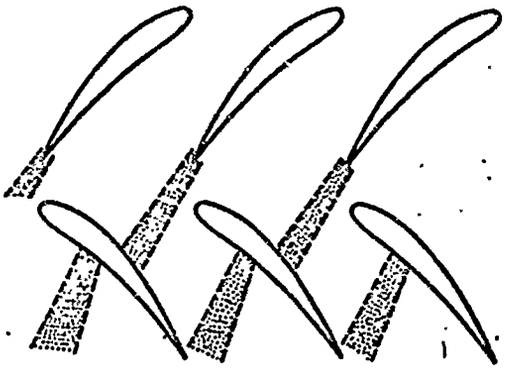


Figure 1.4. Cylindrical section of the aerodynamic cascades of an axial compressor.

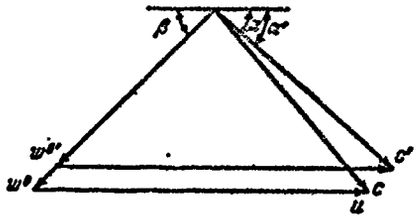


Figure 1.5. Velocity triangles of a compressor stage.

located in a pulsating flow. In contrast to the preceding case, intersection of the wake brings about the appearance of a positive angle of attack, and not a negative one. In this connection, the pressure at the back of the profile of the motionless cascade will decrease, and the pressure at the concave surface will increase in comparison to the calculated pressure. This change of the angle of attack affects the streamline flow conditions more than in a turbine cascade, since compressor turbine cascades have a large relative pitch and thin inlet edges.

Above we have been considering disturbances that can be brought about by the first cascade, which is located in a subsonic stream. The cause of the perturbation was inhomogeneity of the stream, brought about by the viscosity of the fluid.

In many cases the flow at the outlet of the first cascade is supersonic, and then considerable inhomogeneity can be brought about by the appearance of shock waves and decompression waves. Figure 1.6 shows a schematic diagram of the wave system supersonic flow at the outlet from a cascade with converging channels for a supercritical pressure gradient. Since the pressure past the outlet edges is below critical, rarefacation wave 1-2-3 originates. Rarefaction

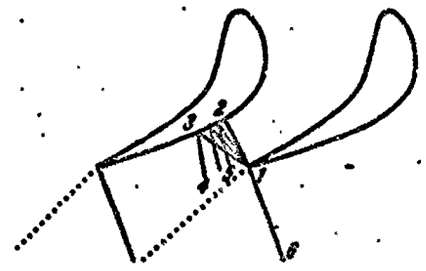


Figure 1.6. Structure of supersonic flow at the outlet from a cascade with convergent channels.

wave 1-2-3 is reflected from the convex surface of the adjacent profile by rarefaction wave 2-3-4-5. Shock wave 1-6 is also being formed at the outlet edges. The trailing wakes are marked by dotted lines. This is a schematic representation of the simplest case, which is realized in the case of a small supersonic gradient and sharp outlet edges.

Thus, in the supersonic velocity case, the inhomogeneity of the flow behind the directing cascade can increase substantially due to the origination of shock waves and rarefacation waves.

In the problems discussed above, consideration was given only to the influence of the first cascade upon the second. Indeed, this influence is the most important one. However, the presence of a second cascade of course distorts the flow emerging from the first one. The trailing wakes are washed out and, by virtue of the turbulent structure, are random in nature. Shock waves and rarefaction waves proceeding from the first cascade are reflected by the second one. In such a case the flow pattern becomes very complicated, and so far it is possible to rely only on experimental research for the overall effects.

Distrubances originating at the cascade profiles bring about a reconstruction of the stream, and the blades become acoustic emitters. The pulses transmitted by the blades propagate with the speed of sound, and consideration of this pattern is of practical interest in the study of vibration stresses, and of the noise created by turbomachines. The blade cascade constitutes a system of sources, and therefore acoustic resonance is possible under certain conditions. Acoustic resonance in a single cascade is a special case. The pattern becomes very complicated, and a large number of possible

cases are possible if the acoustic waves propagate in a system of cascades that are moving with respect to one another.

The acoustic waves emitted by the blades propagate in all directions, including (under specific conditions) the direction of the nozzle cascade, are reflected from solid boundaries, to the working cascade, etc. In the case of certain velocity relationships and combinations of geometrical cascade shapes, regular reflection is possible, which is capable of bringing about blade vibrations. This has been confirmed by direct experiments. Figure 1.7 shows a possible case of regular reflection. In the general case acoustic waves can propagate both in the direction of rotation and against it. Under certain conditions, an acoustic wave running counter to the rotation of the wheel will be motionless with respect to the directing cascade. This case apparently presents the greatest danger, since a standing wave is formed. The actual pattern depends to a considerable extent upon refraction of the waves in the turbulent wakes. The resonance phenomena are considerably weakened by aerodynamic inhomogeneity of the stream and geometrical homogeneity of the cascades. This latter property (for example, change of the spacings) may be used in the design, in order to avoid dangerous consequences.

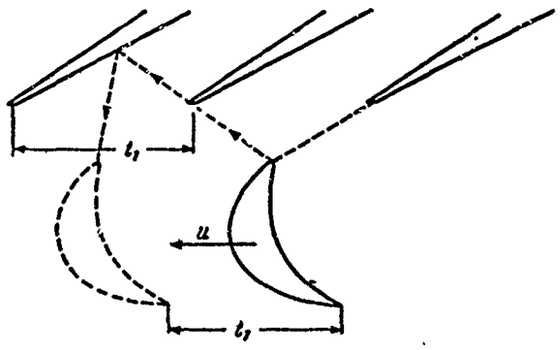


Figure 1.7. Regular reflection of acoustic waves in a turbine stage.

Noise originating in the operation of a turbomachine is determined by at least two causes. In the first place, the blades serve as acoustic emitters and are of the pressure dipole type. In the second place, noise originates along the boundaries of the turbulent edge jets. In the latter case the acoustic sources are quadrupoles. The resonance processes in the stream affect the noise level.

Aside from the inhomogeneities connected with the presence of an trailing wake and waves, a substantial effect can be exerted by an inhomogeneity originating in the potential stream with the shift of the cascades with respect to one another as has been shown by calculations.

Let us consider two cascades, through which a potential stream of ideal fluid flows(Figure 1.8). The working cascade moves in the negative ordinate direction. Obviously, the flow regime in the two cascades depends upon their position with respect to one another. The pressure distribution along the profiles of the directing cascade does not change if the working cascade is shifted by its spacing of t_2. In precisely the same manner, the pressure distribution along the profiles of the working cascade does not change if it is shifted by the spacing of the nozzle cascade — t_1.

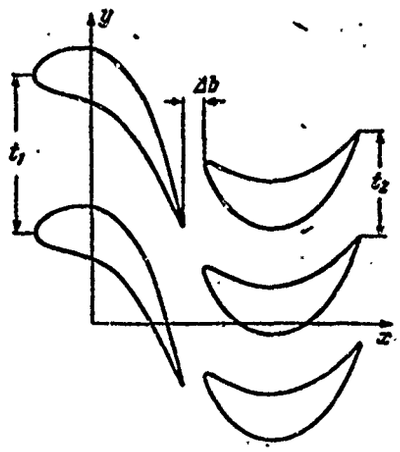


Figure 1.8. Concerning the influence of cascades moving with respect to one another in a potential flow.

Mutual cascade influence of this type becomes much weaker when the gap Δb is increased. The perturbations which are presently being considered also originate in a potential stream. However, since a change of the circulation around the profiles originates as a result of interference, vortex wakes will appear after them. The reason for the appearance of these wakes in an ideal fluid may be explained in the following manner.

The motion of an ideal incompressible fluid, starting from a state of rest under the influence of mass forces, is potential, but may have discontinuities in the velocity fields. These solutions with discontinuities must be considered in order to satisfy the physical requirements at the sharp trailing edge of the profiles. In the contrary case, infinitely large velocities and, consequently, infinite

negative pressures, will originate at the trailing edge. This mathematical model, with a discontinuity proceeding from the rear edge, selects among the possible solutions the one which has the characteristic feature of an actually observed phenomenon. It is known from the solution of many problems of mathematical physics that conditions at sharp edges must be discussed separately, and in addition to observing the usual boundary conditions, special physical hypotheses must be resorted to.

This feature of unsteady streamline flow may also be explained from a somewhat different point of view. The solution of the problem of flow about bodies (in the present instance — cascades) by a stabilized stream of an ideal incompressible fluid may be obtained by placing a vortex layer along the surfaces of the bodies with a density distribution such that the boundary conditions are satisfied. The distributed vortexes are called Zhukovskiy's attached vortexes and are connected with the distribution of local forces (determined by Zhukovskiy's theorem concerning local lifting force). With a change in the conditions of flow about the body, the distribution density of the vortex layer changes. The released vorticity is carried away by the mainstream along the surface of the blades, and then forms a vortex wake which flows off the trailing edge. In the presence of interaction among the vortexes and with shifting of the second cascade, the motion of these vortex wakes will be very complex. In individual cases it is possible to formulate a series of simplifying assumptions and solve the problem approximately. Thus, for example, if the cascade profiles have small curvature, if the flow has a small angle of attack, and if the intensity of the vortex sheet is small, it may be assumed that the vortex wakes propagate from the trailing edges of the blades along straight lines (although the motion of the sheet will be unstable).

The problem of unsteady flow about the working cascade in a nonuniform potential stream which is perturbed by the succeeding nozzle cascade is of practical interest (particularly if the axial

jet is small, and the inlet edges of the second cascade are thick). Such a problem does not differ in principle from the one considered above.

The solution of problems of flow about a cascade by a nonuniform unsteady stream has several technical applications.

The determination of nonsteady forces which cause blade oscillation is necessary in the evaluation of vibration reliability of the blades. Frequently one makes a comparative evaluation of the danger of various types of oscillations.

In formulating the corresponding problems, it is necessary to introduce substantial simplifications. In all cases, only an ideal fluid is considered.

The problem of the displacement of cascades with profiles of arbitrary form with respect to one another is solved in an incompressible liquid in a quasi-steady formulation in order to obtain numerical results. The simplest case is where the spacings of the cascades are identical (although in practice, this case is usually not treated). The case where the cascade spacings are different has been solved in principle, but requires extensive calculations.

The problem of flow about an insulated cascade by a vortex stream has been solved only in a linear formulation for thin profiles with small curvatures.

Problems concerning the motion of cascades in a nonuniform field brought about by the influence of inlet and outlet nozzles are related to this group. Special interest is afforded by the problem of movement of the working cascade with supersonic velocity at the outlet, in a nonuniform stream caused by the outlet nozzle.

A second problem presented by practical considerations is the determination of supplementary losses of kinetic energy connected

with unsteady streamline flow. These losses are brought about by the expenditure of energy for the formation of a vortex wake behind the profile, velocity pulsations in the boundary layer, and acoustic radiation. Losses also originate during smoothing out of the velocity field inside the channels and beyond the cascade due to the influence of viscosity forces. The problem of the expenditure of energy on the formation of a vortex wake may be considered on the basis of an ideal fluid model.

The evaluation of supplemental energy losses in the boundary layer is also possible in principle. For this it is necessary to calculate the external nonsteady potential stream and to resort to the theory of a nonsteady boundary layer.

The energy expenditure for acoustic radiation in a compressible fluid is small in a number of cases, but precise evaluations for an arbitrary case involve considerable difficulties.

It is necessary to note that the experimental determination of supplementary nonsteady losses is also a complex problem. In general these losses are not very great. However, the available experimental investigations yield contradictory results.

Special regimes may originate in turbomachines, in which a strong separation of the stream appears at the cascades. Such regimes represent considerable vibrational danger and bring about a substantial drop in efficiency. Separation regimes are always unsteady. Their theoretical investigation involves considerable difficulties. The available studies are based upon rather crude assumptions. Here it must be noted that a stream which is nonuniform in a circumferential direction will facilitate earlier separation.

It was noted above that acoustic radiation is possibly not even a very large item in the total loss balance. However, the noise originating during the operation of turbomachines is to a considerable degree linked to the generation of acoustic waves on the blades in unsteady streamline flow. The study of noise intensity and of the

structure and characteristics of noise is of great practical significance, particularly for compressors operating at high velocities. A number of experimental studies in this direction are known. The theoretical studies are based upon the introduction of radiating dipoles which are caused by pulsating forces, into the flow field. This problem is in some measure equivalent to studying aircraft propeller noise.

The problem on unsteady flow about cascades is of interest also in the field of hydraulic turbines and turbopumps; in addition to some enumerated problems, there is the problem of the cavitation characteristics of a cascade operating in a nonuniform stream.

The quantity used to characterize the cavitation in hydrodynamic machines is the so-called cavitation number, which is proportional to the difference of the pressure in an unperturbed stream at the moment of the start of cavitation and the saturation pressure at the temperature of the flowing liquid. In flow about blades, cavitation commences earlier, the lower the minimum pressure on the blade, which in a homogeneous stream depends upon the shape of the profile and the incident flow angle. Cavitation originates at the point of minimum pressure on the blade. As the angle β_1 increases, this point moves toward the leading edge. A break of the cavitation curve (the relationship of the cavitation number to the angle of attack) is observed from the moment when cavitation bubbles begin to form on the leading edge of the profile (Figure 1.9). When the cascade of a hydrodynamic machine moves in a nonuniform stream, the blades intersect turbulent jets and operate with a variable entry angle. Since at the moment of intersection of the turbulent wake the angle β_1 increases (for example, in the pump), this brings about an earlier origination of cavitation in comparison with a uniform stream.

The unsteady forces acting upon turbomachine blades are considerably smaller than the static forces, and therefore they are dangerous only in the case of resonance vibrations. Determination of the frequency (but not the value) of the regular perturbing forces is

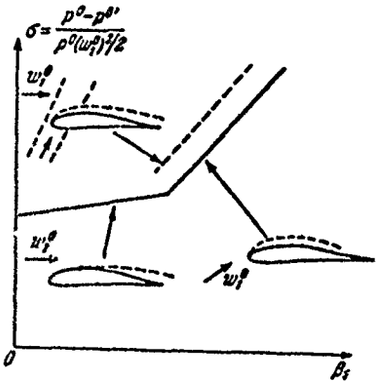


Figure 1.9. Relationship of the cavitation number σ to the incident flow angle β_1; w_1^0 and p^0 are respectively the velocity and pressure in the mainstream, $p^{0'}$ is the saturation pressure. Dotted line indicates the sector of the cavitation curve with circular unevenness of the flow due to the wakes of the preceding cascade.

elementary. However, wave oscillations brought about by random aerodynamic forces also originate in turbomachines. The reason for the manifestation of these forces is understandable, since along the boundaries of turbulent trailing wakes there are the so-called intermittant zones. In these zones, irregular velocity pulsations are observed. In addition, the disintegration of vortex jets under the action of a shifting cascade also brings about irregular pulsations of the stream. Particularly large pulsations originate in the case of separation flow about the cascades. Special measurements, conducted by means of quick-response probes, make it possible to obtain the amplitudes and the frequencies of the pulsations. These pulsations are particularly large behind rotating cascades, which have also been confirmed by direct experiments in which the measurements of relative motion are made. In such measurements, regular velocity dips are observed in the wake behind a rotating cascade, as well as irregular pulsations superimposed both upon the wake and upon the flow core.

Practical interest is afforded by the study of blade oscillations under the action of random aerodynamic forces. The corresponding problems are analogous to problems of the flight of an aircraft in a turbulent stream. However, the presence of cascades and not of a single wing introduces basic difficulties.

In some turbine stages so-called partial supply is used, i.e., the supply of the working medium is not along the entire length of the circumference, but only along a specific arc. Thus, the working

blades periodically enter (and emerge from) a jet of gas flowing at a high velocity. In such a case a very pronounced radical reconstruction of the pattern of flow about the blade of a working cascade takes place. In this case the working blades cannot be tuned out from the resonance frequency in view of the high density of the spectrum of the perturbing force (1 - 2% between adjacent harmonics). Consequently, precise evaluation of the dynamic stresses is of particularly great significance. A second question, also very important, is evaluation of the reduction of economic efficiency. In stages with partial supply, the flow velocities are frequently supersonic not only in terms of absolute motion, but also in terms of relative motion. It may be assumed that in some cases it is of essential significance to take into account the propagation and reflection of shock waves originating at the jet boundaries in the cascade channels.

Let us now devote some attention to the phenomenon of aerodynamic damping. In the excitation of oscillations of elastic blades in a cascade, there originates the possibility of energy exchange between the oscillating blades and the stream. In principle, passage of energy is possible both from the blades to the stream and in the opposite direction. The first of these processes is called aerodynamic.

Let us consider the oscillation of a single wing in a uniform stream (Figure 1.10). The wing performs small oscillations in a direction perpendicular to the chord. If, during oscillation, a blade moves in the direction of arrow 1, the angle of attack decreases; but if the motion takes place in the direction of arrow 2, the angle of attack increases. Change of the angle of attack brings about a change in the lifting force, and an increment of the lifting force will counteract the motion, since it is directed against the rate of movement of the blade. Consequently, an oscillating blade will give energy to the stream, i.e., aerodynamic damping of the oscillations will originate. With a change in the circulation behind the blade, a vortex wake will appear; this will introduce only a quantitative correction into the aerodynamic damping. If the fluid is compressible,

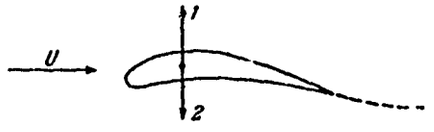


Figure 1.10. Oscillation of a single wing in a stream of fluid.

the damping increases on account of energy scattered by acoustic radiation. The problem of the oscillation of a thin single wing (the limit case of a very sparse cascade) has been solved, and corresponding computation tables exist for an imcompressible fluid, as well as for subsonic and supersonic flow.

In the case of flow about an aerodynamic cascade with oscillating profiles, the problem becomes basically more complex. In the first place, the profiles of the cascade may oscillate with different amplitudes (in a special case, some may be motionless); in the second place, the phases of the oscillations may also differ, and in the third place, a substantial effect may be exerted in the cascade by mutual displacement of profiles.

In the case of high-frequency oscillations in an unloaded cascade (a cascade is called unloaded if the static rotation of the stream is equal to zero), the influence of profile displacement may be disregarded. In such a case the interference consists in the fact that the oscillating profiles bring about mutual induction of velocities. Such a linearized problem is the simplest of all and has been considered in detail. Computation tables are available. In such a case aerodynamic damping origniates with purely translational and purely torsional blade vibrations. Aerodynamic damping depends to a substantial extent upon the distribution of the oscillation phases of the blades. Naturally, the greatest effect is exerted by the neighboring profiles. It is obvious that the greatest aerodynamic damping originates when the blades oscillate in counterphase, since in this case the normal velocities induced by neighboring profiles are directed against the motion of the blades situated between them.

In the oscillation of blades in an aerodynamically loaded cascade (large static rotation of the stream), they move in a nonuniform

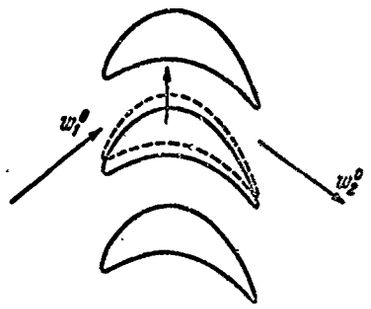


Figure 1.11. Oscillation of profiles in a cascade and the influence of shift.

field (Figure 1.11). Let us at first assume that only one blade is oscillating, and that the rest of them are motionless. The unsteady part of the pressure on the profile will have one component, proportional to the speed of the oscillations, and a second component, proportional to the acceleration (the effect of the vortex wake will be disregarded in these considerations). In addition, since the field of the main stream is nonuniform in the direction of the cascade axis, the pressure distribution will depend upon the shift of the blade under consideration. In practice, the vibration velocities are small in comparison to the velocity of the main stream, and the displacements are small in comparison to the cascade spacing. Therefore, the problem may be linearized, and the three components of the unsteady flow may be considered separately. It is obvious that during the oscillation cycle, work can be performed only by the force which is in phase with the speed of movement of the profile. Since this force is contrary to the direction of the movement, aerodynamic damping of the oscillations will be observed. The situation will change basically if the neighboring profiles oscillate synchronously with the profile under consideration, but there will be a phase shift. In the general case a component of the unsteady force originates which depends upon the displacement of all the profiles and which is in phase with the oscillation rate. Obviously, this force may perform positive or negative work, i.e., it may damp oscillations or excite them.

If the profiles are oscillating in a compressible fluid, then in addition to acoustic radiation, which brings about supplementary energy dispersion, a new phenomenon may be observed in the cascade — resonance oscillations of the gas (which cannot originate for the case of a single wing).

Let us first consider the oscillations of only one profile in the cascade. In the course of the oscillations, the profile will send acoustic waves in all directions, including along the cascade axis (we are considering subsonic conditions). The rate of wave propagation depends upon the speed of sound and the direction of propagation of the waves, since they are carried away by the main stream. The waves will be reflected by motionless profiles and will be returned to the oscillating profile. If the reflected waves are returned in the corresponding phase, which depends upon the relationship among the velocity of sound, the oscillation frequency, the cascade spacing, and the main stream velocity, the onset of acoustic resonance is possible. Thus, for example, if a straight cascade of plates oscillating in counter phase is considered, the (first) resonance will occur if half the wavelength fits between the profiles. In such a case the oscillations of the gas along the cascade axis are analogous to the oscillations of a gas column in a pipe that is closed at one end and is provided with an oscillating piston on the other. The difference will be only in the fact that the main stream is flowing though the cascade, and therefore, the propagation speed of the signal (in the linear formulation) will be equal to the speed of sound multiplied by Prandtl's correction $a\sqrt{1-M^2}$.

A similar, but a somewhat more complex pattern is observed in a cascade with an offset, the profiles of which oscillate with a constant phase shift. Resonance will obviously be observed if the acoustic waves reach each profile in the phase corresponding to it. Since the propagation rates of a signal in an oblique cascade depend upon the direction, two resonances should be observed, each with the corresponding multiplicity factors.

The study of resonance is of practical interest, since under these conditions aerodynamic damping decreases, which facilitates the origination of self-oscillation of the blades.

Let us pass on to the consideration of regimes in which oscillating blades can obtain energy from the stream and, consequently, nondamping oscillations can be maintained. Since the energy is obtained

from a uniform stream, this process differs basically from the forced-oscillation process and bears the name of self-oscillations. In a special case, in the application to aircraft wings and turbomachine blades, this phenomenon is called flutter. It is theoretically clear and has been confirmed in practice that several types of flutter are possible, which differ with respect to the energy-absorption mechanism.

The first type of flutter, also called "classical," was detected in aviation.

Let us consider a single wing, which may perform flexural and torsional oscillations in a uniform stream. The center of torsion does not coincide with the center of mass (Figure 1.12). In such a case, flexural oscillations will bring about torsional ones, and conversely, i.e., combined flexure-torsional oscillations may be observed in the wing. If only purely flexural or purely torsional oscillations were to originate, they would have been damped out by aerodynamic damping (as well as mechanical damping). The appearance of joint flesure-torsional oscillations radically changes the pattern. The point is that flexural oscillations will bring about not only the unsteady lift force $\mathcal{Z}_1$, but also the unsteady moment M_1, and torsional oscillations, in addition to bringing about the moment M_2, will also bring abcut the lift force $\mathcal{Z}_2$. The work of the lift force $\mathcal{Z}_1$ and the aerodynamic moment M_2 in the respective shifts is always negative, since they are in counterphase with the oscillation rates. Consequently, this force and moment bring about aerodynamic damping. The work of force $\mathcal{Z}_2$ and moment M_1 may be positive as well as negative, and this depends upon the phase-shift angle between the torsional oscillations and the flexural oscillations. In case the energy supplied and energy drawn off balance one another, nondamping harmonic oscillations will

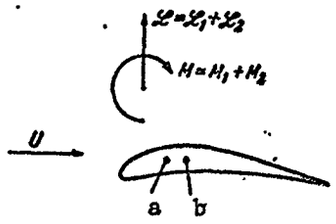


Figure 1.12. Flexure-torsional oscillations of a single profile in a stream.

originate. Since aerodynamic forces and moments depend upon the velocity of the main stream, the energy balance will occur at a specific velocity, which is called the critical velocity. If the velocity exceeds the critical, oscillations with increasing amplitude should be observed. In actual fact, nonlinear factors will become effective, which will retain the amplitude at a certain level.

An analogous flexure torsional flutter may, in principle, exist also in cascades. Calculations show that in view of the great rigidity of the blades , the required critical flow velocities are very great. Nevertheless, this question should not be considered fully solved, since under certain conditions the aerodynamic coherence of the cascades may decrease the velocity.

The second type of experimentally observed flutter can take place only with purely flexural or purely torsional oscillations of the blades in the cascade. The oscillations of each blade take place with one degree of freedom; however, the entire cascade is an elastic solid with many degrees of freedom, this being basically necessary for the origination of this type of flutter, which therefore may be called cascade flutter. In the cascade, oscillation of the blades is possible with a constant phase shift such that the energy will be derived from the stream and nondamping oscilations will originate.

Let us consider the oscillations of blades in the cascade represented in Figure 1.11. It was said above that in the case of oscillation of all the blades, they can be acted upon by a force which depends upon the relative shift. Let us emphasize that this force acts upon the blades from the side of the stream, and therefore, a force acting, for example, upon the n^{th} blade, with the shifting of the $(n-1)^{st}$ blade is altogether not equal to the force acting upon the $(n-1)^{st}$ blade. For an explanation of the phenomenon, let us consider a special case. Let us assume that all the blades oscillate with a constant phase shift, which between neighboring blades is equal to $\pi/2$. Then it is obvious that the force component induced at the n^{th} blade by the shifting of the $(n-1)^{st}$ blade will be in phase

with the vibration rate of the n^{th}. An analogous statement can be made concerning the influence of the $(n+1)^{st}$ blade upon the n^{th}. Since the sum of these forces, in accordance with what has been said above, generally will not be equal to zero, it is obvious that the n^{th} blade can absorb energy from the stream during oscillations. These considerations are valid with respect to all the blades of the cascade. If the absorbed energy is equal to the energy dispersed due to mechanical and aerodynamic damping, undamped oscillations will originate.

Thus, aerodynamic coupling of the cascade is necessary for maintenance of the oscillations. The example considered here was the most simple one, since in actuality a substantial influence is exerted by the compressibility of the fluid, inhomogeneity of the cascade(1), mechanical coupling through the elastic disk, etc. These problems, aside from their practical application, provide a number of interesting examples of the mechanics of the aeroelastic process. We shall immediately emphasize that not only in the study of flutter is it necessary to deal to a considerable extent with aeroelastic processes, but also in the study of forced oscillations, because the amplitude and phase of blade oscillations affect damping since it depends upon aerodynamic coherence. The mechanical and aerodynamic coupling of a cascade also leads to the result that it becomes possible to transmit energy from one oscillating blade to another; study of these phenomena makes it possible to explain the dispersion of instantaneous and maximum stresses in the blades of an inhomogeneous cascade. This dispersion is known from practical experience in the measurement of dynamic stresses in operating turbomachines.

In cascades situated in the streamline flow of fluid, separation flutter can also exist.

Figure 1.13 shows an experimental graph (1) of the change of the coefficient of a force normal to the chord, acting upon the profile

---

Footnote (1) appears on page 31.

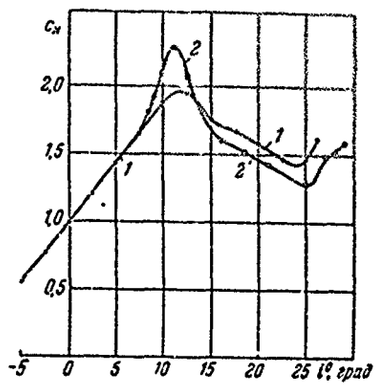


Figure 1.13. (1)-Relationship of the coefficient of normal force to the angle of attack on a motionless blade in a compressor cascade, (2)-for an oscillating blade.

in an aerodynamic compressor cascade, as a function of the angle of attack. Here is represented not the graph of a lift force, but of a normal force, since it is specifically the normal force which excites the oscillations of the blades about the axis of minimal profile inertia, which is parallel to the chord. This relationship is characterized by the fact that when the critical angle of attack is reached, the normal force starts to decrease, since separation of the stream takes place at the profiles. Damping will be observed for oscillations of a blade at the subcritical sector of the characteristic since an increase of the aerodynamic force corresponds to an increase of the angle of attack during motion of the blade. In case the oscillations take place at the decending arm of the curve, the blade may absorb energy from the stream. Steady oscillations will correspond to the case where the absorbed energy will be equal to the dispersed energy. Energy dispersion takes place both on account of mechanical damping, and on account of aerodynamic damping. The origination of separation flutter at supercritical streamline-flow angles takes place at comparatively low stream velocities and is therefore dangerous for turbomachine blades. Self-oscillations of the separation flutter type may take place both in a cascade, and in a case where the blade is isolated. However, the presence of a cascade very strongly affects the flutter characteristics, both on account of change of the static force characteristic and on account of the aerodynamic coherence of the cascade.

The relationship represented by curve (1) in Figure 1.13 was recorded by means of a tensometric balance on a motionless blade (a damper is situated at the apex of the blade). In the same figure curve (2) represents the relationship of the normal force to the

angle of attack in a case where the blade is oscillating in a cascade. The curves do not coincide. This is explained by the presence of hysteresis in the case of separation streamline flow. The hysteresis phenomenon substantially affects the value of the energy transmitted by the stream to the oscillating system during one period. The theoretical investigation of separation flutter is a very complex problem, since it requires determination of the forces in a separating stream with account taken of hysteresis.

Separation flutter has been experimentally investigated by numerous authors. Theoretical considerations, based upon similitude theory with resort to concepts of limit oscillation cycles, are known. As a result of these studies, it is becoming possible to establish the zones of the origination of separation flutter.

When supersonic velocities originate in the cascades of the axial compressor, the appearance of "shock" flutter is possible. Its appearance is explained by instability of the location of shock waves and by interaction of the shock waves with the boundary layer. In this field only experimental research is known.

Also known in addition to the indicated types of flutter is choking flutter, which is detected at Mach numbers and "onflow" angles corresponding to "choking" of the cascade.

Thus, with respect to their physical nature, the last three types of flutter have characteristic restricted areas of existence.

The typical location of these areas is shown in Figure 1.14. Along the abscissa the angle of attack of the compressor cascade is plotted, and along the ordinate the Mach number at the inlet is plotted. Separation flutter originates at large angles of attack and may be excited at relatively low velocities. This area (1) is bounded on the left by the value of the angle of attack at which separation of the stream occurs, and underneath it is bounded by the minimum velocity,

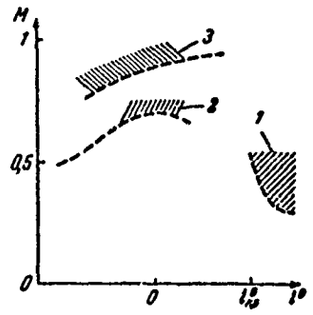


Figure 1.14. Areas where various forms of flutter originate in a compressor cascade.

determined by the balance of supplied and dispersed energy. Shock flutter occupies area (2), somewhat higher than the curve of the critical Mach number, i.e., the Mach number at the inlet at which supersonic zones ending in shock waves originate at the profile in the cascade. Choking flutter originates in the region of the maximum Mach number (area 3), i.e., the Mach number at the inlet, at which the input through the cascade for a given angle of attack attains the maximum value.

Let us now consider a qualitatively new phenomenon which is detected in the cascades of turbomachines — separation due to rotation. The essence of the phenomenon consists in the fact that under certain conditions, an axially symmetrical flow (as a whole) becomes unsteady, and nonsymmetrical forms originate which are more steady. In addition to its practical value, this phenomenon represents an interesting problem in fluid mechanics.

Let an annular aerodynamic diffuser cascade, in the general case a rotating one, be in a streamline flow with a relative velocity w_1^0 and a direction angle of β_1 with respect to the cascade front. The development of a cylindrical section of this cascade is shown in Figure 1.15. If angle β_1 is close to the calculated value, axially symmetrical flow exists in the annular cascade. If angle β_1 changes and approaches the value at which separation of the stream from the blades takes place, separation can be observed not at all blades of the cascade, as may have been expected, but only at a specific group of blades (or several groups). The separation zones do not remain motionless, but shift or rotate (in an annular cascade). Generally, such a phenomenon can exist not only in annular cascades (radial and axial, rotating and motionless), but also in straight cascades. The

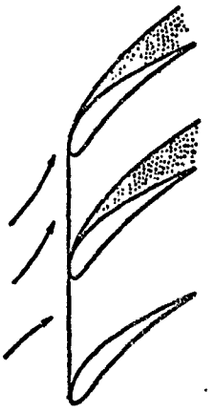


Figure 1.15. Shifting separation in a compressor cascade.

shifting of the separation zone is explained by the fact that during effusion of the main stream (at both sides of the separation point), the angles of attack of the adjacent blades change. On one side the adjacent blades get into a separation regime of streamline flow, and on the other side they come out of it. The gas input through the separation zones is small, is equal to zero, or is even directed against the main stream.

Although simultaneous homogeneous separation at all blades can indeed exist theoretically, experience has shown that it turns out to be unstable. The originating separation zone (or several zones) shifts and includes within itself an equal number of blades at all times. Consequently, the phenomenon as a whole, except for turbulent fluctuations, is stable, i.e., a separation zone is not destroyed during motion. The angular velocity of the shift of the zones with respect to the rotating wheel comprises usually 0.4 - 0.6 of the wheel velocity and is directed counter to the rotation. The study of rotation separation is of practical interest, since it sharply changes the aerodynamic characteristics of the stage and creates dangerous blade vibrations. Rotation separation is a purely aerodynamic phenomenon and may exist in a wheel with absolutely rigid blades.

The basic scheme explaining the existence of rotation separation may be represented in the following manner. We shall not be considering the initial moment of separation, when the choice of location of the separation zone depends upon random phenomena. Let us consider a steadily shifting separation. Let the blades be replaced by equivalent attached Zhukovskiy vortices with a circulation Γ_0 (Figure 1.16). We shall disignate the velocity circulation about the

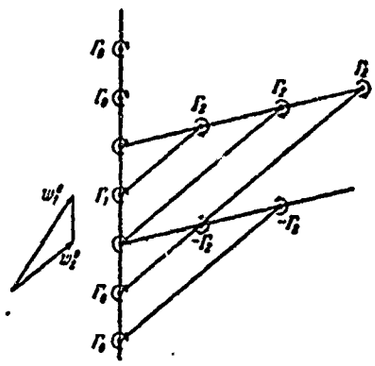


Figure 1.16. The vortex scheme of shifting separation.

blades that are in the separation zone by $\Gamma_1<\Gamma_0$. Since, as the separation zone moves, the blades alternatively enter the separation region and emerge from it, their circulation changes from Γ_0 to Γ_1 and from Γ_1 to Γ_0, respectively. Then at the boundaries of the separation zone there will be situated vortex arrays with circulations of $\Gamma_0-\Gamma_1=\Gamma_2$, $\Gamma_1-\Gamma_0=-\Gamma_2$. We shall assume that the free vortices are carried away by the stream with a velocity behind the cascade of w_2^0. From the drawing it can be seen that the vortex arrays change the velocity direction of the stream flowing onto the cascade. In the upper part of the drawing — it decreases. This explains the shift of the separation zone (according to the diagram — upwards). Within the separation zone bounded by the vortex path, an additional velocity is induced, directed against the velocity of the main stream. From here on, various authors put forth various supplementary physical hypotheses which permit the width of the zone and the rate of its shifting to be determined.

An unstable regime, similar to rotation separation, is also observed in hydraulic turbines. For partial loads a vortex filament is formed in the turbines. It brings about infraction of streamline symmetry, and strong pulsations.

All the unsteady aerodynamic or aeroelastic phenomena take place in the cascades of turbomachines. In this sense surging, the last unsteady process considered here, is distinguished by the fact that the possibility of origination and the character of oscillation of the gas depend not only upon the compressor, but also upon the network connected to the compressor.

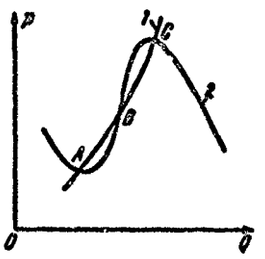


Figure 1.17. Static performance curve of a blower (2) and the network (1) (with regard to the origination of surging).

Surging refers to a self-oscillating process which originates in the entire mass of the gas situated in a compressor (or blower) and in the communicating passages. The possibility of the origination of static instability is determined by the form of the blower curve (i.e., the relationship of the pressure p to the discharge Q). Figure 1.17 shows the static performance curve of a blower (curve 2) and that of the network (curve 1), which intersect at points A, B, and C. Points A and C lie on descending arms of the performance curve, and the operating conditions will be statically stable. Point B lies on the ascending arm, and corresponds to statically unstable conditions. Thus, the origination of this type of instability is linked with nonlinearity of the performance curves. A detailed analysis shows that two types of surging can be distinguished — with soft and hard excitation, as is known from the theory of the self-oscillation of systems with nonlinear performance curves. Soft self-excitation can take place on the ascending arm of the performance curve. Hard excitation is possible under certain conditions on the descending arms of the performance curve.

Self-oscillations which take place in sliding bearings on an oil film have also been detected in turbomachines. Rotor oscillations are known. They are maintained due to forces originating with change of the gaps in the flow-through part and in labyrinth seals.

The problem of the possibility of flutter in the blades of the last stages of superpower steam condensation turbines is a very interesting one. This problem has the special feature that streams pass over frequency blades at high supersonic velocities. The stream is very nonuniform with respect in the radial direction. Shock waves and rarefacation waves can serve as excitation sources, since it is known that when they react with the boundary layer, unsteady

processes originate. In particular, such unsteady processes can originate both at the inlet to the cascade and at the outlet from it during expansion in an oblique section.

Oscillation of relatively thin outlet edges of nozzle units, brought about by turbulent edge wakes, is possible in principle.

Numerous cases of the breakage of high-pressure steam-turbine control-valve stems due to self-oscillations are known.

The most important and typical unsteady phenomena in turbomachines have been given above, with clarification only of the basic features. The actual patterns of the phenomena are considerably more complex, since they take place in annular cascades with blades of variable profile.

In many cases, the superimposition of several phenomena (for example, surging and rotation separation) is observed.

Only the processes themselves have been considered here, but they were not tied to the operating regime of the entire turbomachine. Establishment of this relationship is a very important engineering task, since only after this is it possible to make a judgment concerning the limit regimes with respect to conditions of strength and economy. This question is not discussed, since it would require a classification of a variable turbomachine operational regime, which is beyond the scope of the book.

FOOTNOTES

1. on page 23. An inhomogeneous cascade is called a cascade, the blades of which differ with respect to mass, rigidity, and other mechanical characteristics.

Chapter 2

THE BASIC EQUATIONS AND ELEMENTARY (FUNDAMENTAL) SOLUTIONS OF THE UNSTEADY MOTION OF A FLUID

§ 2.1. Basic Equations and Galileo and Lorentz Transformations

In this chapter we shall consider the two-dimensional motion of an ideal (nonviscous) compressible fluid.

Unsteady motion is described by the Euler Equations:

$$\left.\begin{aligned}\frac{\partial u}{\partial \tau}+u\frac{\partial u}{\partial x}+v\frac{\partial u}{\partial y}&=-\frac{1}{\rho}\frac{\partial p}{\partial x}+X_1,\\ \frac{\partial v}{\partial \tau}+u\frac{\partial v}{\partial x}+v\frac{\partial v}{\partial y}&=-\frac{1}{\rho}\frac{\partial p}{\partial y}+Y_1\end{aligned}\right\} \tag{2.1}$$

and by the equation of continuity

$$\frac{\partial \rho}{\partial \tau}+\frac{\partial (u\rho)}{\partial x}+\frac{\partial (v\rho)}{\partial y}=0. \tag{2.2}$$

Here $u=u(x, y, \tau)$, $v=v(x, y, \tau)$ are projections of the velocity on the coordinate axes; τ is the time; $p=p(x, y, \tau)$, $\rho=\rho(x, y, \tau)$ are respectively the pressure and the density of the fluid; $X_1=X_1(x, y, \tau)$, $Y_1=Y_1(x, y, \tau)$ are the components of the external forces per unit of mass of the fluid. These equations must be supplemented by an equation relating the pressure and the density of the fluid, which is done below. We shall be considering such small perturbations that quadratic terms

may be disregarded and the equations may be linearized. We shall select a system of coordinates which is stationary with respect to the fluid at infinity. Linearizing the Equations (2.1), we obtain

$$\left.\begin{aligned}\rho^0\frac{\partial u}{\partial \tau}&=-\frac{\partial p}{\partial x}+X,\\ \rho^0\frac{\partial v}{\partial \tau}&=-\frac{\partial p}{\partial y}+Y.\end{aligned}\right\} \tag{2.3}$$

Here $p=p(x, y, \tau)$ is regarded as a small perturbation in response to constant pressure in the stream p^0; ρ^0 is the density of the fluid in an unperturbed flow. For the sake of the discussion it is convenient to introduce forces X and Y, which are the external forces acting upon the fluid. Forces X and Y are regarded as distributed forces per unit of volume. In the special case of external forces acting only along a line, they will be surface forces. By X and Y will henceforth be understood forces acting upon the fluid from the direction of the body in the stream.

By linearizing the continuity equation, we obtain

$$\rho^0\left(\frac{\partial u}{\partial x}+\frac{\partial v}{\partial y}\right)+\frac{\partial \rho}{\partial \tau}=0. \tag{2.4}$$

Here $\rho=\rho(x, y, \tau)$ is the perturbation of the density of the fluid, which is small in comparison to the constant density of the unperturbed flow. In order to close the system of Equations (2.3) and (2.4), it is necessary to establish a relationship between the perturbed pressures and densities. Since currents of nonviscous fluid are being considered, and shock waves are not present in linearized flows, the process taking place in the gas must be isoentropic:

$$\frac{p^0+p}{\rho^0}=\left(\frac{\rho^0+\rho}{\rho^0}\right)^{\varkappa}.$$

Here $\varkappa$ is the isoentropic index.

Retaining in the preceding equation terms no higher than the first order of smallness ($p\ll p^0$, $\rho\ll\rho^0$), we obtain

$$\frac{p}{p^0}=\varkappa\frac{\rho}{\rho^0}.$$

From this it follows that perturbed pressures and density are linked by the relationship

$$\frac{p}{\rho} = \varkappa \frac{p^0}{\rho^0} = a_0^2. \tag{2.5}$$

Here a_0 is the velocity of sound in an unperturbed fluid (the rate of propagation of weak perturbations).

We obtain the basic equation for perturbed pressure. We differentiate the first Equation (2.3) with respect to x, and the second with respect to y, and add:

$$\rho^0 \frac{\partial}{\partial \tau}\left(\frac{\partial u}{\partial x} + \frac{\partial v}{\partial y}\right) = -\left(\frac{\partial^2 p}{\partial x^2} + \frac{\partial^2 p}{\partial y^2}\right) + \frac{\partial X}{\partial x} + \frac{\partial Y}{\partial y}.$$

The left-hand part of the equation is expressed by means of (2.4) and (2.5) in terms of pressure, and we finally obtain the wave equation

$$\frac{\partial^2 p}{\partial x^2} + \frac{\partial^2 p}{\partial y^2} - \frac{1}{a_0^2}\frac{\partial^2 p}{\partial \tau^2} = \frac{\partial X}{\partial x} + \frac{\partial Y}{\partial y}. \tag{2.6}$$

We obtain the second basic equation of the problem by eliminating the pressure. We differentiate the first Equation of (2.3) with respect to y, and the second with respect to x. Substracting the former from the latter, we obtain:

$$\rho^0 \frac{\partial}{\partial \tau}\left(\frac{\partial v}{\partial x} - \frac{\partial u}{\partial y}\right) = \frac{\partial Y}{\partial x} - \frac{\partial X}{\partial y}.$$

Into this equation we introduce the expression for the vorticity of the fluid

$$\omega = \frac{1}{2}\left(\frac{\partial v}{\partial x} - \frac{\partial u}{\partial y}\right) \tag{2.7}$$

and obtain

$$2\rho^0 \frac{\partial \omega}{\partial \tau} = \frac{\partial Y}{\partial x} - \frac{\partial X}{\partial y}. \tag{2.8}$$

From this equation it follows that vorticity may originate only at the point of application of forces (if the forces do not have a potential), and the originating vortices remain motionless. The latter remark obviously excludes vortex interaction, and is a consequence of linearization of the problem.

The equations derived above were obtained in a system of coordinates which is motionless with respect to the fluid at infinity, i.e., is not connected to a moving body, which sometimes makes the formulation of boundary conditions more difficult.

Let us connect the system of coordinates x'y' with a moving body. We shall be interested in the motion of the body only at a constant velocity U; and therefore it is possible to use the Galileo transformation:

$$x = x' + U\tau', \quad y = y', \quad \tau = \tau'. \tag{2.9}$$

The advantage of this transformation lies in the fact that the system of coordinates will be connected to the body, while the time remains invariant. However, a drawback will be the fact that the wave Equation (2.6) will not remain invariant. After transformation of Equation (2.6) by means of (2.9), we obtain (the primes are dropped)

$$(1-M^2)\frac{\partial^2 p}{\partial x^2} + \frac{\partial^2 p}{\partial y^2} - 2\frac{M}{a_0}\frac{\partial^2 p}{\partial x\,\partial \tau} - \frac{1}{a_0^2}\frac{\partial^2 p}{\partial \tau^2} = \frac{\partial X}{\partial x} + \frac{\partial Y}{\partial y}. \tag{2.10}$$

The wave equation will remain invariant if use is made of the Lorentz transformation, which for subsonic motion ($M = U/a_0 < 1$) has the form

$$x' = x + U\tau, \quad y' = \sqrt{1-M^2}\,y, \quad \tau' = \tau + \frac{Mx}{a_0}. \tag{2.11}$$

Inverse transformations are given by the formulas

$$x = \frac{x' - U\tau}{1-M^2}, \quad y = \frac{y'}{\sqrt{1-M^2}}, \quad \tau = \frac{\tau' - Mx'/a_0}{1-M^2}. \tag{2.12}$$

Thus the time does not remain invariant, which is inconvenient. When M = 0, the Lorentz transformation passes into the Galileo transformation. Applying the Lorentz transformation to Equation (2.6), we obtain

$$\frac{\partial^2 p}{\partial x'^2}+\frac{\partial^2 p}{\partial y'^2}-\frac{1}{a_0^2}\frac{\partial^2 p}{\partial \tau'^2}=\frac{1}{1-M^2}\frac{\partial Y}{\partial x'}+\frac{M}{a_0(1-M^2)}\frac{\partial X}{\partial \tau'}+\frac{1}{\sqrt{1-M^2}}\frac{\partial Y}{\partial y'}. \tag{2.13}$$

After the transformation of Equation (2.8), by means of the Galileo formulas we have

$$\frac{\partial \omega}{\partial \tau'}+U\frac{\partial \omega}{\partial x'}=\frac{1}{2\rho^0}\left(\frac{\partial Y}{\partial x'}-\frac{\partial X}{\partial y'}\right). \tag{2.14}$$

Integrating this expression and assuming that vorticity and forces are absent at infinity upstream, we obtain an equation which describes a distribution of vorticity in the fluid which originates under the action of nonsteady forces:

$$\omega(x', y', \tau')=\frac{1}{2U\rho^0}Y(x', y', \tau')- \\ -\frac{1}{2U^2\rho^0}\int_{-\infty}^{\tau'}\left[\frac{\partial}{\partial \tau'}Y\left(\xi, y', \tau'+\frac{\xi-x'}{U}\right)+U\frac{\partial}{\partial y'}X\left(\xi, y', \tau'+\frac{\xi-x'}{U}\right)\right]d\xi. \tag{2.15}$$

If the forces are absent, (2.14) becomes the linearized Helmholtz equation, the solution of which is the traveling wave $\omega=\omega(\tau-x/U)$. The first term in (2.15) represents attached vortices situated at the point of action of force Y. Assuming that force Y acts in a certain region Ω and integrating in this region, we obtain

$$Y=2U\rho^0\int\int_{\Omega}\omega\, d\Omega.$$

From Stokes' theorem concerning the fact that twice the vorticity is equal to the circulation of the velocity along the closed curve which surrounds the region, it follows that

$$\Gamma=2\int\int_{\Omega}\omega\, d\Omega.$$

From the last two formulas we obtain the Zhukovskiy formula for the lifting force:

$$Y = \rho^0 U\Gamma.$$

Thus, as is known, the existence of a lift force is connected with attached vortices. If the lifting force does not depend on time, and the drag force (a force parallel to the direction of the main stream) is absent, the flow will be potential everywhere except for the region of the application of the lift forces. It should be emphasized that the action of the drag force, as well as the action of the lift force, is being considered on the basis of an ideal fluid model.

The second term in (2.15) represents free vorticity, originating in the region Ω and carried away by the main stream. These vortices form a vortex wake. The lift force will cause free vorticity only if it changes with respect to time. The drag force can also cause vorticity when it is constant with respect to time.

From a consideration of the argument of the forces $\tau' + (\xi - x')/U$, in the integrand, it follows that the free vortices originating at the point of application of the force ξ, will appear at point $x' > \xi$ with the delay necessary for their transfer at the velocity U. In such a case, if the point x' lies in the region of the vortex wake downstream from the region Ω, the integral does not change when $\tau' - x'/U = \text{const}$, i.e., the free vorticity moves like a traveling wave.

When the main stream has vorticity at infinity (for example, by another system of forces), it is necessary to add a term of the type of $\omega(\tau - x/U)$, to the Solution (2.15), i.e., a vorticity wave traveling from infinity.

For supersonic velocity of the main stream ($M = U/a_0 > 1$), the transformation of Equation (2.6) to a moving system of coordinates is effected also by means of the Galileo transformation in the form

$$(M^2 - 1)\frac{\partial^2 p}{\partial x^2} - \frac{\partial^2 p}{\partial y^2} + 2\frac{M}{a_0}\frac{\partial^2 p}{\partial x \partial \tau} + \frac{1}{a_0^2}\frac{\partial^2 p}{\partial \tau^2} = -\frac{\partial X}{\partial x} - \frac{\partial Y}{\partial y}. \qquad (2.16)$$

In supersonic flow it is impossible to pass to a moving coordinate system and at the same time to leave the wave equation invariant. As has been shown by D. U. Miles [44], in this case it is expedient to use the modified Lorentz transformation:

$$x' = x + U\tau, \quad y' = \sqrt{M^2-1}\,y, \quad \tau' = -\tau - \frac{Mx}{a_0}. \tag{2.17}$$

Here, in comparison to the subsonic case, the factor $\sqrt{1-M^2}$ is replaced by $\sqrt{M^2-1}$, and the sign of τ is changed.

After transforming Equation (2.6) by means of (2.17) we obtain

$$\frac{\partial^2 p}{\partial x'^2} - \frac{\partial^2 p}{\partial y'^2} - \frac{1}{a_0^2}\frac{\partial^2 p}{\partial \tau'^2} = -\frac{1}{M^2-1}\frac{\partial X}{\partial x'} + \frac{M}{a_0\sqrt{M^2-1}}\frac{\partial X}{\partial \tau'} - \frac{1}{\sqrt{M^2-1}}\frac{\partial Y}{\partial y'}. \tag{2.18}$$

For the subsonic case, the perturbed pressure must satisfy the classical wave equation, i.e., a hyperbolic equation. For supersonic velocity of the main stream, the perturbed pressure in the coordinate system that is moving with respect to the fluid at infinity satisfies Equation (2.18).

It is convenient, as before, to use the Galileo transformation for the vortex-propagation equation. After transformation it takes on the same form as in the subsonic case, (2.14).

It was noted above that in the Lorentz transformation the time does not remain invariant. In the final solution it is convenient to retain the coordinates connected with the body, but to return to absolute time. We obtain the transition formula for the subsonic case from (2.11):

$$\tau' = (1-M^2)\tau + \frac{M}{a_0}x'.$$

For the supersonic case, from (2.17) we obtain

$$\tau' = (M^2-1)\tau - \frac{M}{a_0}x'. \tag{2.19}$$

§ 2.2. The Velocity Potential and the Acceleration Potential

Above we obtained equations for the perturbed pressure field and the vorticity field. When solving boundary value problems it is necessary to determine also the perturbation-velocity fields, in order to satisfy the boundary conditions at the bodies in the streamline flow.

As a result of the preceding calculations, it was shown that in the case of unsteady motion, vorticity is created in the fluid at the points of application of the forces. The flow of the fluid may also have vortices in regions located downstream from the points of application of the forces where vortex wakes propagate.

In the remaining regions, the flow of the fluid will be vortex-free, i.e., for a two-dimensional flow the following condition must hold:

$$\omega = \frac{\partial v}{\partial x} - \frac{\partial u}{\partial y} = 0.$$

Consequently, the velocity field has the potential

$$u = \frac{\partial \varphi}{\partial x}, \quad v = \frac{\partial \varphi}{\partial y}, \quad \varphi = \varphi(x, y, t). \tag{2.20}$$

Since a vortex sheet may exist in unsteady fluid flow, the velocity potential may be a discontinuous function.

Let us return to the linearized equations of motion (2.3), written in a system of coordinates which is motionless with respect to the fluid at infinity. Let us consider a region of the stream outside the point of application of the forces and outside the vortex wake. Then from (2.3) and (2.20) we obtain

$$\rho^0 \frac{\partial}{\partial t}\left(\frac{\partial \varphi}{\partial x}\right) = -\frac{\partial p}{\partial x}, \quad \rho^0 \frac{\partial}{\partial t}\left(\frac{\partial \varphi}{\partial y}\right) = -\frac{\partial p}{\partial y}.$$

Hence we find the connection between the velocity potential and the perturbed pressure (in a stationary system of coordinates):

$$\frac{\partial \varphi}{\partial \tau} = -\frac{p}{\rho^0}. \tag{2.21}$$

From the continuity Equation (2.4) and acoustic Condition (2.5), it follows that:

$$\rho^0\left(\frac{\partial u}{\partial x}+\frac{\partial v}{\partial y}\right)+\frac{1}{a_0^2}\frac{\partial p}{\partial \tau}=0. \tag{2.22}$$

Then from (2.22) — (2.20) we find that the velocity potential in a stationary system of coordinates must satisfy the wave equation

$$\frac{\partial^2 \varphi}{\partial x^2}+\frac{\partial^2 \psi}{\partial y^2}-\frac{1}{a_0^2}\frac{\partial^2 \varphi}{\partial \tau^2}=0. \tag{2.23}$$

From Euler's equations it is possible to express the projections of the accelerations by

$$a_x = -\frac{1}{\rho^0}\frac{\partial p}{\partial x}=\frac{\partial u}{\partial \tau}, \quad a_y = -\frac{1}{\rho^0}\frac{\partial p}{\partial y}=\frac{\partial v}{\partial \tau}.$$

From this it follows that the vector acceleration field possesses the potential (as was noted by Euler)

$$\varphi_* = -\frac{p}{\rho^0}, \quad a_x = \frac{\partial \varphi_*}{\partial x}, \quad a_y = \frac{\partial \varphi_*}{\partial y}. \tag{2.24}$$

Since the acceleration potential $\varphi_*=\varphi_*(x, y, \tau)$ is proportional to the perturbed pressure, it must satisfy the wave equation.

The connection between the velocity potential and the acceleration potential for a motionless system of coordinates follows from (2.21) and (2.24):

$$\varphi_* = \frac{\partial \varphi}{\partial \tau}. \tag{2.25}$$

Applying the Galileo transformation to Equation (2.25), we obtain this connection for a moving system of coordinates

$$\frac{\partial \varphi}{\partial \tau} + U \frac{\partial \varphi}{\partial x} = \varphi_*. \tag{2.26}$$

Integrating this equation under the assumption that the perturbations attenuate far upstream from the point of application of the force, we obtain

$$\varphi(x, y, \tau) = \frac{1}{U} \int_{-\infty}^{x} \varphi_*\left(\xi, y, \tau - \frac{x-\xi}{U}\right) d\xi. \tag{2.27}$$

This integral equation makes it possible to find φ from φ_* or, what is the same thing, to find the perturbation-velocity field from a known field of perturbed pressures.

We emphasize that the pressure field at the vortex wake cannot have a discontinuity and, consequently, the acceleration potential is also a continuous function. This affords distinct advantages when using the acceleration potential method.

In many problems it is of interest to study the oscillations in a flow brought about by forces which depend harmonically upon time.

For studying harmonically time-dependent flows, we introduce the designations

$$\varphi(x, y, \tau) = \tilde{\varphi}(x, y) e^{j\nu\tau}, \quad \varphi_*(x, y, \tau) = \tilde{\varphi}_*(x, y) e^{j\nu\tau}. \tag{2.28}$$

Here ν is the angular frequency of the process; j is a imaginary unit used for designations having to do with time. In linear problems, for the sake of abbrevated notation φ is frequently written which is $\tilde{\varphi}$. Therefore, we shall henceforth be writing only φ, and if $\varphi(x, y, \tau)$ is meant by this, it will be noted. Then Formula (2.27), which connects these potentials in the special case of harmonic motion, will take on the form

$$\varphi(x, y) = \frac{1}{U} \int_{-\infty}^{\tilde{x}} e^{j\nu\frac{\xi}{U}} \tilde{\varphi}_*(\xi, y) d\xi. \tag{2.29}$$

The wave equation which is satisfied by the velocity potential, the acceleration potential, and the perturbed pressure with the harmonic law of oscillations will change into the Helmholtz equation.

Thus, in a stationary system of coordinates the velocity potential must satisfy the equation

$$\frac{\partial^2\varphi}{\partial x^2}+\frac{\partial^2\varphi}{\partial y^2}+\frac{\nu^2}{a_0^2}\varphi=0. \tag{2.30}$$

§ 2.3. Green's Theorem and the Kirchhoff Formula

In the solution of boundary value problems in a linear formulation, elementary solutions corresponding to fields evoked by sources and multipoles (and in the first place by dipoles) are of special interest. An analysis of such solutions is of interest from the physical aspect, since perturbation fields far away from the perturbing bodies do not depend upon the specific shape of the bodies, but are determined only by the total action of the forces.

These solutions may also be used as kernels of integral equations which solve the corresponding boundary value problems.

For the boundary value problem of potential theory, use is made of Green's theorem, which reduces the volume integral to a surface integral:

$$\int_V(\psi\Delta\varphi-\varphi\Delta\psi)\,dV=\int_\Omega\left(\psi\frac{\partial\varphi}{\partial n}-\varphi\frac{\partial\psi}{\partial n}\right)d\Omega. \tag{2.31}$$

Here φ and ψ are functions which are bounded, continuous, and single-valued together with their first derivatives; $\partial/\partial n$ signifies differentiation along the external normal.

Selecting the function $\psi=r^{-1}$, for the three-dimensional case, where $r=\sqrt{x^2+y^2+z^2}$, we obtain the expression for the potential:

$$\varphi=\frac{1}{4\pi}\int_\Omega\left[\frac{\partial\varphi}{\partial n}\frac{1}{r}-\varphi\frac{\partial}{\partial n}\left(\frac{1}{r}\right)\right]d\Omega. \tag{2.32}$$

This formula yields the value for the potential, expressed in terms of values of φ and $\partial\varphi/\partial n$ at the boundary. The first integrand term is the potential of simple sources distributed along the boundaries of a region with the density $\partial\varphi/\partial n$, and the second integrand term is the dipole potential with axes normal to the surface and distributed with a density φ.

For the wave equation the Kirchhoff formula is used; this is a mathematical formulation of the Huygens principle:

$$\varphi = \frac{1}{4\pi}\int_{\Omega}\left[\frac{1}{r}\left(\frac{\partial\varphi}{\partial n}\right)_{\tau-r/a_0} - \frac{\partial}{\partial n}\frac{\varphi(\tau-r/a_0)}{r}\right]d\Omega. \qquad (2.33)$$

The integrand may also be written in the form of

$$K = \frac{1}{r}\frac{\partial\varphi}{\partial n} - \varphi\frac{\partial}{\partial n}\left(\frac{1}{r}\right) + \frac{1}{a_0 r}\frac{\partial\varphi}{\partial\tau}\frac{\partial r}{\partial n}$$

and the integral may be represented in the following manner:

$$\varphi = \frac{1}{4\pi}\int_{\Omega} K\left(\tau - \frac{r}{a_0}\right)d\Omega.$$

The value r/a_0 is the delay time, i.e., the time necessary for passage of the signal from the point of excitation to the point of observation.

In the special case of harmonic vibrations, the Kirchhoff formula changes into the formula obtained by Helmholtz.

Formula (2.33) describes the propagation of perturbations in a stationary medium. For generalization for the case of a moving medium, either the Doppler principle is used, or else use is made of the invariance of the wave equation with respect to the Lorentz transformation.

§ 2.4. Elementary Solutions for an Incompressible Fluid

In order to find the basic physical features of unsteady fields of perturbed pressures and velocity, as well as of the vorticity field, let us consider elementary solutions.

Let a stream of ideal incompressible fluid, moving at a constant velocity of U be acted upon by the concentrated impulsive force

$$Y = Y_0\delta(x)\delta(y)\delta(\tau),\quad \delta(x) = 0 \text{ for } x \neq 0,\quad \int_{-\infty}^{+\infty}\delta(x)\,dx = 1.$$

Here δ is the Dirac function.

The pressure field is found on the basis of Equation (2.6), which for an incompressible fluid ($a_0 = \infty$) assumes the form

$$\frac{\partial^2 p}{\partial x^2} + \frac{\partial^2 p}{\partial y^2} = \frac{\partial Y}{\partial y}.$$

In this problem the concentrated force acts at the coordinate origin (x = 0, y = 0) at the moment in time $\tau = 0$; consequently,

$$\frac{\partial^2 p}{\partial x^2} + \frac{\partial^2 p}{\partial y^2} = Y_0\delta(x)\delta'(y)\delta(\tau).$$

Here $\delta'(y)$ is a derivative of the Dirac function, which is regarded as a derivative of the generalized function.

In solving the problems, we shall use the direct Fourier transform and the inverse one according to the formulas

$$p(r) = \int_{-\infty}^{\infty} p(x)e^{-2\pi irx}\,dx,\quad p(x) = \int_{-\infty}^{\infty} p(r)e^{2\pi irx}\,dr. \qquad (2.34)$$

In order not to introduce a new designation for the Fourier transform, we shall use the same designations for the function, but shall denote the corresponding arguments.

The Fourier transform of the derivative function corresponds to multiplication of the representation by $2\pi ir$. In particular, the Dirac δ-function and its derivatives, regarded as generalized functions, have the following Fourier transforms [89]:

$$\mathfrak{F}\delta = 1,\quad \mathfrak{F}\delta^{(m)} = (2\pi ir)^m,\quad \mathfrak{F}\delta(x-a) = e^{-2\pi ra}.$$

Completing transformation of the equation according to the variables x and y, we obtain

$$p(r, s) = \frac{-isY_0\delta(\tau)}{2\pi(r^2+s^2)}.$$

Effecting a double inverse Fourier transform, we find the solution for the perturbed pressure and the acceleration potential:

$$p = \frac{-iV_0\delta(\tau)}{2\pi(x+iy)}, \quad \varphi_* = \frac{iV_0\delta(\tau)}{2\pi\rho^0(x+iy)}. \tag{2.35}$$

The perturbed pressure is represented by the real part of this expression:

$$p = \frac{-V_0 y\delta(\tau)}{2\pi(x^2+y^2)}.$$

Thus we arrive at the conclusion that the concentrated inpulsive force brings about an instantaneous pressure dipole at the point of its application. The lines of constant perturbed pressure in a plane (an instantaneous pattern is being considered) will be circles passing through the coordinate origin, with the centers on the ordinate axis (Figure 2.1). It may be considered that this pattern has been evoked by a directional explosion, the axis of which coincides with the ordinate axis. It may also be imagined that such an acceleration field is brought about by a small plate, placed at the origin of the coordinates and brought into motion by an impact in the direction of the ordinate axis. Since the acceleration potential is proportional to the perturbed pressure, determination of the instantaneous-acceleration components is not difficult. Since the time function $\delta(\tau)$ was not differentiated or integrated, it follows that $\delta(\tau)$ may be replaced by an arbitrary time function. Thus this solution is a general one for an arbitrary force law (in an incompressible fluid). Thus, we arrive at the conclusion that the pressure dipole exists as long as the force is acting.

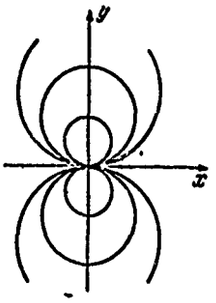


Figure 2.1. Lines of constant perturbed pressure.

This conclusion is valid only for an incompressible fluid, since a signal propagates in it at an infinitely high velocity. However,

the perturbation-velocity field will in all cases depend upon the law of change of the force in time and the velocity of the main stream.

The velocity potential of the disturbed motion originating after the impulsive application of a force is computed by means of Formulas (2.27) and (2.35) and has the form

$$\varphi = \frac{iY_0}{2\pi\rho^0 U}\int_{-\infty}^{x}\frac{\delta\left(\tau-\frac{x-\xi}{U}\right)d\xi}{\xi+i\eta} = \frac{iY_0}{2\pi\rho^0}\frac{1}{(x-U\tau)+iy}.$$

In the integration, the basic property of the Dirac function $\int_{-\infty}^{+\infty} f(\xi)\delta(\xi-x)d\xi = f(x)$ is utilized. The formula is valid for $x-U\tau \geqslant 0$.

This expression is called a complex potential, and the velocity potential is determined by its real part.

Thus, the velocity potential of the induced motion is a dipole which originates at the moment of application of the force and continues to exist after removal of the load and is carried away by the stream with a velocity U.

It can be shown that the motion described by the velocity dipole[1] A/z possesses a finite momentum, equal to $2\pi\rho^0 A$, in the direction of the axis of the dipole action. Consequently, the dipole obtained has a momentum in the direction of the y-axis equal to $2\pi\rho^0 Y_0/2\pi\rho^0 = Y_0$, and this value is numerically equal to the momentum of the force bringing about the motion:

$$\int_{-\infty}^{+\infty} Y(\tau)\,d\tau = \int_{-\infty}^{+\infty} Y_0\delta(\tau)\,d\tau = Y_0.$$

The momentum of the fluid due to the dipole in the direction of the abscissa is equal to zero in view of the symmetry of the flow pattern. The impulse of the forces causes a corresponding momentum in the fluid, which subsequently remains constant, since it does not depend upon the position of the dipole center.

Footnote (1) appears on page 69.

The action of a force that changes with time in an arbitrary manner may be replaced by consecutive impulses. Thus, the perturbed-pressure field will be determined by a pressure dipole located at the point of action of the force, and the velocity field will be determined by the velocities induced by the velocity-dipole sheet which are carried away by the stream and which depend upon the entire history of the motion.

In case the force is applied suddenly at the moment of time $\tau = 0$ and subsequently remains constant, the perturbed pressure is determined by (2.35) in the following manner:

$$p = \frac{-iY_0\sigma(\tau)}{2\pi(x+iy)},$$

where

$$\sigma(\tau) = \int_{-\infty}^{\tau} \delta(\tau)\,d\tau, \quad \begin{cases} \sigma(\tau) = 0 & \text{when } \tau < 0, \\ \sigma(\tau) = 1 & \text{when } \tau > 0. \end{cases}$$

Here $\sigma(\tau)$ is a unit function.

The velocity potential is found from (2.27) and is expressed by the formula

$$\varphi = \frac{Y_0}{2\pi U\rho^0} \ln \frac{x+iy}{(x-U\tau)+iy}, \quad x - U\tau > 0. \tag{2.36}$$

We shall find the vorticity distribution from (2.15) in the form

$$\omega = \frac{Y_0}{2U\rho^0}[\delta(x)\delta(y)\delta(\tau) - \delta(x-U\tau)\delta(y)].$$

The last two formulas show that the disturbed flow is determined by two vortices of identical intensity, but of opposite sign. The first one is motionless and is located at the coordinate origin (attached vortex), and the second moves at the velocity of the main stream (the so-called initial vortex). According to (2.36), the circulation of the vortices is equal to $\Gamma = Y_0/U\rho^0$. From this it follows that the lifting force is equal to the Zhukovskiy force $Y_0 = \rho^0 U\Gamma$.

It is known that the momentum possessed by the vortex pair is equal to $I=\rho\Gamma d$, where Γ is the circulation of the vortices and d is the distance between their centers. The vector of the momentum is perpendicular to the straight line connecting the centers of the vortices, i.e., is directed parallel to the ordinate axis. In this case $\Gamma=\gamma_0 l/U\rho^*$ and $d = Ut$, so that the momentum introduced constantly increases. The derivative of the momentum with respect to time is equal to the acting force

$$I=\gamma_0 t, \quad \frac{dI}{dt}=\gamma_0.$$

After much time has passed, the flow pattern becomes stabilized, and the flow will be determined only by the Zhukovskiy attached vortex. The action of a wing upon the stream of fluid may be represented by the action of a distributed load. The sudden application of a load must evoke an initial vortex. The appearance of such a vortex can be found experimentally. Figure 2.2 shows a photograph taken during the sudden origination of motion of the wing by a camera which is stationary with respect to the unperturbed fluid. A trailing initial vortex can be seen behind the trailing edge. After this the wing was stopped, and the photograph in Figure 2.3 shows the trailing vortex, which has a circulation opposite in sign to the initial vortex. The momentum imparted to the fluid by the impulse of forces applied to the wing is equal to the momentum of the vortex pair which is formed.

Let us now consider still another case of practical importance of a concentrated force which depends harmonically upon time. The pressure dipole is determined in the conventional manner:

$$p=\frac{-iV_0\cos\nu t}{2\pi(x+iy)}.$$

We compute (according to 2.27) the real part of the complex velocity potential at an infinite distance downstream from the point of action of the force:

$$\varphi=\pm\frac{\gamma_0}{2U\rho^*}e^{-\frac{\nu}{U}|y|}\cos\frac{\nu}{U}(x-Ut). \qquad (2.37)$$



Figure 2.2. The appearance of an initial vortex for the sudden motion of the wing.

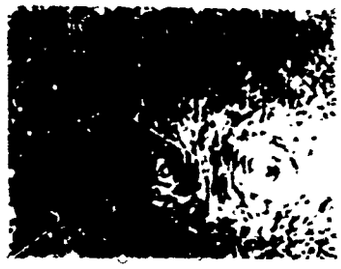


Figure 2.3. The appearance of a second vortex when the wing suddenly stops.

The $\pm$ signs refer to the upper and lower half-planes, respectively.

The vorticity in this current is determined by the formula

$$\omega = \frac{\gamma_0}{2U\rho^2}\left[\delta(x)\delta(y)\cos\nu\tau + \frac{1\cdot\nu}{U}\delta(y)\sin\frac{\nu}{U}(x-U\tau)\right]. \qquad (2.38)$$

Here a dimensional unit of length is placed in front of ν, in order to emphasize that the second term represents a distribution of linear vorticity.

For the latter, we shall obtain the law governing distribution of vertical perturbation velocities along the x-axis, which is found by the above-described methods (the transforms are omitted) in the form

$$v(x,0) = \frac{\gamma_0}{2\pi U\rho^2}\left\{\frac{1}{x} - ie^{-i\nu\frac{x}{U}}\frac{\nu}{U}\left[\mathrm{Ci}\left(\frac{\nu x}{U}\right) + j\,\mathrm{Si}\left(\frac{\nu x}{U}\right) + \frac{\pi i}{2}\right]\right\}e^{i\nu\tau}.$$

Here Ci and Si are, respectively, the integral cosine and the integral sine functions:

$$\mathrm{Ci}(x) = -\int_x^\infty \frac{\cos x}{x}dx, \quad \mathrm{Si}(x) = \int_0^x \frac{\sin x}{x}dx.$$

When the frequency of the process tends towards zero ($\nu \to 0$), the vortex wake disappears and this expression passes into the well-known formula which yields the velocity distribution of a single vortex. Far upstream, the perturbation velocity vanishes $v(-\infty, 0) = 0$. For points

lying downstream ($x \to +\infty$), using the well-known asymptotic estimates

$$\mathrm{Ci}(x) \to \frac{\sin x}{x}, \quad \mathrm{Si}(x) \to \frac{\pi}{2} - \frac{\cos x}{x},$$

we find

$$v(+\infty, 0) = \frac{\nu Y_0}{2U^2\rho^0} e^{\frac{\beta\nu}{U}(tU-n)}, \quad tU - x \geqslant 0, \tag{2.39}$$

which corresponds to the vertical velocity for an infinite moving vortex sheet with a harmonic vorticity distribution.

Thus, in this case, in addition to a concentrated vortex at the coordinate origin, there is an infinite vortex wake with a periodic distribution of vorticity. In connection with this, the velocity potential has a discontinuity at the x-axis. We emphasize that the acceleration potential and the perturbed pressure do not have a discontinuity, i.e., the pressure on both sides of the traveling vortex sheet is the same.

The action of concentrated forces upon a stream of fluid has been considered above. It is obvious that a wing may be replaced by a system of forces in order to satisfy the boundary conditions at the contour. If, however, the behavior of the stream far from the body in the stream is being studied, then obviously the action of the wing is equivalent to a perturbation induced by a resultant concentrated force. However, the moment of the forces is also transmitted to the fluid from the wing. To study the flow pattern at a distance from the body, the concentrated moment may also be considered. Corresponding solutions are obtained from a consideration of the action of a force couple. Let us assume that the fluid is acted upon by two concentrated forces Y_0, located at the points $x = \pm h, y = 0$. Let us let the arm become zero ($2h \to 0$), keeping the moment constant: $M = 2hY_0$. Then we shall obtain, at the limit, the expression of the perturbed pressure:

$$p = -\frac{iM}{2\pi} \frac{1}{(x+iy)^2}.$$

§ 2.5. Elementary Solutions for Subsonic Flow

In a compressible fluid, in distinction to an incompressible fluid, the acceleration potential is determined not by the Laplace equation, but by a wave equation, which results in essential special features. Let us first consider the action of a concentrated impulse force upon a motionless gas:

$$Y = Y_0 \delta(x)\delta(y)\delta(\tau).$$

Above Fourier transformations were used with respect to coordinates as well as with respect to time for obtaining the solution. These transformations are necessary when considering a range of change of variables that is infinite in both directions. In the problem under consideration, the time changes within the range of $\tau > 0$. Below, in the study of supersonic flow, the change of space coordinates will also be restricted within definite ranges. In such cases it is natural to apply the Laplace transformation

$$f(t) = \int_0^\infty e^{-tx} F(x)\,dx. \tag{2.40}$$

The basic equation of this problem has the form

$$\frac{\partial^2 p}{\partial x^2} + \frac{\partial^2 p}{\partial y^2} - \frac{1}{a_0^2}\frac{\partial^2 p}{\partial \tau^2} = Y_0 \delta(x)\delta'(y)\delta(\tau).$$

Applying Fourier transformations (with respect to coordinates) and Laplace transformations (with respect to time) to the wave equation, we obtain

$$p(r, s, t) = \frac{-i2\pi a_0^2 s Y_0}{4\pi^2(r^2+s^2)+t^2}. \tag{2.41}$$

Here r, s, t are, respectively, the equivalents of variables x, y, τ. By carrying out an inverse Laplace transformation [21], we find

$$p(r, s, \tau) = \frac{-ia_0 s Y_0}{\sqrt{r^2+s^2}} \sin\left(2\pi a_0 \sqrt{r^2+s^2}\,\tau\right).$$

Inverse Fourier transformations with respect to r and s lead to the following formulas:

$$\left.\begin{aligned} p(\tau, s, \tau) &= i\pi^2 s Y_0 J_0\left(2\pi s \sqrt{a_0^2\tau^2 - x^2}\right), \\ p(x, y, \tau) &= \frac{a_0 Y_0}{2\pi} \frac{\partial}{\partial y} \frac{\sigma\left(a_0^2\tau^2 - x^2 - y^2\right)}{\sqrt{a_0^2\tau^2 - x^2 - y^2}}. \end{aligned}\right\} \tag{2.42}$$

In the numerator of the last expression there is a unit function and, thus, the perturbations are at any given moment of time bounded by the circle $a_0^2\tau^2 - x^2 - y^2 \geqslant 0$. This is explained by the fact that, in a compressible fluid, a signal propagates with a finite velocity equal to the speed of sound. Under the differentiation sign in (2.42) there is a discontinuous function, equal to

$$\left(a_0^2\tau^2 - x^2 - y^2\right)^{-1/2} \text{ when } a_0^2\tau^2 - x^2 - y^2 > 0 \text{ and } 0 \text{ when } a_0^2\tau^2 - x^2 - y^2 < 0.$$

According to the rule for the differentiation of discontinuous functions regarded as generalized function [89], we find

$$p(x, y, \tau) = -\frac{a_0 Y_0}{2\pi} \frac{y\sigma\left(a_0^2\tau^2 - x^2 - y^2\right)}{\left(a_0^2\tau^2 - x^2 - y^2\right)^{3/2}} + \frac{a_0 Y_0}{2\pi} \frac{y\delta\left(a_0^2\tau^2 - x^2 - y^2\right)}{\sqrt{a_0^2\tau^2 - x^2 - y^2}}. \tag{2.43}$$

The first term of the formula describes an aftereffect, characteristic of two-dimensional problems, which is expressed in the fact that behind the wave front perturbations also remain within the circle. When $a_0^2\tau^2 \gg x^2 + y^2$, these perturbations rapidly diminish. This feature of two-dimensional problems is explained when one considers the effect of a two-dimensional impulse distributed in a three-dimensional space along the z coordinate axis. After the passage of time τ in an arbitrary plane z, a signal sent by a perturbation source lying in this plane will cover a circle $a_0^2\tau^2 - x^2 - y^2 \geqslant 0$. The same plane will be reached by perturbations sent by a source lying on an axis with the z coordinates $|z| \leqslant a_0\tau$. Each of these perturbations will be located in a selected plane within the circle $x^2 + y^2 \leqslant a_0^2\tau^2 - z^2$. It is the interference of the indicated waves that explains the aftereffect.

Since in the subsonic case the wave equation remains invariant, the solution obtained in a stationary gas can, by means of a

substitution of variables, be transformed into a solution for a moving stream. Let, for example, the field of perturbed pressures for a given type of perturbations in a stationary gas be described by the solution of $p=\gamma_0 F(\tau, x, y)$. It may be assumed that this solution $p=\gamma_0' F(\tau', x', y')$ remains invariable for a moving stream, if the new coordinates are connected to the old ones by Lorentz transformations, while $\gamma_0'=\gamma_0\sqrt{1-M^2}$.

Consequently,

$$x'=x+U\tau,\quad y'=\beta y,\quad \tau'=\tau+\frac{Mx}{a_0},\quad \beta=\sqrt{1-M^2}. \tag{2.44}$$

In the solution obtained we shall be measuring the coordinates in a moving system, but we shall return to absolute time. From (2.44) we obtain

$$\tau'=\tau+\frac{M}{a_0}(x'-U\tau)=(1-M^2)\tau+\frac{M}{a_0}x'=\beta^2\tau+\frac{M}{a_0}x'.$$

Then it is obvious that the solution for a subsonic stream is obtained from the solutions for U = 0 by the substitution (we drop the primes):

$$\gamma_0 \text{ for } \frac{\gamma_0}{\beta},\ y \text{ for } \beta y \text{ and } \tau \text{ for } \beta^2\tau+\frac{Mx}{a_0}.$$

We effect the change of variables in the denominator of (2.43) in the expression which is encountered in problems with the initial conditions

$$a_0^2\left(\beta^2\tau+\frac{M}{a_0}x\right)^2-x^2-\beta^2y^2=\beta^2\left[a_0^2\tau^2-(x-U\tau)^2-y^2\right].$$

Naturally, the circle in which the perturbations are contained moves with the velocity of the main stream in the coordinates linked with the body (force). Taking this into account, from (2.43) we obtain

$$p=-\frac{a_0\gamma_0}{2\pi\beta^3}\frac{y\sigma(z)}{z^{3/2}}+\frac{a_0\gamma_0}{2\pi\beta}\frac{\delta(z)}{\sqrt{z}},\quad z=a_0^2\tau^2-(x-U\tau)^2-y^2.$$

Let us define the perturbation brought about by the concentrated force suddenly applied at the moment of time $\tau = 0$ and by the subsequently remaining constant $\gamma=\gamma_0\delta(x)\delta(y)\sigma(\tau)$. The Laplace transformation

of a unit function is equal to $\varphi_0(\tau) = 1/l$. Effecting the Fourier transformation according to the coordinates, we find the representation of the wave equation in the form

$$p(r, s, l) = -\frac{iY_0}{2\pi}\frac{s}{l\left(r^2+s^2+l^2/4\pi^2a_0^2\right)}.$$

The inverse Fourier transformation on the basis of the variable r leads to the formula

$$p(x, s, l) = -\frac{iY_0}{2}\frac{s}{l}\frac{\exp\left(-2\pi|x|\sqrt{s^2+l^2/4\pi^2a_0^2}\right)}{\sqrt{s^2+l^2/4\pi^2a_0^2}}.$$

Taking advantage of the fact that differentiation of the function with respect to y is equivalent to multiplying the Fourier transformation by $2\pi is$, and employing the inversion formula, we obtain

$$p(x, y, l) = \int_{-\infty}^{\infty}\frac{-Y_0(2\pi is)}{4\pi l}\frac{\exp(-2\pi isy)\exp\left(-2\pi|x|\sqrt{s^2+l^2/4\pi^2a_0^2}\right)ds}{\sqrt{s^2+l^2/4\pi^2a_0^2}} =$$
$$= -\frac{Y_0}{2\pi l}\frac{\partial}{\partial y}K_0\left(\frac{l}{a_0}\sqrt{x^2+y^2}\right) = \frac{Y_0}{2\pi a_0}\frac{y}{\sqrt{x^2+y^2}}K_1\left(\frac{l}{a_0}\sqrt{x^2+y^2}\right).$$

Here K_0 and K_1 are cylindrical functions of the third kind, of an imaginary argument.

Applying the formula for inversion of the Laplace transformation [22] to the obtained representation, we find the solution(2):

$$p(x, y, \tau) = \frac{Y_0}{2\pi a_0}\frac{y}{\sqrt{x^2+y^2}}\mathfrak{L}^{-1}K_1\left(\frac{l}{a_0}\sqrt{x^2+y^2}\right) =$$
$$= \frac{a_0Y_0\tau y}{2\pi(x^2+y^2)\sqrt{a_0^2\tau^2-x^2-y^2}}. \qquad (2.45)$$

After the transition to a moving system of coordinates, we obtain

$$p = \frac{Y_0\alpha\beta}{2\pi}\frac{\tau+\mu x}{(x^2+\beta^2y^2)\sqrt{a_0^2\tau^2-(x-U\tau)^2-y^2}}. \qquad (2.46)$$

Here $\mu = \frac{M^2}{U\beta^2}$, $a_0^2\tau^2-(x-U\tau)^2-y^2>0$.

Footnote (2) appears on page 69.

In the special case of an incompressible stream ($a_0 \to \infty$), the solution passes into the pressure-dipole formula obtained above. With a boundless time increase ($\tau \to \infty$), Solution (2.46) describes a field of perturbed pressures brought about by a constant force in a stream of compressible fluid:

$$p(x, y) = \frac{Y_0 y}{2\pi (x^2 + \beta^2 y^2)}.$$

Let us consider a case which is of considerable interest in problems dealing with unsteady flow about cascades. We define the perturbations brought about in a subsonic stream by a concentrated force which depends harmonically upon time,

$$Y = Y_0 \delta(x) \delta(y) \exp(j\nu\tau).$$

Applying the Fourier transform to the wave equation, we obtain

$$p(r, s, t) = \frac{jY_0 s \delta(t - r/2\pi)}{2\pi \left(t^2/a_0^2 - r^2 - s^2\right)}. \tag{2.47}$$

Here j is an imaginary unit connected to time processes. The Dirac function in the numerator is a Fourier transformation of exp $(j\nu\tau)$.

Successive inversions of (2.47) are found from the expression (the transformations are omitted)

$$\left.\begin{aligned} p(r, s, \tau) &= \frac{jY_0 s \exp(j\nu\tau)}{2\pi \left[(\nu/2\pi a_0)^2 - r^2 - s^2\right]}, \\ p(r, y, \tau) &= -\frac{Y_0}{2} e^{j\nu\tau} e^{-2\pi |y| \sqrt{r^2 - (\nu/2\pi a_0)^2}}, \\ p(x, y, \tau) &= \frac{j\nu y Y_0}{4a_0} \frac{\exp(j\nu\tau)}{\sqrt{x^2 + y^2}} H_1^{(2)}\left(\frac{\nu}{a_0} \sqrt{x^2 + y^2}\right). \end{aligned}\right\} \tag{2.48}$$

Here $H_1^{(2)}(z) = J_1(z) - jN_1(z)$ is a Hankel function of the second kind, which is expressed in terms of a combination of a Bessel function of the first kind and a Neumann function.

The latter formula is a solution of the problem concerning the propagation of perturbations in a stationary gas medium. By the method described above we pass to a moving system of coordinates in

(2.48) and to absolute time. We do not denote this by special indexes:

$$p(x, y, \tau) = \frac{\nu g \Gamma_0 \exp\left[i\nu\left(\beta^2\tau + Ux'_0\right)\right]}{4a_0\sqrt{x^2+\beta^2y^2}} H_1^{(2)}\left(\frac{\nu}{a_0}\sqrt{x^2+\beta^2y^2}\right).$$

Introducing the new frequency $\nu_1=\beta^2\nu$ (and then dropping the index), we obtain the final solution:

$$p = \frac{\rho g \Gamma_0}{4\beta^2 a_0} \frac{\exp\left[i(\nu\tau + \mu x)\right]}{\sqrt{x^2+\beta^2y^2}} H_1^{(2)}\left(\varkappa\sqrt{x^2+\beta^2y^2}\right). \qquad (2.49)$$

Here the designations $\varkappa = \frac{\nu M}{U\beta^2}$, $\mu = \frac{\nu M^2}{U\beta^2}$ have been introduced. The frequency replacement has been brought about by the Doppler effect.

Let us consider the limits toward which (2.49) tends in an incompressible fluid ($a_0 \to \infty$). We shall make use of the Handel function representation for a small value of the argument

$$H_1^{(2)}(z) = \frac{2i}{\pi z} + \frac{z}{\beta\pi}\ln z + \ldots$$

Then, retaining only the first term, we obtain

$$H_{1\,\varkappa\to 0}^{(2)}\left(\varkappa\sqrt{x^2+\beta^2y^2}\right) \to \frac{2i}{\pi\varkappa\sqrt{x^2+\beta^2y^2}}.$$

Substituting this expression into (2.49), we find ($\varkappa \to 0$, $\mu \to 0$, $\beta \to 1$)

$$p = -\frac{\rho g \Gamma_0 \exp(i\nu\tau)}{2\pi(x^2+y^2)},$$

This coincides with the perturbed-pressure dipole obtained above. Let us recollect that since a signal propagates instantaneously in an incompressible fluid, an analogous solution is valid for any law of change of a force in time. This conclusion at the same time shows that at a low oscillation frequency (more precisely, at a low value of $\varkappa$) and at small distances from the focus of perturbations, the fluid behaves like an incompressible fluid.

In order to represent the solution a great distance from the source of the perturbations, we may use the asymptotic representation for the Hankel function:

$$jH_1^{(2)}(z) \sim j\sqrt{\frac{2}{\pi z}}\exp\left[-j\left(z-\frac{\pi}{4}\right)\right].$$

Let us find the perturbation velocity field far downstream from the acting force.

We express the perturbation velocity potential by means of (2.29) and (2.49) in the form

$$\varphi = -\frac{f_0\gamma_0}{4\pi\alpha\beta U\gamma^2}e^{j(\alpha x-\beta\gamma y)}\int_{-\infty}^{+\infty}\frac{\exp j(\nu/U+\mu)\xi}{\sqrt{\xi^2+\beta^2\gamma^2}}H_1^{(2)}\left(\alpha\sqrt{\xi^2+\beta^2\gamma^2}\right)d\xi.$$

Here the upper limit is taken as $+\infty$, since the velocity potential is calculated at an infinite distance behind the perturbation source. At an infinite distance in front of the perturbation source the velocities are equal to zero, since the perturbations attenuate; this follows from the asymptotic behavior of the Hankel function. Taking the representation of the Hankel function $H_1^{(2)}(z)=J_1(z)-jN_1(z)$ and the Euler formula $\exp jx=\cos x+j\sin x$ into account, this integral may be written as the integral of the sum (the arguments are omitted)

$$J_1\cos(\ )+N_1\sin(\ )+j[-N_1\cos(\ )+J_1\sin(\ )].$$

Functions J_1 sin, N_1 sin are odd and their integrals are equal to zero.

The integral of the first term is also equal to zero, since it is known [19] that

$$\int_0^\infty (x^2+b^2)^{-1/2}J_1\left(a\sqrt{x^2+b^2}\right)\cos(cx)\,dx=0,$$

if $0<a<c,\ b>0$. In this case this condition is always satisfied, since

$$a=x=\frac{\nu M}{U(1-M^2)},\quad c=\frac{\nu}{U}+\mu=\frac{\nu}{U}\left(1+\frac{M^2}{1-M^2}\right)=\frac{\nu}{U}\frac{1}{1-M^2}.$$

The computation of the integral of N_1 cos ( ) remains, which when $0<a<c,\ b>0$ is equal [19] to

$$I=\int_0^{\infty}(x^2+b^2)^{-1/2}N_1(a\sqrt{x^2+b^2})\cos(cx)\,dx=$$

$$=-\sqrt{\frac{2b}{\pi}}\frac{\sqrt[4]{c^2-a^2}}{ab}K_{1/2}(b\sqrt{c^2-a^2}).$$

The cylindrical function of the imaginary argument with the index 1/2 is expressed in terms of the elementary functions:

$$K_{1/2}(b\sqrt{c^2-a^2})=\sqrt{\frac{\pi}{2b}}\frac{1}{\sqrt[4]{c^2-a^2}}e^{-b\sqrt{c^2-a^2}}.$$

Therefore the computed integral is equal to

$$I=-\frac{1}{ab}e^{-b\sqrt{c^2-a^2}}.$$

Collecting the computations and making the transformations, we finally obtain the perturbation-velocity potential at an infinite distance downstream from the perturbation source:

$$\varphi=\mp\frac{\gamma_0}{2U\rho^0}e^{\frac{-\nu|y|\sqrt{1+M^2}}{U}}e^{i\nu\left(\tau-\frac{x}{U}\right)}. \qquad (2.50)$$

The signs $\pm$ pertain to the upper and lower half-planes. It should be noted that, as the distance downstream increases, the perturbation of the velocity field along the abscissa continues indefinitely. This perturbation is brought about by a vortex sheet which has its origin at the point of application of the periodic force. From the last cofactor in (2.50), it follows that the vortex sheet constitutes a traveling wave. The length of the wave is equal to $\lambda=2\pi U/\nu$. When $|y|\to\pm\infty$ the perturbations attenuate. The sheet serves as a line of discontinuity for the tangential velocities. The fields of the normal perturbation velocities and pressures are continuous. Computing the tangential velocities according to (2.50) when $y\to\pm 0$, we obtain

$$u=\frac{\partial\varphi}{\partial x}=\pm\frac{i\nu\gamma_0}{2U^2\rho^0}e^{i\nu\left(\tau-\frac{x}{U}\right)}.$$

The intensity of the vortex sheet which brings about this velocity jump can be found from formula

$$\gamma(x,\tau)=-\frac{i\nu\gamma_0}{U^2\rho^0}e^{i\nu\left(\tau-\frac{x}{U}\right)}. \qquad (2.51)$$

This same vorticity distribution law may be found on the basis of considerations concerning the preservation of vortices in an ideal fluid.

The acting force brings about the appearance of an attached vortex, and according to Zhukovskiy's theorem concerning a lifting force we have

$$Y = Y_0 e^{i\nu\tau} = \rho^0 U \Gamma_0 e^{i\nu\tau} = \rho^0 U \Gamma. \tag{2.52}$$

With a change in the circulation of the attached vortex, the liberated vorticity trails off into the vortex wake. Let the circulation increment during the time $d\tau$ be equal to $d\Gamma$, and let the vortex wake increase by the length dx; then from the condition of the preservation of vortices it follows that

$$\frac{d\Gamma}{d\tau} d\tau + \gamma dx = 0.$$

Since the movement of a vortex trail takes place with the velocity of the main stream, the intensity of the vortex sheet at the point of its origin is equal to

$$\gamma(0, \tau) = -\frac{1}{U}\frac{d\Gamma}{d\tau}.$$

Employing (2.52) and taking into account the fact that the intensity of the vortex sheet at point x may be expressed in terms of its intensity at the coordinate origin taking account of lag with respect to time $\gamma(x, \tau) = \gamma(0, \tau - x/U)$, we obtain

$$\gamma(x, \tau) = -\frac{i\nu Y_0}{U^2\rho^0} e^{i\nu\left(\tau - \frac{x}{U}\right)}.$$

This expression coincides with the one found above.

§ 2.6. Elementary Solutions for Supersonic Flow

Let us consider perturbations excited in a supersonic stream by

a suddenly applied force which subsequently remains constant:

$$Y = Y_0 \delta(x)\delta(y)\sigma(\tau).$$

Since the basic wave equation is written for a supersonic stream, the perturbations must be found in the semiplane $x > 0$. By applying to Equation (2.18) a Laplace transformation with respect to the variable x and Fourier transformations with respect to the variables y and τ, we find

$$p(r, s, t) = \frac{-2\pi i s Y_0}{\beta t\left(t^2 + 4\pi^2 s^2 + 4\pi^2 t^2/a_0^2\right)}.$$

Applying the Laplace inversion formulas with respect to the variable r yields

$$p(x, s, t) = \frac{-isY_0}{\beta t \sqrt{s^2 + t^2/a_0^2}} \sin\left(2\pi x \sqrt{s^2 + t^2/a_0^2}\right).$$

Henceforth we shall denote the coordinates and the time by primes in order to emphasize that they pertain to the wave equation obtained by the generalized Lorentz transformation.

Applying the Fourier inversion formula with respect to the variable s, and taking into account the fact that the factor $2\pi is$ corresponds to differentiation with respect to y, we obtain

$$p(x', y', t) = -\frac{Y_0}{2\beta t}\frac{\partial}{\partial y'} J_0\left(\frac{2\pi t}{a_0}\sqrt{x'^2 - y'^2}\right).$$

In view of the parity of the function, the formula for inversion of the Fourier transformation with respect to the variable t may be written in the following manner:

$$p(x', y', \tau') = -\frac{Y_0}{\beta}\frac{\partial}{\partial y'}\int_0^\infty J_0\left(\frac{2\pi t}{a_0}\sqrt{x'^2 - y'^2}\right)\frac{\sin 2\pi\tau' t}{t}\,dt. \qquad (2.53)$$

Replacing the integration variable $2\pi\sqrt{x'^2 - y'^2}\,t/a_0 = z$, we reduce the integral to the form

$$I = \int_0^{\infty} J_0(z) \sin \frac{a_0 \tau' z}{\sqrt{x'^2 - y'^2}} dz.$$

In computing the integral, two cases may be encountered:

1) $\frac{a_0 \tau'}{\sqrt{x'^2 - y'^2}} \geq 1, \quad I = \frac{\pi}{2}.$

2) $\frac{a_0 \tau'}{\sqrt{x'^2 - y'^2}} < 1, \quad I = \arcsin\left(\frac{a_0 \tau'}{\sqrt{x'^2 - y'^2}}\right).$

In the first case the perturbed pressure is equal to zero. In the second case, from (2.53), carrying out the differentiation, we find

$$p(x', y', \tau') = \frac{-a_0 \gamma \tau' \gamma_0}{2\pi\beta (x'^2 - y'^2) \sqrt{x'^2 - y'^2 - a_0^2 \tau'^2}}. \tag{2.54}$$

The coordinates with primes correspcnd to the generalized Lorentz transform:

$$x' = x + U\tau, \quad y' = \beta y, \quad \tau' = -\tau - U\frac{x}{a_0}, \quad \beta^2 = M^2 - 1. \tag{2.55}$$

In the final solution, just as in the subsonic case, it is convenient to transfer to absolute time, but to retain the coordinate x', which is linked to a moving system.

From (2.55) we find

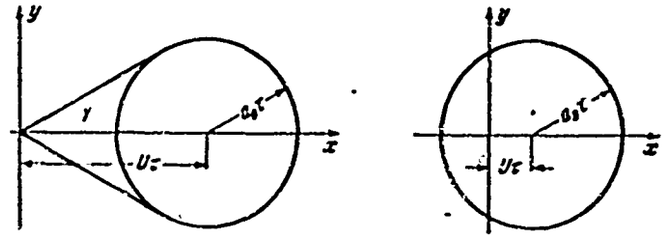
$$\tau' = \beta^2 \tau - \frac{Ux'}{a_0^2}.$$

Making the substitution in (2.54) and discarding the prime, we obtain the solution

$$p(x, y, \tau) = -\frac{\beta a_0 \gamma}{2\pi} \frac{\tau - \frac{Ux}{a_0^2}}{(x^2 - \beta^2 y^2) \sqrt{a_0^2 \tau^2 - (x - U\tau)^2 - y^2}}.$$

The perturbations are concentrated in the circle $a_0^2\tau^2 - (x - U\tau)^2 - y^2 \leqslant 0$, which is carried away by the supersonic stream ($U > a_0$), and thus the point of application of the force is now no longer located within the circle, as it was in the subsonic case. The difference consists

in the fact that at any moment of time the perturbations cannot pass beyond the Mach wedge $x^2>\beta^2y^2$. At any finite moment of time the perturbation region is bounded on the left by the straight lines $x^2 = \beta^2y^2$, and on the right by the arc of the circle $a_0^2\tau^2-(x-U\tau)^2-y^2=0$. In zone (1) (Figure 2.4a) the process is already stabilized and the perturbed pressure is equal to zero (with the exception of the boundaries of this region).



a b

Figure 2.4. (a) Perturbation zones for supersonic and (b) for subsonic flow.

In the case of supersonic streamline flow, the attached vortex is located at the apex of the wedge, and the free vortex is shifted together with a circular zone, which is located in its center. The perturbations at the straight-line segments which bound region (1) are determined by the transformation of the basic equation for stabilized flow.

The hyperpolic equation for stabilized flow has the form (after transformation for a moving system)

$$\frac{\partial^2 p}{\partial x^2} - \frac{\partial^2 p}{\partial y^2} = -\frac{1}{\beta}\frac{\partial Y}{\partial y}.$$

In this case we are considering the concentrated stabilized force, $Y=Y_0\delta(x)\delta(y\beta)$, which acts at the coordinate origin. Applying the Laplace transformation (for the x-coordinate) and the Fourier transformation (for the y-coordinate), to this equation we obtain

$$p(r, s) = \frac{-2\pi i s Y_0}{r^2+4\pi^2 s^2}.$$

The Laplace transformation has been selected, because the perturbations are located only in the right half-plane ($x > 0$).

Carrying out an inverse Laplace transformation, we find

$$p(x, s) = -iY_0 \sin(2\pi s x).$$

Further, employing the Euler formula $\sin(2\pi s x) = (e^{2\pi i s x} - e^{-2\pi i s x})/2i$ and taking advantage of the fact that the Fourier transformation of 1 yields the delta function

$$\int_{-\infty}^{\infty} e^{\pm 2\pi i s y}\, ds = \delta(y),$$

we find the expression for the perturbed pressure:

$$p(x, y) = \frac{1}{2} Y_0 [\delta(x - \beta y) - \delta(x + \beta y)], \quad x \geqslant 0.$$

Thus, the pressure field undergoes a discontinuity and the perturbations are concentrated along the straight lines $x^2 = \beta^2 y^2$. These discontinuities are inclined at the angle $\operatorname{tg} \alpha = \pm 1/\beta$, i.e., at the Mach angle $\sin \alpha = \pm 1/M$.

Since this case corresponds to the effect of the action of a concentrated force, it follows that the object in the stream has vanishingly small dimensions. The function $\delta(x - \beta y)$ describes (in a linearized formulation) the pressure change in the front shock and in the tail rarefacation wave which has merged with it: the pressure first increases, and then drops to the previous value. The function $-\delta(x + \beta y)$ represents the merged rarefacation and tail shock waves. For a clarification of this, let us consider the flow under study after the passage of an infinitely great amount of time, when it has become completely stabilized. Then the perturbations from the concentrated force are observed only along the semi-infinite straight line $x^2 = \beta^2 y^2$. Let us now assume that at first y_0 is uniformly distributed along the segment $y = 0,\ 0 \leqslant x \leqslant b$, i.e., the load intensity is equal to y_0/b.

The perturbed pressure is determined by integration along the segment:

$$p(x, y) = \frac{1}{2b} Y_0 \int_0^b [\delta(x-\xi-\beta y) - \delta(x-\xi+\beta y)]\, d\xi =$$
$$= \frac{1}{2b} Y_0 [\sigma(x-\beta y) - \sigma(x-b-\beta y)] + \frac{1}{2b} Y_0 [\sigma(x-b+\beta y) - \sigma(x+\beta y)].$$

The obtained equation describes the pressure perturbation in the field of a supersonic stream in flow about a plate at the angle of attack. Perturbations are absent before the frontal waves ($p = 0$); after the tail waves they are also equal to zero.

From the preceding formula it follows that in the region bounded by the straight lines $x=\beta y$, $x-b=\beta y$, $0 \leqslant x \leqslant b$ and the condition $y \geqslant 0$, the perturbation pressure is constant and is equal to $p^+ = Y_0/2b$. Similarly in the region $x=-\beta y$, $x-b=-\beta y$, $0 \leqslant x \leqslant b$, under the condition of $y \leqslant 0$, the perturbation pressure is equal to $p^- = -Y_0/2b$.

Supersonic streamline flow (including such flow at nonsteady regimes) is characterized by the absence of infinitely large rarefaction at the sharp leading edge.

Figure 2.4b also shows the perturbation zone for the subsonic case.

Let us consider the perturbations brought about in a supersonic stream by a concentrated force which changes harmonically in time:

$$Y = Y_0 \delta(x)\, \delta(y) \exp(j\nu\tau).$$

Applying to the wave equation the Laplace transformation with respect to the variable x and Fourier transformations with respect to y and τ, we obtain

$$p(r, s, l) = -\frac{2\pi j \nu_e}{\beta} \frac{s\delta\left(l - \frac{\nu}{2\pi}\right)}{r^2 + 4\pi^2 s^2 + \frac{4\pi^2 l^2}{a_0^2}}.$$

Using the transformation inversion formulas, we find

$$p(r, s, \tau) = -\frac{2\pi i V_0}{\beta} \frac{s \exp(i\nu\tau)}{r^2 + 4\pi^2 s^2 + \frac{\nu^2}{a_0^2}},$$

$$p(x, s, \tau) = -\frac{i V_0 \exp(i\nu\tau)}{\beta} \cdot \frac{s \sin\left(2\pi x \sqrt{s^2 + \frac{\nu^2}{4\pi^2 a_0^2}}\right)}{\sqrt{s^2 + \frac{\nu^2}{4\pi^2 a_0^2}}},$$

$$p(x, y, \tau) = \frac{-\nu V_0}{2\beta a_0} \frac{y \exp(i\nu\tau)}{\sqrt{x^2 - y^2}} J_1\left(\frac{\nu}{a_0}\sqrt{x^2 - y^2}\right).$$

The sequence of the inversion operations may be followed on the basis of the arguments.

Effecting the transition to absolute time and an undistorted ordinate, we obtain the final formula

$$p(x, y, \tau) = \frac{-\nu V_0}{2\beta^2 a_0} \frac{y \exp(i\nu\tau - i\mu x)}{\sqrt{x^2 - \beta^2 y^2}} J_1(\varkappa \sqrt{x^2 - \beta^2 y^2}). \tag{2.56}$$

Here we set

$$\beta^2 = M^2 - 1, \quad \mu = \frac{\nu M}{a_0 \beta^2}, \quad \varkappa = \frac{\nu}{a_0 \beta^2}.$$

In the case of supersonic streamline flow, the perturbations are concentrated within the wedge $x^2 - \beta^2 y^2$. When the frequency of the process tends toward zero, the perturbations within the wedge also tend toward zero. In the case of stabilized streamline flow, the perturbations will be concentrated only in the Mach waves at the boundaries of the waves.

§ 2.7. Energetic Interaction Between Stream and Body

Before passing on to consideration of the process of energy exchange between an oscillating body and a stream of fluid, let us discuss the manner in which the action of the body upon the stream can be replaced by the action of a system of forces. Up to now we have been studying perturbations brought about forces that are perpendicular to the direction of the main stream. The point of application of the force was assumed motionless. In actuality, a variable

force can act upon a wing only in a case where the velocity of the wing also changes in time (or if the wing is encountering a stream the velocity of which changes in time).

We will be particularly interested in two cases: (1) the wing is in a stream of constant velocity U and oscillates in a direction perpendicular to the main stream, and (2) the wing is motionless, but is situated in a stream in which transverse velocity pulsations occur.

We shall now treat the first case, and we shall assume that the action of the wing upon the stream is replaced by the action of a single concentrated force. Obviously, the point of application of the force must move with the velocity of oscillation of the wing v_0. In this case the point of application of the force moves with respect to the fluid with a velocity equal to the geometrical difference of the velocities of the wing and the stream. Since the force $\mathcal{P}$ is a lift force (drag is absent), it must be perpendicular to the speed of motion of the wing with respect to the fluid. It was found above that the force creates a pressure dipole with the axis directed along the axis of action of the force. Thus, the axes of pressure dipoles originating during oscillation of the wing will not be perpendicular to the direction of the main stream.

Velocity dipoles are formed simultaneously with pressure dipoles, which exist while the force is acting. The axes of velocity dipoles are parallel to the instantaneous direction of the force. Later the velocity dipoles are carried away by the main stream and form a wake. In this case, the wake behind the body will consist of a sheet of dipoles, the axes of which are inclined at different angles in the general case.

From Figure 2.5 it is clear that the influence of the stream on the wing has a component directed in the principal direction of motion of the wing, i.e., the oscillating wing is acted upon by a thrust force. This force is a propulsive force (for example, in bird flight).

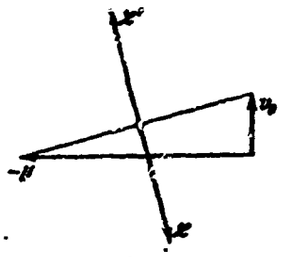


Figure 2.5. The effect of an oscillating body on the stream.

If one considers a stream flowing over an oscillating wing, the wing will be acting upon the fluid with a force $\mathcal{L}'=-\mathcal{L}$, which is directed in the direction of the flow, i.e., it will accelerate the stream. From the diagram it also follows that work must be expended for the oscillation of the wing in the fluid, since the direction of the oscillation velocity has a component which is opposite to the force. Energy is expended by formation of the vortices of the sheet behind the wing and by creation of thrust. In a compressible fluid, the energy input due to the formation of acoustic waves is an additional factor.

Let us consider the harmonic oscillations of a body in an incompressible fluid. The energy input on the formation of a vortex wake may be determined by computing the kinetic energy of the perturbed motion. The energy input per oscillation cycle is equal to the kinetic energy contained in an infinite vertical band with a width equal to the wavelength of the wake.

It is known that the kinetic field energy in a potential flow may be expressed in terms of the contour integral

$$E=\frac{1}{2}\rho^0\oint\varphi\frac{\partial\varphi}{\partial n}ds.$$

Here φ is the velocity potential, s is the curvilinear contour coordinate, n is a normal directed outward. We shall apply this integral only to the upper half-band and shall double the result. The flow field has a period along the abscissa equal to the wake wavelength; thus, the integrals along vertical straight lines will cancel. The integral along the upper boundary of the band will be equal to zero, since $(\partial\varphi/\partial y)\to 0$ when $y\to\infty$.

We obtain as a final result:

$$E = -\rho^0 \int_0^{\lambda} \varphi_{y=0} \left(\frac{\partial \varphi}{\partial y}\right)_{y \to 0} dx, \quad \lambda = \frac{2\pi U}{\nu}.$$

The velocity potential of a vortex wake at an infinite distance from the body has the form (the inessential time factor is discarded):

$$\varphi = A \exp\left(-|y| \frac{\nu}{U}\right) \cos \frac{\nu x}{U}.$$

Consequently, the kinetic energy of perturbed motion contained in one period is equal to

$$E = \pi \rho^0 A^2.$$

This calculation may be extended also to the case where the axes of the velocity dipoles are not perpendicular to the wake axis.

FOOTNOTES

1. on page 46. The complex coordinate is $Z = x + iy$.

2. on page 54. It should be kept in mind that in the quoted source, the connection between the original and the representation differs from the one adopted here.

Chapter 3

GENERAL PROPERTIES OF UNSTEADY FLOW IN A CASCADE

§ 3.1. Preliminary Remarks

Let us consider a system of singular points (vortices or dipoles), situated along a straight line. We shall be calling such a system a singularity cascade, and the straight line will be called the cascade axis, while the constant distance t between adjacent singular points is the cascade spacing.

The flow field around the cascade possesses specific properties (periodicity, conditions of perturbations at infinity, the possibility of the origination of resonance) which are not characteristic of an isolated singularity, and therefore deserve special study.

In addition, elementary solutions corresponding to a singularity cascade are used as kernels of integral equations.

§ 3.2. The Singularity Cascade in a Incompressible Fluid

Let us consider a field created by a vortex cascade with a circulation that is constant in time.

Let the cascade axis be directed along the ordinate. Since blade oscillation with a phase shift will no longer be of interest to us, we shall study the velocity field from a vortex cascade with a circulation which changes according to a harmonic law (Figure 3.1a):

$$\Gamma_m = \Gamma_0 \exp(-jm\alpha), \quad m = 0, \pm 1, \pm 2, \ldots \tag{3.1}$$

Here α is the phase shift between adjacent vortices, m is the number of the vortex, read off from the basic vortex which has the circulation Γ_0 and which is located at the origin of the coordinates. Here and subsequently the imaginary unit j will be used for writing down time processes in complex form. The imaginary unit i, which does not interact with j, will be used, as usual, for complex numbers in the plane of the coordinates. In determining the law of change of vortex circulation, the imaginary unit j has been selected, since it will henceforth be assumed that the intensity of the vortices can change in time.

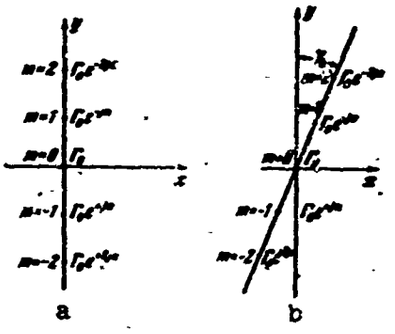


Figure 3.1. (a) Cascade of vortices without offset, (b) with offset.

The field created by the cascade of attached vortices may be regarded as a perturbation field evoked by a cascade of forces that are constant in time (under the condition that the main stream is superimposed).

The complex velocity induced by the vortex cascade may be represented by the infinite sum:

$$w(z)=\frac{\Gamma_0}{2\pi i}\sum_{m=1}^{\infty}\left(\frac{e^{ima}}{z+imi}+\frac{e^{-ima}}{z-imi}\right)+\frac{\Gamma_0}{2\pi iz}. \tag{3.2}$$

This expression may be transformed and summed:

$$\begin{aligned} w(z)&=\frac{\Gamma_0}{2\pi i}\left[\frac{1}{z}+\frac{2z}{l^2}\sum_{m=1}^{\infty}\frac{\cos ma}{m^2+z^2/l^2}-\frac{2il}{l}\sum_{m=1}^{\infty}\frac{m\sin ma}{m^2+z^2/l^2}\right]= \\ &=\frac{\Gamma_0}{2\pi i}\left\{\frac{\pi}{l}\frac{\operatorname{ch}\left[(\pi-a)\frac{z}{l}\right]}{\operatorname{sh}\pi\frac{z}{l}}-ij\frac{\pi}{l}\frac{\operatorname{sh}\left[(\pi-a)\frac{z}{l}\right]}{\operatorname{sh}\left(\pi\frac{z}{l}\right)}\right\},\quad 0<a<2\pi. \end{aligned} \tag{3.3}$$

Obviously, the velocity field possesses generalized periodicity in the sense introduced in Reference [57]:

$$w(z+imi)=e^{-ima}w(z). \tag{3.4}$$

The perturbation velocity at an infinite distance from the cascade ($x\to\pm\infty$) strives to zero according to an exponential law:

$$w(z)\to\pm\frac{\Gamma_0}{2il}(1\mp ij)e^{\mp ia\frac{x}{l}},\quad (y=0).$$

Let us note some interesting special cases. In the absence of a phase shift ($\alpha = 0$) the result may be obtained by direct summation (3.1) when $\alpha = 0$:

$$w(z,\,0,\,l)=\frac{\Gamma_0}{2il}\operatorname{cth}\frac{\pi z}{l}.$$

In case the vortices are in counterphase ($\alpha = \pi$), we find

$$w(z,\,\pi,\,l)=\frac{\Gamma_0}{2il}\operatorname{csch}\frac{\pi z}{l}.$$

When the cascade spacing increases to infinity by a limit transition we obtain the velocity field brought about by a single vortex in the form

$$w(z,\,\infty)=\frac{\Gamma_0}{2\pi i}\frac{i}{z}.$$

The case of the absence of a phase shift ($\alpha = 0$) is a special one, since here the perturbations created by the cascade propagate to infinity:

$$w(z, 0, t) = \pm \frac{\Gamma_0}{2it} \text{ for } x \to \pm \infty.$$

In some cases it is more convenient to consider a cascade with aerodynamic offset γb (Figure 3.1b) instead of changing the direction of the main stream velocity. Obviously, the singular points will then have the coordinates $imt\exp(-i\gamma_b)$, where $m=0, \pm 1; \pm 2; \ldots$ Then the corresponding formulas, describing the velocity field of an oblique cascade, are obtained from the preceding ones by replacing t by $t\exp(-i\gamma_b)$. The use of a vortex cascade with offset does not introduce any fundamental changes, and is expedient in some cases only due to the compactness of the formulas.

Expression (3.3) may be represented in the form of a series of exponential functions; this is starting to find application in problems dealing with the mutual influence of cascades. Let us utilize the well-known expansion for the denominator of (3.3):

$$\frac{1}{\operatorname{sh}\frac{\pi z}{t}} = \pm 2 \sum_{m=0}^{\infty} e^{\mp (2m+1)\pi z/t}.$$

Here the upper and the lower signs pertain respectively to the right-hand ($x > 0$) semiplane and the left-hand ($x < 0$) semiplane.

We shall represent the numerator of Formula (3.2) in the following manner:

$$\operatorname{ch}\frac{\pi - \alpha}{t} z - i \operatorname{sh}\frac{\pi - \alpha}{t} z = \frac{1}{2}(1 - i) e^{\frac{\pi - \alpha}{t} z} + \frac{1}{2}(1 + i) e^{-\frac{\pi - \alpha}{t} z}.$$

After simple transformations we obtain the final formula:

$$w(z) = \frac{\Gamma_0}{2it}\left[(\pm 1 - i) e^{\mp \alpha z/t} \sum_{m=0}^{\infty} e^{\mp 2mz\pi/t} + (\pm 1 - i) e^{\pm \alpha z/t} \sum_{m=0}^{\infty} e^{\mp 2(m+1)\pi z/t}\right].$$

For the case of $\alpha = 0$ we obtain an analogous formula, utilizing the expansion of the hyperbolic cotangent:

$$w(z) = \pm \frac{\Gamma}{2it}\left(1 + 2\sum_{m=1}^{\infty} e^{\mp 2m\pi z/t}\right).$$

Here the upper and the lower signs also pertain respectively to the right-hand semiplane and the left-hand semiplane.

From the obtained expressions it follows that the perturbations brought about by the singularity cascade are periodic and attenuate exponentially as the distance from the cascade axis increases. The intensity of the amplitude decrease depends on the wavelength; the greater the wavelength, the slower the attenuation. A wave, the period of which is equal to t/α, attenuates most slowly of all. When $\alpha = 0$, the perturbations brought about by the cascade are finite at an arbitrary distance from the cascade axis.

These conclusions are valid for a cascade of arbitrary profiles, since an arbitrary cascade can be replaced by a corresponding combination of singularities. Such considerations are of practical interest when studying the mutual influence of a system of aerodynamic cascades in turbomachines.

Let us consider one more case which has a practical application. Let there be an infinite cascade of vortices that are situated along the ordinate (the cascade axis). Let the distance between (n+1) successively situated vortices $t_1, t_2, \ldots, t_n$ (the cascade spacings) and the circulation of vortices $\Gamma_1, \Gamma_2, \ldots, \Gamma_n$ be given. Let us assume that further on, the pattern is cyclically repeated. Such a non-uniform cascade may be replaced by a system of n cascades, each of which has a constant spacing equal to $t = t_1 + t_2 + \ldots + t_n$ and consists of vortices with equal circulation $\Gamma_1, \Gamma_2, \ldots, \Gamma_n$.

The field of complex velocity brought about by such a cascade system may be represented by the sum

$$w(z) = \frac{1}{2it}\sum_{m=1}^{n} \Gamma_m \operatorname{cth}\frac{\pi}{t}(z - ib_m).$$

Here b_m is the ordinate determining the position of the "basic" vortex of the m^{th} cascade.

Placing the basic vortex of the first cascade at the origin of the coordinates, we obtain $b_1=0,\ b_2=t_1,\ \ldots,\ b_n=t_1+t_2+\ldots+t_n=t$.

In the special case where $t_1 = t_2 = \ldots = t_n$ and

$$\Gamma_2=\Gamma_1\exp(-j\alpha),\quad \Gamma_3=\Gamma_1\exp(-2j\alpha),\ \ldots,\ \Gamma_n=\Gamma_1\exp(-nj\alpha),$$

after summation we arrive at Formula (3.3).

It has already been mentioned that a field created by a cascade of attached vortices may be regarded as a turbulence field in the stream, brought about by the action of constant forces. Let us emphasize that the replacement of bodies in a streamline flow by a system of vortices is possible also in the case of large perturbations, i.e., in a nonlinearized problem as well. In such a case, if the forces vary in time, a vortex wake is situated behind each vortex. The perturbation fields may be found on the basis of the obtained solution by means of integration along the vortex sheet.

If a linearized problem is considered, the acceleration-potential method may be used.

Let a plane-parallel stream of an incompressible fluid, having a velocity of U, be acted upon by a system of concentrated forces Y_m, which change according to a harmonic law with a phase shift and are applied at the points $(0,\ y_m)$

$$Y_m=Y_0e^{i(\nu t-m\alpha)},\quad y_m=lm,\quad m=0;\pm1;\pm2;\ldots$$

Each of the forces creates a field of perturbed pressure equivalent to a dipole situated at the point of its application. Then the total perturbed-pressure field (or the complex acceleration potential) may be expressed by means of Formula (3.3):

$$p = \frac{\gamma_0}{2il}\left\{\frac{\operatorname{ch}\left[(\pi-\alpha)\frac{z}{l}\right]}{\operatorname{sh}\left(\pi\frac{z}{l}\right)} - ij\frac{\operatorname{sh}\left[(\pi-\alpha)\frac{z}{l}\right]}{\operatorname{sh}\left(\pi\frac{z}{l}\right)}\right\}. \qquad (3.5)$$

Here use has been made of the fact that (3.3) constitutes the total action of an infinite series of dipoles, which in this case are regarded as pressure dipoles. The constant factor in (3.5) is expressed in terms of force by means of the known solution for a single dipole (see Chapter 2).

§ 3.3. A Singularity Cascade in a Subsonic Stream

Let us now consider the action of a force cascade[1] upon a subsonic stream [62]. We assume that the main stream is parallel to the x-axis, the cascade offset is equal to γb, the harmonic forces are arranged with the spacing intervals t and have the phase shift α.

We consider the perturbation problem in a linearized formulation.

The acceleration potential brought about by a single periodic concentrated force applied at the origin of coordinates is, for a subsonic stream, expressed in terms of the Hankel function $H_1^{(2)}$ (see Chapter 2).

On the basis of the known property of cylindrical functions

$$\frac{dZ_n}{dx} = \frac{n}{2}Z_n - Z_{n+1}$$

the formula for perturbation pressure may be expressed in terms of a derivative of a zero-order Hankel function in the form of

$$p = Ae^{i(\alpha x+\omega t)}\frac{\partial}{\partial y}H_0^{(2)}\left(\varkappa\sqrt{x^2+\beta^2y^2}\right), \qquad (3.6)$$

where $A = -jV_\infty M\beta^2$; the rest of the designations are the same as in Chapter 2. Let us note that if function $H_1^{(2)}$ represents a perturbed dipole field, then function $H_0^{(2)}$ describes the field of pressure

Footnote (1) appears on page 121.

perturbations brought about by a pulsating source in a compressible fluid. Here the derivative must be taken in the direction of the action of the field. In the case under consideration it is assumed that the forces are perpendicular to the main stream, i.e., are parallel to the ordinate.

The perturbation pressure brought about by the action of the force cascade is represented by the series

$$p = Ae^{j(\nu t+\mu x)}\frac{\partial}{\partial y}\sum_{n=-\infty}^{\infty} e^{j(-n\ell\sin\gamma_0-\alpha)x}\times$$
$$\times H_0^{(2)}\left[\varkappa\sqrt{(x-n\ell\sin\gamma_0)^2+\beta^2(y-n\ell\cos\gamma_0)^2}\right].$$

Let us apply the Poisson summation method to this series, and let us represent the perturbation pressure by a series of Fourier representations of the summed-up function

$$p = Ae^{j(\nu t+\mu x)}\frac{\partial}{\partial y}\sum_{m=-\infty}^{\infty}\mathfrak{F}(m). \tag{3.7}$$

By $\mathfrak{F}(m)$ is meant a Fourier transformation of the summed-up function, represented in the form

$$\mathfrak{F}(m) = \frac{1}{2\pi}\int_{-\infty}^{\infty}\exp\xi[-j\mu\ell\sin\gamma_0-j\alpha-im]\times$$
$$\times H_0^{(2)}\left[\varkappa\sqrt{[x-(\xi\ell/2\pi)\sin\gamma_0]^2+\beta^2[y-(\xi\ell/2\pi)\cos\gamma_0]^2}\right]d\xi. \tag{3.8}$$

Here the imaginary unit i has been introduced, which does not interact with the imaginary unit j. However, the imaginary unit i in Formula (3.8) may be replaced by j. This is possible since summation along m proceeds for all whole positive and negative values. The exponential factor in the integrand may be grouped for values of $\pm$ m, and it can be shown that only cosine transformation takes place with the exponent m. Let us replace the integration variable

$$\xi = \frac{2\pi x}{\ell\sqrt{\sin^2\gamma_0+\beta^2\cos^2\gamma_0}}+\frac{2\pi(x\sin\gamma_0+\beta^2y\cos\gamma_0)}{\ell(\sin^2\gamma_0+\beta^2\cos^2\gamma_0)}$$

and designate

$$b^2 = \beta^2 \frac{(x\cos\gamma_b - y\sin\gamma_b)^2}{\sin^2\gamma_b + \beta^2\cos^2\gamma_b}, \quad c_m = \frac{-\mu t\sin\gamma_b - 2\pi m - \omega}{t\sqrt{\sin^2\gamma_b + \beta^2\cos^2\gamma_b}},$$
$$d_m = \frac{\exp jc_m(x\sin\gamma_b + \beta^2 y\cos\gamma_b)}{t\sqrt{\sin^2\gamma_b + \beta^2\cos^2\gamma_b}}. \qquad (3.9)$$

Then the integral is reduced to the form

$$\mathfrak{F}(m) = d_m \int_{-\infty}^{\infty} e^{jc_m z} H_0^{(2)}(x\sqrt{z^2+b^2})\,dz. \qquad (3.10)$$

The function $H_0^{(2)}$ may be represented as a combination of Bessel and Neumann functions

$$H_0^{(2)}(x\sqrt{z^2+b^2}) = J_0(x\sqrt{z^2+b^2}) - jN_0(x\sqrt{z^2+b^2}).$$

Since these functions are even functions of z, in the integration along the interval $-\infty$, $+\infty$ it is necessary to take into account only the Fourier cosine transformation.

With account taken of what has been said, Integral (3.10) is represented by a sum of two integrals:

$$\mathfrak{F}(m) = 2d_m \times$$
$$\times\left[\int_{-\infty}^{\infty} J_0(x\sqrt{z^2+b^2})\cos(c_m z)\,dz - j\int_{-\infty}^{\infty} N_0(x\sqrt{z^2+b^2})\cos(c_m z)\,dz\right].$$

The reduced definite integrals are expressed in terms of elementary functions, two cases being possible for the integration:

a) $0 < x < |c_m|, \quad b > 0,$

$$\mathfrak{F}(m) = \frac{-2jd_m}{\sqrt{c_m^2 - x^2}} e^{-b\sqrt{c_m^2 - x^2}}, \qquad (3.11)$$

b) $0 < |c_m| < x, \quad b > 0,$

$$\mathfrak{F}(m) = \frac{2d_m}{\sqrt{x^2 - c_m^2}} e^{-jb\sqrt{x^2 - c_m^2}}. \qquad (3.12)$$

The denominators of these expressions increase arbitrarily when $x^2 \to c_m^2$. This case deserves special attention, since it corresponds physically to the phenomenon of resonance in a gas stream. The oscillations of the gas, brought about by finite harmonic forces, must

increase arbitrarily in the absence of attenuation. Consequently, the resonance condition is the equality ($x=\pm c_m$):

$$x = \pm \frac{\mu l \sin\gamma_b + 2\pi m + \alpha}{l\sqrt{\sin^2\gamma_b + \beta^2\cos^2\gamma_b}}.$$

After the substitution $x = \nu M/U\beta^2$, $\mu = \nu M^2/U\beta^2$, $\beta^2 = 1 - M^2$, $M = U/a_0$ and transformations, we find

$$\frac{\nu M}{U(1-M^2)} = \pm \frac{2\pi m + \alpha}{l(\mp M\sin\gamma_b + \sqrt{1 - M^2\cos^2\gamma_b})}.$$

The left-hand part of this expression is always positive. Since the numerator of the right-hand part is also always positive, the sign in front of the entire right-hand part must be selected in such a manner that for the selected m, the numerator also be positive. After transformations, the formula for determination of the resonance frequency may be written down as follows [62]:

$$\nu = \pm a_0(\pm M\sin\gamma_b + \sqrt{1 - M^2\cos^2\gamma_b})\frac{2\pi m + \alpha}{l}. \qquad (3.13)$$

Here the $\pm$ signs in front of the parenthesis should be selected in such a manner that the oscillation frequency is a positive value.

This formula has a simple physical interpretation, since the product of the first two cofactors constitutes the rate of propagation of the perturbations along the cascade axis, i.e., in the direction of a straight line drawn at the angle γb.

The $\pm$ signs correspond to propagation of the signal in one direction and in the other, i.e., in the direction of the rays γb and $\gamma_b+\pi$.

Actually, if a signal is sent from the coordinate origin, then after the time τ the region of perturbations will be bounded by a circle (Figure 3.2a):

$$(x - U\tau)^2 + y^2 = a^2\tau^2.$$

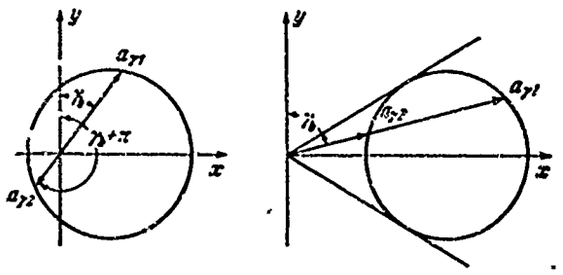


Figure 3.2. (a) The determination of the propagation rate of a perturbation in subsonic flow and (b) in supersonic flow.

We make the replacement $x=r\sin\gamma$, $y=r\cos\gamma$ (remember that the angle γ_b — the cascade offset — is measured clockwise from the ordinate). Then, differentiating with respect to time, from this equation it is possible to determine the rate of propagation of the signal in the direction of ray γ ($\gamma=\gamma_b$ or $\gamma=\gamma_b+\pi$):

$$a_\gamma=\frac{r}{\tau}=a_0(M\sin\gamma+\sqrt{1-M^2\cos^2\gamma}). \tag{3.14}$$

Formula (3.13) may also be written in the form

$$\nu=2\pi\frac{a_\gamma}{l},$$

where the relationship of the frequency ν to the rate of propagation of the wave a_γ and its length $l=\pm t/(m+\alpha/2\pi)$ is obvious.

Returning to Formula (3.13), we note that there are two resonance frequencies which correspond to waves traveling forward and backwards. In a cascade without offset, the two frequencies coincide ($\gamma_b=0$). In a cascade with offset $\gamma_b=\pi/2$ the speeds forwards and backwards of the traveling waves are respectively equal to $a_0 \pm U$.

In the straight cascade ($\gamma b = 0$) and with the action of forces without a phase shift, resonance should be observed when a whole number of waves is situated along the cascade spacing:

$$\nu=a_0\sqrt{1-M^2}\frac{2\pi m}{t}.$$

This problem is applicable in the theory of aerodynamic cascades which consist of thin profiles, and are in a subsonic streamline flow of gas, since the arbitrary profiles are replaced by a dipole system.

Let us also consider the application of the above considerations to the problem of flow resonance in a turbomachine stage. In Figure 3.3 line (1) conventionally represents a directing cascade, and line (2) represents a working cascade. The points on these lines denote blades, situated in accordance with spacing t_1 and t_2. The stream, which is assumed to be subsonic, emerges from the directing cascade with a velocity of c_1. The working cascade moves with respect to the directing cascade with the peripheral velocity u. The stream enters the working cascade with the relative velocity w_1^0.

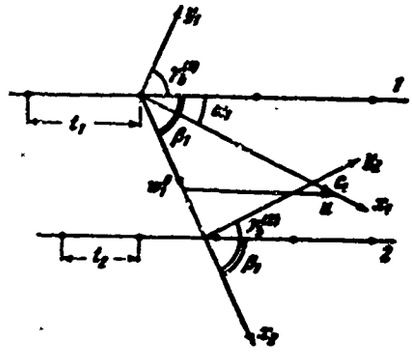


Figure 3.3. The origination of resonance in a turbomachine stage.

Let us consider the conditions of the development of resonance in the space between the cascades.

The blades of the working cascade move in a periodically inhomogeneous stream which is perturbed by the directing cascade. The angular frequency of the pulses acting upon the working blades is equal to $2\pi n z_1$, where n is the number of rotations of the turbomachine wheel, and z_1 is the number of blades in the directing cascade. The phase shift of the action of the aerodynamic force upon the adjacent blades of the second cascade is equal to $\alpha = 2\pi t_2/t_1$.

At resonance, Condition (3.13) must be satisfied in the stream; this condition is written in conventional notation in the following manner:

$$2\pi n z_1 = \pm a_0 \left(\pm M \cos\beta_1 + \sqrt{1 - M^2 \sin^2\beta_1}\right) \frac{2\pi m - 2\pi t_2/t_1}{t_2}.$$

Here the offset angle of the second cascade is found on the basis of condition $\gamma_b^{(2)} = \pi/2 - \beta_1$, the orientation of the coordinate axes x_2y_2 being selected in the manner that has been adopted above. The Mach number in this case must be determined on the basis of the relative stream velocity $M = w_1^0/a_0$. The minus sign in front of $2\pi t_2/l_1$ is used because the phase shift is opposite in sign to the phase shift selected in the derivation of Formula (3.13).

The number of blades in the first cascade is equal to $z_1 = \pi d/t_1$, where d is the diameter of an annular cascade. Then from the basic formula (when m = 0) we shall obtain the result that resonance will be observed under the condition of

$$\pi nd = a_0(-M\cos\beta_1 + \sqrt{1 - M^2\sin^2\beta_1}).$$

This relationship establishes the equality of the circular velocity $u = \pi dn$ and the velocity of the backwards traveling wave $a_y = a_0(-M\cos\beta_1 + \sqrt{1 - M^2\sin^2\beta_1})$.

Since these velocities have different directions, the traveling wave will be motionless with respect to the first cascade. Consequently, resonance will originate when the wave is a standing wave. This phenomenon is analogous to the phenomenon of resonance in a rotating disk.

§ 3.4. A Singularity Cascade in a Supersonic Stream

A concentrated force acting at the origin of the coordinates and changing harmonically in time brings about a pressure perturbation which is described by the Bessel function J_1 (see Chapter 2). By means of a simple transformation, analogous to the one cited in § 3.2, the perturbation may be expressed by the formula

$$p = Ae^{i(\omega t - \mu x)}\frac{\partial}{\partial y}J_0(\varkappa\sqrt{x^2 - \beta^2 y^2}).$$

Here

$$A=i\frac{\gamma_0}{2\beta^2},\quad \mu=\frac{\nu M}{a_0\beta^2},\quad \varkappa=\frac{\nu}{a_0\beta^2},\quad \beta^2=M^2-1.$$

Let us consider a cascade of forces acting with a phase shift, and let us determine the resonance frequency [62].

With supersonic velocity of the main stream, perturbations created by any of the forces propagate only within the Mach wedge. Thus, a force denoted by the index m (i.e., applied to the cascade axis at the point $x=mt\sin\gamma_0$, $y=mt\cos\gamma_0$), brings about perturbations only within a wedge bounded by the straight lines

$$x-mt\sin\gamma_0=\pm\beta(y-mt\cos\gamma_0)$$

under the condition $x\geqslant mt\sin\gamma_0$, since the perturbations propagate only downstream.

In this equation the value $\pm\beta$ is the angular coefficient of the Mach lines and, consequently, $\pm 1/\beta=\pm 1/\sqrt{M^2-1}$ is equal to the tangents of the inclination angle of these lines. In connection with this, two characteristic regimes of flow about a cascade by a supersonic stream are possible:

(a) $\beta>\operatorname{tg}\gamma_0$ — the cascade axis lies (Figure 3.4) within the region of unperturbed flow (except for the points of application of the forces);

(b) $\beta<\operatorname{tg}\gamma_0$ — the Mach waves emerge into the space in front of the cascade, and the cascade axis lies within the region of perturbed flow (Figure 3.5).

Let us consider the latter case. In view of the periodicity of the pattern, it is possible to study only the perturbations within bands bounded by adjacent Mach lines, for example, $x=\beta y$, $x-t\sin\gamma_0=\beta(y-t\cos\gamma_0)$ and $x=-\beta y$, $x=-\beta(y-t\cos\gamma_0)$. Within the band under consideration, only forces with indexes from m = 0 to m = $-\infty$ participate in the formation of perturbations.

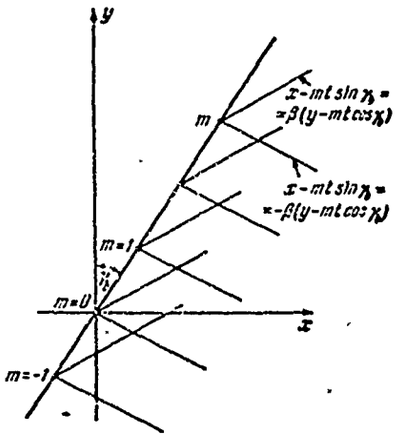


Figure 3.4. Singularity cascade in supersonic flow when $\beta > \tan\gamma$

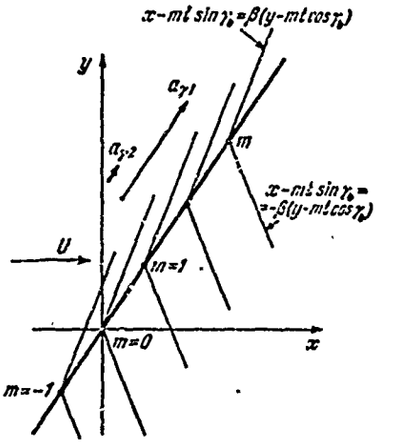


Figure 3.5. Singularity cascade in supersonic flow. Arrows indicate the flow velocity (U) and the propagation rates of perturbations along the cascade axis ($a_\gamma 1$ and $a_\gamma 2$).

To reduce the computations, let us consider the perturbations only at one point of this band — at the origin of the coordinates, and we shall naturally exclude the effect of a force with an index m = 0. In case resonance occurs at the point under consideration, it will simultaneously originate at other points of the band.

The perturbed pressure may be represented by the following series:

$$p = Ae^{i(\alpha x-\mu t)}\frac{\partial}{\partial y}\sum_{m=1}^{\infty} e^{i(\mu mt\sin\gamma_0-m\alpha)}J_0\left(\varkappa mt\sqrt{\sin^2\gamma_0-\beta^2\cos^2\gamma_0}\right).$$

This series is transformed into a series [19], the general term of which has the form

$$\{\varkappa^2t^2(\sin^2\gamma_0-\beta^2\cos^2\gamma_0)-[2\pi n\pm(\mu t\sin\gamma_0-\alpha)^2]\}^{-1/2}. \qquad (3.15)$$

When the expression in the parenthesis tends toward zero, the series diverges, which corresponds to the origination of infinitely large oscillations during resonance.

Equating Expression (3.15) to zero and taking into account the fact that

$$\beta^2 = M^2 - 1, \quad \mu = \frac{\nu M}{a_0 \beta^2}, \quad \varkappa = \frac{\nu}{a_0 \beta^2},$$

we obtain the formula for the resonance frequency in a supersonic stream [62]:

$$\nu = \pm a_0 (M \sin \gamma_0 \pm \sqrt{1 - M^2 \cos^2 \gamma_0}) \frac{(2\pi m + \alpha)}{t}. \tag{3.16}$$

Formula (3.16) differs from Formula (3.13) by the position of the double sign. This is explained by the fact that in supersonic flow the perturbations propagate in only one direction (see Figure 3.2).

Since now $M > 1$, the condition $1 - M^2 \cos^2 \gamma_0 > 0$, is additionally set forth, whence follows that resonance is possible only when the condition $\beta < \operatorname{tg} \gamma_0$ is satisfied.

The double sign at the second term indicates the possibility of two resonance frequencies for the given regime of flow about a cascade (not counting the possibility of varying the number of waves m). This corresponds to two possible rates of propagation of the perturbations along the cascade axis, as was also the case in subsonic flow. Now, however, the perturbations propagate along the cascade axis only in one direction.

It is of interest to study the behavior of perturbation functions at a very large distance from the cascade axis.

If the observation point is situated at a distance that is much greater than the cascade spacing, it may be considered that the perturbation forces replace the real profiles, i.e., the asymptotic behavior of the perturbation functions should not depend upon the specific shape of the blades.

Analyzing Formulas (3.11) and (3.12), conclusions may be drawn concerning the attenuation intensity of perturbations with different wavelengths (in comparison to the cascade spacing and the total period of the forces, the action of which has been shifted by the

angle α). Corresponding remarks are made below for some special cases.

§ 3.5. A Cascade as a Singular Line

Above we considered the effect of individual concentrated forces upon a stream. The limiting problem of flow about a cascade with an infinitely small spacing is of interest. In order to solve such a problem, it is necessary first to consider the perturbations brought about by forces distributed along a straight line. The solution may be obtained in two ways: direct integration of the wave equation, which in this simple case is feasible, or by using the solution for a single singularity. Let us pick the second way, and let us consider the problem for subsonic flow.

Let us assume that the main stream is moving parallel to the abscissa, the forces are perpendicular to the x-axis, depend harmonically upon time, and are distributed along the cascade axis also according to a harmonic law. The cascade axis has an offset of γ_0. We shall write the acceleration potential of such a flow by using the well-known solution for the acceleration potential due to the action of a concentrated harmonic force.

Distributing the singularity along the cascade axis and replacing the discrete phase shift $m\alpha (m = 0; \pm 1; \pm 2; \ldots)$ by a continuous change, we write the acceleration potential in the form of the integral:

$$\varphi_* = B\frac{\partial}{\partial y}\int_{-\infty}^{+\infty} e^{-i\left(\mu \sin\gamma_0 + \frac{2\pi}{t}\right)\xi} \times \\ \times H_0^{(2)}\left[\varkappa\sqrt{(x-\xi\sin\gamma_0)^2 + \beta^2(y-\xi\cos\gamma_0)^2}\right] d\xi.$$

Here t is the period of the cascade (the period of load distribution), the integration variable ξ passes along the cascade axis; B is the linear load.

From a consideration of the integral it follows that it is possible to use the solution obtained above for a singularity cascade. For this solution it is necessary to retain only the one term of Series (3.7) which corresponds to the given wavelength.

In Designations (3.9) it should be assumed:

$$\left.\begin{aligned} b^2 &= \beta^2\frac{(x\cos\gamma_0 - y\sin\gamma_0)^2}{\sin^2\gamma_0+\beta^2\cos^2\gamma_0}, \quad c = \frac{\mu l\sin\gamma_0 + 2\pi n}{l\sqrt{\sin^2\gamma_0+\beta^2\cos^2\gamma_0}}, \\ d &= \frac{\exp jc(x\sin\gamma_0+\beta^2 y\cos\gamma_0)}{\sqrt{\sin^2\gamma_0+\beta^2\cos^2\gamma_0}}. \end{aligned}\right\} \tag{3.17}$$

Then, making use of Formulas (3.7), (3.10), and (3.17), we obtain the final solution. Two cases must be considered:

a) $x<|c|, \quad b>0,$

$$\varphi_0 = B\frac{\partial}{\partial y}\frac{-2\pi d}{\sqrt{c^2-x^2}}e^{-b\sqrt{c^2-x^2}}, \tag{3.18}$$

b) $x>|c|, \quad b>0,$

$$\varphi_0 = B\frac{\partial}{\partial y}\frac{2d}{\sqrt{x^2-c^2}}e^{-jb\sqrt{x^2-c^2}}. \tag{3.19}$$

Let us consider an analogous problem with supersonic velocity of the main stream. Let the stream be directed along the abscissa, and let the load be distributed along the cascade axis perpendicular to the main stream. The acceleration potential (for the case of $\beta<\operatorname{tg}\gamma_0$) is determined by the formula

$$\left.\begin{aligned} \varphi_0 &= B_1\frac{\partial}{\partial y}\int_{-\infty}^{\xi_1} e^{j\left(\mu\sin\gamma_0-\frac{2\pi}{l}\right)\xi}\times \\ &\quad\times J_0\left[x\sqrt{(x-\xi\sin\gamma_0)^2-\beta^2(y-\xi\cos\gamma_0)^2}\right]d\xi, \\ B_1 &= \frac{j\Gamma_0}{2\beta^2 p^0}e^{j(\nu t-\mu x)} \end{aligned}\right\} \tag{3.20}$$

Here use is made of the solution for the acceleration potential created by a single concentrated force, expressed in terms of the Bessel function J_0. In this case the upper integration limit is not infinite, as in subsonic flow, since the perturbation at the observation point x, y is created only by the forces (situated at the cascade axis) for which the observation points are within the Mach wedge. The integration variable ξ runs through the cascade axis and, consequently, may be found as a coordinate of the point of intersection of a Mach line passing through the observation point with the cascade axis.

For determining ξ_1 it is necessary to solve the equations:

$$x-\xi_1\sin\gamma_0 = \pm\beta(y-\xi)\cos\gamma_0, \quad y = x\operatorname{ctg}\gamma_0.$$

Here the $\pm$ signs pertain respectively to cases where the observation point lies at the left (1) or at the right(2) of the cascade (Figure 3.6a). Hence

$$\xi_1 = \frac{x-\beta y}{\sin\gamma_b - \beta\cos\gamma_b} \text{ and } \xi_1 = \frac{x+\beta y}{\sin\gamma_b + \beta\cos\gamma_b}.$$

Obviously, for $\xi \leqslant \xi_1$ the radicand in the formula for the acceleration potential is non-negative. We replace the variable in (3.20):

$$\xi = \frac{z}{\sqrt{\sin^2\gamma_b - \beta^2\cos^2\gamma_b}} + \frac{x\sin\gamma_b - \beta^2 y\cos\gamma_b}{\sin^2\gamma_b - \beta^2\cos^2\gamma_b},$$

and designate

$$b^2 = \beta^2\frac{(x\cos\gamma_b - y\sin\gamma_b)^2}{\sin^2\gamma_b - \beta^2\cos^2\gamma_b}, \quad c = \frac{\mu\sin\gamma_b + \frac{2\pi}{l}}{\sqrt{\sin^2\gamma_b - \beta^2\cos^2\gamma_b}},$$
$$d = \frac{\exp jc(x\sin\gamma_b - \beta^2 y\cos\gamma_b)}{\sqrt{\sin^2\gamma_b - \beta^2\cos^2\gamma_b}}.$$

Then the acceleration-potential integral is reduced to the form

$$I = -d\int_b^\infty e^{-lcz} J_0\left(\varkappa\sqrt{z^2-b^2}\right)dz, \quad b>0.$$

In integration, two cases are possible:

a $\quad \varkappa<c, \quad b>0, \quad I = -jdl\frac{1}{\sqrt{c^2-\varkappa^2}}e^{-lb\sqrt{c^2-\varkappa^2}},$

b $\quad \varkappa>c, \quad b>0, \quad I = -d\frac{1}{\sqrt{\varkappa^2-c^2}}e^{-b\sqrt{\varkappa^2-c^2}}.$

The case of $c = \varkappa$, as has already been said above, corresponds to resonance.

The obtained expressions differ from the subsonic variant with respect to one fundamental feature. In the case of subsonic streamline flow, oscillations with a frequency below the critical attenuate far away from the cascade, while those with a frequency above the critical propagate to infinity.

In the case of supersonic streamline flow, the pattern is reversed: oscillations with a subresonance frequency are observed in

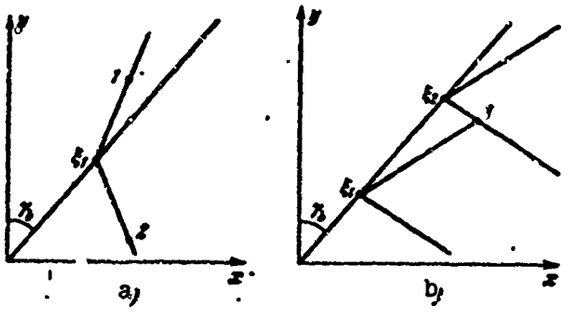


Figure 3.6. Determination of the integration limits in cases (a) $\beta < \operatorname{tg}\gamma_b$, (b) $-\beta > \operatorname{tg}\gamma_b$.

the entire flow field, whereas oscillations with a frequency above the resonance attentuate at a distance from the cascade.

Let us dwell on the second possible variant of flow about a cascade, when $\beta > \operatorname{tg}\gamma_b$, i.e., the variant where perturbations do not penetrate into the region to the left of the cascade (Figure 3.6b). Now both limits in the fundamental integral will be finite and equal to ξ_1, ξ_2.

These limits are found as coordinates of the points of intersection of Mach waves (from the first and second family), passing through the observation point, with the cascade axis.

We replace the integration variable:

$$\xi = \frac{x}{\sqrt{\beta^2\cos^2\gamma_b - \sin^2\gamma_b}} - \frac{x\sin\gamma_b - \beta^2 y\cos\gamma_b}{\beta^2\cos^2\gamma_b - \sin^2\gamma_b}.$$

We introduce the designations

$$\delta^2 = \beta^2\frac{(x\cos\gamma_b - y\sin\gamma_b)^2}{\beta^2\cos^2\gamma_b - \sin^2\gamma_b}, \quad c = \frac{\mu\sin\gamma_b + \frac{2\pi}{t}}{\sqrt{\beta^2\cos^2\gamma_b - \sin^2\gamma_b}},$$

$$d = \frac{\exp jc(\beta^2 y\cos\gamma_b - x\sin\gamma_b)}{\sqrt{\beta^2\cos^2\gamma_b - \sin^2\gamma_b}}.$$

Then the integral of the acceleration potential turns out equal to

$$d\int_{-b}^{+b} e^{ikz} J_0(\varkappa\sqrt{b^2-z^2})\,dz = 2d\,\frac{\sin b\sqrt{\varkappa^2+c^2}}{\sqrt{\varkappa^2+c^2}},\quad b>0.$$

In this case, resonance cannot originate in the stream, since this value remains restricted at any values of the determining parameters. Physically, this is explained by the fact that at any point of the stream, interference of waves emitted from the restricted sector of the cascade axis is observed.

We shall find the equations for calculating the velocity field and shall find the connection between the oscillation rate and the value of the force. Formulas were established above, which determine the field of perturbed pressures of cascades with an arbitrary offset. Now, in order to obtain more graphic formulas, we shall find the perturbation-velocity potential only for the special case of a cascade without offset and for a subsonic stream.

For $\gamma_0=0$, from (3.17) we have

$$b=|x|,\quad c=\frac{2\pi}{\beta t},\quad d=\frac{1}{\beta}\exp\left(j2\pi\frac{y}{t}\right). \tag{3.21}$$

The acceleration potential for subsonic flow and for a subresonance oscillation frequency ($\varkappa<|c_1|$) is determined by Formula (3.18). Substituting Conditions (3.21) into (3.18), differentiating with respect to y and transforming, we obtain the acceleration potential

$$\varphi_*=\frac{jV_0}{2\rho^0\sqrt{\beta^2-k^2M^2}}\exp\left[j\left(\nu\tau+\mu x+2\pi\frac{y}{t}\right)-\left(\frac{2\pi|x|}{t\beta^2}\right)\sqrt{\beta^2-k^2M^2}\right].$$

Here the Strouhal number $k=\nu t/2\pi U$ has been introduced; it characterizes the unsteadiness of the process. The wavelength in the distribution of the perturbing forces has been taken as the linear dimension of t.

On the basis of the acceleration potential, we determine the vertical-acceleration field by differentiation with respect to y

$$a_y=\frac{-2\pi V_0}{2\rho^0 t\sqrt{\beta^2-k^2M^2}}\exp\left[j\left(\nu\tau+\mu x+2\pi\frac{y}{t}\right)-\frac{2\pi|x|}{t\beta^2}\sqrt{\beta^2-k^2M^2}\right]. \tag{3.22}$$

On the basis of the acceleration field it is possible to determine the field of vertical perturbed velocities. For this it is necessary to integrate the linearized equation of motion all the way through.

$$\frac{\partial v_2}{\partial y} = a_y = \frac{\partial v}{\partial t} + U\frac{\partial v}{\partial x}. \tag{3.23}$$

When using this equation it is necessary to bear in mind that the vertical velocity has a discontinuity at the cascade axis, which is a singular line. We represent the derivative of the discontinuous function on the basis of the theory of generalized functions in the form

$$\frac{\partial v}{\partial x} = \left(\frac{\partial v}{\partial x}\right) + \Delta\delta(x). \tag{3.24}$$

Here $(\partial v/\partial x)$ is a derivative, understood in the conventional sense; $\Delta = v(+0, y, t) - v(-0, y, t)$ is the value of the function discontinuity, i.e., the difference of the limits on the right and to the left of the discontinuity line. The value of the vertical-velocity discontinuity is determined by the value of the acting force from the relationship

$$\Delta = \frac{\gamma_0}{\rho U} e^{j\left(\nu t + \varphi_0 - \frac{x}{l}\right)}, \tag{3.25}$$

since only the component of the vertical velocity which is in phase with the local acting force has a discontinuity.

For the case of harmonic oscillations it may be assumed that:

$$\left.\begin{aligned} a_y = a'_y(x)\exp j\left(\nu t + 2\pi\frac{x}{l}\right), \quad v = v'(x)\exp j\left(\nu t + 2\pi\frac{x}{l}\right), \\ \gamma_0 = \gamma'_0 \exp j\left(\nu t + 2\pi\frac{x}{l}\right). \end{aligned}\right\} \tag{3.26}$$

Then from Equation (3.23), by means of (3.24) - (3.26) we obtain (again discarding the prime index)

$$a_y = j\nu v + U\frac{\partial v}{\partial x} + \gamma_0\frac{\delta(x)}{\rho U}. \tag{3.27}$$

Here a_y is a known function and is determined by Formula (3.22), in which the factor $\exp j\left(\nu\tau + 2\pi\frac{y}{t}\right)$ should be discarded.

We integrate (3.27) first in the left-hand semiplane, assuming that perturbation velocities at infinity in front of the cascade are absent $v(-\infty)=0$. During integration in the left-hand semiplane, the last term of (3.27) is equal to zero in accordance with the well-known property of the Dirac Function.

The total integral has the form

$$v(x)=\frac{j}{U}e^{-j\nu\frac{x}{U}}\int_{-\infty}^{x}a_y e^{j\nu\frac{\xi}{U}}d\xi.$$

Performing calculations and effecting transformations, we obtain the value of the perturbation velocity in the left-hand semiplane

$$v(x)=\frac{-Y_0\beta^2}{2\rho^0 U}\frac{\exp\left[j\mu x+(2\pi\nu/t\beta^2)\sqrt{\beta^2-k^2M^2}\right]}{\sqrt{\beta^2-k^2M^2}\,(jk+\sqrt{\beta^2-k^2M^2})}. \qquad (3.28)$$

On the basis of (3.28) we find the perturbation velocity immediately in front of the cascade:

$$v(-0)=\frac{-Y_0\beta^2}{2\rho^0 U\sqrt{\beta^2-k^2M^2}\,(jk+\sqrt{\beta^2-k^2M^2})}.$$

At the intersection of the cascade axis (from x = -0 to x = +0) the vertical-velocity jump determines the last term of (3.27), and when integrating we obtain $\Delta v=Y_0/U\rho^0$. In passage through the discontinuity line, only that part of the vertical velocity undergoes a jump, which is in phase with the force. Computing the velocity component before the cascade ($x\to-0$), which is in phase with the force, and adding the jump, we find the same component after the cascade ($x\to+0$). Adding to this the component which does not have a discontinuity, we find the boundary value of the vertical velocity. Integrating and making transformations, we obtain the value of the perturbed vertical velocity in the right-hand semiplane in the form of

$$v(x)=\frac{Y_0k^2}{\rho^0U(1+k^2)}e^{-j\nu x/U}-\frac{Y_0\beta^2}{2\rho^0U}\frac{\exp\left[j\mu x-(2\pi x/t\beta^2)\sqrt{\beta^2-k^2M^2}\right]}{\sqrt{\beta^2-k^2M^2}\,(jk-\sqrt{\beta^2-k^2M^2})}. \qquad (3.29)$$

The first term of this expression constitutes velocity induced by free vortices, and is therefore a traveling wave and does not vanish when $x \to +\infty$. In this case the entire right-hand semiplane is filled by free vortices.

Let us remember that these relationships have been obtained for a subresonance oscillation frequency of $\beta^2 > k^2M^2$. We find analogous relationships for an above-resonance frequency.

The acceleration potential is written in the following form:

$$\varphi_1 = \frac{\gamma_0}{2\rho^2\sqrt{k^2M^2-\beta^2}} \exp i\left[\gamma x + \mu x + \left(2\pi\frac{y}{t}\right) - \left(\frac{2\pi x}{t\beta^2}\right)\sqrt{k^2M^2-\beta^2}\right].$$

In this case the perturbations do not attenuate at an infinite distance in front of the cascade. The perturbation-velocity field in the left-hand semiplane is periodic and is yielded by the formula

$$v(x) = \frac{\beta^2\gamma_0}{2\rho^2 U} \frac{\exp i\left[\mu x + (2\pi x/t\beta^2)\sqrt{k^2M^2-\beta^2}\right]}{\sqrt{k^2M^2-\beta^2}\left(k+\sqrt{k^2M^2-\beta^2}\right)}. \qquad (3.30)$$

We shall find the velocity in the right-hand semiplane in the same manner as above, in order that the jump condition be satisfied. Then we shall obtain

$$v(x) = \frac{\gamma_0 k^2}{\beta^2 U(1+k^2)} e^{-i\gamma x/U} + \frac{\gamma_0\beta^2}{2\rho^2 U} \frac{\exp i\left[\mu x - (2\pi x/t\beta^2)\sqrt{k^2M^2-\beta^2}\right]}{\sqrt{k^2M^2-\beta^2}\left(k-\sqrt{k^2M^2-\beta^2}\right)}. \qquad (3.31)$$

In the same way, by means of the formulas presented in this section, it is possible to consider the general case of a cascade with offset, as well as supersonic flow about a cascade.

Let us consider a straight cascade, composed of plates. Let the cascade have very high density, so that the spacing t_1 is smaller than the chord ($t_1 \ll b$). The cascade is in a streamline flow with a velocity of U, parallel to the chords. Let the profiles oscillate with a certain phase shift α, which is constant from profile to profile. The flow pattern will be repeated at intervals of a period equal to $t = 2\pi t_1/\alpha$. We shall be considering only the case where the cascade

spacing is much smaller than this period: $t_1 \ll t$. If at the same time it is assumed that $b \ll t$, it is then easy, on the basis of the preceding conclusions, to obtain an approximate solution of the problem. Let us emphasize already now that the problem can be generalized in a sufficiently simple manner, thus giving up the last-mentioned restriction.

Under the assumptions set forth, the cascade can be replaced by a system of forces distributed along its axis.

Let the plates make small harmonic oscillations along the ordinate; then, in view of the smallness of the spacing, it may be assumed that the vertical component of velocity at the outlet of the cascade is equal to

$$v_0 e^{i\left(\nu t - 2\pi \frac{y}{t}\right)},$$

where v_0 is the modulus of the blade oscillation velocity $v_0 \ll U$.

The boundary condition at the outlet from the cascade requires equality of the vertical velocities of the plates and the fluid $v_0 = v(+0)$. Here $v(+0)$ is the vertical velocity according to (3.29) with tendency toward the cascade axis from the right-hand side.

For a subresonance oscillation frequency, the vertical velocity of the fluid at the cascade outlet will be found from (3.29), assuming $x = 0$, in the following form:

$$v(+0) = \frac{\gamma_0}{2\rho^0 U} \frac{(2k^2+1)\sqrt{\beta^2 - k^2M^2} + ik}{\sqrt{\beta^2 - k^2M^2}(1+k^2)}.$$

We introduce the force coefficient

$$c_y = \frac{\gamma_0}{\rho^0 U v_0},$$

which in the general case is a complex number, so that the force induced at the blades during oscillation acts out of phase with the velocity.

Then for the subresonance oscillation frequency ($kM<\beta$) we obtain

$$c_y = \frac{2\sqrt{\beta^2 - k^2M^2}(1+k^2)}{(2k^2+1)\sqrt{\beta^2 - k^2M^2} + jk}, \quad k = \frac{\omega l}{2\pi U}. \tag{3.32}$$

For a super-resonance oscillation frequency ($kM>\beta$), the boundary value of the velocity in the case of an approach from the right is found from (3.31), for the condition $x = 0$, according to the formula

$$v(+0) = \frac{k + (2k^2+1)\sqrt{k^2M^2 - \beta^2}}{2\sqrt{k^2M^2 - \beta^2}(1+k^2)}, \quad k = \frac{\omega l}{2\pi U}.$$

Analogously to the preceding, the force coefficient is expressed by the relationship

$$c_y = \frac{2\sqrt{k^2M^2 - \beta^2}(1+k^2)}{(2k^2+1)\sqrt{k^2M^2 - \beta^2} + k}. \tag{3.33}$$

In this case the force coefficient is a real number.

Let us emphasize that by the force Y_0 is understood a force acting upon the fluid. Thus, a body in a streamline flow is acted upon by the force $-Y_0$.

Let us consider first the special case of an incompressible stream. When $M = 0$, it follows from (3.32) that:

$$c_y = \frac{2(1+k^2)}{2k^2+1+jk}. \tag{3.34}$$

The real part and the imaginary part of this function are represented in Figure 3.7. First of all, let us note that the real part of c_y is positive over the entire range of the change of k, i.e., oscillation damping is observed, as well as energy transmission from the oscillating plates to the stream. When $k = 0$, $c_y = 2$ and when $k \to \infty$ $c_y \to 1$. Thus, at a very high oscillation frequency the absolute value of the force coefficient decreases. Let us note one more important special case, which is singular. When the cascade profiles oscillate as a single whole, i.e., without a phase shift, the force-distribution period $t = \infty$ and, no matter what the oscilation frequency

is, we have $c_y = 1$. On the other hand, when the oscillation frequency decreases to zero ($\nu = 0$), the solution must tend toward the solution of a static problem of flow about a cascade. An indeterminacy originates with the value of k when $t \to \infty$ and $\nu \to 0$.

The case of oscillations without a phase shift is singular, since only when $\alpha = 0$ do perturbations, induced by the cascade in an incompressible flow, not tend toward zero at infinity. If, however, it is required that, just as in the other cases, the vertical velocity far in front of the cascade be equal to zero, it is necessary to superpose a vertical flow which nullifies this velocity (this flow will double the velocity at the right of the cascade). Determining the change of momentum, we find $Y_0 = \rho^0 U v_+$ and, consequently, when $\alpha = 0$ we obtain $c_y = 1$.

Thus, the problem of profile oscillation in a dense cascade with a small phase shift is reduced to the problem of steady streamline flow, since the influence of trailing free vortices may be disregarded.

When the cascade oscillates in a compressible fluid, a new phenomenon — resonance — appears, which originates at $k^2M^2 = \beta^2$. With resonance $c_y = 0$, which indicates an absence of aerodynamic damping of the oscillations. A substantial deviation of the curves for a compressible fluid and an incompressible fluid is observed specifically in the resonance region (Figure 3.8). In limit cases ($k = 0$ and $k = \infty$) the force coefficients for a compressible fluid coincide with the corresponding values for an incompressible fluid, as follows from Formulas (3.32) and (3.33). Figure 3.8 shows the real parts, and Figure 3.9 shows the imaginary parts of the force coefficient for three values of the Mach number.

From Formulas (3.32) and (3.33) it follows that when passing through resonance, the phase-shift angle between the force and the velocity changes by $\pi/2$.

The approximate theory that has been set forth describes

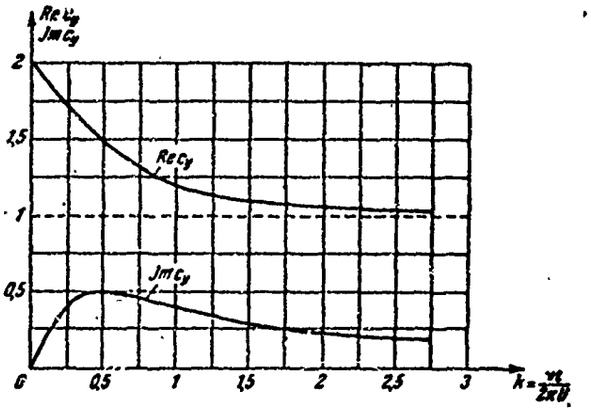


Figure 3.7. Relationship of the real and imaginary parts of the force coefficient to the Strouhal number for a cascade of very great density $t_1 \ll b$, $t_1 \ll t = 2\pi t_1/\alpha$. The dotted curve corresponds to a phase shift equal to zero ($\alpha = 0$).

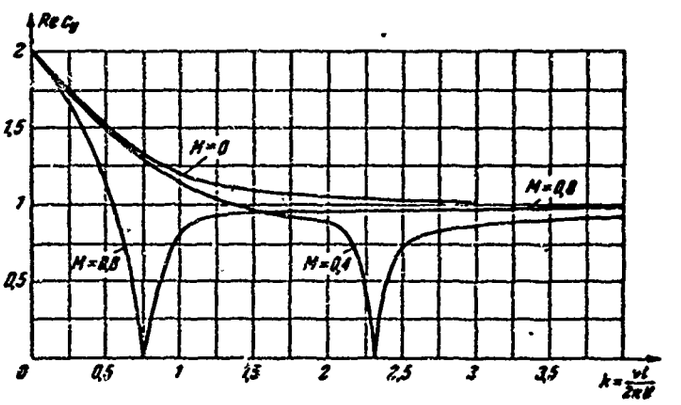


Figure 3.8. Relationship of the real part of the force coefficient to the Strouhal number and the Mach number for a cascade of very great density.

correctly, in general terms, the laws governing the action of the cascade upon a compressible flow.

By means of the formulas of this chapter, analogous calculations may be made for a cascade with offset, as well as for a cascade in a supersonic flow.

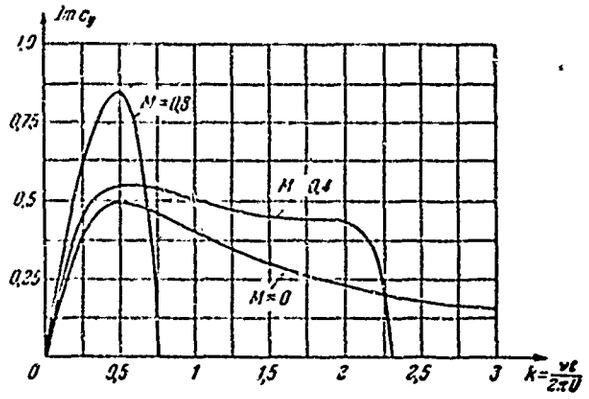


Figure 3.9. Relationship of the imaginary part of the force coefficient to the Strouhal number and the Mach number for a cascade of very great density.

Problems concerning dense cascades have been dealt with by other methods by Songen [139], Songen and Quick [141], and Whitehead [145].

§ 3.6. A Dense Cascade in a Nonuniform Vortex Stream

In the problems considered in this chapter, it was assumed that the main stream is homogeneous, and that its angle of turn in the cascade is negatively small. In real turbomachines the stream has circumferential nonuniformity, and turns by a considerable angle in the aerodynamic cascade. This introduces substantial singularities into the problem.

Let us consider the problem of flow about an aerodynamic cascade with a very small spacing (in the sense defined in § 3.5) by a nonuniform unsteady vortex stream of incompressible fluid.

We shall replace the cascade by discontinuity lines with tangential velocities; however, in distinction from the previous problems, we shall consider that the main stream turns in the cascade by an arbitrary angle. This problem was considered in Reference [68].

Let us consider a moving aerodynamic cascade in which a vortex stream flows with nonuniform velocity. The nonuniform vortex stream may be brought about by edge wakes of the preceding cascade, may originate during flow about motionless struts, etc. We shall replace the vortex trails originating in viscous fluid flow about the indicated bodies by a distributed vorticity transported by a stream of ideal fluid.

Let us designate by c_1 the absolute velocity of the main stream, u is the velocity shift of the cascade, w_1^0 is the relative motion velocity of the main stream running in the cascade. We shall henceforth be considering the cascade in terms of relative motion. Then it can be considered that a uniform main stream flows in at a constant complex rate of $w_{1c}^0 e^{-i\beta_1}$ and transports the vorticity waves ω, which may also be characterized by a supplementary complex velocity $w_{01}e^{-i\alpha_1}$, which are directed at the angle of inclination of the absolute velocity. The cascade under consideration constitutes a cylindrical cross section of the wheel blades; and therefore the vorticity waves will have, along the cascade axis, a period equal to $2\pi R/z$ (R is the radius of the annular section, z is the number of perturbing bodies — blades, struts, etc.) and a repetition frequency of $\nu = zU/2\pi R$.

After turning, the main stream is determined in terms of relative motion by the constant complex velocity $w_{2c}^0 e^{-i\beta_2}$, as well as by vorticity waves, which will be defined below.

Let us formulate the problem in the following manner. We connect the coordinate system xy to a movable cascade, and shall consider the vortex stream of ideal fluid in terms of relative motion. We shall replace the system of edge wakes by vorticity waves flowing in from infinity. The vorticity is $\omega(x, y, \tau)$, here τ — the time, is determined by the known nonuniformity of the flow in edge wakes. The velocity perturbations are assumed everywhere to be small in comparison to the velocity of the main stream $\omega \ll w^0$; in this manner we disregard the distortion of the flow lines by the main stream.

We replace the cascade by the tangential-velocity discontinuity line (x = 0) (Figure 3.10). The traveling vorticity waves in the left-hand semiplane are described by the equation

$$\omega = \omega\left[\nu\tau + \frac{2\pi}{l_1}(-x\sin\alpha_1 + y\cos\alpha_1)\right].$$

Then the equation of motion of the wave front will be

$$\nu\tau + \frac{2\pi}{l_1}(-x\sin\alpha_1 + y\cos\alpha_1) = \text{const}.$$

Differentiating this expression with respect to τ and replacing $\partial y/\partial\tau = \omega_1^0 \sin\beta_1$, $\partial x/\partial\tau = \omega_1^0\cos\beta_1$, we obtain the expression for the wave frequency or for its length

$$\nu = \frac{2\pi}{l_1}\omega_1^0 \sin(\alpha_1 - \beta_1), \quad l_1 = \frac{2\pi}{\nu}\omega_1^0 \sin(\alpha_1 - \beta_1).$$

Henceforth we shall consider only one harmonic of vorticity waves (the results are generalized by the use of a Fourier series)

$$\omega_1(x, y, \tau) = \omega_1 = \omega_{01}\exp j\nu(\tau - p_1 x - q_1 y). \tag{3.35}$$

The imaginary unit j does not interact with i. On the basis of the preceding calculations we obtain

$$p_1 = \frac{\sin\alpha_1}{\omega_1^0 \sin(\alpha_1 - \beta_1)}, \quad q_1 = \frac{-\cos\alpha_1}{\omega_1^0 \sin(\alpha_1 - \beta_1)}. \tag{3.36}$$

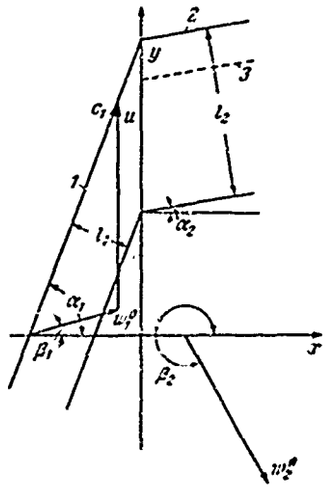


Figure 3.10. Diagram of flow about a cascade by an inhomogeneous vortex stream. The y-axis is a discontinuity line replacing the cascade; (1)-front of approaching and (2)-front of the receding vorticity waves; (3)-front of vorticity waves originating on the cascade.

In the general case, refraction of traveling vorticity waves originates at the discontinuity line. It follows from the condition of the maintenance of vortices that in receding waves the amplitude and frequency must be maintained, and the condition $q_2 = q_1$ must also be observed. Then the vorticity waves behind the cascade (in the right-hand semiplane) will be described by the equation

$$\omega_2(x, y, \tau) = \omega_2 = \omega_{02} \exp jv(\tau - p_2 x - q_2 y), \quad q_2 = q_1. \tag{3.37}$$

The values p_2 and q_2 are determined in a like manner according to (3.36). Utilizing (3.36), (3.37), and the continuity equation $\omega_1^0 \cos\beta_1 = \omega_2^0 \cos\beta_2$, we find the equation for determining the angle of inclination of the receding-wave front (the condition of wave refraction)

$$\operatorname{tg}\alpha_2 - \operatorname{tg}\alpha_2 = \operatorname{tg}\beta_2 - \operatorname{tg}\beta_1. \tag{3.38}$$

The refraction of vorticity waves is an essential singularity of a cascade in which the mainstream turns by a finite angle. The discontinuity line constitutes a vortex sheet and replaces the influence of the blades which turn the stream. Let us note that the streams in regions before and after the cascade cannot be considered independent, since wave systems (3.35) and (3.37) induce velocity in the right-hand semiplane and the left-hand semiplane, respectively.

According to Stokes' theorem the circulation around the elementary area with vorticity is equal to $d\Gamma = 2\omega\, dx\, dy$. Then the complex velocity in the region of $x \geqslant 0$, induced by the wave system (3.35), is equal to

$$\omega_1(z) = \frac{\omega_{01}}{\pi i} \int\int \frac{\exp jv(\tau - p_1\xi - q_1\xi)\, d\xi\, d\eta}{z - (\xi + i\eta)}. \tag{3.39}$$

Here integration is performed along the entire semiplane $x < 0$. Making the substitution $y - \eta = s$, we reduce the integral to the following form:

$$\omega_1(z) = \frac{\omega_{01}}{\pi i} e^{jv(\tau - q_1 y)} \int_{-\infty}^{0} e^{-jvp_1\xi}\, d\xi \int_{-\infty}^{\infty} \frac{[(x-\xi) - i(y-\eta)]\, e^{jvq_1 s}\, ds}{(x-\xi)^2 + s^2}.$$

Integrating along s (with account taken of $x \geqslant 0$, $\xi \leqslant 0$, $y > 0$), we obtain

$$\omega_1(z) = -\omega_{01}(\quad + j)\, e^{jv(\tau - q_1 y)} \int_0^{\infty} e^{-v(|q_1| - jp_1)\xi}\, d\xi. \tag{3.40}$$

Here the $\pm$ signs in front of j pertain respectively to the cases of $q_1 > 0$ and $q_1 < 0$.

Completing integration along ξ, we finally find

$$w_1(z) = -\frac{(\pm j + 1)\,\omega_{01}}{\nu(|q_1| - jp_1)} e^{-\nu|q_1|x} e^{j\nu(z - q_1 y)}. \tag{3.41}$$

If the right-hand semiplane were also taken up by waves (3.35), they would induce in the left-hand semiplane the velocity

$$w(z) = -\frac{(\pm j - 1)\,\omega_{01}}{\nu(|q_1| + jp_1)} e^{\nu|q_1|x} e^{j\nu(z - q_1 y)}. \tag{3.42}$$

This result may be obtained from (3.40), (3.41) if account is taken of the fact that the vorticity is situated to the right of point z (this changes the sign of the imaginary unit i), and also of the fact that when integrating (3.40) from 0 to $+\infty$ the sign in front of p_1 changes and $\nu|q_1|x$.

In this case the total velocity at the ordinate axis will be equal to the sum of (3.41) and (3.42) (when x = 0). By virtue of periodicity along x, the velocity in the entire plane taken up by Waves (3.35) will be equal to the sum of (3.41) and (3.42) when x = 0 with the addition of the multiplier $\exp(-jvp_1x)$. Obviously, this will be the velocity at an infinite distance in front of the cascade, independently of what wave system is situated in the right-hand semiplane (according to (3.42) $w(z) \to 0$ when $x \to -\infty$).

Making the indicated transformations and utilizing the obvious relationship $\pm|q_1| = q_1$, we obtain the perturbation velocity far in front of the cascade

$$w_{1\infty}(z) = -\frac{2j\omega_{01}}{\nu(q_1 - jp_1)} e^{j\nu(z - p_1 x - q_1 y)}. \tag{3.43}$$

The latter result is also easy to obtain by means of direct application of the continuity and vortex equations; however, we will need the intermediate Formulas (3.41) and (3.42).

Recollect that actually the left-hand semiplane contains the wave System (3.35), and the right-hand semiplane contains the wave System (3.37). We find the velocities at the cascade axis, as well as far in front of and behind the cascade, for the wave system under consideration.

According to (3.36) and (3.43) the perturbation velocity at infinity in front of the cascade is equal to

$$w_{1\infty}(z) = \frac{2\omega_{01}w_1^0}{\nu} e^{-i\alpha_1} \sin(\alpha_1 - \beta_1)\, e^{i\nu(\tau - px - qy)},$$
$$w_{01} = \frac{2\omega_{01}w_1^0}{\nu} \sin(\alpha_1 - \beta_1). \tag{3.44}$$

Here w_{01} is the modulus of the perturbation velocity at infinity in front of the cascade. The replacement of α_1 by $\alpha_1+\pi$ does not change the value of p and q according to (3.36). Therefore, we henceforth consider that $(\alpha_1 - \beta_1) > 0$.

The perturbation velocity at infinity behind the cascade (only from the stream carrying the vorticity ω_{01}) will be found analogously by replacement of the indexes 1 by 2:

$$w_{2\infty} = \frac{2\omega_{01}w_2^0}{\nu} e^{-i\alpha_2} \sin(\alpha_2 - \beta_2)\, e^{i\nu(\tau - px - qy)}. \tag{3.45}$$

The modulus of the perturbation velocity may be expressed in terms of the initial perturbation by means of (3.45), (3.38), and the continuity equation in the form of

$$w_{02} = \frac{2\omega_{01}w_2^0 \sin(\alpha_2 - \beta_2)}{\nu}. \tag{3.46}$$

We shall express the perturbation velocity at the cascade axis (x = 0), brought about by the system of vortex waves (3.35), by means of (3.41), (3.36), and (3.44) in terms of the perturbation velocity far in front of the cascade:

$$w_1(0, y, \tau) = -\frac{1}{2}(\pm j + i)\, w_{01} e^{i\alpha_1^0} e^{i\nu(\tau - qy)}. \tag{3.47}$$

Here the $\pm$ signs pertain respectively to the cases of $q_1 > 0$ and $q_1 < 0$. Here and henceforth we shall designate $\exp(j\alpha^*_{1,2}) = |\cos\alpha_{1,2}| + j\sin\alpha_{1,2}$, i.e., $\alpha^*_{1,2} = \alpha_{1,2}$ when $-\pi/2 \leqslant \alpha_{1,2} \leqslant \pi/2$ and $\alpha^* = \pi - \alpha_{1,2}$ when $\pi/2 < \alpha_{1,2} < 3\pi/4$

The perturbation velocity at the outlet from the cascade of wave System (3.37) is found by means of (3.42) and (3.36) with the replacement of p_1 and q_1 by p_2 and q_2 according to the formula

$$w_2(0, y, \tau) = -\frac{1}{2}(\pm j - i) w_{02} e^{-j\alpha^*_2} e^{j\nu(\tau - q_1 y)}. \tag{3.48}$$

The value w_{02} may be expressed in terms of the initial perturbation according to (3.46).

With the passage and refraction of a vorticity-wave system, attached vortices originate at the cascade; these yield the unsteady component of circulation $d\Gamma(y, \tau) = 2\gamma(y, \tau)dy$. The attached vortex sheet must have the same frequency of change with respect to time and the same wavelength as the cause bringing it about:

$$\gamma(y, \tau) = \gamma_0 e^{i\varepsilon} e^{j\nu(\tau - q_1 y)}. \tag{3.49}$$

Here ε is the phase shift. The attached vortex sheet determines the unsteady part of the aerodynamic force acting upon the cascade. Such a phase shift is characteristic of unsteady processes and is brought about by the influence of free vorticity.

The velocity induced by the vortex sheet will be found by integrating along the cascade axis

$$w_3(z) = \frac{1}{\pi i}\int_{-\infty}^{\infty} \frac{\gamma(y, \tau)\,d\eta}{z - i\eta} = \frac{1}{\pi i}\gamma_0 e^{i\varepsilon} e^{j\nu\tau} \int_{-\infty}^{\infty} \frac{[x - i(y - \eta)e^{-j\nu q_1 \eta}\,d\eta}{x^2 + (y - \eta)^2}. \tag{3.50}$$

Completing the integration, we obtain

$$w_3(z) = -\gamma_0 e^{i\varepsilon}(\pm j \pm i) e^{-\nu|q_1 x|} e^{j\nu(\tau - q_1 y)}. \tag{3.51}$$

Here the $\pm$ signs in front of i pertain respectively to the right-hand semiplane and the left-hand semiplane. Let us note that the sheet

does not cause an accelerated velocity field at infinity. With the appearance of the time-dependent, attached distributed vorticity (3.49), a vortex sheet originates behind the cascade, consisting of free vortices carried away by the stream at a velocity of w_2^0. This sheet will occupy the entire right-hand semiplane. The circulation change of an element of the vortex sheet γ with a length of dy for the time $d\tau$ is equal to $2\frac{\partial\gamma}{\partial\tau}d\tau dy$. The circulation of the vortices in the wake behind the cascade during the same time will change by $2\omega_1 dx dy = 2\omega_1 w_2^0 \cos\beta_2 dy d\tau$. We find the value of the trailing vorticity immediately behind the cascade (x = 0), by equating the total circulation change

$$\omega_3(y, \tau) = -\frac{1}{w_2^0 \cos\beta_2}\frac{d\gamma}{\partial\tau} = \frac{-j\nu\gamma_0}{w_2^0\cos\beta_2}e^{jq_1\nu(\tau-p_2x-q_1y)} \qquad (3.52)$$

to zero in accordance with Thompson's theorem.

Downstream the vorticity is carried away by waves traveling with the velocity of the main stream w_2^0.

Waves of free vorticity will have a rectilinear front, parallel to the front of the refracted waves which have been described above, and their propagation in terms of xy coordinates can be expressed by the formula

$$\omega_3 = -j\omega_{03}e^{jk}\exp j\nu(\tau - p_2x - q_1y), \quad \omega_{03} = \frac{\nu\gamma_0}{w_2^0\cos\beta}. \qquad (3.53)$$

Figure 3.10 shows fronts of vorticity waves: oncoming (1), refracted (2), and those which have originated during the change of an attached vortex sheet (3). A phase shift is possible between wave systems (2) and (3)

Obviously, the perturbations velocity of wave system (3.53) far past the cascade can be found according to formula analogous to (3.43) or (3.45):

$$\omega_{4\omega} = -j\frac{2\gamma_0}{\cos\beta_2}e^{-i\alpha_2}\sin(\alpha_2-\beta_2)e^{jk}e^{j\nu(\tau-p_2x-q_1y)}. \qquad (3.54)$$

Here $\omega_{01}=2\gamma_0\sin(\alpha_2-\beta_2)/\cos\beta_2$ is the modulus of the perturbation velocity of this wave system at infinity past the cascade. Just as before, it may always be considered that $\sin(\alpha_2-\beta_2)\geqslant 0$.

The perturbation velocity of wave system (3.53) at the cascade axis can be found according to Formula (3.42) with the replacement of p_1 and q_1 by p_2 and q_2, and ω_{01} by ω_3 according to (3.53). After transformation with the use of Formula (3.36) we obtain

$$w_1(0, y, \tau)=(\mp 1-j\bar{i})\frac{\gamma_2\sin(\alpha_2-\beta_2)}{\cos\beta_2}e^{-j\alpha_2^{*}y/t}e^{jv(\tau-q_1y)}. \qquad (3.55)$$

Here the signs in front of j and α_2^{*} are selected in the same manner as in (3.47).

When considering the boundary conditions at the cascade we shall assume that in the general case the blades can oscillate, and also that the stream-emergence angle can change on account of inhomogeneity of the blades. Since a velocity that is normal to the cascade axis undergoes no discontinuity, the continuity equation is satisfied automatically for perturbed flow. The tangential component of velocity to the right of the cascade must be found according to the known emergence angle $\beta_2=\beta_2(y, \tau)$. The relationship $\beta_2(y, \tau)$ is determined, generally speaking, on the basis of a given law of profile oscillation in the cascade, as well as on the basis of a given inhomogeneity of the emergence angle.

The perturbed velocity at the outlet from the cascade ($x\to 0$, $x>0$) must satisfy the condition (stationary blades)

$$v_+=u'\operatorname{tg}\beta_2. \qquad (3.56)$$

Here v_+ and u' are projections of the velocity w on the coordinate axes.

Above the frequency of the process plays no part in the determination of all the desired values in terms of the velocity of the

perturbed stream. Therefore, the results may be applied directly to nonuniformities of arbitrary shape. This remark naturally pertains to the case of a cascade with maximum density.

Let us consider a motionless cascade in an unsteady vortex field. In this case perturbation velocities at the cascade are brought about by systems of vortex waves (3.35), (3.37), and (3.53), as well as by the unsteady vortex sheet (3.49). Separating the imaginary terms (on the basis of i) and the real terms in (3.47), (3.48), (3.51) and (3.55), we obtain on the basis of (3.56) the equation for determining the intensity of the attached vortex sheet γ_0 and the phase-shift angle ε. After transformations, by means of (3.46) we find

$$\gamma_0 e^{j\varepsilon} = \frac{\omega_{01}\cos\beta_1}{2\cos\alpha_1}\frac{\cos\alpha_2 e^{-j\left(\alpha_2^\circ \pm \beta_2\right)} - \cos\alpha_1 e^{j\left(\alpha_1^\circ \pm \beta_2\right)}}{\cos\beta_2 e^{\pm j\beta_2} + j\sin\left(\alpha_2 - \beta_2\right) e^{-j\left(\alpha_2^\circ \pm \beta_2\right)}}. \tag{3.57}$$

Here the $\pm$ signs pertain respectively to the cases of $q_1 > 0$ and $q_1 < 0$.

The modulus of the distributed force acting along the cascade axis is found on the basis of the equation of momentum

$$l_0 = 2\rho^\circ \gamma_0 w_1^\circ \cos\beta_1. \tag{3.58}$$

We denote several special cases:

1. Let us consider flow about a cascade of plates without offset by a stream with a zero angle of attack ($\beta_1 = 0$), which carries vertical vortex wakes ($\alpha_1 = \pi/2$). Obviously, the angle of emergence is $\beta_2 = 0$ and $w_1^\circ = w_2^\circ$. In this case, according to (3.38) $\alpha_2 = \pi/2$, i.e., the waves are not refracted. According to (3.57) we determine the intensity of the attached vortex sheet $\gamma_0 = \omega_{01}/2$ and the phase-shift angle $\varepsilon = -\pi/2$.

The initial vorticity of the stream according to (3.44) is equal to $\omega_1 = \nu\omega_{01}/2w_1^\circ$. The factor $\exp j\nu(\tau - p_1 x - q_1 y)$ is discarded. On the basis of (3.53) we find the free vorticity, evoked at the cascade and

carried away by the stream $\omega_2 = -\nu\omega_{01}/2\omega_1^0$. Since $\omega_1 + \omega_2 = 0$, it follows that there is no vortex wake behind the cascade (the initial vorticity is destroyed by the vorticity, opposite in sign, which has been brought about on the cascade). The distributed lift force, acting upon a unit of cascade length, is according to (3.58) equal to $l = \rho^0\omega_{01}\omega_1^0 \exp[j\nu \times (\tau - q_1 y)]$, i.e., coincides with a quasi-steady force. The singularities of streamline flow noted above are mentioned in [58, 60] (in which is considered a precise linearized solution for a cascade of plates in a velocity burst) as the limit case of a dense cascade.

2. For a typical reactive cascade: $\beta_1 = 0$, $\beta_2 = -70°$, , $\alpha_1 = 70°$. On the basis of (3.38) we find the inclination of the receding wave $\alpha_2 = 0$. We determine the intensity of the vortex-sheet attachments and the phase shift on the basis of (3.53) $\gamma_0 = 0{,}555\omega_{01}$, $\varepsilon = -99°$. The modulus of the distributed force acting upon the cascade axis is, according to (3.58), equal to $l_0 = 1{,}11\rho\omega_{01}\omega_{01}^0$.

3. For a typical active cascade: $\beta_1 = 65°$, $\beta_2 = -65°$, $\alpha_1 = 75°$. On the basis of (3.38) we find the inclination of the receding wave $\alpha_2 = -23°$. The intensity of the attached vortex sheet is, according to (3.53), equal to $\gamma_0 = 0{,}850\,\omega_{01}$; the phase shift is equal to $\varepsilon = -94°$. The modulus of the distributed force along the y-axis is found according to (3.58) as $l_0 = 0{,}85\rho\omega_{01}\omega_1^0$.

Let us make an estimate of the value of the forces acting upon the cascade in cases 2 and 3, at an equal absolute velocity of the main stream. Vorticity is formed when the flow velocity about perturbing bodies is c_1; and therefore, the perturbation velocity is proportional to the absolute velocity: $w_{01} = k_1 c_1$. The proportionality coefficient k_1 may be found from a calculation of the edge wake or experimentally. The relative velocity of the main stream can also be expressed in terms of the absolute velocity $\omega_1^0 \cos\beta_1 = c_1 \cos\alpha_1$. Then for cases 1 and 2 we find respectively, the following force values:

2) $l_0 = 0{,}380 k_1 \rho^0 c_1^2$.

3) $l_0 = 0{,}520 k_1 \rho^0 c_1^2$.

In estimating, it is logical to consider that the specific work of both stages is the same. In the active stage, thermal energy is transformed into kinetic energy in the directing cascade. In a typical reactive stage with congruent blades in a directing cascade, only half the available energy is used. Since the squares of the absolute velocities are related as correspoinding differences of gas enthalpies, the ratio of the perturbing forces for cases 2 and 3 will be equal to 0.365.

Let us consider flow about a cascade by a steady vortex stream. In steady flow the wave front coincides with the flow lines, and along each flow line the vorticity remains constant. Hence, on the basis of geometrical considerations, we obtain the equation of a vorticity wave incident on the cascade,

$$\omega_1(x, y) = \omega_{01} e^{j\nu_1(-x\sin\beta_1 + y\cos\beta_1)}. \tag{3.59}$$

Here $\nu_1 = 2\pi/l_1$, l_1 is the wavelength of the incoming vorticity. As previously, we shall be considering one harmonic.

After passage of the wave (3.59) through the cascade, the vorticity along the flow lines should remain constant. Consequently, the period of the wave along the y-axis should also be retained:

$$\nu_2 = \nu_1 \frac{\cos\beta_1}{\cos\beta_2}, \quad l_2 = l_1 \frac{\cos\beta_2}{\cos\beta_1}. \tag{3.60}$$

From (3.59) and (3.60) we obtain the equation of the vorticity wave behind the cascade in the form

$$\omega_2(x, y) = \omega_{01} \exp\left[j\nu_1 \frac{\cos\beta_1}{\cos\beta_2}(-x\sin\beta_2 + y\cos\beta_2)\right]. \tag{3.61}$$

To compute the velocities, use may be made of the conclusions presented above.

The velocity at infinity in front of the cascade will be found according to (3.43) by the replacement $p_1 = \sin\beta_1$ and $q_1 = -\cos\beta_1$, $\nu = \nu_1$ according to the formula

$$w_{1\infty} = \frac{2}{v_1}\omega_{21} e^{-i\beta_1} e^{jv_1(-x\sin\beta_1 + y\cos\beta_1)}. \qquad (3.62)$$

The velocity at infinity behind the cascade will be found in a like manner:

$$w_{2\infty} = \frac{2j\omega_{21}\cos\beta_2}{v_1\cos\beta_1}\exp(-i\beta_2)\exp\left[jv_1\frac{\cos\beta_1}{\cos\beta_2}(-x\sin\beta_2 + y\cos\beta_2)\right]. \qquad (3.63)$$

The perturbation velocity at the cascade axis, brought about by vorticity (3.59), is found by means of the same substitutions and the condition $q_1 < 0$ from (3.41):

$$w_1(0, y) = \frac{(j-i)\omega_{21}}{v_1} e^{i\beta_1} e^{jv_1 y\cos\beta_1}. \qquad (3.64)$$

For vorticity (3.61) the velocity at the cascade axis is found in a like manner with the aid of (3.42):

$$w_2(0, y) = \frac{(j+i)\omega_{21}\cos\beta_2}{v_1\cos\beta_1} e^{-i\beta_2} e^{jv_1 y\cos\beta_1}. \qquad (3.65)$$

In all formulas, the initial vorticity may be replaced according to (3.62) via the modulus of the perturbation velocity at infinity in front of the cascade $\omega_{01} = 2\omega_{21}w_1^0/v_1$. If the stream does not turn in the cascade ($\beta_1 = \beta_2$), then (3.63) naturally passes into (3.61), and the sum (3.64) and (3.65) is also equal to (3.62) when x = 0. When the non-uniform stream passes through the cascade, a supplementary attached vorticity γ_0 originates. The induced velocity to the right of the cascade will be found by means of (3.51):

$$w_3(0, y) = \gamma_0 e^{i\beta}(j-i) e^{jv_1 y\cos\beta_1}. \qquad (3.66)$$

The boundary conditions at the outlet of the cascade ($x \to +0$) require that the perturbation velocity be directed along the basic flow lines. Hence we obtain, by means of (3.64) - (3.66), by means of transformations, the formula for determination of the attached vorticity (the result is expressed in terms of the modulus of the perturbation velocity of the main stream)

$$\gamma_0 e^{i\varepsilon} = \frac{1}{2} w_{01} \left(\frac{\cos \beta_2}{\cos \beta_1} e^{i\beta_2} - e^{i\beta_1} \right). \qquad (3.67)$$

The formula may also be obtained by the limit transition $\alpha_1 \to \beta_1$, $\alpha_2 \to \beta_2$ from (3.57).

The supplementary distributed force is found according to Zhukovskiy's theorem

$$I(y) = -\frac{i}{2} \rho^0 \gamma_0 \left(w_1^0 e^{-i\beta_2} + w_2^0 e^{-i\beta_1} \right) e^{i(\omega y \cos \beta_1 + \varepsilon)}. \qquad (3.68)$$

It was assumed above that the vorticity propagates along the flow lines of the main stream. Actually, however, the flow lines will become distorted. This distortion may be obtained only in a second approximation, which will not be considered here.

Let us consider the oscillation of a cascade in a uniform main stream. Instead of Condition (3.56) we shall use the condition $v_+ = v_0(y)$, where $v_0(y)$ is the velocity modulus of the oscillations along the y-axis. Then, with account taken of (3.51) and (3.55), we obtain

$$\gamma_0 e^{i\varepsilon} \left[(1 + j \operatorname{tg} \beta_2) + \frac{\sin(\alpha_2 - \beta_1)}{\cos \beta_2} e^{-i\alpha_2} (j + \operatorname{tg} \beta_2) \right] = v_0. \qquad (3.69)$$

If the cascade oscillates as a single rigid system, the front of the trailing vorticity waves must be situated at an angle of $\alpha_2 = \pi/2$. Then we shall find from (3.69) that the attached vorticity depends only upon the oscillation velocity of the blades $\gamma_0 = v_0/2$. The trailing vorticity will be found according to (3.53):

$$\omega_3 = -i \frac{\gamma v_0}{2 w_2^0 \cos \beta_2} e^{i\omega x}. \qquad (3.70)$$

In spite of the fact that behind the cascade there is free vorticity, defined by Formula (3.70), the problem for the limit case of a dense cascade may be regarded as a quasi-static one. This is explained by the fact that the velocities induced by free vorticity are constant in the left-hand semiplane. This property is proved by

the limit transition in precise-solution formulas for a plate cascade [58, 60].

§ 3.7. Singularities of Three-dimensional Flow About a Cascade

Above we have considered only two-dimensional streams and, correspondingly, flow about two-dimensional cascades, i.e., the assumption was being made that the flow in any plane z = const. is the same. In practical cases this condition is, of course, not maintained, since the blades which comprise the cascade may have a variable profile, the oscillation amplitude is not constant along the z-axis, etc. Let us now consider a simple problem, in order to make clear the singularities of unsteady three-dimensional flow about cascades.

In the case of three-dimensional perturbation and with the condition that the coordinate system is motionless with respect to the fluid at infinity, the field of perturbed pressures must satisfy the wave equation

$$\frac{\partial^2 p}{\partial x^2}+\frac{\partial^2 p}{\partial y^2}+\frac{\partial^2 p}{\partial z^2}-\frac{1}{a_\infty^2}\frac{\partial^2 p}{\partial t^2}=\frac{\partial X}{\partial x}+\frac{\partial Y}{\partial y}+\frac{\partial Z}{\partial z}. \tag{3.71}$$

The derivation of this equation is completely analogous to the one presented above for the two-dimensional case.

Let us define the pressure field brought about in an incompressible fluid by a concentrated force. It was found out that for an incompressible fluid the field of perturbed pressures (and accelerations) does not depend upon the velocity of the main stream. It was also noted above that in this special case a solution may be obtained in the general form for an arbitrary law of change of the force in time.

Let us consider, for the sake of specificity, the action of a concentrated force, applied at the origin of the coordinates, which

is parallel to the y-axis and communicates to the fluid the instantaneous impulse:

$$Y = Y_0 \delta(x)\delta(y)\delta(z)\delta(\tau).$$

Integrating Equation (3.71) with the indicated right-hand part, we find that the perturbed pressure is described by a three-dimensional dipole with the axis parallel to the axis of action of the force

$$p = \frac{Y_0}{4\pi} y (x^2 + y^2 + z^2)^{-3/2} \delta(\tau). \tag{3.72}$$

The velocity potential is determined according to a formula which is analogous to the one derived for the two-dimensional case

$$\varphi(x, y, z, \tau) = -\frac{1}{\rho^0 U} \int_{-\infty}^{x} p\left(\xi, y, z, \tau - \frac{x-\xi}{U}\right) d\xi. \tag{3.73}$$

Here it is assumed that the main stream moves in the direction of the abscissa with a velocity of U.

Integrating (3.73) by means of (3.72), we find

$$\varphi = \frac{Y_0}{4\pi\rho^0} y [(x - U\tau)^2 + y^2 + z^2]^{-3/2} \sigma(\tau). \tag{3.74}$$

This velocity potential corresponds to a three-dimensional dipole with an axis parallel to the direction of the force. Consequently, the impulse force creates a vortex ring of infinitely small radius, which is carried away by the stream (Figure 3.11).

Since a force which changes arbitrarily in time can be replaced by successive pulses, solution of (3.72) and (3.74) makes it possible to present a three-dimensional pattern of unsteady streamline flow.

In an xyz system of coordinates, let us represent a three-dimensional cascade of blades, in a main stream flow in the direction of the x-axis (Figure 3.12). The oscillating blades act upon the fluid by means of forces distributed along their surface. Vortex rings,

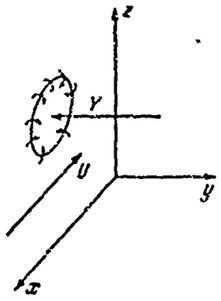


Figure 3.11. Formation of vortex ring in the plane xz of an impulse force parallel to the y-axis.

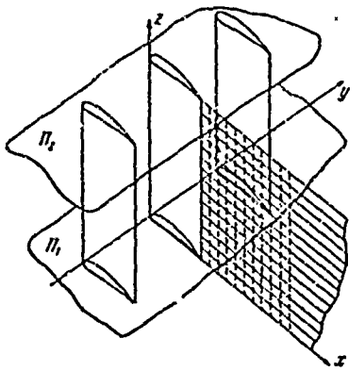


Figure 3.12. Diagram of flow about a three-dimensional cascade with the formation of vortex wakes.

forming a vortex layer, originate at the points of application of the forces on the boundary of the solid surface and the fluid. Since the forces change in time, the intensity of the vortex sheet covering each blade also changes. The three-dimensional velocity dipoles are carried away by the main stream and form a vortex sheet behind each blade. The value of the forces distributed along a blade depends, in the general case, upon the z coordinate, since each blade cross section has its own oscillation velocity. Consequently, the intensity of the trailing vortex sheet changes along the z coordinate.

Thus, the vortex sheet will consist of two vortex systems. The vortex axes of the first system are parallel to the z-axis. The appearance of these vortices is explained by the nonsteady nature of the flow about the given blade cross section. It is specifically these vortices which form the wake in the case of unsteady flow about a two-dimensional blade. The vortex axes of the second system are parallel to the x-axis. The appearance of these vortices is brought about by a change in circulation with respect to the blade span (along the z-axis). The latter vortex system can also originate in the case of steady streamline flow, if, for example, the blade profile changes with respect to height.

In the steady case, the indicated coordinate system does not change with respect to time, since the law of circulation changes with respect to span is steady.

With oscillations of the blade, the intensity of the vortices of the two systems changes periodically with a frequency equal to the frequency of the blade. If there is a gap at the free end of the blade, which oscillates at the first harmonic, the vortex sheet of the second system will be particularly intensive there. This is explained by the fact that here (over a relatively short sector) the modulus of velocity circulation will fall from the maximum value to zero. In general, an analogous pattern will also be observed in a cascade bounded by end walls, since in an actual case the lift force at the end of the blade should be equal to zero.

Thus, the three-dimensional effect is manifested in the appearance of a vortex system with axes parallel to the x-axis and, consequently, within the mutual influence of the cross sections. For investigation of the general governing rules, the cascade may be replaced by the discontinuity plane of tangential velocities, analogous to replacement of the two-dimensional cascade by a discontinuity line.

The perturbed pressure evoked by a concentrated force which depends harmonically upon time is found according to (3.72):

$$p = \frac{\gamma_0}{4\pi} y (x^2 + y^2 + z^2)^{-3/2} e^{i\nu t}. \qquad (3.75)$$

Let us now consider the influence of a force distributed along a straight line upon the flow. In view of the linearity of the problem, it is sufficient to study only the harmonic law of distribution in space, and subsequently, if necessary, to use Fourier series or Fourier integrals.

The perturbed-pressure field, evoked by a force parallel to the y-axis and distributed along the z-axis, is defined by the expression

$$p = -\frac{\gamma_0}{4\pi} y e^{i\nu t} \int_{-\infty}^{+\infty} e^{i \frac{2\pi\zeta}{l_1}} [x^2 + y^2 + (z-\zeta)^2]^{-3/2} d\zeta.$$

Here t_2 is the period of the distributed forces.

After integration and transformation we obtain

$$p = \frac{-\gamma\gamma_0}{t_2\sqrt{x^2+y^2}} e^{i\left(\omega t+\frac{2\pi z}{t_2}\right)} K_1\left(\frac{2\pi}{t_2}\sqrt{x^2+y^2}\right). \tag{3.76}$$

Here K_1 is a modified Bessel function.

This expression may be conveniently represented in terms of the zero-order function K_0 in the form

$$p = \frac{\gamma_0}{2\pi} e^{i\left(\omega t+\frac{2\pi z}{t_2}\right)} \frac{d}{dy} K_0\left(\frac{2\pi}{t_2}\sqrt{x^2+y^2}\right).$$

It can be shown that when $t_2 \to \infty$ the solution tends toward the known solution for the two-dimensional case.

Desiring to apply the problems under consideration to the theory of a cascade with a very small spacing, we obtain the field of perturbed pressures that has been evoked by forces distributed along a plane. For the sake of brevity, we shall call this plane a cascade.

Let the forces be distributed along the plane x = 0 and be parallel to the y-axis; let them have a period of t_1 along the y-axis and a period of t_2 along the z-axis.

The perturbed pressure is determined by means of (3.76) by the integral

$$p = \frac{\gamma_0}{2\pi} e^{i\left(\omega t+\frac{2\pi z}{t_2}\right)} \frac{d}{dy} \int_{-\infty}^{+\infty} e^{i\frac{2\pi\eta}{t_1}} K_0\left[\frac{2\pi}{t_2}\sqrt{x^2+(y-\eta)^2}\right] d\eta.$$

After calculations we obtain

$$p = \frac{i\gamma_0}{2\sqrt{1+(t_1/t_2)^2}} e^{i\left(\omega t-2\pi\frac{y}{t_1}+2\pi\frac{z}{t_2}\right)} e^{-2\pi|x|\frac{\sqrt{1+(t_1/t_2)^2}}{t_1}}.$$

The acceleration potential is determined in terms of the perturbed pressure by the formula

$$\varphi_*(x, y, z, \tau) = -\frac{p(x, y, z, \tau)}{\rho^0}.$$

Then the velocity potential in the semispace $x < 0$ is expressed by the integral

$$\varphi(x, y, z, \tau) = \frac{1}{U} e^{-j\frac{\nu x}{U}} \int_{-\infty}^{x} \varphi_*(\xi, y, z) e^{j\frac{\nu\xi}{U}} d\xi.$$

After computation we obtain the value of the velocity potential in the semispace in front of the cascade in the form

$$\varphi = \frac{jY_0 t_1}{4\pi\rho^0 U} \frac{\exp[j(\nu\tau + 2\pi y/t_1 + 2\pi z/t_2)] \exp\left[2\pi x \frac{\sqrt{1+(t_1/t_2)^2}}{t_1}\right]}{\sqrt{1+(t_1/t_2)^2}\,[jk+\sqrt{1+(t_1/t_2)^2}\,]}.$$

Differentiating with respect to y and assuming $x = 0$, we find the velocity component v when approaching the cascade from the left ($x \to -0$):

$$v(-0) = \frac{Y_0}{2\rho^0 U} \frac{\exp[j(\nu\tau + 2\pi y/t_1 + 2\pi z/t_2)]}{\sqrt{1+(t_1/t_2)^2}\,[jk+\sqrt{1+(t_1/t_2)^2}\,]}. \qquad (3.77)$$

Here the Strouhal number $k = \nu t_1/2\pi U$ has been introduced, the period t_1 being selected as the linear dimension.

The flow in front of the cascade (in the left-hand semispace $x < 0$) will be potential; the flow behind the cascade ($x > 0$) is of the vortex type. The plane $x = 0$, which replaces the cascade, is a discontinuity plane for velocities v, since forces parallel to the y-axis are acting in this plane. Only the velocity component which is in phase with the force should undergo a discontinuity. The value of the velocity-function discontinuity is determined by the momentum equation according to the formula

$$v(+0) - v(-0) = \frac{Y_0}{\rho^0 U} e^{j\left(\nu\tau + 2\pi\frac{y}{t_1} + 2\pi\frac{z}{t_2}\right)}. \qquad (3.78)$$

From Equation (3.77) and (3.78) we determine the velocity component v (+0), which is in phase with the force (to the right of the cascade)

$$v(+0)=-\frac{Y_0}{2\rho^0 U}\frac{1+2k^2+2(l_1/l_2)^2}{1+k^2+(l_1/l_2)^2}\ldots.$$

Here and henceforth, in order to abridge the notation, the factor

$$\exp[j(\nu\tau+2\pi y/l_1+2\pi z/l_2)]$$

is omitted.

The velocity component which has a phase shift with respect to the force by the angle $\pi/2$, is according to Formula (3.77) equal to

$$\frac{jkY_0}{2\rho^0 U}\cdot\frac{1}{[1+k^2+(l_1/l_2)^2]\cdot\sqrt{1+(l_1/l_2)^2}}$$

and does not undergo a discontinuity when passing through the plane $x = 0$. Consequently, the velocity at the right of the cascade is equal to

$$v(+0)=-\frac{Y_0}{2\rho^0 U}\frac{1+2k^2+2(l_1/l_2)^2\sqrt{1+(l_1/l_2)^2}+jk}{\sqrt{1+(l_1/l_2)^2}[1+k^2+(l_1/l_2)^2]}\ldots. \qquad (3.79)$$

Let us apply the obtained result to an evaluation of the influence of the finite length of the blades. We shall consider flow about a three-dimensional aerodynamic cascade (Figure 3.11) without offset, consisting of blades of finite length l, bounded on the ends by the planes Π_1, Π_2. The blades are considered to be fastened at the point of their intersection of plane Π_1. The other ends of the blades may be either fastened or free, depending upon the conditions of the problem. We introduce a series of restriction; these will simplify the problem. Let the cascade have very great density, so that the blade spacing t is much smaller than the chord of the plates $t \ll b$. The cascade is in a flow main stream of incompressible ideal fluid at velocity U which is parallel to the chords. The profiles may in the general case oscillate with the phase shift α, constant from profile to profile. The flow pattern will be repeated along the y-axis at intervals of a period equal to $l_1=2\pi l/\alpha$. We shall assume the phase shift to be so small that $\alpha \ll 2\pi$ (or, what is the same, $l_1 \gg l$). We

assume that the profile oscillations are harmonic, and that the oscillation amplitude is small. We shall consider the law of velocity change along the height of the plates to be given and arbitrary. In order to make planes Π_1 and Π_2 flow planes, we extend the blades to $\pm\infty$ along the z-axis, and shall consider the flow pattern also to be periodic along the z-axis with a period of $t_2 = 2l$.

With such a formulation of the problem, the action of the cascade upon the flow may be approximately replaced by the action of a system of forces situated in the plane $x = 0$ and parallel to the y-axis. Free vortices occupy the entire semispace $x > 0$ and are carried away by the stream with a velocity of U. Two causes which bring about the appearance of free vortices are acting in the three-dimensional case. In the first place, free vortices appear in accordance with the Helmholtz theorem due to the variability of circulation of the velocity along the blade span (along the z-axis). Second, free vortices originate in accordance with Thompson's theorem when the blade circulation changes in time. The first case brings about the vorticity ω_x (the vortex axes are parallel to the x axis); the second cause brings about veoticity ω_z (the vortex axes are parallel to the z-axis).

Let us define the distribution law of the oscillation velocity of the plates in the cascade as the Fourier series

$$v_0(z) = \sum_{n=0}^{\infty} A_n e^{i\pi n \frac{z}{l}}. \tag{3.80}$$

Consequently, the coefficients A_n are henceforth considered to be known.

For each harmonic of velocity (3.80), it is possible by means of (3.79) to find the force corresponding to it

$$Y_{0n} = 2\rho U A_n \frac{\sqrt{1+(\pi n/2l)^2}\,[1+k^2+(\pi n/2l)^2]}{1+2k^2+2(\pi n/2l)^2\sqrt{1+(\pi n/2l)^2}+ik}. \tag{3.81}$$

The law of distribution of forces along the span of the plates may be expressed by a Fourier series with the obtained coefficients

$$\gamma_0(z) = \sum_{n=0}^{\infty} \gamma_{cn} e^{i2n\frac{z}{t}}. \qquad (3.82)$$

In the special case of a two-dimensional paroblem $A_0 = v_0$, $A_n = 0$ when $n > 1$. In the two-dimensional problem $t_1 n/2l \to 0$ and Formula (3.81) charges into the formula

$$\gamma_0 = 2\rho^0 v_0 U \frac{1+k^2}{1+2k^2+jk}$$

Then the coefficient of the forces is equal to

$$c_y = \frac{2(1+k^2)}{1+2k^2+jk},$$

which coincides with Formula (3.34).

An obtained solution of the problem of flow about a dense three-dimensional cascade is considered in [60].

The problem in a linearized presentation for a cascade of plates has been studied by V. N. Gorelov [17].

FOOTNOTES

1. on page 76. If the points of application of the forces are situated along one straight line with a definite spacing. Such a system will, for the sake of abbreviation, be called a force cascade.

PART II

UNSTEADY FLOW ABOUT CASCADES

Chapter 4

A TWO-DIMENSIONAL CASCADE OF THIN SLIGHTLY BENT PROFILES IN AN UNSTEADY STREAM OF INCOMPRESSIBLE FLUID

§ 4.1. Preliminary Remarks

The problem of a two-dimensional cascade with thin slightly bent profiles in an unsteady stream of ideal incompressible fluid has been dealt with in a large number of studies [5, 6, 12, 16, 35, 48, 58, 59, 85, 121, 130, 131, 137, 140, 145, 150], etc. The problem under consideration is reduced to a solution of the Laplace equation in a cascade region formed on the plane by an infinite system of thin rectilinear sections. The methods employed by the authors have made use of the velocity potential, the acceleration potential, the vortex pattern, etc.

For a cascade without offset and with oscillation of the profiles without a phase shift, the solution may be obtained in closed form. The problem of the incidence of vorticity waves upon a cascade without offset has also been solved. It is assumed that the vorticity is low, and that the wave front is parallel to the cascade axis.

Such solutions have the advantage that they permit limit cases to be studied: cascades which have very large and very small density, a very large Strouhal number and a very small one. Such solutions should also be used for estimating the accuracy of various numerical methods. It is expedient to solve the general problem for a cascade with offset and small oscillation of the profiles with an arbitrary constant phase shift, as well as the problem of the incidence of arbitrarily oriented vorticity waves upon the cascade.

In this case, with a view to the utilization of computers, it is preferable to reduce the problem to an integral equation in which the unknown function may be the perturbation velocity or distributed vorticity.

Methods also exist, which are based upon utilization of the known solution for a single wing and successive allowance for the interference of profiles in the cascade.

§ 4.2. Use of the Acceleration Potential Method

Let us consider a cascade of thin slightly bent profiles situated in the complex variable plane $\zeta=\xi+i\eta$ (Figure 4.1). The cascade axis is inclined at an angle of γb to the ordinate. We shall designate the profile spacing by t, and we shall assume the profile chord equal to $2b = 2$.

Let us consider the problem of flow about the cascade by a stream of ideal incompressible fluid, incident at a small angle of attack, with a basic velocity U parallel to the abscissa. In the general case, the incident stream can have vorticity. The cascade profiles can oscillate arbitrarily or can be deformed with small amplitudes. In view of the fact that the perturbations introduced by the cascade are small, and the profiles are thin and slightly bent, we shall replace the profile cascade with a plate cascade. Thus, the problem is considered in a linearized formulation.

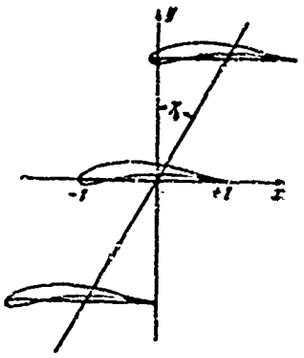


Figure 4.1. A cascade of thin slightly bent profiles, replaced by sections.

If the velocity potential or the acceleration potential are introduced as the desired function, they must satisfy the Laplace equation. This makes it possible to apply conformal transformation and to map the oblique cascade onto the cascade without offset ($\gamma_b = 0$), located in the plane $z = x + iy$.

The indicated transformation is yielded by the Formula [74]

$$\zeta = z\cos\gamma_b - \frac{it\sin\gamma_b}{\pi}\operatorname{arch}\frac{\operatorname{ch}(\pi z/t)}{\operatorname{ch}(\pi/t)}.$$

A sectional cascade in plane z without offset will correspond to the section cascade in plane ζ. Expressing the inverse hyperbolic function in terms of a logarithm, the preceding relationship can be represented in the following form:

$$\zeta = z\cos\gamma_b - \frac{t\sin\gamma_b}{q}\ln\frac{\operatorname{ch}qz + \sqrt{\operatorname{ch}^2 qz - \operatorname{ch}^2 q}}{\operatorname{ch} q}.$$

here the designation $q = \pi/t$ is introduced. We shall call the dimensionless parameter $\bar{q} = b/t = \pi/t$ the cascade density.

Henceforth, we shall be considering only a straight cascade, without dwelling on the computational difficulties which will arise in the calculation of an oblique cascade.

We introduce the complex acceleration potential in terms of which the acceleration field can be expressed,

$$w(z) = \varphi + i\psi, \quad a = a_x - ia_y = \frac{dw}{dz}.$$

The real part of the acceleration potential is proportional to the pressure perturbation:

$$\varphi = -\frac{p}{\rho^2}.$$

We find the boundary condition on the faired profiles. The coordinates of profiles that are vibrating and are being deformed may be given by the function

$$F(x, y, \tau) = y - f(x, \tau), \quad (-1 \leqslant x \leqslant 1).$$

Since at any moment of time the point belongs to the contour, it is obvious that

$$F(x+dx, y+dy, \tau+d\tau) = 0.$$

Expanding the obtained expression into a series and restricting ourselves to the first terms, we obtain

$$\frac{\partial F}{\partial x}dx + \frac{\partial F}{\partial y}dy + \frac{\partial F}{\partial \tau}d\tau = 0.$$

Dividing by $d\tau$ and introducing the projections of the velocity of a particle of fluid $dx/d\tau = v_x$, $dy/d\tau = v_y$, we find the boundary condition for velocity:

$$\frac{\partial F}{\partial x}v_x + \frac{\partial F}{\partial y}v_y + \frac{\partial F}{\partial \tau} = 0.$$

Noting that

$$\frac{\partial F}{\partial x} = -\frac{\partial f}{\partial x}, \quad \frac{\partial F}{\partial y} = 1, \quad \frac{\partial F}{\partial \tau} = -\frac{\partial f}{\partial \tau},$$
$$v_x = U + u, \quad v_y = v,$$

and discarding terms of the second order of smallness, we write the boundary condition for velocity in another form:

$$v = \frac{\partial f}{\partial \tau} + U\frac{\partial f}{\partial x}. \tag{4.1}$$

In using the acceleration potential, it is necessary to obtain also the boundary conditions of the acceleration of fluid particles

on the surface of the faired blades. Utilizing the linearized Euler equation and the preceding condition, we obtain the boundary condition for acceleration:

$$a_y = \frac{\partial v}{\partial t} + U\frac{\partial v}{\partial x} = \frac{\partial^2 f}{\partial t^2} + 2\dot{U}\frac{\partial^2 f}{\partial x \partial t} + U\frac{\partial^2 f}{\partial x^2}. \qquad (4...)$$

In view of the fact that the profiles are thin and slightly bent, and that the amplitude of their oscillations and the angle of attack are small, the boundary conditions on the contour may be transferred to the upper and lower boundaries of the sections, which coincide with the chords of the profiles.

The solution of the problem consists in determining the unsteady velocity, oscillation, pressure, and vorticity fields, and in computing the forces and moments acting upon the profiles in the cascade. In view of the linearity of the problem the velocity field v, the acceleration field a, the pressure field p, and the vorticity field ω for the general case of fluid motion may be regarded as the sum of the corresponding like fields brought around by various causes.

We shall consider the following fields [58].

1. The main stream field. The stream moves with a velocity of U and carries away the given system of free vortices. The velocity field induced by the vortices may be restored in the conventional manner; the perturbations are naturally assumed to be small. Pressure in the fluid will be constant.

2. The velocity, acceleration, and pressure perturbation fields brought about by flow about a cascade of profiles with a given thickness and curvature at a velocity U with an average angle of attack.

3. The perturbation fields v, a, p and ω brought about by unsteady flow around a cascade of plates with profiles of zero thickness and curvature. The perturbation fields are brought about: (a) by velocity pulsations of the main stream, (b) by vibration and

deformation of the profiles, and (c) by the presence of a vortex sheet which trails from the profiles in the case of unsteady streamline flow.

Calculation of the fields noted in points 1 and 2 pertains to problems of steady streamline flow. These problems can be solved by any of the known methods of aerodynamic cascade theory and are not considered here.

Let us note the properties which the desired function — the acceleration potential which describes an unsteady flow — must have. As the distance upstream from the cascade increases, the real part of the acceleration potential must tend toward zero, since the flow must be unperturbed. From the condition that when $x \to -\infty$ the pressure perturbation must vanish $p \to 0$, it follows that $\varphi \to 0$.

The acceleration potential must be a periodic function with a period equal to the cascade spacing; it stands to reason that this pertains to the case where all the profiles oscillate synchronously, in phase, and with the same amplitude.

The acceleration potential must satisfy the Zhukovskiy-Chaplygin postulate, i.e., it must satisfy specific conditions at the exit edge of the profiles. In the case of steady streamline flow in the use of a model of ideal fluid, on both sides of the sharp exit edge it is necessary to equalize the velocities of the trailing stream or the pressures, which is the same on the basis of the Bernoulii equation. In the case of unsteady, streamline flow, the requirement concerning the equalization of pressures remains; however, the stream velocities on the two sides of the edge will, generally speaking, not be equal. This is explained by the fact that as the circulation changes in time, a vortex wake which is the discontinuity line of the velocity field will, in accordance with Thomson's theorem, trail from the profile. Since the acceleration potential is proportional to the perturbed pressure, it is obvious that the Chaplygin-Zhukovskiy condition will be satisfied at the trailing edge if the velocity potential undergoes

no discontinuity there. Since the constant term in the acceleration-potential function is insignificant, it may be considered that at the trailing edge $\varphi=0$. The perturbed-pressure field (and, consequently, the acceleration potential as well) must be continuous everywhere, with the exception of the infinitely sharp leading edges of the plates. Singular points are situated on sharp leading edges similarly to the manner in which this takes place in the theory of steady flow about a thin profile.

Thus, we consider the plate cascade and find the integral representation of the velocity potential [59]. Since the complex acceleration potential is represented by an analytic function, it can be represented, up to an insignificant constant, by a Cauchy integral, written for a cascade region

$$w(z)=\frac{q}{2\pi i}\int_L w(\zeta)\operatorname{cth}[q(z-\zeta)]\,d\zeta. \tag{4.3}$$

Here $w(\zeta)$ is the boundary value of complex acceleration. Integration is carried out along an arbitrary contour which encloses one of the profiles of the cascade, but which does not intercept the other profiles. Expression (4.3) may also be represented in the form of a function series [56].

For this we shall expand $\operatorname{cth}(z-\zeta)$ in the vicinity of point $\zeta=0$ according to powers of ζ:

$$\operatorname{cth}[q(z-\zeta)]=\sum_{n=0}^{\infty}\frac{1}{n!}\left[\frac{d^n}{d\zeta^n}\operatorname{cth}q(z-\zeta)\right]_{\zeta=0}\zeta^n=$$

$$=-\sum_{n=0}^{\infty}\frac{(-1)^n}{n!}\left(\frac{d^n}{dz^n}\operatorname{cth}qz\right)\zeta^n.$$

This series converges absolutely and uniformly in the entire region of determinacy of w(z). Substituting the series into Integral (4.3), we obtain

$$\int_L w(\zeta)\operatorname{cth}[q(z-\zeta)]\,d\zeta=\int_L w(\zeta)\sum_{n=0}^{\infty}\frac{(-1)^n}{n!}\left(\frac{d^n}{dz^n}\operatorname{cth}qz\right)\zeta^n\,d\zeta=$$

$$=2\pi i\sum_{n=0}^{\infty}\frac{(-1)^n}{n!}c_{-(n+1)}\frac{d^n}{dz^n}\operatorname{cth}qz.$$

Here the coefficients of the expansion may be expressed by means of residues according to the formula

$$c_{-n} = \frac{1}{2\pi i} \oint_L w(\zeta) \zeta^{n-1} d\zeta.$$

We shall finally obtain the expression of the complex acceleration potential in the form

$$w(z) = q \sum_{n=0}^{\infty} \frac{(-1)^n}{n!} c_{-(n+1)} \frac{d^n}{dz^n} \operatorname{cth} qz.$$

On the profiles, only the normal acceleration component a_y is known. Therefore, in order to obtain an effective solution it is necessary to express the acceleration potential in terms of a_y. In order to obtain the solution in closed form we shall use the method of isolation of singularities [74].

Let us consider the function [68]

$$a(z, \tau) \sqrt{\operatorname{sh}^2 qz - \operatorname{sh}^2 q}.$$

Here τ is time, which is a real parameter and does not depend upon the complex coordinate z. The introduced function will be periodic, with a period equal to the cascade spacing. At an infinite distance from the cascade the function under consideration tends toward zero, since on the basis of (4.3) we obtain for a the following asymptotic representation:

$$a_{z \to \infty} = \frac{dw}{dz}_{z \to \infty} \sim qc_1 \frac{d}{dz} \operatorname{cth} qz \sim -\frac{q^2 c_1}{\operatorname{sh}^2 qz}.$$

From this we have

$$(a \sqrt{\operatorname{sh}^2 qz - \operatorname{sh}^2 q})_{z \to \infty} \sim -\frac{q^2 c_1}{\operatorname{sh} qz}.$$

Let us note one more property of the function under consideration that is important for what follows. The radical $\sqrt{\operatorname{sh}^2 qz - \operatorname{sh}^2 q}$ assumes, at the upper and lower boundaries of the sections, values that are

purely imaginary and opposite in sign. At the sections, complex acceleration has the symmetry property

$$a_x(x,\ y+0) = -a_x(x,\ y-0).\quad a_y(x,\ y+0) = a_y(x,\ y-0).$$

Consequently, the real part of the function under concideration $a_y\sqrt{\operatorname{sh}^2 q - \operatorname{sh}^2 qx}$ assumes, at the corresponding points of the two boundaries, values which are equal in magnitude and opposite in sign. On the other hand, the imaginary part of function $a_x\sqrt{\operatorname{sh}^2 q - \operatorname{sh}^2 qx}$ has identical values at the corresponding points of the section. Then, using the Cauchy integral to express the function under consideration in a cascade region, selecting the section contour as the path of integration, and utilizating the conditions of symmetry, we obtain an integral representation of complex acceleration in terms of the known boundary values of normal acceleration:

$$a(z,\ \tau) = \frac{q}{i\pi\sqrt{\operatorname{sh}^2 qz - \operatorname{sh}^2 q}} \int_{-1}^{+1} a_y(\xi,\ \tau)\sqrt{\operatorname{sh}^2 q - \operatorname{sh}^2 q\xi}\operatorname{cth}[q(\xi - z)]\,d\xi.$$

The obtained expression does not yet completely solve the problem, since at the profiles it is necessary to satisfy the boundary conditions not only for acceleration, but also for velocity.

The acceleration field constructed on the basis of the boundary value of acceleration at the profiles is not the only possibl one. The function of a complex valuable may be added to the solution. The imaginary part of this function is equal to zero at the plates. In the construction of this function it is necessary to take into account the conditions imposed upon the acceleration field or upon the complex acceleration potential: (a) the function must have a period equal to the cascade spacing, (b) at an infinite distance in front of the cascade the real part of the complex acceleration potential must tend towards zero, (c) at the trailing edges of the plates the real part of the complex potential must equal zero, (d) the real part of the acceleration potential must be restricted everywhere except at the singular points, which may be located at the entering edges of the blades.

The supplementary complex acceleration potential and complex acceleration, which satisfy the imposed conditions, are determined by the formulas

$$w_1(z) = iB\sqrt{\frac{\operatorname{sh}[q(z-1)]}{\operatorname{sh}[q(z+1)]}},$$

$$a_1(z) = \frac{iqB\operatorname{sh}2q}{2\operatorname{sh}[q(z+1)]\sqrt{\operatorname{sh}[q(z-1)]\operatorname{sh}[q(z+1)]}}.$$

Here B is a real constant.

Thus, finally the complex acceleration field about the cascade is determined by the following expression [58]:

$$a(z,\tau) = \frac{q}{i\pi\sqrt{\operatorname{sh}^2 qz - \operatorname{sh}^2 q}}\int_{-1}^{+1} a_y(\xi,\tau)\sqrt{\operatorname{sh}^2 q - \operatorname{sh}^2 q\xi}\operatorname{cth}[q(\xi-z)]\,d\xi + \frac{iqB(\tau)\operatorname{sh}^2 q}{2\operatorname{sh}[q(z+1)]\sqrt{\operatorname{sh}[q(z-1)]\operatorname{sh}[q(z+1)]}}. \quad (4.4)$$

The complex acceleration potential is found by integrating (4.4) along an arbitrary curve from point z = +1, where the real part of w(z) may be assumed equal to zero, and the insignificant imaginary constant may be discarded:

$$w(z,\tau) = \frac{q}{\pi i}\int_{+1}^{z}\frac{dz}{\sqrt{\operatorname{sh}^2 qz - \operatorname{sh}^2 q}}\int_{-1}^{+1} a_y(\xi,\tau)\sqrt{\operatorname{sh}^2 q - \operatorname{sh}^2 q\xi}\times \operatorname{cth}[q(\xi-z)]\,d\xi + iB(\tau)\sqrt{\frac{\operatorname{sh}[q(z-1)]}{\operatorname{sh}[q(z+1)]}}. \quad (4.5)$$

The second term of this formula does not change the value of normal acceleration on the plates. Consequently, the constant with respect to the coordinates $B(\tau)$ may be determined from the boundary value of the velocity on the plates.

Let us consider a special case of (4.5) for a single profile. When q = 0, (4.5) passes into the following formula:

$$w(z,\tau) = \frac{1}{\pi i}\int_{1}^{z}\frac{dz}{\sqrt{z^2-1}}\int_{-1}^{+1}\frac{a_y(\xi,\tau)\sqrt{1-\xi^2}}{\xi-z}\,d\xi + iB(\tau)\sqrt{\frac{z-1}{z+1}}.$$

In view of the fact that only one integral is singular, the order of integration may be changed:

$$w(z,\tau)=\frac{1}{\pi i}\int_{-1}^{+1}a_y(\xi,\tau)\sqrt{1-\xi^2}\,d\xi\int_{1}^{\infty}\frac{dz}{\sqrt{z^2-1}(\xi-z)}+iB(z)\sqrt{\frac{z-1}{z+1}}.$$

Designating the first integral by I and substituting in it the variables $\xi - z = x$, we reduce it to the form

$$I=-\int_{\xi-1}^{\xi-z}\frac{dx}{x\sqrt{(\xi^2-1)-2\xi x+x^2}}=$$

$$=-\frac{\pi}{2}\frac{1}{\sqrt{1-\xi^2}}+\frac{1}{\sqrt{1-\xi^2}}\arcsin\frac{\xi z-1}{\xi-z}.$$

Then the acceleration potential of a single wing may be expressed in terms of the known boundary condition of normal acceleration on the profile:

$$w(z,\tau)=\frac{1}{\pi i}\int_{-1}^{+1}a_y(\xi,\tau)\arcsin\frac{\xi z-1}{\xi-z}\,d\xi+iB(\tau)\sqrt{\frac{z-1}{z+1}}.$$

Here the term

$$-\frac{1}{2i}\int_{-1}^{+1}a_y(\xi,\tau)\,d\xi,$$

had been discarded, since it is an imaginary constant and, consequently, does not affect the law of distribution of the perturbed pressure. In the special case of acceleration that is constant with respect to the profile, the computations are easily carried out until an algebraic formula is obtained. Effecting in the last integral the change of variables $(\xi z-1)/(\xi-z)=x$, we obtain when $a_y = a_y(\tau)$ the complex acceleration potential in the form of

$$w(z,\tau)=\frac{1}{\pi i}(1-z^2)a_y(\tau)\int_{-1}^{+1}\frac{\arcsin x\,dx}{(z-x)^2}+iB(\tau)\sqrt{\frac{z-1}{z+1}}.$$

Integrating, we finally find that with progressive oscillations of the wing, the acceleration potential is expressed by the formula

$$w=ia_y(\tau)\left(\sqrt{z^2-1}+z\right)+iB(\tau)\sqrt{\frac{z-1}{z+1}}.$$

Returning to the general case of (4.5), we derive the formula for determining the constant B. The connection between the velocity and the acceleration of the fluid particles is established by the linearized Euler equation

$$a_y = \frac{\partial v}{\partial \tau} + U \frac{\partial v}{\partial x}. \tag{4.6}$$

We shall henceforth consider only harmonic oscillations of the blade and shall express the velocities and accelerations in an explicit manner in terms of time

$$a_y(z, \tau) = a'_y(z)\, e^{j\nu\tau}, \quad v(z, \tau) = v'(z)\, e^{j\nu\tau}. \tag{4.7}$$

Here ν is the circular frequency of the oscillation process, j is an imaginary unit pertaining only to description of the time processes and which does not interact with the imaginary unit i, which has been introduced for designation of the complex coordinate. τ is time.

From (4.6) and (4.7) we obtain (the primes have been discarded)

$$a_y = j\nu v + U \frac{\partial v}{\partial x}. \tag{4.8}$$

Integrating this linear equation all the way through under the condition that far in front of the cascade the stream is not perturbed (v = 0), and that the oscillation velocity on the profiles in the cascade is known, we obtain

$$v(x, y) = \frac{1}{U} e^{-j\nu\frac{x}{U}} \int_{-\infty}^{x} a_y(\xi, y) e^{j\nu\frac{\xi}{U}} d\xi.$$

In a case where the point x, y is situated on the profile, the normal velocity of a fluid particle must be equal to the normal velocity of the contour.

We introduce a dimensionless criterion which characterizes the unsteadiness of the process — the Strouhal number $k = \nu b/U$. Here

the semichord b of the profile is selected as the linear dimension. Recollect that in the computations above, 2b = 2 was assumed and, consequently, k = ν/U. Then we obtain the basic formula for determining the constant B in the following form:

$$v(x, y) \approx \frac{1}{U} e^{-ikx} \int_{-\infty}^{x} \gamma_y(\xi, y) e^{ik\xi} d\xi. \tag{4.9}$$

The representation of the complex acceleration field and the acceleration potential by Formulas (4.4) and (4.5) has the advantage of integral formulas. However, in some cases it is convenient, from the computational point of view, to represent the solution in the form of a series.

Let us consider the function of the complex variable z and the real parameter q, which is known in cascade theory [59]:

$$F(z, q) = \frac{1}{q} \ln\left[\frac{(\operatorname{ch} qz + \sqrt{\operatorname{ch}^2 qz - \operatorname{ch}^2 q})}{\operatorname{ch} q}\right]. \tag{4.10}$$

After elementary transformations, this function may be given the following form:

$$F(z, q) = \frac{1}{q} \operatorname{arch} \frac{\operatorname{ch} qz}{\operatorname{ch} q}, \quad q = \frac{\pi}{\tau}. \tag{4.11}$$

Function F(z, q) possesses the following properties:

(1) Function F(z, q) is periodic with a purely imaginary period equal to $i\tau/q = it$;

(2) When $|x| \to \infty$ function $F(z, q) \to z - q^{-1} \ln \operatorname{ch} q \mp \ldots$;

(3) In the limit case when $\tau \to 0 (t \to \infty)$ function $F(z, 0) \to \sqrt{z^2 - 1}$;

(4) At the segment $y = 0, -1 < x < 1$ function F(z, q) assumes purely imaginary values.

The latter property is obvious, since from (4.10) when $|x| < 1$ and $y = 0$ we obtain

$$\left|\frac{(\operatorname{ch} qx + i\sqrt{\operatorname{ch}^2 q - \operatorname{ch}^2 qx})}{\operatorname{ch} q}\right| = 1,$$

from which follows the consequence that at the indicated segment the function is expressed by the formula

$$F(x, q) = \frac{i}{q} \operatorname{arctg} \frac{\sqrt{\operatorname{ch}^2 q - \operatorname{ch}^2 qx}}{\operatorname{ch} qx}, \tag{4.12}$$

or also by the formula which follows from the known relationship between inverse trigonometric functions

$$F(x,q) = \frac{i}{q} \arccos \frac{\operatorname{ch} qx}{\operatorname{ch} q}.$$

On this segment the function may be expanded into the series

$$F(x, q) = i \sum_{n=1}^{\infty} a_n (1 - x^2)^{n/2}. \tag{4.13}$$

Next we introduce a second function of the complex variable z and the real parameter q:

$$P(z, q) = \ln \left| \frac{(\operatorname{sh} qz + \sqrt{\operatorname{sh}^2 qz - \operatorname{sh}^2 q})}{\operatorname{sh} q} \right|. \tag{4.14}$$

Making use of the connection between logarithmic and inverse hyperbolic functions, we obtain

$$P(z, q) = \operatorname{arch} \frac{\operatorname{sh} qz}{\operatorname{sh} q}.$$

This function possesses the following properties:

(1) Function P(z, q) is periodic with a purely imaginary period, equal to $i\pi/q = it$;

(2) In the limit case when $q \to 0$ $(t \to \infty)$ function

$$P(x, q) \to \ln(z + \sqrt{z^2 - 1});$$

(3) On the segment $y=0$, $-1<x<+1$ function P(z, q) assumes purely imaginary values

$$P(x, q) = i \operatorname{arctg} \frac{\sqrt{\operatorname{sh}^2 q - \operatorname{sh}^2 qx}}{\operatorname{sh} qx} = i \arccos \frac{\operatorname{sh} qx}{\operatorname{sh} q}.$$

The properties of the introduced functions have been selected in such a manner that the acceleration potential for the cascade could be expressed in terms of them.

Let the profiles of a straight cascade oscillate synchronously and cophasally in the direction perpendicular to the chords, i.e., in the direction parallel to the ordinate. In this case the acceleration component a_y will be constant along the chord of the profile or, what is the same, the imaginary part of the complex potential must be a linear function of x. There it is obvious that the acceleration potential for the cascade may be expressed in terms of the function F(z, q),

$$w(z, \tau) = iA(\tau)[F(z, q) - z].$$

Assuming $A(\tau)$ to be a real constant with respect to the ordinate and taking into account that at plates $y = ik_1 l$, $-1 < x < 1$, $k_1 = 0, \pm 1, \pm 2, \ldots$ function F(z, q) assumes purely imaginary values, we find that the real part of F(z, q) is a linear function of x. The remaining requirements for the acceleration potential are also satisfied. Function $w(z, \tau) = w(z + il, \tau)$, i.e., has a period equal to the cascade spacing. At an infinite distance in front of the cascade the perturbations vanish $\lim_{x \to -\infty} \operatorname{Re} w(z, \tau) \to 0$. However, the obtained expression is a partial solution. To obtain the general solution, it is necessary to add to it the function of a complex variable. The imaginary part of this function has a constant value on the paired profiles. Obviously, the addition of such a function will not change the boundary values of normal accelerations.

The function which represents the second partial solution may be expressed in terms of the derivatives of functions F(z, q) and P(z, q):

$$w(z, \tau) = iB_1 F'(z, q) + iB_2 P'(z, q) = -iB_1 \frac{\operatorname{sh} qz}{\sqrt{\operatorname{sh}^2 qz - \operatorname{sh}^2 q}} + iB_2 \frac{q \operatorname{ch} qz}{\sqrt{\operatorname{sh}^2 qz - \operatorname{sh}^2 q}}. \quad (4.15)$$

Here B_1, B_2 are real constants with respect to the coordinates.

Function (4.15) possesses the properties necessary for representing the acceleration potential: (a) The imaginary part of the function is equal to zero on the plates which comprise the cascades; (b) at an infinite distance in front of the cascade $(x \to -\infty)$ the real part of (4.15) tends toward zero. The relationship among the constants must be so selected as to satisfy the Chaplygin-Zhukovskiy condition at the trailing edges $(x=+1,\ y=ik_1l,\ k_1=0,\ \pm 1, \ldots)$.

Assuming $\frac{B_1}{B_2} = -\frac{q \operatorname{ch} q}{\operatorname{sh} q}$ or $B_1 = B \operatorname{ch} q,\ B_2 = -\frac{B \operatorname{sh} q}{q}$, where B is the new real constant, we provide for continuity of the function at the trailing edges:

$$w(x, \tau) = iB \frac{\operatorname{ch} q \operatorname{sh} qx - \operatorname{sh} q \operatorname{ch} qx}{\sqrt{\operatorname{sh}^2 qx - \operatorname{sh}^2 q}} = iB \sqrt{\frac{\operatorname{sh}[q(x-1)]}{\operatorname{sh}[q(x+1)]}}.$$

Then the final expression for the acceleration potential will be written in the following manner:

$$w(x, \tau) = iA(\tau)\left[\frac{1}{q} \ln \frac{\operatorname{ch}(qx) + \sqrt{\operatorname{ch}^2 qx - \operatorname{ch}^2 q}}{\operatorname{ch} q} - x\right] + iB(\tau) \sqrt{\frac{\operatorname{sh}[q(x-1)]}{\operatorname{sh}[q(x+1)]}}. \tag{4.16}$$

This formula yields the solution of the problem. The time function $A(\tau)$ is determined on the basis of the boundary value of the acceleration, while $B(\tau)$ is determined on the basis of the boundary value of the velocity. Determination of these functions will be carried out later, and at present we shall indicate a possible generalization for the case of a different law of plate motion in the cascade.

Let us consider the series

$$w(x, \tau) = i \sum_{n=1}^{\infty} A_n [F(x, q) - x]^n + iB(\tau) \sqrt{\frac{\operatorname{sh}[q(x-1)]}{\operatorname{sh}[q(x+1)]}}. \tag{4.17}$$

Here the real coefficients may be determined on the basis of the boundary value of the normal accelerations at the plates. Thus, employment of the series makes it possible to solve the problem not only for translational laws of motion of plates in the cascade, but

for others as well. Let us consider the behavior of functions F(z, q) and P(z, q) when z changes to the extent of half the period $i\pi/2q=il/2$.

From known formulas it follows that

$$ch(z+i\pi/2q)=i\,sh\,qz,\ sh[q(z+i\pi/2q)]=i\,ch\,qz.$$

Then by means of (4.10) we obtain

$$F(z+i\pi/2q)=\frac{1}{q}\ln\frac{sh\,qz+\sqrt{sh^2qz+ch^2q}}{ch\,q}+\frac{i\pi}{2q}, \qquad (4.18)$$

or

$$F(z+i\pi/2q)=\frac{1}{q}\,arsh\frac{sh(qz)}{ch\,q}+\frac{i\pi}{2q}.$$

At the segment $y=0,\ -1<x<1$ the real part of the function is expanded into the series

$$Re\,F(x+i\pi/2q)=\sum_{n=1}^{\infty}b_nx^n,\quad n=1,\ 3,\ 5,\ \ldots$$

Omitting the calculations, we reduce the first terms of the series:

$$Re\,F(x+i\pi/2q)=\frac{1}{ch\,q}\left[x+\frac{q^2}{3!}(th^2q)\,x^3+\frac{q^4}{5!}\left(1-\frac{9}{ch^2q}\right)x^5+\ldots\right].$$

Analogously for function P(z) we obtain

$$P(z+i\pi/2q)=\ln\frac{ch\,qz+\sqrt{ch^2qz+sh^2q}}{sh\,q}+\frac{i\pi}{2},$$

or

$$P(z+i\pi/2q)=arsh\frac{ch\,qz}{sh\,q}+\frac{i\pi}{2}.$$

§ 4.3. Attached Cascade Masses

In a case where the profiles in an aerodynamic cascade vibrate

(here we shall be considering only cophasal oscillations), but a main stream is absent, the profiles are acted upon by forces of fluid pressure that are proportional to the acceleration of the profiles themselves. Actually, in the absence of a main stream (U = 0), the convective acceleration is also equal to zero and the local accelerations of all the particles of the fluid are proportional to the same value. Since in this case $a_y=\partial v/\partial t$, satisfaction of the boundary conditions with respect to acceleration simultaneously means the boundary conditions with respect to velocity are satisfied.

Let us consider synchronous cophasal movements of the plates in a cascade without offset in a direction which is normal to the chords, i.e., a direction parallel to the ordinate. In the general Solution (4.16) only the first term has been retained. Differentiating it all the way through with respect to z, we determine the complex acceleration:

$$a=a_x-ia_y=iA\left(\frac{\operatorname{ch}\varepsilon z}{\sqrt{\operatorname{sh}^2\varepsilon z-\operatorname{sh}^2\varepsilon}}-1\right).$$

Since the first term in the parentheses in the sections $-1<x<1$, $y=ik_1l$ is purely imaginary, the coefficient in front of the parentheses is equal to the boundary value of normal acceleration: $A = a_y$.

Utilizing the condition that the perturbed pressure is proportional to the real part of the complex potential $p=-\rho^2\varphi$ and to the boundary values of function $F(z)$ in accordance with (4.13), we find the pressure distribution on the plates:

$$p=\frac{c_y\rho^2}{\varepsilon}\arccos\frac{\operatorname{ch}\varepsilon x}{\operatorname{ch}\varepsilon}. \qquad (4.19)$$

On both boundaries of the section the obtained pressure has the same magnitude, but opposite signs. Integrating the pressure distribution all the way through along the plate, we find the acting force. This force is proportional to the acceleration of the plate. It is customary to call the proportionality coefficient the attached mass, since it may be assumed that this mass of fluid is, as it were, added

to the mass of the moving plate. In the case under consideration (motion of the cascade in the fluid as a single whole), by means of integration of the pressure distribution it is possible to obtain the known precise solution [74]:

$$m = \rho^0 \frac{2l^2}{\pi} \ln \operatorname{ch} \frac{\pi b}{l}. \tag{4.20}$$

In the final formula it is convenient to drop the condition 2b = 2 and to assume an arbitrary chord of 2b, as has been done here and henceforth in the corresponding places.

With an unlimited increase in the cascade spacing ($2b/t \to \infty$) we obtain the known value of the attached mass for an isolated plate:

$$m = \rho^0 \pi b^2.$$

In the other limit case, for a cascade with very small spacing ($2b/t \to \infty$) we obtain

$$m = 2\rho^0 bl.$$

This limit value is explained by the fact that in cascades with very small spacing, only the fluid situated between the plates is entrained. In the rest of the fluid mass, as the distance from the cascade increases the perturbations attenuate very rapidly (according to an exponential law). The value $2\rho^0 bl$ represents precisely the mass of the liquid contained between the plates, i.e., the mass added to each oscillating profile.

We shall also obtain an approximate formula in order to estimate the accuracy of the calculation and the possibility of applying the calculation henceforth.

Figure 4.2 shows a graph of the value of function F(x) on a plate according to the exact Formula (4.12) (curve 1) and the approximate Formula (4.13), where only the first term of the series

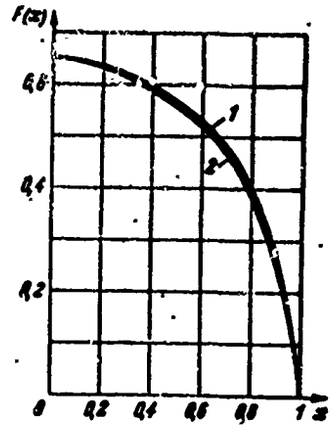


Figure 4.2. Exact (1) and approximate (2) value of function F(x) at a section in a cascade without offset ($\gamma_b = 0$) when q = 2.

$$F(x) = i\sqrt{1-x^2}\,\frac{\operatorname{arcig}(\operatorname{sh} q)}{q}. \qquad (4.21)$$

has been considered (curve 2).

When q = 0 this expression coincides with the exact value $F(x) = i\sqrt{1-x^2}$. The greater the density, the greater the error.

The calculations were made for a comparatively dense cascade of q = 2, i.e., $2b/t = 4/\pi$. It can be seen that the curves practically coincide, and this indicates the fact that the law of change of pressure over the Profile (4.19) depends very weakly upon the cascade density. More precisely, with a change in the cascade spacing, the pressure at all points of the plate changes proportionally to the same coefficient $((\operatorname{arcig}\operatorname{sh} q)/q)$. Such a singularity is explained in the following manner. The attached mass of a single plate differs from the attached mass of the same plate in a cascade, since the remaining plates induce a supplemental acceleration field in the fluid. Obviously, in this case the induced acceleration field is almost constant along the plate, and this brings about a change only of the proportionality coefficient.

On the basis of a known acceleration potential, the attached mass is found by integration:

$$m = -2\rho^0 \int_{-b}^{+b} \varphi\, dx. \qquad (4.22)$$

In the example under consideration, we obtain the approximate formula

$$m = \rho^0 bl \operatorname{arcig}\operatorname{sh}\frac{\pi b}{t},$$

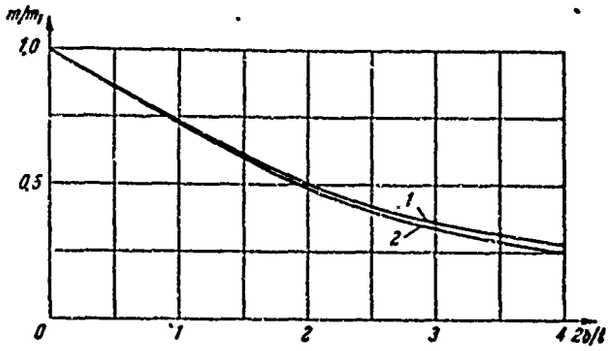


Figure 4.3. Exact (1) and approximate (2) relationship of the attached mass to the cascade density.

which coincides sufficiently well with the exact Solution (4.20) even for dense cascades (Figure 4.3). Curve (1) was computed according to the exact formula; curve (2) was computed according to the approximate one, $m_1 = \pi\rho^0 b^2$.

In the case of torsional oscillation of a plate, the concept of the attached moment of inertia is introduced in a manner analogous to the concept of attached mass. In the case of torsional oscillation of the plates around their centers, the moment acting from the direction of the fluid may be computed according to the formula

$$\Theta = -2\rho^0 \int_{-b}^{+b} \varphi x \, dx. \tag{4.23}$$

If the plates oscillate torsionally other than about their centers, the superposition principle of (4.22) and (4.23) should be used.

Let us consider the determination of attached moments of inertia in the case of synchronous cophasal torsional oscillation of plates about their centers. In the case of torsional oscillation about the center, the distribution of normal accelerations along the plate is represented by the formula

$$a_y(x, \tau) = \frac{x}{b} a_{y0}(\tau). \tag{4.24}$$

To represent the acceleration potential, we shall make use of Series (4.17). We shall show that in order to obtain a solution with greater accuracy, it is necessary to restrict oneself to the first term with an even index

$$\omega = iA_2(F-z)^2.$$

Differentiating this expression with respect to z, we obtain the complex acceleration:

$$a = 2iA_2\left(\frac{dF}{dz}F - F\frac{1}{z}z\frac{dF}{dz} + z\right).$$

For instance we determine the normal acceleration, taking advantage of the fact that on a plate the functions F and dF/dz assume purely imaginary values:

$$a_y = -2A_2\left(F\frac{dF}{dz} + x\right).$$

From the approximate Formula (4.21), it follows that $F\cdot dF/dz = xq^{-2}(\operatorname{arcctg}\operatorname{sh} q)^2$. Then A_2 is determined in terms of the boundary value of the acceleration according to (4.24):

$$A_2 = -\frac{q^2 a_{y0}}{2\left[q^2 + (\operatorname{arcctg}\operatorname{sh} q)^2\right]b}.$$

Then, in the conventional manner the real part of the acceleration potential is found and, according to (4.23), the attached moment of inertia is:

$$\Theta = \frac{\pi\rho^2 b^4}{4}\frac{q\operatorname{arcctg}\operatorname{sh} q}{q^2 + (\operatorname{arcctg}\operatorname{sh} q)^2}.$$

When the cascade spacing increases without limit ($q \to 0$), this expression passes into the known exact solution for an isolated plate which carries out rotational motion around the center:

$$\Theta = \frac{\pi\rho^2 b^4}{8}.$$

Let us now consider the determination of the attached masses for the case where adjacent plates in the cascade oscillate with a phase shift equal to π (henceforth this case will be called oscillation in counterphase). Let us find an approximate solution of the problem and estimate the error. In the case of oscillation in counterphase, the acceleration potential must have a period equal to twice the cascade spacing. The values of the normal oscillations on adjacent blades must have equal moduli and opposite sign.

We define the acceleration potential by the following expression:

$$w = iA\,[F(z,\ q/2) - F(z + ix/q,\ q/2)],\quad q = \pi b/t.$$

Obviously the requirement of $w(z) = w(z + 2it)$ is satisfied. The condition at an infinite distance from the cascade is also satisfied, since $w \to 0$ when $|x| \to \infty$ (the condition of perturbation damping).

To obtain the complex acceleration we differentiate this expression with respect to z and replace $F(z)$ by (4.10):

$$a = iA\left[\frac{\operatorname{sh}(qz/2)}{\sqrt{\operatorname{sh}^2(qz/2) - \operatorname{sh}^2(q/2)}} - \frac{\operatorname{ch}(qz/2)}{\sqrt{\operatorname{ch}^2(qz/2) - \operatorname{sh}^2(q/2)}}\right].$$

It can be easily seen that on even plates $-1 < x < 1$, $y = ik_1 t$, $k_1 = 0, \pm 2, \pm 4, \ldots$ the normal acceleration is equal to

$$a_y = \frac{A \operatorname{ch}(qx/2)}{\sqrt{\operatorname{ch}^2(qx/2) + \operatorname{sh}^2(q/2)}}. \qquad (4.25)$$

On odd plates $-1 < x < 1$, $y = ik_1 t$, $k_1 = \pm 1, \pm 3$, the normal acceleration has the same absolute magnitude, but the opposite sign. If a_y did not depend upon $x (-1 \leqslant x \leqslant 1)$, the solution would be exact. In actuality, a_y depends on x according to (4.25). However, in the indicated range of the change of x the acceleration changes only little. The ratio of the maximum acceleration $a_y(1)$ (along the edges of the plate when $x = \pm 1$) to the minimum acceleration $x_y(0)$ (in the center of the plate when $x = 0$) is equal to $\sqrt{1 + \operatorname{th}^2(q/2)}$.

Then the maximum deviation from the average value, expressed in terms of this average, is the error

$$\frac{\sqrt{1+\mathrm{th}^2(q/2)}-1}{\sqrt{1+\mathrm{th}^2(q/2)}+1}.$$

With a relative cascade spacing of t/2b = 1 the relative error will be about 9%, and when t/2b = 1.5 it would be about 3%.

Omitting the intermediate calculations, we cite the approximate formula for the attached mass with oscillation of the plates in counterphase:

$$m=2\rho bl\left(\mathrm{ch}\frac{\pi b}{t}\right)\left(\mathrm{arctg\,sh}\frac{\pi b}{2t}\right).$$

When $2b/t\to 0$ we approach the known expression for the attached mass of an isolated plate. It is obvious that with oscillation in counterphase, the attached mass is greater than with oscillation in phase. This is explained by the appearance of large accelerations with the shift of fluid among adjacent channels. Thus, for example, with a relative cascade spacing of t/2b = 1, the indicated ratio of attached masses comprises 3.1.

A conception of the acceleration potential in a more general case can be obtained by using a series similar to Series (4.17):

$$w=i\sum_{n=1}^{\infty}A_n\{[F(z)-z]^n-[F(z+i\pi/2q)-i\pi/2q-z]^n\}. \qquad (4.26)$$

Without dwelling on the computations, we shall cite the formula for determining the attached moment of inertia in the case of torsional oscillation of plates in counterphase about their centers:

$$\Theta=\frac{\pi\rho b^4}{4}\,\frac{\frac{q}{2}\,\mathrm{ch}^2\left(\frac{q}{2}\right)\mathrm{arctg\,sh}\left(\frac{q}{2}\right)}{\left(\frac{q}{2}\right)^2+\mathrm{ch}^2\left(\frac{q}{2}\right)\cdot\left[\mathrm{arctg\,sh}\left(\frac{q}{2}\right)\right]^2}.$$

Computation of the attached masses for a cascade is necessary in some fields of technology, for example in the determination of eigenfrequencies of thin blades rotating in a heavy fluid. For steam and

gas turbines, as well as for axial compressors, the attached masses are very small in comparison with the mass of the blade.

The currents which are considered in this section have zero circulation. We emphasize that the force brought about by attached masses acts in phase with the acceleration (and not with the velocity), and therefore cannot produce work.

The question considered here has been studied in Reference [59].

Some precise solutions for the attached mass of cascades have been obtained by M. I. Gurevich [74].

§ 4.4. A Cascade in an Unsteady Vortex Stream

The problem of flow about a cascade by an unsteady vortex stream is of special interest for turbomachine theory. Here we shall consider some basic problems, while questions of an applied nature will be carried over into Chapter 9.

Let a cascade of plates (chord b = 2) with zero offset ($\gamma b = 0$) be situated in the plane of the complex valuable $z = x + iy$. The main stream with a constant velocity of U flows about the cascade with a zero angle of attack and transports free vortices of low intensity. The vorticity is homogeneous along the cascade axis, which is parallel to the ordinate.

Let us consider the flow field in the absence of a cascade. From the Helmholtz equation it follows that the vorticity follows a traveling wave

$$\frac{\partial \omega}{\partial \tau} + U \frac{\partial \omega}{\partial x} = 0, \quad \omega = \omega(\tau - x/U).$$

The wave front is perpendicular to the direction of the main stream.

The vertical velocity $v (v \ll U)$ is related to the vorticity by the condition:

$$w=-\frac{1}{\rho}\frac{\partial p}{\partial x}.$$

A jump of vertical velocity also constitutes a traveling wave

$$v=v(\tau-x/U).$$

Then according to the Euler equation the vertical acceleration is everywhere equal to zero:

$$a_y=\frac{\partial v}{\partial \tau}+U\frac{\partial v}{\partial x}=0.$$

We assume the pressure in the main stream to be everywhere constant. If a cascade is placed in such a stream, it will bring about perturbations, since its profiles are impermeable, and at them the normal velocity component must be equal to zero. With the incidence of vertical velocity jumps, the local angle of attack will be a variable; this will bring about a change of the circulation about the profiles in time. Consequently, behind the profiles vortex wakes will appear, the intensity of which will also vary in time.

The problem consists in determining the variable forces which act upon the cascade profiles, as well as in determining the perturbations introduced by the cascade.

We shall solve the problem by the acceleration-potential method, which in this particular case has a special advantage, since the boundary value of normal accelerations at the profiles is equal to zero ($a_y = 0$). Consequently [58], in accordance with (4.5) the acceleration potential assumes a particularly simple form:

$$w(z,\tau)=iB(\tau)\sqrt{\frac{\operatorname{sh}[q(z-1)]}{\operatorname{sh}[q(z+1)]}}. \qquad (4.27)$$

Coefficient B is determined from the condition that the perturbed vertical velocity at the profile is equal to $-v(\tau-x/U)$. Then the

total vertical velocity of the fluid particles at the profile will be equal to zero, i.e., the profile may be considered motionless and impermeable. In view of the linearity of the problem, we shall consider only the case where the velocity of a vertical jump changes according to the harmonic law

$$v = v_0 \exp jv(\tau - x/U). \tag{4.28}$$

A general case may be obtained by expanding the jump into a series or into a Fourier integral. Explicity separating in $B(\tau)$ the time function, we assume $B(\tau) = B_0 \exp(jv\tau)$, where B_0 is a complex (with respect to j) constant. Constant B_0 is determined from the boundary condition for velocity (4.28) according to the formula

$$v_0 e^{ik} = \frac{1}{U} e^{ik} \int_{-\infty}^{-1} a_y(\xi) e^{ik\xi} d\xi. \tag{4.29}$$

Here $v_0 e^{ik}$ is the vertical velocity at the leading edge (the time factor is discarded).

Vertical acceleration must be expressed in terms of the complex acceleration potential:

$$a_y = \frac{\partial \varphi}{\partial y} = -\frac{\partial \psi}{\partial x}. \tag{4.30}$$

In this case let us use the expression of a_y in terms of the imaginary part of the complex acceleration potential. We substitute this expression into (4.29) and integrate by parts from $x = -\infty$ to a point on the leading edge of the profile $x = -1$. Integration by parts permits the integral to be taken directly from the function ψ, and not from its derivative:

$$v_0 = -\frac{1}{U}\{e^{ik\xi}[\psi(\xi) - \psi(-\infty)]\}_{-\infty}^{-1} + \\ + \frac{ik}{U} \int_{-\infty}^{-1} e^{ik\xi}[\psi(\xi) - \psi(-\infty)]\, d\xi. \tag{4.31}$$

Here to the function ψ, to which an arbitrary constant may be added, has been added the value $\psi(-\infty) = B_0 \exp q$, equal to the value of this function far in front of the cascade ($x = -\infty$). As follows from

Formula (4.27), everywhere on the profile the smallest part of the complex acceleration potential, is equal to zero; consequently $\psi(-1)=0$.

On the integration path the function $\psi(x)$ is defined by means of (4.27) by the relationship

$$\psi(x)=B_0\sqrt{\frac{\operatorname{sh}|q(x-1)|}{\operatorname{sh}|q(x-1)|}}.$$

Taking these remarks into account and after simple transformations of Formula (4.31), we find the desired expression for $B(\tau)$:

$$B(\tau)=B_0e^{i\nu\tau}=a_0Ue^{i\nu\tau}R(k, q).$$

The function R(k, q) is introduced which is basic to this problem, and which depends upon two dimensionless parameters: the Strouhal number $k=\nu b/U$, which characterizes the unsteadiness, and $q=\pi b/t$, which determines the cascade density. Function R(k, q) is defined by the Formula [58]

$$R(k, q)=\frac{e^{ik}}{e^{ik}+ik\pi^{ik}I_1(k, q)}. \tag{4.32}$$

$I_1(k, q)$ designates the improper integral:

$$I_1(k, q)=\int_0^\infty\left(\sqrt{\frac{\operatorname{sh}|q(x+1)|}{\operatorname{sh}|q(x-1)|}}-e^x\right)e^{-ikx}dx. \tag{4.33}$$

The pressure field is found by isolating the real part (with respect to i) from (4.27). In particular, the pressure distribution on a profile in the cascade is described by the expression

$$p=\rho^0B(\tau)\sqrt{\frac{\operatorname{sh}|q(1-x)|}{\operatorname{sh}|q(1+x)|}}. \tag{4.34}$$

The signs in front of the radical at the upper and lower boundaries of the section are taken respectively as + and −. Worthy of note is the fact that the law of pressure distribution does not depend, in the linear formulation, upon the shape of the jump and the incidence frequency of the vorticity waves.

The unsteady lifting force acting upon a profile in the cascade is found by integrating (4.34) along the profile contour:

$$\mathscr{L} = 2\rho^0 B(\tau) \int_{-1}^{+1} \sqrt{\frac{\operatorname{sh}[q(1-x)]}{\operatorname{sh}[q(1+x)]}}\, dx.$$

We break down the integrand function into two terms, integrate, and obtain:

$$\mathscr{L} = 2\rho^0 B(\tau) \int_{-1}^{+1} \left(\frac{\operatorname{sh} q \operatorname{ch}(qx)}{\sqrt{\operatorname{sh}^2 q - \operatorname{sh}^2(qx)}} - \frac{\operatorname{ch} q \operatorname{sh}(qx)}{\sqrt{\operatorname{sh}^2 q - \operatorname{sh}^2(qx)}} \right) dx =$$

$$= 2\rho^0 B(\tau) \left[\frac{\operatorname{sh} q}{q} \arcsin \frac{\operatorname{sh}(qx)}{\operatorname{sh} q} - \operatorname{ch} q \cdot \arcsin \frac{\operatorname{ch}(qx)}{\operatorname{ch} q} \right]_{-1}^{+1} = \frac{2\pi\rho^0 \operatorname{sh} q}{q} B(\tau).$$

In the final expression for the lift force we introduce the arbitrary semichord b

$$\mathscr{L} = 2\rho^0 v_0 U t \operatorname{sh}\left(\frac{\pi b}{t}\right) e^{i\omega\tau} R(k, q). \tag{4.35}$$

We now analyze the obtained solution.

Integral (4.33) may be expressed in terms of a hypergeometric function. We break down Expression (4.33) into two integrals and, carrying out a change of variable in the first integral $\xi = \exp[2q(1-x)]$, we obtain

$$\int_1^\infty \sqrt{\frac{\operatorname{sh}[q(x+1)]}{\operatorname{sh}[q(x-1)]}}\, e^{-ikx}\, dx = \frac{e^{q-ik}}{2q} \int_0^1 (1-\xi)^{-1/2} (1 - e^{-4q\xi})^{1/2} \xi^{\frac{ik}{2q}-1}\, d\xi =$$

$$= \frac{1}{2q} e^{q-ik} B(a, b) F(\alpha, \beta, \gamma, z). \tag{4.36}$$

Here B(a, b) is a beta-function, and $F(\alpha, \beta, \gamma, z)$ is a hypergeometric function.

In the case under consideration

$$\left.\begin{aligned} a &= \frac{ik}{2q}, \quad b = \frac{1}{2}, \\ \alpha &= -\frac{1}{2}, \quad \beta = \frac{ik}{2q}, \quad \gamma = \frac{1}{2} + \frac{ik}{2q}, \quad z = e^{-4q}. \end{aligned}\right\} \tag{4.37}$$

This integral can be expressed in terms of a hypergeometric

function if $\mathrm{Re}(jk/2q)>0$. In the case under consideration, the real part of this expression is strictly equal to zero. However, if it is assumed from the very start that the process in the physical plane during flow about the cascade was a weakly attenuating process, and not a periodic one, the succeeding calculations are possible. After they have been carried out, it is necessary to pass to the limit, making the damping coefficient go to zero.

The second integral constitutes a Fourier transform of a unit function and is computed by the same kind of passage to the limit:

$$e^{q}\int_{1}^{\infty} e^{-jkx}\,dx = e^{q}\lim_{\varepsilon\to 0}\int_{-\infty}^{\infty} e^{-\varepsilon x - jkx}\sigma(x-1)\,dx = \frac{1}{jk}e^{q-jk}.$$

After simple transformation we obtain the final formula:

$$I_1(k, q) = e^{q-jk}\left[\frac{1}{2q}B\left(\frac{jk}{2q}, \frac{1}{2}\right)F\left(-\frac{1}{2}, \frac{jk}{2q}, \frac{1}{2}+\frac{jk}{2q}, e^{-2q}\right)-\frac{1}{jk}\right]. \qquad (4.38)$$

The hypergeometric function is expressed by the series

$$F(\alpha, \beta, \gamma, z) = 1+\frac{\alpha\cdot\beta}{\gamma\cdot 1}z+\frac{\alpha(\alpha+1)\beta(\beta+1)}{\gamma(\gamma+1)\cdot 1\cdot 2}z^2+\ldots \qquad (4.39)$$

In the case under consideration $\mathrm{Re}(\alpha+\beta-\gamma)=-1<0$ and, consequently, the series must converge (absolutely) within the entire unit circle, including point $z = 1$. The beta-function, in the special case where $b = 1/2$, i.e., precisely in the case under consideration, may be represented by the series

$$B\left(a, \frac{1}{2}\right)=\sum_{n=0}^{\infty}\frac{(2n+1)!!}{2^n n!}\frac{1}{a+n}. \qquad (4.40)$$

Thus, for computing the lift force acting upon a profile in a cascade for a sinusoidal velocity jump, it is necessary to compute function R(k, q) according to Formula (4.32). This in its turn requires computation of the hypergeometric Function (4.38).

Let us first consider some interesting limit cases:

(a) A very dense cascade. Let us assume that the cascade spacing $l \to 0$, i.e., $q \to \infty$, the relative frequency of the process being such that $k/2q \to 0$. Let us first estimate the behavior of the integral expressed by Formula (4.38).

For the limit case under consideration $\alpha = -1/2$, $\beta \to 0$, $\gamma \to 1/2$, $z \to 0$. Then hypergeometric Series (4.39) has as its limit the unit $F(\alpha, \beta, \gamma, z) \to 1$. The beta-function when $a = jk/2q \to 0$ may, according to (4.40) be represented thus:

$$B\left(\frac{jk}{2q}, \frac{1}{2}\right) \to \frac{2q}{jk} + \text{const.}$$

Consequently,

$$\frac{1}{2q} B\left(\frac{jk}{2q}, \frac{1}{2}\right) \to \frac{1}{jk} \text{ with } q \to \infty.$$

From this it follows that the expression in the brackets of (4.38) tends toward zero. In this manner it may be asserted that when $q \to \infty$, the condition

$$I_1(k, q) e^{-q} \to 0.$$

will be satisfied

Then from Formula (4.32) we obtain the limit value of function R(k, q) when $q \to \infty$:

$$R(k, q) \to e^{-q+jk}.$$

Finally, by means of this relationship and Formula (4.35), we establish a formula for the lift force in the case of a very dense cascade [59]

$$\mathcal{Y} \to U\rho^0 v_0 l c^{j(\nu\tau+k)}. \tag{4.41}$$

This formula establishes an important fact: For a dense lattice

the lift force does not depend upon the frequency of the process. The value $v_0 \exp j(\nu\tau+k)$ represents the velocity of a vertical jump at point x = -b (since $k=\nu b/U$), i.e., on the leading edge. Consequently, Formula (4.41) follows from the equation of momentum applied to steady fluid flow through one channel between plates. From the derivation, it follows that the turn of the stream takes place instantaneously at the leading edges, since the lift force is proportional to the current value of the jump velocity at point x = -b. The value $\rho^0 Ut$ represents the mass flowing into a single channel per unit of time. Function $v_0 \exp j(\nu\tau+k)$ represents the current value of the vertical velocity of the fluid immediately before the entrance into the cascade. Consequently, the stream introduces the momentum (in direction of the y-axis) equal $Up^0 t \exp j(\nu\tau+k)$ into the channel between the plates. The vertical velocity of the liquid within the channel must equal zero in a dense lattice with stationary plates. Consequently, the obtained value is equal to the change of the momentum of the fluid in a unit of time, i.e., is equal to the force acting upon the plate in the direction of the ordinate. We shall also emphasize that this result is valid, as was stipulated above, when $k/q \to 0$, i.e., when the Strouhal number, computed on the basis of the cascade spacing $\nu t/U \to 0$, tends toward zero.

In view of the importance of this result for practical applications, we shall explain its physical aspect from the point of view of vortex theory.

A vertical velocity jump that reaches the leading edges brings about the appearance of vorticity which, as usual, consists of attached and free vortices. The attached vortices obtain the same sign as do the incident ones, and the newly formed free vortices naturally get the opposite sign. In a very dense lattice the vortices at the leading edges of the plate comprise almost a solid sheet. Then the vertical velocity induced by them does not depend upon the distance from the leading edges. Obviously, in order to satisfy the boundary conditions at the blades it is necessary that the free vorticity completely cancel the incident vorticity. Consequently, the flow behind a dense cascade will be nonvertical, the process of streamline flow will be quasi-steady, and there will be no effect characteristic of unsteady regimes.

(b) Steady flow about a cascade of arbitrary density. When $k = 0$, it follows from (4.38) that the cascade will be in a steady stream at a constant angle of attack $\operatorname{arctg}(v_0/U)$. When $k = 0$, from (4.32) we obtain $R(0, q) = \exp(-q)$. Then the lift force acting upon the profile in the steady flow about a cascade of plates without offset will, according to Formula (4.35), be equal to

$$\mathcal{Y} = 2\pi\rho^0 v_0 U b \frac{3h q}{qe^q}, \tag{4.42}$$

whence when $q \to 0$ we obtain the formula for steady flow about an isolated profile $\mathcal{Y} = 2\pi\rho^0 v_0 U b$, and when $q \to \infty$ we obtain the formula for the lift force of the very dense cascade $\mathcal{Y} = \rho^0 v_0 U l$, which agrees with (4.41) when $\nu = 0$ and $k = 0$.

(c) A single profile. When the cascade spacing tends toward zero, all formulas must pass into formulas for a single profile. In the special case when $q = 0$, Integral (4.33) is expressed in terms of Hankel functions. We represent (4.33) in the form of a sum

$$I_1(k, 0) = \int_1^\infty \left(\sqrt{\frac{x+1}{x-1}} - 1\right) e^{-jkx}\,dx = \int_1^\infty \sqrt{\frac{x+1}{x-1}}\, e^{-jk}\,dx - \int_1^\infty e^{-jkx}\,dx.$$

Making use of the definition of the Hankel functions, we write:

$$H_1^{(2)}(k) = -\frac{2}{\pi}\int_1^\infty \frac{xe^{-jkx}\,dx}{\sqrt{x^2-1}}, \quad H_0^{(2)}(k) = \frac{2j}{\pi}\int_1^\infty \frac{e^{-jkx}\,dx}{\sqrt{x^2-1}}.$$

We obtain the value of the first integral:

$$\int_1^\infty \sqrt{\frac{x+1}{x-1}}\, e^{-jkx}\,dx = \frac{\pi}{2}\left[H_1^{(2)}(k) + jH_0^{(2)}(k)\right].$$

The second integral constitutes a Fourier transform of a single function, and is computed by the limit method:

$$\int_1^\infty e^{-jkx}\,dx = \frac{1}{jk}e^{-jk}.$$

Finally we obtain

$$I_1(k,\ 0)=\frac{\pi}{2}\left[H_1^{(2)}(k)+jH_0^{(2)}(k)\right]-\frac{1}{jk}e^{-jk}.$$

Then the function R(k, q) passes into the function

$$R(k,\ 0)=\frac{-2j}{\pi k\left[H_1^{(2)}(k)+jH_0^{(2)}(k)\right]}. \tag{4.43}$$

The formula for the lift force (4.35) when q = 0 passes into the known formula for a thin wing:

$$\mathcal{Y}=2\pi\rho^0 b v_0 U e^{j\omega t}R(k,\ 0), \tag{4.44}$$

The first six cofactors yield the steady value of the lift force, which may be obtained according to the Zhukovskiy theorem. The last cofactor takes into account the unsteadiness of the process and, for a single wing and a burst of sinusoidal shape, was defined by Kuessner and then in a somewhat different form by Sears. The function introduced by Sears and transformed by Kemp coincides with the special case (4.43) under consideration.

We shall make use of expressions for the Hankel functions at small values of the argument in the following form:

$$\left.\begin{aligned} H_0^{(2)}(k)&=\frac{2}{j\pi}\ln k-\frac{2}{j\pi}\ln\frac{2}{\gamma}+1+\ldots,\\ H_1^{(2)}(k)&=-\frac{2}{\pi jk}+\frac{k}{\pi j}\ln k+\ldots,\ \ln\frac{2}{\gamma}=0{,}1159\ldots \end{aligned}\right\} \tag{4.45}$$

We write the approximate value of function (4.43) for a small Strouhal number:

$$R(k,\ 0)=\frac{2}{2-k^2\ln k-2jk\ln k}.$$

As was to have been expected, under steady conditions of streamline flow we obtain R(0, 0) = 1.

We write the Hankel functions for large values of the argument:

$$H_0^{(2)} = \sqrt{\frac{2}{\pi k}} e^{-i(k-\pi/4)},$$

$$H_1^{(2)} = i\sqrt{\frac{2}{\pi k}} e^{-i(k-\pi/4)},$$

Then Function (4.43) for very large values of k will have the form

$$R(k, 0) \approx \frac{1}{\sqrt{2\pi k}} e^{i(k-\pi/4)}.$$

The modulus of function R determines the reduction of the modulus of the lift force due to the effect of unsteadiness, and the argument of R determines the phase shift between the traveling wave of the jump of vertical velocity and the lift force vector. In many applications it is sufficient to know only the modulus of function R(k, 0). The approximate formula applicable within the entire range of the variation of k, has the form [81]

$$|R(k, 0)| = \frac{a+k}{a+(\pi a+1)k+2\pi k^2}, \quad a = 0{,}1811.$$

(d) The cascade in vorticity waves with a very large Strouhal number. We obtain an asymptotic formula for a very large frequency of the process $k \to \infty$.

We return to Integral (4.33), which has the form of a Fourier integral; the integrand function has a singularity at the left end of the interval. We isolate this singularity, expressing $\mathrm{sh}[q(x-1)]$ by the infinite product:

$$\mathrm{sh}[q(x-1)] = q(x-1)\prod_{n=1}^{\infty}\left[1+\frac{q^2(x-1)^2}{n^2\pi^2}\right].$$

We reduce Integral (4.33) to the expression

$$I_1(k, q) = \int_1^{\infty} e^{-ikx}(x-1)^{-1/2}\varphi(x, q)\,dx.$$

Here the function $\varphi(x, q)$ on the integration segment has no singularity and is represented by the formula

$$\varphi(x, q) = \sqrt{\frac{\operatorname{sh}[q(x+1)]}{q\prod\left[1+\frac{q^2(x-1)^2}{n^2\pi^2}\right]}} - e^q\sqrt{x-1}.$$

When $k \to \infty$, the method of asymptotic expansion [95] may be used for evaluation of the integral:

$$I_1(k, q) = \sum_{n=0}^{N-1} j\frac{\Gamma(n+1/2)}{n!}e^{j\frac{\pi}{2}\left(n-\frac{3}{2}\right)}\varphi^{(n)}(1)\,k^{-n-1/2}e^{-jk} + O\left(k^{-N}\right).$$

Here it is assumed that the function $\varphi(x, q)$ has continuous derivatives up to the N^{th} order inclusively.

Restricting ourselves to the first term of the series, we find

$$I_1(k, q) = j\Gamma(1/2)e^{-3j\pi/4}\sqrt{\frac{\operatorname{sh} 2q}{kq}}e^{-jk}.$$

We find the final value of function R(k, q) in the limit case of $k \to \infty$ by means of (4.32). After the replacement $\Gamma(1/2) = \sqrt{\pi}$ and transformations, we obtain

$$R(k, q) = \frac{e^{jk}}{e^q + \sqrt{\frac{\pi k \operatorname{sh}(2q)}{q}}e^{j\pi/4}}, \quad k \to \infty. \tag{4.46}$$

If, in addition, the cascade spacing increases without limit ($l \to \infty$, $q \to 0$), we obtain the formula

$$R(k, q) = \frac{1}{\sqrt{2\pi k}}e^{j(k-\pi/4)}, \quad k \to \infty, \quad q \to 0,$$

which coincides with the formula found above for a single wing.

If, under the condition of $k \to \infty$ it is assumed that $q \to \infty$ (i.e., a cascade with an infinitely small spacing $t \to 0$ is considered) and it is required that $k/q \to 0$, we obtain

$$R(k, q) = e^{-q+jk}, \quad k \to \infty, \quad q \to \infty, \quad k/q \to 0.$$

This formula also agrees with the one found above. Thus, the streamline may be regarded as being quasi-steady, if only $k/q = \nu l/\pi U \to 0$, i.e., if

the Strouhal number, computed on the basis of the cascade spacing, is sufficiently small.

We shall obtain one more asymptotic formula by taking advantage of the fact that even for a cascade of relatively low density it may be assumed that $\mathrm{sh}(2q) \approx e^{2q}/2$; for example, when 2b/t = 1 the error with such a substitution comprises less than 1%. Then for large Strouhal numbers and large cascade density, the following formula is valid:

$$R(k, q) \approx \frac{\exp(-q + jk - j\pi/4)}{1 + \sqrt{\pi k/2q}}, \quad k \to \infty, \quad q > \pi.$$

If when $k \to \infty$ it is also true that $k/q \to \infty$, then from (4.46) it follows that

$$R(k, q) \approx \sqrt{\frac{2q}{\mathrm{sh}(2q)}} \frac{1}{\sqrt{2\pi k}} e^{j(k - \pi/4)}.$$

This formula differs from the asymptotic formula for a single wing only by virtue of the multiplier which depends upon the cascade density. Taking (4.35) into account, we find the formula for the lift force when $k \to \infty$ and $k/q \to \infty$:

$$\mathcal{Z} \approx 2\pi\rho^0 v_0 U b \sqrt{\frac{\mathrm{th}\, q}{q}} \frac{1}{\sqrt{2\pi k}} e^{j(\omega t + k - \pi/4)}.$$

When $q \to 0$, the asymptotic formula for a single wing is found as a consequence.

Let us return to the general case. Function $I_1(k, q)$ is encountered in many problems of unsteady flow about a plate cascade, and therefore it is desirable to have tables for it. Integral (4.33) was computed on a digital electronic computer [1], and the results of computation of the real part and the imaginary part of the function are presented in Table 4.1 (a, b). The integral may also be computed by means of hypergeometric Series (4.38), and furthermore such a series

---

Footnote (1) appears on page 195.

TABLE 4.1a

h \ M	0,1	0,2	0,3	0,4	0,5	0,6	1,0	1,5	2,0	2,5	3,0	4,0	5,0	6,0
0	0,94850	0,90085	0,86254	0,80549	0,71681	0,63692	0,56656	0,43301	0,33777	0,27482	0,23045	0,17339	0,13879	0,11568
0,05	0,94127	0,89555	0,84883	0,80264	0,71468	0,63514	0,56539	0,42925	0,33722	0,27439	0,23010	0,17315	0,13860	0,11553
0,10	0,91409	0,88006	0,83787	0,79117	0,70906	0,63105	0,56188	0,42698	0,33558	0,27312	0,22908	0,17241	0,13803	0,11506
0,20	0,83786	0,82439	0,79651	0,76151	0,68625	0,61367	0,51736	0,41795	0,32906	0,26808	0,22500	0,16947	0,13573	0,11317
0,40	0,66720	0,66701	0,66113	0,64674	0,60110	0,54726	0,49419	0,38264	0,30346	0,24828	0,20891	0,15798	0,12669	0,10576
0,60	0,49145	0,49398	0,49599	0,49461	0,47726	0,44651	0,41081	0,32682	0,26250	0,21644	0,18307	0,13917	0,11207	0,09377
0,80	0,31811	0,32138	0,32581	0,33029	0,33248	0,32301	0,30578	0,25381	0,20861	0,17430	0,14870	0,11423	0,09254	0,07773
1,00	0,15170	0,15500	0,16053	0,16761	0,18136	0,18844	0,18798	0,16908	0,14489	0,12408	0,10755	0,08421	0,06897	0,05836
2,00	−0,44978	−0,44543	−0,43814	−0,42821	−0,40164	−0,36875	−0,33332	−0,25191	−0,19236	−0,15172	−0,12367	−0,08895	−0,06891	−0,05606
5,00	0,32209	0,31942	0,31539	0,30984	0,29521	0,27731	0,25782	0,20979	0,16957	0,13851	0,11498	0,08325	0,06374	0,05095

TABLE 4.1b

β \ ξ	0,1	0,2	0,3	0,4	0,6	0,8	1,0	1,5	2,0	2,5	3,0	4,0	5,0	6,0
0	0	0	0	0	0	0	0	0	0	0	0	0	0	0
0,05	−0,09154	−0,07668	−0,06664	−0,05921	−0,04818	−0,04079	−0,03491	−0,02495	−0,01891	−0,01508	−0,01246	−0,00920	−0,00725	−0,00602
0,10	−0,17888	−0,15085	−0,13196	−0,11762	−0,09655	−0,08132	−0,06961	−0,04981	−0,03782	−0,03012	−0,02483	−0,01837	−0,01454	−0,01202
0,20	−0,30981	−0,28335	−0,25113	−0,22912	−0,18695	−0,16063	−0,13785	−0,09883	−0,07513	−0,05985	−0,04947	−0,03653	−0,02891	−0,02391
0,40	−0,49066	−0,47422	−0,41714	−0,41611	−0,35653	−0,30659	−0,26168	−0,19150	−0,14613	−0,11675	−0,09652	−0,07138	−0,05653	−0,04678
0,60	−0,60168	−0,59064	−0,57209	−0,51599	−0,48136	−0,42408	−0,37115	−0,27240	−0,20915	−0,16731	−0,13889	−0,10294	−0,08163	−0,06759
0,80	−0,66309	−0,65545	−0,61182	−0,62198	−0,56817	−0,50796	−0,45075	−0,33693	−0,26097	−0,20990	−0,17453	−0,12976	−0,10307	−0,08547
1,00	−0,68873	−0,67901	−0,66317	−0,64326	−0,60964	−0,55557	−0,50015	−0,38181	−0,29873	−0,24177	−0,20177	−0,15066	−0,11968	−0,09962
2,00	−0,37614	−0,37539	−0,37396	−0,37187	−0,36545	−0,35542	−0,34156	−0,29715	−0,25258	−0,21551	−0,18637	−0,14337	−0,11869	−0,10015
5,00	+0,28893	+0,28784	+0,28595	+0,28337	+0,27642	+0,26757	+0,25746	+0,23031	+0,20165	+0,18241	+0,16368	+0,13169	+0,11376	+0,09865

of approximate formulas can be obtained for special cases. By means of the obtained table, function R(k, q) can be computed on the basis of (4.32), and the lift force can be computed on the basis of (4.35).

It is convenient, by means of simple transformations, to put Formula (4.35) into the following form

$$\mathcal{Y} = 2\pi\rho^{*}\omega_{0}bU\frac{\mathrm{sh}\,q}{q}R(k, q).$$

The first five cofactors determine the lift force of an isolated plate in a stabilized stream. The last cofactors yield a correction for the fact that the plate is situated in a cascade, and also take into account the unsteadiness of the streamline flow.

The value of the real part and the imaginary part of function R(k, q) are presented in Table 4.2 (a, b). Graphs of the real part and the imaginary part of function $\mathrm{sh}(q)\cdot R(k, q)/q$ are presented in Figure 4.4 and Figure 4.5, and in the polar coordinate system in Figure 4.6. The values of the real part and the imaginary part of function R(k, 0) according to the data of Reference [152] are presented in Table 4.2 (c).

The problem considered in this section has been solved in Reference [58].

§ 4.5. Flow about a Cascade of Thin Vibrating Profiles

The theory of flow about a cascade of vibrating plates has been considered in a large number of works (Section 4.1). We shall now dwell on the application of the acceleration potential method on the basis of Reference [59]. The principal advantage of the acceleration potential method in this case is the possibility of obtaining formulas which can be analyzed.

TABLE 4.2a

h \ q	0,1	0,2	0,3	0,4	0,6	0,8	1,0	1,5	2,0	2,5	3,0	4,0	5,0	6,0
0	0,90181	0,81871	0,74082	0,67032	0,54881	0,44933	0,36788	0,22313	0,13533	0,08208	0,04979	0,01832	0,00674	0,00248
0,05	0,87815	0,80731	0,73189	0,66690	0,54742	0,44863	0,36747	0,22295	0,13523	0,08202	0,04974	0,01830	0,00673	0,00248
0,10	0,81880	0,77725	0,71833	0,65709	0,54331	0,44652	0,36623	0,22240	0,13491	0,08182	0,04962	0,01825	0,00671	0,00247
0,20	0,70337	0,69557	0,66597	0,62315	0,52815	0,43860	0,36140	0,22024	0,13363	0,08102	0,04911	0,01805	0,00663	0,00244
0,40	0,56715	0,56517	0,55696	0,53906	0,49055	0,41060	0,34335	0,21176	0,12851	0,07795	0,04711	0,01725	0,00632	0,00232
0,60	0,48752	0,48383	0,47713	0,46571	0,42653	0,37311	0,31677	0,19815	0,12012	0,07270	0,04381	0,01593	0,00582	0,00213
0,80	0,42515	0,42108	0,41429	0,40440	0,37371	0,33137	0,28449	0,18008	0,10934	0,06559	0,03910	0,01420	0,00514	0,00187
1,00	0,36781	0,36388	0,35737	0,34831	0,32233	0,28749	0,24838	0,15831	0,09575	0,05707	0,03393	0,01201	0,00431	0,00155
2,00	0,09017	0,07903	0,07668	0,07353	0,06537	0,05555	0,04515	0,02212	0,00775	0,00037	−0,00167	−0,00195	−0,00108	$-0{,}495 \cdot 10^{-3}$
5,00	−0,08038	−0,07913	−0,07789	−0,07593	−0,07010	−0,06382	−0,05672	−0,03362	−0,02602	−0,01638	−0,00990	−0,00314	−0,00110	$-0{,}220 \cdot 10^{-3}$

TABLE 4.2b

h \ ε	0,1	0,2	0,3	0,4	0,6	0,8	1,0	1,5	2,0	2,5	3,0	4,0	5,0	6,0
0	0	0	0	0	0	0	0	0	0	0	0	0	0	0
0,05	−0,81525	−0,01856	−0,02812	−0,01517	−0,00208	+0,00359	+0,00581	+0,00601	+0,00112	+0,00296	+0,00191	$+0{,}757\cdot10^{-3}$	$+0{,}29\cdot10^{-3}$	$+0{,}109\cdot10^{-3}$
0,10	−0,13622	−0,08651	−0,05192	−0,02896	−0,00365	+0,00733	+0,01167	+0,01201	+0,00883	+0,00592	+0,00382	+0,00151	$+0{,}579\cdot10^{-3}$	$+0{,}219\cdot10^{-3}$
0,20	−0,14986	−0,11615	−0,07699	−0,01463	−0,00362	+0,01579	+0,02367	+0,02397	+0,01760	+0,01180	+0,00762	+0,00301	+0,00115	$+0{,}436\cdot10^{-3}$
0,40	−0,08191	−0,07105	−0,05143	−0,02763	+0,01393	+0,03470	+0,01953	+0,01755	+0,03172	+0,02225	+0,01500	+0,00593	+0,00227	$+0{,}857\cdot10^{-3}$
0,60	−0,00331	+0,00151	+0,01015	+0,02212	+0,05008	+0,06939	+0,07788	+0,07024	+0,05089	+0,03562	+0,02193	+0,00866	+0,00331	+0,00125
0,80	+0,06573	+0,06914	+0,07328	+0,079187	+0,09332	+0,10392	+0,10718	+0,09113	+0,06553	+0,01378	+0,02818	+0,01111	+0,00125	+0,00160
1,0	+0,12656	+0,12741	+0,12883	+0,13082	+0,13551	+0,13790	+0,13522	+0,11136	+0,07819	+0,05221	+0,03357	+0,01322	+0,00505	+0,00190
2,0	+0,26752	+0,26515	+0,26127	+0,25660	+0,24187	+0,22104	+0,20383	+0,15039	+0,10313	+0,06750	+0,04271	+0,01661	+0,00625	+0,00232
5,0	−0,15872	−0,15723	−0,15481	−0,15151	−0,14281	−0,13196	−0,11992	−0,08938	−0,06323	−0,04328	−0,02897	−0,01236	−0,00503	−0,00199

TABLE 4.2c

k	Re $R(k, 0)$	Im $R(k, 0)$	k	Re $R(k, 0)$	Im $R(k, 0)$
0	1,00000	0	26	+0,07793	+0,00678
1	+0,36865	+0,12594	27	+0,03573	+0,06795
2	+0,03157	+0,26797	28	−0,03719	+0,06559
3	−0,14479	+0,17727	29	−0,07403	+0,00944
4	−0,10802	+0,02067	30	−0,01266	−0,05904
5	−0,03116	−0,15863	31	+0,02620	−0,06671
6	+0,08127	−0,14098	32	+0,06915	−0,01390
7	+0,15050	−0,00765	33	+0,04883	+0,05004
8	+0,09235	+0,11443	34	−0,01575	+0,06657
9	−0,04863	+0,12373	35	−0,06360	+0,02241
10	−0,12365	+0,02477	36	−0,05246	−0,04081
11	−0,08357	−0,08635	37	+0,00587	−0,06534
12	+0,02618	−0,11212	38	+0,05735	−0,03000
13	+0,10121	−0,03712	39	+0,05550	+0,03162
14	+0,08139	+0,06512	40	+0,00335	+0,06301
15	−0,00882	+0,10261	41	−0,05061	+0,03639
16	−0,08320	+0,04634	42	−0,05647	−0,02345
17	−0,08420	−0,04760	43	−0,01175	−0,05970
18	−0,00539	−0,09390	44	+0,04355	−0,04170
19	+0,07401	−0,05350	45	+0,05785	+0,01384
20	+0,08312	+0,03240	46	+0,01937	+0,05554
21	+0,01728	+0,08530	47	−0,03589	+0,04582
22	−0,06161	+0,05930	48	−0,05715	−0,00536
23	−0,05101	−0,01887	49	−0,02627	−0,05056
24	−0,02730	−0,07670	50	+0,02815	−0,04588
25	+0,01875	−0,06314			

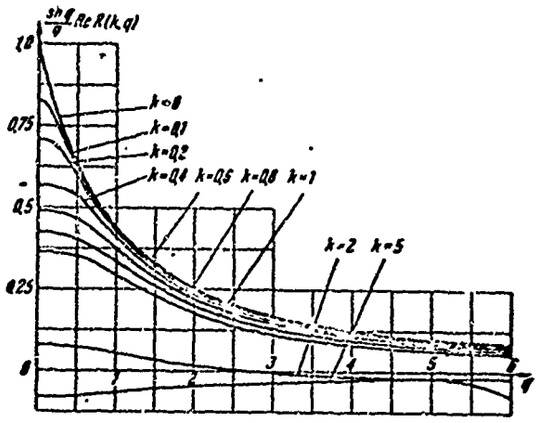


Figure 4.4. Relationship of the real part of function $q^{-1}shqR(k,q)$ to the Strouhal number and the cascade density.

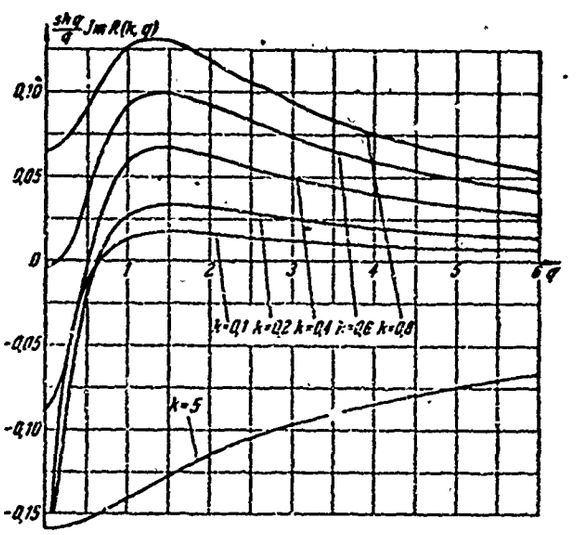


Figure 4.5. Relationship of the imaginary part of function $q^{-1}shqR(k,q)$ to the Strouhal number and the cascade density.

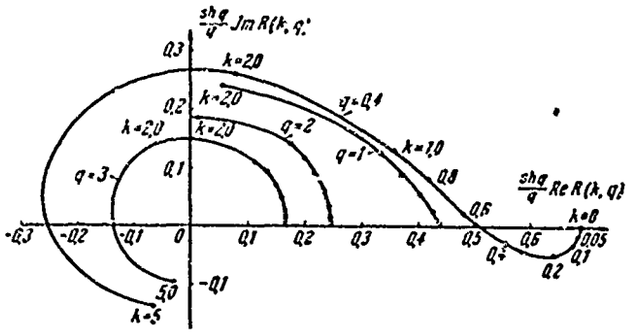


Figure 4.6. Graph of function $q^{-1}\operatorname{sh} qR(k, q)$ in a polar system of coordinates.

We shall consider flow about a straight cascade of plates which oscillate synchronously in phase in a direction perpendicular to the chord. We consider the normal velocities and accelerations of the plates to be given:

$$v_0(\tau) = v_{0e}e^{j\nu\tau}, \quad a_y = j\nu v_{0e}e^{j\nu\tau}$$

Since the normal velocity and acceleration are constant along a plate, the acceleration potential may be given in the following form:

$$w(z) = iA\left[\frac{1}{q}\ln\frac{\operatorname{ch} qz + \sqrt{\operatorname{ch}^2 qz - \operatorname{ch}^2 q}}{\operatorname{ch} q} - z\right] + iB\sqrt{\frac{\operatorname{sh}[q(z-1)]}{\operatorname{sh}[q(z+1)]}}. \qquad (4.47)$$

Here it is assumed that the chord of the plates is 2b = 2, and that the origin of the coordinates is located in the center of one of the plates. The abscissa coincides with the plate. In all transformations we shall be discarding the multiplier $\exp(j\nu\tau)$; and therefore we shall henceforth be considering A and B as complex (with respect to j) constants. Coefficient A is, as before, determined on the basis of the normal acceleration on the plate. Coefficient B, which is now not equal to zero, does not enter in these calculations, since the expression by which it is multiplied will yield only the acceleration component a_x on the plates. This is obvious, since the derivative of the last term, which is the complex acceleration

$$\frac{iqB\sin 2q}{2\operatorname{sh}[q(z+1)]\sqrt{\operatorname{sh}[q(z-1)]\operatorname{sh}[q(z+1)]}}$$

on the sections $y=inl, -1<x<1$ assumes real (with respect to i) values, where n = 0; $\pm$ 1; ...

The derivative of the first term of (4.47) is equal to:

$$iA\left(\frac{\operatorname{sh} qx}{\sqrt{\operatorname{sh}^2 qx-\operatorname{sh}^2 q}}-1\right).$$

On the sections, the imaginary part (with respect to i) of this derivative is equal to -iA.

Since the derivative of the acceleration potential Function (4.47) is equal to the complex acceleration, it is obvious that on the sections the equality

$$A=a_y=jv_0=jkU$$

is valid.

Coefficient B must be selected in such a manner as to satisfy the boundary value for velocity. From Formula (4.9), on the basis of the obtained normal accelerations, we determine the normal velocity on the plates:

$$v_0=jke^{jk}\int_{-\infty}^{-1}\left[\frac{\operatorname{sh} qx}{\sqrt{\operatorname{sh}^2 qx-\operatorname{sh}^2 q}}-1\right]e^{jkx}\,dx+$$

$$+\frac{jkB_0}{U}e^{jk}\int_{-\infty}^{-1}\frac{q\sin 2qe^{jkx}\,dx}{2\operatorname{sh}[q(x+1)]\sqrt{\operatorname{sh}[q(x-1)]\cdot\operatorname{sh}[q(x+1)]}}$$

Here v_0 is the boundary value of the oscillation velocity modulus; the time multiplier is everywhere discarded.

In this case it is assumed that perturbations far in front of the cascade are absent. Since all the plates are under the same conditions, the integral is written for the basic plate, i.e., integration is conducted along the abscissa. The second integral is taken by parts, as has been shown above. After transformation we obtain the expression for B:

$$B = e^{j\nu\tau}\beta_0 = -v_0 U e^{j\nu\tau} T(k, q). \tag{4.48}$$

Here T(k, q) is a function that is complex with respect to j, equal [59] to

$$T(k, q) = \frac{1 + jke^{jk} I_2(k, q)}{e^q + jke^{jk} I_1(k, q)}. \tag{4.49}$$

In the formula the designations are: $I_1(k, q)$ is the improper integral introduced above (4.33); $I_2(k, q)$ is an improper integral defined by the expression

$$I_2(k, q) = \int_1^\infty \left(\frac{\operatorname{sh} qx}{\sqrt{\operatorname{sh}^2 qx - \operatorname{sh}^2 q}} - 1 \right) e^{-jkx}\, dx. \tag{4.50}$$

The pressure distribution along the profile is found by isolating, from the complex acceleration Potential (4.47), the real (with respect to i) part:

$$p = \frac{1}{q} A\rho^0 \arccos \frac{\operatorname{ch} qx}{\operatorname{ch} q} + \rho B \sqrt{\frac{\operatorname{sh}[q(1-x)]}{\operatorname{sh}[q(1+x)]}}. \tag{4.51}$$

The pressures at the upper side and the lower side of the profile are equal in magnitude, but are opposite in sign. The force acting upon the blade is found by integrating (4.51) along the blade contour. The force obtained with integration of the first term is not connected with circulation, but is equal to the attached mass multiplied by the acceleration. Computation of the attached mass for this type of oscillation has already been carried out (4.20). Integration of the second term in (4.51) yields the component of the lift force which depends upon the circulation:

$$\mathcal{Z} = -2\rho^0 v_0 U l e^{j\nu\tau} \operatorname{sh}\left(\frac{\pi b}{l}\right) T(k, q). \tag{4.52}$$

The improper integral entering into the basic function T(k, q) may be expressed in terms of hypergeometric functions. For the integral $I_1(k, q)$ this was done in Formulas (4.33) and (4.38). We break integral $I_2(k, q)$ into a sum of two integrals and, replacing in the first integral the integration variable $\xi = \exp[2q(1-x)]$, we obtain

$$\int_1^\infty \frac{\operatorname{sh}(qx)\, e^{-jkx}\, dx}{\sqrt{\operatorname{sh}^2 qx - \operatorname{sh}^2 q}} = \frac{e^{-jk}}{2q} \int_0^1 (1-\xi)^{-1/2} (1 - e^{-4q}\xi)^{-1/2} (1 - e^{-2q}\xi)\, \xi^{\frac{jk}{2q}-1}\, d\xi. \tag{4.53}$$

The last integral is also broken down into two integrals, each of which is expressed in terms of the hypergeometric function $F(\alpha, \beta, \gamma, z)$ and the beta-function B(a, b)

$$\int_0^1 (1-\xi)^{-1/2} (1 - e^{-4q}\xi)^{-1/2}\, \xi^{\frac{jk}{2q}-1}\, d\xi = B(a, b)\, F(\alpha, \beta, \gamma, z).$$

Here
$$a = \frac{jk}{2q},\ b = \frac{1}{2},\ \alpha = \frac{1}{2},\ \beta = \frac{jk}{2q},$$
$$\gamma = \frac{1}{2} + \frac{jk}{2q},\quad z = e^{-4q}.$$
$$\int_0^1 (1-\xi)^{-1/2} (1 - e^{-4q}\xi)\, \xi^{\frac{jk}{2q}}\, d\xi = B(a', b')\, F(\alpha', \beta', \gamma', z).$$

Here
$$a' = 1 + \frac{jk}{2q},\ b' = \frac{1}{2},\ \alpha' = \frac{1}{2},\ \beta' = 1 + \frac{jk}{2q},$$
$$\gamma' = \frac{3}{2} + \frac{jk}{2q},\quad z = e^{-4q}.$$

With account taken of these expressions, as well as of the expression for the Fourier integral of a unit function, we obtain the formula for determining $I_2(k, q)$:

$$I_2(k, q) = \frac{1}{2q} e^{-jk} \left[B(a, b)\, F(\alpha, \beta, \gamma, z) - e^{-2q} B(a', b')\, F(\alpha', \beta', \gamma', z) - \frac{2q}{jk} \right]. \tag{4.54}$$

We shall consider the interesting limit cases.

(a) A dense cascade. For a dense cascade when $\exp(-q) \ll 1$, in the integrand of (4.53) the second and the third parenthesis may be discarded. Under the same condition, the third parenthesis may be discarded in the integrand of (4.36). It is easy to show [59] that discarding the parentheses is equivalent to assuming $\operatorname{ch} qx = \operatorname{sh} qx = 1/2 \exp qx$, which in the limit is exact, and in practice is fulfilled already under the condition q > 1 when $x \geqslant 1$. Here the integrals $I_1(k, q)$ and $I_2(k, q)$ are reduced to the following form:

$$I_1(k, q) = e^q \int_1^\infty \left(\frac{1}{\sqrt{1 - e^{2q(1-x)}}} - 1 \right) e^{-jkx}\, dx,$$

$$I_2(k, q) = \int_1^\infty \left(\frac{1}{\sqrt{1 - e^{2q(1-x)}}} - 1 \right) e^{-jkx}\, dx.$$

With this taken into consideration, it follows from Formula (4.49) that when $\exp(-q) \ll 1$ the function $T(k, q) = e^{-q}$ does not depend upon the oscillation frequency. Consequently, the lift force acting upon a plate which oscillates without phase shift in a dense lattice is equal to the steady lift force:

$$\mathcal{L} = \rho^0 v_0 U l e^{j\nu\tau}. \tag{4.55}$$

This formula differs from Formula (4.41) only by the multiplier exp(jk), which is not a basic difference, and is explained by the fact that now the argument of the boundary value of the velocity does not change. Consequently, for calculation of the forces acting upon the profiles in a dense cascade which are oscillating in phase, it is possible to employ the equation of momentum directly:

$$\mathcal{L} = \int_\sigma v\rho^0 U\, d\sigma + \int_f \frac{\partial}{\partial\tau}(\rho^0 v)\, df. \tag{4.56}$$

Here U is the velocity of the stabilized main stream, v is the oscillation velocity of the blade in a direction perpendicular to the velocity of the main stream, τ is time, ρ^0 is the density of the fluid; the force $\mathcal{L}$ acts upon the mass of the fluid contained within the closed curve σ which encompasses the area f.

For synchronous and cophasal ($v = v_0 \exp j\nu\tau$) oscillation of plates in a dense cascade without offset we consider the velocity v_0 to be constant in the channel. We integrate along the contour of σ, which is composed of adjacent plates and straight lines connecting their ends, and the area f contained within the contour:

$$\mathcal{L} = \rho^0 l v_0 U e^{j\nu\tau} + 2j\rho^0 b l \nu v_0 e^{j\nu\tau}.$$

Here t is the cascade spacing, 2 b is the chord of the plate.

The first term of the obtained expression coincides with the limit case (4.55). The second term yields the force caused by the attached mass, and can also be obtained from the exact solution (4.20) by a limit transition t/2b → 0.

(b) Stabilized Flow about a Cascade of Arbitrary Density. With stabilized streamline flow, acceleration is absent ($a_y = 0$) and, consequently, A = 0.

From Formula (4.49) it follows that T(0, q) = exp (-q), and then from (4.52) we obtain

$$\mathscr{Y} = -2\pi\rho^0 v_0 U b \frac{\operatorname{sh} q}{q \exp q}.$$

This expression differs from (4.42) only by the sign. The appearance of the minus sign is explained by the fact that when the cascade moves upward, the lift force is directed downwards.

(c) A Single Profile. With an increase without limit of the cascade spacing ($t \to \infty$, $q \to 0$) we obtain the limit values of the integrals:

$$I_1(k, 0) = \int_1^\infty \left(\sqrt{\frac{x+1}{x-1}} - 1\right) e^{-jkx}\, dx,$$

$$I_2(k, 0) = \int_1^\infty \left(\frac{x}{\sqrt{x^2-1}} - 1\right) e^{-jkx}\, dx,$$

which are expressed in terms of the Hankel function in the form

$$\begin{aligned} I_1(k, 0) &= -\frac{\pi}{2}\left[H_1^{(2)}(k) + jH_0^{(2)}(k)\right] - \frac{1}{jk} e^{-jk}, \\ I_2(k, 0) &= -\frac{\pi}{2} H_1^{(2)}(k) - \frac{1}{jk} e^{-jk}. \end{aligned} \tag{4.57}$$

Substituting (4.57) into (4.49), it becomes clear that function T(k, q) passes into the Theodorsen function C(k), which plays a basic part in the study of oscillations of an isolated profile:

$$T(k, 0) = C(k) = \frac{H_1^{(2)}(k)}{H_1^{(2)}(k) + jH_0^{(2)}(k)}. \tag{4.58}$$

The formula for lift force (4.52) when q = 0 passes into the well-known formula for a thin wing [81]:

$$\mathcal{Y} = 2\pi\rho^0 b v_0 U e^{i\omega t} C(k). \tag{4.59}$$

The first cofactors yield the quasi-steady value of the lift force obtained under the assumption that there is no vortex wake. The last cofactor takes into account the unsteadiness of the process and was first defined by Birnbaum in a somewhat different form. Utilizing the expansion of Hankel function with a small value of the argument (4.45), we obtain the limit value of C(k) when k → 0:

$$C(k) \to \left(1 - \frac{\pi k}{2}\right) + jk\left(\ln\frac{k}{2} + \gamma\right), \quad \gamma = 0{,}5772\ldots$$

Analogously, by means of asymptotic formulas we obtain the values of C(k) when k → ∞:

$$C(k) \to \frac{1}{2}\left[\left(1 + \frac{1}{8k^2}\right) - \frac{j}{4k}\right].$$

The values of the real part and the imaginary part of function C(k) = F(k) + jG(k) are presented in Table 4.3.

(d) The Oscillations of a Lattice with a Very Large Strouhal Number. We obtain the asymptotic formula for a very high frequency of the process k → ∞. We return to the basic Formula (4.49). The asymptotic formula for the integral $I_1(k, q)$ was obtained above. We shall make an asymptotic estimate of integral $I_2(k, q)$. For this we shall isolate the singularity at the end of the integration interval. Using trigonometric formulas, we reduce Integral (4.50) to the form

$$I_2(k, q) = \int_1^\infty \left(\frac{\operatorname{sh} qx}{\sqrt{\operatorname{sh}[q(x+1)] \cdot \operatorname{sh}[q(x-1)]}} - 1\right) e^{-jkx}\, dx.$$

Representing sh[q(x-1)] in terms of an infinite product, we obtain

$$I_2(k, q) = \int_1^\infty e^{-jkx} \varphi(x, q)(x-1)^{-1/2}\, dx.$$

TABLE 4.3

h	F	−G	h	F	−G	h	F	−G
0,000	1,00000	0,00000	0,48	0,60259	0,15347	0,98	0,54062	0,10171
0,002	0,99671	0,01258	0,50	0,59795	0,15071	1,00	0,53943	0,10027
0,02	0,96373	0,07521	0,52	0,59359	0,14800	1,1	0,53421	0,09361
0,04	0,92670	0,11600	0,54	0,58953	0,14535	1,2	0,52996	0,08771
0,06	0,89204	0,14259	0,56	0,58572	0,14277	1,3	0,52644	0,08247
0,08	0,86043	0,16040	0,58	0,58215	0,14024	1,4	0,52349	0,07777
0,10	0,83192	0,17230	0,60	0,57880	0,13779	1,5	0,52101	0,07356
0,12	0,80333	0,18007	0,62	0,57565	0,13539	1,6	0,51890	0,06977
0,14	0,78337	0,18489	0,64	0,57269	0,13305	1,7	0,51709	0,06632
0,16	0,76277	0,18757	0,66	0,56989	0,13078	1,8	0,51552	0,06318
0,18	0,74426	0,18867	0,68	0,56725	0,12857	1,9	0,51415	0,06032
0,20	0,72758	0,18862	0,70	0,56476	0,12642	2,0	0,51295	0,05768
0,22	0,71252	0,18772	0,72	0,56240	0,12433	2,5	0,50874	0,04730
0,24	0,69889	0,18619	0,74	0,56017	0,12229	3,0	0,50628	0,04000
0,26	0,68651	0,18420	0,76	0,55806	0,12031	3,5	0,50472	0,03462
0,28	0,67525	0,18188	0,78	0,55605	0,11838	4,0	0,50367	0,03050
0,30	0,66497	0,17932	0,80	0,55415	0,11650	4,5	0,50294	0,02724
0,32	0,65557	0,17659	0,82	0,55234	0,11468	5,0	0,50240	0,02460
0,34	0,64695	0,17376	0,84	0,55062	0,11290	10	0,50062	0,01245
0,36	0,63902	0,17086	0,86	0,54898	0,11117	20	0,50016	0,00625
0,38	0,63172	0,16792	0,88	0,54741	0,10949	30	0,50007	0,00417
0,40	0,62498	0,16498	0,90	0,54593	0,10785	40	0,50004	0,00312
0,42	0,61874	0,16206	0,92	0,54451	0,10626	50	0,50003	0,00250
0,44	0,61296	0,15915	0,94	0,54315	0,10470	100	0,50001	0,00125
0,46	0,60759	0,15629	0,96	0,54186	0,10319	∞	0,50000	0,00000

Here the function $\varphi(x, q)$, has been introduced which has no singularities in the integration interval. It is defined by the formula

$$\varphi(x, q) = \frac{\operatorname{sh} qx}{\sqrt{q \prod_{n=1}^{\infty} \left[1 + \frac{q^2 (x-1)^2}{n^2 \pi^2}\right] \frac{1}{x+1}}} - \sqrt{x-1}.$$

Omitting further operations, which are analogous to those carried out in estimating integral $I_1(k, q)$, we reduce the final expression to the form

$$I_2(k, q) = j\Gamma(1/2) e^{-3j\pi/4} \frac{\operatorname{sh} q}{\sqrt{q \operatorname{sh} 2q}} e^{-jk} + O(k^{-1}), \; k \to \infty.$$

We shall obtain the resultant formula for $T(k, q)$ when $k \to \infty$ from (4.49), using the asymptotic estimates of integrals $I_1(k, q)$ and $I_2(k, q)$:

$$T(k, q) \sim \frac{1 + \operatorname{sh} q \sqrt{\frac{\pi k}{q \operatorname{sh} 2q}} e^{j\pi/4}}{e^q + \sqrt{\pi k \cdot \frac{\operatorname{sh} 2q}{q}} e^{j\pi/4}}, \; k \to \infty.$$

Let us consider special cases of this formula. For a single profile ($q = 0$) with a very high relative oscillation frequency ($k \to \infty$) we obtain the known value $T(k, 0) \to 1/2$. For a very dense cascade $\exp(-q) \ll 1$, with a supplementary condition concerning the smallness of the Strouhal number computed on the basis of cascade spacing $k/q \to 0$, we find $T(k, q) \to \exp(-q)$. This agrees with the derivation obtained above in another way.

We return to the general case. The value of function $I_2(k, q)$ enters into many problems dealing with unsteady flow about cascades. The real and imaginary parts of $I_2(k, q)$, computed on an electronic digital computer directly on the basis of (4.50), are presented in Table 4.4 (a, b). The calculations may also be made by taking advantage of the expression of the integral in terms of the hypergeometric function on the basis of (4.54).

The lift force acting upon a vibrating plate in the cascade may be defined by (4.52). It is convenient to reduce (4.52) to the form

$$\mathcal{Y} = -2\pi\rho^0 v_0 b U \frac{\operatorname{sh} q}{q} T(k, q).$$

TABLE. 4.4a

a \ σ	0,1	0,2	0,3	0,4	0,5	0,6	1,0	1,5	2,0	2,5	3,0	4,0	5,0	6,0
0	3,30058	2,73437	2,40311	2,19566	1,96597	1,87216	1,86025	2,06871	2,56227	3,38059	4,64523	9,47173	20,60011	46,6896
0,05	3,27679	2,70846	2,38927	2,18637	1,96017	1,86765	1,85631	2,06504	2,55812	3,37540	4,63834	9,45828	20,57161	46,6061
0,10	3,06665	2,63428	2,34857	2,15879	1,94286	1,85416	1,84453	2,05405	2,54567	3,35983	4,61769	9,41798	20,48622	46,4160
0,20	2,54668	2,38111	2,19738	2,05306	1,87496	1,80069	1,79779	2,01034	2,49611	3,29781	4,53542	9,25737	20,14565	45,6580
0,40	1,89890	1,73652	1,72510	1,68991	1,62328	1,59783	1,61735	1,83954	2,30162	3,05396	4,21155	8,62141	18,80362	42,8678
0,60	1,06395	1,13847	1,19381	1,22820	1,26217	1,29139	1,33825	1,56870	1,99048	2,66221	3,69032	7,60261	16,63407	37,8308
0,80	0,54062	0,62059	0,69290	0,75479	0,84778	0,91861	0,98786	1,21688	1,58111	2,14358	2,99714	6,23963	13,73513	31,3601
1,00	0,03364	0,17064	0,24312	0,31031	0,42470	0,51628	0,59661	0,80778	1,09726	1,52557	2,16757	4,60014	10,23744	23,5405
2,00	−1,21143	−1,17658	−1,14821	−1,12593	−1,09806	−1,09058	−1,10239	−1,21669	−1,46157	−1,86730	−2,49329	−4,85903	−10,22850	−22,6182
5,00	0,79693	0,77911	0,77200	0,76941	0,77721	0,80150	0,84162	1,01063	1,28794	1,70184	2,31826	4,54772	9,46120	20,5528

TABLE 5.4b

λ \ φ	0,1	0,2	0,3	0,4	0,6	0,8	1,0	1,5	2,0	2,5	3,0	4,0	5,0	6,0
0	0	0	0	0	0	0	0	0	0	0	0	0	0	0
0,05	−0,10039	−0,28512	−0,21163	−0,17105	−0,13749	−0,12177	−0,11536	−0,11983	−0,14308	−0,18151	−0,21956	−0,49867	−1,07089	−2,10494
0,10	−0,89223	−0,55510	−0,41765	−0,31522	−0,27374	−0,21275	−0,23017	−0,23919	−0,28567	−0,36812	−0,49839	−0,99586	−2,13879	−4,80330
0,20	−1,38126	−1,00805	−0,79111	−0,66858	−0,53716	−0,47920	−0,45550	−0,47158	−0,56737	−0,73211	−0,99068	−1,98027	−4,25363	−9,55363
0,10	−1,77091	−1,31216	−1,31215	−1,19036	−1,00231	−0,91021	−0,87318	−0,91933	−1,10346	−1,42676	−1,93303	−3,86925	−8,31739	−18,6901
0,00	−1,89826	−1,76461	−1,63162	−1,51302	−1,31796	−1,25623	−1,22231	−1,30709	−1,57910	−2,01868	−2,78130	−5,58008	−12,0101	−27,6093
0,80	−1,90698	−1,82692	−1,75099	−1,67768	−1,56140	−1,49620	−1,48636	−1,61569	−1,96921	−2,56683	−3,49177	−7,03150	−15,1677	−34,1490
1,00	−1,83366	−1,78869	−1,74708	−1,71001	−1,65171	−1,62528	−1,63689	−1,82918	−2,25129	−2,95614	−4,03981	−8,16660	−17,6507	− 39,7988
2,00	−0,71555	−0,77031	−0,79759	−0,82873	−0,89982	−0,98139	−1,08353	−1,11123	−1,39364	−2,03017	−3,72652	−7,87018	−17,4156	−39,9817
5,00	+0,57060	+0,58123	+0,59527	+0,61480	+0,65879	+0,72031	+0,79884	+1,08325	+1,53229	+2,22051	+3,26679	+7,28334	+16,7063	+29,1505

The real and imaginary values of function T(k, q) are presented in Table 4.5. The graph of the real part of function $\frac{\mathrm{sh}\, q}{q} T(k, q)$ is presented in Figure 4.7. With a cascade density of $q = \pi b/l > 2$, the curves corresponding to different values of Strouhal numbers k = γb/U coincide. The reason for this was explained above.

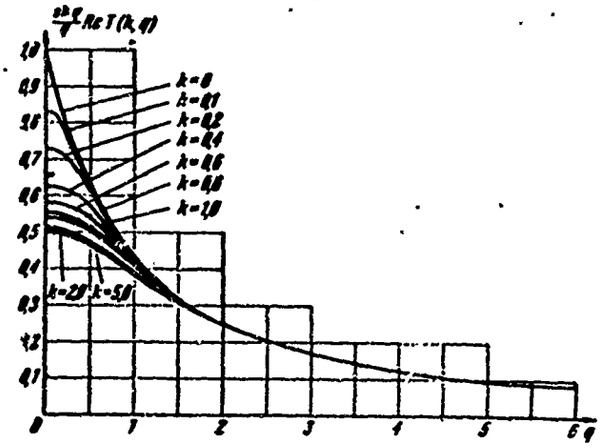


Figure 4.7. Relationship of the real part of function $q^{-1} \mathrm{sh}\, q\, T(k, q)$ to the Strouhal number and the cascade density.

A graph of the imaginary part of T(k, q) is given in Figure 4.8. Here it can be seen that when q > 2, the imaginary parts are small. In Figure 4.9 the latter relationship is reconstructed; the Strouhal number is plotted as the argument along the abscissa. This makes the graph easier to visualize. The relationship corresponding to the limit case q = 0 (an isolated wing) is also plotted on the basis of the data of Table 4.3.

We shall finish our study of the problem of the oscillations of a cascade without phase shift with a comparison of the numerical results obtained by various authors. In Figures 4.10 and 4.11 the solution under consideration is compared with data obtained from four known studies.

TABLE 4.5a

k \ q	0,1	0,2	0,3	0,4	0,6
0	0,90184	0,81873	0,74082	0,67032	0,54881
0,05	0,88082	0,80017	0,73521	0,66789	0,54804
0,10	0,82822	0,78106	0,72338	0,66095	0,54576
0,20	0,72827	0,71720	0,66351	0,63752	0,53745
0,40	0,62399	0,61905	0,60023	0,58267	0,51322
0,60	0,57745	0,57119	0,56033	0,54307	0,48992
0,80	0,55262	0,54599	0,53183	0,51885	0,47239
1,00	0,53792	0,53115	0,51970	0,50398	0,46014
2,00	0,51035	0,50375	0,49196	0,47613	0,43480
5,00	0,50112	0,49373	0,48185	0,46600	0,42866

k \ q	0,5	1,0	1,5	2,0	2,5
0	0,44933	0,36788	0,22313	0,13533	0,08208
0,05	0,41905	0,36777	0,22312	0,13533	0,08208
0,10	0,41824	0,36716	0,22299	0,13533	0,08208
0,20	0,41515	0,36527	0,22297	0,13532	0,08209
0,40	0,43505	0,36209	0,22250	0,13528	0,08209
0,60	0,42847	0,35576	0,22183	0,13522	0,08210
0,80	0,41323	0,35146	0,22103	0,13512	0,08210
1,00	0,40511	0,34680	0,22019	0,13501	0,08209
2,00	0,38533	0,33328	0,21617	0,13115	0,08187
5,00	0,37678	0,32650	0,21385	0,13318	0,08179

k \ q	3,0	4,0	5,0	6,0
0	0,04979	0,01832	0,00674	0,00218
0,05	0,04979	0,01832	0,00674	0,00248
0,10	0,04979	0,01832	0,00674	0,00218
0,20	0,04979	0,01832	0,00674	0,00218
0,40	0,04979	0,01832	0,00674	0,00218
0,60	0,04980	0,01832	0,00674	0,00248
0,80	0,04981	0,01833	0,00674	0,00248
1,00	0,04982	0,01833	0,00674	0,00248
2,00	0,04974	0,01830	0,00674	0,00248
5,00	0,04977	0,01833	0,00674	0,00248

TABLE 4.5b

h \ q	0,1	0,2	0,3	0,4	0,5
0	0	0	0	0	0
0,05	−0,08737	−0,05296	−0,03372	−0,02206	−0,00987
0,10	−0,11383	−0,09563	−0,0[illegible]387	−0,01257	−0,01933
0,20	−0,17804	−0,14393	−0,10553	−0,07499	−0,03[illegible]13
0,40	−0,16105	−0,14821	−0,12617	−0,10037	−0,05[illegible]78
0,60	−0,13553	−0,12797	−0,11529	−0,09853	−0,06281
0,80	−0,11490	−0,10945	−0,10052	−0,08[illegible]7	−0,05123
1,00	−0,09639	−0,09144	−0,08782	−0,07857	−0,05391
2,00	−0,05515	−0,05354	−0,05221	−0,04940	−0,03563
5,00	−0,02226	−0,02157	−0,02010	−0,01845	−0,01455

h \ q	0,6	1,0	1,5	2,0	2,5
0	0	0	0	0	0
0,05	−0,00457	−0,00216	$-0{,}352 \cdot 10^{-3}$	$-0{,}608 \cdot 10^{-4}$	$-0{,}110 \cdot 10^{-4}$
0,10	−0,00901	−0,00423	$-0{,}701 \cdot 10^{-3}$	$-0{,}121 \cdot 10^{-3}$	$-0{,}215 \cdot 10^{-4}$
0,20	−0,01732	−0,00831	−0,00138	$-0{,}240 \cdot 10^{-3}$	$-0{,}423 \cdot 10^{-4}$
0,40	−0,02933	−0,01497	−0,00252	$-0{,}458 \cdot 10^{-3}$	$-0{,}793 \cdot 10^{-4}$
0,60	−0,03579	−0,01915	−0,00355	$-0{,}639 \cdot 10^{-3}$	$-0{,}104 \cdot 10^{-3}$
0,80	−0,03715	−0,02116	−0,00428	$-0{,}765 \cdot 10^{-3}$	$-0{,}115 \cdot 10^{-3}$
1,00	−0,03[illegible]1	−0,02162	−0,00466	$-0{,}814 \cdot 10^{-3}$	$-0{,}111 \cdot 10^{-3}$
2,00	−0,02543	−0,01672	−0,00447	$-0{,}846 \cdot 10^{-3}$	$-0{,}433 \cdot 10^{-3}$
5,00	−0,01058	−0,00714	−0,00198	$-0{,}241 \cdot 10^{-3}$	$+0{,}149 \cdot 10^{-3}$

h \ q	3,0	4,0	5,0	6,0
0	0	0	0	0
0,05	$-0{,}204 \cdot 10^{-5}$	$-0{,}743 \cdot 10^{-7}$	$-0{,}218 \cdot 10^{-6}$	$+0{,}178 \cdot 10^{-6}$
0,10	$-0{,}404 \cdot 10^{-5}$	$-0{,}132 \cdot 10^{-6}$	$+0{,}111 \cdot 10^{-6}$	$+0{,}224 \cdot 10^{-6}$
0,20	$-0{,}768 \cdot 10^{-5}$	$-0{,}138 \cdot 10^{-6}$	$+0{,}455 \cdot 10^{-7}$	$+0{,}194 \cdot 10^{-7}$
0,40	$-0{,}123 \cdot 10^{-4}$	$+0{,}695 \cdot 10^{-6}$	$+0{,}122 \cdot 10^{-6}$	$+0{,}153 \cdot 10^{-6}$
0,60	$-0{,}116 \cdot 10^{-4}$	$+0{,}324 \cdot 10^{-5}$	$+0{,}138 \cdot 10^{-6}$	$+0{,}487 \cdot 10^{-6}$
0,80	$-0{,}432 \cdot 10^{-5}$	$+0{,}782 \cdot 10^{-5}$	$+0{,}303 \cdot 10^{-5}$	$+0{,}106 \cdot 10^{-5}$
1,00	$+0{,}908 \cdot 10^{-5}$	$+0{,}142 \cdot 10^{-4}$	$+0{,}530 \cdot 10^{-5}$	$+0{,}184 \cdot 10^{-5}$
2,00	$+0{,}715 \cdot 10^{-4}$	$+0{,}102 \cdot 10^{-4}$	$+0{,}142 \cdot 10^{-4}$	$+0{,}486 \cdot 10^{-5}$
5,00	$+0{,}172 \cdot 10^{-3}$	$+0{,}906 \cdot 10^{-4}$	$+0{,}303 \cdot 10^{-4}$	$+0{,}110 \cdot 10^{-4}$

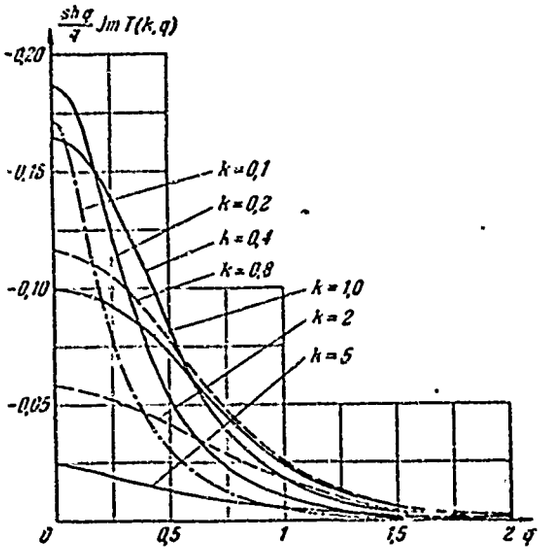


Figure 4.8. Relationship of the imaginary part of function $q^{-1}\,sh\,qT(k,q)$ to the Strouhal number and the cascade density.

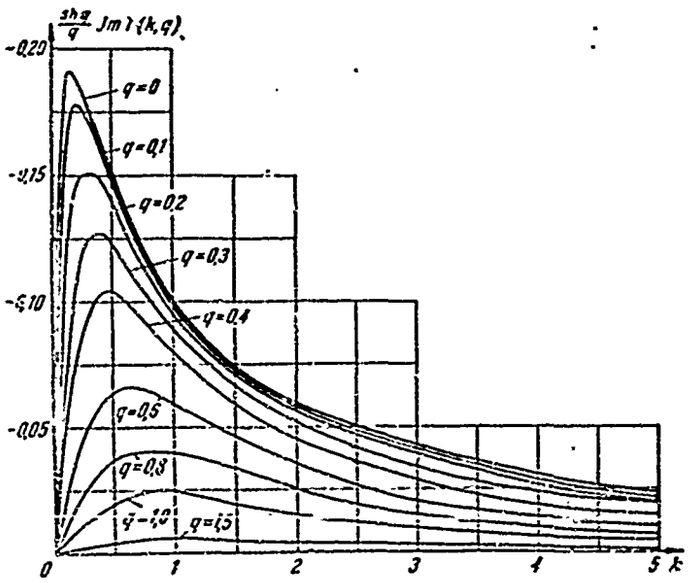


Figure 4.9. Relationship of the imaginary part of function $q^{-1}\,sh\,qT(k,q)$ to the Strouhal number and the cascade density.

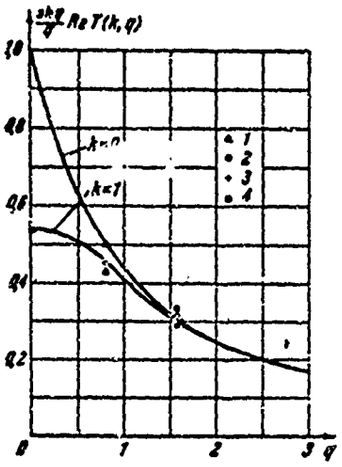


Figure 4.10. Comparison of results of the calculation of function $q^{-1}\operatorname{sh} q\,T(k, q)$ by various authors. The solid curve is plotted according to Formula (4.49), (1)-according to [6], (2)-according to [145], (3)-according to [132], (4)-according to D. N. Gorelov.

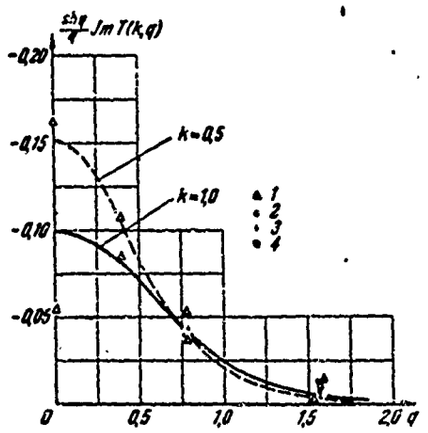


Figure 4.11. Comparison of results of the calculation of function $q^{-1}\operatorname{sh} q\,\operatorname{Im} T(k, q)$ by various authors. The solid curve is plotted according to Formula (4.49), (1)-according to [6], (2)-according to [145], (3)-according to [132], (4)-according to D. N. Gorelov.

Problems dealing with torsional oscillations of plates may be considered with application of the expansion of the complex acceleration potential into Series (4.17).

Let us consider cophasal torsional oscillations of the blades in a cascade in the same formulation as in the case of translational vibration. Let the blades oscillate according to the law

$$y = y_0 x e^{j\omega t}. \tag{4.60}$$

Here y0 is the oscillation amplitude of the ends of the plate.

The normal component of the stream velocity at the profile depends upon the instantaneous velocity and the instantaneous position of the plate in accordance with the formula

$$v = y_0 U (1 + jkx) e^{j\omega t}. \tag{4.61}$$

The normal acceleration component will be equal to

$$a_y = jv\upsilon + U\frac{\partial \upsilon}{\partial x} = jy_0 kU^2(2 + jkx)e^{jvt}. \tag{4.62}$$

We shall show that even for dense cascades, it is possible to be restricted in the complex acceleration potential to the first two terms of Series (4.17) in the solution:

$$w = i\sum_{n=1}^{2} A_n [F(z, q) - z]^n + iB \sqrt{\frac{\operatorname{sh}[q(z-1)]}{\operatorname{sh}[q(z+1)]}}. \tag{4.63}$$

We find the complex acceleration by differentiation with respect to z:

$$a = \frac{dw}{dz} = iA_1\frac{dw_1}{dz} + iA_2\frac{dw_2}{dz} + iB\frac{dw_3}{dz}, \tag{4.64}$$

where w_1, w_2 and w_3 represent the corresponding parts of complex acceleration potential (4.30)

The normal acceleration component at the profile is found by isolating the imaginary part of Expression (4.64). The third term in (4.64) was found above and it was shown that it assumes real values on plates. The imaginary parts of the first term and the second term can be found with the aid of the formulas of Section 4.3:

$$a_y = -A_1 - 2A_2\left(\frac{\operatorname{sh} qx}{q\sqrt{\operatorname{sh}^2 q - \operatorname{sh}^2 qx}}\arcsin\frac{\sqrt{\operatorname{sh}^2 q - \operatorname{sh}^2 qx}}{\operatorname{ch} q} + x\right).$$

In the limit case of a cascade with an infinitely large spacing (q = 0), the expression in parenthesis passes into 2x, i.e., on the basis of (4.62) it can give an exact solution of the problem for an isolated wing. However, it is easy to notice that the function in parentnesis is close to a linear one, i.e., it yields a practically exact solution even in the case of a dense cascade.

This is confirmed by the graph presented in Figure 4.12, where the value of a_{y2} is plotted in terms of fractions of the value of this function at the edges of the plate:

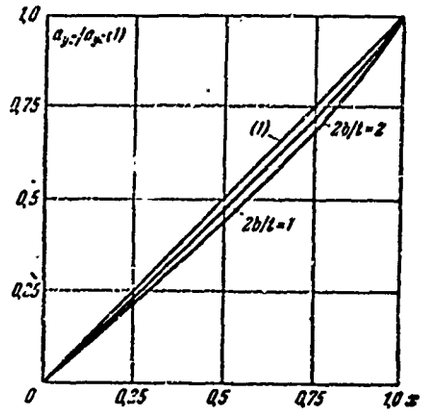


Figure 4.12. Comparison of the precise relationship of normal accelerations at a plate in the case of torsional oscillation (1) with approximate curves computed for cases of 2b/t = 1 and 2b/t = 2.

$$a_{y2}(1) = 2\left(1 + \frac{1}{q}\,\mathrm{th}\,q\right). \qquad (4.65)$$

Then the coefficients A_n in the expression for the complex potential are determined on the basis of the known boundary acceleration (4.62):

$$A_1 = -2jy_0kU^2e^{jvt},$$

$$A_2 = \frac{1}{2}\frac{q}{q+\mathrm{th}\,q}\,y_0k^2U^2e^{jvt}.$$

The coefficient B in (4.63) must be defined in such a manner as to satisfy the normal velocities at the plates. Employing (4.9) and utilizing (4.63), (4.64), (4.10), and (4.65), we obtain

$$B = -y_0U^2e^{jvt}\frac{1 - jk + 2jke^{jk}I_1 + \frac{1}{2}jk^2q\,(q+\mathrm{th}\,q)^{-1}I_3}{1 + jke^{jk}I_2}.$$

Here functions $I_1(k, q)$ and $I_2(k, q)$ were introduced above, and function $I_3(k, q)$ is expressed by the integral:

$$I_3(k, q) = \int_1^\infty \left[\frac{1}{q}\ln\left(\mathrm{ch}\,qx + \sqrt{\mathrm{sh}^2qx - \mathrm{sh}^2q}\right) - x\right]^2 e^{-jkx}\,dx.$$

The pressure distribution on the vibrating profiles is found by isolating the imaginary part (with respect to i) from (4.63):

$$p = \rho^0(A_1 - 2jI_2x)\frac{1}{q}\arcsin\frac{\sqrt{\mathrm{sh}^2q - \mathrm{sh}^2qx}}{\mathrm{ch}\,q} + \rho^0B\sqrt{\frac{\mathrm{sh}\,[q\,(1-x)]}{\mathrm{sh}\,[q\,(1+x)]}}. \qquad (4.66)$$

Integration of the first term of (4.66) along the plate contour yields the force in phase with the acceleration, the action of which is reduced to the effect of the attached moment of inertia. Integration of the second term yields the component of the force which depends upon the circulation:

$$\mathscr{L} = 2\rho^0 B \frac{l}{b} \operatorname{sh} \frac{\pi b}{l}.$$

In Reference [59] approximate methods for solving the problem of oscillation of the plates in a cascade in counterphase are also considered.

§ 4.6. Solution of the Problem of Unsteady Flow about a Cascade by the Vortex Method.

The vortex method considered in this section permits the problem to be reduced to an integral equation which is solved on an electronic digital computer. The advantage of the method consists in the fact that the equations for the case of a cascade with offset are easily derived, and in the case of oscillation of the plates with an arbitrary phase shift only the computation work increases. The drawback consists in the impossibility of carrying out analysis in a general form, as also in all cases solved by the numerical method. The vortex method has been used in the studies of Sisto [137], Whitehead [145], S. M. Belotserkovskiy, A. S. Ginevskiy, and Ya. Ye. Polonskiy [6], and others. The most detailed results are available in the work by Whitehead.

Studies based upon the utilization of vortex schemes are distinguished by the method of compiling the integral equations and by the calculation programs. It is possible to utilize schemes consisting of discrete vortices or of a continuous vortex sheet. The kernel of the integral equation may be constructed by various methods: (1) as a singularity cascade which has the same spacing and offset angle as the cascade being calculated, (2) as the above singularity cascade with the addition of an infinite vortex sheet behind each vortex, etc.

Let us consider an aerodynamic cascade with the offset γb, consisting of plates with a chord of 2b, situated with a spacing of t. In some cases it will be more convenient to speak of the complex

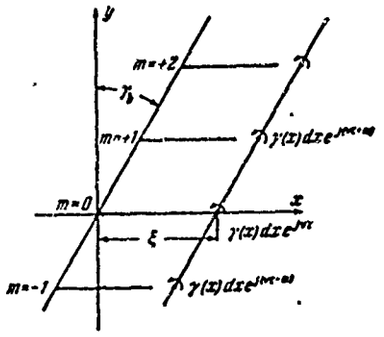


Figure 4.13. A plate cascade and a vortex cascade having the same spacing and the same offset.

spacing $l\exp(i\gamma_b)$. We shall place the origin of the coordinates at the leading edge of one of the profiles (Figure 4.13), to which we shall assign the number m = 0 and which we shall call the basic profile. We shall formulate the problem of unsteady flow about the cascade under the assumption that the profiles oscillate (and in the general case are deformed) according to a harmonic law with respect to time in such a manner that between adjacent profiles there is a phase shift α, constant from profile to profile. We shall solve the problem in a linear formulation with the same assumptions that had been made above.

The vertical velocity at the m^{th} profile $v_m(x, y, \tau)$ may be expressed in terms of the velocity of the basic profile:

$$v_m(x, y, \tau) = v_{0m}(x, y)e^{j\nu\tau} = v_0(x)e^{j\nu(\tau - m\theta)}. \qquad (4.67)$$

Here $v_0(x)$ is the given distribution function of the oscillation-velocity modulus or the deformation of the basic profile, ν is the circular frequency of the oscillations, τ is time.

It is obvious that the flow field will be described by a periodic function with a period equal to $Nl\exp(j\gamma_b)$, where $N = 2\pi/\alpha$ is the number of blades in a period (in real cases N is an integer, since the two-dimensional cascade under consideration is a cross section of an annular cascade which has a finite number of blades).

In view of the fact that in the general case the circulation about the blades changes within time, vortex wakes will originate behind the blades, formed by free vortices, which are carried away

by the stream with the basic velocity U which is parallel to the abscissa. It is obvious from what has been said that if there is an elementary vortex with a circulation of $\gamma(x)\exp(j\nu\tau)dx$, on the basic profile or in its wake, it follows that at all similar points $x_m=x+ml\sin\gamma_0$, $y_m=y+ml\cos\gamma_0$ vortices with a circulation of $\gamma(x)\exp j(\nu\tau+mu)dx$ must be present. In other words, the elementary-vortex cascade must have the same complex spacing as the profile cascade, and the intensity of the vortices must change with the same phase shift.

From the cascades of elementary vortices, we shall furthermore construct a complete vortex system which originates during unsteady flow about a plate cascade. Then it is obvious that when the boundary conditions on the basic profile are satisfied, the boundary conditions on the remaining profiles are satisfied automatically, since the flow field is periodic. A cascade of elementary vortices may be recorded by a single coordinate ζ — the distance of the basic elementary vortex from the origin of the coordinates. Since we are interested in vertical velocity, induced only on the basic profile, the point at which the velocity is determined is also measured by only a single coordinate x.

We introduce the function $K(x,\xi)$, which determines the vertical velocity at point x from the unit-intensity vortex at point ξ. We shall employ such terminology for the sake of contraction, since it would be more correct to speak of the determination of vertical velocity at point x, y = 0 and all similar points $x_m=x+ml\sin\gamma_0$, $y_m=ml\cos\gamma_0$ from the vortex cascade measured by the coordinate ξ. The function $K(x, \xi)$ determines the reaction at point x from a unit perturbation at point ξ.

To proceed, we shall take up the physical considerations and the construction of a vortex system for this problem. Two approaches are possible, which are based upon different descriptions of the aerodynamic phenomena [48]. These two methods were proposed even before the theory of unsteady flow about a single wing was developed:

the first method was used by Birnbaum, and then by Kuessner, while the second method was developed by Karman and Sears.

In brief, the idea of the methods is contained in the following. In the first method the vorticity is broken down into attached vorticity γ_0, free vorticity situated at the profile ε_0, and free vorticity situated in the wake ε_1. The attached vorticity consists of attached Zhukovskiy vortices and determines the force acting upon the profile. The free vorticity ε_0 consists of the free vortices carried away by the stream and, at a given moment, situated at the blade contour. The free vorticity in the wake is formed by all the free vortices trailing from the profile.

In the method of Karman and Sears the vorticity is also broken down into three components: quasi-steady vorticity at the profile γ_0', vorticity induced at the profile by the vortex wake γ_1, and free vorticity in the wake ε_1. Quasi-steady vorticity is called the vorticity which originates at the profile if its movement according to a given law is considered, but in the absence of a vortex wake. Vorticity γ_1 is induced at the profile by the vortex wake and is selected in such a manner as to satisfy the zero boundary values with respect to normal velocity at the profile. In other words, γ_1 is the vorticity which must be inevitably present on a motionless profile about which flows a perturbed stream brought about by the vortex wake in addition to the main stream.

The two methods naturally yield identical final results and, consequently, the total vorticity at the profile must be equal to $\gamma_0+\varepsilon_0=\gamma_0'+\gamma_1$. The Karman-Sears method is advantageous when it is possible, in the general case, to express γ_1 in terms of ε_1.

We shall compile the equation of unsteady flow about a cascade on the basis of the first method and Reference [145]. In the case of steady streamline flow, the profile may be replaced by attached vorticity $\gamma(x)$ which does not depend upon time, and the problem consists in determining function $\gamma(x)$, which satisfies the boundary

conditions with respect to normal velocity. In the case of unsteady flow the pattern becomes more complex, since the attached vorticity $\gamma(x,\tau)$ changes within time and, consequently, free vorticity is formed at the profile. This free vorticity is continuously carried away along the profile by the main stream and, having come off the trailing edge, forms a vortex wake. The change of the attached vorticity at an arbitrary point x of the profile during the small amount of time $\Delta\tau$ is equal to $(\partial\gamma/\partial\tau)\Delta\tau$. As a result of this free vorticity is formed, which is distributed over the sector from x to $x + \Delta x$. The total change of the vorticity must be equal to zero; consequently,

$$\frac{\partial\gamma(x,\tau)}{\partial\tau}\Delta\tau = -\varepsilon(x,\tau)\Delta x.$$

Since Δx is the path traveled by the fluid during the time $\Delta\tau$ with a velocity of U, it follows that

$$\varepsilon(x,\tau) = -\frac{1}{U}\frac{\partial\gamma(x,\tau)}{\partial\tau}. \qquad (4.68)$$

Since vorticity ε is free, it is carried away by the stream with a velocity U without changing its intensity. This means that the free vorticity formed at the moment of time τ at the point x_1 reaches the point $x > x_1$ at the moment of time $\tau+(x-x_1)/U$, or, on the contrary, free vorticity formed at points $x_1 < x$ at the moment of time $\tau-(x-x_1)/U$ arrives at point x simultaneously. Consequently, the free vorticity at point x in the moment of time τ will be expressed by the integral, taken from the leading edge to the observation point:

$$\varepsilon(x,\tau) = -\frac{1}{U}\int_0^x \frac{\partial}{\partial\tau}\gamma\left(x_1, \tau-\frac{x-x_1}{U}\right)dx_1.$$

We consider the harmonic dependence upon time,

$$\gamma(x,\tau) = \gamma(x)\exp j\nu\tau, \quad \varepsilon(x,\tau) = \varepsilon(x)\exp j\nu\tau,$$

We introduce the Strouhal number $k = \nu b/U$, and assume a semichord as the unit of length. Then after simple transformations, we obtain the expression for free vorticity at any point of the plate:

$$\varepsilon(x) = -jke^{-jkx}\int_0^x \gamma(x_1)e^{jkx_1}dx_1. \tag{4.69}$$

The vorticity running off the trailing edge (x = 2) is equal to

$$\varepsilon(2) = -jke^{-jk2}\int_0^2 \gamma(x_1)e^{jkx_1}dx_1. \tag{4.70}$$

If the point at which the free vorticity is determined lies in the vortex wake, i.e., $x > 2$, it follows that the value of the preceding integral will not change, since when $x_1 > 2$ we have $\gamma(x_1) = 0$ (attached vorticity exists only at the profile). From this it follows that the free vorticity in the wake constitutes a traveling wake, since when $x > 2$ we obtain

$$\varepsilon(x) = \varepsilon(2)e^{jk(2-x)}. \tag{4.71}$$

Utilizing the function $K(x, \xi)$, we determine the normal velocity induced at the main profile:

$$v(x) = \int_0^2 \gamma(\xi)K(x, \xi)d\xi + \int_0^2 \varepsilon(\xi)K(x, \xi)d\xi + \int_2^\infty \varepsilon(\xi)K(x, \xi)d\xi. \tag{4.72}$$

Here the integrals express the normal velocity induced, respectively, by the attached vorticity, free vortices moving along the profile, and free vortices situated in the vortex wake.

Then, utilizing Formulas (4.69) - (4.71), from Formula (4.72) we find the integral equation of the problem:

$$v(x) = \int_0^2 \gamma(\xi)K(x, \xi)d\xi - jk\int_0^2 e^{-jk\xi}K(x, \xi)d\xi\int_0^\xi \gamma(x_1)e^{jkx_1}dx_1 - \\ - e^{j2k}\int_0^2 \gamma(x_1)e^{jkx_1}dx_1\int_2^\infty e^{-jk\xi}K(x, \xi)d\xi. \tag{4.73}$$

Here function v(x) is regarded as being the known one, and function $\gamma(x)$ as the desired one. During the solution, it must be required that the value of the vorticity at the trailing edge of the profiles be finite. If a function corresponding to a single vortex $K(x, \xi) =$

$-(x-\xi)^{-1}(2\pi)^{-1}$, is selected as the function $K(x, \xi)$ integral Equation (4.73) will pass into Birnbaum's equation for unsteady flow about a single profile. For solution of the problem of unsteady flow about a profile cascade, $K(x \quad \xi)$ should be selected as follows for vortex cascade (3.3):

$$K(x)=\operatorname{Re}\left[\frac{\pi}{t_1}\frac{\operatorname{ch}\left[(\pi-\alpha)\frac{\xi}{t_1}\right]}{\operatorname{sh}\pi x/t_1}-ij\frac{\pi}{t_1}\frac{\operatorname{sh}\left[(\pi-\alpha)\frac{x}{t_1}\right]}{\operatorname{sh}\pi x/t_1}\right]. \tag{4.74}$$

Here, for the sake of brevity, we do not isolate the real part and the imaginary part.

If in integral Equation (4.73) the last two integrals, which take into account the influence of the free vortices, are defined, we shall obtain the equation for the steady-state problem of flow about a cascade. The equation for unsteady streamline flow may be reduced to an analogous form by substituting the kernel.

Let us assume that a unit singularity cascade is given, which is determined by the coordinate ξ. This may be expressed in terms of the Dirac delta function $\gamma=\delta(x-\xi)$. This cascade of attached vortices will bring about the formation of infinite vortex wakes, with the wake at the basic profiles starting at point $x = \xi$. Then the intensity of the wake is defined by means of a formula analogous to Formula (4.70):

$$\varepsilon(x)=-jke^{-jk(x-\xi)}, \quad \xi>x.$$

We define the normal velocity induced at the basic profile by a unit singularity, located at point ξ, and by its vortex wake:

$$v(x, \xi)=K(x, \xi)-jke^{-jkx}\int_{-\infty}^{\xi}e^{jk\xi}K(x, \xi)\,d\xi. \tag{4.75}$$

Here the kernel is obtained from (4.74) by the replacement of x by $x - \xi$. We assume this function to be the kernel of the integral equation $v(x,\xi)=H(x,\xi)$. Then it is obvious that the distribution of

normal velocities on the basic profile, induced by the attached vorticity and by the wake engendered by it, will be expressed by the integral

$$v(x) = \int_0^2 \gamma(\xi) H(x, \xi)\, d\xi. \tag{4.76}$$

The obtained integral equation must be solved for $\gamma(x)$ with a given distribution law of normal velocities $v(x)$. Kernel $H(x, \xi)$ undergoes a discontinuity at point $x = \xi$; therefore, it is necessary to speak of the principal value of the integral.

We obtain the formulas for calculating the force and the moment acting upon the profile in the cascade. The pressure distribution along the plate is determined on the basis of the linearized Euler equation:

$$\frac{\partial w}{\partial t} + U\frac{\partial w}{\partial x} = -\frac{1}{\rho^2}\frac{\partial p}{\partial x}. \tag{4.77}$$

The limit values of the perturbed tangential velocities when the profile is approached from above ($y = +0$) and from below ($y = -0$) may be expressed in terms of linear vorticity.

The stream function in the vorticity region is expressed in terms of the area integral [49]:

$$\psi(x, y) = \frac{1}{2\pi}\iint \omega(\xi, \eta) \ln \sqrt{(x-\xi)^2 + (y-\eta)^2}\, d\xi\, d\eta.$$

If the vorticity is distributed over a thin strip along the abscissa, the stream function may be computed in terms of the linear vorticity ($2b = 2$ is the length of the strip);

$$\psi(x, y) = \frac{1}{2\pi}\int_0^2 \gamma(\xi) \ln \sqrt{(x-\xi)^2 + y^2}\, d\xi.$$

The horizontal velocity on the basis of the known formula is expressed in terms of the derivative of the stream function by the relationship

$$u = -\frac{\partial \psi}{\partial y} = -\frac{1}{2\pi}\int_0^2 \gamma(\xi)\frac{\partial \xi}{(x-\xi)^2+y^2} = \frac{1}{2\pi}\int_0^2 \gamma(\xi)\frac{d\left(\frac{x-\xi}{y}\right)}{1+\left(\frac{x-\xi}{y}\right)^2}.$$

Substituting the variable $z=(x-\xi)/y$ and then directing y toward the strip from above ($y \to +0$), we obtain the value of the tangential velocity directly at the boundary of the strip:

$$u^+ = \frac{1}{2\pi}\lim_{y\to+0}\int_{(x+1)/y}^{(x-1)/y}\gamma(x-zy)\frac{dz}{1+z^2} = \int_{+\infty}^{-\infty}\gamma(x)\frac{dz}{1+z^2} = -\frac{1}{2}\gamma(x).$$

When y tends toward -0, we shall correspondingly find $u^-=1/2\gamma(x)$. In the case under consideration the attached vorticity and the free vorticity are situated on the profile and consequently

$$u^+ = -\frac{1}{2}(\gamma+\varepsilon),\quad u^- = \frac{1}{2}(\gamma+\varepsilon),\quad u^- - u^+ = \gamma+\varepsilon. \tag{4.78}$$

The tangential velocities depend upon the total vorticity, which consists of attached vorticity and free vorticity.

When the last of Expressions (4.78) is substituted into Equation (4.77), we obtain the relationship for the pressure difference on the two sides of the plate:

$$\left(\frac{\partial \gamma}{\partial \tau}+U\frac{\partial \gamma}{\partial x}\right)+\left(\frac{\partial \varepsilon}{\partial \tau}+U\frac{\partial \varepsilon}{\partial x}\right) = -\frac{1}{\rho^2}\frac{\partial \Delta p}{\partial x}. \tag{4.79}$$

We simplify this expression, taking advantage of the fact that at a fixed point of the profile the total change of the vorticity must be equal to zero $d(\gamma+\varepsilon)/d\tau=0$. As time passes, both the attached vorticity and the free vorticity change at the point. Since the attached vorticity depends upon time, and free vorticity is carried out by the stream, we obtain

$$\frac{d\gamma}{d\tau} = \frac{\partial \gamma}{\partial \tau},\quad \frac{d\varepsilon}{d\tau} = \frac{\partial \varepsilon}{\partial \tau}+U\frac{\partial \varepsilon}{\partial x}.$$

Consequently,

$$\frac{\partial \gamma}{\partial \tau}+\frac{\partial \varepsilon}{\partial x}+U\frac{\partial \varepsilon}{\partial x} = 0.$$

Then we obtain the result that the pressure gradient at the plate depends only upon the attached vorticity (this is, essentially, the Zhukovskiy theorem concerning the lift force, written for an elementary vortex)

$$\Delta p = -\rho^0 U \gamma. \tag{4.80}$$

We emphasize once again that the lift force is created only by the attached vorticity, while the discontinuity of the tangential velocities depends both upon the attached vorticity and upon the free vorticity.

Integrating along plate (4.80), we find the acting force:

$$\mathcal{Z}(x, \tau) = -\rho^0 U \int_0^\infty \gamma(x, \tau)\, dx. \tag{4.81}$$

Since the force applied at the element of length is equal to $d\mathcal{Z} = -\rho^0 U \gamma dx$, it follows that the moment acting upon the profile with respect to the leading edge, which is situated at the origin of the coordinates, is equal to

$$M(x, \tau) = -\rho^0 U \int_0^\infty \gamma(x, \tau)\, x\, dx. \tag{4.82}$$

FOOTNOTES

1. On page 158. The programming and calculations were carried out by B. E. Kapelovich.

CHAPTER 5

TOTAL CHARACTERISTICS OF CASCADES IN THE CASE OF UNSTEADY STREAMLINE FLOW

§ 5.1. Basic Problems and Total Characteristics

Three basic problems of unsteady flow about cascades are of special interest in practical applications: (a) the profiles carry out translational oscillations in a direction perpendicular to the chords, (b) the profiles oscillate torsionally about an assigned center, and (c) the cascade is in a streamline flow which carries vortex wakes. These problems have applications in the theory of flexural-torsional flutter, in the determination of aerodynamic damping forces, and in determination of the unsteady forces which induce blade oscillations in a nonuniform stream. In all cases it is necessary to add up the total characteristics of the force $\mathcal{P}$ and the moment M in the case of various phase shifts among adjacent profiles. In view of the linearity of the problem, it is sufficient to perform calculations only for the harmonic relationship to time.

We shall consider the assignment of boundary conditions at the profile for the enumerated problems,

(a) Translational oscillations. The normal velocity at the basic profile is given by the following law:

$$v_0(x, \tau) = v_0 e^{j\nu\tau}. \tag{5.1}$$

(b) Torsional oscillations about the leading edge. The normal velocity at the basic profile is given by the law:

$$v_0(x, \tau) = \theta_0 U\left(1 + jk\frac{x}{b}\right)e^{j\nu\tau}. \tag{5.2}$$

Here θ_0 is the amplitude of the angular shift.

(c) A cascade in an unsteady vortex stream. The vertical velocity of a jump v_0 will be a traveling wave, moving with a velocity U. Since the blade is motionless and impermeable, it must induce in the field a velocity that is the same in magnitude, but opposite in sign:

$$v(x, \tau) = -v_0 e^{j\nu(\tau - x/U)}. \tag{5.3}$$

It is convenient to express the total characteristics in terms of the dimensionless functions:

$$\left.\begin{aligned} \mathcal{Y}_0 &= 2\pi\rho^0 v_0 UbT_{\gamma_0}, \quad \mathcal{Y}_\theta = 2\pi\rho^0\theta_0 UbT_{\gamma_\theta}, \\ \mathcal{Y} &= -2\pi\rho^0 v_0 UbR_\gamma. \end{aligned}\right\} \tag{5.4}$$

$$\left.\begin{aligned} M_0 &= 4\pi\rho^0 v_0 Ub^2 T_{M_0}, \quad M_\theta = 4\pi\rho^0\theta_0 Ub^2 T_{M_\theta}, \\ M &= -4\pi\rho^0 v_0 Ub^2 R_M. \end{aligned}\right\} \tag{5.5}$$

Here the functions $R(k, q, \gamma_b, \alpha)$ and $T(k, q, \gamma_b, \alpha)$ depend on four dimensionless criteria: the Strouhal number $k = \nu b/U$, the cascade density $q = \pi b/t$, the cascade offset γb and the phase shift α. These functions are multiplied by the value of the lift force and the moment of an isolated plate in the case of steady streamline flow.

Some solutions where R and T were expressed in closed form have been considered above. Let us note some general properties and limit values of functions R and T.

These properties can be ascertained by considering the function K(x) for the cascade Region (3.3), since this very function is the

kernel of an integral equation which solves the problem of determining the functions under study:

$$K(x_1, t, \gamma_b, \alpha) = \mathrm{Re}\left\{\frac{\pi}{t_1}\frac{\mathrm{ch}\left[(\pi-\alpha)\frac{x_1}{t_1}\right]}{\mathrm{sh}\left(\pi\frac{x_1}{t_1}\right)} - ij\frac{\pi}{t_1}\frac{\mathrm{sh}\left[(\pi-\alpha)\frac{x_1}{t_1}\right]}{\mathrm{sh}\left(\pi\frac{x_1}{t_1}\right)}\right\}. \qquad (5.6)$$

Here $t_1 = t\exp j\gamma_b$ is the complex spacing of the singularity cascade $x_1 = \xi - x$.

1. When the spacing increases without limit $t \to \infty$ we obtain $K(x_1, \gamma_b, \alpha) \to x_1^{-1}$. Consequently, functions R and T pass into the corresponding solution for an isolated profile. In particular, function R_α passes into the Sears function S(k) and function T_α passes into the Theodorsen function C(k).

2. Functions R and T do not change in case of the simultaneous substitution of α by $2\pi-\alpha$ and γb by $-\gamma b$:

$$R(k, q, \gamma_b, \alpha) = R(k, q, -\gamma_b, 2\pi-\alpha),$$
$$T(k, q, \gamma_b, \alpha) = T(k, q, -\gamma_b, 2\pi-\alpha).$$

This is a consequence of the fact that the same property is possessed by the function $K(x_1, \gamma_b, \alpha)$, since with the indicated substitution the expression in the braces of (5.6) changes to a conjugate one with respect to i. This property of functions R and T is obvious also from the consideration of symmetry in the replacement of the direction of motion of the main stream by the contrary one.

3. For a cascade with zero offset $(\gamma_b = 0)$, the characteristics with a phase shift of $\alpha = \pi$ coincide with the characteristics of a cascade with twice as small a relative spacing with a phase shift of $\alpha = \pi/2$:

$$R(k, q, 0, \pi) = R(k, 2q, 0, \pi/2), \quad T(k, q, 0, \pi) = T(k, 2q, 0, \pi/2).$$

This follows from the fact that when $\alpha = \pi$, the function K(x, t, 0, π) is determined according to (5.6) only by the first term and may

be replaced by $K(x, 2l, 0, \pi/2)$. Such a behavior of function R and T is explained by considerations of streamline-flow symmetry.

It was assumed above that the point about which the torsional oscillations of the profile take place is located on the leading edge. The selection of a specific center of torsion is necessary in order to be able to tabulate functions R and T. In practical applications, the profiles carry out torsional oscillations about a center of torsion, the position of which depends upon the geometrical shape of the blade. Reduction of the formulas for calculating the unsteady forces and moments with a new position of the center of rotation is based upon the linearity of the problem and, naturally, does not require the computation of new characteristics.

Let the position of the center of torsion be fixed by the coordinate x', measured from the leading edge(1). Then the normal velocity at the basic blade in the case of torsional oscillation is expressed by the formula

$$v_0(x, \tau) = \theta U + \dot{\theta}(x - x') = [U\theta_0(1 + jkx/b) - jk\theta_0 Ux'/b]e^{j\omega\tau}.$$

Here the dot signifies differentiation with respect to time. Thus, the motion may be represented as torsional oscillation about the leading edge and translational oscillation with a velocity of $-jkUx'/b$.

The force $\mathcal{Z}$, acting upon the profile, does not depend upon the center of rotation, and the moment must be recalculated according to the formula

$$M = M^0 - x'L.$$

Here and henceforth, the index zero denotes the value assumed when the axis of rotation is situated on the leading edge. Taking these remarks into consideration, by means of Formulas (5.4) and (5.5) we obtain the value of functions R and T with a new position of the

---

Footnote (1) appears on page 238.

axis of rotation in terms of the values of functions R^0 and T^0:

$$\left.\begin{aligned} T_{x_0} &= T^0_{x_0}, \quad T_{x_0} = T^0_{x_0} - (2jkx'/b)\,T^0_{x_0}, \\ R_x &= R^0_x, \quad T_{M_0} = T^0_{M_0} - (x'/b)\,T^0_{x_0}, \\ T_{\mu_0} &= T^0_{M_0} - (2jkx'/b)\,T^0_{M_0} - (x'/b)\,T^0_{x_0} + (2jkx'^2/b^2)\,T^0_{x_0}, \\ R_M &= R^0_M - (x'/b)\,R^0_x. \end{aligned}\right\} \qquad (5.7)$$

Individual total characteristics for a cascade of plates were computed by Sisto [137], Belotserkovskiy S. M., Ginevskiy A. S., and Polonskiy Ya. Ye. [6], and Gorelov D. N. [16]. Detailed tables of the function for solution for the three basic problems were computed by Whitehead [145]. Table 5.1 shows the values of the total characteristics in relation to the relative cascade spacing $t = t/2b$, the offset angle γb, the Strouhal number $k = 2\nu b/U$, and the phase shift angle α[(2)].

§ 5.2. Influence Coefficients

Up to now we have been considering a problem of the synchronous oscillation of profiles with the same oscillation amplitude. In real problems, however, the blades in the cascade oscillate at different amplitudes, for example, due to differing rigidity. Therefore, it is of practical interest to formulate the problem of unsteady flow about a cascade, the profiles of which oscillate with an arbitrarily small amplitude[(3)]. The solution of this problem is also of interest because it permits the characteristics of unsteady streamline flow to be expressed in a different manner.

As was noted in [57], solution of the problem of flow about a cascade of profiles that oscillate with an arbitrary phase shift makes it possible to solve the problem of flow about a cascade with profiles that oscillate according to an arbitrary law. Let us assume that the oscillation velocity moduli of all the profiles are given. We designate the oscillation velocity of an arbitrary m^{th} profile by $v_0(m)$. Here the velocity $v_0(m)$ is also the deformation rate of the profile or the negative vertical velocity jump. Let us also assume that the

---

Footnotes (2) and (3) appear on page 238.

TABLE 5.1a

$l/2b = 1, \quad \nu_b = 0$

h	a/2b	T_{σ_x}		T_{σ_θ}		R_σ		T_{M_x}		T_{M_θ}		R_M	
0,2	0,0	−0,3015	−0,0365	−0,3009	−0,0864	−0,3038	0,0134	−0,0550	−0,0185	−0,0529	−0,0394	−0,0542	0,0024
	0,1	−0,0667	0,5411	−0,6909	0,0378	−0,6338	0,2417	−0,1504	0,0198	−0,1513	−0,0156	−0,1429	0,0545
	0,2	−0,9289	0,1289	−0,9507	−0,0101	−0,8657	0,2653	−0,2339	0,0201	−0,2378	−0,0273	−0,2255	0,0668
	0,3	−1,1110	0,1210	−1,1313	−0,0123	−1,0801	0,2817	−0,2977	0,0196	−0,3016	−0,0367	−0,2888	0,0753
	0,4	−1,2303	0,1178	−1,2500	−0,0605	−1,1963	0,2935	−0,3390	0,0195	−0,3428	−0,0425	−0,3296	0,0809
	0,5	−1,2703	0,1170	−1,2896	−0,0661	−1,2360	0,2978	−0,3533	0,0195	−0,3571	−0,0445	−0,3437	0,0828
	0,6	−1,2303	0,1178	−1,2500	−0,0605	−1,1963	0,2935	−0,3390	0,0195	−0,3428	−0,0425	−0,3296	0,0809
	0,7	−1,1110	0,1210	−1,1313	−0,0123	−1,0801	0,2817	−0,2977	0,0196	−0,3016	−0,0367	−0,2888	0,0753
	0,8	−0,9289	0,1289	−0,9507	−0,0101	−0,8957	0,2653	−0,2339	0,0201	−0,2378	−0,0273	−0,2255	0,0668
	0,9	−0,0667	0,1111	−0,6909	−0,0378	−0,6338	0,2417	−0,1504	0,0198	−0,1543	−0,0156	−0,1429	0,0545
0,5	0,0	−0,3042	−0,0913	−0,2817	−0,2159	−0,2997	0,0328	−0,0550	−0,0463	−0,0116	−0,0985	−0,0542	0,0059
	0,1	−0,5032	0,0555	−0,5397	−0,1393	−0,4276	0,2352	−0,1135	−0,0177	−0,1123	−0,0918	−0,0964	0,0530
	0,2	−0,7421	0,1222	−0,8033	−0,1551	−0,6263	0,3774	−0,1569	−0,0002	−0,1926	−0,1011	−0,1577	0,0950
	0,3	−0,9327	0,1502	−1,0036	−0,1915	−0,7951	0,4658	−0,2193	0,0084	−0,2583	−0,1147	−0,2125	0,1245
	0,4	−1,0539	0,1628	−1,1290	−0,2190	−0,9046	0,5166	−0,2903	0,0125	−0,3010	−0,1250	−0,2492	0,1423
	0,5	−1,0955	0,1665	−1,1718	−0,2289	−0,9424	0,5334	−0,3016	0,0138	−0,3157	−0,1287	−0,2621	0,1483
	0,6	−1,0539	0,1628	−1,1290	−0,2190	−0,9046	0,5166	−0,2903	0,0127	−0,3010	−0,1250	−0,2492	0,1423
	0,7	−0,9327	0,1502	−1,0036	−0,1915	−0,7951	0,4658	−0,2193	0,0084	−0,2583	−0,1147	−0,2125	0,1245
	0,8	−0,7421	0,1222	−0,8033	−0,1551	−0,6263	0,3774	−0,1869	−0,0002	−0,1926	−0,1011	−0,1577	0,0950
	0,9	−0,5032	0,0555	−0,5397	−0,1393	−0,4274	0,2352	−0,1135	−0,0177	−0,1123	−0,0918	−0,0964	0,0530
1,0	0,0	−0,3034	−0,1828	−0,2132	−0,4313	−0,2863	0,0614	−0,0518	−0,0926	−0,0012	−0,1970	−0,0517	0,0111
	0,1	−0,1397	−0,1171	−0,4093	−0,4577	−0,3368	0,1839	−0,0992	−0,0867	−0,0515	−0,2239	−0,0759	0,0415
	0,2	−0,0004	−0,0580	−0,6190	−0,5073	−0,4146	0,3201	−0,1512	−0,0766	−0,1171	−0,2516	−0,1044	0,0807
	0,3	−0,7439	−0,0163	−0,7956	−0,5614	−0,4910	0,4349	−0,1988	−0,0679	−0,1739	−0,2771	−0,1320	0,1162
	0,4	−0,8112	0,0081	−0,9118	−0,6013	−0,5513	0,5096	−0,2318	−0,0624	−0,2109	−0,2950	−0,1519	0,1404
	0,5	−0,8755	0,0161	−0,9522	−0,6159	−0,5720	0,5335	−0,2435	−0,0606	−0,2213	−0,3014	−0,1591	0,1489
	0,6	−0,8112	0,0081	−0,9118	−0,6013	−0,5513	0,5096	−0,2318	−0,0624	−0,2109	−0,2950	−0,1519	0,1404
	0,7	−0,7139	−0,0163	−0,7956	−0,5614	−0,4910	0,4349	−0,1988	−0,0679	−0,1739	−0,2771	−0,1320	0,1162
	0,8	−0,6091	−0,0580	−0,6190	−0,5073	−0,4146	0,3201	−0,1512	−0,0766	−0,1171	−0,2516	−0,1044	0,0807
	0,9	−0,4397	−0,1171	−0,4093	−0,4577	−0,3368	0,1839	−0,0992	−0,0867	−0,0515	−0,2239	−0,0759	0,0415
2,0	0,0	−0,3009	−0,3671	0,0626	−0,8602	−0,2170	0,0981	−0,0511	−0,1854	0,1607	−0,3935	−0,0146	0,0178
	0,1	−0,1171	−0,3814	−0,0676	−1,0275	−0,2732	0,1636	−0,0911	−0,2067	0,1360	−0,4731	−0,0616	0,0369
	0,2	−0,5358	−0,3854	−0,2069	−1,1873	−0,2941	0,2395	−0,1319	−0,2209	0,1029	−0,5167	−0,0741	0,0503
	0,3	−0,6382	−0,3816	−0,3288	−1,3198	−0,3105	0,3093	−0,1706	−0,2298	0,0707	−0,6069	−0,0830	0,0827
	0,4	−0,7074	−0,3526	−0,4113	−1,4076	−0,3211	0,3578	−0,1949	−0,2347	0,0178	−0,6164	−0,0885	0,0986
	0,5	−0,7318	−0,3817	−0,4109	−1,4352	−0,3249	0,3752	−0,2035	−0,2362	0,0395	−0,6602	−0,0963	0,1013
	0,6	−0,7074	−0,3526	−0,4116	−1,4076	−0,3211	0,3578	−0,1949	−0,2347	0,0178	−0,6164	−0,0885	0,0986
	0,7	−0,6382	−0,3816	−0,3288	−1,3198	−0,3105	0,3093	−0,1706	−0,2298	0,0707	−0,6069	−0,0830	0,0827
	0,8	−0,5358	−0,3854	−0,2069	−1,1873	−0,2941	0,2395	−0,1319	−0,2209	0,1029	−0,5167	−0,0741	0,0503
	0,9	−0,1171	−0,3814	−0,0676	−1,0275	−0,2732	0,1636	−0,0911	−0,2067	0,1360	−0,4731	−0,0616	0,0359

TABLE 5.1b

$t/2b = 1$, $\gamma_0 = 15°$

k	a/2b	T_{P_0}		$T_{P\theta}$		R_P		T_{N_0}		T_{M_0}		R_M	
0,2	0,0	−0,3150	−0,0373	−0,3113	−0,0687	−0,3142	0,0140	−0,0580	−0,0189	−0,0358	−0,0404	−0,0578	0,0026
	0,1	−0,7215	0,0456	−0,7292	−0,0663	−0,7043	0,1563	−0,1618	0,0071	−0,1630	−0,0302	−0,1569	0,0440
	0,2	−0,9505	0,0329	−0,9613	−0,1105	−0,9308	0,1752	−0,2396	0,0089	−0,2409	−0,0394	−0,2338	0,0568
	0,3	−1,1260	0,0487	−1,1334	−0,1165	−1,1052	0,2126	−0,2998	0,0121	−0,3016	−0,0445	−0,2928	0,0683
	0,4	−1,2310	0,0780	−1,2435	−0,1006	−1,2040	0,2546	−0,3381	0,0155	−0,3410	−0,0464	−0,3301	0,0768
	0,5	−1,2607	0,1132	−1,2796	−0,0689	−1,2270	0,2927	−0,3505	0,0186	−0,3541	−0,0449	−0,3411	0,0814
	0,6	−1,2100	0,1494	−1,2356	−0,0258	−1,1703	0,3215	−0,3312	0,0216	−0,3388	−0,0396	−0,3240	0,0820
	0,7	−1,0918	0,1832	−1,1134	0,0251	−1,0373	0,3378	−0,2910	0,0250	−0,2966	−0,0303	−0,2806	0,0794
	0,8	−0,8823	0,2113	−0,9188	0,0798	−0,8351	0,3365	−0,2250	0,0287	−0,2313	−0,0173	−0,2145	0,0738
	0,9	−0,6015	0,2169	−0,6390	0,1243	−0,5564	0,3056	−0,1387	0,0293	−0,1448	−0,0043	−0,1293	0,0620
0,5	0,0	−0,3147	−0,0933	−0,2917	−0,2217	−0,3099	0,0345	−0,0579	−0,0473	−0,0443	−0,1010	−0,0570	0,0063
	0,1	−0,5613	0,0189	−0,5803	−0,1990	−0,4976	0,2249	−0,1255	−0,0191	−0,1221	−0,0981	−0,1094	0,0569
	0,2	−0,7039	0,0668	−0,8290	−0,2313	−0,6089	0,3477	−0,1976	−0,0034	−0,1998	−0,1065	−0,1709	0,0968
	0,3	−0,9668	0,1015	−1,0148	−0,2538	−0,8485	0,4354	−0,2563	0,0056	−0,2621	−0,1001	−0,2220	0,1251
	0,4	−1,0689	0,1543	−1,1306	−0,2536	−0,9313	0,4970	−0,2932	0,0106	−0,3019	−0,1276	−0,2537	0,1420
	0,5	−1,0912	0,1636	−1,1664	−0,2309	−0,9396	0,5293	−0,3036	0,0132	−0,3142	−0,1285	−0,2612	0,1472
	0,6	−1,0303	0,1848	−1,1162	−0,1878	−0,8726	0,5274	−0,2852	0,0131	−0,2972	−0,1223	−0,2432	0,1404
	0,7	−0,8907	0,1905	−0,9609	−0,1345	−0,7378	0,4857	−0,2406	0,0098	−0,2522	−0,1097	−0,2021	0,1220
	0,8	−0,6852	0,1665	−0,7677	−0,0883	−0,5536	0,3949	−0,1755	0,0016	−0,1841	−0,0949	−0,1445	0,0917
	0,9	−0,4482	0,0790	−0,4964	−0,0036	−0,3656	0,2345	−0,1029	−0,0181	−0,1031	−0,0683	−0,0854	0,0483
1,0	0,0	−0,3139	−0,1869	−0,2216	−0,4430	−0,2969	0,0646	−0,0578	−0,0946	−0,0030	−0,2020	−0,0545	0,0119
	0,1	−0,4768	−0,1285	−0,4322	−0,4079	−0,3745	0,2045	−0,1074	−0,0638	−0,0621	−0,2273	−0,0819	0,0506
	0,2	−0,6121	−0,0766	−0,6380	−0,5582	−0,4626	0,3405	−0,1601	−0,0725	−0,1252	−0,2542	−0,1117	0,0919
	0,3	−0,7765	−0,0337	−0,8069	−0,6041	−0,5345	0,4193	−0,2061	−0,0641	−0,1791	−0,2782	−0,1380	0,1255
	0,4	−0,8575	−0,0009	−0,9162	−0,6332	−0,5724	0,5171	−0,2353	−0,0597	−0,2140	−0,2943	−0,1548	0,1450
	0,5	−0,8724	0,0188	−0,9505	−0,6110	−0,5684	0,5357	−0,2425	−0,0593	−0,2210	−0,2989	−0,1580	0,1489
	0,6	−0,8188	0,0215	−0,9031	−0,5709	−0,5238	0,5019	−0,2265	−0,0628	−0,2072	−0,2911	−0,1470	0,1353
	0,7	−0,7060	0,0022	−0,7783	−0,5137	−0,4500	0,4185	−0,1901	−0,0700	−0,1661	−0,2728	−0,1245	0,1070
	0,8	−0,5564	−0,0433	−0,5935	−0,4381	−0,3684	0,2966	−0,1413	−0,0804	−0,1082	−0,2486	−0,0966	0,0695
	0,9	−0,1081	−0,1146	−0,3852	−0,4301	−0,3090	0,1609	−0,0923	−0,0917	−0,0169	−0,2245	−0,0717	0,0324
2,0	0,0	−0,3114	−0,3751	0,0603	−0,8833	−0,2512	0,1036	−0,0573	−0,1896	0,1622	−0,4036	−0,0468	0,0191
	0,1	−0,4372	−0,3958	−0,0717	−1,0604	−0,2822	0,1879	−0,1109	−0,2031	0,1298	−0,4767	−0,0613	0,0459
	0,2	−0,5577	−0,3875	−0,2101	−1,2200	−0,3033	0,2702	−0,1415	−0,2137	0,0936	−0,5103	−0,0726	0,0720
	0,3	−0,6550	−0,3810	−0,3313	−1,3127	−0,3167	0,3354	−0,1757	−0,2222	0,0618	−0,5036	−0,0810	0,0929
	0,4	−0,7142	−0,3769	−0,4138	−1,4152	−0,3218	0,3717	−0,1970	−0,2287	0,0417	−0,4811	−0,0866	0,1041
	0,5	−0,7262	−0,3752	−0,4425	−1,4239	−0,3192	0,3727	−0,2019	−0,2335	0,0378	−0,4539	−0,0887	0,1036
	0,6	−0,6902	−0,3749	−0,4111	−1,3758	−0,3104	0,3393	−0,1937	−0,2354	0,0510	−0,6102	−0,0874	0,0917
	0,7	−0,6134	−0,3784	−0,3244	−1,2791	−0,2982	0,2797	−0,1690	−0,2339	0,0783	−0,6022	−0,0825	0,0715
	0,8	−0,5109	−0,3837	−0,1991	−1,1511	−0,2851	0,2080	−0,1272	−0,2273	0,1129	−0,5153	−0,0745	0,0484
	0,9	−0,4030	−0,3859	−0,0583	−1,0129	−0,2716	0,1428	−0,0803	−0,2136	0,1448	−0,4767	−0,0630	0,0288

TABLE 5.1c

$l/2b = 1, \quad \gamma_b = 30°$

h	a/2b	T_{H_0}		T_{H_θ}		R_H		T_{M_0}		T_{M_θ}		R_M	
0,2	0,0	−0,3504	−0,1100	−0,3165	−0,0961	−0,3495	0,0164	−0,0683	−0,0203	−0,0659	−0,0137	−0,0681	0,0032
	0,1	−0,3593	−0,0773	−0,3163	−0,1917	−0,3624	0,0496	−0,1724	−0,0122	−0,1700	−0,0513	−0,1711	0,0269
	0,2	−0,3598	−0,0800	−0,3112	−0,2236	−0,3614	0,0641	−0,2409	−0,0071	−0,2387	−0,0556	−0,2386	0,0415
	0,3	−1,1132	−0,0354	−1,1059	−0,1989	−1,1071	0,1279	−0,2961	0,0011	−0,2953	−0,0549	−0,2917	0,0569
	0,4	−1,2085	0,0209	−1,2125	−0,1495	−1,1902	0,2032	−0,3314	0,0088	−0,3325	−0,0519	−0,3248	0,0690
	0,5	−1,2292	0,1014	−1,2103	−0,0762	−1,1976	0,2767	−0,3112	0,0156	−0,3144	−0,0193	−0,3325	0,0768
	0,6	−1,1686	0,1733	−1,1988	0,0013	−1,1217	0,3389	−0,2834	0,0222	−0,2886	−0,0372	−0,3128	0,0807
	0,7	−1,0293	0,2367	−1,0708	0,0867	−0,9757	0,3823	−0,2792	0,0292	−0,2862	−0,0241	−0,2673	0,0815
	0,8	−0,8180	0,2824	−0,8671	0,1613	−0,7591	0,3985	−0,2127	0,0365	−0,2210	−0,0076	−0,2002	0,0795
	0,9	−0,5278	0,2785	−0,5759	0,1982	−0,4733	0,3542	−0,1263	0,0391	0,1314	0,0064	−0,1150	0,0689
0,5	0,0	−0,3502	−0,1900	−0,3255	−0,2110	−0,3115	0,0402	−0,0082	−0,0507	−0,0537	−0,1093	−0,0671	0,0078
	0,1	−0,6255	−0,0101	−0,6182	−0,2827	−0,5822	0,1938	−0,1404	−0,0256	−0,1330	−0,1110	−0,1268	0,0577
	0,2	−0,8386	−0,0081	−0,8339	−0,3339	−0,7728	0,2966	−0,2078	−0,0110	−0,2018	−0,1201	−0,1853	0,0946
	0,3	−0,9901	0,0383	−1,0095	−0,3263	−0,8974	0,3875	−0,2609	−0,0005	−0,2622	−0,1277	−0,2305	0,1216
	0,4	−1,0729	0,0955	−1,1173	−0,2915	−0,9514	0,4641	−0,2929	0,0067	−0,2987	−0,1310	−0,2563	0,1380
	0,5	−1,0767	0,1535	−1,1478	−0,2354	−0,9208	0,5183	−0,2989	0,0112	−0,3088	−0,1282	−0,2681	0,1430
	0,6	−0,9974	0,2014	−1,0916	−0,1587	−0,8210	0,5299	−0,2771	0,0130	−0,2901	−0,1187	−0,2350	0,1364
	0,7	−0,8103	0,2259	−0,9175	−0,0794	−0,6752	0,4981	−0,2297	0,0115	−0,2138	−0,1036	−0,1898	0,1185
	0,8	−0,6221	0,2052	−0,7228	−0,0244	−0,4783	0,4051	−0,1629	0,0038	−0,1743	−0,0850	−0,1302	0,0895
	0,9	−0,3927	0,0940	−0,4492	−0,0562	−0,3074	0,2253	−0,0925	−0,0190	−0,0937	−0,0858	−0,0746	0,0438
1,0	0,0	−0,3493	−0,2603	−0,2504	−0,4816	−0,3281	0,0756	−0,0681	−0,1014	−0,0098	−0,2186	−0,0639	0,0147
	0,1	−0,5215	−0,1530	−0,4559	−0,5390	−0,4286	0,2224	−0,1185	−0,0814	−0,0703	−0,2375	−0,0915	0,0602
	0,2	−0,6819	−0,1018	−0,6303	−0,6197	−0,5185	0,3350	−0,1699	−0,0701	−0,1321	−0,2592	−0,1202	0,1024
	0,3	−0,8056	−0,0551	−0,8109	−0,6197	−0,5759	0,4392	−0,2121	−0,0604	−0,1836	−0,2783	−0,1436	0,1340
	0,4	−0,8685	−0,0089	−0,9151	−0,6101	−0,5896	0,5227	−0,2370	−0,0556	−0,2158	−0,2901	−0,1562	0,1501
	0,5	−0,8629	0,0261	−0,9116	−0,5973	−0,5577	0,5359	−0,2395	−0,0556	−0,2230	−0,2915	−0,1548	0,1488
	0,6	−0,7891	0,0108	−0,8901	−0,5293	−0,4879	0,1915	−0,2290	−0,0502	−0,2031	−0,2819	−0,1395	0,1305
	0,7	−0,6603	0,0253	−0,7519	−0,4557	−0,3985	0,4012	−0,1793	−0,0693	−0,1588	−0,2636	−0,1143	0,0984
	0,8	−0,5061	−0,0280	−0,5393	−0,4052	−0,3191	0,2695	−0,1297	−0,0827	−0,0984	−0,2429	−0,0869	0,0589
	0,9	−0,1787	−0,1203	−0,3564	−0,4130	−0,2888	0,1519	−0,0960	−0,0981	−0,0398	−0,2279	−0,0683	0,0235
2,0	0,0	−0,3167	−0,1021	0,0513	−0,9604	−0,2784	0,1216	−0,0676	−0,2631	0,1660	−0,4366	−0,0542	0,0237
	0,1	−0,1671	−0,1010	−0,0729	−1,1193	−0,3003	0,2183	−0,1080	−0,2038	0,1265	−0,4905	−0,0627	0,0562
	0,2	−0,5799	−0,3917	−0,2699	−1,2369	−0,3136	0,3021	−0,1473	−0,2067	0,0956	−0,5163	−0,0704	0,0839
	0,3	−0,6662	−0,3778	−0,3331	−1,3533	−0,3172	0,3690	−0,1785	−0,2114	0,0522	−0,5935	−0,0769	0,1023
	0,4	−0,7117	−0,3610	−0,4189	−1,3933	−0,3121	0,3818	−0,1961	−0,2176	0,0322	−0,6219	−0,0815	0,1083
	0,5	−0,7092	−0,3549	−0,4179	−1,3795	−0,3010	0,3650	−0,1969	−0,2242	0,0326	−0,6314	−0,0836	0,1013
	0,6	−0,6605	−0,3513	−0,4120	−1,3132	−0,2881	0,3148	−0,1811	−0,2301	0,0509	−0,6209	−0,0827	0,0833
	0,7	−0,5773	−0,3610	−0,3162	−1,2137	−0,2790	0,2415	−0,1524	−0,2335	0,0810	−0,5873	−0,0792	0,0592
	0,8	−0,1795	−0,3520	−0,1802	−1,1056	−0,2761	0,1732	−0,1178	−0,2323	0,1231	−0,5399	−0,0736	0,0360
	0,9	−0,3936	−0,1006	−0,0190	−1,0153	−0,2791	0,1245	−0,0863	−0,2238	0,1561	−0,4873	−0,0659	0,0216

TABLE 5.1d

$t/2b = 1$, $\gamma_b = 45°$

h	a/2b	T_{X_0}		T_{XQ}		R_X		T_{M_0}		T_{MQ}		R_M	
0,2	0,0	−0,4271	−0,0153	−0,4226	−0,1123	−0,4259	0,0217	−0,0920	−0,0229	−0,0894	−0,0505	−0,0917	0,0047
	0,1	−0,7642	−0,2374	−0,7258	−0,3543	−0,7929	−0,1178	−0,1796	−0,0440	−0,1720	−0,0815	−0,1837	−0,0030
	0,2	−0,9225	−0,2126	−0,8832	−0,3502	−0,9473	−0,0725	−0,2345	−0,0310	−0,2260	−0,0787	−0,2367	0,0170
	0,3	−1,0641	−0,1334	−1,0405	−0,2836	−1,0747	0,0241	−0,2831	−0,0155	−0,2790	−0,0694	−0,2821	0,0385
	0,4	−1,1527	−0,0310	−1,1468	−0,1986	−1,1447	0,1364	−0,3144	−0,0018	−0,3135	−0,0596	−0,3101	0,0558
	0,5	−1,1669	0,0836	−1,1812	−0,0882	−1,1391	0,2477	−0,3220	0,0103	−0,3244	−0,0484	−0,3144	0,0684
	0,6	−1,0987	0,1892	−1,1322	0,0301	−1,0524	0,3445	−0,3033	0,0217	−0,3089	−0,0314	−0,2927	0,0769
	0,7	−0,9509	0,2818	−1,0006	0,1435	−0,8902	0,4150	−0,2507	0,0335	−0,2680	−0,0167	−0,2467	0,0826
	0,8	−0,7329	0,3434	−0,7925	0,2358	−0,6647	0,4453	−0,1950	0,0454	−0,2053	0,0039	−0,1807	0,0855
	0,9	−0,4445	0,3296	−0,5007	0,2630	−0,3831	0,3908	−0,1118	0,0487	−0,1220	0,0189	−0,0988	0,0774
0,5	0,0	−0,4269	−0,1133	−0,3989	−0,2808	−0,4194	0,0533	−0,0919	−0,0573	−0,0756	−0,1263	−0,0903	0,0115
	0,1	−0,6960	−0,1417	−0,6469	−0,4097	−0,6882	0,1278	−0,1600	−0,0436	−0,1444	−0,1375	−0,1526	0,0496
	0,2	−0,8674	−0,1185	−0,8224	−0,4443	−0,8443	0,2065	−0,2157	−0,0285	−0,2039	−0,1410	−0,2010	0,0822
	0,3	−0,9926	−0,0196	−0,9747	−0,4160	−0,9356	0,3088	−0,2603	−0,0139	−0,2545	−0,1406	−0,2370	0,1092
	0,4	−1,0569	0,0393	−1,0776	−0,3160	−0,9589	0,4082	−0,2864	−0,0023	−0,2875	−0,1368	−0,2550	0,1269
	0,5	−1,0414	0,1315	−1,1070	−0,2466	−0,9077	0,4843	−0,2882	0,0062	−0,2961	−0,1282	−0,2505	0,1337
	0,6	−0,9193	0,2104	−1,0486	−0,1324	−0,7844	0,5208	−0,2637	0,0118	−0,2771	−0,1139	−0,2225	0,1293
	0,7	−0,7777	0,2558	−0,8902	−0,0247	−0,6036	0,5027	−0,2148	0,0138	−0,2312	−0,0952	−0,1739	0,1143
	0,8	−0,5499	0,2415	−0,6666	0,0404	−0,3566	0,4103	−0,1478	0,0062	−0,1624	−0,0780	−0,1131	0,0868
	0,9	−0,3322	0,1923	−0,3930	−0,0229	−0,2479	0,2100	−0,0810	−0,0188	−0,0834	−0,0822	−0,0626	0,0403
1,0	0,0	−0,4261	−0,2267	−0,3140	−0,5511	−0,3976	0,1008	−0,0917	−0,1147	−0,0266	−0,2525	−0,0856	0,0217
	0,1	−0,5918	−0,2035	−0,4813	−0,6594	−0,5136	0,2332	−0,1358	−0,0930	−0,0794	−0,2514	−0,1097	0,0684
	0,2	−0,7318	−0,1558	−0,6500	−0,7069	−0,5923	0,3356	−0,1806	−0,0740	−0,1358	−0,2719	−0,1332	0,1097
	0,3	−0,8317	−0,0913	−0,8006	−0,7063	−0,6245	0,4570	−0,2167	−0,0602	−0,1839	−0,2809	−0,1507	0,1390
	0,4	−0,8734	−0,0232	−0,9027	−0,6805	−0,6062	0,5208	−0,2300	−0,0525	−0,2139	−0,2845	−0,1569	0,1519
	0,5	−0,8158	0,0315	−0,9309	−0,5779	−0,5108	0,5332	−0,2334	−0,0506	−0,2192	−0,2797	−0,1493	0,1471
	0,6	−0,7503	0,0662	−0,8710	−0,4756	−0,4121	0,4869	−0,2084	−0,0545	−0,1974	−0,2663	−0,1285	0,1256
	0,7	−0,6037	0,0559	−0,7210	−0,3821	−0,3358	0,3836	−0,1654	−0,0644	−0,1506	−0,2175	−0,0998	0,0909
	0,8	−0,4446	−0,0118	−0,5146	−0,3110	−0,2621	0,2384	−0,1154	−0,0818	−0,0875	−0,2320	−0,0736	0,0493
	0,9	−0,3481	−0,1368	−0,3176	−0,4054	−0,2761	0,0962	−0,0799	−0,1060	−0,0294	−0,2337	−0,0658	0,0143
2,0	0,0	−0,4231	−0,4547	0,0266	−1,1191	−0,3293	0,1626	−0,0912	−0,2256	0,1697	−0,5045	−0,0709	0,0350
	0,1	−0,5162	−0,4314	−0,0719	−1,2253	−0,3311	0,2601	−0,1207	−0,2123	0,1269	−0,5222	−0,0682	0,0691
	0,2	−0,6079	−0,3931	−0,2053	−1,3127	−0,3289	0,3394	−0,1532	−0,2022	0,0807	−0,5516	−0,0683	0,0960
	0,3	−0,6756	−0,3187	−0,3355	−1,3606	−0,3131	0,3853	−0,1789	−0,1990	0,0433	−0,5799	−0,0709	0,1108
	0,4	−0,7011	−0,3376	−0,4087	−1,3569	−0,2804	0,3833	−0,1914	−0,2014	0,0228	−0,5977	−0,0729	0,1109
	0,5	−0,6796	−0,3180	−0,4506	−1,3020	−0,2671	0,3518	−0,1875	−0,2080	0,0239	−0,5998	−0,0737	0,0971
	0,6	−0,6151	−0,3168	−0,4157	−1,2111	−0,2513	0,2826	−0,1680	−0,2171	0,0468	−0,5853	−0,0731	0,0730
	0,7	−0,5248	−0,3081	−0,3021	−1,1123	−0,2303	0,2005	−0,1377	−0,2268	0,0871	−0,5581	−0,0719	0,0453
	0,8	−0,4370	−0,3591	−0,1104	−1,0127	−0,2083	0,1320	−0,1038	−0,2350	0,1316	−0,5280	−0,0712	0,0227
	0,9	−0,3596	−0,1310	−0,0018	−1,0399	−0,3018	0,1086	−0,0852	−0,2386	0,1717	−0,5066	−0,0718	0,0156

TABLE 5.1e

$l/2b = 1, \quad \gamma_0 = 60°$

λ	$x/2b$	$T_{Y\Phi}$		$T_{Y\Phi}$		R_Y		$T_{M\Phi}$		$T_{M\Phi}$		R_M	
0,2	0,0	−0,5993	−0,0552	−0,5938	−0,1449	−0,5973	0,0345	−0,1506	−0,0279	−0,1475	−0,0644	−0,1501	0,0087
	0,1	−0,7014	−0,4105	−0,6329	−0,5156	−0,7698	−0,3301	−0,1756	−0,0991	−0,1596	−0,1381	−0,1876	−0,0570
	0,2	−0,8213	−0,3611	−0,7602	−0,4859	−0,8701	−0,2378	−0,2122	−0,0686	−0,1937	−0,1130	−0,2205	−0,0233
	0,3	−0,9543	−0,2454	−0,9135	−0,3858	−0,9833	−0,1021	−0,2519	−0,0414	−0,2437	−0,0906	−0,2556	0,0083
	0,4	−1,0401	−0,1027	−1,0232	−0,2550	−1,0443	0,0503	−0,2785	−0,0182	−0,2749	−0,0705	−0,2772	0,0342
	0,5	−1,0522	0,0499	−1,0617	−0,1638	−1,0300	0,2019	−0,2841	0,0021	−0,2852	−0,0507	−0,2781	0,0545
	0,6	−0,9811	0,1958	−1,0160	0,0528	−0,9345	0,3350	−0,2660	0,0212	−0,2717	−0,0292	−0,2557	0,0707
	0,7	−0,8314	0,3173	−0,8868	0,1961	−0,7663	0,4331	−0,2355	0,0402	−0,2352	−0,0019	−0,2116	0,0841
	0,8	−0,6169	0,3939	−0,6840	0,3038	−0,5428	0,4776	−0,1667	0,0585	−0,1792	0,0211	−0,1506	0,0944
	0,9	−0,3472	0,3715	−0,4086	0,3206	−0,2818	0,4169	−0,0926	0,0613	−0,1050	0,0370	−0,0775	0,0903
0,5	0,0	−0,5991	−0,1380	−0,5649	−0,3622	−0,5870	0,0849	−0,1505	−0,0697	−0,1311	−0,1611	−0,1475	0,0213
	0,1	−0,7561	−0,3316	−0,6360	−0,6177	−0,8141	−0,0808	−0,1839	−0,0914	−0,1503	−0,1550	−0,1920	0,0149
	0,2	−0,8503	−0,2668	−0,7108	−0,6049	−0,8915	0,0439	−0,2140	−0,0677	−0,1865	−0,1800	−0,2145	0,0459
	0,3	−0,9170	−0,1782	−0,8781	−0,5281	−0,9404	0,1751	−0,2456	−0,0424	−0,2280	−0,1634	−0,2349	0,0779
	0,4	−0,9957	−0,0161	−0,9832	−0,1117	−0,9334	0,3104	−0,2613	−0,0212	−0,2576	−0,1470	−0,2425	0,1012
	0,5	−0,9730	0,0886	−1,0195	−0,2665	−0,8569	0,4222	−0,2627	−0,0014	−0,2664	−0,1286	−0,2311	0,1160
	0,6	−0,8691	0,2052	−0,9676	−0,1107	−0,7134	0,4896	−0,2374	0,0087	−0,2500	−0,1066	−0,1990	0,1163
	0,7	−0,6911	0,2797	−0,8225	0,0290	−0,5141	0,4937	−0,1901	0,0176	−0,2082	−0,0821	−0,1491	0,1085
	0,8	−0,4623	0,2758	−0,5918	0,1080	−0,3035	0,4098	−0,1267	0,0169	−0,1451	−0,0518	−0,0898	0,0874
	0,9	−0,2395	0,1072	−0,3210	0,0106	−0,1807	0,1863	−0,0661	−0,0158	−0,0703	−0,0748	−0,0175	0,0389
1,0	0,0	−0,5981	−0,2761	−0,4617	−0,7241	−0,5521	0,1609	−0,1503	−0,1394	−0,0727	−0,3220	−0,1387	0,0304
	0,1	−0,6919	−0,3263	−0,4989	−0,8485	−0,6662	0,2135	−0,1567	−0,1243	−0,0877	−0,3185	−0,1507	0,0681
	0,2	−0,7791	−0,2613	−0,6116	−0,8511	−0,7014	0,3121	−0,1922	−0,0969	−0,1280	−0,3051	−0,1578	0,1034
	0,3	−0,8452	−0,1688	−0,7497	−0,7977	−0,6982	0,4169	−0,2163	−0,0734	−0,1702	−0,2939	−0,1618	0,1310
	0,4	−0,8626	−0,0629	−0,8567	−0,6079	−0,6255	0,4922	−0,2276	−0,0570	−0,1990	−0,2816	−0,1569	0,1436
	0,5	−0,8135	0,0316	−0,9032	−0,5622	−0,5184	0,5152	−0,2196	−0,0181	−0,2054	−0,2650	−0,1400	0,1391
	0,6	−0,6668	0,0925	−0,8559	−0,1133	−0,3847	0,4735	−0,1910	−0,0166	−0,1853	−0,2135	−0,1119	0,1185
	0,7	−0,5311	0,0953	−0,6807	−0,2903	−0,2575	0,3651	−0,1458	−0,0533	−0,1372	−0,2214	−0,0798	0,0815
	0,8	−0,3651	0,0122	−0,4521	−0,2566	−0,1907	0,2027	−0,0963	−0,0750	−0,0711	−0,2115	−0,0513	0,0416
	0,9	−0,2120	−0,1729	−0,2560	−0,1111	−0,2748	0,0164	−0,0738	−0,1169	−0,0173	−0,2423	−0,0558	0,0035
2,0	0,0	−0,5958	−0,5529	−0,0187	−1,1152	−0,4382	0,2615	−0,1497	−0,2790	0,1611	−0,6133	−0,1101	0,0657
	0,1	−0,6981	−0,5122	−0,0612	−1,1378	−0,4101	0,3259	−0,1466	−0,2396	0,1351	−0,5953	−0,0875	0,0876
	0,2	−0,6531	−0,4429	−0,1851	−1,1265	−0,3532	0,3834	−0,1616	−0,2087	0,0961	−0,5759	−0,0731	0,1079
	0,3	−0,4871	−0,3691	−0,3289	−1,3000	−0,3116	0,4159	−0,1766	−0,1900	0,0417	−0,5659	−0,0651	0,1168
	0,4	−0,4815	−0,3016	−0,4101	−0,3107	−0,2570	0,3952	−0,1815	−0,1823	0,0152	−0,5618	−0,0506	0,1104
	0,5	−0,6364	−0,2626	−0,4796	−1,1917	−0,2128	0,3332	−0,1718	−0,1811	0,0135	−0,5482	−0,0575	0,0900
	0,6	−0,5193	−0,2556	−0,4254	−1,0681	−0,1919	0,2104	−0,1482	−0,1939	0,0485	−0,5282	−0,0553	0,0602
	0,7	−0,4176	−0,2911	−0,2801	−0,5556	−0,2067	0,1130	−0,1168	−0,2105	0,0597	−0,5081	−0,0580	0,0294
	0,8	−0,3743	−0,3795	−0,0832	−0,9177	−0,2614	0,0781	−0,0902	−0,2310	0,1470	−0,5014	−0,0472	0,0085
	0,9	−0,3956	−0,4933	0,0672	−1,1051	−0,3588	0,0963	−0,0899	−0,2621	0,1932	−0,5415	−0,0469	0,0130

TABLE 5.1f

$l/2b = 1$, $\gamma_b = 75°$

h	e/2b	T_{N_0}		T_{N_0}		R_N		T_{M_0}		T_{M_0}		R_M	
0,2	0,0	−1,1428	−0,0765	−1,1352	−0,2324	−1,1382	0,0796	−0,3631	−0,0385	−0,3589	−0,1022	−0,3616	0,0252
	0,1	−0,5012	−0,6674	−0,4060	−0,7407	−0,5900	−0,5868	−0,1345	−0,1914	−0,1072	−0,2250	−0,1585	−0,1558
	0,2	−0,6002	−0,5212	−0,5222	−0,6111	−0,6703	−0,4253	−0,1506	−0,1314	−0,1304	−0,1671	−0,1672	−0,0943
	0,3	−0,7246	−0,3616	−0,6688	−0,4741	−0,7710	−0,2510	−0,1773	−0,0852	−0,1636	−0,1241	−0,1872	−0,0454
	0,4	−0,8084	−0,1840	−0,7307	−0,3064	−0,8257	−0,0599	−0,1962	−0,0451	−0,1891	−0,0932	−0,1934	−0,0038
	0,5	−0,8236	0,0081	−0,8270	−0,1166	−0,8096	0,1318	−0,2000	−0,0090	−0,1994	−0,0503	−0,1966	0,0320
	0,6	−0,7607	0,1906	−0,7938	0,0757	−0,7180	0,3021	−0,1860	0,0248	−0,1917	−0,0145	−0,1766	0,0635
	0,7	−0,6267	0,3400	−0,6833	0,2457	−0,5625	0,4289	−0,1556	0,0670	−0,1667	0,0216	−0,1410	0,0913
	0,8	−0,4410	0,4303	−0,5100	0,3646	−0,3669	0,4896	−0,1127	0,0853	−0,1278	0,0555	−0,0947	0,1137
	0,9	−0,2240	0,4028	−0,2859	0,3702	−0,1596	0,4302	−0,0608	0,0934	−0,0759	0,0706	−0,0434	0,1147
0,5	0,0	−1,1428	−0,1912	−1,0953	−0,5811	−1,1141	0,1953	−0,3630	−0,0962	−0,3371	−0,2555	−0,3539	0,0620
	0,1	−0,6951	−0,6979	−0,4562	−0,9524	−0,8762	−0,4047	−0,1859	−0,2201	−0,1110	−0,3231	−0,2347	−0,1067
	0,2	−0,6929	−0,5347	−0,5021	−0,7952	−0,8248	−0,2446	−0,1719	−0,1532	−0,1168	−0,2507	−0,2023	−0,0488
	0,3	−0,7674	−0,3599	−0,6361	−0,6507	−0,8328	−0,0526	−0,1859	−0,1014	−0,1488	−0,2021	−0,1982	0,0027
	0,4	−0,8133	−0,1734	−0,7563	−0,4519	−0,8016	0,1361	−0,1963	−0,0694	−0,1761	−0,1621	−0,1919	0,0431
	0,5	−0,7949	0,0120	−0,8132	−0,2890	−0,7148	0,2984	−0,1930	−0,0245	−0,1887	−0,1250	−0,1736	0,0725
	0,6	−0,7018	0,1739	−0,7864	−0,0907	−0,5651	0,4112	−0,1725	0,0047	−0,1820	−0,0885	−0,1412	0,0917
	0,7	−0,5419	0,2845	−0,6704	0,0814	−0,3756	0,4530	−0,1359	0,0274	−0,1555	−0,0537	−0,0972	0,1004
	0,8	−0,3392	0,3029	−0,4726	0,1772	−0,1845	0,3959	−0,0878	0,0362	−0,1104	−0,0290	−0,0495	0,0933
	0,9	−0,1626	0,1154	−0,2210	0,0524	−0,0945	0,1554	−0,0415	−0,0053	0,0501	−0,0550	−0,0255	0,0414
1,0	0,0	−1,1425	−0,3824	−0,9525	−1,1619	−1,0317	0,3711	−0,3629	−0,1924	−0,2591	−0,5110	−0,3278	0,1179
	0,1	−0,8278	−0,6711	−0,4043	−1,2781	−0,9774	0,0165	−0,2205	−0,2475	−0,0638	−0,4794	−0,2611	0,0060
	0,2	−0,7606	−0,5298	−0,4147	−1,1043	−0,8474	0,1011	−0,1861	−0,1858	−0,0649	−0,3904	−0,2034	0,0350
	0,3	−0,7773	−0,3552	−0,5523	−0,9167	−0,7476	0,2144	−0,1858	−0,1302	−0,1007	−0,3323	−0,1726	0,0715
	0,4	−0,7751	−0,1793	−0,6853	−0,7687	−0,6259	0,3552	−0,1857	−0,0835	−0,1329	−0,2872	−0,1459	0,0959
	0,5	−0,7170	−0,0210	−0,7560	−0,5639	−0,4729	0,4311	−0,1741	−0,0600	−0,1486	−0,2467	−0,1148	0,1047
	0,6	−0,5952	0,0913	−0,7307	−0,3535	−0,3013	0,4211	−0,1474	−0,0412	−0,1415	−0,2084	−0,0786	0,0981
	0,7	−0,4251	0,1339	−0,5956	−0,1836	−0,1561	0,3354	−0,1079	−0,0362	−0,1093	−0,1770	−0,0431	0,0766
	0,8	−0,2552	0,0185	−0,3666	−0,0403	−0,0943	0,1624	−0,0664	−0,0369	−0,0531	−0,1710	−0,0248	0,0390
	0,9	−0,2469	−0,2514	−0,1304	−0,4310	−0,2877	−0,0628	−0,0673	−0,1379	0,0062	−0,2358	−0,0768	−0,0173
2,0	0,0	−1,1410	−0,7616	−0,3813	−2,3217	−0,7539	0,6032	−0,3625	−0,3848	0,6530	−1,0213	−0,2395	0,1913
	0,1	−0,8322	−0,7696	−0,0202	−1,9937	−0,6592	0,4369	−0,2201	−0,3131	0,1805	−0,8086	−0,1754	0,1177
	0,2	−0,7351	−0,6121	−0,0197	−1,7287	−0,5017	0,4230	−0,1767	−0,2694	0,1457	−0,6710	−0,1159	0,1064
	0,3	−0,7009	−0,4501	−0,2292	−1,5224	−0,3565	0,4227	−0,1617	−0,2112	0,0985	−0,5483	−0,0767	0,1056
	0,4	−0,6556	−0,3095	−0,3937	−1,3095	−0,2313	0,3860	−0,1556	−0,1785	0,0130	−0,5203	−0,0507	0,0958
	0,5	−0,5725	−0,2093	−0,4751	−1,0762	−0,1391	0,3027	−0,1390	−0,1605	0,0216	−0,4808	−0,0338	0,0735
	0,6	−0,4540	−0,1713	−0,4386	−0,8531	−0,0998	0,1853	−0,1130	−0,1596	0,0381	−0,1117	−0,0254	0,0433
	0,7	−0,3301	−0,2205	−0,2464	−0,7134	−0,1363	0,0616	−0,0837	−0,1786	0,0871	−0,1232	−0,0335	0,0128
	0,8	−0,2686	−0,3321	0,0123	−0,7822	−0,2741	−0,0064	−0,0585	−0,2284	0,1658	−0,4573	−0,0961	−0,0350
	0,9	−0,4255	−0,5581	0,2595	−1,2769	−0,5314	0,0830	−0,1160	−0,3156	0,2458	−0,6212	−0,1421	0,0213

problem of streamline flow with an arbitrary, but constant phase shift α among the oscillating profiles is solved for the given profiles. We designate by $v_0(m, \alpha)$ the velocity of the m^{th} profile with a phase shift α and with the condition that the profiles oscillate with a constant phase shift. In this case the oscillation velocity of the m^{th} profile may be expressed in terms of the velocity of the basic profile:

$$v_0(m, \alpha) = e^{im\alpha} v_0(0, \alpha).$$

Regarding $v_0(0, \alpha)$ as the spectral density, the oscillation velocity of the m^{th} profile may be expressed as the result of addition of the oscillation velocities for all phase shifts:

$$v_0(m) = \int_0^{2\pi} e^{im\alpha} v_0(0, \alpha)\, d\alpha. \tag{5.8}$$

Considering $v_0(m)$ as the coefficients of a Fourier series, this expression may be converted to:

$$v_0(0, \alpha) = \frac{i}{2\pi} \sum_{m=-\infty}^{\infty} v_0(m) e^{-im\alpha}. \tag{5.9}$$

The combination of Formulas (5.8) and (5.9) essentially represents a Fourier transform with finite limits. Thus, the spectrum $v_0(0, \alpha)$ is determined on the basis of the given profile-oscillation velocity, i.e., to every infinitely small interval of change of the phase-shift angle $d\alpha$ is juxtaposed an infinitely small oscillation velocity of the basic profile $v_0(0, \alpha)d\alpha$.

Now the problem of determining the aerodynamic characteristics of a cascade with given profile-oscillation velocities $v_0(m)$ will be presented. By aerodynamic characteristics we mean: the force and moment acting upon the profiles, the velocity circulation about the profiles, the law of pressure distribution, etc. It is assumed that these characteristics are known for the case of flow about a cascade with an arbitrary, but constant phase shift among the profiles. Let us assume that for a fixed angle α the value of the characteristic for the basic profile $Z(0, \alpha)$ is known. We shall stipulate that this value corresponds to a unit oscillation velocity. Here by Z is understood any of the enumerated characteristics.

Then the value of this characteristic for profile m with a constant phase shift will be equal to

$$Z(m, \alpha) = e^{jm\alpha} Z(0, \alpha).$$

The value of this characteristic for profile m with an arbitrary given profile-oscillation law is determined by an integral in which the obtained spectral density is included:

$$Z(m) = \int_0^{2\pi} e^{jm\alpha} v_0(\Sigma, \alpha) Z(0, \alpha) d\alpha. \qquad (5.10)$$

The obtained expression and (5.9) solve the problem.

If, for example, the profiles in the cascade oscillate as a single rigid system, i.e., if $v_0(m) = v_0(0) = 1$, then from (5.9) we obtain

$$v_0(0, \alpha) = \frac{1}{2\pi} \sum_{m=-\infty}^{\infty} e^{-jm\alpha}.$$

Utilizing the Poisson summation method, i.e., replacing the infinite series of functions by a series of Fourier transforms, we obtain

$$v_0(0, \alpha) = \frac{1}{2\pi} \sum_{m=-\infty}^{\infty} \delta(m - \alpha/2\pi).$$

Here use has been made of the well-known condition that from $\exp(-jm\alpha)$ a Fourier transform yields the delta function $\delta(m - \alpha/2\pi)$.

Since m assumes integer values and $0 \leqslant \alpha < 2\pi$, when this expression is substituted into Integral (5.10) it may be considered that $\alpha = 0$. Then we obtain

$$Z(m) = \frac{1}{2\pi} \int_0^{2\pi} e^{jm\alpha} \delta(m) Z(0, 0) d\alpha = Z(0, 0).$$

From the last formula the obvious condition follows that the characteristics of all the profiles are identical.

If the profiles in the cascade oscillate with the constant phase

shift α_0, the spectral density on the basis of (5.9) turns out equal to

$$v_0(0, \alpha) = \frac{v_0(0)}{2\pi} \sum_{m=-\infty}^{\infty} e^{-jm(\alpha-\alpha_0)},$$

and the characteristics are obtained one from the other with the phase shift

$$Z(m) = Z(0)\, e^{jm\alpha_0}.$$

Let us now consider a case which is of special interest. Let all the profiles of the cascade be motionless ($v(m) = 0$ when $m \neq 1$), with the exception of the basic profile, which oscillates with the unit velocity $v_0(0) = 1$. In such a case it follows from Formula (5.9) that the spectral function must be constant: $v(0, \alpha) = 1/2\pi$.

Then the characteristic for any profile is obtained by means of (5.10):

$$Z(m) = \frac{1}{2\pi} \int_0^{2\pi} e^{jm\alpha} Z(0, \alpha)\, d\alpha. \qquad (5.11)$$

Function Z(m) determines the influence of the basic profile upon the m^{th} profile. Since any profile can be selected as the basic one, it is obvious that function Z(m) also takes into account the influence of the fixed profile n upon profile m + n. In particular, when m = 0 we determine the influence of the profile upon itself Z(0) or, more precisely, the influence of all the other motionless profiles upon the selected one.

Inverting Formula (5.11), we obtain the relationship of characteristic $Z(0, \alpha)$ in terms of Z(m):

$$Z(0, \alpha) = \sum_{m=-\infty}^{\infty} e^{-jm\alpha} Z(m). \qquad (5.12)$$

Above have been considered the conditions of recalculation when a single profile oscillates in a cascade with an infinite number of

blades. Real cascades employed in turbomachines are annular and contain a finite number of blades. If, out of z blades in an annular cascade, let us say, the zeroth blade oscillates, then when the intersecting cylindrical surface is unfolded into a plane, it must be considered that blades with the number nz, where nz = 0, $\pm$ 1, $\pm$ 2, ... oscillate in the same manner. In such a case the aerodynamic pattern of flow about a cascade with an infinite number of blades will be periodically repeated every z blades.

Assuming the oscillation velocity to be $v_0(nz) = 1$ and $v_0(m) = 0$ when $m \neq nz$ and substituting in (5.9) m = nz, we obtain the spectral density:

$$c_0(0, \alpha) = \frac{1}{2\pi} \sum_{n=-\infty}^{\infty} e^{-inz\alpha} = \frac{1}{2\pi} \sum_{n=-\infty}^{\infty} \delta\left(n - \frac{z\alpha}{2\pi}\right).$$

Here the series of exponential functions has been replaced by an equivalent series of δ-functions, analogous to the manner in which this was done above. Substituting this expression into (5.10) and integrating, we find the value of the characteristics:

$$Z(m) = \frac{1}{2\pi} \int_0^{2\pi} e^{im\alpha} Z(0, \alpha) \sum_{n=-\infty}^{\infty} \delta\left(n - \frac{z\alpha}{2\pi}\right) d\alpha =$$
$$= \frac{1}{z} \sum_{n=-\infty}^{\infty} e^{\frac{im2\pi n}{z}} Z\left(0, \frac{2\pi n}{z}\right), \quad n = 0, 1, 2, \ldots, (z-1). \tag{5.13}$$

In the case under consideration the phase shift is expressed by the formula $\alpha = 2\pi n/z$. Thus there can be only discrete values of the shift; this follows from considerations of symmetry. In the special case of z = 1, Formula (5.13) passes into the formula for the case where all the profiles oscillate. Formulas (5.11) - (5.13), just as the entire preceding derivation, pertain not only to a cascade of thin plates. They can be applied also for recalculation of the distribution of pressure or circulation in a cascade of profiles of arbitrary form. In the general case the characteristics are complex (with respect to j) values.

In some problems connected with the determination of forces, it is more convenient to consider not the influence of the basic

profile upon the m^{th} profile but, on the contrary, to consider the influence of the m^{th} profile upon the basic one. Out of simple considerations it is clear that the m^{th} profile affects the basic profile (m = 0) in the same manner as the basic profile affects the $(-m)^{th}$ one. Thus, in this case it is necessary to change the sign in front of m in the presented formulas.

Applying Formula (5.11) to force and moment characteristics and considering a special case of the problem solved above, we obtain the so-called influence coefficients, introduced by V. B. Kurzin [33]:

$$r(m) = \frac{1}{2\pi}\int_0^{2\pi} e^{-im\alpha} R(\alpha)\, d\alpha, \quad t(m) = \frac{1}{2\pi}\int_0^{2\pi} e^{-im\alpha} T(\alpha)\, d\alpha. \tag{5.14}$$

Here r(m) = r(k, q, γ_b, m), t(m) = t(k, q, γ_b, m) are the influence coefficients determining the forces and moments originating at the profile m, if all the profiles are motionless, and only the profile m = 0 is oscillating.

The total characteristics are determined according to the formulas:

$$\left.\begin{aligned} \mathcal{Y}_a(m) &= 2\pi\rho^0 v_0 U b l_{\mathcal{Y}_a}, & M_a(m) &= 4\pi\rho^0 v_0 U b^2 l_{M_a}, \\ \mathcal{Y}_b(m) &= 2\pi\rho^0 v_0 U b l_{\mathcal{Y}_b}, & M_b(m) &= 4\pi\rho^0 v_0 U b^2 l_{M_b}, \\ \mathcal{Y}(m) &= -2\pi\rho^0 v_0 U b r_{\mathcal{Y}}, & M(m) &= -4\pi\rho^0 v_0 U b^2 r_M. \end{aligned}\right\} \tag{5.15}$$

The formula determining the relationship of R and T in terms of the influence coefficients is obtained from (5.12):

$$R(\alpha) = \sum_{m=-\infty}^{\infty} e^{im\alpha} r(m), \qquad T(\alpha) = \sum_{m=-\infty}^{\infty} e^{im\alpha} t(m). \tag{5.16}$$

Extending the influence coefficients to the case of a cascade with a finite number of blades, Formula (5.13) should be used:

$$\left.\begin{aligned} r(m) &= \frac{1}{z}\sum_{n=-\infty}^{\infty} e^{-\frac{2\pi i m n}{z}} R\left(\frac{2\pi n}{z}\right), \\ t(m) &= \frac{1}{z}\sum_{n=-\infty}^{\infty} e^{-\frac{2\pi i m n}{z}} T\left(\frac{2\pi n}{z}\right). \end{aligned}\right\} \tag{5.17}$$

In Table 5.2 are presented the influence coefficients determined by D. N. Gorelov for a cascade with an infinite number of blades.

TABLE 5.2a

$l_{x_0}(m)$ $\gamma_b = 0°$

x	m \ l	0,5	1,0	1,5	2,0
0,1	3	0,015 +0,022	0,010 +0,036	0,005 +0,033	0,003 +0,032
	2	0,017 +0,047	0,008 +0,068	0,005 +0,067	0,004 +0,067
	1	0,005 +0,137	0,001 +0,251	0,009 +0,359	0,018 +0,468
	0	−0,160 −1,095	−0,147 −1,198	−0,139 −1,340	−0,137 −1,501
	−1	0,005 +0,137	0,001 +0,251	0,009 +0,359	0,018 +0,468
	−2	0,017 +0,137	0,008 +0,068	0,005 +0,067	0,004 +0,067
	−3	0,015 +0,022	0,010 +0,036	0,005 +0,033	0,003 +0,032
0,25	3	0,025 +0,012	0,034 +0,037	0,031 +0,049	0,026 +0,054
	2	0,055 +0,043	0,062 +0,103	0,053 +0,126	0,046 +0,136
	1	0,127 +0,250	0,128 +0,555	0,139 +0,814	0,158 +1,056
	0	−0,250 −2,212	−0,333 −2,465	−0,389 −2,609	−0,410 −3,192
	−1	0,127 +2,250	0,128 +0,555	0,139 +0,814	0,158 +1,056
	−2	0,055 +0,013	0,062 +0,103	0,053 +0,126	0,046 +0,136
	−3	0,025 +0,012	0,034 +0,037	0,031 +0,049	0,026 +0,054
0,5	3	0,018 +0,015	0,025 +0,045	0,024 +0,058	0,021 +0,067
	2	0,046 +0,040	0,064 +0,117	0,058 +0,155	0,049 +0,176
	1	0,201 +0,272	0,256 +0,809	0,265 +1,271	0,277 +1,694
	0	0,263 −3,755	0,338 −4,036	0,150 −4,559	5,177
	−1	0,201 +0,272	0,256 +0,809	0,265 +1,271	0,277 +1,694
	−2	0,046 +0,040	0,064 +0,117	0,058 +0,155	0,049 +0,176
	−3	0,018 +0,015	0,025 +0,045	0,024 +0,058	0,021 +0,067
1,0	3	0,003 +0,033	−0,014 +0,079	−0,033 +0,101	−0,050 +0,115
	2	0,009 +0,076	−0,027 +0,190	−0,073 +0,251	−0,111 +0,285
	1	0,080 +0,364	−0,020 +1,182	−0,241 +1,952	−0,468 +2,654
	0	4,991 −6,777	4,804 −7,030	4,660 −7,778	4,625 −8,688
	−1	0,080 +0,364	−0,020 +1,182	−0,241 +1,952	−0,468 +2,654
	−2	0,009 +0,076	−0,027 +0,190	−0,073 +0,251	−0,111 +0,285
	−3	0,003 +0,033	−0,014 +0,079	−0,033 +0,101	−0,050 +0,115

TABLE 5.2b

t_{x_0} (m) $\gamma_0 = 0°$

h	m \ l	0,5	1,0	1,5	2,0
0	3	−0,032	−0,073	−0,467	−0,093
	2	0,020	−0,177	−0,240	−0,291
	1	−0,325	−0,953	−1,575	−2,122
	0	6,310	6,554	7,057	7,704
	−1	−0,325	−0,953	−1,575	−2,122
	−2	−0,020	−0,177	−0,240	−0,291
	−3	−0,032	−0,073	−0,467	−0,098
0,1	3	−0,112 +0,074	−0,180 +0,040	−0,167 +0,018	−0,158 +0,007
	2	−0,238 +0,077	−0,339 +0,027	−0,337 +0,009	−0,333 +0,005
	1	−0,680	−1,252 −0,039	−1,794 −0,017	−2,338 +0,009
	0	5,531 −0,526	6,042 −0,445	6,750 −0,384	7,557 −0,354
	−1	−0,680	−1,252 −0,039	−1,794 −0,017	−2,338 +0,009
	−2	−0,238 +0,077	−0,339 +0,027	−0,337 +0,009	−0,333 +0,005
	−3	−0,112 +0,074	−0,180 +0,040	−0,167 +0,018	−0,158 +0,007
0,25	3	−0,030 +0,049	−0,085 +0,060	−0,109 +0,048	−0,128 +0,038
	2	−0,100 +0,102	−0,222 +0,101	−0,269 +0,076	−0,291 +0,059
	1	−0,530 +0,206	−1,140 +0,156	−1,663 +0,136	−2,157 +0,135
	0	4,584 +0,503	5,106 +0,073	5,803 −0,132	6,574 −0,175
	−1	−0,530 +0,206	−1,140 +0,156	−1,663 +0,136	−2,157 +0,135
	−2	−0,100 +0,102	−0,222 +0,101	−0,269 +0,076	−0,291 +0,059
	−3	−0,030 +0,049	−0,085 +0,060	−0,109 +0,048	−0,123 +0,038
0,5	3	−0,021 +0,018	−0,057 +0,017	−0,072 +0,012	−0,086 +0,006
	2	−0,054 +0,042	−0,143 +0,041	−0,183 +0,024	−0,209 +0,009
	1	−0,328 +0,158	−0,891 +0,119	−1,369 +0,050	−1,815 −0,011
	0	4,002 +1,459	4,334 +1,314	4,901 +1,203	5,554 +1,147
	−1	−0,328 +0,158	−0,891 +0,119	−1,369 +0,050	−1,815 −0,011
	−2	−0,054 +0,042	−0,143 +0,041	−0,183 +0,024	−0,209 +0,009
	−3	−0,021 +0,018	−0,057 +0,017	−0,072 +0,012	−0,086 +0,006
1,0	3	−0,021 −0,003	−0,051 −0,020	−0,065 −0,035	−0,071 −0,050
	2	−0,050 −0,006	−0,120 −0,044	−0,156 −0,084	−0,173 −0,116
	1	−0,238 −0,003	−0,705 −0,191	−1,125 −0,433	−1,505 +0,666
	0	3,711 +4,134	3,916 +4,121	4,336 +4,139	4,861 +4,246
	−1	−0,238 −0,003	−0,705 −0,191	−1,125 −0,433	−1,505 +0,666
	−2	−0,050 −0,006	−0,120 −0,044	−0,156 −0,084	−0,173 −0,116
	−3	−0,021 −0,003	−0,051 −0,020	−0,065 −0,035	−0,071 −0,050

TABLE 5.2c

$l_{M_0}(m)$ $\gamma_b = 0°$

h	m \ l	0,5	1,0	1,5	2,0
0	3	−0,004	−0,012	−0,017	−0,020
	2	−0,010	−0,029	−0,043	−0,056
	1	−0,041	−0,141	−0,248	−0,350
	0	1,573	1,599	1,659	1,745
	−1	−0,044	−0,141	−0,248	−0,350
	−2	−0,010	−0,029	−0,043	−0,056
	−3	−0,004	−0,012	−0,017	−0,020
0,1	3	−0,028 +0,018	−0,047 +0,011	−0,043 +0,004	−0,041 +0,001
	2	−0,056 +0,018	−0,080 +0,005	−0,078	−0,078 −0,001
	1	−0,138 −0,003	−0,223 −0,013	−0,302 −0,004	−0,392 +0,009
	0	1,374 −0,282	1,456 −0,268	1,563 −0,253	1,678 −0,245
	−1	−0,138 −0,003	−0,223 −0,013	−0,302 −0,004	−0,392 +0,009
	−2	−0,056 +0,018	−0,080 +0,005	−0,078	−0,078 −0,001
	−3	−0,028 +0,018	−0,047 +0,011	−0,043 +0,004	−0,041 +0,001
0,25	3	−0,004 +0,014	−0,020 +0,019	−0,027 +0,017	−0,031 +0,015
	2	−0,019 +0,028	−0,050 +0,030	−0,063 +0,026	−0,068 +0,023
	1	−0,103 +0,054	−0,205 +0,050	−0,289 +0,050	−0,370 +0,074
	0	1,152 +0,277	1,241 +0,404	1,350 −0,418	1,467 −0,433
	−1	−0,103 +0,054	−0,205 +0,050	−0,289 +0,050	−0,370 +0,074
	−2	−0,019 +0,028	−0,050 +0,030	−0,063 +0,026	−0,068 +0,023
	−3	−0,004 +0,014	−0,020 +0,019	−0,027 +0,017	−0,031 +0,015
0,5	3	−0,002 +0,006	−0,011 +0,011	−0,016 +0,012	−0,020 +0,009
	2	−0,008 +0,015	−0,029 +0,023	−0,041 +0,025	−0,048 +0,018
	1	−0,055 +0,052	−0,154 +0,072	−0,235 +0,091	−0,311 +0,065
	0	1,046 −0,400	1,096 −0,454	1,182 −0,491	1,281 −0,335
	−1	−0,055 +0,052	−0,154 +0,072	−0,235 +0,091	−0,311 +0,065
	−2	−0,008 +0,015	−0,029 +0,023	−0,041 +0,025	−0,048 +0,018
	−3	−0,002 +0,006	−0,011 +0,011	−0,016 +0,012	−0,020 +0,009
1,0	3	−0,004 +0,004	−0,006 +0,006	−0,014 +0,007	−0,016 +0,007
	2	−0,007 +0,007	−0,022 +0,013	−0,032 +0,016	−0,039 +0,018
	1	−0,035 +0,030	−0,115 +0,058	−0,191 +0,065	−0,263 +0,115
	0	1,122 −0,524	1,146 −0,553	1,203 −0,586	1,279 −0,621
	−1	−0,035 +0,030	−0,115 +0,058	−0,191 +0,065	−0,263 +0,115
	−2	−0,007 +0,007	−0,022 +0,013	−0,032 +0,016	−0,039 +0,018
	−3	−0,004 +0,004	−0,009 +0,006	−0,014 +0,007	−0,016 +0,007

TABLE 5.2d

$l_{M_0}(m)$ $\gamma_b = 0°$

h	m \ l	0,5	1,0	1,5	2,0
0,1	3	0,004 +0,005	0,033 +0,009	0,001 +0,009	0,003
	2	0,004 +0,011	0,002 +0,016	0,001 +0,016	0,016
	1	0,028	−0,022 +0,045	0,061	0,002 +0,079
	0	−0,036 −0,272	−0,320 −0,236	−0,049 −0,310	−0,018 −0,333
	−1	0,028	−0,022 +0,045	0,061	0,002 +0,079
	−2	0,011 +0,011	0,032 +0,116	0,001 +0,016	0,016
	−3	0,004 +0,005	0,033 +0,009	0,001 +0,009	0,008
0,25	3	0,007 +0,031	0,010 +0,008	0,010 +0,012	0,009 +0,014
	2	0,015 +0,008	0,017 +0,023	0,015 +0,030	0,014 +0,033
	1	0,031 +0,043	0,031 +0,100	0,034 +0,142	0,010 +0,182
	0	−0,159 −0,550	−0,176 −0,593	−0,186 −0,647	−0,195 −0,705
	−1	0,031 +0,013	0,031 +0,100	0,034 +0,142	0,010 +0,183
	−2	0,015 +0,003	0,017 +0,023	0,015 +0,030	0,014 +0,033
	−3	0,007 +0,031	0,010 +0,008	0,010 +0,012	0,009 +0,014
0,5	3	0,006	0,011 +0,036	0,013 +0,012	0,013 +0,016
	2	0,014 +0,004	0,025 +0,022	0,027 +0,034	0,027 +0,041
	1	0,055 +0,043	0,051 +0,137	0,038 +0,216	0,115 +0,268
	0	−0,219 −0,936	−0,290 −0,975	−0,343 −1,034	−0,383 −1,146
	−1	0,056 +0,043	0,081 +0,137	0,093 +0,216	0,115 +0,268
	−2	0,014 +0,004	0,025 +0,022	0,027 +0,034	0,027 +0,041
	−3	0,006	0,011 +0,008	0,013 +0,012	0,013 +0,016
1,0	3	0,005 +0,032	0,011 +0,012	0,013 +0,019	0,014 +0,024
	2	0,012 +0,007	0,025 +0,038	0,030 +0,048	0,031 +0,059
	1	0,057 +0,045	0,114 +0,180	0,148 +0,312	0,178 +0,435
	0	−0,332 −1,691	−0,376 −1,720	−0,448 −1,809	−0,517 −1,935
	−1	0,057 +0,045	0,114 +0,180	0,148 +0,312	0,178 +0,435
	−2	0,012 +0,007	0,025 +0,038	0,030 +0,048	0,031 +0,050
	−3	0,005 +0,032	0,011 +0,012	0,013 +0,019	0,014 +0,020

TABLE 5.2e

$t_{x_0}(m)\ \gamma_0 = 30°$

h	m \ l	0,5		1,0		1,5		2,0	
0,1	3	−0,005	+0,013	−0,012	+0,014	−0,010	+0,014	−0,008	+0,015
	2	−0,015	+0,018	−0,021	+0,022	−0,015	+0,030	−0,009	+0,037
	1	−0,044	+0,034	−0,040	+0,121	−0,019	+0,263	−0,002	+0,408
	0	−0,138	−1,077	−0,115	−1,162	−0,113	−1,319	−0,119	−1,514
	−1	0,068	+0,212	0,076	+0,349	0,050	+0,458	0,048	+0,565
	−2	0,032	+0,059	0,039	+0,086	0,027	+0,873	0,021	+0,057
	−3	0,024	+0,020	0,029	+0,038	0,020	+0,041	0,015	+0,040
0,25	3	0,008	+0,010	0,004	+0,031	0,002	+0,037	0,002	+0,041
	2	0,008	+0,032	−0,001	+0,071	0,001	+0,089	0,005	+0,100
	1	−0,017	+0,125	−0,026	+0,359	0,021	+0,692	0,072	+0,986
	0	−0,221	−2,214	−0,271	−2,446	−0,339	−2,824	−0,410	−3,259
	−1	0,205	+0,286	0,303	+0,685	0,278	+0,972	0,270	+1,231
	−2	0,003	+0,006	0,119	+0,095	0,103	+0,133	0,087	+0,148
	−3	0,030	−0,012	0,037	+0,022	0,055	+0,043	0,049	+0,054
0,5	3	0,007	+0,007	0,009	+0,035	0,006	+0,048	0,003	+0,056
	2	0,016	+0,029	0,016	+0,093	0,012	+0,129	0,009	+0,149
	1	−0,031	+0,178	0,034	+0,621	0,081	+1,138	0,137	+1,644
	0	0,579	−3,754	0,370	−0,036	0,154	−4,620	−0,027	−5,342
	−1	0,424	+0,143	0,582	+0,870	0,549	+1,427	0,516	+1,908
	−2	0,051	−0,015	0,121	+0,068	0,122	+0,130	0,111	+0,165
	−3	0,013	−0,007	0,041	+0,015	0,048	+0,037	0,048	+0,053
1,0	3	−0,001	+0,012	−0,012	+0,052	−0,029	+0,078	−0,044	+0,093
	2		0,011	−0,032	+0,140	−0,075	+0,205	−0,019	+0,245
	1	−0,012	+0,248	−0,161	+0,986	−0,361	+1,846	−0,563	+2,669
	0	5,002	−6,768	4,772	−7,029	4,560	−7,821	4,501	−8,990
	−1	0,235	+0,095	0,471	+1,060	0,234	+2,020	−0,067	+2,848
	−2	0,015	+0,020	0,038	+0,111	0,016	+0,191	−0,016	+0,241
	−3	0,004	+0,005	0,008	+0,040	0,001	+0,068	−0,006	+0,087

TABLE 5.2f

$t_{x_0}(m)\ \gamma_0 = 30°$

h	m \ l	0,5		1,0		1,5		2,0	
0	3	−0,176		−0,211		−0,199		−0,136	
	2	−0,308		−0,404		−0,412		−0,416	
	1	−0,861		−1,549		−2,070		−2,544	
	0	6,139		6,279		6,914		7,759	
	−1	0,235		−0,281		−1,111		−1,913	
	−2	0,216		0,128		−0,907		−0,094	
	−3	0,161		0,130		0,057		0,060	
0,1	3	−0,054	−0,055	−0,064	−0,064	−0,065	−0,053	−0,071	−0,039
	2	−0,080	−0,076	−0,105	−0,109	−0,145	−0,076	−0,179	−0,049
	1	−0,149	−0,217	−0,590	−0,199	−1,303	−0,103	−2,033	−0,032
	0	5,441	−0,419	5,851	−0,295	6,638	−0,267	7,609	−0,272
	−1	−1,078	+0,290	−1,758	+0,196	−2,304	+0,137	−2,842	+0,106
	−2	−0,298	+0,247	−0,438	+0,172	−0,445	+0,113	−0,430	+0,080
	−3	−0,099	+0,170	−0,200	+0,135	−0,211	+0,091	−0,205	+0,063
	3	−0,023	+0,013	−0,062	+0,003	−0,074	−0,003	−0,080	−0,004
	2	−0,065	+0,011	−0,139	−0,014	−0,175	+0,077	−0,198	−0,007

TABLE 5.2f

k	m \ t̄	0,8		1,0		1,5		2,0	
0,25	1	−0,245	−0,051	−0,704	−0,070	−1,316	+0,001	−1,936	+0,072
	0	4,578	+0,110	5,018	+0,045	5,812	−0,039	6,716	−0,118
	−1	−0,618	+0,512	−1,452	+0,440	−2,025	+0,321	−2,543	+0,248
	−2	−0,035	+0,186	−0,223	+0,215	−0,256	+0,062	−0,324	+0,135
	−3	−0,016	+0,061	−0,059	+0,169	−0,101	+0,039	−0,124	+0,083
0,5	3	−0,069	+0,067	−0,039	+0,005	−0,063	−0,062	−0,075	−0,007
	2	−0,031	+0,013	−0,109	+0,063	−0,137	−0,017	−0,160	−0,017
	1	−0,188	+0,012	−0,631	−0,090	−1,170	+0,005	−1,702	+0,008
	0	3,999	+1,516	4,218	+1,346	4,914	+1,208	5,710	+1,129
	−1	−0,258	+0,394	−1,034	+0,377	−1,601	+0,210	−2,092	+0,069
	−2	0,001	+0,057	−0,101	+0,107	−0,171	+0,090	−0,205	+0,068
	−3	0,003	+0,016	−0,028	+0,039	−0,051	+0,030	−0,084	+0,034
1,0	3	−0,008		−0,032	−0,011	−0,047	−0,024	−0,056	−0,031
	2	−0,026	−0,003	−0,083	−0,291	−0,122	−0,061	−0,147	−0,097
	1	−0,145	−0,021	−0,683	−0,126	−1,037	−0,283	−1,507	−0,474
	0	3,703	+4,192	3,890	+4,100	4,349	+4,086	4,965	+4,196
	−1	−0,125	+0,106	−0,590	−0,008	−1,214	−0,358	−1,635	−0,697
	−2	−0,019	+0,006	−0,082	−0,003	−0,128	−0,037	−0,153	−0,069
	−3	−0,006	+0,003	−0,030	−0,003	−0,047	−0,015	−0,057	−0,026

Influence coefficients are given for the basic profile and for three adjacent profiles on each side of the initial profile. The values of the Strouhal number k, the relative spacings $\bar{t}$, and the incidences are given in the table. In the case at hand, influence coefficients are given only for translational and torsional oscillation of plates (about the center of the plate)[4].

The lift force and the moment applied to the center of the basic profile, when all the profiles oscillate with a constant phase shift, are equal to

$$\mathcal{Z} = \rho^0 U^2 b c_y, \quad M = 2\rho^0 U^2 b^2 c_m.$$

Here the coefficients of the forces and of the moment

$$c_y = \mathrm{Re}\left(\vartheta c_{y\vartheta} + \frac{y}{2b} c_{yy}\right), \quad c_m = \mathrm{Re}\left(\vartheta c_{m\vartheta} + \frac{y}{2b} c_{my}\right).$$

are introduced

Footnote (4) appears on page 238.

TABLE 5.2g

$t_{M_0}(m)\ \gamma_0 = 30°$

k	m \ $\bar{t}$	0,5		1,0		1,5		2,0	
0,1	3	−0,002	+0,003	−0,001	+0,002	−0,004	+0,001	−0,001	+0,001
	2	−0,031	+0,001	−0,007	+0,002	−0,006	+0,002	−0,005	+0,003
	1	−0,012	+0,001	−0,013	+0,001	−0,009	+0,005	−0,005	+0,021
	0	−0,658	−0,268	−0,642	−0,278	−0,010	−0,293	−0,061	−0,325
	−1	0,017	+0,052	0,016	+0,086	0,015	+0,112	0,015	+0,136
	−2	0,013	+0,015	0,011	+0,022	0,008	+0,021	0,007	+0,023
	−3	0,009	+0,005	0,008	+0,010	0,001	+0,011	0,005	+0,012
0,25	3	0,002	+0,002		0,006	−0,001	+0,008	−0,001	+0,008
	2	0,002	+0,006	0,003	+0,012	−0,003	−0,076	−0,002	+0,016
	1	−0,006	+0,016	−0,015	+0,025	−0,008	+0,041	0,004	+0,072
	0	−0,151	−0,551	−0,155	−0,586	−0,165	−0,639	−0,178	−0,702
	−1	0,077	+0,068	0,082	+0,165	0,681	+0235	0,083	+0,292
	−2	0,021		0,033	+0,023	0,030	+0,124	0,027	+0,039
	−3	0,008	−0,001	0,016	+0,005	0,017	+0,011	0,015	+0,015
0,5	3	0,002		0,001	+0,005	0,005	+0,008	0,019	+0,010
	2	0,035	+0,003	0,007	+0,013	0,008	+0,020	0,010	+0,025
	1	0,009	+0,019	0,013	+0,012	0,032	+0,077	0,057	+0,129
	0	−0,215	−0,937	−0,281	−0,976	−0,221	−1,054	−0,308	−1,155
	−1	0,110	+0,030	0,164	+0,205	0,174	+0,339	0,134	+0,447
	−2	0,014	−0,006	0,035	+0,015	0,040	+0,032	0,010	+0,042
	−3	0,001	−0,003	0,013	+0,002	0,017	+0,000	0,032	+0,014
1,0	3	0,002		0,006	+0,005	0,008	+0,009	0,010	+0,013
	2	0,005	+0,003	0,013	+0,013	0,019	+0,023	0,721	+0,032
	1	0,020	+0,015	0,150	+0,046	0,114	+0,102	0,172	+0,190
	0	−0,319	−1,591	−0,356	−1,714	−0,439	−1,806	−0,516	−1,945
	−1	0,077	+0,012	0,060	+0,234	0,205	+0,475	0,211	+0,664
	−2	0,009	+0,001	0,027	+0,022	0,033	+0,045	0,033	+0,061
	−3	0,003	−0,001	0,010	+0,007	0,013	+0,015	0,014	+0,022

TABLE 5.2h

$l_{M_0}(m)\ \gamma_k = 30°$

k	m \ $\bar{l}$	0,5		1,0		1,5		2,0	
0	3	−0,016		−0,058		−0,099		−0,055	
	2	−0,079		−0,168		−0,113		−0,114	
	1	−0,215		−0,393		−0,521		−0,634	
	0	1,522		1,514		1,585		1,704	
	−1	0,116		0,160		0,020		−0,085	
	−2	0,067		0,053		0,044		0,020	
	−3	0,047		0,052		0,081		0,026	
0,1	3	−0,014	−0,008	−0,009	−0,022	−0,005	−0,021	−0,005	−0,017
	2	−0,016	−0,022	−0,005	−0,036	−0,006	−0,029	−0,013	−0,021
	1	−0,003	−0,059	0,011	−0,061	−0,035	−0,038	−0,117	−0,015
	0	1,352	−0,261	1,400	−0,223	1,499	−0,213	1,631	−0,214
	−1	−0,262	+0,074	−0,133	+0,059	−0,565	+0,053	−0,683	+0,032
	−2	−0,076	+0,053	−0,114	+0,019	−0,120	+0,036	−0,118	+0,028
	−3	−0,027	+0,043	−0,053	+0,038	−0,059	+0,029	−0,059	+0,022
0,25	3	−0,004	+0,004	−0,012		−0,014	−0,003	−0,014	−0,002
	2	−0,012	+0,003	−0,021	−0,007	0,135	−0,007	−0,029	−0,003
	1	−0,030	−0,014	−0,038	−0,025	−0,072	−0,001	−0,136	+0,030
	0	1,152	−0,361	1,221	−0,366	1,325	−0,382	1,408	−0,485
	−1	−0,154	+0,139	−0,352	+0,131	−0,492	+0,121	−0,698	+0,122
	−2	−0,007	+0,048	−0,055	+0,061	−0,256	+0,054	−0,066	+0,017
	−3	0,005	+0,017	−0,014	+0,031	−0,027	+0,031	−0,034	+0,028
0,5	3	−0,001	+0,003	−0,005	+0,001	−0,008	+0,001	−0,010	+0,019
	2	−0,001	+0,005	−0,013	+0,006	−0,019	+0,009	−0,023	+0,013
	1	−0,019	+0,008	−0,037	+0,018	−0,069	+0,032	−0,123	+0,064
	0	1,017	−0,304	1,090	−0,435	1,173	−0,475	1,280	−0,516
	−1	−0,058	+0,166	−0,258	+0,129	−0,388	+0,126	−0,501	+0,131
	−2	0,002	+0,017	−0,025	+0,035	−0,044	+0,037	−0,051	+0,036
	−3	0,002	+0,005	−0,006	+0,014	−0,014	+0,017	−0,019	+0,031
1,0	3		0,002	−0,004	+0,001	−0,006	+0,005	−0,005	+0,007
	2	−0,002	+0,004	−0,008	+0,008	−0,012	+0,013	−0,017	+0,019
	1	−0,010	+0,012	−0,021	+0,100	−0,048	+0,099	−0,099	+0,160
	0	1,121	−0,522	1,138	−0,548	1,194	−0,585	1,277	−0,627
	−1	−0,026	+0,043	−0,177	+0,002	−0,307	+0,054	−0,414	+0,056
	−2	−0,003	+0,006	−0,019	+0,014	−0,034	+0,015	−0,043	+0,015
	−3		0,003	−0,007	+0,006	−0,012	+0,007	−0,016	+0,007

The expression of these coefficients in terms of the influence coefficients is constructed by the method described above:

$$c_{y\theta} = \sum_{n=-\infty}^{\infty} l_\theta e^{ln\alpha}, \quad c_{yy} = \sum_{n=-\infty}^{\infty} l_y e^{ln\alpha},$$

$$c_{m\theta} = \sum_{n=-\infty}^{\infty} m_\theta e^{ln\alpha}, \quad c_{my} = \sum_{n=-\infty}^{\infty} m_y e^{ln\alpha}.$$

§ 5.3. Unsteady Motion for an Arbitrary Relationship to Time

Solutions obtained under the assumption of a harmonic relationship of the form of the jump or of the oscillation velocity to time can, in view of the linearity of the problem, be extended to a random relationship. In such a case, if the action of the velocity jump of the profile oscillation is described by a periodic law, a Fourier series is used. If the action is aperiodic, the solution is expressed in terms of a Fourier integral. In turbomachines, in view of the periodicity of the processes, the use of Fourier series is of the greatest significance. However, in some cases it becomes necessary to study aperiodic processes as well.

Let us assume that there is a solution for the harmonic law of oscillation $v_0 \exp j\nu\tau$, expressed in terms of the function $Z_0(k, q, \gamma_b, \alpha) = Z_0$. It is required to find a solution where the boundary conditions change with time according to the given law $f(\tau)$. We assume that $f(\tau)$ satisfies the conditions necessary for the application of Fourier transforms.

The spectrum of the given time function is found from the formula

$$s(k) = \int_{-\infty}^{\infty} v(\varphi) e^{-ik\varphi} d\varphi. \tag{5.18}$$

Then the desired solution is determined by the Fourier integral:

$$Z(\varphi) = \frac{1}{2i} \int_{-\infty}^{\infty} Z_0(k) s(k) e^{ik\varphi} dk. \tag{5.19}$$

Here $k = \nu b/U$ is the Strouhal number, $\varphi = U\tau/b$ is dimensionless time. We shall consider the two most important cases.

1. Up to $\tau<0$ the profiles in the cascade were motionless, and when $\tau>0$ they suddenly acquired a velocity of $v_0 \exp j\alpha$. In this case the time function is a unit step function $\sigma(\tau)$ and its spectrum is

$$s(k)=\int_{-\infty}^{\infty}\sigma(\varphi)e^{-jk\varphi}d\varphi=\frac{1}{jk}.$$

Consequently, the solution is determined by the formula

$$Z_0(\varphi)=\frac{1}{2\pi j}\int_{-\infty}^{\infty}\frac{1}{k}Z_0(k)e^{-jk\varphi}dk. \tag{5.20}$$

The problem of a sudden change of the angle of attack for an isolated wing was first considered (by the vortex method) by Wagner. Obviously, according to (5.20) the Wagner function can be expressed in terms of the Theodorsen function:

$$W(\varphi)=\frac{1}{2\pi j}\int_{-\infty}^{\infty}\frac{1}{k}C(k)e^{jk\varphi}dk. \tag{5.21}$$

The value of the Wagner function is presented in Table 5.3.

TABLE 5.3

φ	$W(\varphi)$	φ	$W(\varphi)$	φ	$W(\varphi)$
0,0	0,5000	5,5	0,8010	12	0,8911
0,5	0,5537	6,0	0,8125	15	0,9148
1,0	0,6006	6,5	0,8230	20	0,9366
1,5	0,6378	7,0	0,8325	25	0,9501
2,0	0,6693	7,5	0,8412	30	0,9591
2,5	0,6952	8,0	0,8491	40	0,9702
3,0	0,7195	8,5	0,8564	50	0,9767
3,5	0,7399	9,0	0,8631	100	0,9891
4,0	0,7579	9,5	0,8693	500	0,9980
4,5	0,7739	10	0,8750	1000	0,9990
5,0	0,7882	11	0,8853	∞	1,0000

The lift force acting upon a plate is equal to

$$\mathcal{Y}=2\pi b\rho^0 U v_0[W(\varphi)+b\,\delta(\varphi)].$$

Function $W(\varphi)$ determines the increment of the lift force as the flow becomes stabilized. The value φ may be treated as the path

traveled by the wing (or by the stream) after the change of the stream. This path is measured in terms of wing semichords. Thus, for example, it follows from Table 5.3 that when $\varphi=1$, the lift force reaches 60% of the stabilized value. The rate of stabilization of the circulation is linked with the influence of the acceleration vortex. The delta function in the formula for the lift force is due to the origination of infinite accelerations in the fluid at the moment of reconstruction of the current $\varphi=0$.

2. The cascade passes through a vertical velocity jump, which moves at the velocity of the main stream (Figure 5.1). The vertical velocity (at the basic profile is given by the condition:

$$\left.\begin{array}{ll}\text{when } x>U\tau-b & v_0=0,\\ \text{when } x<U\tau-b & v_0=1.\end{array}\right\}$$

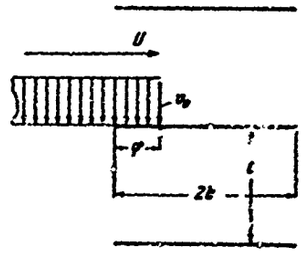


Figure 5.1. The incidence of a vertical velocity jump onto a cascade.

Then the time function is described by the unit function $\sigma(\varphi-1-x/b)$ and its spectrum is

$$s(k)=\int_{-\infty}^{\infty}\sigma\left(\varphi-1-\frac{x}{b}\right)e^{-jk\varphi}d\varphi=\frac{1}{jk}e^{-\left(1+\frac{x}{b}\right)jk}.$$

Consequently, we obtain

$$Z(\varphi)=\frac{1}{2\pi j}\int_{-\infty}^{\infty}\frac{1}{k}Z_0(k)e^{jk\left(\varphi-1-\frac{x}{b}\right)}dk. \qquad (5.22)$$

For an isolated wing the analogous problem was first considered by Kuessner, and his function is also expressed in terms of the

function C(k):

$$K(\varphi)=\frac{1}{2\pi i}\int_{-\infty}^{\infty}\frac{1}{k}C(k)e^{ik\left(\varphi-1-\frac{\pi}{b}\right)}dk. \tag{5.23}$$

The value of Kuessner's function is presented in Table 5.4.

TABLE 5.4

φ	$K(\varphi)$	φ	$K(\varphi)$	φ	$K(\varphi)$	φ	$K(\varphi)$
−1,0	0,0000	7,0	0,8225	0,6	0,5057	25	0,9190
−0,8	0,1950	8,0	0,8408	0,8	0,5293	30	0,9383
−0,6	0,2757	9,0	0,8561	1,0	0,5508	40	0,9608
−0,4	0,3321	10	0,8691	2,0	0,6351	50	0,9765
−0,2	0,3782	11	0,8801	3,0	0,6915	100	0,9890
0,0	0,4167	12	0,8897	4,0	0,7388	500	0,9979
0,2	0,4509	15	0,9117	5,0	0,7731	1000	0,9990
0,4	0,4791	20	0,9319	6,0	0,8004	∞	1,0000

In turn, the Wagner function or the Kuessner function (or, in the general case, Z) can serve as fundamental functions for the expression of new solutions in terms of m. For this it is necessary to apply the superposition principle, written in the form of the Duhamel integral:

$$Y(\varphi)=v_0(0)Z(\varphi)+\int_0^{\varphi}\frac{\partial v}{\partial\sigma}Z(\varphi-\sigma)\,d\sigma. \tag{5.24}$$

If the Duhamel integral is written in terms of the Kuessner function, we obtain the solution for an arbitrary velocity jump $v(\varphi)$, defined for $\varphi>0$. This solution will be obtained as a result of the addition of a series of step jumps. An analogous result may be written for a cascade, where each profile has a jump with a phase shift.

The increment of the lift force when a single profile encounters a jump (the limit case of a very sparse cascade 2b/t = 0) is shown in Figure 5.2. In the other limit case for a very dense cascade ($\exp \pi b/t \gg 1$) the problem, as has been shown above, may be treated as a quasi-steady one. When the jump occurs the lift force attains the stabilized value in a stepwise fashion. The graphs of the lift force

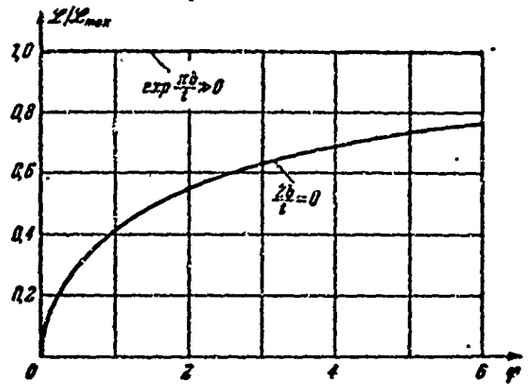


Figure 5.2. Reaction of a very thin cascade and a very dense cascade to a velocity jump.

are plotted in fractions of its steady-state value $\mathcal{Y}_{max}$ in the two above mentioned special cases.

The change of the lift force with the incidence of a rectangular wake, which may be presented as two consecutive jumps, is shown in Figure 5.3. The maximum value of the force attained in a thin cascade depends upon the width of the jump, which in this case is equal to $\Delta/2b=1/2$. The lift force in Figure 5.3 is expressed in terms of the stabilized lift force $\mathcal{Y}_{max}$ in the case of a jump of infinite length. In particular, the reaction of a single profile to a rectangular shaped jump with a length of Δ is equal (here the Kuessner function is used) to

$$\mathcal{Y}=2\pi b\rho^0 U v_0[K(\varphi)-K(\varphi-\varphi_1)],\quad \varphi-\varphi_1=\Delta/2b. \tag{5.25}$$

In some cases applicable to turbomachines, it is convenient to consider an infinitely narrow jump. In (5.25) we shall direct the length of the jump toward zero ($\Delta\to 0$), retaining $v_0\Delta=\text{const}$ in the transition. Then the jump will be given by the Dirac δ-function, and the stream force may be expressed in terms of the derivative of the Kuessner function:

$$\mathcal{Y}=2\pi\rho^0\Delta v_0 U\frac{dK(\varphi)}{d\varphi}. \tag{5.26}$$

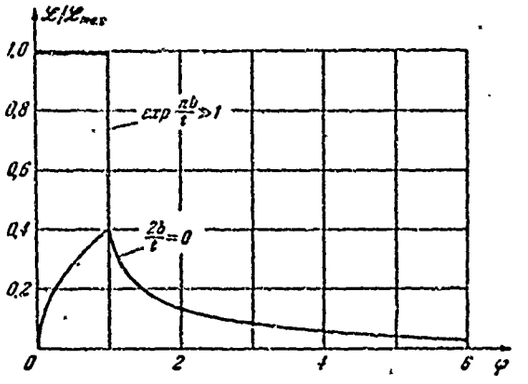


Figure 5.3. Reaction of a very thin cascade and a very dense cascade to a velocity jump of limited width.

Function $\frac{dK(\varphi)}{d\varphi}$ has been tabulated by Mayer [119] and, in greater detail, by Lefert [115], which is necessary for numerical integration in the solution of practical problems. At the moment of encounter of the wake with a sharp leading edge the force will be infinitely great; however, the impulse will be finite and is expressed in terms of the Kuessner function (or a cascade analogous to it).

An analogous series of solutions may also be obtained in another way, since the problem of a jump of arbitrary shape can generally be solved by means of the function Z_0, derived for a jump of sinusoidal shape. It is necessary only to keep in mind, when computing the spectrum, that the solution for a jump of sinusoidal shape already assumes the existence of a traveling wave. Thus, for example, the spectrum for a vertical jump is defined by the formula

$$s(k) = \int_{-\infty}^{\infty} \sigma(\varphi) e^{-jk\varphi} d\varphi = \frac{1}{jk}.$$

Then the solution may be expressed in terms of Z_0 (where by Z_0 are already understood to be functions of the R type) in the form

$$Z(\varphi) = \frac{1}{2\pi j} \int_{-\infty}^{\infty} \frac{1}{k} Z_0(k) e^{jk\varphi} dk.$$

In particular, for an isolated profile the solution may be expressed in terms of S(k). Consequently, the connection between the Kuessner function and the Sears function is found as:

$$K(\varphi) = \frac{1}{2\pi j} \int_{-\infty}^{\infty} \frac{1}{k} S(k) e^{jk\varphi} dk.$$

For a jump given by a δ-function, the spectrum is equal to 1 and, consequently, we obtain a solution of the type of (5.26) in another form:

$$\frac{dK(\varphi)}{d\varphi} = \frac{1}{2\pi} \int_{-\infty}^{\infty} S(k) e^{jk\varphi} dk.$$

§ 5.4. The Influence of a Shift of Profiles in a Cascade

In the calculations of cascades considered above, the shift of profiles was disregarded. This simplification causes a small error if around the profile flow has zero angle of attack, and the oscillation frequency is sufficiently large. Actually, defining the profile shift by the function $y = h \exp j\nu\tau$, we find the boundary value of velocity $v_0 = j\nu h \exp j\nu\tau$. From this it follows that the velocity may be great even with a small shift. The influence of a profile shift will be most significant of all with a low oscillation frequency, a high cascade density, and a large turning angle of the main stream.

Analysis of the problem of unsteady streamline flow taking into account the shift of profiles is of considerable interest, since in this case the origination of flutter with one degree of freedom is possible. The problem taking the shift of profiles into account has been studied by Whitehead [146], V. V. Musatov [48], V. E. Saren [73], and D. N. Gorelov. The influence of the shift upon unsteady forces is characteristic for a cascade and is insignificant for a single wing.

Let us consider a cascade (Figure 5.4) with the offset γb, the plate spacing t and the chord 2b. The plates can oscillate harmonically in a direction perpendicular to the chord. The oscillation of

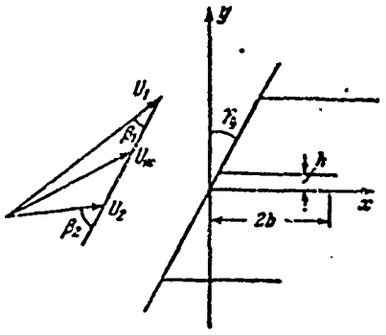


Figure 5.4. Concerning flow about an aerodynamically loaded cascade.

the plates takes place with a phase shift in such a manner that the shift of plate m from the central position is given by the formula $h\exp j(\nu\tau+m\alpha)$. The cascade is in a stream of ideal fluid which has the velocity U_1 at an infinite distance in front of the cascade and U_2 far behind it. From the continuity equation it follows that the projections of these velocities onto a normal to the cascade axis must be equal. Figure 5.4 shows the modulus of the mean geometric velocity before and after the cascade in terms of U_m.

We shall assume that the profile is small in comparison to the spacing $h \ll l$ and that the oscillation velocity is small in comparison to the main stream velocity $v_0 \ll U$. The attached vorticity originating at the profiles may be broken down into two components, of which the first one, γ_0, does not depend upon time, while the second component, γ, depends upon time. Since in practical problems the influence of the shift of the blades will manifest itself in the case of a small reduced oscillation frequency and a large angle of turn of the main stream, we shall consider the case of $\gamma \ll \gamma_0$.

In the subsequent calculations we shall disregard the squares and derivatives of small values. From this it may be concluded that the influence of shift may be regarded only as an effect of a shift of the constant part of the attached vorticity. The part of the attached vorticity that is variable in time may be referred to the central position of the profile. Since the intensity of the vortices in the wakes is of the same small order as γ, it is possible, as before, to disregard the shift of the wakes and to consider them situated along the flow lines of the main steady stream.

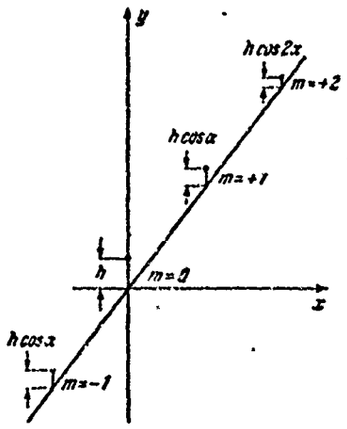


Figure 5.5 A vortex cascade with shift.

In order to obtain the kernel of the integral equation, let us first consider a cascade of vortices with the offset γb and the spacing t, situated in the region of the complex variable $z = x + iy$ (Figure 5.5). Having in view subsequently to study the shift of the blades, let us assume that the vortices have a vertical shift of $h \exp jm\alpha$ and, consequently, are situated at the points

$$z_m = lmte^{-i\gamma_b} + ihe^{lm\alpha}. \tag{5.27}$$

Let all the vortices have the unit circulation $\Gamma(m)=1$.

The complex velocity induced by the vortex cascade will be expressed by the series

$$w(z) = \frac{1}{2\pi i} \sum_{m=-\infty}^{\infty} \frac{1}{z - lmte^{-i\gamma_b} - ihe^{lm\alpha}}.$$

It is convenient to introduce a system of coordinates linked to the main vortex, i.e., to transform the coordinates. We pass to the new system of coordinates and, discarding the index, we obtain

$$w(z) = \frac{1}{2\pi i} \sum_{m=-\infty}^{\infty} \frac{1}{z - lmte^{-i\gamma_b} + ih\left(1 - e^{lm\alpha}\right)}.$$

We expand this expression into a Taylor series and retain the term of the first order of smallness with respect to the vortex shift amplitude:

$$w(z) = \frac{1}{2\pi i} \sum_{m=-\infty}^{\infty} \frac{1}{z - lmt_1} + \frac{h}{2\pi} \sum_{m=-\infty}^{\infty} \frac{e^{lm\alpha} - 1}{(z - lmt_1)^2}.$$

Here we have introduced the designation of the complex spacing $t_1 = t \exp(-i\gamma_b)$. The first series is summed and is equal to $(\pi/it_1)\operatorname{ctg}(\pi z/t_1)$. After the transformations the second series can also be summed:

$$\sum \frac{e^{jm\alpha}-1}{(z-imt_1)^2} = -\frac{d}{dz}\left(\sum \frac{e^{jm\alpha}}{z-imt_1} - \sum \frac{1}{z-imt_1}\right) =$$
$$= \frac{\pi}{t_1}\frac{d}{dz}\left\{\frac{\operatorname{ch}\left[(\pi-\alpha)\frac{z}{t_1}\right]+ij\operatorname{sh}\left[(\pi-\alpha)\frac{z}{t_1}\right]-\operatorname{ch}\pi\frac{z}{t_1}}{\operatorname{sh}\pi\frac{z}{t_1}}\right\}. \qquad (5.28)$$

In the last transformation Formula (3.3) has been used; it is valid under the condition of $0<\alpha<2\pi$.

Thus, the cascade of vortices which are situated with the shift $ih\exp jm\alpha$ induces the same kind of a velocity field as if the vortices were situated without shift, and a supplementary field (when h << t), defined by (5.28).

We designate (the sign Im designates the imaginary part with respect to i)

$$K_0(x) = \operatorname{Im}\frac{1}{2t_1}\frac{d}{dz}\left\{\frac{\operatorname{ch}\left[(\pi-\alpha)\frac{x}{t_1}\right]-\operatorname{ch}\pi\frac{x}{t_1}+ij\operatorname{sh}\left[(\pi-\alpha)\frac{x}{t_1}\right]}{\operatorname{sh}\pi\frac{x}{t_1}}\right\}. \qquad (5.29)$$

Here z is replaced by x, since calculation of the vertical velocities is necessary only at the basic profile of the cascade, which is situated on the abscissa. On the basis of (5.28) and (5.29) it may be concluded that the vertical velocity at the point x, y = 0 of the vortex cascade, the main vortex of which has the coordinates $\xi, \eta=0$, is defined by the expression

$$v(x, 0) = \operatorname{Re}\frac{1}{2t_1}\operatorname{cth}\frac{\pi}{t_1}(x-\xi)+hK_0(x-\xi). \qquad (5.30)$$

The second term determines the supplementary vertical velocity induced by the vortex shift. These supplemental velocities are proportional to the shift, for the adopted degree of accuracy. The second term has no singularities; this is physically understandable, since it takes into account the shifts of the adjacent profiles. In the absence of a phase shift ($\alpha = 0$) we obtain $K_0 = 0$, which is obvious, since the cascade oscillates as a single system.

Let us now pass on to consideration of the basic problem. When the plates in the cascade oscillate with a shift, attached vorticity

will be induced at the plates; this vorticity can be broken down into the component γ_0, which does not depend upon time, and the component γ, which depends upon time:

$$\gamma_0(x) + \gamma(x)e^{j\omega t}.$$

Here $\gamma(x)$ is a complex value with respect to j.

The constant attached vorticity is determined from the solution of the static problem for a cascade in a main stream with a large angle of turn:

$$U_{my} + \mathrm{Re}\frac{1}{2t_1}\int_0^{2b} \gamma_0(\xi)\operatorname{ctg}\frac{\pi}{t_1}(x-\xi)\,d\xi = 0.$$

Here U_{my} is the vertical projection of the main geometric velocity. The solution of this problem for a cascade of plates is known, and for a cascade of plates without offset $(\gamma_0=0)$ may be expressed by simple formulas. Thus, we consider $\gamma_0(X)$ to be a known function. With shift of the profiles (and the attached vorticity), supplemently velocity normals are induced at the profiles. These supplemental velocities may be defined by means of the second term of Formula (5.30), considering it as a kernel:

$$v(x) = h\int_0^{2b} \gamma_0(\xi)K_0(x-\xi)\,d\xi. \qquad (5.31)$$

Consequently, with a shift of oscillating profiles it is necessary, in addition to the oscillation velocity, to take into account the normal induced Velocities (5.31). A shift modulus may be replaced by the oscillation-velocity modulus $h=v_0/jv$. Then the basic integral equation, from which the attached vorticity $\gamma(\xi)$ is determined, may be written in the following manner:

$$v_0(x) + [v_0(x)/jv]\int_0^2 \gamma_0(\xi)K_0(x-\xi)\,d\xi = \int_0^2 \gamma(\xi)H(x-\xi)\,d\xi. \qquad (5.32)$$

Here it is assumed that 2b = 2.

This equation differs from the analogous equation, written without taking into account the profile shift, by virtue of the second term in the left-hand part which takes into account the supplemental normal velocities. For a high oscillation frequency the coefficient in front of this term tends toward zero, and we obtain the initial special case.

Thus, in the case of small shift the problem differs from the analogous problem without taking into account shifts only due to a simple change of the boundary conditions.

The formula for determining the forces and moments acting upon the profiles in the streamline flow do not differ from those cited above, since they are expressed in terms of the attached vorticity. All that must be added are the static forces and the moment brought about by that part of the attached vorticity which does not depend upon time. Determination of these forces and this moment is carried out on the basis of the same formulas, and encounters no difficulty.

Some results of the calculation of plate cascades with taking shift into account are presented in the works cited above.

§ 5.5. Determination of the Total Quasi-Steady Characteristics of Cascades by Means of an Electrohydrodynamic Analogy

Use of the electrohydordynamic analogy method for solving problems in hydromechanics is a method of analysis that is carried out experimentally.

The solution of the problem may be reduced to finding the stream function $\psi(x,y)$, which satisfies the Laplace equation and satisfies the necessary boundary conditions. We shall consider the stream function of a perturbed stream, since the superposition of the basic homogeneous stream can be performed separately, taking advantage of the linearity of the problem.

In view of the fact that the perturbations tend towards zero far from the perturbing bodies in the streams under consideration, the boundary condition for the stream function at infinity will be

$$\frac{\partial \psi}{\partial x} = 0, \quad \frac{\partial \psi}{\partial y} = 0. \tag{5.33}$$

The boundary conditions at the contour are determined by equality of the normal surface and fluid velocities $\partial\psi/\partial s = v_n$ or

$$\psi = v_x y - v_y x - \frac{1}{2}\Omega(x^2 + y^2) + \text{const.} \tag{5.34}$$

Here v_x and v_y are projections of the oscillation velocity of the point of the contour on the abscissa and ordinate; Ω is the angular velocity of the oscillation.

Two basic methods of employment of the electrohydrodynamic analogy are possible. In the first method the electrical potential is compared with the velocity potential; in the second method the electrical potential is compared with the stream function. In the first case the body in the streamline flow must be replaced by an insulator situated in the electrical field. In the second case the body must be replaced by a conductor with a given distribution of electrical potential along the surface. The law of distribution of the electrical potential must be selected in such a manner as to satisfy boundary Condition (5.34). The second method is convenient in the problems under consideration.

When using the analogy according to the second method, to the circulation velocity is compared the strength of the electric current supplied to a model of the body in the streamline flow:

$$\Gamma = mJ \cdot R_0, \tag{5.35}$$

where R_0 is the ohmic resistance of the paper, J is the intensity of the current passing through the model, m is the proportionality coefficient.

Studying unstabilized flow about cascades, it is of interest to study a quasi-steady problem which may be considered as a limit case. In the quasi-steady formulation, to Conditions (5.33) and (5.34) is added the Chaplygin-Zhukovskiy condition at the trailing edge. If, as has been done below, a solution is sought only for a perturbed stream, the Chaplygin-Zhukovskiy condition may be formulated as equality of the tangential components of the perturbed velocities at both sides of the edge.

Let us consider the method of conducting the experiment on the basis of the example of constructing a perturbed field about a vibrating plate. When vibration is spoken of, it is meant that the plate is motionless, but that the boundary conditions on it are given according to Condition (5.34), as is considered in linearly formulated problems. In the case of translational vibrations, it follows from (5.34) that $\psi = -vx + \text{const}$. Since the stream function is equivalent to an electrical potential, it is necessary to assign a distribution of the electrical potential according to a linear law.

Current-conducting paper is taken as the electrically conductive medium. The plate consists of narrow pieces of foil, the electrical resistance of which is much less than the specific resistance of the paper. Electric current is fed through voltage dividers to each strip, in this case in such a manner that the voltage drop from strip to strip is linear. The line is replaced by stepwise sectors (in this case by ten). The second electrode is a ring and is situated at a large distance from the plate, so that the region under consideration will be internal to it. The total force of the current passing along all the plates is regulated in such a manner (without changing the linear law of voltage drop) that the lines of equal electrical potential, corresponding to the stream line in the fluid (A), are normal to the trailing edge (Figure 5.6).

The line of equal electric potential is determined by means of a probe and a zero instruemnt. In this case a series of stream lines is plotted. For determining the total force it is necessary to plot

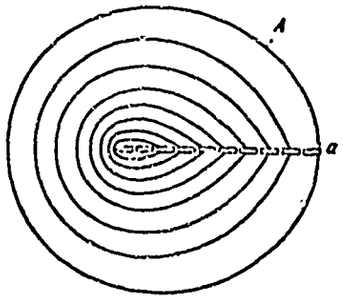


Figure 5.6. Stream lines of perturbed flow in the case of vibration of a plate, constructed by means of electrohydrodynamic analogy.

only the sectors of the stream lines (A) adjacent to the trailing edge (a) to be convinced that the Chaplygin-Zhukovskiy condition is fulfilled. Determining the force of the current supplied to the model, we find the value of the circulation. Then the force which acts upon an oscillating profile which is in a uniform stream with a velocity of U is defined, in the quasi-steady formulation, by the Zhukovskiy theorem:

$$\mathcal{Y} = \rho^* U \Gamma.$$

Experiments show that the practical accuracy of determination of the circulation lies within the limits of 1.5 - 3%. (Such an accuracy can be obtained on electrically conductive paper with the measurement of integral characteristics such as, for example, circulation.)

When studying the oscillation of profiles in counterphase in a cascade without offset, advantage may be taken of the fact that this problem is equivalent to the oscillation of a wing in a channel. When the electrohydrodynamic analogy method is used, the channel walls are replaced by current-conducting buses (1) and (2) (Figure 5.7). In Figure 5.8, results of experimental measurements conducted with various cascade densities are compared with the theoretical formula [74]. The ratio of the circulation of a plate in a cascade to that of an isolated plate is plotted along the ordinate. Comparison shows that the measurement accuracy is entirely satisfactory. The formula of L. I. Sedov [74] for circulation about a plate in a channel in terms of our motation has the form (2b - chord)

$$\Gamma = \frac{4l}{\pi^2} v_0 \operatorname{sh} 2q \left[\int_0^{\pi/2} \frac{d\theta}{\sqrt{1 + \operatorname{sh}^2 q \sin^2 \theta}} \right]^2, \quad q = \frac{\pi b}{t}. \tag{5.36}$$

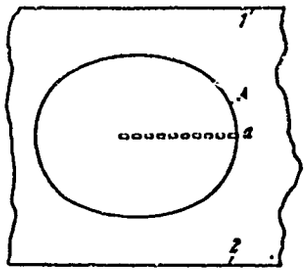


Figure 5.7. Diagram of an experiment in studying the oscillation of blades in counterphase.

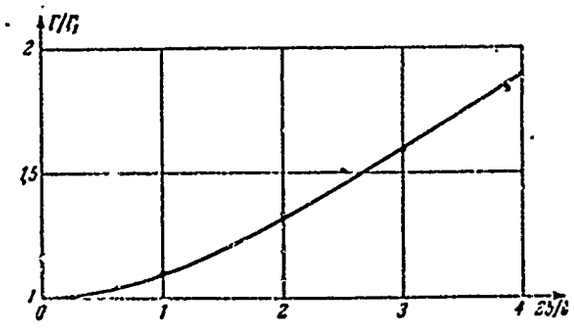


Figure 5.8. Comparison of the experimental value and the theoretical value of circulation in case of the oscillation of blades in counterphase (quasi-steady approximation).

Since the cited formula is one of the few precise solutions for a cascade, it is expedient to utilize it not only in experiments, but also in evaluating the accuracy of the approximate theoretical calculation methods.

In order to obtain a convenient calculation formula, we effect in (5.36) the substitution of variables $x=\sin^2\theta$ and express the integral in terms of a hypergeometric function:

$$I(q)=\frac{1}{2}\int_0^1 x^{-1/2}(1-x)^{-1/2}(1-x\,\mathrm{sh}^2 q)^{-1/2}\,dx=$$
$$=\frac{1}{2}B\left(\frac{1}{2},\frac{1}{2}\right)F\left(\frac{1}{2},\frac{1}{2},1,-\mathrm{sh}^2 q\right)$$

The value of the beta-function when its arguments are equal to 1/2 is known: $B(1/2, 1/2)=\pi$. We represent the result in terms of a hypergeometric series, using the formula for the conversion of a hypergeometric function

$$F(\alpha,\beta,\gamma,z)=(1-z)^{-\alpha}F\left(\alpha,\gamma-\beta,\gamma,\frac{z}{z-1}\right),$$

in order to replace the argument $z = -\mathrm{sh}^2 q$ with an infinite interval by a new argument, $z/(z-1) = \mathrm{th}^2 q$, which varies within the limits of 0 to 1.

Utilizing the expansion

$$F(\alpha, \beta, \gamma, z) = 1 + \frac{\alpha \cdot \beta}{\gamma \cdot 1} z + \frac{\alpha(\alpha+1)\beta(\beta+1)}{\gamma(\gamma+1) \cdot 1 \cdot 2} z^2 + \ldots,$$

after transformation we obtain the final formula for determining the circulation when the blades are oscillating in counterphase:

$$\Gamma(q) = 2lv_0 \operatorname{th} q \left(1 + \frac{1}{4} \operatorname{th}^2 q + \frac{9}{64} \operatorname{th}^4 q + \frac{25}{256} \operatorname{th}^6 q + \ldots\right)^2. \qquad (5.37)$$

In a special case of an isolated plate ($l \to \infty$, $q \to 0$) we obtain the known solution

$$\Gamma(0) = 2\pi b v_0.$$

The analogy method may also be used for the determination of influence coefficients. The experiment is conducted according to the setup shown in Figure 5.9. In this case it is necessary to create a model in the case of which one blade (the central one) oscillates, while the rest are motionless (actually, the model has 11 blades). The central blade is split, and the difference in potential along the sectors is established by the selection of resistances R. The conditions at the trailing edge of this blade are controlled by the construction of a stream line, as described above. The remaining blades are motionless; consequently they must coincide with the streamlines. This corresponds to streamline flow without separation. Therefore, they are made of continuous foil. The force of the current fed to them is regulated by resistances R_1, R_2, ... (only four blades are shown). For these blades the Chaplygin-Zhukovskiy postulate will be satisfied if the stream line is tangent to the trailing edge. The selection of resistances for satisfying this condition is made by successive approximations. Since the profiles are flowed about with a circulation induced by the perturbing field of the central blade, the front branch points of the stream do not coincide with the front points of the plates.

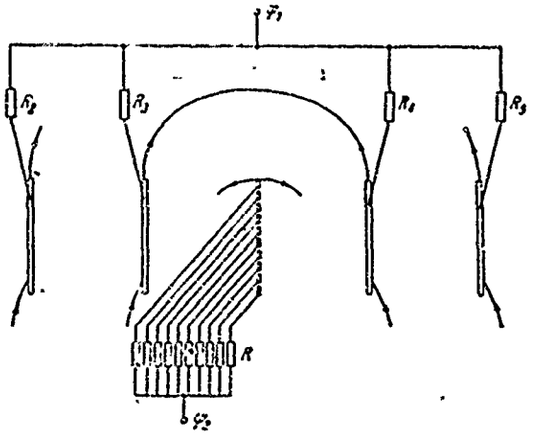


Figure 5.9. Diagram of determination of influence coefficients on an electrohydrodynamic model.

The results of an experiment for a cascade without offset with a relative spacing of t/2b = 1 are presented in Table 5.5. Experimentally obtained ratios of the circulation of the m^{th} blade to that of the central blade (m = 0) are also presented in the table. For comparison, the last line shows the ratios determined by the theoretical method on an electronic computer for a low Strouhal number (k = 0, 1). The results coincide in a completely satisfactory way.

TABLE 5.5

blade number	-3	-2	-1	0	1	2	3
Γ_m/Γ_0	0,012	0,032	0,159	1	0,119	0,030	0,011
Γ_m/Γ_0	0,01115	0,0270	0,1455	1	0,1455	0,0270	0,01115

Table 5.6 shows analogous results for a case where the central blade was shifted along the cascade axis by a relative distance equal to y/t = 0,037.

TABLE 5.6

blade number	-3	-2	-1	0	1	2	3
Γ_m/Γ_0	0,009	0,023	0,121	1	0,151	0,028	0,010

In an analogous manner it is possible to obtain the influence coefficients for cascades with offset. In principle, if the main

stream is superimposed, aerodynamically loaded cascades can be studied. The problem of determination of the total quasi-steady characteristics for a cascade of plates by the electrohydrodynamic analogy method was studied in Reference [66a].

With a sufficient number of voltage dividers R, the problem of the mutual influence of cascades can be solved by the same means.

The solution of a quasi-steady problem was discussed above, but it is also possible to take into account the influence of a vortex wake, which is replaced by a split conductor. However, it is simpler to use only a one point conductor (an imitation of a vortex), to make the profiles continuous and, essentially, to construct Green functions by means of the electrohydrodynamic analogy method. Then the summation, when counting up the influence of all the wakes, is performed on the basis of linearity of the problem. The electrohydrodynamic analogy method may also be used for constructing an acceleration potential. In this case, construction of a vortex wake is unneccessary.

FOOTNOTES

1. on page 199. The position of the coordinate axes remains the same — on the leading edge of the plate.

2. on page 200. Here it is assumed that the profiles oscillate according to the law $\exp(\nu t+m\alpha)$.

3. on page 200. Here the problem of asynchronous motion of the profiles is also solved.

4. on page 217. Here it is assumed that the profiles oscillate according to the law $\exp(\nu t+m\alpha)$.

CHAPTER 6

A CASCADE OF VIBRATING PROFILES IN A SUBSONIC STREAM

§ 6.1. Formulation of the Problem

Let us consider flow by a two-dimensional subsonic stream of compressible fluid about a cascade of plates oscillating with small amplitudes according to a harmonic law. Adjacent plates oscillate with an arbitrary constant phase shift α. We designate by t the spacing of the plates, 2b is the chord of the plates, and γb is the offset of the cascade. At an infinite distance from the cascade the incoming stream is homogeneous and has a velocity of U, parallel to the chords of the plates. We shall connect the system of coordinates with the center of a plate to which we shall assign the number $m = 0$.

In the system of coordinates connected with the cascade, the velocity potential of perturbed motion $\varphi(x, y, \tau)$ must satisfy the equation obtained by the Galileo transform:

$$(1-M^2)\frac{\partial^2\varphi}{\partial x^2}+\frac{\partial^2\varphi}{\partial y^2}-2\frac{M}{a_0}\frac{\partial^2\varphi}{\partial x\,\partial\tau}-\frac{1}{a_0^2}\frac{\partial^2\varphi}{\partial\tau^2}=0. \tag{6.1}$$

Here $M = U/a_0$, a_0 is the velocity of sound in an unperturbed stream.

The boundary conditions are based upon the requirements of streamline flow without separation and impermeability of the plates:

$$\left.\begin{aligned} \frac{\partial \varphi}{\partial y} &= v_{0y}(x)\, e^{i(\omega t + \alpha)}, \\ y - mt\cos\gamma_b &= 0. \end{aligned} \quad \begin{aligned} |x - mt\sin\gamma_b| &\leqslant b, \end{aligned}\right\} \tag{6.2}$$

This condition is insufficient to guarantee uniqueness of the solution of the problem. Other conditions are formulated when the physical considerations are considered.

The perturbed pressure is defined by the linearized Lagrange integral:

$$p = -\rho^0\left(\frac{\partial \varphi}{\partial \tau} + U\frac{\partial \varphi}{\partial x}\right). \tag{6.3}$$

Here $p = p(x, y, \tau)$, ρ^0 is the density of the unperturbed fluid.

Behind the profiles vortex wakes propagate, which are discontinuity lines of the tangential velocity and the potential. The perturbation-pressure field is continuous at the wake; and therefore the condition

$$\frac{\partial \varphi}{\partial \tau} + U\frac{\partial \varphi}{\partial x} = 0 \tag{6.4}$$

must be satisfied.

At the trailing edges of the profiles the condition of finiteness of the velocity at any moment of time must be satisfied (or the equivalent requirement that the pressure gradient be equal to zero). To these conditions, in contrast to the case of an incompressible fluid flow, we must add the requirement concerning the absence of radiation from infinity (the Sommerfeld principle). In other words, the physical condition must be maintained according to which the energy radiation from the oscillation sources recedes from the cascade to infinity and does not return in the form of an "echo". At a sharp leading edge the pressure tends toward infinity. It is assumed that this condition

does not differ from the analogous condition in an incompressible fluid.

Let us pass on to the dimensionless coordinates of time, potential, velocities, and pressure:

$$\left.\begin{aligned} x = b\bar{x},\ \ y = \frac{b}{\sqrt{1-M^2}}\bar{y},\ \ \tau = \frac{b}{U}\bar{\tau}, \\ \varphi(x, y, \tau) = bU\bar{\varphi}(\bar{x}, \bar{y}, \bar{\tau}),\ \ \bar{v} = \frac{v}{U},\ \ \bar{p} = \frac{p}{\rho^0 U^2}. \end{aligned}\right\} \tag{6.5}$$

Subsequently, we shall be writing new dimensionless values, discarding the bar.

In dimensionless form, the equation of the velocity potential assumes the form

$$\frac{\partial^2\varphi}{\partial x^2} + \frac{\partial^2\varphi}{\partial y^2} - \frac{2M^2}{1-M^2}\frac{\partial^2\varphi}{\partial x\,\partial\tau} - \frac{M^2}{1-M^2}\frac{\partial^2\varphi}{\partial\tau^2} = 0. \tag{6.6}$$

We introduce the designation of dimensionless criteria:

$$k = \frac{\nu b}{U},\ \ \varkappa = \frac{kM}{1-M^2},\ \ \mu = \frac{kM^2}{1-M^2}.$$

We shall seek a solution in the following form:

$$\varphi(x, y, \tau) = \Phi(x, y)\,e^{j(k\tau+\mu x)}. \tag{6.7}$$

Only the desired function should satisfy the Helmholtz equation:

$$\frac{\partial^2\Phi}{\partial x^2} + \frac{\partial^2\Phi}{\partial y^2} + \varkappa^2\Phi = 0. \tag{6.8}$$

We shall represent the boundary conditions at the profiles and at the wakes in terms of the new desired function:

$$\frac{\partial\Phi}{\partial y} = \frac{v_{0y}(x)}{\sqrt{1-M^2}}\,e^{-j(\mu x+j\varkappa a)}, \tag{6.9}$$

$$\frac{\partial\Phi}{\partial x} + j\delta\Phi = 0,\quad \delta = \frac{k}{1-M^2}. \tag{6.10}$$

The function $\Phi(x, y)$ must satisfy the indicated postulate at the trailing edges and at infinity must satisfy the radiation principle. The Lagrange integral in terms of the new designation will assume the following form:

$$p = -\left(\frac{\partial \Phi}{\partial z} + j\delta\Phi\right). \tag{6.11}$$

Let us consider the possible ways of solving the problem.

In the Cartesian system of coordinates the variable Helmholtz equations can be separated, and the partial solution, as well as the general solution, can be obtained without difficulty. The principal difficulty, as always in problems of this kind, is the construction of functions which satisfy the boundary conditions. In order to obtain the solution in a form which permits the boundary conditions to be satisfied in a relatively simple manner, it is necessary to select coordinates which follow the shape of the region being studied. It is also necessary that the selected system of coordinates makes it possible to separate the variables.

However, in this manner it is possible to solve only some partial problems, since the number of coordinate systems which allow separated variables is small. It was specifically by the method of the separation of variables that M. D. Khaskind [84] solved the problem of the oscillation of a single thin wing in a subsonic stream. A direct solution of the problem by an analogous method for a cascade is impossible. However, interation methods have been developed in acoustics which make it possible to take into account the acoustic interaction of a system of bodies, if the problem of an isolated body in unrestricted space is solved first.

For the calculation of a perturbed field in a cascade with oscillating blades, a similar method has been developed by G. N. Gorelov [18]. The velocity potential of the perturbed unsteady motion of fluid about a cascade is represented by a sum of potentials, induced by oscillating isolated profiles, and a supplementary potential which

takes the interference into account.

A second possible way is compilation of the integral equation of the problem for the acceleration potential within the physical plane. Each of the methods has definite advantages and drawbacks.

Let us consider the first way, which is based upon the solution for a single wing. Therefore, we shall first consider the problem of unsteady flow about a single wing, which at the same time makes it possible to ascertain important physical singularities.

§ 6.2. A Single Vibrating Profile in a Subsonic Stream

In the plane $z = x + iy$ let us consider a single wing (Figure 6.1), which is represented by an interval drawn along the abscissa between the points ± 1. We place the trailing edge at point (-1) and, consequently, change the direction of the main stream velocity. The equation of the problem (6.8) remains the same. Instead of (6.7) we shall assume

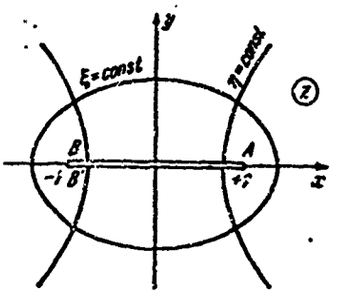


Figure 6.1. A section representing a thin, slightly bent profile in a Cartesian and elliptical system of coordinates.

$$\varphi(x, y, \tau) = \Phi(x, y) e^{i(\alpha\tau - \mu x)}. \qquad (6.12)$$

The boundary conditions at the profile and at the wake will be written in the following manner:

$$\frac{\partial \Phi}{\partial y} = \frac{v_{0y}(x)}{\sqrt{1 - M^2}} e^{i\mu x}, \qquad (6.13)$$

$$\frac{\partial \Phi}{\partial x} - j\delta\Phi = 0. \qquad (6.14)$$

The Sommerfeld principle concerning radiation is formulated mathematically in the following manner (for the two-dimensional case):

$$\lim_{r\to\infty}\sqrt{r}\left(\frac{\partial\Phi}{\partial r}-ik\Phi\right)=0. \tag{6.15}$$

Satisfying this condition simultaneously provides for a limited nature of the solution

$$\lim_{r\to\infty}\sqrt{r}\,\Phi<\infty. \tag{6.16}$$

The pressure at the sharp leading edge in a subsonic stream tends toward infinity as $s^{-1/2}$, where s is the distance from the leading edge.

Let us consider the basic considerations concerning the perturbed velocity potential for an isolated wing, based on the method of M. D. Khaskind [84]. Since in this case the boundary value problem is solved for an interval $-1\leqslant x\leqslant 1$, it is convenient to introduce elliptical coordinates. The connection between the regions of complex variables $z = x + iy$ and $\zeta=\xi+i\eta$ is established by the relationship

$$z=\operatorname{ch}\zeta,\quad x=\operatorname{ch}\xi\cos\eta,\quad y=\operatorname{sh}\xi\sin\eta. \tag{6.17}$$

A set of confocal ellipses corresponds to the coordinate lines $\xi=\text{const}$ in plane z and a set of confocal hyperbolas (Figure 6.2) corresponds to the coordinate lines $\eta=\text{const}$:

$$\frac{x^2}{\operatorname{ch}^2\xi}+\frac{y^2}{\operatorname{sh}^2\xi}=1,$$
$$-\frac{y^2}{\sin^2\eta}+\frac{x^2}{\cos^2\eta}=1.$$

The plate is represented in plane z by the section (+1, -1), which is a degenerate ellipse with semiaxes 1 and 0. In plane ζ, section BB' corresponds to the two ends of the interval.

For conversion of the boundary conditions we utilize the transformation Function (6.17) and obtain

$$\left.\begin{aligned}\frac{\partial\Phi}{\partial x}&=\frac{1}{\operatorname{ch}^2\xi-\cos^2\eta}\left(\frac{\partial\Phi}{\partial\xi}\operatorname{sh}\xi\cos\eta-\frac{\partial\Phi}{\partial\eta}\operatorname{ch}\xi\sin\eta\right),\\ \frac{\partial\Phi}{\partial y}&=\frac{1}{\operatorname{ch}^2\xi-\cos^2\eta}\left(\frac{\partial\Phi}{\partial\xi}\operatorname{ch}\xi\sin\eta+\frac{\partial\Phi}{\partial\eta}\operatorname{sh}\xi\cos\eta\right).\end{aligned}\right\} \tag{6.18}$$

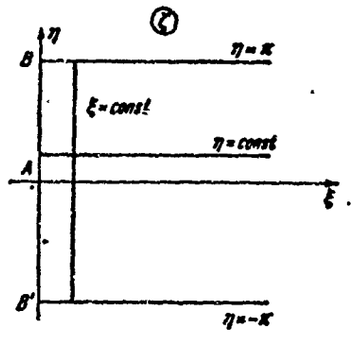


Figure 6.2. Conformal mapping of the stream region.

Since segment $\xi=0,\ -\pi\leqslant\eta\leqslant\pi$ corresponds to both sides of the plate, the boundary conditions in the auxiliary plate are defined by the relationship

$$\left(\frac{\partial\Phi}{\partial\xi}\right)_{\xi=0}=\left(\frac{\partial\Phi}{\partial y}\right)_{y=0}\sin\eta.$$

After transformation into an elliptical system of coordinates, Helmholtz's Equation (6.8) assumes a form which permits separation of the variables,

$$\frac{\partial^2\Phi}{\partial\xi^2}+\frac{\partial^2\Phi}{\partial\eta^2}+\varkappa^2(\operatorname{ch}^2\xi-\cos^2\eta)\Phi=0.$$

Consequently, a partial solution may be sought in the form of a product of functions, each of which depends upon one variable $\Phi(\xi,\eta)=F_1(\xi)F_2(\eta)$. The equation breaks down into Mathieu equations:

$$\frac{d^2F_1}{d\xi^2}-\left(m-\frac{1}{2}\varkappa^2\operatorname{ch}2\xi\right)F_1=0,$$
$$\frac{d^2F_2}{d\eta^2}+\left(m-\frac{1}{2}\varkappa^2\cos2\eta\right)F_2=0.$$

Here m is the separation constant.

Function $F_1(\xi)$ must satisfy the condition of radiation, since to points $\xi\to\infty$ correspond infinitely remote points in a physical region.

Function $F_2(\eta)$ must be periodic with a period of 2π, in order that the flow in the physical plane be represented by single-valued functions. This imposes certain conditions upon the separation constant, since the periodicity corresponds to so-called eigenvalues.

Thus, the solutions must be combined out of periodic Mathieu functions[1] $se_n(\eta)$, $ce_n(\eta)$, where n = 0, 1, 2, ..., and modified Mathieu-Hankel functions $Se_n(\xi)$, $Ce_n(\xi)$, which satisfy the condition of radiation and are analogues of Hankel functions. Cosine-type solutions $ce_n(\eta,\ \varkappa^2/4)$

Footnote (1) appears on page 268.

and sine-type solutions $se_n(\eta, \varkappa^2/4)$ may be considered. These functions are, respectively, even and odd, and when $\varkappa=0$ degenerate into cos nη and sin nη. Only functions with an odd index have a period of 2π. The eigenvalues for constant m at which a periodic solution is possible depend upon $\varkappa$ and n. Since the eigenfunctions are different for functions ce_n and se_n, these functions cannot be periodic solutions of a single equation.

It is convenient to represent the velocity potential as a sum of two functions:

$$\Phi(x, y) = \Phi_0(x, y) + \Phi_1(x, y).$$

Here Φ_0 is a velocity potential corresponding to flow without circulation flow about an isolated plate.

Function Φ_0 must satisfy the Helmholtz equation and the radiation condition

$$\frac{\partial^2\Phi_0}{\partial x^2} + \frac{\partial^2\Phi_0}{\partial y^2} + \varkappa^2\Phi_0 = 0, \quad \lim_{r\to\infty}\sqrt{r}\left(\frac{\partial\Phi_0}{\partial r} - j\delta\Phi_0\right) = 0, \quad r^2 = x^2 + y^2,$$

as well as the boundary conditions on a vibrating wing:

$$\frac{\partial\Phi_0}{\partial y} = \frac{1}{\sqrt{1-M^2}} v_{0y}(x) e^{j\omega t} = V(x) \text{ for } y = 0, \ |x|<1. \tag{6.19}$$

On the abscissa when y = 0 and $x>1$ we shall have $\Phi_0=0$. Function Φ_1 corresponds to the circulation flow originating from the vortex sheets situated along the abscissa from x = -1 to $x=-\infty$, in the presence of a motionless impermeable plate. Obviously, function Φ_1 must also satisfy the Helmholtz equation and the radiation condition

$$\frac{\partial^2\Phi_1}{\partial x^2} + \frac{\partial^2\Phi_1}{\partial y^2} + \varkappa^2\Phi_1 = 0, \quad \lim_{r\to\infty}\sqrt{r}\left(\frac{\partial\Phi_1}{\partial r} - j\delta\Phi_1\right) = 0.$$

The normal velocity on the plate should be equal to zero, since the plate is motionless. The wake trails should not have a pressure-field discontinuity:

$$\left.\begin{aligned}&\frac{\partial\Phi_0}{\partial y}=0 \text{ for } y=0,\ |x|<1;\ \Phi_1=0 \text{ for } y=0,\ x>1;\\&\frac{\partial\Phi_1}{\partial x}-j\delta\Phi_1=0 \text{ for } y=0,\ x<-1.\end{aligned}\right\} \tag{6.20}$$

We shall now pass on to the determination of potentials Φ_0 and Φ_1.

In the solution under consideration for Φ_0 the boundary conditions are odd, which follows from (6.19); and therefore, function $se_{2n+1}(\eta, \kappa^2/4)$ should be taken as the solution. In final form, the potential of circulationless streamline flow may be represented by the following series:

$$\Phi_0=\sum_{n=0}^{\infty} a_{2n+1}\frac{Se_{2n+1}(\xi)}{Se'_{2n+1}(0)}se_{2n+1}(\eta),\quad Se'_n(0)=\left[\frac{d\,Se_n(\xi)}{d\xi}\right]_{\xi=0}. \tag{6.21}$$

The constant coefficients of this series are determined from the boundary conditions on the Plate (6.19). When $|x|<1$ and $y = 0$ we have $\xi = 0$, $x = \cos\eta$, and then from (6.19) and (6.21) we obtain

$$\sum_{n=1}^{\infty} a_{2n+1}\,se_{2n+1}(\eta)=V(\cos\eta)\sin\eta. \tag{6.22}$$

The Mathieu functions as well as the right-hand part of Equality (6.22) may be expanded into Fourier series, and a_{2n+1} may be found by comparison of coefficients. Function $se_{2n+1}(\eta)$ is odd and is represented by the series

$$se_{2n+1}=\sum_{k=0}^{\infty} B_{(2n+1),k}\cdot\sin k\eta. \tag{6.23}$$

Function $V(\cos\eta)\sin\eta$ is also odd $(-\pi<\eta<\pi)$:

$$V(\cos\eta)\sin\eta=\sum_{r=1}^{\infty} a_r\sin r\eta. \tag{6.24}$$

Hence it follows:

$$a_{2n+1}=\sum_{k=0}^{\infty} a_k B_{(2n+1),k}. \tag{6.25}$$

Thus, the potential of flow without circulation about the plate has been determined. In the absence of the main stream, this potential

yields the solution of the problem of perturbations induced by the vibrations of the plate in quiescent air.

To ascertain the singularities of the solution, as a special example we shall consider the case, which is of practical importance, of the translational vibration of a plate $v_{0y}(x)=v_0=\text{const}$. With the condition of constant normal velocity at the plate, from (6.24) there follows: $\alpha_1=v_0$, $\alpha_r=0$ when r = 2, 3, 4, ... Consequently, on the basis of (6.21) and (6.25) we obtain

$$\Phi_0 = v_0 \sum_{n=0}^{\infty} B_{(2n+1),1} \frac{Se_{2n+1}(\xi)}{Se'_{2n+1}(0)} se_{2n+1}(\eta). \tag{6.26}$$

Utilizing the Lagrange integral (for U = 0) and Formula (6.18), we find the pressure distribution with respect to the profile, and the acting force

$$Y = \rho^0 b \frac{d}{d\tau}\left[e^{j\nu\tau}\int_{-\pi}^{+\pi} \Phi_0 \sin\eta\, d\eta\right] = -j\pi\nu\rho^0 b^2 \sum_{n=0}^{\infty} \frac{Se_{2n+1}(0)}{Se'_{2n+1}(0)} B^2_{(2n+1),1}. \tag{6.27}$$

In the integration of Φ_0, use was made of Relationships (6.23) and (6.26). Functions Se assume a complex value; therefore, the force will consist of a real part and an imaginary part. The real part of the force will agree in phase with the velocity, and the imaginary part will agree with the acceleration. At low frequencies for long waves ($\nu \ll a_0/b$), it is possible to obtain from (6.27), retaining the first terms of the expansions (the multiplier exp $j\nu\tau$ has been discarded)

$$Y_0 = -\frac{\pi^2 b^4 \nu^2 \rho^0 v_0}{32 a_0^2} - j\pi\rho^0 b^2 \nu v_0. \tag{6.28}$$

Since there is a term which is in phase with the velocity, it follows that in order to maintain the oscillation of the plate it is necessary to expend energy. This energy consumption is spent on the formation of acoustic waves which recede to infinity. Consequently, in the case of oscillation in a compressible fluid a new type of damping appears, which is connected with acoustic radiation. In an incompressible fluid, the first term in Formula (6.28) vanishes ($a_0=\infty$) and

damping does not originate (recollect that the main stream is absent and that the fluid is nonviscous).

The second term in Formula (6.28) is in phase with the acceleration and cannot produce work. This component of the force is induced by the appearance of accelerations in the fluid and may be defined as the effect of the attached mass $\pi\rho^0 b^2$. The latter function coincides (in this approximation) with the previously found value of the attached mass for a plate oscillating in an incompressible fluid.

Let us consider the dimensionless value of the force

$$\frac{Y_0}{\pi\rho^0 b^2 v_0 \omega} = -\frac{\pi}{32} k^2 - j, \quad k = \frac{\omega b}{a_0}. \tag{6.29}$$

From this it follows that for small values of k (this approximation is valid when $k \ll 1$), the unsteady force induced by acoustic radiation is considerably smaller than the force induced by the attached mass. Since the value of k for the blades of an air compressor is very small (0.04 - 0.03), the influence of acoustic radiation on the damping coefficient may be disregarded. At very high oscillation frequencies ($k = \omega b/a_0 \gg 1$) the radiation constitutes a plane wave which propagates in a direction normal to the two surfaces of the plate. The limit value of the real part of the force will in this case be equal to $2\rho^0 a_0 b v_0$, and the attached mass will tend toward zero. For intermediate values of the frequency parameter k, calculation can proceed on the basis of (6.27) with the aid of tables.

In the general case, the unsteady force may be represented by the formula [74]

$$Y = -m(k)\frac{dv}{dt} - \lambda(k)v. \tag{6.39}$$

Here m is the attached mass, λ is the proportionality coefficient which characterizes damping. A calculated graph for the relative values $\bar{m} = m/m_0$ and $\bar{\lambda} = \lambda/\omega m_0$ ($m_0 = \pi\rho^0 b^2$ is the attached mass in an

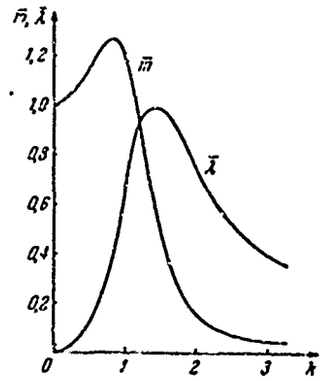


Figure 6.3. The relationship of the attached mass and the damping coefficient to the Strouhal number for a plate oscillating in a gas.

incompressible fluid), which depend upon the frequency parameter, is shown in Figure 6.3. From the graph it can be seen that $\bar{\lambda}$ first increases sharply, and when $k \to \infty$ must go toward zero as $2/\pi k$, according to the estimate cited above.

Let us now undertake the determination of the second component of the velocity potential, which determines the flow about the plate, with account taken of the circulation component. The previous method cannot be used now, since at the ends of the plate the function will tend toward infinity. In this case a different method has been proposed by M. D. Khaskind.

We introduce the auxiliary function g(x, y), which has finite values in the interval $y=0$, $|x| \leqslant 1$ and is connected to the desired function by the relationship (the introduction of this function is analogous to use of the acceleration-potential method)

$$\frac{\partial g}{\partial y} = \frac{\partial \Phi_1}{\partial x} - j\delta\Phi_1; \tag{6.31}$$

This function satisfies the wave equation and the radiation condition

$$\frac{\partial^2 g}{\partial x^2} + \frac{\partial^2 g}{\partial y^2} + \varkappa^2 g = 0, \quad \lim_{r\to\infty} \sqrt{r}\left(\frac{\partial g}{\partial r} - j\delta g\right) = 0.$$

At the leading edge the function g(x, y) must tend toward infinity as $s^{-1/2}$, where s is the distance from the leading edge.

We compile the boundary conditions for g on the abscissa, using Conditions (6.20) for functions Φ_1:

$$\frac{\partial g}{\partial y} = 0 \text{ for } |x| > 1, \quad \frac{\partial^2 g}{\partial y^2} = 0 \text{ for } |x| < 1. \tag{6.32}$$

The second condition, jointly with the wave equation which must be satisfied by function g(x, y), leads to equation

$$\frac{\partial^2 g}{\partial x^2} + \varkappa^2 g = 0 \text{ for } y = 0, \ |x| < 1;$$

Integrating this equation, we obtain ($|x|<1$):

$$g(x, 0) = Ce^{j\varkappa x} + De^{-j\varkappa x}. \tag{6.33}$$

Here C and D are arbitrary constants, defined below. When passing the auxiliary plane, we substitute x = cos η. Consequently, function g(x, y) may be expressed in terms of a series with respect to even Mathieu functions:

$$g(x, y) = \sum_{n=0}^{\infty} b_n \frac{Ce_n(\xi)}{Ce_n(0)} ce_n(\eta). \tag{6.34}$$

This solution satisfies the Helmholtz equation, the radiation condition, and the first condition of (6.32). The coefficients b_n in the expansion of (6.34) must be defined in such a manner as to satisfy the second condition of (6.32) or, what is the same, Condition (6.33)

$$\sum_{n=0}^{\infty} b_n ce_n(\eta) = Ce^{j\varkappa\cos\eta} + De^{-j\varkappa\cos\eta}.$$

Coefficients b_n may be computed by taking advantage of the orthogonality of the Mathieu functions, multiplying the left-hand part and the right-hand part by $ce_n(\eta)$ and integrating from $\eta=-\pi$ to $\eta=+\pi$:

$$\left.\begin{aligned} b_n &= 2\left[C\beta_+^n + D\beta_-^{(n)}\right], \\ \beta_{\pm}^{(n)} &= \frac{1}{\pi}\int_0^{\pi} e^{\pm j\varkappa\cos\eta} ce_n(\eta)\, d\eta. \end{aligned}\right\} \tag{6.35}$$

Here use is made of the property that functions $ce_n(\eta)$, including $ce_0(\eta)$, have the normalization

$$\int_{-\pi}^{+\pi} [ce_n(\eta)]^2 d\eta = \pi.$$

The even periodic function $ce_n(\eta)$ may be represented by a Fourier series:

$$ce_n(\eta) = \sum_{k=0}^{\infty} A_{nk} \cos k\eta. \qquad (6.36)$$

Substituting (6.36) into (6.35) and utilizing the Bessel integral

$$(\pm i)^k J_k(x) = \frac{1}{\pi} \int_0^{\pi} e^{\pm ix\cos\eta} \cos k\eta \, d\eta,$$

we obtain a different expression for the coefficients,

$$\beta_{\pm}^{(n)} = \sum_{k=0}^{\infty} (\pm i)^k A_{nk} J_k(q), \quad \beta_{+}^{(n)} = (-1)^k \beta_{-}^{k}. \qquad (6.37)$$

Thus, function g(x, y) is defined in such a manner that it satisfies the Helmholtz equation and the radiation condition. However, function g(x, y) and, consequently, $\Phi_1(x, y)$ as well, contains the two so far arbitrary constants C and D. For their determination two physical conditions must be satisfied: the normal velocity on a motionless plate is zero, and the postulate concerning infiniteness of the velocities at the trailing edge.

Let us undertake the determination of these constants. We solve the differential Equation (6.31) for the function Φ_1:

$$\Phi_1(x, y) = e^{i\delta x} \int_{-\infty}^{x} e^{-i\delta u} \frac{\partial g(u, y)}{\partial y} \, du. \qquad (6.38)$$

We differentiate the left-hand part and the right-hand part of this equation with respect to y and, taking advantage of the condition $\partial^2 g/\partial y^2 = -\partial^2 g/\partial x^2 - \varkappa^2 g$, which proceeds from the wave equation, we integrate the result by parts:

$$-\frac{\partial \Phi_1}{\partial y} = \frac{\partial g(x, y)}{\partial x} + i\delta g(x, y) + (\varkappa^2 - \delta^2) e^{i\delta x} \int_{-\infty}^{x} e^{-i\delta u} g(u, y) \, du. \qquad (6.39)$$

These transformations are analogous to those used in the acceleration-potential method when determining the velocity field on the basis of the acceleration field. Assuming in (6.39) that y = 0 and $|x|<1$, we

equate the derivative to zero, $\partial\Phi_1/\partial y=0$, as required by the boundary conditions

$$\frac{\partial g(x, 0)}{\partial x}+j\delta g(x, 0)+(x^2-\delta^2)e^{j\delta x}\int_{-\infty}^{x}e^{-j\delta x}g(u, 0)\,du=0.$$

From this, utilizing Expression (6.33) for function g(x, 0), we find the equation linking the constants C and D:

$$\int_{0}^{1}e^{-j\delta u}g(u, 0)\,du+\frac{jC}{x-\delta}e^{j(x-\delta)}-\frac{jD}{x+\delta}e^{j(x-\delta)}=0. \tag{6.40}$$

The definite integral entering into this expression can be computed [83, 74]. The second equation linking the constants C and D is found from the condition of finiteness of the stream velocity at the trailing edge ($\partial\Phi/\partial x-j\delta\Phi$ is finite when y = 0 x = -1). We express this combination in terms of the first and second solutions:

$$\frac{\partial\Phi}{\partial x}-j\delta\Phi=\frac{\partial\Phi_0}{\partial x}-j\delta\Phi_0+\frac{\partial g}{\partial y}.$$

Taking advantage of expansions of (6.26) and (6.34), as well as Formula (6.19) for recalculating the derivative, we obtain

$$\frac{\partial\Phi}{\partial x}-j\delta\Phi=-\sum_{n=1}^{\infty}a_n\left[\frac{se_n'(\eta)}{\sin\eta}+j\delta se_n(\eta)\right]\frac{Se_n(0)}{Se_n'(0)}+\\+\sum_{n=0}^{\infty}b_n\frac{Ce_n'(0)}{Ce_n(0)}\frac{ce_n(\eta)}{\sin\eta}. \tag{6.41}$$

The condition of finite velocity is written in the form

$$\lim_{x\to-1}\sqrt{1+x}\left(\frac{\partial\Phi}{\partial x}-j\delta\Phi\right)=0.$$

Utilizing the expression for coefficients b_n (6.35), we obtain the second equation connecting coefficients C and D

$$CK_++DK_-=\gamma_1. \tag{6.42}$$

Here we have introduced the designations:

$$\left.\begin{aligned} K_{\pm} &= 2\sum_{n=0}^{\infty}\frac{Ce_n'(0)}{Ce_n(0)}\beta_{\pm}^{(n)}ce_n(\pi),\\ \gamma_1 &= \sum_{n=1}^{\infty}\frac{Se_n(0)}{Se_n'(0)}\cdot se_n'(\pi)a_n. \end{aligned}\right| \qquad (6.43)$$

Thus two Equations, (6.40) and (6.42), are available for determining the two constants.

The perturbed pressure is determined by means of the Lagrange integral

$$p = -\rho^0 U^2\left(\frac{\partial\Phi}{\partial x} - jk\Phi\right)e^{j(k\tau-\mu x)}.$$

The unsteady lift force and the moment acting upon the profile are expressed by the formulas:

$$Y = 2\rho^0 Ub\int_{-1}^{+1}\left(\frac{\partial\Phi}{\partial x} - jk\Phi\right)e^{j(k\tau-\mu x)}dx,$$

$$M = 2\rho^0 Ub^2\int_{-1}^{+1}x\left(\frac{\partial\Phi}{\partial x} - jk\Phi\right)e^{j(k\tau-\mu x)}dx.$$

In a special case, when $a_0 = \infty$ the solution under consideration passes into the corresponding formulas which describe the behavior of a profile in an incompressible fluid.

§ 6.3. A Cascade of Vibrating Profiles in a Subsonic Stream

We shall consider the problem of the vibrations of profiles in a cascade in a linear formulation. We shall employ the method developed in several studies by D. N. Gorelov [15, 18] which is based upon a known solution of the problem for a single profile and will successively take into account the interference of the profiles in the cascade.

We shall call one of the cascade profiles the main one and shall assign to it the number m = 0. We shall situate the origin of

coordinates x, y in the center of this profile, directing the abscissa against the stream. We shall also introduce the coordinate systems x_m, y_m connected to the cascade profiles and obtained from the initial system by a parallel shift along the cascade axis by the value of the spacing (Figure 6.4)

$$x_m = x - ml\sin\gamma_0, \quad y_m = y - ml\cos\gamma_0. \tag{6.44}$$

The velocity potential of the perturbed motion in the system of coordinates x, y satisfies the wave equation

$$(1-M^2)\frac{\partial^2\varphi}{\partial x^2} + \frac{\partial^2\varphi}{\partial y^2} + 2\frac{M}{a_0}\frac{\partial^2\varphi}{\partial x\,\partial\tau} - \frac{1}{a_0^2}\frac{\partial^2\varphi}{\partial\tau^2} = 0. \tag{6.45}$$

We shall write the condition of impermeability of the profiles in the coordinate system connected to the given profile

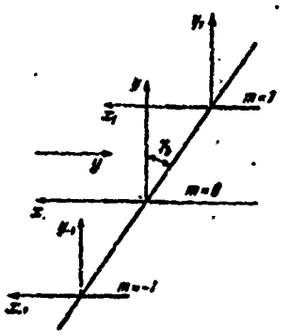


Figure 6.4. Coordinate systems connected to the plates in a cascade.

$$\frac{\partial\varphi}{\partial y} = v_{0y}(x_m)\,e^{i(\omega\tau+m\alpha)}$$

when

$$y_m = 0, \quad |x_m| \leqslant b. \tag{6.46}$$

The conditions at the discontinuity lines of the velocities, as well as the conditions at the trailing edges, do not differ from analogous requirements for a single profile.

We pass to dimensionless coordinate systems

$$x_m = b\bar{x}_m, \quad y_m = \frac{b}{\sqrt{1-M^2}}\,y_m, \qquad m = 0; \pm 1; \pm 2; \ldots \tag{6.47}$$

Henceforth we shall discard the bar over the dimensionless coordinates.

We shall seek the velocity potential of the unsteady perturbed motion in the form of the sum of the potentials which correspond to

flow about isolated profiles and the potential which takes into account the interference of the profiles in the cascade:

$$\varphi(x, y, \tau) = e^{i\nu\tau} \sum_{m=-\infty}^{\infty} e^{-i\lambda x_m} [\Phi_m^{(0)}(x_m, y_m) + \Phi_m(x_m, y_m)]. \tag{6.48}$$

We designate:

$$\lambda = \frac{kM^2}{1-M^2}, \quad k = \frac{\nu b}{U}, \quad \mu = \frac{kM}{1-M^2}, \quad \delta = \frac{k}{1-M^2}$$

The velocity potentials Φ_m^0 and Φ_m must satisfy the Helmholtz equation

$$\frac{\partial^2 \Phi_m^{(0)}}{\partial x_m^2} + \frac{\partial^2 \Phi_m^{(0)}}{\partial y_m^2} + \mu^2 \Phi_m^{(0)} = 0, \quad \frac{\partial^2 \Phi_m}{\partial x_m^2} + \frac{\partial^2 \Phi_m}{\partial y_m^2} + \mu^2 \Phi_m = 0, \tag{6.49}$$

the boundary conditions on the profiles

$$\left.\begin{aligned} \frac{\partial \Phi_m}{\partial y_m} &= \frac{b}{\sqrt{1-M^2}} v_{0y}(x_m) e^{i(\lambda x_m + m\alpha)}, \\ \frac{\partial \Phi_m^{(0)}}{\partial y_m} &= \frac{b}{\sqrt{1-M^2}} v_{0y}^{(0)}(x_m) e^{i(\lambda x_m + m\alpha)}, \end{aligned}\right\} \tag{6.50}$$

when $\qquad y_m = 0, \ (\tau_m) \leqslant 1,$

and the property of symmetry

$$\Phi_m^{(0)}(x_m, y_m) = -\Phi_m^{(0)}(x_m, -y_m), \quad \Phi_m(x_m, y_m) = -\Phi_m(x_m, -y_m)$$

Here $v_{0y}^{(0)}(x_m)$ is the given law of distribution of normal velocity on the profiles due to oscillation, $v_{0y}(x_m)$ are the velocities induced due to interference.

The functions must satisfy the condition of continuity of the pressure field along the vortex wakes, which are discontinuity lines of the velocity field

$$\frac{\partial \Phi_m^{(0)'}}{\partial x_m} - i\delta \Phi_m^{(0)} = \frac{\partial \Phi_m}{\partial x_m} - i\delta \Phi_m = 0 \text{ for } y_m = 0, \ x_m < -1. \tag{6.51}$$

Functions Φ_m^{Φ} and Φ_m must also satisfy the radiation condition and the condition on the trailing edges. Since the conditions on all the profiles are identical and differ only with respect to the multiplier $\exp(jn\alpha)$, all considerations may be conducted with respect to the main profile. We differentiate (6.48) with respect to y and determine the normal velocity on the main profile:

$$\frac{\partial \varphi}{\partial y} = e^{j\omega t} \sum_{m=-\infty}^{\infty} e^{-jh x_m} \left[\frac{\partial \Phi_m^{\Phi}}{\partial y_m} + \frac{\partial \Phi_m}{\partial y_m} \right]. \tag{6.52}$$

This normal velocity is not yet compared with the boundary value. Note is taken only of the fact that if the velocity potentials are given in terms of the Cartesian coordinate systems connected to the profiles, the normal velocity on the main profile may be determined by means of Equation (6.52).

As has already been said, it is assumed that the problem for a single profile has been solved. In this case it is considered that it has been solved by the method of M. B. Khaskind by means of series in an elliptical coordinate system. The elliptical systems of coordinates ξ_m, η_m are linked to each profile; the Cartesian coordinates are expressed in terms of the elliptical ones by the known formulas:

$$x_m = \operatorname{ch} \xi_m \cos \eta_m, \quad y_m = \operatorname{sh} \xi_m \sin \eta_m. \tag{6.53}$$

The coordinates of the main profile, just as before, will not be denoted by an index. Solving Equations (6.53) with respect to the elliptical coordinates, we find

$$\left.\begin{aligned} \operatorname{sh}^2 \xi_m &= -\frac{1}{2}(1 - x_m^2 - y_m^2) + \sqrt{\frac{1}{4}(1 - x_m^2 - y_m^2)^2 + y_m^2}, \\ \sin \eta_m &= \frac{y_m}{\operatorname{sh} \xi_m}. \end{aligned}\right\} \tag{6.54}$$

The connection between the Cartesian coordinates of the main profile and those of profile number m is given by the Equations (6.44). After the introduction of dimensionless coordinates, Equations (6.44) will assume the form

$$x_\kappa = x - m\frac{b}{t}\sin\gamma_b, \quad y_\kappa = y - m\frac{b}{t}\sqrt{1-M^2}\cos\gamma_b. \tag{6.55}$$

Combining (6.44) and (6.55), we find the relationship between the elliptical coordinates connected with two profiles. This relationship between coordinates is necessary when considering interference.

The idea of the calculation method consists in the following. The solution of the problem for an isolated profile consists in determining the acceleration potential according to a given normal velocity potential on the profile. The method of solving such a problem with an arbitrary distribution law of the normal velocity has been described above. As a result of solving the problem according to the method of M. B. Khaskind, the perturbed potential of acceleration and the perturbation velocities themselves can be found within the entire region of the stream. In the formulated problem about a cascade, the law of oscillation of all the plates is the same and differs only with respect to the phase shift. Therefore, when the boundary conditions on an arbitrary profile (for example, the main profile) are satisfied, the boundary conditions on the remaining profiles will be automatically satisfied.

Let all the profiles first oscillate according to a given law. Then, having the solution of the problem for an isolated profile (see § 6.2) and Equations (6.54) and (6.55), which connect the coordinates, it is possible to find the supplementary normal velocities induced on the main profile by all the profiles of the cascade. In order to satisfy the boundary conditions, we assume that the profiles also oscillate in such a manner that the total induced normal velocities are equal to zero. It is assumed that functions Φ_n^0 and Φ_n are solutions of the Helmholtz equation and satisfy all the conditions linked to flow about a single profile. The only remaining requirement which must be satisfied is the condition of impermeability of the cascade profiles.

On the basis of the boundary condition for the main profile, from (6.50) we may write (we discard the index zero)

$$\frac{\partial \Phi}{\partial y} = \frac{k}{\sqrt{1-M^2}} v_{0y}(x) e^{j\lambda x}. \tag{6.56}$$

Then the condition of the impermeability of the main profile is established by means of (6.52) and (6.56):

$$\frac{\partial \Phi}{\partial y} e^{-j\lambda x} + \sum_{m=-\infty}^{\infty}{}' e^{-j\lambda x_m} \left(\frac{\partial \Phi_m^{(0)}}{\partial y_m} + \frac{\partial \Phi_m}{\partial y_m} \right) = 0. \tag{6.57}$$

Here the prime with the summation sign signifies that when summing, the term with index zero is omitted.

The potentials $\Psi_m^{(0)}$ are considered to be known, since the laws of oscillation of all the profiles are given. The supplemental potentials differ from the supplemental potentials in the main profile (each in its own system of coordinates) only with respect to the multiplier $\exp(jm\alpha)$. Therefore, Equation (6.57) can serve for finding the distribution law of the supplemental potential along the main profile. The first term of Expression (6.57) may be represented, for the sake of clarity, as a supplemental normal velocity on the main profile, induced only by the potential Φ.

We represent the given normal velocity $v_{0y}^{(0)}(x)\exp(j\lambda x)$ and the desired normal velocity $v_{0y}(x)\exp(j\lambda x)$ by Fourier series:

$$\left.\begin{aligned} v_{0y}^{(0)}(x) e^{j\lambda x} &= \frac{1}{2}\theta_0 + \sum_{k=1}^{\infty} \theta_k \cos k\eta, \\ v_{0y}(x) e^{j\lambda x} &= \frac{1}{2}\delta_0 + \sum_{k=1}^{\infty} \delta_k \cos k\eta. \end{aligned}\right\} \tag{6.58}$$

Then utilizing Equation (6.57), representation of the velocity potentials by Series (6.24) and (6.34), the condition for recalculation of the Derivatives (6.18), and the equation relating the Coordinates (6.54), it is possible to obtain an infinite system of equations for determining δ_k:

$$\frac{1}{2}\delta_0 + \sum_{k=1}^{\infty}\delta_k \cos k\eta + \sum_{k=0}^{\infty}(\delta_k - \theta_k)f(\eta) = 0. \qquad (6.59)$$

Here $f(\eta) = f(\alpha, \gamma, 2b/t, k, \theta_k, \eta)$ is a function which depends upon the given law of oscillation θ_k, the phase-shift angle α, the cascade offset γb, the relative spacing $2b/t$, the relative oscillation frequency $k = \omega b/U$, and the coordinates of the point on the profile. An explicit expression of this function is very cumbersome [15].

It is convenient to seek the solution of System (6.59) by the collocation method, restricting oneself in the expansion of (6.58) to N times and requiring satisfaction of the boundary conditions at N previously indicated points. It should be emphasized that the principal time is spent on computation of the components of function $f(\eta)$, which do not depend upon the phase shift. After this computation work has been accomplished, solution of the problem for a specific phase shift requires relatively little time.

D. N. Gorelov and L. V. Dominas [18] carried out computation of the influence coefficients for translational and torsional oscillations of profiles in a cascade. In practice it has turned out sufficient to satisfy the boundary condition at six points on the initial profile and to take into account the influence of 30 profiles on each side of the initial profile. The values of the influence coefficients are presented in Table 6.1. All the calculations have been carried out for a constant cascade density of $t/2b = 1$ and a constant Strouhal number of $k = 0.2$. During the calculations the Mach number was varied: $M = 0$, 0.5, 0.7, and 0.8, and the offset angle of the cascade $\gamma b = 0$, 30°, 60°. For each value of the selected parameters, three influence coefficients, set forth in Chapter 5, are also applicable.

The problem of unsteady flow about a cascade by a stream of gas may be solved also by the method of integral equations. We obtain an integral equation which must be satisfied by the acceleration potential or by the perturbed pressure. We introduce the acceleration potential, which in dimensionless form may be obtained from Equation (6.11):

TABLE 6.1

	φ_0	$n=0$		$n=0.5$		$n=0.7$		$n=0.8$	
l_{x_0} (m)	0	−1,18 5,37 −1,18	+0,11 −0,10 +0,11	−1,66 6,33 −1,66	+0,09 −0,83 +0,09	−2,42 7,32 −2,42	+0,32 −1,51 +0,32	−3,23 8,23 −3,23	+0,63 −2,93 +0,63
	30	−0,63 5,23 −1,85	−0,03 −0,11 +0,26	−1,09 5,93 −1,95	−0,23 −0,58 +0,12	−1,63 7,12 −2,72	−0,14 −1,51 +0,77	−2,58 7,77 −3,26	+0,17 −2,42 +0,88
	60	0,20 4,78 −1,86	−0,14 +0,16 +0,69	0,16 5,32 −2,12	−0,40 +0,19 +0,81	−0,01 6,42 −2,42	−0,55 −0,22 +1,14	−0,86 7,48 −3,08	−1,86 −0,94 +1,56
l_{y_0} (m)	0	−0,21 1,29 −0,21	+0,03 −0,37 +0,03	−0,31 1,47 −0,31	+0,05 −0,63 +0,05	−0,45 1,58 −0,45	+0,27 −1,05 +0,27	−0,55 1,42 −0,55	+0,66 −1,80 +0,66
	30	−0,03 1,27 −0,38	−0,01 −0,03 +0,11	−0,09 1,38 −0,19	−0,08 −0,54 +0,17	−0,15 1,52 −0,67	−0,01 −0,99 +0,43	−0,24 1,41 −0,80	+0,27 −1,49 +0,78
	60	0,18 1,14 −0,53	−0,06 −0,18 +0,16	0,18 1,25 −0,81	−0,14 −0,32 +0,26	0,09 1,48 −0,66	−0,29 −0,61 +0,42	−0,28 1,56 −0,70	−0,27 −1,13 +0,73
l_{x_0} (m)	0	0,09 −0,32 0,00	+0,47 −2,07 +0,47	0,09 −0,56 0,09	+0,65 −2,11 +0,65	0,20 −0,85 0,20	+0,16 +0,94 +0,16	0,33 −1,40 0,33	+1,24 −3,09 +1,24
	30	−0,03 −0,20 0,33	+0,29 −2,05 +0,59	−0,08 −0,45 0,24	+0,45 −2,31 +0,75	−0,03 −0,81 0,41	+0,86 +2,72 +1,09	0,10 −1,18 0,27	+1,01 −2,39 +1,29
	60	−0,09 −0,06 0,37	−0,06 −1,99 +0,70	−0,19 −0,12 0,42	−0,04 −2,09 +0,98	−0,40 −0,31 0,56	+0,06 −2,49 +0,91	−0,65 −0,61 0,75	−0,43 −2,86 +1,14
l_{y_0} (m)	0	0,03 −0,23 0,03	+0,05 −0,50 +0,05	0,03 −0,23 0,03	+0,12 −0,56 +0,12	0,11 −0,35 0,11	+0,17 −0,59 +0,17	0,26 −0,61 0,26	+0,20 +0,51 +0,20
	30	−0,01 −0,12 0,06	+0,02 −0,49 +0,14	−0,03 −0,13 0,05	+0,01 −0,51 +0,19	−0,35 0,19	+0,05 −0,57 +0,25	0,11 −0,52 0,31	+0,09 −0,52 +0,28
	60	−0,03 −0,05 0,10	−0,07 −0,46 +0,20	−0,05 −0,10 0,13	−0,07 −0,49 +0,23	−0,11 −0,20 0,20	−0,03 −0,57 +0,24	−0,09 −0,39 0,32	+0,11 −0,59 +0,24

$$\Phi_{*m} - \rho_m = \frac{\partial \varkappa}{\partial x} + j\delta\Phi. \qquad (6.60)$$

From the symmetry of the problem it follows that when the sections are approached from above and from below, the acceleration potential must assume values that are equal in absolute magnitude but are opposite in sign. On lines y = const going from the trailing edges and which are discontinuity lines in the acceleration field, the perturbed pressure and, consequently, the acceleration potential as well must be continuous. The normal derivative of the acceleration potential as well must be continuous. The normal derivative of the acceleration potential on a contour is equal to the normal acceleration. Consequently, the value of the acceleration potential at like points of the main blade and blade m correspond to the condition

$$\Phi_*(m) = \Phi_*(0)\exp(jm\alpha). \qquad (6.61)$$

From the presented considerations it follows that the kernel of the integral equation must provide for a discontinuity on the potential and on the potential and must satisfy the given periodicity. The acceleration potential must satisfy the Helmholtz equation, as is established by means of (6.60) and (6.8), and the solution must contain only waves diverging from the cascade. From what has been said, it follows that the acceleration potential may be represented by an integral expression where integration is carried out only along the main profile

$$\Phi_*(x, y) = \int_{-l}^{+l} \Phi_*^{(0)}(\xi) K_1(x-\xi)\, d\xi. \qquad (6.62)$$

The kernel constitutes a cascade of pressure dipoles, the axes of which are parallel to the ordinate, and the intensity is shifted in phase. For a harmonic law of oscillations the dipoles are expressed in terms of the Hankel function

$$K_1(x, y) = \frac{\partial}{\partial y} \sum_{m=-\infty}^{\infty} e^{jm\alpha} H_0^{(2)}\left[\varkappa \sqrt{(x - mt\sin\gamma_b)^2 + \beta^2 (y - mt\cos\gamma_b)^2}\right]. \qquad (6.63)$$

The desired function is Φ_* — the distribution intensity of the pressure dipoles along the main profile. Each of the terms of this

series satisfies the Helmholtz equation and the radiation principle.

For compiling the integral equation it is necessary to use the known boundary values of the normal velocity on the profiles. For this we shall solve differential Equation (6.60), regarding the velocity potential as the unknown function

$$\Phi(x, y) = e^{-i\beta x} \int_{-\infty}^{x} e^{i\beta u} \Phi_0(u, y)\, du. \tag{6.64}$$

Combining (6.62) and (6.64), we obtain the expression of the velocity potential in terms of the acceleration potential

$$\Phi(x, y) = e^{-i\beta x} \int_{-1}^{+1} \Phi_c^0(\xi) \int_{-\infty}^{x} e^{i\beta u} K_1(u-\xi)\, du\, d\xi. \tag{6.65}$$

Differentiating this expression with respect to v and assuming that $y = 0$ when $|x| \leqslant 1$, we replace the left-hand part of (6.9) by the boundary value of normal acceleration on the main profile ($m = 0$)

$$a_{n_0}(x) = \sqrt{1-M^2}\, e^{-i\beta x} \int_{-1}^{+1} \Phi_c^{(0)}(\xi) K_2(x-\xi)\, d\xi. \tag{6.66}$$

Here we have set:

$$K_2(x) = \int_{-\infty}^{x} e^{i\beta u} \left[\frac{\partial^2}{\partial y^2} \sum_{m=-\infty}^{\infty} e^{i\alpha m} H_0^{(2)}(u, y) \right]_{y=0} du. \tag{6.67}$$

This derivation is analogous to the derivation of Possio's equation [84, 49] for the oscillation of an isolated wing in a compressible stream. The difference lies only in the fact that in this equation it is not the distribution of isolated dipoles that is being accounted for, but the dipole cascade. In passage to the limit in the case of parameterless growth of the spacing, Equations (6.66) and (6.67) pass into the Possio equation. The method of integral equations for calculating cascades was used by Woolston Runyan [149], who considered a partial problem of the oscillation of profiles in a cascade without offset and counterphase (it has already been noted above that this simultaneously solves the problem of the oscillation of profiles with a phase shift of $\alpha = \pi/2$ with a halved spacing). The

problem of the oscillation of a plate cascade with offset was studied in the works of V. B. Kurzin [33, 34]. In the limit case of an incompressible fluid, when the velocity of sound increases without limit, the Hankel function $\varkappa H_0^{(2)}(\varkappa r)$ and its derivative $-\varkappa H_1^{(2)}(\varkappa r)$ pass into the expressions in r and r. Then the basic equation passes into the integral formula for the calculation of cascades in an incompressible stream.

Let us return again to the general case, and let us note that the kernel of the integral equation is complex, and that a solution in closed form is not obtained even for a single profile (when solving by the integral-equation method). Let us note that even a direct passage to the limit $y \to 0$ is possible, since a diverging integral is obtained. In order to avoid this complication, in the theory of a single profile use is made of a substitution of the differential operator, which proceeds from the Helmholtz equation

$$\frac{\partial^2}{\partial y^2} = \frac{\partial^2}{\partial x^2} + \mu^2.$$

Subsequent transformations of the kernel consist in getting rid of the infinite sum of improper integrals and isolating the singularity. These transformations are brought about by the requirements of computer engineering; and therefore, for details we refer the reader to Reference [34]. Let us note that in contrast to the method adopted in the work of V. B. Kurzin, the Poisson method may be used for the summation of Hankel functions (see the transformations presented in § 3.2), and then the conditions of resonance become obvious.

Let us analyze some numerical results obtained in calculating a cascade of oscillating plates in a subsonic stream. Let us consider the results of Woolston and Runyan [149], who carried out calculations to determine the influence of the walls of a wind tunnel upon the unsteady force acting upon an oscillating wing. As has already been noted, this case may be regarded as oscillation in

counterphase in a cascade without offset. The distance between the walls is equal to the cascade spacing. Figure 6.5 shows the change of the modulus of the unsteady lifting force in the case of translational oscillation as a function of the Strouhal number $k = \omega b/u$ (2b is the chord of the blades). The solid curve corresponds to the

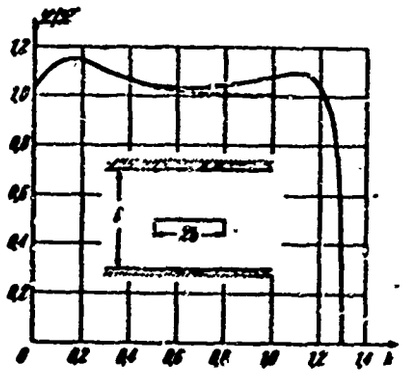


Figure 6.5. Relative lift force in the oscillation of plates in a cascade with a phase shift $\varepsilon = \pi$ as a function of the Strouhal number. Mach number M = 0.3, and 2b/t = 3.8.

Mach number of the main stream M = 0.3 and the cascade density $\bar{t} = t/2b = 3.80$. Along the ordinate the ratios of the modulus of the unsteady lift force $\mathcal{Y}$ to the modulus of the lifting force of a single wing $\mathcal{Y}_0$ are plotted, which is in an infinite stream of incompressible fluid. The dotted curve corresponds to the calculations of Reissner, carried out for the case of the oscillation of plates in a cascade which is flowed about by an incompressible fluid (M = 0). In the latter case the cascade density did not differ very greatly and was equal to $\bar{t} = 3.14$.

At small Strouhal numbers coincidence of the two curves is observed; this indicates very weak influence of compressibility. This is evidently explained by the fact that for small Strouhal numbers the parameter $\varkappa = kM/\beta'$ is also small and, as has been noted in § 2.5, the compressible fluid in the vicinity of an oscillating profile behaves like an incompressible fluid. At a large distance from the oscillating profile the perturbations in compressible fluid and in incompressible fluid differ; however, the absolute value of these perturbations, and therefore also the interference among the profiles, is small. It must be kept in mind that this comparison has been carried out for a relatively thin cascade. In the case

of steady streamline flow (k = 0) the curves do not pass into 1; this is brought about by the effect of the cascade. The ratio of the lift forces may be determined according to Formula (5.38), dividing it by $\Gamma = 2\pi b w_0$ — the circulation of the velocity about a single plate; this, when t/2b = 3.80 yields

$$\frac{\mathcal{Y}}{\mathcal{Y}^0} = \frac{\Gamma}{\Gamma^0} = \frac{2}{\pi}\frac{t}{2b}\operatorname{th}\frac{\pi b}{t}\left(1+\frac{1}{4}\operatorname{th}^2\left(\frac{\pi b}{t}\right)+\ldots\right)^2 = 1{,}03.$$

Considerable divergence of the curves is observed only close to resonance, when the aerodynamic damping in the cascade tends toward zero.

According to Formula (3.13), for oscillation in counterphase $\alpha = \pi$ and with a cascade offset of $\gamma b = 0$ we obtain the resonance frequency

$$\nu = \frac{\pi c_0 \sqrt{1-M^2}}{t}.$$

Transforming this formula to the form

$$k = \frac{\pi}{2}\frac{\sqrt{1-M^2}}{M}\frac{2b}{t},$$

for M = 0.3 and t/2b = 3.80, we find k = 1.31; this is in agreement with the detailed solution. It must be noted that solution of the integral equation close to resonance will obviously not be very precise. The calculations carried out in the cited article show that the effect of compressibility naturally increases with an increase in the Mach number. However, in a thin cascade ($\bar{t}$ = 3.8), the maximum lift force when m = 0.8 differs from the lift force in an incompressible fluid by approximately 15%. The calculations also show that the phase shift between the oscillation velocity and the aerodynamic force far from resonance does not differ from the corresponding shift for the oscillation of a single wing. Close to resonance and at large Mach numbers the phase shift changes substantially. This fact is of practical significance, since it brings

about a decrease in the critical flutter velocity. Calculations cited in [18] show that in dense cascades the influence of compressibility increases substantially.

It should be emphasized that the influence of compressibility may be very considerable also in the case of a small Mach number (or may be even equal to zero with a main stream velocity equal to zero), if the oscillation frequency is sufficiently large.

FOOTNOTES

1. on page 245. Information on Mathieu functions can be found in the book by McLaughlan [45].

CHAPTER 7

FLOW ABOUT A CASCADE OF ARBITRARY PROFILES, OSCILLATING WITH AN ARBITRARY PHASE SHIFT

§ 7.1. Preliminary Remarks

In this chapter we consider problems concerning synthesis of the flow of an ideal incompressible fluid around a cascade of arbitrary oscillating profiles.

Two methods of calculation are set forth. In the first method, the region of the stream is conformally transformed into a canonical region — the exterior of a cascade of circles. Calculation in the canonical region is reduced to the solution of an infinite system of equations. In principle, other canonical regions used in the calculation of a stabilized flow about cascades can be used. In particular, it is known that it is convenient to select as a canonical region an infinite strip, extensively used in the calculation of aerodynamic cascades [78].

In the second method set forth in this chapter, the problem is reduced to the solution of an integral equation. This method has advantages with the use of computers.

With the use of the first method, the problem is considered only in a quasi-steady formulation, i.e., without taking account of the

influence of vortex wakes. In principle, the method can be generalized for the general case of the use of Green functions (flow about a cascade in the presence of vortex-type singularities) or by reduction to a problem with mixed boundary conditions. This, however, leads to computational difficulties.

We emphasize that when studying flow about a cascade of oscillating profiles, the influence of profile displacement can in many cases turn out to be significant. Usually, in turbomachine cascades this displacement is small; and therefore, the corresponding effect can be taken into account either by a small deformation of the profiles or by determination of supplemental normal velocities at the contour. In view of the smallness of the displacement the perturbing function can be linearized, and it can be considered that the supplemental velocities are induced by displacements in the main stream field. In application to turbomachine cascades, usually only the study of such small oscillation is of interest, so that this assumption is entirely justified. For determination of the perturbed velocities induced by the shift of profiles in the cascade, the method set forth in § 5.4 can be used. With the use of the method of small deformations of the contour, the ideas developed by M. A. Lavrent'yev [38] can be used. Calculation of flow about cascades with small equal deformation of all the profiles has been developed by G. Yu. Stepanov [78]. When $a \to 0$ Reference [57] can be used.

When studying the oscillation of profiles in a cascade with a phase shift, it is necessary also to consider deformations with a phase shift. In this case one might consider deformation in the canonical region upon which the cascade is mapped, and a function with generalized periodicity may be used (see Chapter 2). We emphasize that for calculating the oscillation of a cascade with account taken of a small displacement of the profiles, both methods (that of conformal transformations and integral equations) are applicable without changes. The difference will consist only in the fact that account must be taken of the sum of the perturbations, which now depend both on the velocity of the profiles and upon their displacement

In conclusion, we note that the calculation of cascades with account taken of a large displacement of the profiles may be based upon the consideration of flow about a system of "inserted" cascades. The method of solution of this problem pertains to Chapter 8.

§ 7.2. Formulation of the Quasi-steady Problem of Flow about a Cascade of Arbitrary Profiles with Account Taken of Their Displacement

Let us consider, in the plane of the complex variable $z = x + iy$, an aerodynamic cascade consisting of random profiles (Figure 7.1). The cascade axis is parallel to the y-axis; we shall designate the profile spacing by t.

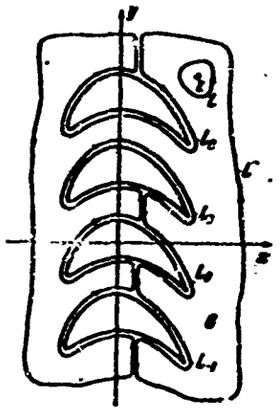


Figure 7.1. A cascade of arbitrary profiles and the integration contour.

We shall be studying the potential motion of an ideal incompressible fluid in an infinitely connected region G, which is the exterior of the indicated cascade.

A stream which is uniform at infinity comes from the left, onto the cascade. The cascade profiles oscillate arbitrarily with a small amplitude. We are considering a case where all the profiles oscillate synchronously with a frequency ν, but with an arbitrary constant phase shift α between adjacent profiles. The case of an arbitrary law of profile oscillation can be reduced to the formulated problem. When formulating the boundary conditions, in view of the smallness of the oscillation amplitude it is possible to consider separately the influence of the velocity of the profiles and the influence of the displacement. First we shall assume that the profiles are not displaced, but move at given velocities, and then we shall consider

the influence of the displacement of the profiles, assuming that they are stationary. When studying flow about profiles with circulation, we shall be considering the quasi-steady problem. We shall consider the influence of vortex wakes for a cascade of arbitrary profiles later. The problem in such a formulation is considered in Reference [57].

We introduce the complex velocity potential

$$f=\varphi+i\psi,\quad u=\frac{\partial\varphi}{\partial x}=\frac{\partial\psi}{\partial y},\qquad v=\frac{\partial\varphi}{\partial y}=-\frac{\partial\psi}{\partial x}. \tag{7.1}$$

Here, u, v are the components of the velocity w of the fluid, the velocity potential $\varphi=\varphi(x, y, \tau)$ and the stream function $\psi=\psi(x, y, \tau)$ depend upon the coordinates and the time τ. We decompose functions φ and ψ into a sum of two functions

$$\varphi=\varphi_0(x, y)+\varphi_1(x, y, \tau),$$
$$\psi=\psi_0(x, y)+\psi_1(x, y, \tau).$$

Here φ_0 and ψ_0 do not depend upon time, and we solve the problem of stabilized flow about the cascade. This problem may be considered solved. Henceforth, it is assumed that it has been solved using the exterior of the circle cascade as the canonical region [56]. Functions $\varphi_1(x, y, \tau)$, $\psi_1(x, y, \tau)$ are the velocity potential and the stream function of the absolute perturbed motion of the fluid, induced by the vibration of the profiles. It is convenient to represent function φ_1 in a form analogous to the Kirchhoff form [39, 52, 57],

$$\varphi_1=v_x\varphi_{01}+v_y\varphi_{02}+\Omega\varphi_{03}+\Gamma\varphi_{04}+\varphi_{05}.$$

Here v_x, v_y are the velocity components of the oscillation of an arbitrary profile along the axes of an immobile system of coordinates, Ω is the angular velocity of rotation of the profile; Γ is the circulation of the velocity about the profile. The values depend only upon time. Functions $\varphi_{01}, \varphi_{02}, \varphi_{03}, \varphi_{04}$ depend only upon the coordinates of the point at which the velocity potential is being computed.

Function φ_ω is the potential of flow about the profile by a stream induced by the vortex wakes which appear when the circulation changes in accordance with the Thompson theorem. Obviously, $\varphi_\omega = \varphi(x, y, \tau)$ depends both upon the coordinate and upon time. In considering this problem, we shall assume that φ_ω may be assumed equal to zero.

The boundary conditions at the profiles in the streamline flow state that the normal velocity components of the contour and of the fluid are equal. These conditions may be written in terms of the stream function. On impermeable contours we have the following obvious boundary conditions:

$$\frac{\partial \psi}{\partial s} = v_n(s, \tau).$$

Here s is a curvilinear coordinate measured along a contour; v_n is a velocity component normal to the contour. Integrating, we obtain

$$\psi = f(s, \tau) + \text{const.}$$

As one of the geometrical considerations, the normal velocity of the contour points may be expressed in terms of oscillation velocities

$$v_n = v_x \frac{dy}{ds} - v_y \frac{dx}{ds} - \\ -\Omega\left(x \frac{dx}{ds} + y \frac{dy}{ds}\right).$$

From this, after integration, we obtain the boundary value of the stream function

$$\psi = v_x y - v_y x - \frac{1}{2}\Omega(x^2 + y^2) + \text{const.} \qquad (7.2)$$

At an infinite distance from the cascade, the perturbation induced by the profile oscillation should attenuate. Only in a case where the profiles oscillate cophasally and the circulation is not equal to zero will the perturbations at an infinite distance on the right remain finite.

The obtained boundary values have been found under the condition that the influence of the displacement of the profiles may be

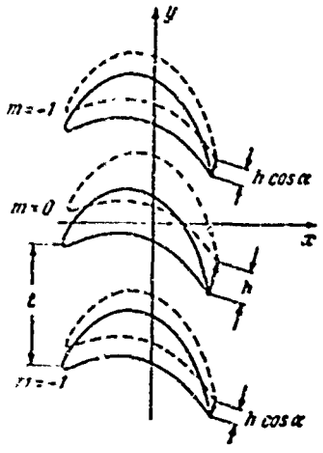


Figure 7.2. Displacements of profiles in a cascade.

disregarded. Now we shall consider the influence of the displacement.

Let it be possible for the cascade profiles to have displacements given by the vectors $h\exp(-jm\alpha)$ where h is a complex constant (with respect to i), m is the number of the profile. The profiles in the initial position are shown by a solid line (Figure 7.2), and when shifted — by a dotted line. The modulus of the displacement vector is much smaller than the cascade spacing: $|h|\ll t$. It is assumed that a solution of flow about the initial cascade by a stabilized stream is available, i.e., the distribution of velocities at the profiles has been found. The velocity in the entire field of the stream is expressed in terms of the known boundary values by a Cauchy integral, taken along all the contours,

$$w(z)=\frac{1}{2\pi i}\sum_{m=-\infty}^{\infty}\oint_{L_m}\frac{w^0(\zeta)\,d\zeta}{\zeta_m-z}+\text{const.}$$

Here $w^0(\zeta)=w^0(\zeta+imt)$ does not depend upon the profile number, since all the profiles are subjected to the same conditions; ζ_m is a complex coordinate at the m^{th} profile L_m; z lies outside the profiles.

In a case where the profiles are displaced, the preceding expression must be replaced by the following one:

$$w(z,h)=\frac{1}{2\pi i}\sum_{m=-\infty}^{\infty}\oint_{L_m}\frac{w_0(\zeta)\,d\zeta}{\zeta_m-z}+\text{const.}\qquad(7.3)$$

Here $w_0(\zeta)=w^0(\zeta)+w^{(m)}(\zeta)$, $w^{(m)}(\zeta)$ is a supplemental velocity at the profiles, induced by their displacement. Functions $w^{(m)}(\zeta)$ are unknown, and their construction is the final aim of the formulated problem. For the construction of $w^{(m)}(\zeta)$, use may be made of the method of successive

approximations, since in the case of a small displacement $|h| \ll l$ it may be expected that $|w^{(m)}(\zeta)| \ll |w^0(\zeta)|$. In a null approximation we assume $w^{(m)}(\zeta) = 0$ and then determine the perturbed acceleration field at the profiles which is induced by the displacement.

We designate by ζ_0 the complex coordinate of the points of the profile with the number zero; then the coordinates of like points of the displaced profiles are determined by the relationship

$$\zeta_m = \zeta_0 + lml + h\exp(-jm\alpha), \quad m = 0; \pm 1; \pm 2; \ldots$$

Analogously, if a coordinate of a point situated in the vicinity of the zero profile is designated by z_0, the coordinate of a like point (in relation to the profile) in the vicinity of profile m will be

$$z_m = z_0 + lml + h\exp(-jm\alpha), \quad m = 0; \pm 1; \pm 2; \ldots$$

Henceforth, we shall discard the index zero for ζ and z, but as before, we shall consider that they pertain to the zero profile.

The perturbed velocities are the difference of velocities $\Delta w = w(z, h) - w^0(z)$, determined at points similar in relation to the given profile, for cases where the profiles are shifted ($h \neq 0$) and when they occupy the initial position ($h = 0$). On the basis of (7.3) we find the velocity in the vicinity of the n^{th} profile in a cascade with displaced profiles

$$w(z, h) = \frac{1}{2\pi i}\sum_{m=-\infty}^{\infty}\oint \frac{w^0(\zeta)\,d\zeta}{\zeta + l(m-n)t + h\left(e^{-jm\alpha} - e^{-jn\alpha}\right) - z} + \text{const}.$$

Then the perturbation of the velocity in the vicinity of the n^{th} profile, induced by the shift of all the profiles in the cascade, will be equal to

$$\Delta w(z) = w(z, h) - w^0(z) = \frac{1}{2\pi i}\sum_{m=-\infty}^{\infty}\oint\left[\frac{1}{\zeta - l(m-n)t + h\left(e^{-jm\alpha} - e^{-jn\alpha}\right) - z} - \frac{1}{\zeta - l(m-n)t - z}\right] w^0(\zeta)\,d\zeta. \qquad (7.4)$$

In the integrand, terms with m = n are mutually eliminated. This is brought about by the fact that the perturbations in the vicinity of the n^{th} profile are determined not by its own shift, but by the relative shift of the remaining profiles, i.e., by the value $h[\exp(-jm\alpha)-\exp(-jn\alpha)]$. Here it should be recalled that perturbations of the velocity are determined not at fixed points of the plane of the stream, but at points, the position of which is coordinated with respect to the moveable profile under consideration. Since terms with m = n are removed from consideration, point $\zeta = z$ ceases to be singular and z may belong not only to the vicinity of the contour, but to the contour itself. Retaining terms of the first order of smallness ($|h|/t \ll 1$, $m \neq n$) in the brackets of (7.4) and replacing the summation index by m - n = k, we find

$$\Delta w(z) = -\frac{1}{2\pi i} h e^{-jn\alpha} \sum_{k=-\infty}^{\infty}{}' \oint \frac{(e^{jk\alpha}-1)\, w^0(\zeta)\, d\zeta}{(\zeta - z + ikt)^2}. \qquad (7.5)$$

Here the prime at the summation sign signifies that in summation, the term with k = 0 is omitted. In Formula (7.5) ζ and z belong to the zero profile. Consequently, and this is important for construction of the solution, the velocity perturbations at the n^{th} profile differ from the perturbations at the main profile only by the multiplier $\exp(-jn\alpha)$. Let us also note that the displacement of the profiles does not change the stream an infinite distance from the cascade. Changing the order of summation and integration in (7.5), the integrand can be summed. The values of the perturbation velocity at the profiles, obtained by means of (7.5), are used in compilation of the boundary conditions. These conditions may be given in terms of the value of the stream function at the profile or directly in terms of the perturbed normal velocities.

The solution of the problem consists in determining the complex potential, which satisfies the cited boundary conditions at oscillating profiles.

The velocity field is found by means of (7.1), and the pressure field is represented by the Lagrange integral

$$p = p_0(\tau) - \rho^0 \frac{\partial \varphi}{\partial \tau} - \frac{1}{2}\rho^0(u^2 + v^2).$$

Computation of the forces and moments acting upon the profile may be carried out according to the general formulas of L. I. Sedov for unstabilized motion.

§ 7.3. Derivation of the Basic Formulas

Before passing on to the solution, we obtain the formula for a function which has the properties that must be possessed by the complex acceleration potential in the formulated problem.

In the region G we introduce for consideration the function $F(z, t, \alpha)$ of the complex variable z, depending upon two real parameters, t and α, which possesses the following properties.

1. Function $F(z, t, \alpha)$ satisfies the condition of generalized periodicity in the following sense [57]

$$F(z + lmlj) = e^{-lm\alpha} F(z), \quad m = \pm 1; \pm 2; \pm 3; \ldots \tag{7.6}$$

Here j is an imaginary unit which does not interact with the imaginary unit i.

2. Function $F(z, t, \alpha)$ does not have singular points in the region G.

3. Function $F(z, t, \alpha) \to 0$ when

$$x \to \pm\infty, \ (\alpha \neq 0), \tag{7.7}$$

We obtain the integral representation of this function. We write the Cauchy formula:

$$F(z) = \frac{1}{2\pi i} \oint_L \frac{F(\zeta)\, d\zeta}{\zeta - z}.$$

Here L is any contour which may be drawn around the arbitrary point z without intersecting the contour profiles. We draw contour L in the manner shown in Figure 7.1 and, excluding the sections, which are passed through twice indifferent directions, we replace L by the sum of the contours

$$L = L' + \sum_{m=-N}^{N} L_m.$$

Here L' embraces all the selected profiles, and L_m is only the profile with the number m. Then we obtain

$$F(z) = -\frac{1}{2\pi i}\oint_{L'}\frac{F(\zeta)\,d\zeta}{\zeta - z} + \frac{1}{2\pi i}\sum_{m=-N}^{N}\oint_{L_m}\frac{F_m(\zeta)\,d\zeta}{\zeta - z}. \qquad (7.8)$$

Expanding L' taking (7.7) into account, we discard the first integral. Here $F_m(\zeta)$ signifies the boundary value of function F(z) on contour L_m. We reduce the integration to integration only along contour L_0, which will subsequently be called the main contour. Effecting in (7.8) the replacement of variable $\zeta = \zeta_0 + im\ell$, utilizing Condition (7.6)

$$F_m(\zeta) = e^{-\ell m\alpha}F_0(\zeta)$$

and letting $N \to \infty$, we obtain (we discard the index zero in the integration variable)

$$F(z) = \frac{1}{2\pi i}\oint_{L_0}\sum_{m=-\infty}^{\infty}\frac{F_0(\zeta)\,e^{-\ell m\alpha}\,d\zeta}{\zeta - z + im\ell}.$$

The integrand may be transformed and summed (when $0<\alpha<2\pi$). Then we obtain the final integral formula, which expresses the value of function F(z) in the region G in terms of its value on the main contour

$$F(z) = \frac{1}{4i}\int_{L_0} F_0(\zeta)\,\Phi(z-\zeta, \alpha, q)\,d\zeta. \qquad (7.9)$$

Here is designated q = 2/t and the function $\Phi(z, \alpha, q)$ is introduced, which is the kernel of

$$\Phi(z, \alpha, q) = q\left\{\frac{\operatorname{ch}[1/2(\pi-\alpha)qz]}{\operatorname{sh}[1/2\pi qz]} - i\frac{\operatorname{sh}[1/2(\pi-\alpha)qz]}{\operatorname{sh}[1/2\pi qz]}\right\}. \tag{7.10}$$

Function $\Phi(z, \alpha, q)$ possesses the following basic property:

$$\Phi\left(z + \frac{2im}{q}\right) = e^{-im\alpha}\Phi(z). \tag{7.11}$$

Function $\Phi(z, \alpha, q)$ has simple bands at points 2im/q and is expanded into the simple fractions

$$\Phi(z, \alpha, q) = \frac{1}{z} + q\sum_{m=1}^{\infty}\left(\frac{e^{im\alpha}}{qz+2im} + \frac{e^{-im\alpha}}{qz-2im}\right). \tag{7.12}$$

As the distance from the cascade increases to the left and to the right, we have

$$\Phi(z, \alpha, q) \to \pm(1 \mp i\beta)e^{\mp i\alpha q z} \qquad z \to \pm\infty. \tag{7.13}$$

We expand function $\Phi(z-\zeta)$ in the vicinity of point $\zeta = 0$ according to powers of ζ:

$$\Phi(z-\zeta, \alpha, q) = \sum_{n=0}^{\infty}\frac{(-1)^n\zeta^n}{n!}\frac{d^n\Phi(z)}{dz^n}. \tag{7.14}$$

We substitute this expression into Integral (7.9)

$$\begin{aligned}\oint_{L_0} F_0(\zeta)\Phi(z-\zeta)\,d\zeta &= \oint_{L_0} F_0(\zeta)\sum_{n=1}^{\infty}\frac{(-1)^n}{n!}\left[\frac{d^n}{dz^n}\Phi(z)\right]\zeta^n\,d\zeta = \\ &= \sum_{n=1}^{\infty}\frac{(-1)^n}{n!}\frac{d^n}{dz^n}\Phi(z)\oint_{L_0} F_0(\zeta)\zeta^n\,d\zeta.\end{aligned} \tag{7.15}$$

Here the order of integration and summation has been changed; this is possible due to the absolute and uniform convergence of the series.

Utilizing (7.14) and (7.15), we arrive at the result that function F(z) may be represented by the functional series

$$F(z) = \frac{1}{M}\sum_{n=2}^{\infty}\frac{(-1)^n}{n!}N_{n+1}\frac{d^n\Phi(z)}{dz^n}. \tag{7.16}$$

Here, coefficients N_n are defined by the formula

$$N_n = \frac{1}{2\pi i}\int F(\zeta)\zeta^{n-1}\,d\zeta. \tag{7.17}$$

Series (7.16) in the special case of $\alpha = 0$ passes into a series with respect to derivatives of cth z and is used in cascade theory [56]

$$F(z) = q\sum_{n=0}^{\infty}\frac{(-1)^n}{n!}N_{n+1}\frac{q^n}{2^n}\operatorname{cth}\frac{\pi q z}{2}$$

When q = 0, Series (7.16) passes into the main part of a Laurent series outside a single contour

$$F(z) = \sum_{n=0}^{\infty} N_{n+1}z^{-(n+1)}.$$

We obtain the expansion of $\Phi(z, \alpha, q)$ in the vicinity of the poles. We note first of all that on the basis of the property of (7.11), the expansion in the vicinity of pole m differs from the expansion in the vicinity of pole m = 0 only by the multiplier $\exp(-jm\alpha)$.

First we expand into a Taylor series (in the vicinity of pole m = 0) the expression in the parentheses of (7.12)

$$\cos m\alpha\sum_{k=1}^{\infty}\frac{(-1)^{k+1}q^{2k}}{2^{2k-1}m^{2k}}z^{2k-1} - ij\sin m\alpha\sum_{k=1}^{\infty}\frac{(-1)^k q^{2k+1}}{2^{2k}m^{2k+1}}z^{2k+1}.$$

Here the constant, which is henceforth insignificant, has been discarded. Substituting this series into (7.12) and changing the order of summation, we find the expansion of $\Phi(z, \alpha, q)$ in the vicinity of pole m = 0:

$$\Phi(z, \alpha, q) = \frac{1}{z} + \sum_{k=1}^{\infty}\frac{c_k q^{2k}}{2^{2k-1}}z^{2k-1} - ij\sum_{k=1}^{\infty}\frac{s_k q^{2k+1}}{2^{2k}}z^{2k}. \tag{7.18}$$

The series must converge all the way to the closest singular point, i.e., under the condition $|z| < 1 = 2/q$. Here we have introduced the designations:

$$\left.\begin{aligned} c_k &= c_k(\alpha) = (-1)^{k+1}\sum_{m=1}^{\infty}\frac{\cos m\alpha}{m^{2k}},\\ s_k &= s_k(\alpha) = (-1)^k\sum_{m=1}^{\infty}\frac{\sin m\alpha}{m^{2k-1}}. \end{aligned}\right\} \tag{7.19}$$

These relationships may be expressed in terms of Bernoulli polynomials ($0<\alpha<2\pi$):

$$c_k = \frac{1}{2}\frac{(2\pi)^{2k}}{(2k)!}B_{2k}\left(\frac{\alpha}{2\pi}\right), \quad s_k = \frac{1}{2}\frac{(2\pi)^{2k+1}}{(2k+1)!}B_{2k+1}\left(\frac{\alpha}{2\pi}\right).$$

The Bernoulli polynomials may be written in terms of the Bernoulli numbers:

$$B_n(x) = \sum_{k=0}^{n}\binom{n}{k}B_k x^{n-k}.$$

In particular, the first numbers c_k and s_k are expressed (for $0<\alpha<2\pi$) by polynomials with powers of α according to the following formulas:

$$\left.\begin{aligned} c_1 &= \frac{\pi^2}{6} - \frac{\pi\alpha}{2} + \frac{\alpha^2}{4}, \quad c_2 = -\frac{\pi^4}{90} + \frac{\pi^2\alpha^2}{12} - \frac{\pi\alpha^3}{12} - \frac{\alpha^4}{48}, \\ s_0 &= \frac{\pi-\alpha}{2}, \quad s_1 = -\frac{\pi^2\alpha}{6} + \frac{\pi\alpha^2}{4} - \frac{\alpha^3}{12}, \\ s_2 &= \frac{\pi^4\alpha}{90} - \frac{\pi^2\alpha^3}{36} + \frac{\pi\alpha^4}{48} - \frac{\alpha^5}{240}. \end{aligned}\right\} \qquad (7.20)$$

Functions $c_k(\alpha)$ and $s_k(\alpha)$ are given in Tables (7.1) and (7.2). Series (7.19) converge so rapidly that when $k > 5$ we may write

$$c_k = (-1)^{k+1}\cos\alpha, \quad s_k = (-1)^k\sin\alpha.$$

In order to obtain the expansion of function $F(z, \alpha, q)$ into a Laurent series in the vicinity of pole $m = 0$, we differentiate (7.18) n times with respect to z. After transformations we obtain

$$\frac{d^n\Phi(z)}{dz^n} = \frac{(-1)^n n!}{z^{n+1}} + \sum_k^{\infty}\frac{q^{2k}c_k}{2^{2k-1}}\frac{(2k-1)!}{(2k-n-1)!}z^{2k-n-1} - ij\sum_k^{\infty}\frac{s_k q^{2k+1}}{2^{2k}}\frac{(2k)!}{(2k-n)!}z^{2k-n}. \qquad (7.21)$$

Here summation with respect to k is conducted in such a manner that the powers of z are greater than zero (insignificant constants may be discarded).

Then on the basis of (7.16) and (7.21) function F(z) in the vicinity of pole $m = 0$ may be represented by the series (the intermediate transformations are omitted)

TABLE 7.1

α	k=1	k=2	k=3	k=4	k=5
0	1,63309	−1,08232	1,01731	−1,00107	1,00106
10	1,37609	−1,05861	1,00091	−0,99862	0,98199
20	1,12671	−0,99293	0,95225	−0,94276	0,93989
30	0,89106	−0,89285	0,87363	−0,86796	0,86673
40	0,67029	−0,76559	0,73777	−0,72562	0,76649
50	0,46437	−0,61788	0,63865	−0,64196	0,64283
60	0,27422	−0,45597	0,48074	−0,49788	0,49987
70	0,09965	−0,28558	0,32297	−0,33890	0,34198
80	−0,05103	−0,11234	0,15349	−0,16991	0,17358
90	−0,20554	0,05918	−0,01539	0,00389	−0,00092
100	−0,33506	0,22449	−0,18751	0,17723	−0,17322
110	−0,44938	0,37962	−0,35280	0,34487	−0,34155
120	−0,54824	0,52111	−0,50657	0,50180	−0,49815
130	−0,63208	0,64594	−0,64151	0,64334	−0,64195
140	−0,70057	0,75155	−0,76282	0,76530	−0,76591
150	−0,75385	0,83595	−0,85629	0,86107	−0,86575
160	−0,79203	0,89723	−0,92836	0,92677	−0,93815
170	−0,81469	0,93452	−0,97115	0,98125	−0,98356
180	−0,82239	0,94703	−0,98455	0,99623	−0,99605

TABLE 7.2

α	k=1	k=2	k=3	k=4	k=5
0	0	0	0	0	0
10	−0,26351	0,18750	−0,17660	0,17434	−0,17377
20	−0,48203	0,36709	−0,34751	0,34332	−0,34268
30	−0,65792	0,53210	−0,50728	0,50174	−0,50017
40	−0,79394	0,67717	−0,65033	0,64175	−0,64293
50	−0,89274	0,79815	−0,77393	0,76759	−0,76652
60	−0,95693	0,89203	−0,87272	0,85771	−0,85649
70	−0,98982	0,95643	−0,94112	0,94091	−0,93988
80	−0,99212	0,99157	−0,97705	0,98512	−0,98500
90	−0,96894	0,99815	−0,99575	0,99994	−1,00023
100	−0,92154	0,97128	−0,98178	0,99109	−0,98511
110	−0,85266	0,91838	−0,93149	0,93811	−0,93591
120	−0,76539	0,83956	−0,85930	0,86133	−0,86051
130	−0,66235	0,73745	−0,75858	0,76114	−0,76055
140	−0,51783	0,61529	−0,63516	0,61090	−0,61297
150	−0,41818	0,47635	−0,49314	0,49835	−0,50052
160	−0,28354	0,32176	−0,33731	0,33989	−0,34201
170	−0,11310	0,16155	−0,17117	0,17390	−0,17388
180	0	0	0	0	0

$$F(z,\alpha,q)=\sum_{n=1}^{\infty}\frac{(-1)^{n-1}(n-1)!N_n}{z^n}+\sum_{n=0}^{\infty}\sum_{k}^{\infty}\frac{(2k-1)!q^{2k}c_k}{n!2^{2k-1}}N_{2k-n}z^n-$$

$$-ij\sum_{n=2}^{\infty}\sum_{k}^{\infty}\frac{(2k+1)!q^{2k+1}s_k}{n!2^{2k}}N_{2k-n+1}z^n. \qquad (7.22)$$

This series converges in the circle $|z|<2/q$ or $|z|<t$, where t is the spacing of the cascade singularities, i.e., is the distance between

adjacent poles. In a special case, with a zero phase shift ($\alpha = 0$) direct use may be made of the expansion of cth qz with respect to the powers of qz in the circle $|qz|<\pi$ or $|z|<l$:

$$\operatorname{cth} qz = \sum_{k=0}^{\infty} \frac{2^{2k}}{k!} B_k (qz)^{k-1}.$$

Here B_k are Bernoulli numbers. Then for the special case under consideration, instead of (7.22), we obtain

$$F(z, 0, q) = \sum_{n=1}^{\infty} \frac{N_n}{z^n} + \sum_{n=0}^{\infty} \sum_{k=n+1}^{\infty} \frac{(-1)^{n+1} 2^{2k} B_k N_{-(k+n)} q^k}{k(k-n-1)!\,n!} z^n. \qquad (7.23)$$

Thus, the coefficients of the regular part of a Laurent series depend upon the coefficients of the main part. This relationship will be used when establishing the conformal correspondence between the exterior of the cascade profile and the exterior of the circle profile which is selected as the canonical region.

Before considering the flow around a cascade of arbitrary profiles, we obtain the solution in the canonical region — the exterior of a circle cascade.

§ 7.4. A Circle in a a Nonstabilized Stream

Let a circle cascade be given (Figure 7.3) with radii r = 1, which oscillates harmonically with a small amplitude. Without restricting the generality, we may consider that the cascade axis coincides with the ordinate.

The law of oscillation of any circle of the cascade may be written in the following manner:

$$v_x = v_{0x} e^{i(\nu\tau - m\theta)}, \quad v_y = v_{0y} e^{i(\nu\tau - m\theta)}.$$

Then the stream function on the main circumference must, in accordance with (7.2), take the following form:

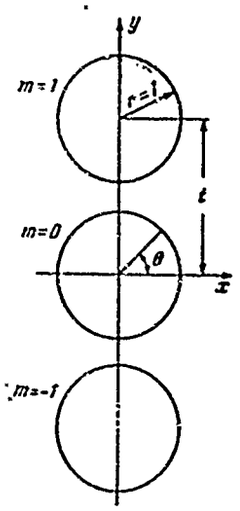


Figure 7.3. A circle cascade.

$$\psi = v_{0x}\sin\theta - v_{0y}\cos\theta.$$

Here θ is the polar angle of the main circles; the time-dependent multiplier has been omitted. Since the exterior of the circle cascade has been selected as the canonical region, let us immediately consider the more general case where a boundary value is assigned value to the stream function

$$\psi = \sum_{n=1}^{\infty} \delta_n \cos n\theta + \sum_{n=1}^{\infty} \gamma_n \sin n\theta. \qquad (7.24)$$

The complex velocity potential of the nonsteady zero circulation stream around a cascade of circles that are vibrating with a phase shift α must possess the following properties. The imaginary part of the complex potential on the main circle must satisfy boundary Condition (7.24). The boundary condition on the left of the circles differs from (7.24) by the multiplier $\exp(-jm\alpha)$. At an infinite distance from the cascade, the perturbations must tend toward zero. Consequently, outside the circle cascade the complex potential must possess the same properties as the constructed function $F(z, \alpha, q)$. That means that outside the circle cascade the complex potential must expand into functional Series (7.16), and in the vicinity of pole m = 0 it must expand into the Laurent Series (7.22). The expansion of $F(z, \alpha, q)$ into a Laurent series in the vicinity of pole m differs from Expansion (7.22), as follows from (7.6), only by the multiplier $\exp(-jm\alpha)$. Consequently, the problem consists in determining such coefficients N_n in (7.22) as to satisfy the boundary Condition (7.24).

In the general case coefficients N_n must be complex numbers with respect to two imaginary units:

$$N_n = (A_n + jB_n) + i(C_n + jD_n). \qquad (7.25)$$

Substituting (7.25) into (7.22) and assuming $z=re^{j\theta}$, we separate the imaginary (with respect to i) part and find the series into which the stream function must expand in the vicinity of the main pole (the constants have been discarded):

$$\begin{aligned}\psi(r,\theta)=\sum_{n=1}^{\infty}\Bigg\{&\Bigg[(-1)^{n-1}(n-1)!\,(C_n+jD_n)r^{-n}+\\&+\sum_{k}^{\infty}\frac{(2k-1)!\,q^{2k}c_k}{n!\,2^{2k-1}}(C_{2k-n}+jD_{2k-n})r^n-\\&-j\sum_{k}^{\infty}\frac{(2k)!\,q^{2k+1}s_k}{n!\,2^{2k}}(A_{2k-n+1}+jB_{2k-n+1})r^n\Bigg]\cos n\theta-\\&-\Bigg[(-1)^n(n-1)!\,(A_n+jB_n)r^{-n}-\\&-\sum_{k}^{\infty}\frac{(2k-1)!\,q^{2k}c_k}{n!\,2^{2k-1}}(A_{2k-n}+jB_{2k-n})r^n-\\&-j\sum_{k}^{\infty}\frac{(2k)!\,q^{2k+1}s_k}{n!\,2^{2k}}(C_{2k-n+1}+jD_{2k-n+1})r^n\Bigg]\sin n\theta\Bigg\}.\end{aligned}\tag{7.26}$$

Comparing the boundary values (when r = 1) of the real (with respect to j) part of Series (7.26) with the given Condition (7.24) and setting the boundary conditions of the imaginary part equal to zero, we obtain the system of equations:

$$\left.\begin{aligned}&(-1)^{n-1}(n-1)!\,C_n+\sum_{k}^{\infty}\frac{(2k-1)!\,q^{2k}c_k}{n!\,2^{2k-1}}C_{2k-n}+\\&\qquad+\sum_{k}^{\infty}\frac{(2k)!\,q^{2k+1}s_k}{n!\,2^{2k}}B_{2k-n+1}=\delta_n,\\&-(-1)^{n-1}(n-1)!\,A_n+\sum_{k}^{\infty}\frac{(2k-1)!\,q^{2k}c_k}{n!\,2^{2k-1}}A_{2k-n}-\\&\qquad-\sum_{k}^{\infty}\frac{(2k)!\,q^{2k+1}s_k}{n!\,2^{2k}}D_{2k-n+1}=\gamma_n,\end{aligned}\right\}\tag{7.27}$$

$$\left.\begin{aligned}&(-1)^{n-1}(n-1)!\,D_n+\sum_{k}^{\infty}\frac{(2k-1)!\,q^{2k}c_k}{n!\,2^{2k-1}}D_{2k-n}-\\&\qquad-\sum_{k}^{\infty}\frac{(2k)!\,q^{2k+1}s_k}{n!\,2^{2k}}A_{2k-n+1}=0,\\&-(-1)^{n-1}(n-1)!\,B_n+\sum_{k}^{\infty}\frac{(2k-1)!\,q^{2k}c_k}{n!\,2^{2k-1}}B_{2k-n}+\\&\qquad+\sum_{k}^{\infty}\frac{(2k)!\,q^{2k+1}s_k}{n!\,2^{2k}}C_{2k-n+1}=0.\end{aligned}\right\}$$

From the four series of infinite equations, four series of unknowns can be found. Without investigating the question of convergence of the process of successive approximations, we shall note that in practice the approximations converge very rapidly. Let us note that the systems break down into two groups, with two series of unknowns in each, the unknowns with an even index being linked to the unknowns of the other series with an odd index. The computations are greatly shortened by the diagonal symmetry of the coefficients. We introduce the supplemental designations:

$$\mathscr{L}(k, n) = \frac{(2k-1)!\, q^{2k}}{n!\, 2^{2k-1}}, \quad M(k, n) = \frac{(2k)!\, q^{2k+1}}{n!\, 2^{2k}}.$$

These functions do not depend on the boundary conditions and therefore may be computed once and for all; this greatly simplifies the solution of the equations.

The basic equations in terms of the new designations are written in the following manner:

$$\left.\begin{aligned}
&(-1)^{n-1}(n-1)!\, C_n + \sum_k^{\infty} \mathscr{L}(k, n)\, c_k C_{2k-1} + \\
&\qquad + \sum_k^{\infty} M(k, n)\, s_k B_{2k-n+1} = \delta_n, \\
&-(-1)^{n-1}(n-1)!\, A_n + \sum_k^{\infty} \mathscr{L}(k, n)\, c_k A_{2k-1} - \\
&\qquad - \sum_k^{\infty} M(k, n)\, s_k D_{2k-n+1} = \gamma_n, \\
&(-1)^{n-1}(n-1)!\, D_n + \sum_k^{\infty} \mathscr{L}(k, n)\, c_k D_{2k-1} - \\
&\qquad - \sum_k^{\infty} M(k, n)\, s_k A_{2k-n+1} = 0, \\
&-(-1)^{n-1}(n-1)!\, B_n + \sum_k^{\infty} \mathscr{L}(k, n)\, c_k B_{2k-1} + \\
&\qquad + \sum_k^{\infty} M(k, n)\, s_k C_{2k-n+1} = 0.
\end{aligned}\right\} \qquad (7.28)$$

The distribution of velocity at the circumferences in the cascade is found in terms of the stream function

$$v_\tau = -\frac{\partial \psi}{\partial r} \text{ for } r = 1. \qquad (7.29)$$

Here v_s is the tangential component of the absolute velocity of the fluid. Making use of (7.26), (7.22) and (7.27), after transformations which are omitted here, we obtain the law of velocity distribution at the arbitrary circumference m

$$\begin{aligned} v_s = \cos(v\tau - m\alpha) \sum_{n=1}^{\infty} \{ [2(-1)^{n-1} n! C_n - n\delta_n] \cos n\theta - \\ - [2(-1)^{n-1} n! A_n + n\gamma_n] \sin n\theta \} - \\ - 2\sin(v\tau - m\alpha) \sum_{n=1}^{\infty} (-1)^{n-1} n! [D_n \cos n\theta - B_n \sin n\theta]. \end{aligned} \tag{7.30}$$

The radial velocity at the circumference is known according to the condition of the problem.

Since at the circumference $v_s = (\partial\varphi/r\partial\theta)_{r=1}$, we obtain from (7.30) the expression for the velocity potential

$$\begin{aligned} \varphi = \cos(v\tau - m\alpha) \sum_{n=1}^{\infty} \{ [2(-1)^{n-1} (n-1)! C_n - \delta_n] \sin n\theta + \\ + [2(-1)^{n-1} (n-1)! A_n + \gamma_n] \cos n\theta \} - \\ - 2\sin(v\tau - m\alpha) \sum_{n=1}^{\infty} (-1)^{n-1} (n-1)! [D_n \sin n\theta + B_n \cos n\theta]. \end{aligned} \tag{7.31}$$

The pressure distribution is found from the Lagrange equation according to the known distribution of Potentials (7.31) and the square of the total velocity. The velocity field outside the cascade is determined on the basis of (7.9) or by means of (7.16).

Let us consider as an example the problem of velocity distribution for the perturbed movement of fluid, induced by vibration of the circles in the cascade in the direction of the cascade axis with a velocity of $v_{0y} = 1$, $v_y = v_{0y} \exp j(v\tau - m\alpha)$. The cascade density is given by the parameter $q = 2/t = 0.7$.

We shall carry out the computations for three phase shifts: $\alpha = 0$; $\alpha = \pi$; $\alpha = \pi/4$.

From (7.24) and (7.4) it follows that for all cases of $\delta_1 = -1$ and $\delta_n = \gamma_n = 0$ when $n \geqslant 2$.

(a) For $\alpha = 0$ from (7.19) or the table we obtain

$$c_1 = 1{,}633,\ c_2 = -1{,}082,\ c_3 = 1{,}017,\ c_4 = -1{,}004,\ s_n = 0.$$

From (7.27) it is obvious that $A_n = B_n = D_n = 0$, $C_{2n} = 0$, which is in agreement with the considerations of streamline symmetry. Coefficients C_{2n-1} are found from the solution of the first system of Equations (7.27).

$$\left.\begin{aligned} C_1 + 0{,}400C_1 - 0{,}194C_3 + \ldots &= -1, \\ 2C_3 - 0{,}0324C_1 + 0{,}0746C_3 + \ldots &= 0, \\ \cdots\cdots\cdots\cdots\cdots\cdots & \end{aligned}\right\}$$

We shall restrict ourselves to computation of the first two coefficients

$$C_1 = -0{,}714; \quad C_3 = -0{,}0117; \ldots$$

The distribution of absolute velocity on the circumferences is found from (7.30):

$$v_z = -(0{,}428\cos\theta + 0{,}129\cos 3\theta + \ldots)\cos\nu\tau.$$

(b) For $\alpha = \pi$ we obtain

$$c_1 = -0{,}322;\ c_2 = 0{,}917;\ c_3 = -0{,}985;\ c_4 = 0{,}996,\ s_n = 0.$$

From (7.27) it follows that $A_n = B_n = D_n = 0$, $C_{2n} = 0$. Coefficients C_{2n-1} are found from the solution of the first system of equations

$$C_1 = -1{,}25; \quad C_3 = 0{,}0192; \ldots$$

The absolute velocity at the circumferences according to (7.30) is equal to

$$v_z = (-1{,}52\cos\theta + 0{,}230\cos 3\theta - \ldots)\cos(\nu\tau - m\pi).$$

(c) For $\alpha = \pi/4$, according to (7.20) or the tables we find

$$c_1 = 0{,}575;\ c_2 = -0{,}694;\ c_3 = 0{,}705;\ c_4 = -0{,}707;$$
$$s_1 = 0{,}845;\ s_2 = 0{,}740;\ s_3 = 0{,}715;\ s_4 = 0{,}709.$$

From (7.27) it follows that $A_n = D_n = B_{2n-1} = C_{2n} = 0$.

Coefficients C_{2n-1} and B_{2n} are found from the solution of the first and the fourth system of Equations (7.27):

$$C_1 = -0{,}895;\ C_3 = -0{,}00795;\ B_2 = -0{,}0675;\ B_4 = 0{,}00337; \ldots;$$

The distribution of the absolute velocities at the circumference is yielded by the series

$$v_\theta = -(0{,}790\cos 3\theta + 0{,}035\cos 3\theta + \ldots)\cos(\nu\tau - 1/4m\pi) + \\ + (0{,}270\sin 2\theta - 0{,}162\sin 4\theta + \ldots)\sin(\nu\tau - 1/4m\pi).$$

In the case of such streamline flow, there are eight groups of circumferences at which the velocity distribution will differ. Figure 7.4 shows the curves for four characteristic values of $\beta = \nu\tau - 1/4m\pi$.

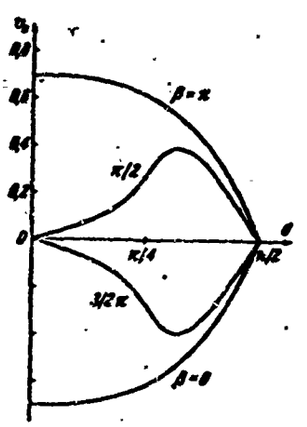


Figure 7.4. Velocity distribution on oscillating circles in a cascade with phase shift.

§ 7.5. Purely Circulatory Flow About a Cascade of Circles With a Phase Shift

Let us consider purely circulational stabilized flow about a cascade of circles under the condition that the circulation of velocity about the m^{th} circle is equal to $\Gamma_m = \Gamma_0 \exp jm\alpha$. On the basis of the analysis carried out above, it is obvious that the complex velocity potential for this streamline flow may be represented in this manner:

$$f = \frac{\Gamma_0}{2\pi i}\left[\int \Phi(z, a, q)\,dz + \sum_n^{\infty} \frac{(-i)^n}{n!} N_{n+1} \frac{d^n}{dz^n} \Phi(z, a, q)\right]. \qquad (7.32)$$

We obtain the expansion of the first term of (7.32) in the vicinity of z = 0 by integrating (7.18):

$$\int \Phi(z)\,dz = \ln z + \sum_{n=1}^{\infty} \frac{c_n q^{2n}}{2^{2n} n} z^{2n} - ij \sum_{n=1}^{\infty} \frac{s_n q^{2n+1}}{2^{2n}(2n+1)} z^{2n+1}. \qquad (7.33)$$

In the problem under consideration, the cascade circumferences are flow lines and, consequently, the stream function at them assumes constant values. Coefficients N_n in (7.32) must in the general case be double complex numbers of the type (7.35); the circulation Γ_0 can in the general case be the complex number $\Gamma_0 = \Gamma_0' + j\Gamma_0''$. Substituting (7.32) and (7.33) into (7.32) and separating the imaginary (with respect to i) part, we obtain the expansion for a stream function in the vicinity of the main pole. Setting the boundary value of the stream function at the main circle equal tc zero, we obtain four series of infinite equations. Pairs of these equations relate the unknowns A, D and B, C. From these equations it follows that

$$A_{2n} = B_{2n} = C_{2n-1} = D_{2n-1} = 0; \quad A_{2n-1} = -B_{2n-1}, \; C_{2n} = D_{2n}. \qquad (7.34)$$

Thus, the unknowns are two series of infinite equations with the unknowns C_{2n} and B_{2n-1} (or D_{2n} and A_{2n-1})

$$\left.\begin{aligned} -(n-1)!\,C_n + \sum_k^{\infty} \frac{(2k-1)!\,q^{2k} c_k}{n!\,2^{2k-1}} C_{2k-1} + \\ + \sum_k^{\infty} \frac{(2k)!\,q^{2k+1} s_k}{n!\,2^{2k}} B_{2k-n+1} = \frac{c_n n q^n}{2^{n-1}} \end{aligned}\right| \qquad (7.35)$$

(Equation continued on next page)

$$-(n-1)!\,B_n+\sum_k^{\infty}\frac{(2k-1)!\,q^{2k}c_k}{n!\,2^{2k-1}}B_{2k-n}+\sum_k^{\infty}\frac{(2k)!\,q^{2k+1}s_k}{n!\,2^{2k}}C_{2k-n+1}\Bigg\}\qquad(7.35)$$

In the first equation n = 2, 4, 6, ..., in the second equation n = 1, 3, 5 .... Summation with respect to k is carried out in such a manner that the unknowns have indices greater than zero. On the basis of (7.32), (7.21), (7.33) and (7.35) we find the series into which the complex potential of a purely circulatory stream in the vicinity of the main pole must be expanded:

$$f=\frac{\Gamma_0'+j\Gamma_0''}{2\pi j}\left[\ln z-\sum_{n=2,4,6\ldots}^{\infty}(n-1)!\,C_n(z^n-z^{-n})+ij\sum_{n=1,3,5,\ldots}^{\infty}(n-1)!\,B_n(z^n+z^{-n})\right].\qquad(7.36)$$

Multiplying this expression by $\exp(-jm\alpha)$, we obtain an expansion of the complex potential in the vicinity of pole m. We separate from the obtained expression the real (with respect to i and j) part and find the expression for the velocity potential at the circumference of number m:

$$\varphi=\left[\frac{\Gamma_0'}{2\pi}\theta-2\frac{\Gamma_0'}{2\pi}\sum_n^{\infty}(n-1)!\,C_n\sin n\theta-2\frac{\Gamma_0''}{2\pi}\sum_n^{\infty}(n-1)!\,B_n\cos n\theta\right]\cos m\alpha+\left[\frac{\Gamma_0''}{2\pi}\theta-2\frac{\Gamma_0''}{2\pi}\sum_n^{\infty}(n-1)!\,C_n\sin n\theta+2\frac{\Gamma_0'}{2\pi}\sum_n^{\infty}(n-1)!\,B_n\cos n\theta\right]\sin m\alpha.\qquad(7.37)$$

The tangential velocities at the circumferences are found by differentiating the complex potential with respect to the polar angle θ when r = 1:

$$v_\tau=\left[\frac{\Gamma_0'}{2\pi}-2\frac{\Gamma_0'}{2\pi}\sum_n^{\infty}n!\,C_n\cos n\theta+2\frac{\Gamma_0''}{2\pi}\sum_n^{\infty}n!\,B_n\sin n\theta\right]\cos m\alpha+\left[\frac{\Gamma_0''}{2\pi}-2\frac{\Gamma_0''}{2\pi}\sum_n^{\infty}n!\,C_n\cos n\theta-2\frac{\Gamma_0'}{2\pi}\sum_n^{\infty}n!\,B_n\sin n\theta\right]\sin m\alpha.\qquad(7.38)$$

When using the circle cascade as a canonical region and when considering a quasi-steady problem, in Expression (7.38) sin mα and cos mα should be replaced by $\sin(\nu\tau - m\alpha)$ and $\cos(\nu\tau - m\alpha)$.

Let us also note the behavior of the solution at infinity. In purely circulatory flow and a phase shift not equal to zero and perturbation at an infinite distance from the cascade attenuates. The case of $\alpha = 0$ is singular, since the total circulation about the cascade is not equal to zero. When $\alpha = 0$ the complex potential, in place of (7.32), is represented by the series

$$f(z) = \frac{\Gamma_0}{2\pi i} \ln \frac{1}{q} \operatorname{sh} \pi q z = \frac{\Gamma_0}{2\pi i} \ln z + \sum_{k=1}^{\infty} \frac{2^{2k-1} B_k q^{2k}}{k\,(2k)!} z^{2k}.$$

The complex velocity will be found by differentiating this expression with respect to z

$$w(z) = \frac{\Gamma_0}{2\pi i} q \operatorname{cth} \pi q z, \quad (q = 2/t).$$

At an infinite distance to the left and to the right from the cascade $(x \to \mp\infty) \operatorname{cth} \pi q z \to \mp 1$. Consequently, the velocity at infinity in front of and behind the cascade has values that have equal moduli, by are opposite in sign $\mp\Gamma_0/2ti$. The last-mentioned magnitude is also determined easily by the contour circulation integral.

As an example, let us find the velocity distribution on the circumferences in a cascade. if the circulation $\Gamma_m = \Gamma_0 \cos m\alpha$ changes with a shift phase equal to $\alpha=0$; $\alpha=\pi$; $\alpha=\pi/4$. The cascade density is given, but the parameter $q = 2/t = 0.7$.

(a) For $\alpha = 0$ we obtain $s_n = 0$ and, consequently, $B_n = 0$. Solving the first equation of (7.35), we find

$$C_2 = -0{,}184; \quad C_4 = 0{,}00012; \ldots$$

Then according to (7.35) we find the law of velocity distribution

$$v_\theta = \frac{\Gamma_0}{2\pi}(1 + 0{,}736\cos 2\theta - \\ - 0{,}0057\cos 4\theta + \ldots).$$

(b) For $\alpha = \pi$ we obtain $s_n = 0$ and $B_n = 0$. From (7.35) we have

$$C_2 = 0{,}110; \quad C_4 = 0{,}000345; \ldots$$

According to (7.38) it is obvious that the distribution of velocities on the neighboring circles differs with respect to sign

$$v_\theta = \frac{\Gamma_0}{2\pi}(1 - 0{,}441\cos 2\theta - 0{,}046\cos 4\theta - \ldots)\cos m\pi.$$

(c) For $\alpha = \pi/4$ we obtain

$$B_1 = 0{,}00753; \; B_2 = 0{,}0175; \ldots; \; C_2 = -0{,}0060; \; C_4 = 0{,}00073, \ldots,$$
$$v_\theta = \frac{\Gamma_0}{2\pi}(1 + 0{,}240\cos 2\theta - 0{,}035\cos 4\theta + \ldots)\cos 1/4\, m\pi + \\ + \frac{\Gamma_0}{2\pi}(-0{,}015\sin\theta - 0{,}210\sin 3\theta - \ldots)\sin 1/4 m\pi.$$

Figure 7.5 gives graphs of the velocity distribution on the circumferences m = 0 — curve 1, and m = 2 — curve 2. Circumference m = 2 has a circulation equal to zero. There is a total of eight groups of circumferences with a different velocity-circulation law.

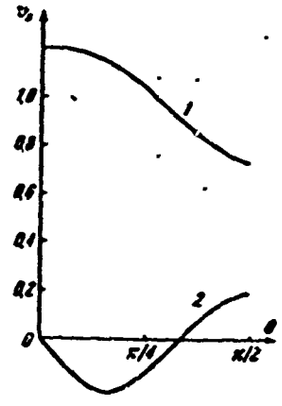


Figure 7.5. Velocity distribution on the circumference with purely circulatory flow about the cascade with a phase shift (1)-for m = 0; (2)-for m = 2.

§ 7.6. The Problem of Flow Around a Cascade with Arbitrary Profiles, Oscillating with a Phase Shift, in a Quasi-steady Formulation

Let us consider the problem of small harmonic oscillation of arbitrary profiles in a cascade with a phase shift. In the presence of circulation about the profiles, we shall consider the problem in a quasi-steady formulation, disregarding the influence of vortex trails which, according to Thompson's theorem, run off the trailing edges. The complex velocity of the stream flowing about the cascade of vibrating blades may be represented as the sum of the complex velocities of the stabilized stream and the perturbed motion. We shall consider the problem of stabilized streamline flow to be solved, and shall turn to plotting the perturbed motion.

The complex velocity w(z) of the perturbed motion must possess the following properties:

1. The function w(z, τ) must be periodic with respect to spacing and with respect to time:

$$w(z, \tau) = w(z)e^{i\nu\tau}, \quad w(z + lml) = w(z)e^{-i\nu\alpha}.$$

2. Function w(z) should not have singular points in the region of the stream, with the exception, possibly, of sharp leading edges of the profiles.

3. Perturbed velocities attenuate at an infinite distance from the cascade.

For solving the problem we shall employ the method of conformal transformation, selecting as the canonical region the exterior of the circle cascade in plane z. The connection between the cascade regions is established by the functional series [56]

$$\zeta = az + \frac{n}{l}\sum_{n=0}^{\infty}\frac{(-1)^n}{n!}a_{-(n+1)}\frac{d^n}{dz^n}\operatorname{ctg}\frac{\pi z}{l}. \qquad (7.39)$$

In the vicinity of poles, (7.39) may be represented by the series

$$\zeta = az + \sum_{n=1}^{\infty} \frac{a_{-n}}{z^n} + \sum_{n=0}^{\infty} a_n z^n. \tag{7.40}$$

The coefficients of the regular part depend upon the coefficients of the main part:

$$a_n = \sum_{k}^{\infty} \frac{(-1)^n 2^{2k} B_k}{2k(k-n-1)!\,n!} \left(\frac{\pi}{t}\right)^{2k} a_{-(2k-n)}. \tag{7.41}$$

Here B_k are Bernoulli numbers.

Conformal transformation of the exterior of a cascade of arbitrary profiles to the exterior of a circle cascade is reduced to the determination of such coefficients a_{-n} and a_n, that when $z=\exp i\theta$ is substituted into Series (7.40) it would be transformed into a parametric equation of the profile. The methods of solving this problem have been considered in [56] and [24]. We consider this problem solved.

Assuming

$$a = a' + ia'', \quad a_n = a'_n + ia''_n, \quad a_{-n} = a'_{-n} + ia''_{-n}, \tag{7.42}$$

the contour of the profiles may be given by two parametric equations:

$$\left.\begin{aligned} \xi &= a'\cos\theta + \sum_{n=1}^{\infty} (a'_{-n} + a''_n)\cos n\theta + \sum_{n=1}^{\infty} (a''_{-n} - a''_n)\sin n\theta, \\ \eta &= a''\sin\theta + \sum_{n=1}^{\infty} (a''_{-n} + a''_n)\cos n\theta + \sum_{n=1}^{\infty} (a'_n - a'_{-n})\sin n\theta. \end{aligned}\right\} \tag{7.43}$$

Here the polar angle of the main circle in the cascade has been taken as the parameter.

Let the profiles carry out arbitrary, but small, oscillations with an arbitrary shift. The boundary conditions of the stream function on the main profile in the case of translational and torsional oscillation are defined by Formula (7.2) in terms of the profile coordinates

$$\psi = v_\xi \eta - v_\eta \xi - \frac{1}{2}\Omega(\xi^2+\eta^2) + \text{const.}$$

When the coordinates of the profile are replaced by parameter θ in accordance with Condition (7.43), we obtain the boundary values of the stream function on the circumferences in the canonical region in the form of a trigonometric series (7.24). The corresponding problem in the canonical region has been solved. The distribution of velocity from the circulationless flow and the purely circulatory flow is known. The value of the circulation is established on the basis of the Chaplygin-Zhukovskiy postulate in a quasi-steady formulation. The method set forth can be extended to a case where the cascade profiles are subjected to small deformations with a phase shift (this problem is of interest when determining the exciting forces in a non-uniform stream). The boundary conditions for the stream function for motion with deformations and with a normal velocity at the boundary v_n are established via the relationship $\partial\psi/\partial s = v_n(0, \tau)$.

Above have been considered problems in which the phase shift changed from blade to blade by a constant value. Such a generalization is analogous to the one considered in § 5.2.

We shall demonstrate the calculation method on the basis of an example.

We find the velocity distribution on the blades in the cascade (Figure 7.6), which are oscillating with the phase shift $\alpha = \pi$ in a direction perpendicular to the chord[1].

We select the components of the oscillation velocities along the coordinate axes $v_{0\xi} = v_{0\eta} = 1$, which naturally does not limit the generality of the calculation, since the oscillation takes place in an incompressible fluid.

Footnote (1) appears on page 324a.

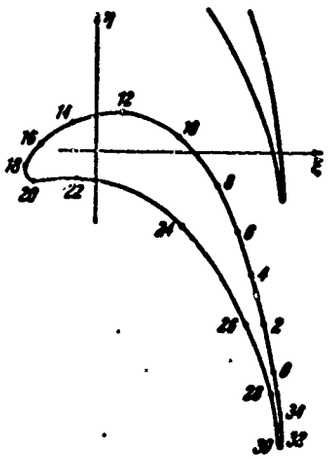


Figure 7.6. Reactive cascade of vibrating profiles.

Utilizing the principle of superposition, we shall consider first only the perturbed flow induced by vibrations of the profiles about the axis of the main stream.

Conformal transformation of the circle cascade exterior to the exterior of a profile cascade may be conducted by any of the known methods. We omit the corresponding operations, which are known from the theory of stabilized flow about a cascade, and shall write the coefficients $(a'_{-n}+a'_n)$, $(a'_n-a'_{-n})$, $(a''_n-a''_{-n})$, $(a''_{-n}-a''_n)$ of Series (7.43) which establish the parametric correspondence between the main circumference and the main profile (Table 7.3).

The points marked on the profile in the cascade (see Figure 7.6) correspond to points uniformally distributed along the main circumference of the circle cascade (every second point is marked, since 36 points were located on the circumference). The density of the equivalent cascade of circles is characterized by the parameter $q = 0.853$. All the calculations are conducted with an accuracy to terms with an index not higher than 5.

TABLE 7.3

$a'_{-n}+a'_n$	0,5210	−0,1779	0,0197	0,0278	−0,0004
$a'_{-n}-a'_n$	0,3960	0,1119	−0,0212	−0,0082	0,0161
$a''_n+a''_n$	−0,4993	−0,0170	0,0914	−0,0296	−0,0060
$a''_{-n}-a''_n$	−0,1089	−0,0170	0,0330	−0,0270	0,0058

Then, on the basis of the given condition of oscillations, by the method described above we determine the boundary condition of the stream function on the profiles. Omitting the calculations, we present the corresponding coefficients of Series (7.24):

$$\begin{aligned}
&\delta_1 = 1{,}0203, && \gamma_1 = +0{,}5049,\\
&\delta_2 = +0{,}1609, && \gamma_2 = +0{,}1289,\\
&\delta_3 = -0{,}0717, && \gamma_3 = -0{,}0542,\\
&\delta_4 = -0{,}0574, && \gamma_4 = +0{,}0188,\\
&\delta_5 = +0{,}0119, && \gamma_5 = +0{,}0093.
\end{aligned}$$

According to the condition of the problem, the oscillation takes place with a phase shift of $\alpha = \pi$; therefore from (7.19) follows $s_k = 0$, and from (7.27) we obtain

$$B_n = D_n = 0.$$

Substituting δ_n and γ_n into (7.27), we obtain a system of linear equations, and we obtain

$$\begin{aligned}
&C_1 = -1{,}535, && C_2 = -0{,}2090, && C_3 = +0{,}0950,\\
&C_4 = +0{,}0120, && C_5 = +0{,}000358, && A_1 = -0{,}3850,\\
&A_2 = +0{,}1100, && A_3 = +0{,}0134, && A_4 = +0{,}00411,\\
&A_5 = -0{,}000275.
\end{aligned}$$

Then we solve the first equation of (7.35) and find

$$C_2^{(0)} = +0{,}188\,\frac{\Gamma_0}{2\pi}, \quad C_4^{(0)} = -0{,}00479\,\frac{\Gamma_0}{2\pi}.$$

Here the upper index indicates that these coefficients pertain to purely circulational flow.

On the basis of the computed coefficients, we find the distribution of the perturbed velocities along the circumference by means of (7.30) and (7.38), i.e., separately for the circulationless flow and the purely circulational flow. The sum of (7.30) and (7.38) yields the distribution of absolute perturbed velocities on the main circumference. This sum includes the multiplier $\Gamma_0/2\pi$, which must be determined according to the condition on the trailing edge. In the case of quasi-steady formulation of the problem at the trailing edge, the Chaplygin-Zhukovskiy condition must be satisfied.

Substituting into the sum of (7.30) and (7.38) the angular coordinate of the trailing edge ($\theta_0 = 310°$, as follows from the conformal mapping), we set the result equal to zero and determine: $\Gamma_0/2\pi = 2{,}41$.

The final distribution of the perturbed tangential velocities on the circumference is given by the series

$$v_s = \sum_{n=1}^{4} C_n^* \cos n\theta + \sum_{n=1}^{4} A_n^* \sin n\theta + 2{,}41.$$

Here:

$$C_1^* = -2{,}050; \quad C_2^* = -1{,}300; \quad C_3^* = +0{,}925; \quad C_4^* = +0{,}210;$$
$$A_1^* = +0{,}265; \quad A_2^* = +0{,}172; \quad A_3^* = 0; \quad A_4^* = +0{,}160.$$

Recalculation of the velocities into the plane of the cascade is conducted according to the rules of conformal transformation in terms of the modulus of the mapping function derivative.

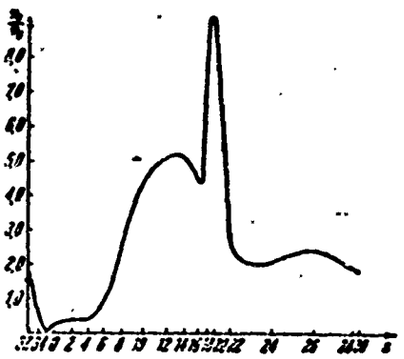


Figure 7.7. Distribution of perturbed tangential velocities in case of vibration of the profiles in a cascade with a phase shift $\alpha = \pi$.

Figure 7.7. shows the distribution of absolute velocities on the profile v_s in relation to the modulus of the profile-oscillation velocity $v_0 = \gamma\overline{v_{0x}^2 + v_{0y}^2}$. An expansion of the profile has been carried out along the abscissa, the point numbers corresponding to the data in Figure 7.6. The considerable velocity peak originates in the case of flow about the leading edge. Branching of the stream takes place between points 0 and 34. The graph in Figure 7.7 is an auxiliary one, since it refers to the perturbed stream with a circulation that varies in time, while the main stream is absent.

We omit calculation of the main stream, since it is carried out by conventional methods for steady streamline flow.

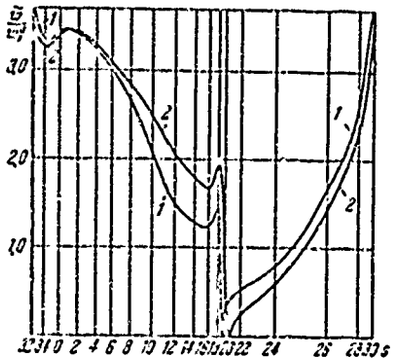


Figure 7.8. Distribution of velocities of a reactive cascade in the case of vibration with a phase shift of $\varphi = \pi$.

Figure 7.8 gives a conception of the manner in which vibration of the profile acts upon the conditions of flow about it. The solution is obtained by addition of the perturbed stream calculated above, brought about by vibration of the profiles in counterphase, and the stabilized stream which flows about the cascade. In plotting the velocity distribution curves $\bar{w}_1/w_1^0$, it is assumed that the maximum vibration velocity comprises 0.05 of the velocity of the stream incident upon the cascade w_1^0. In Figure 7.8, curve (1) corresponds to the moment of time at which the profile during oscillation is moving with the maximum velocity forward with the convex side, and curve (2) represents the same for the concave side. A particularly intensive change of velocity is observed at the leading edge. The velocity peaks would be even greater if the leading edge were sharper. The front critical point moves along the profile, and the rear critical point is, by condition, motionless.

At the small Strouhal numbers typical of many practical problems, the influence of the vortex wake will be small.

However, as has already been noted above, the influence of the shift of a profile in an aerodynamically loaded cascade can turn out to be significant. The influence of a profile shift can be taken into account by the same calculation method. In view of the fact that the shift is small, supplemental perturbation velocities are found according to the given distribution of the steady velocity.

Let us consider the results of calculation of the vibrating profiles in a typical active cascade (Figure 7.9). The equivalent cascade of circles has a density of q = 0.846. The position of the points

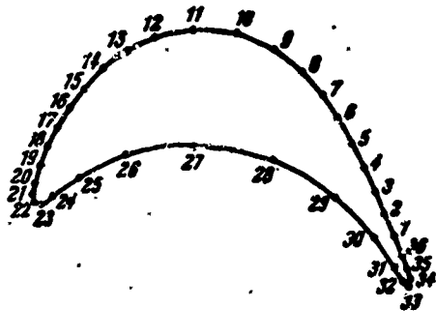


Figure 7.9. A profile in an active cascade.

on the profile corresponds to a uniform position of the points on the circumference in a cascade with the polar coordinate $\theta=10n$ (n is the point number). The blade profile is a TR-ZA type, the relative spacing is $\bar{t}=0,60$, the incidence is $\beta_y = 77°30'$, the calculated inflow and outflow angles of the main stream are $\beta_1=27°$, $\beta_2=24°$. In the calculations it is assumed that the vibration velocity comprises 0.10 (for $\alpha = 0$) and 0.05 (for $\alpha=\pi$) of the velocity of the stream incident upon the cascade.

From the obtained results, we note the fact, important for practical application, that when the blade oscillates in counterphase, the velocity change is considerably more significant (particularly for dense cascades). Consequently, the energy exchange between the blades and the stream for counterphase will be considerably greater than for oscillation in phase. Recollect that the calculations were conducted without taking account of the blade displacement. The considerably greater mutual influence of profiles for oscillation in counterphase has a simple physical explanation. In the case of the indicated oscillation in counterphase has a simple physical explanation. In case of the indicated oscillation the fluid is, as it were, displaced from the internal blade channel. The rate of displacement is greater the less the cascade spacing is and the greater the channel length is. This rate of displacement brings about the appearance of supplemental circulation necessary for maintaining the trailing conditions of the stream from the trailing edge. In the case of oscillation in phase, essentially only the angle of attack changes and, thus, this problem practically does not differ from the conventional problems considered in the theory of steady flow about a cascade.

In the theory of unsteady flow about cascades, determination of the unsteady forces acting upon the profiles is of greatest significance

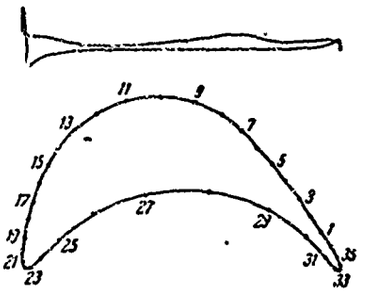


Figure 7.10. Distribution of perturbed pressures along the profile of an active cascade in the case of oscillation with a phase shift of $\alpha=0$.

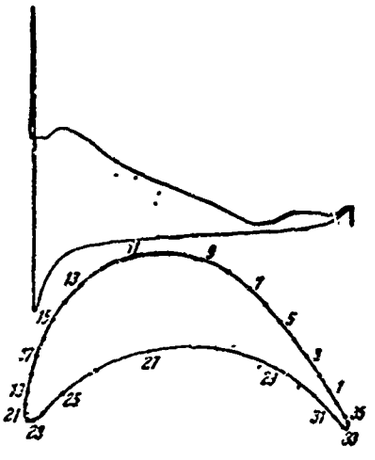


Figure 7.11. Distribution of perturbed pressures along the profile of an active cascade in the case of oscillation with a phase shift of $\alpha=\pi$.

in practice. Figure 7.10 shows the distribution of perturbed pressures along a profile which is in phase with the oscillation velocity for $\alpha = 0$. An analogous graph for the case of oscillations in counter-phase is given in Figure 7.11.

For evaluating the relative intensity of the energy exchange between an oscillating blade and the stream, the aerodynamic damping coefficient can be intro iced. This coefficient may be represented as the ratio of the work performed by the aerodynamic force during one oscillation cycle to twice the energy of the oscillating blade. The aerodynamic force which is in phase with the acceleration of the oscillation may be determined by integrating the perturbed pressure along the profile contour. Utilizing the Bernoulli equation (in the quasi-steady formulation), as well as the smallness of the perturbation velocities in comparison to the velocity of the main stream, we arrive at the following formula for the coefficient of aerodynamic damping:

$$\delta = 2\pi^2 \frac{\rho^0 w_1^0 b}{\rho_1 \nu^2} K, \quad K = \frac{1}{2\pi b} \int_{-b}^{+b} \frac{w^0}{w_1} \frac{v_s}{v_0} d\xi, \tag{7.44}$$

where ρ^0 and ρ_1 are, respectively, the density of the fluid and the density of the blade material, 2b is the blade chord, ν is the circular frequency of the oscillations, w_1^0 is the velocity of the stream

at infinity in front of the cascade, $w^0 = w^0(\xi)$ is the distribution of velocity along the profile in the case of steady flow about the cascade, $v_1 = v_1(\xi)$ is the distribution of the perturbation velocity along the profile, v_0 is the modulus of the oscillation velocity, F is the area of the blade cross section, ξ is a coordinate measured along the blade chord. Here we take into account the fact that the oscillation takes place about the axis of minimum inertia of the cross section, which, as is known, is practically parallel to the chord.

In the specific example under consideration, with a steam pressure of p = 30 absolute atmospheres and a stream velocity of w_1^0 = 164 m/sec, the following values of aerodynamic damping coefficients were obtained:

$\delta = 0{,}007$ (when $\alpha = 0$) and $\delta = 0{,}040$ (when $\alpha = \pi$).

§ 7.7. Solution of the Problem of the Oscillation of Arbitrary Profiles in a Cascade, with a Phase Shift, by the Method of Integral Equations

In the preceding sections, the problem of flow about a cascade of oscillating profiles was solved by the method of conformal transformation onto a cascade of circles, with subsequent solution of an infinite system of linear equations. When highly numerous calculations must be made, it is sometimes more expedient to solve the problem directly in the physical plane. In such a case it is more convenient for the application of computers, and permits account to be taken, in a rather simple manner, of the influence of vortex wakes propagating beyond the profile.

Let us consider an infinite cascade of random profiles in the plane of the complex variable z = x + iy in a steady stream of ideal incompressible fluid. The profiles carry out small synchronous harmonic oscillations with a frequency ν and an arbitrary phase shift ε.

During flow about a cascade of oscillating profiles, the stream velocity ϖ is composed of the velocity of the main steady stream w^0

(we consider the problem of steady streamline flow to be solved) and the perturbation velocity w, induced by the oscillation of the profile. velocities w^0 and w are the absolute velocities of the stream, i.e., velocities measured with respect to a motionless system of coordinates. We designate by w_1^0 and w_2^0, respectively, the velocities of the steady streamline flow in front of and behind the cascade.

We assume that the blade has a piecewise-smooth contour. The complex velocity of the perturbed stream w(z) is found in the flow region, which constitutes the exterior of the profile cascade S. When the circulation about the oscillating profiles changes, a vortex sheet trails off their trailing edges in accordance with Thompson's theorem; this vortex sheet is the velocity discontinuity line (Figure 7.12).

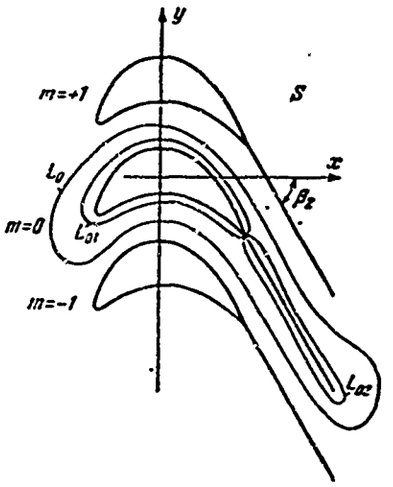


Figure 7.12. A cascade of arbitrary profiles with vortex wakes.

The value of the perturbed complex velocity at any point belonging to S may be determined on the basis of the generalized Cauchy formula. Making the same transformations as at the preceding points, we obtain the formula

$$w(z)+\frac{1}{\omega t}\oint_{L_0} w_0(\zeta)\Phi(\zeta-z,\alpha,t)\,d\zeta=0. \qquad (7.45)$$

Here $w_0(\zeta)$ is the boundary value of the represented function on contour L_0. Contour L_0, along which integration is conducted, encloses only the main profile and the wake after it. The kernel is represented by the expression

$$\Phi(\zeta-z,\alpha,t)=\frac{\operatorname{ch}\left[(\pi-\alpha)\frac{\zeta-z}{t}\right]}{\operatorname{sh}\left[\pi\frac{\zeta-z}{t}\right]}-i\frac{\operatorname{sh}\left[(\pi-\alpha)\frac{\zeta-z}{t}\right]}{\operatorname{sh}\left[\pi\frac{\zeta-z}{t}\right]}. \tag{7.46}$$

We break down contour L_0 into two contours L_{01} and L_{02}, where L_{01} is the contour enclosing only the main profile, and L_{02} is the contour which encloses only the wake after the main profile.

We direct point $z\to L_{01}$, and $L_{01}\to L$, where L is the profile contour. In accordance with the theorem concerning limit values of a Cauchy-type integral, we find that at each regular point $z\in L$

$$w(z)=\frac{1}{2}w(z)-\frac{1}{2\pi i}\oint_{L+L_\infty}w(\zeta)\Phi(\zeta-z,\alpha,t)\,d\zeta.$$

From this we obtain

$$w(z)+\frac{1}{\pi i}\oint_{L+L_\infty}w(\zeta)\Phi(\zeta-z,\alpha,t)\,d\zeta=0. \tag{7.47}$$

Here $w(\zeta)$ is the boundary value of the represented function on the profile and on the wake after it. It is further assumed that function $w(\zeta)$ satisfies the Hoelder condition with the index $\mu<1$.

Equation (7.47) may be written in another form [57a], breaking down the contour integral into two integrals: one integral is computed along contour L, and the other — only along contour L_{02}:

$$w(z)+\frac{1}{\pi i}\oint_{L}w(\zeta)\Phi(\zeta-z,\alpha,t)\,d\zeta+\frac{1}{\pi i}\oint_{L_{02}}w(\zeta)\Phi(\zeta-z,\alpha,t)\,d\zeta=0. \tag{7.48}$$

We write the expression for the velocity of the absolute perturbed motion for points $z\in L$ in the following form

$$w(z)=v(z)+v_0(z). \tag{7.49}$$

Here $\hat{v}(z)$ is the velocity of the fluid on the contour for relative motion, $v_0(z)$ is the local velocity of the contour. Then in accordance with Condition (7.49), Equation (7.48) is rewritten in the following form:

$$\hat{v}(z)+\frac{1}{i\pi}\oint_L \hat{v}(\zeta)\Phi[\zeta-z,\alpha,t]\,d\zeta+\frac{1}{i\pi}\oint_{L_m} w(\zeta)\Phi[\zeta-z,\alpha,t]\,d\zeta=$$
$$=-v_0(z)-\oint_L v_0(\zeta)\Phi[\zeta-z,\alpha,t]\,d\zeta. \tag{7.50}$$

The equation for the complexiy conjugate velocity is obtained from (7.50) with the replacement of $\hat{v}(z)$ by $\overline{\hat{v}(z)}$ and with the replacement of $w(\zeta)$ by $\overline{w(\zeta)}$.

By virtue of the fact that

$$\frac{dz}{d\bar{s}}=\frac{dx}{d\bar{s}}+i\frac{dy}{d\bar{s}}=e^{i\beta(\bar{s})},\quad \frac{\overline{dz}}{d\bar{s}}=e^{-i\beta(\bar{s})}, \tag{7.51}$$

we have

$$\overline{\hat{v}(z)}=\hat{v}(\bar{s})\bar{z}'(\bar{s})=v(\bar{s})e^{-i\beta(\bar{s})}, \tag{7.52}$$
$$\overline{\hat{v}(\zeta)}\,d\bar{\zeta}=\hat{v}(\bar{\sigma})e^{-i\beta(\bar{\sigma})}e^{i\beta(\bar{\sigma})}d\bar{\sigma}=\hat{v}(\bar{\sigma})\,d\bar{\sigma}. \tag{7.53}$$

Here $\bar{s}$ and $\bar{\sigma}$ are arc coordinates at points zero and ζ of contour L, measured along the main profile from a certain point fixed on it, β is the angle between the tangent to the profile at point $\bar{s}$ and the abscissa, $\hat{v}(\bar{s})$ is the modulus of the velocity of the perturbed motion of the fluid on the contour in terms of relative motion, $\bar{z}(\bar{s})=d\bar{z}/d\bar{s}$.

Expression (7.52) follows from the boundary condition of profile impermeability

$$\mathrm{Re}[i\bar{z}'(\bar{s})\overline{\hat{v}(z)}]=0 \tag{7.54}$$

Taking into account (7.52) and (7.53), from (7.50) we obtain

$$v(\bar{s})+\frac{z'(\bar{s})}{ii}\oint_L v(\bar{\sigma})\Phi[\zeta(\bar{\sigma})-z(\bar{s}),\ \alpha,\ t]\,d\bar{\sigma}+$$
$$+\frac{z'(\bar{s})}{ii}\oint_{L_m}\overline{w(\zeta)}\Phi[\zeta-z,\ \alpha,\ t]\,d\zeta=$$
$$=-\overline{v_0(\bar{s})}z'(\bar{s})-\frac{z'(\bar{s})}{ii}\oint_L\overline{v_0(\zeta)}\Phi[\zeta-z,\ \alpha,\ t]\,d\zeta. \qquad (7.55)$$

For points $\zeta\in L_m$, vector $\overline{w(\zeta)}$ in the coordinate system connected to the contour which embraces the wake may be represented in the form

$$\overline{w(\zeta)}=\overline{w_n(\zeta)}+\overline{w_s(\zeta)},$$

where $\overline{w_n(\zeta)}$ and $\overline{w_s(\zeta)}$ are projections of $\overline{w(\zeta)}$ respectively upon the normal and the tangent to the wake.

Since vector $\overline{w_n(\zeta)}$ is perpendicular to the direction of passage along contour L_{02}, it follows that

$$\oint_{L_m}\overline{w(\zeta)}\Phi[\zeta-z,\ \alpha,\ t]\,d\zeta=\oint_{L_m}\overline{w_s(\zeta)}\Phi[\zeta-z,\ \alpha,\ t]\,d\zeta. \qquad (7.56)$$

The integral of the normal component in passage along contour L_{02} will be equal to zero, since the normal component does not undergo discontinuity and is the same on both sides of the section enclosed by contour L_{02}. Introducing the independent variables σ and s, analogously to (7.53), for the wake contour we obtain

$$\overline{w_s(\zeta)}\,d\zeta=w_s(\sigma)\,d\sigma. \qquad (7.57)$$

Here σ and s are arc coordinates of points z and ζ of contour L_{02}.

By means of (7.56) and (7.57) the integral along the contour will assume the form

$$\oint_{L_m}\overline{w(\zeta)}\Phi[\zeta-z,\ \alpha,\ t]\,d\zeta=\oint_{L_m}w_s(\sigma)\Phi[\zeta_0(\sigma)-z(s),\ \alpha,\ t]\,d\sigma. \qquad (7.58)$$

We introduce on contour L, in place of the independent variables $\tilde{s}$ and δ, the new independent variables $0\leqslant\theta<2\pi$ and $0\leqslant\varepsilon<2\pi$. The connection between $\tilde{s}$ and θ is established by the relationship

$$d\bar{s} = \left[\left(\frac{dx}{d\theta}\right)^2 + \left(\frac{dy}{d\theta}\right)^2\right]^{1/2} d\theta = \Omega(\theta)\, d\theta. \tag{7.59}$$

Taking into account that $z'(\bar{s}) = z'(\theta)/\Omega(\theta)$ and introducing the new function $\gamma(\theta) = \bar{v}(\theta)\Omega(\theta)$, we write (7.55) in the following manner:

$$\begin{aligned} \bar{v}(\theta) + \frac{z'(\theta)}{i\Gamma} \int_0^{2\pi} \bar{v}(\varepsilon)\, \Phi[\zeta(\varepsilon) - z(\theta), \alpha, t]\, d\varepsilon + \\ + \frac{z'(\theta)}{i\Gamma} \oint_{L_m} w_s(\sigma)\, \Phi[\zeta(\sigma) - z(s), \alpha, t]\, d\sigma = -\overline{v_0(\theta)}\, z'(\theta) - \\ - \frac{z'(\theta)}{i\Gamma} \oint_L \overline{v_0(\zeta)}\, \Phi[\zeta - z, \alpha, t]\, d\zeta. \end{aligned} \tag{7.60}$$

Separating the real (with respect to i) part in Equation (7.60), we obtain

$$\begin{aligned} \bar{v}(\theta) + \int_0^{2\pi} \bar{v}(\varepsilon)\, \mathrm{Im}\left\{\frac{z'(\theta)}{t}\, \Phi[\zeta(\varepsilon) - z(\theta), \alpha, t]\right\} d\varepsilon + \\ + \oint_{L_m} \mathrm{Im}\left\{w_s(\sigma)\frac{z'(\theta)}{t}\, \Phi[\zeta(\sigma) - z(s), \alpha, t]\right\} d\sigma = \\ = \mathrm{Re}\left\{-\overline{v_0(\theta)}\, z'(\theta) - \frac{z'(\theta)}{i\Gamma} \oint_L \overline{v_0(\zeta)}\, \Phi[\zeta - z, \alpha, t]\, d\zeta\right\}. \end{aligned} \tag{7.61}$$

We transform the integral along the wake contour L_{02}. The value of the velocity discontinuity $w_s(\sigma)$ at the wake must be determined on the basis of Thompson's theorem concerning the constant property of circulation along a closed contour which encloses the profile and the wake, as well as on the basis of the condition that free vortices are carried away by the main stream.

Let us consider the conditions of motion of vortices behind the cascade. From the theory of flow about a cascade of arbitrary profiles in a stabilized stream, it is known that two models are successfully used for plotting the stream of ideal fluid behind the cascade [20, 24, 78].

In the first model, if the trailing edge is absolutely sharp, the Chaplygin-Zhukovskiy postulate concerning the finiteness of the velocities on the edge is employed directly. However, if the edge

has a finite thickness, either the position of the rear point of stream branching in the middle of the trailing edge is prescribed, or else, which is preferable, the velocities at both sides of the edge are equal. The points at which the velocities are equal are selected on both sides of the edge at places where a considerable change of the contour curvature commences.

In the second model, the theory of jet streamline flow is used. It is assumed that from the trailing edge a jet descends which at first has the thickness of the trailing edge, and maintains constant velocity at the boundaries everywhere.

These methods, of course, are based primarily upon the Chaplygin-Zhukovskiy postulate. Numerous calculations show that not only the value of the lift force, but also the distribution of velocity along the profiles in the cascade in all cases are in good agreement with the experimental values (with the exception, of course, of a very small zone directly adjacent to the trailing edge).

In the case of unsteady flow with variable circulation, a vortex wake is located behind each profile. If the intensity of the wake is low (the Strouhal number is small), and the edge is infinitely sharp, it may be assumed that the line of discontinuity of the tangential velocities coincides with the streamline emanating from the trailing edge. In this case, in the transfer of vorticity the continuity equation

$$\frac{\partial \gamma}{\partial \tau} + \frac{\partial (\gamma w^0)}{\partial s} = 0 \qquad (7.62)$$

must be satisfied for it. In this equation $\gamma(s, \tau)$ is the intensity of the vortex sheet, $w^0(s)$ is the time-independent velocity of the main stream along the selected streamline, s is a curvilinear coordinate along this streamline.

For the periodic relationship of the trailing vorticity to time $\gamma(s, \tau) = \gamma(s)\exp(j\nu\tau)$ we obtain

$$\gamma(s)\frac{\partial\omega^0}{\partial s}+\omega^0\frac{\partial\gamma(s)}{\partial s}+j\nu\gamma(s)=0.$$

Integrating, we find

$$\gamma(s)=\gamma(0)\exp\left[-\int_0^s\frac{1}{\omega^0(s)}\left(\frac{\partial\omega^0}{\partial s}+j\nu\right)ds\right],$$

where $\gamma(0)$ is the free vorticity immediately behind the trailing edge.

If the edge has a finite thickness and the first of the above-described schemes of a stabilized stream is used, the selected streamline goes from the branching point. The velocity of the main stream is equal to zero at the branching point, increases greatly over a very short sector, and later along the entire stream line this velocity remains practically constant and equal to the velocity of the main stream at an infinite distance behind the cascade.

If the jet theory is used, it may be considered that the trailing free vortices are situated along the boundaries of the jet and are carried away with the constant velocity prevalent at these boundaries without distorting the jet itself. In this case the stream will not contain one discontinuity line, but two close vortex sheets will exist.

It has been emphasized above that schemes of nonseparating and jet flow about thick edges in a stabilized stream are equivalent in the sense of the velocity distribution law along the profile. However, they are not equivalent from the point of view of the transfer of free vorticity in the immediate vicinity of the trailing edge. From the physical point of view, preference should be given to the jet scheme, in the case of which the vorticity is transported at the constant velocity of the external stream. The construction of cascades in a stabilized stream with a jet current at the exit has been investigated in detail by G. Yu. Stepanov [78]. Thus, the boundary of the jet and the velocity of the main stream at this boundary may be considered known, and a calculation model may be constructed on the

basis of the described scheme. However, further simplification of the calculation scheme is expedient and possible without decreasing the accuracy of the results. For further simplification it may be assumed that the boundaries of the jet are practically rectilinear, and that the thickness of the stagnation zone is so small that it may be replaced by a discontinuity line. The main stream velocity along this line is naturally assumed constant. Here it is appropriate to emphasize that flow about the cascade is affected only by the initial sector of the vortex wakes, since attenuation of the perturbations induced by the wakes takes place exponentially (see Chapter 2).

With the indicated assumption, the equation of vorticity distribution in the wakes will take the form of a travelling wave

$$\gamma(s, \tau) = \gamma(0)\, e^{j\nu\left(\tau - s/w_2^0\right)}. \tag{7.63}$$

Thus, we shall consider the velocity of the stabilized stream behind the cascade $w_2^0 \exp(-i\beta_2)$ to be constant with respect both to value and direction.

Then the value of the velocity discontinuity should be equal to

$$2w_s(\sigma) = \frac{1}{w_2^0}\left(\frac{d\Gamma}{d\tau}\right)_{\tau_1}, \quad \tau_1 = \tau - \frac{x - x_0}{w_2^0 \cos\beta_2}. \tag{7.64}$$

Here $\Gamma = \Gamma_0 \exp(j\nu\tau)$ is that part of the circulation about the main profile which is variable in time, x_0 is the abscissa of the trailing edge, ν is the oscillation frequency of the profile. From Expression (7.64) it follows that if it is necessary to compute the value of the velocity discontinuity in a vortex wake at a point with the coordinate x at the moment of time τ, the derivative of the circulation with respect to time on the main profile should be taken at the time $\tau_1 < \tau$. The value $(x - x_0)/w_2^0 \cos\beta_2$ corresponds to the time interval necessary for the vorticity which has come off the profile to reach a fixed point.

Consequently, the velocity discontinuity is equal to

$$2w_s(\sigma, \tau) = j\frac{\nu}{\omega_2^0}\Gamma_0\left[\left(\tau - \frac{x - x_0}{\omega_2^0 \cos\beta_2}\right)j\nu\right]. \tag{7.65}$$

With account taken of (7.65), the integral along the contour of the vortex wake assumes the form

$$\oint_{L_w} w_s(\sigma)\,\mathrm{Im}\left\{\frac{z'(\theta)}{l}\Phi[\zeta(\sigma) - z(s), \alpha, l]\right\}d\sigma = \\ = \delta(\theta, \alpha, l)\left\{\int_0^{2\pi} \vartheta(\varepsilon)\Omega(\varepsilon)\,d\varepsilon + \int_L \overline{v_0(\zeta)}\,d\zeta\right\}. \tag{7.66}$$

Here we have set:

$$\left.\begin{aligned} \Gamma_0 &= \int_0^{2\pi} \vartheta(\varepsilon)\Omega(\varepsilon)\,d\varepsilon + \int_L \bar{v}_0(\zeta)\,d\zeta, \\ \delta(\theta, \alpha, l) &= \oint_{L_w} \mathrm{Im}\left\{\frac{z'(\theta)}{2l} j\frac{\nu}{\omega_2^0} e^{j\nu\left(\tau - \frac{x - x_0}{\omega_2^0 \cos\beta_2}\right)}\Phi[\zeta(\sigma) - z(s), \alpha, l]\right\}d\sigma. \end{aligned}\right\} \tag{7.67}$$

Here Im signifies isolation of the imaginary part only with respect to the imaginary unit i.

Taking these transformations into account, we write the integral Equation (7.61) in the following form:

$$\bar{v}(\theta) - \int_0^{2\pi} \bar{v}(\varepsilon)[K(\varepsilon, \theta, \alpha, l) + \delta(\theta, \alpha, l)]\,d\varepsilon = F(\theta). \tag{7.68}$$

Here the following designations have been introduced:

$$F(\theta) = -\mathrm{Re}\left[\overline{\bar{v}_0(\theta)}z'(\theta) + \frac{z'(\theta)}{il}\int_L \overline{v_0(\zeta)}\Phi[\zeta - z, \alpha, l]\,d\zeta\right] - \\ - i(0, \alpha, l)\int_L \overline{\bar{v}_0(\zeta)}\,d\zeta, \tag{7.69}$$

$$K(\varepsilon, \theta, \alpha, l) = -\mathrm{Im}\left\{\frac{z'(\theta)}{l}\Phi[\zeta(\varepsilon) - z(\theta), \alpha, l]\right\}. \tag{7.70}$$

At point $\theta = \varepsilon$ kernel $K(\varepsilon, 0, \alpha, l)$ has the removable singularity

$$K(\varepsilon, \varepsilon) = \frac{1}{2\pi}\frac{x'(\varepsilon)y''(\varepsilon) - y'(\varepsilon)x''(\varepsilon)}{[x'(\varepsilon)]^2 + [y'(\varepsilon)]^2} = \frac{1}{2r}, \tag{7.71}$$

where 1/r is the curvature of the contour at point $\varepsilon = \theta$.

Equation (7.68) is a singular integral equation with respect to the boundary value of the velocity of a perturbed stream with a removable singularity in the kernel.

The kernel of the integral equation is continuous and bounded, function $F(\theta)$ is continuous and bounded, while function $\delta(\theta)$ is expressed by a convergent integral.

This integral equation has been reduced to the same form as the integral equation used in the calculation of stabilized flow about a cascade. In Reference [80] it has been shown that the solution of an equation of the type of (7.68) is a solution of integral Equation (7.72) computed by the method of successive approximations

$$\bar{v}(\theta)-\int_0^{2\pi}\bar{v}(\varepsilon)\{K(\varepsilon,\theta,\alpha,t)+\delta(\theta,\alpha,t)\}d\varepsilon+ \\ +\varkappa\int_0^{2\pi}\bar{v}(\varepsilon)d\varepsilon=F(\theta)+\varkappa\Gamma_0. \tag{7.72}$$

if $\varkappa$ satisfies the condition $0<\varkappa\leqslant 1/l$, where l is the length of contour L. In this case the solution of integral Equation (7.72) exists and is unique.

The part of the kernel designated by $K(\varepsilon, \theta, \alpha, t)$, takes into account the quasi-steady perturbation velocity, i.e., the velocity induced by the oscillation of profiles in the absence of vortex wakes. This quasi-steady part of the induced velocity originates both as a result of oscillation of the profile under consideration and as a result of interference of all the other profiles of the cascade. Thus, when $\delta(\theta, \alpha, t)=0$ we obtain from (7.72) the solution of a quasi-steady problem, i.e., a problem in which the influence of vortex wakes behind the profiles is not taken into account.

Equation (7.72) must be solved on a digital electronic computer.

Let us further consider the special case of translational oscillation of the profiles in a cascade. The expression for the

complex oscillation velocity is written in the form

$$v_0(z) = jv\gamma \exp(j\nu\tau) \cdot \exp(i\beta_0),$$

where y = const is the oscillation amplitude, β_0 is the angle formed by vector $v_0(z)$ with the abscissa axis. In this case, taking (7.80) into account, the integral in the right-hand part of (7.69) is computed, and function $F(\theta)$ assumes the form

$$F(\theta) \sim -4\,\mathrm{Re}\,[j\nu\gamma z'(\theta)\exp(-i\beta_0)].$$

We pass to the dimensionless form, introducing new functions:

$$\left.\begin{aligned} U(\theta) &= \frac{v(\theta)}{\gamma w_2^0} \cdot \frac{\Omega(\theta)}{t}, \quad \bar{F} = 2k \cdot \bar{t}\,\mathrm{Re}\{z'(\theta)e^{-i\beta_0}\}, \\ \bar{\Gamma} &= \frac{\Gamma}{\gamma w_2^0 t}. \end{aligned}\right\} \tag{7.73}$$

Here we have set: $\bar{t}=t/2b$ is the relative spacing, 2b is the profile chord, $k=\nu b/w_2^0$ is the Strouhal number, computed on the basis of the flow velocity behind the cascade, $\bar{\gamma}=\gamma/t$ is the dimensionless amplitude of oscillation. Then the integral equation will be written as follows:

$$U(\theta) - \int_0^{2\pi} U(\varepsilon)[K(\varepsilon, \theta, \alpha, \bar{t}) + \delta(\theta, \alpha, \bar{t})]\,d\varepsilon + \varkappa \int_0^{2\pi} U(\varepsilon)\,d\varepsilon = \bar{F}(\theta) + \varkappa\bar{\Gamma}_0. \tag{7.74}$$

The kernel of the integral equation may be broken down into a real part and an imaginary part (with respect to j)

$$K(\varepsilon, \theta, \alpha, \bar{t}) = K_1(\varepsilon, \theta, \alpha, \bar{t}) + jK_2(\varepsilon, \theta, \alpha, \bar{t}). \tag{7.75}$$

The values of the real part and the imaginary part of the kernel are expressed by the functions

$$\left.\begin{aligned} K_1 &= -\left\{\frac{x'(0)}{t}\left[\frac{a_1a_4 - a_2a_3}{2} - a_6\right] + \frac{y'(0)}{t}\cdot\left[\frac{a_1a_3 + a_2a_4}{2} - a_5\right]\right\}, \\ K_2 &= \left\{\frac{y'(0)}{t}\left[\frac{a_1a_4 - a_2a_3}{2} - a_4\right] + \frac{x'(0)}{t}\left[\frac{a_1a_3 + a_2a_4}{2} - a_3\right]\right\}. \end{aligned}\right\} \tag{7.76}$$

Here we have set

$$\left.\begin{aligned} &a_1=\frac{\operatorname{sh}2\varphi}{\operatorname{sh}^2\varphi+\sin^2\varphi}, \quad a_2=\frac{\sin 2\psi}{\operatorname{sh}^2\varphi+\sin^2\varphi}, \quad a_3=\operatorname{ch}\alpha\bar{\varphi}\cos\alpha\bar{\psi},\\ &a_4=\operatorname{sh}\alpha\bar{\varphi}\sin\alpha\bar{\psi}, \quad a_5=\operatorname{sh}\alpha\bar{\varphi}\cos\alpha\bar{\psi}, \quad a_6=\operatorname{ch}\alpha\bar{\varphi}\sin\alpha\bar{\psi},\\ &\varphi=\frac{\pi}{t}[x(\varepsilon)-x(0)], \quad \psi=\frac{\pi}{t}[y(\varepsilon)-y(0)], \quad \bar{\varphi}=\frac{\varphi}{\pi}, \quad \bar{\psi}=\frac{\psi}{\pi}. \end{aligned}\right\} \tag{7.77}$$

As has already been said, kernel $K(\varepsilon, 0, \alpha, t)$ has a removable singularity at the point $\varepsilon = 0$. It can be easily seen that this singularity belongs to the real (with respect to j) part of the kernel. The imaginary (with respect to j) part of the kernel does not have a singularity and at the point $\varepsilon=0$ is computed according to the formula

$$K_2(\varepsilon, \varepsilon)=\frac{x'(\varepsilon)}{t}\left[1-\frac{c}{\pi}\right]. \tag{7.78}$$

This property may be explained from the standpoint of a vortex sheet. The real part of kernel K_1 contains a term of the type $\text{const}/(s-\sigma)$, which is characteristic for a vortex sheet distributed along the profile with a density proportional to $\mu(\sigma)$. This part of the kernel is what creates the singularity. The imaginary part of kernel K_2 takes into account the supplemental velocities induced by the remaining profiles in the cascade, which are oscillating and not in phase with the main profile, as well as the wakes. If $\alpha = 0$ or $\alpha = \pi$, it follows that $K_2(\varepsilon, 0)=0$ (when $\alpha = 0$ the insignificant constant in $K_2(\varepsilon, 0)$ must be discarded); this coincides with the symmetry of the problem, since the part included in K_1 does not take into account the influence of vortex wakes, but determines only the quasi-steady component of perturbed velocity. If, on the other hand, all the profiles oscillate in phase or in counterphase, a quasi-steady component, which is also only in phase or counterphase, is induced on the main profile.

The computation of K_1 at the point $\varepsilon=0$ may be carried out according to formula

$$K_1(0, 0)=\frac{\pi}{2\pi}-\sum_{i}^{n-1}K(\varepsilon, 0)_{\varepsilon\neq 0}. \tag{7.79}$$

This is explained by the fact that with corresponding normalization we may set

$$\frac{1}{\pi}\int_L \Phi[\zeta - z, \alpha, t]\,dz = 1. \qquad (7.80)$$

Calculations have shown that the values of kernel $K_1(\theta, \varepsilon)$ at point $\theta=\varepsilon$, determined according to Formula (7.79) in the case of a smooth contour have coincided well with the values obtained on the basis of Formula (7.71).

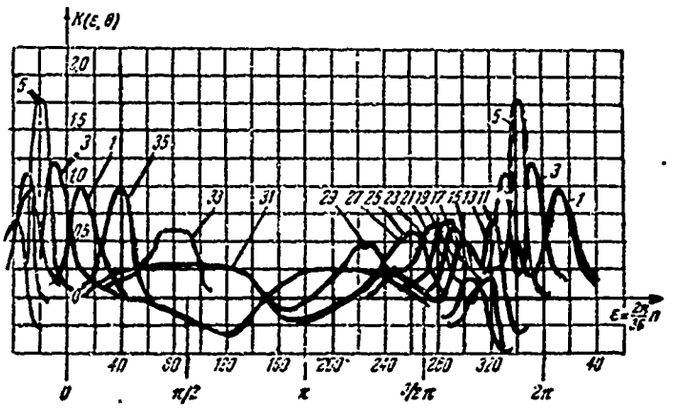


Figure 7.13. Graph of the real part of kernel $K(\varepsilon, \theta)$computed for the cascade shown in Figure 7.14. The numbers on the curves correspond to the points represented on the profile (see Figure 7.14).

Figure 7.13 shows the real part of kernel $K(\varepsilon, \theta)$. The abscissa shows the variable ε, related to the arc length, measured along the contour given by Formula(7.59). The numbers on the curves correspond to the points marked or the profile of the cascade for which the calculations were made (Figure 7.14).

We transform Expression (7.67) to a form convenient for calculations. The term $\delta(\theta, \alpha, t)$ takes into account the influence of the vortex wakes upon the streamline flow about the cascade.

We separate in (7.67) the real and the imaginary part (with respect to j):

$$\delta(\theta, \alpha, t) = -(\Lambda_1 + j\Lambda_2).$$

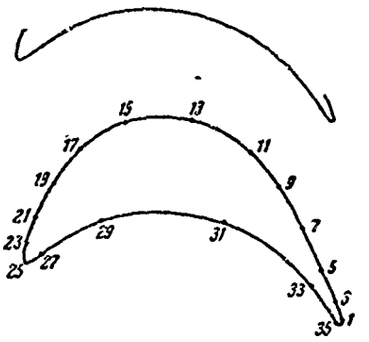


Figure 7.14. An aerodynamic cascade of active profiles pertaining to the example of calculation by means of intgral equations).

Assuming that the oscillations continue for an infinitely long period of time, we find expressions for Λ_1 and Λ_2:

$$\Lambda_1(0, a, t) = 2k\int_0^\infty \left\{\frac{x'(\theta)}{t}[V\cos k\mu - S\sin k\mu] + \frac{y'(\theta)}{t}[-Q\cos k\mu - W\sin k\mu]\right\} d\mu, \tag{7.81}$$

$$\Lambda_2(0, a, t) = 2k\int_0^\infty \left\{\frac{x'(\theta)}{t}[-S\cos k\mu - V\sin k\mu] + \frac{y'(\theta)}{t}[-W\cos k\mu + Q\sin k\mu]\right\} d\mu. \tag{7.82}$$

Here $\mu = a/b$ is the relative distance from the trailing edge,

$$S = \frac{1}{2}(a_1a_4 - a_2a_3) - a_6, \quad W = \frac{1}{2}(a_1a_3 + a_2a_4) - a_5,$$
$$V = \frac{1}{2}(a_1a_5 + a_2a_3) - a_3, \quad Q = \frac{1}{2}(a_1a_6 - a_2a_5) - a_4.$$

The expressions for a_1, a_2, a_3, a_4, a_5, a_6 are given in (7.77); in this case

$$\varphi = \pi\left[\frac{x(0_+) - x(0)}{t} + \mu\frac{b}{t}\cos\beta_2\right], \quad \bar{\varphi} = \frac{\varphi}{\pi},$$
$$\psi = \pi\left[\frac{y(0_+) - y(0)}{t} + \mu\frac{b}{t}\sin\beta_2\right], \quad \bar{\psi} = \frac{\psi}{\pi}.$$

Here β_2 is the angle of emergence of the stream from the cascade, θ_0 is a coordinate of the trailing edge. Integration along contour L_{02} is replaced by integration along a straight line starting from the trailing edge and extending to infinity behind the cascade. With this substitution we have taken into account the direction of passage around the contour and the sign of the tangential velocity component discontinuity. The values of the velocities induced by the wake vortices at the profile decrease rapidly as the distance from the vortex to the trailing edge increases.

We break down the functions contained in integral Equations (7.74) into the real and imaginary parts (with respect to j):

$$\left.\begin{aligned} U(\theta, \alpha, t) &= U(\theta) = U_1(\theta) + jU_2(\theta), \\ K(\theta, \varepsilon, \alpha, t) &= K(\theta, \varepsilon) = K_1(\theta, \varepsilon) + jK_2(\theta, \varepsilon), \\ \delta(\theta, \alpha, t) &= \delta(\theta) = -\Lambda_1(\theta) - j\Lambda_2(\theta), \\ \bar{\Gamma}_0(\alpha, t) &= \bar{\Gamma}_1 + j\bar{\Gamma}_2. \end{aligned}\right\} \tag{7.83}$$

Substituting these expressions into (7.74) and separating the real part and the imaginary part (with respect to j), we obtain a system of two integral equations:

$$\left.\begin{aligned} U_1(\theta) - \int_0^{2\pi} \{U_1(\varepsilon)[H_1(\varepsilon, \theta) - \varkappa] - U_2(\varepsilon) H_2(\varepsilon, \theta)\} d\varepsilon &= \varkappa\bar{\Gamma}_1, \\ U_2(\theta) - \int_0^{2\pi} \{U_1(\varepsilon) H_2(\varepsilon, \theta) + \\ + [H_1(\varepsilon) - \varkappa] U_2(\varepsilon)\} d\varepsilon &= \varkappa\bar{\Gamma}_2 + \bar{F}(\theta). \end{aligned}\right\} \tag{7.84}$$

Here we have set

$$\left.\begin{aligned} H_1(\varepsilon, \theta) &= K_1(\varepsilon, \theta) - \Lambda_1(\theta), \\ H_2(\varepsilon, \theta) &= K_2(\varepsilon, \theta) - \Lambda_2(\theta). \end{aligned}\right\} \tag{7.85}$$

A system of two integral equations with respect to the unknown functions $U_1(\theta)$ and $U_2(\theta)$ is obtained.

In the case of numerical solution the integral equations are replaced by a system of linear algebraic equations. For this the blade contour is broken down into sectors. To increase the calculation accuracy, the singularity points should be situated more densely in the vicinity of the leading edge and the trailing edge,

where a sharper change of the perturbation velocities can be observed. The solution is effected by the method of successive approximations. The basic equations of (7.84) contain the constants $\bar{\Gamma}_1$ and $\bar{\Gamma}_2$, which constitute the real part and the imaginary part of the complex circulation $\bar{\Gamma}_0=\bar{\Gamma}_1+j\bar{\Gamma}_2$.

The pressure is defined by the Lagrange integral

$$\frac{\partial\varphi}{\partial\tau}+\frac{\bar{w}^2}{2}+\frac{\bar{p}}{\rho^0}=f(\tau). \tag{7.86}$$

The stream at the left of the cascade is considered stabilized, the velocity and the pressure are considered known,

$$\frac{\partial\varphi}{\partial\tau}=0, \quad \bar{w}=w_1^0, \quad \bar{p}=p_1^0.$$

Then from (7.86) we obtain (disregarding terms of the second order of smallness)

$$jv\varphi+w^0w+\frac{p}{\rho^0}=0. \tag{7.87}$$

Here ν is the oscillation frequency, φ is the velocity potential of perturbed motion, w^0 is the velocity of the stabilized stream, w and p are respectively the perturbation velocity and the pressure ($|w|\ll|w^0|$)

Setting the pressure difference on both sides of the trailing edge equal to zero (at points where jet convergence is assumed), from (7.87) we find the condition at the edge:

$$-jv\Delta\varphi=-jv\Gamma_0=w_2^0\Delta w. \tag{7.88}$$

Here w_2^0 is the velocity of the stream behind the cascade, Δw is the value of the velocity discontinuity.

The force acting upon the profile in the cascade is found by integrating (7.87) along the contour

$$\mathcal{P} = -i \oint_L p \, dz. \tag{7.89}$$

Since the pressure will be a complex (with respect to j) value, the force vector is a complex value with two imaginary units (i and j). Separating in (7.89) the real and the imaginary parts, we find the dimensionless forces:

$$\bar{\mathcal{P}}_{x1} = \bar{l} \int_0^{2\pi} \left[\frac{\omega^0(0)}{\omega_2^0} w_1(0) - 2k\bar{l}\varphi_2(0) \right] y'(0)\, d\theta,$$

$$\bar{\mathcal{P}}_{y1} = -\bar{l} \int_0^{2\pi} \left[\frac{\omega^0(0)}{\omega_2^0} w_1(0) - 2k\bar{l}\varphi_2(0) \right] x'(0)\, d\theta,$$

$$\bar{\mathcal{P}}_{x2} = \bar{l} \int_0^{2\pi} \left[\frac{\omega^0(0)}{\omega_2^0} w_2(0) + 2k\bar{l}\varphi_1(0) \right] y'(0)\, d\theta,$$

$$\bar{\mathcal{P}}_{y2} = -\bar{l} \int_0^{2\pi} \left[\frac{\omega^0(0)}{\omega_2^0} w_2(0) + 2k\bar{l}\varphi_1(0) \right] x'(0)\, d\theta.$$

Here $w_1(0)$, $\varphi_1(0)$ and $w_2(0)$, $\varphi_2(\theta)$ are respectively the real and the imaginary parts of the velocity function and the velocity potential induced by the oscillation of the profiles; $\bar{\mathcal{P}}_{x1}$, $\bar{\mathcal{P}}_{y1}$, and $\bar{\mathcal{P}}_{x2}$, $\bar{\mathcal{P}}_{y2}$ are respectively the real and the imaginary (with respect to j) parts of the force components along the coordinate axes; $\bar{\mathcal{P}} = \mathcal{P}/\rho_2 \rho^0 b\bar{y}(\omega_2^0)^2$ is the expression of dimensionless force in terms of dimensional force; $\bar{y} = y/t$ and y are respectively the dimensionless and the dimensional amplitude of the oscillations, $k = \nu b/\omega_2^0$ is the Strouhal number.

Taking into account the influence of shift of the profiles in the cascade brings about only a change of the boundary value of the perturbation velocity, and is carried out in the manner set forth in § 7.2.

Let us consider the results of calculations [57a] carried out for the cascade represented in Figure 7.14. The cascade is composed of TRZA profiles, situated with a relative spacing of $\bar{t} = 0.6$ and an attitude of $\beta_y = 76°$. The calculations are carried out at a stream entry angle of $\beta_1 = 27°30'$ and an exit angle of $\beta_2 = 24°$.

Figures 7.15 and 7.16 contain graphs of distribution of the supplemental tangential velocities on a profile in a cascade with

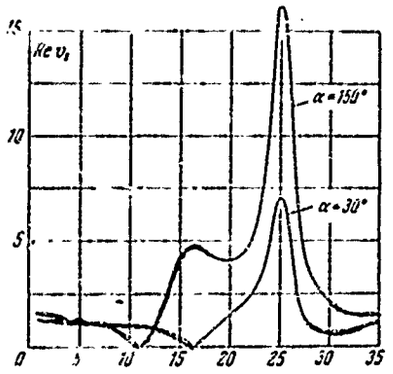


Figure 7.15. Distribution of the real (with respect to j) part of tangential velocities along the profile in a cascade with a phase shift of $\alpha = 30°$ and $\alpha = 150°$, $\mathrm{Re}\, v_s = \mathrm{Re}(v_s/v_0)$, v_s — tangential velocity, v_0 is the modulus of the oscillation velocity of the profile. Quasi-steady solution.

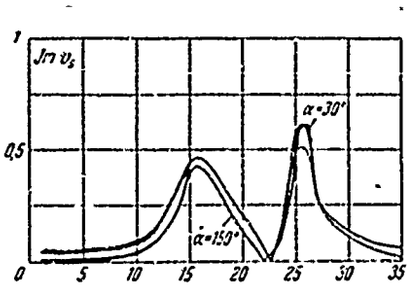


Figure 7.16. Distribution of the imaginary (with respect to j) part of tangential velocities along the profile in a cascade with a phase shift of $\alpha = 30°$ and $\alpha = 150°$, $\mathrm{Im}\, c_s = \mathrm{Im}(c_s/c_0)$, v_s is the tangential velocity, v_0 is the modulus of the oscillation velocity of the profile. Quasi-steady solution.

phase shifts of $\alpha = 30°$ and $\alpha = 150°$. Figure 7.15 shows the real parts of the tangential velocities (i.e., those that are in phase with the oscillation velocity of the profile), and Figure 7.16 shows their imaginary parts. Along the abscissa the numbers of the points on the profile are indicated in accordance with Figure 7.14, and along the ordinate the ratio of the tangential velocities to the velocity modulus of the profile oscillation is plotted. In this calculation and in the succeeding ones it is assumed that the profile oscillates in a direction perpendicular to its chord. These calculations were made without taking into account the influence of the vortex wakes, i.e., the problem is solved in a quasi-steady formulation. The results obtained here by the solution of the integral equation coincide with the results obtained by means of conformal mapping. When the problem was solved in a quasi-steady formulation, the complex values of the tangential velocities at profile points 1 and 35 on the trailing edge (see Figure 7.14) were set equal to zero.

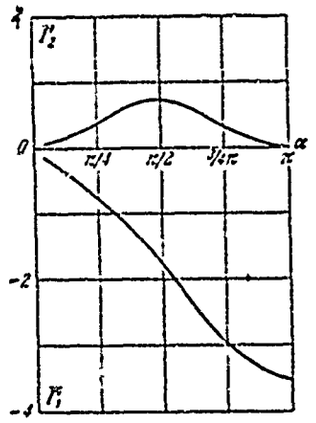


Figure 7.17. Relationship of dimensionless circulations $\bar{\Gamma}_1=\Gamma_1/\bar{y}t\omega_2^0$, $\bar{\Gamma}_2=\Gamma_2/\bar{y}t\omega_2^0$ to the phase shift in the case of oscillation (for the cascade represented in Figure 7.14), $\bar{y}=y/t$, y is the oscillation amplitude, t is the cascade spacing, ω_2^0 is the modulus of the main stream velocity at the exit from the cascade. Quasi-steady problem.

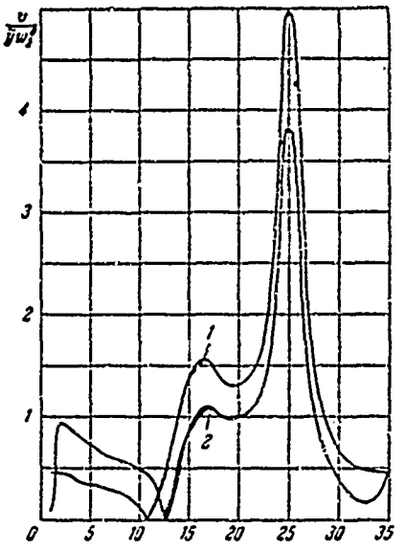


Figure 7.18. Distribution of the real (with respect to j) part of tangential velocity: 1) — quasi-steady solution, 2) — solution taking into account the influence of vortex wakes.

The maximal supplemental tangential velocities induced by oscillations are observed on the leading edge in the vicinity of point 25. When added to the main stream velocities, these supplemental-velocity peaks will bring about a shift of the forward critical point.

Figure 7.17 contains graphs of the real part and the imaginary part of dimensionless circulation when the cascade blades oscillate with different phase shifts in the quasi-steady formulation

$$\bar{\Gamma}_1=\frac{\Gamma_1}{\bar{y}t\omega_2^0},\quad \bar{\Gamma}_2=\frac{\Gamma_2}{\bar{y}t\omega_2^0}.$$

The real part of the circulation reaches a maximum (with respect to absolute value) with a phase shift of $\alpha=\pi$, and the imaginary part —

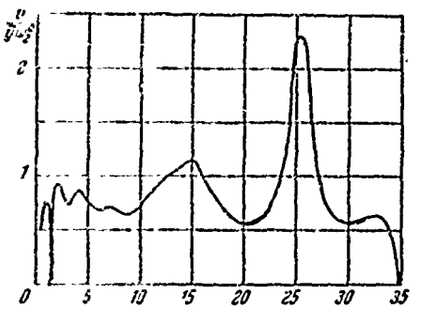


Figure 7.19. Distribution of the imaginary (with respect to j) part of the tangential velocity (solution taking into account the influence of vortex wakes).

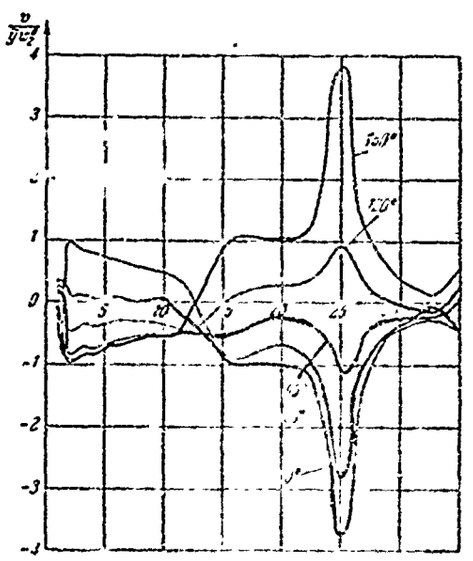


Figure 7.20. Distribution of supplemental velocities on a profile in a cascade (Figure 7.14a) in the case of oscillation with a phase shift of [illegible]. The numbers correspond to different moments of time: 1) [illegible]

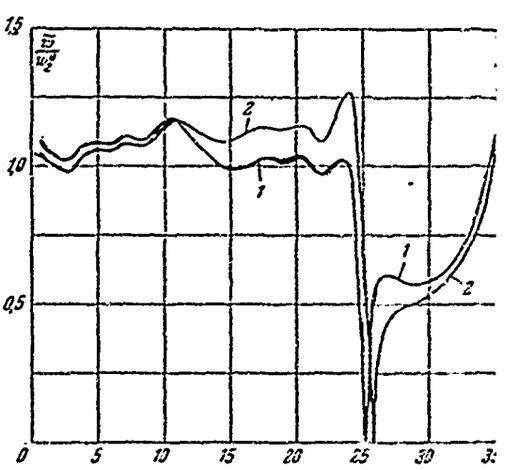


Figure 7.21. Distribution of total velocities when the profile oscillates in a cascade with a phase shift of $\varkappa = \pi$ when $k = 0.25$ and $v_0/w_2^0 = 0.02$.

when $\alpha=\pi/2$; this is explained by the influence of the adjacent blades.

Figure 7.18 shows the distribution of the real part of the tangential velocity induced by oscillation of the profiles with a phase shift of $\alpha=\pi$. Curve (1) was obtained when the problem was solved in a quasi-steady formulation; curve (2) was obtained with account taken of the influence of the vortex wakes. The calculations were made with a Strouhal number of $k=\nu b/w_2^2=0{,}25$.

The distribution of the imaginary part of the tangential velocity is shown in Figure 7.19. This graph pertains to the second calculation (with a quasi-steady formulation of the problem and $\alpha=\pi$ the imaginary part of the velocity is equal to zero). For the same conditions, in Figure 7.20 the distribution of the supplemental velocities on a profile for various moments of time has been plotted. Figure 7.21 shows the distribution of the total velocities on a cascade profile. Curve (1) corresponds to the moment of time when, during oscillation, the profile moves with the convex part forward with maximum velocity, and curve (2) corresponds to the moment of time when it does the same with the concave part forward.

Recollect that these calculations were carried out without taking the displacement into account. Calculations with taking displacements into account are carried out by the same method, but by considering the supplemental perturbations (Section 7.2).

FOOTNOTES

1. on page 296. Here we disregard the displacements. In the general case, displacements should be considered in accordance with Section 7.2.

CHAPTER 8

INTERFERENCE OF TWO CASCADES MOVING IN RELATION TO EACH OTHER IN A POTENTIAL STREAM (QUASI-STEADY PROBLEM)

§ 8.1. Calculation of Flow About Two Moving Cascades by the Method of Conformal Transformation

Let us consider, in the plane of the complex variables $z = x + iy$, two cascades (Figure 8.1) which represent a two-dimensional model of a turbomachine stage. The axes of the cascades are parallel to the ordinate.

Let us first consider a special case where the spacings of the cascades are equal to t. The cascade system is in a stream of ideal incompressible fluid. The first (directing) cascade is motionless in the coordinate system xy, the second (working) cascade is moving at a constant velocity of u in the negative direction of the ordinate axis. Since interference will be observed when the second cascade moves, the circulation about the profiles must change in time. This brings about vortex wakes of variable intensity, which propagate behind the exit edges of the two cascades. For the sake of simplification, we shall not take these vortex wakes into account, i.e., we shall

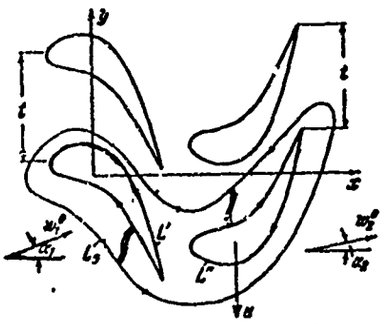


Figure 8.1. Cascades moving with respect to one another, with identical spacings, L is the profile of the stationary cascade, L" is the profile of a cascade moving at the velocity u, w_1^0 and w_2^0 are flow velocities (with respect to the stationary cascade) at infinity in front of and behind the cascades.

consider the problem in a quasi-steady formulation. It should be noted that the influence of the vortex wakes coming from the first cascade upon the distribution of pressures and velocities along the second cascade may be particularly significant.

Thus, after disregarding the influence of the wakes, interference due only to the transmission of perturbations in the potential stream will be considered.

Problems dealing with cascades moving in relation to each other in such a formulation have been considered by Feindt [104-106], Oellers [127], Kasimierski [110], etc. Note that in the simplified formulation (the absence of vortex wakes), the problem under consideration will differ from the known problem of static flow about a two-stage cascade only with respect to the boundary condition. The latter problem, under the condition of equality of the spacing of the two cascades, is reduced to study of the stream about a biplane and is considered in the monographs of L. I. Sedov [74] and G. Yu. Stepanov [78] (for stationary cascades).

Thus, we shall first consider the special case where the cascades have the same spacing t.

We conformally map the exterior of the cascades onto a doubly connected region by means of the most simple periodic function

$$\eta = e^{\frac{2\pi}{t} z}. \tag{8.1}$$

This function maps the infinitely connected region outside the cascade onto an infinite layered surface. A biconnected contour is situated on each sheet, which corresponds to the two adjacent profiles. One sheet of the surface corresponds to the strip of one period of the cascade.

The images of straight lines x = const and y = const are circles and rays with the center in the origin of the coordinates, where there is a logarithmic singularity. Infinite points on the left ($x = -\infty$) correspond to the coordinate origin, infinite points on the right ($x = +\infty$) correspond to the point $\eta=\infty$. The boundaries of a strip of one period correspond to the sides of a sheet section. This section extends from the coordinate origin to an infinitely remote point. The profiles become closed spiral curves. To plot the flow, it is necessary to map the doubly connected region onto a selected canonical biconnected region, for example, an annulus. In view of the fact that the contour of a doubly connected region in the plane η has a very grotesque shape, it is in practice necessary, before transformation into the annulus, to perform a series of smoothing transformations. For the transformation of biconnected regions it is expedient to employ the method developed by G. Yu. Stepanov, which is based upon electrical simulation [78].

From the very start it is convenient, particularly with the employment of electrical simulation, to operate with a finite region. Therefore, in place of Transformation (8.1) it is more convenient to employ the following one:

$$\eta=\operatorname{cth}\frac{\pi z}{t}. \qquad (8.2)$$

If the origin of the coordinates in plane z is placed inside one of the profiles, the flow region will be mapped onto a limited doubly connected region, since to the point Z = 0 corresponds the point $\eta=\infty$. The points at infinity to the right and to the left of the cascade ($x = \pm\infty$) pass into the points $\eta = \pm 1$. Let us note that Transformations (8.1) and (8.2) possess the substantial drawback that they bring about a very nonuniform deformation of the contours. This

decreases the accuracy of the calculations and even makes impossible the use of electrical simulation prior to preliminary smoothing of the contours.

Thus, let us assume that after transformation, the exterior of the contour is mapped onto an annulus in the plane η. The infinitely remote points $x = \pm \infty$) correspond to points η_1 and η_2. At these points the vortex source must be situated as well as the vortex sink. The yields of the source and of the sink must be equal in order to satisfy the continuity equation

$$Q_1 = -Q_2 = tw_1^0 \cos\alpha_1 = tw_2^0 \cos\alpha_2 \tag{8.3}$$

The circulations of the vortices are defined by the formulas

$$\Gamma_1 = w_1^0 t \sin\alpha_1, \quad \Gamma_2 = -w_2^0 t \sin\alpha_2 \tag{8.4}$$

Here w_1^0 and w_2^0 are moduli of the stream velocity at infinity before and after the cascades, respectively, α_1 and α_2 are angles formed by the corresponding velocities with respect to the abscissa.

We shall now dwell on the boundary conditions of the problem. The first cascade is stationary and, consequently, the normal velocity on the profiles must be equal to zero. The second cascade moves with a constant velocity u and, consequently, the boundary value of the normal velocity $w_n(z)$ is equal to a projection of the displacement velocity onto a normal to the profile.

In the plane η let the contour of the directing blade correspond to the external circumference. Then it is obvious that the normal component of velocity on this circumference must be equal to zero, i.e., the circumference will be a streamline. The normal component of velocity on the internal circumference is determined on the basis of the known $w_n(z)$ and the conformal transformation condition

$$|w_n(\eta)| = |w_n(z)| \left|\frac{dz}{d\eta}\right|. \tag{8.5}$$

For plotting the flow from the vortex source and the vortex sink in plane η it is convenient to map the annulus onto a rectangle in plane ξ, employing the transformation

$$\xi = \ln \eta. \tag{8.6}$$

The external circumference will pass into a segment of the imaginary axis AB (it is always possible to select the scale in such a manner that the radius of the external circumference will be equal to unity) with a length of $2\pi i$ (Figure 8.2). The smaller circumference ($r=r_2<1$) will, after transformation, pass into segment CD, and the points of the annulus will have images in the rectangle ABCD. In particular, let the points η_1 and η_2, in which the vortex source and the vortex sink are located, pass into points ξ_1 and ξ_2.

The analytic function representing the complex potential of flow in the rectangle may be continued in the entire plane ξ. Then, in order to express the complex potential, we may use the biperiodic functions with periods equal to

$$AB = 2\pi i, \quad CC' = 2CB = -2\ln r_2. \tag{8.7}$$

The function of complex velocity must have simple poles at points ξ_1 and ξ_2, with residues respectively equal to Γ_1+iQ_1 and Γ_2+iQ_2. We add simple poles at points $-\xi_1$ and $-\xi_2$ with the residues Γ_1+iQ_1 and Γ_2+iQ_2. Then four simple poles will be situated within the period rectangle with given residues, and the complex velocity is expressed in terms of the Weierstrass zeta function ζ

$$w_1(\xi) = \frac{\Gamma_1+iQ_1}{2\pi i}\zeta(\xi-\xi_1) + \frac{-\Gamma_2+iQ_1}{2\pi i}\zeta(\xi+\xi_1) + \\ + \frac{\Gamma_2+iQ_2}{2\pi i}\zeta(\xi-\xi_2) + \frac{-\Gamma_2+iQ_2}{2\pi i}\zeta(\xi+\xi_2). \tag{8.8}$$

For the plotted flow the straight lines AB and CD are streamlines, i.e., the normal velocities on them are equal to zero. Consequently, the complex potential plotted in plane ξ solves the problem of a double cascade with stationary profiles. In order to satisfy the

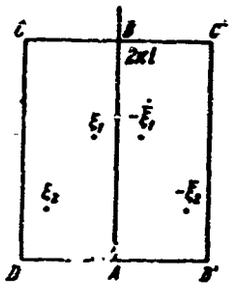


Figure 8.2. Plotting a flow in a rectangle: AB is the image of the profile of the motionless cascade, CD is the image of the profile of the moving cascade.

boundary conditions with respect to normal velocity on the straight line CD (which is an image of profile L" of the movable cascade), we place on it distributed sources with the intensity

$$q(\xi) = 2\omega_n(\xi) = 2|w_n(z)|\left|\frac{dz}{d\xi}\right|.$$

The complex flow velocity induced by the distributed sources may also be expressed in terms of the Weierstrass function

$$w_2(\xi) = \frac{1}{2\pi}\int_0^{2\pi l} q(x)\zeta(\xi - x)\,dx. \tag{8.9}$$

Here x is the integration variable. The integral must be understood in the sense of the Cauchy principal value. In view of the symmetry, the flow described by Integral (8.9) does not change the normal velocity on segment AB.

To the complex velocities represented by Formulas (8.8) and (8.9) we may add an arbitrary imaginary constant, and this will not change the normal velocities on boundaries AB and CD. The addition of such a constant in the physical plane corresponds to the introduction of a purely circulational flow about the two cascades; the total circulation about the cascades does not change, i.e., the velocity circulation about an arbitrary contour of the first cascade is equal in moduli, but is opposite in sign to the circulation about an arbitrary profile of the second cascade.

The resultatt complex velocity in plane ξ is equal to

$$w(\xi) = w_1(\xi) + w_2(\xi) + iC. \tag{8.10}$$

Let us consider an arbitrary closed contour in plane z which encloses only one profile of the first cascade and one profile of the second cascade. A triply connected region is formed, which is composed of the selected contour L_0 and two blade contours L' and L", contained within the first contour. The flow within the isolated region is potential, and therefore, the curvilinear integral taken along contour $L = L_0 + L' + L''$, after making the division (see Figure 8.1) must be equal to zero:

$$\Gamma = \oint_L w_1 ds = \oint_{L_0} w_1 ds + \oint_{L'} w_1 ds + \oint_{L''} w_1 ds = 0.$$

Selecting as the path of integration L_0 the equidistant curves situated at the distance of the spacing, and two straight lines parallel to the ordinate, which connect the curves at infinity in front of and behind the cascade ($x \pm \infty$), we obtain

$$\oint_{L_0} w_1 ds = \Gamma_2 - \Gamma_1.$$

Here Γ_1 and Γ_2 are defined by Formulas (8.4).

Taking the change in the passage around contour L' and L" into account, we find

$$\oint_{L'} w_1 ds = -\Gamma', \quad \oint_{L''} w_1 ds = -\Gamma'',$$

where Γ' and Γ'' are circulations of the velocity along the profiles under consideration. Hence, we obtain the connection between the velocity circulations as follows

$$\Gamma' + \Gamma'' = \Gamma_2 - \Gamma_1. \tag{8.11}$$

The value and direction of the velocity at infinity in front of the cascades may be considered as given. Then on the basis of Conditions (8.3) and (8.4), Q_1, Q_2, and Γ_1 are known. The circulations of velocities Γ', Γ'' should be selected in such a manner as to satisfy the Zhukovskiy-Chaplygin condition on the trailing edges of the

first and the second cascades. Then, in accordance with (8.11) we determine Γ_2 and by means of (8.3) and (8.4) we find the value and direction of the velocity behind the cascades w_2^0 and α_2. The selection of Γ', Γ'' is obviously equivalent to the selection of independent values of Γ_2 and C on the basis of (8.10). The determination of Γ_2 and C proceeds on the basis of two equations, obtained from the condition that the velocities at points which are images of trailing edges in the plane ξ are zero.

Drawbacks of the method under consideration lie in the fact that in practice, such a means of solution is applicable only for cascades with identical spacing, and in the fact that the conformal transformation of a double cascade of arbitrary profiles is a very laborious process.

§ 8.2. Calculation of Flow About Two Moving Cascades by the Method of Integral Equations

Let us return to the general case where the cascade spacings are not equal. This problem may be reduced to the solution of a system of integral Fredholm equations, as has been shown by Kazimierski [110]. With this approach, the problem can be solved only with the aid of a digital electronic computer.

In view of the finiteness of the number of blades on a turbomachine wheel, a least common period always exists for two cascades (Figure 8.3)

$$t = nt_1 = mt_2 \tag{8.12}$$

Here n and m are natural numbers. The analytic function of conjugate velocity has no singular points in the flow region

Let us consider a multiply connected contour (see Figure 8.3) consisting of an external contour L, which encloses the profiles of the two cascades included in the least common period, and n + m internal contours L_k, each of which encloses only one of the profiles.

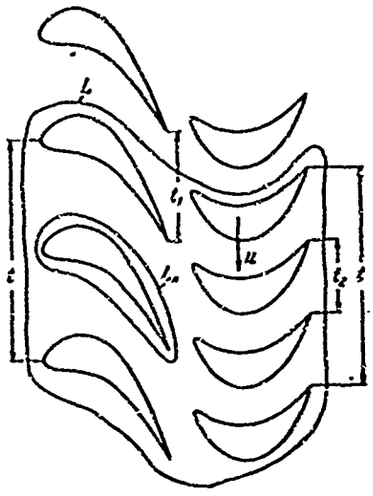


Figure 8.3. Cascades moving with respect to each other, with stages t_1 and t_2; t is the least common spacing, u is the velocity of the second cascade.

Within this multiply connected contour, the complex velocity can be expressed in terms of its boundary values by means of Cauchy integrals (point z lies within L and outside L_k)

$$w(z) = \frac{1}{2\pi i}\int_L \frac{w(\zeta)\,d\zeta}{\zeta - z} - \\ -\frac{1}{2\pi i}\sum \int_{L_{kl}} \frac{w(\zeta)\,d\zeta}{\zeta - z}. \qquad (8.13)$$

Here, the internal contours have double indexation L_{kl}, the first index k = 1, 2, ..., (n + m) corresponds to the profile number in the group of profiles belonging to one period. The second index l denotes the number of the group.

We sum the second term in groups

$$w(z) = w_0 - \frac{1}{2\pi i}\sum_{k=1}^{n+m}\sum_{l=-\infty}^{\infty}\int_{L_{kl}} \frac{w(\zeta)\,d\zeta}{\zeta - z}. \qquad (8.14)$$

The first integral in (8.13) is replaced by a constant, since the remaining terms are a function which is bounded within the entire region.

The complex velocity must be a periodic function with a period equal to t, i.e., the condition

$$w(z + lt) = w(z), \quad l = \pm 1; \pm 2; \pm 3; \ldots \qquad (8.15)$$

must be satisfied.

From this, it follows that the boundary values of the velocity on the corresponding profiles in different groups are identical.

Then, changing the order of summation and integration in (8.14), and taking (8.15) into account as well as the known relationship

$$\frac{\pi}{l}\operatorname{cth}\frac{\pi z}{l}=\sum_{i=-\infty}^{\infty}\frac{1}{z-ili},$$

we obtain

$$w(z)=w_0-\frac{1}{2il}\sum_{k=1}^{n+m}\int_{L_k}w(\zeta)\operatorname{cth}\frac{\pi}{l}(\zeta-z)\,d\zeta. \tag{8.16}$$

Up to now it has been assumed that the arbitrary point z does not lie on the integration contour and, consequently, w(z) were not regarded as boundary values of the velocity.

Let us now assume that contours L_K coincide with the contours of the blades, and we let z approach the contour r. Utilizing Yu. V. Sokhotskiy's formula for the limit value (the contour contains no angular points), we obtain

$$w_r(z)=2w_0-\frac{1}{il}\sum_{k=1}^{n+m}\int_{L_k}w(\zeta)\operatorname{cth}\frac{\pi}{l}(\zeta-z)\,d\zeta. \tag{8.17}$$

Here r = 1, 2, 3, ..., (n + m).

Let us now consider the boundary values for velocity. The normal component of velocity on a contour may be expressed in the following manner:

$$w_n=v_x\frac{dy}{ds}-v_y\frac{dx}{ds}. \tag{8.18}$$

Here, v_x and v_y are projections of the velocity in a Cartesian system of coordinates x, y; s is a cuvilinear coordinate, read off counterclockwise along the contour. We represent the same expression in terms of complex variables:

$$\left.\begin{aligned}z'(s)&=\frac{dx}{ds}+i\frac{dy}{ds},\\ w_n(s)&=\operatorname{Im}[z'(s)\,w(s)].\end{aligned}\right\} \tag{8.19}$$

For the profiles of the stationary directing cascade, $w_n = 0$ and the condition of streamline flow may be expressed in the following manner

$$w(s) = w^0(s)\overline{z'(s)}. \tag{8.20}$$

Here, $w^0(s)$ is the tangential velocity on the profile; it is a real value, which has a plus sign or a minus sign, depending upon whether or not its direction coincides with the direction along the contour arc.

For the profiles of the movable working cascade, $w_n = -u\, dx/ds$ and the condition of streamline flow require satisfaction of the condition

$$w(s) = w^0(s)\overline{z'(s)} - iu. \tag{8.21}$$

In the integral Expression (8.17), w_r^0 is the boundary value of the velocity on a profile with the number r, and $w^0(\xi)$ is the boundary value of the velocity at any one of n + m profiles of a fixed group.

We shall now obtain the system of the integral equations of the problem.

We shall replace in (8.17) the boundary values of the velocities for stationary contours by means of Condition (8.20), and for moving contours — by means of (8.21). Then, if a point fixed by coordinate s is situated on a stationary contour, we obtain (r = 1, 2, 3, ..., n)

$$\overline{z'(s)}\, w_r^0(s) = 2w_0 - \frac{1}{ii}\sum_{k=1}^{n+m}\int_{L_k} w^0(\sigma)\operatorname{cth}\frac{\pi}{t}(\zeta - z)\, d\sigma. \tag{8.22}$$

Analogously, for a point lying on a moving contour, we find (r = n + 1, n + 2, ..., m)

$$\overline{z'(s)}\, w_r^0(s) = 2(w_0 + iu) - \frac{1}{ii}\sum_{k=1}^{n+m}\int_{L_k} w^0(\sigma)\operatorname{cth}\frac{\pi}{t}(\zeta - z)\, d\sigma. \tag{8.23}$$

In the derivation of (8.22) and (8.23), use was made of the condition that for $z \in L_{n+1}, L_{n+2}, \ldots, L_{n+m}$ and $k \leqslant n$

$$\int_{L_k} \operatorname{cth} \frac{\pi}{l}(\zeta - z)\, d\zeta = 0$$

should hold. Use was also made of the expression for the principal value of the integral in the sense of Cauchy. Finally, we used the obvious fomulas:

$$d\zeta = z'(\sigma)\, d\sigma, \quad w(\zeta)\, d\zeta = \overline{z'(\sigma)}\, w^0(\sigma)\, z'(\sigma)\, d\sigma = w^0(\sigma)\, d\sigma.$$

Expressions (8.22) and (8.23) define a system of n + m integral equations. The unknown functions are the boundary values of velocity on n + m profiles of the group. Let us note that for moving profiles of the working cascade, the relative velocity enters into the equations. To determine the hydrodynamic meaning of the constant w_0, let us consider the limit values of Expression (8.16) an infinite distance from the cascade $x = \pm\infty$. The velocity at infinity behind of and in front of the cascade will be equal to

$$w^0_{1,2} = w_0 \mp \frac{1}{2il} \sum_{k=1}^{n} \Gamma_k, \quad \Gamma_k = \int_{L_k} w(\zeta)\, d\zeta. \tag{8.24}$$

Here, Γ_k is the velocity circulation around profile number k in a group of one period. Utilizing (8.24), we obtain

$$w_0 = \frac{1}{2}(w^0_1 + w^0_2). \tag{8.25}$$

Consequently, w_0 is the velocity of the main circulationless stream, and the expression

$$\mp \frac{1}{2il} \sum_{k=1}^{n+m} \Gamma_k$$

represents the velocity induced by the cascades at infinity.

Returning to the integral equations, we note some special cases. If the working cascade is discarded, (8.22) passes into the known integral equation used in the calculation of an isolated cascade. If

the directing cascade is discarded, (8.23) passes into an analogous equation, but with a main stream velocity equal to $w_0 + iu$, since the second cascade is in relative motion.

Let us note (this is important for practical applications) that the basic integral equation is applicable to problems of flow about vibrating profiles in a cascade with displacements taken into account and in a quasi-steady formulation. For solving the problem of the vibration of profiles in counterphase with displacement, it should be assumed that the shape of the profile, its incidence in the cascade, and the spacings of the two cascades are identical. Further, it may be assumed that one cascade is located inside the other and, in the general case, is displaced along the axis. From this, it is clear that in this case the problem may be considered without being restricted to small displacements. Generalizations are possible in principle, if n cascades with identical profiles and identical spacing located inside one another are considered. The spacing of each of the inserted cascades is equal to nt, where t is the true spacing of a cascade of the vibrating profiles. The problem considered in this section, as well as the corresponding generalizations, is restricted only by computational difficulties. In practice, the calculations become very much more complicated if the spacings of cascades moving with respect to each other are not equal.

Let us consider the results obtained by Kazimierski [110] in a calculation of interference of the two cascades presented in Figure 8.4. The cascades consist of identical profiles and have an identical spacing. The shape of the profile with an indication of the points is presented in Figure 8.5. The theoretical turn of the velocity distribution along the profile for a single cascade $(\Delta b/l \to \infty)$ coincides with the experimental values (Figure 8.6). An involute of the profile with indication of the points in accordance with Figure 8.5 is shown along the abscissa. Along the ordinate the ratio of the velocity on the profile to the velocity at the entry into the cascade is plotted. The calculation of simultaneous flow about the first stationary cascade and the second moving cascade by a potential stream in a quasi-steady formulation was carried out for the following values of

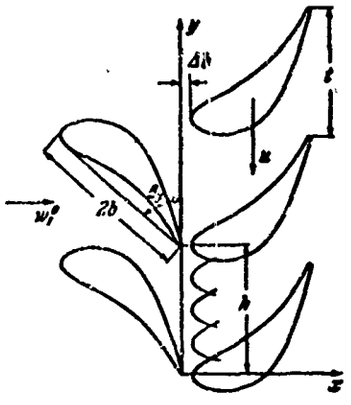


Figure 8.4. Cascade for the calculation example.

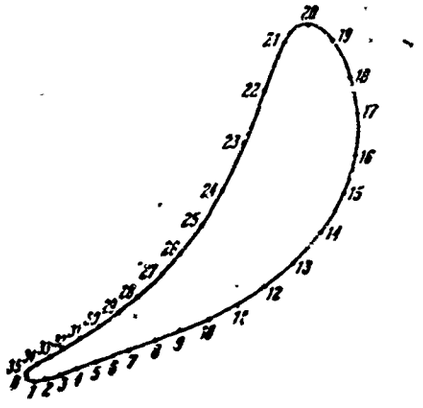


Figure 8.5. Profile of directing plate and working plate. Points on profile correspond to points Figures 8.6 — 8.8.

the geometrical parameters: relative density $2b/t = 1.265$, the incidence of the profile $\beta_1 = 48°$, the relative axial gap between the cascade $\Delta b/t = 0{,}051$. The stream enters the directing cascade at an angle of $\alpha_1 = 0$.

Figures 8.7 and 8.8 show the distribution of velocity along the profiles, respectively, of the directing cascade and the working cascade. Curve (1) pertains to the case of flow about an isolated cascade. The remaining curves correspond to various positions of the working cascade with respect to the directing cascade; this is fixed by the coordinate h/t (see Figure 8.4). The curves correspond to:

$$(2) - h/t = 0,\ (3) - h/t = 0{,}25,\ (4) - h/t = 0{,}50,\ (5) - h/t = 0{,}75.$$

From the calculation graphs it can be seen that on the directing cascade, considerable velocity perturbations exist at the trailing edge. Analogous perturbations at the working cascade naturally originate in the region of the leading edge, a shift of the stream

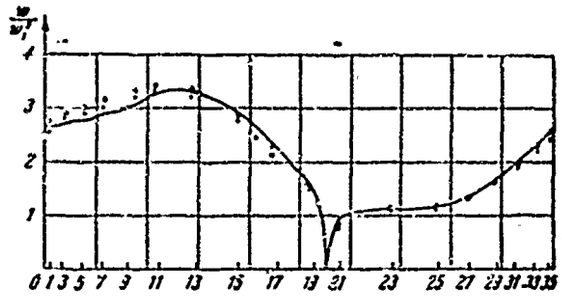


Figure 8.6. Comparison of calculated (solid line) and experimental distribution of velocities in an isolated cascade, w is the velocity on the profile, w_1^0 is the velocity at infinity in front of the cascade.

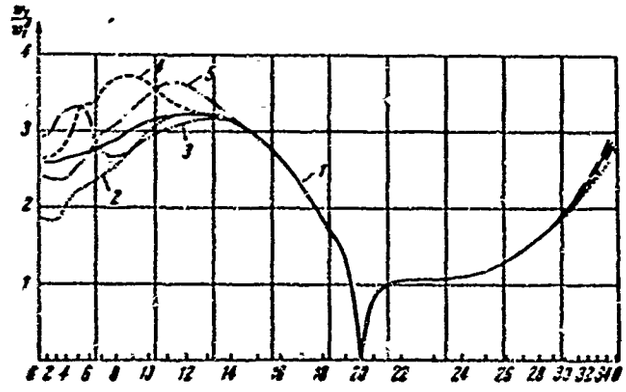
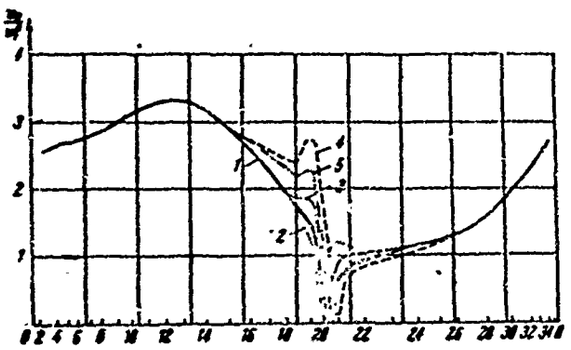


Figure 8.7. Distribution of velocity on the profile of a stationary cascade for various positions of the moving cascade. The figures on the curves correspond to the following conditions (see Figure 8.4):

1) the moving cascade is absent ($\lambda/t \to \infty$); 2) $h/t = 0$; 3) $h/t = 0.25$; 4) $h/t = 0.50$; 5) $h/t = 0.75$.

In cases 2) to 5) $2b/t = 0.051$.



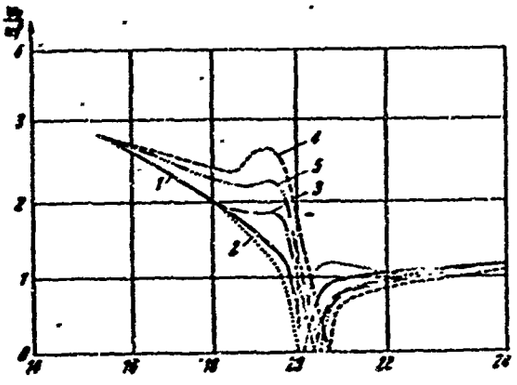


Figure 8.8. a) Distribution of velocities on the profile of a moving cascade at various positions with respect to the stationary cascade. Numbers on curves correspond to: 1) the directing cascade has been removed to infinity; 2) $\Delta/t = 0$; 3) $\Delta/t = 0.25$; 4) $\Delta/t = 0.50$; 5) $\Delta/t = 0.75$. In cases of 2) — 5), $2b/t = 0.051$.

b) Distribution of velocities on the profile of a moving cascade for various positions with respect to the stationary cascade in the vicinity of the leading edge. The numbers on the curves correspond to Figure 8.8a.

branching point being observed. In the example under consideration, the cascades had rather thick edges. With sharper edges, the perturbations brought about by cascades in a potential stream will decrease; however, the sharp leading edge of the working cascade will be more sensitive to a change of the entry angle. Since velocity perturbations in some cases increase the diffusion action of the flow, in a viscous fluid the appearance of boundary-zone separation is possible, which must be kept in mind when calculating turbomachine cascades.

The effect brought about by edge wakes will also be very significant in a viscous liquid. Let us note that the perturbations transmitted in a potential stream will rapidly decrease with an increase of the axial gap between the cascades. However, the influence of an edge wake upon the conditions of flow about the working cascade will be felt at a large distance.

The problem of the mutual influence of cascades with account taken of vortex wakes has been solved for thin profiles in a linearized formulation. In the latter case, the vortex wakes trailing from a directing cascade may be considered rectilinear, in spite of the fact that they are cut up by thin blades of a working cascade.

§ 8.3. Calculation of Flow About Two Moving Cascades by the Method of Successive Approximations

Let us consider the question of the mutual influence of cascades, employing a different approach.

Let there first be a single cascade. The complex velocity, regarded as an analytic, bounded and single-valued function along the entire exterior of the profile cascade, may be represented by the integral

$$w(z)=\frac{1}{2it_1}\oint_{L_0} w(\zeta)\operatorname{cth}\frac{\pi}{t_1}(z-\zeta)\,d\zeta+\frac{w(-\infty)+w(+\infty)}{2}. \qquad (8.26)$$

Here, w (- ∞) and w (+ ∞) are constant values of w(z) when $x\to\mp\infty$. This expression has been given by N. Ye. Kochin [31].

The integral Formula (8.26) may be replaced by the series [56]

$$w(z) = \frac{\pi}{t_1}\sum_{n=0}^{\infty}\frac{(-1)^n}{n!}C_{-(n+1)}\frac{d^n}{dz^n}\operatorname{cth}\frac{\pi z}{t_1} + C_0. \tag{8.27}$$

The coefficients of this series are found on the basis of the theorem

$$C_n = \frac{1}{2\pi i}\oint w(\zeta)\zeta^{n-1}d\zeta, \quad C_0 = \frac{1}{2}[w(-\infty) + w(+\infty)].$$

The constant C_0 is equal to the velocity of a circulationless stream. We take advantage of the expansion:

$$\operatorname{cth}\frac{\pi z}{t_1} = \pm 1 \pm 2\sum_{n=1}^{\infty} e^{\mp 2n\pi i N_1}. \tag{8.28}$$

Here, the upper sign pertains to the case of $x>0$, and the lower sign pertains to the case of $x<0$.

By means of (8.26) and (8.28) we obtain an expansion of the perturbed velocity into a series

$$w(z) = \pm\sum_{n=0}^{\infty} a_n e^{\mp 2n\pi i N_1}, \quad a_n = \pm\oint_{L_0} e^{\mp 2n\pi i(z-\zeta)/t_1} w(\zeta)\,d\zeta, \quad n = 1, 2, 3\ldots \tag{8.29}$$

Let the velocity distribution on the profiles of cascade $w(\zeta)$ be known. Then Series (8.29), the coefficients of which can be computed, yields the value of the perturbed velocity w(z) at point z. This perturbation is brought about by a cascade situated in a plane-parallel homogeneous stream. Thus, the perturbations induced by the cascade are represented by a sum of periodic functions. The greatest period is equal to the spacing of the cascade.

If a second cascade is placed next to the first one, the velocity distributions on the profiles of both cascades will change as a result of interference.

Let the least common period of the cascades be equal to $t = nt_1 = mt_2$. Then, the perturbation field induced by the first cascade,

having periods $t_1/k (k = 1, 2, 3 \ldots)$, will bring about perturbed flow about the second cascade with phase shifts in the general case.

In flow about the second cascade, the phase shift will be equal to

$$\alpha_2 = 2\pi \frac{t_2 - \tau_1/k}{t_1/k} = 2\pi \frac{kt_2 - t_1}{t_1},$$

or, discarding the trivial term 2π, we obtain

$$\alpha_2 = 2\pi k \frac{t_2}{t_1} = 2\pi k \frac{n}{m}.$$

Here, for k = 1, 2, 3, ..., (m-1) there will be m-1 different phase shifts.

Thus, the perturbation waves induced by the first cascade, which have a length equal to or greater than $t_1/(m-1)$, induce perturbed flow about the second cascade with corresponding phase shifts α_2. Perturbation waves, the length of which is less than $t_1/(m-1)$, induce perturbed flow about the second cascade only in phase.

Analogously, the presence of the second cascade will induce perturbations on the first cascade. The corresponding values of the phase shift in the case of streamline flow will be equal to

$$\alpha_1 = 2\pi k \frac{t_1}{t_2} = 2\pi k \frac{m}{n}.$$

In this case there will be n-1 different phase shifts.

It has been shown in Chapter 2 that the shorter the perturbation wavelength induced by the cascade, the more rapidly its amplitude diminishes with increasing distance from the cascade axis. Consequently, in the case of mutual influence of cascades, perturbations with a wavelength equal to the spacings of the cascades will be the most significant ones.

With the approach described above, the method of successive approximations can be applied to the most difficult problem of the mutual influence of cascades with different spacings. Each of the approximations consist in solving a problem of flow about an isolated cascade with a given perturbation on the profiles. The value of the perturbation changes from profile to profile by the multiplier $\exp(j\alpha)$. The latter has been considered in Chapter 7.

The following way of carrying out the successive approximations is expedient.

The problem of flow about two isolated cascades by a uniform stream is solved as the zero approximation. In this case, if one of the cascades moves, the flow about it is considered in terms of relative motion. Then the mutual perturbations induced by the influence of one cascade upon the other are computed. After this, the problems of flow about isolated cascades with given perturbations and constant phase shifts are solved. The sum of the solution for each cascade yields the value of the perturbations in the first approximation. If necessary, a refinement of the mutual influence is obtained, since the velocity distribution along the cascades has changed, and the calculation cycle is repeated.

We shall mention one practical circumstance which can greatly decrease these calculations.(1)

In many cases, determination of the perturbation velocities is not required. All that is necessary is the computation of the force due to interaction of the cascades. In the determination of the force, only a single harmonic is of interest with a wavelength equal to the spacing of the perturbing cascade. This problem is of practical interest in turbines, for example, when estimating the danger of blade oscillation which may be induced by a cascade of blades (situated downstream) with thick leading edges.

Footnote (1) appears on page 345.

FOOTNOTES

1. on page 344. The velocity perturbations are assumed small in comparison with the main stream velocity.

PART III

OSCILLATIONS OF TURBOMACHINE BLADES

CHAPTER 9

FORCED BLADE OSCILLATIONS IN A NONUNIFORM FLOW

§ 9.1 Trailing Wake and its Characteristics

The stage of a turbine (Figure 1.1) and the stage of an axial compressor (Figure 1.4) were examined in Chapter 1. Now let us look, for example, at the stage of an axial flow compressor, consisting of a directing and operating cascade. We shall examine the two-dimensional case by looking at the annular cross section of the stage.

In this case, let the second cascade move with respect to the directing cascade at a velocity u (circumferential velocity) and intersect the vortex wakes forming behind the edges of the blades of the directing cascade when a viscous liquid flows around them.

The moving cascade operates in a nonuniform flow. A similar picture is observed in all turbomachines, i.e., steam and gas turbines,

axial and centrifugal compressors, hydraulic turbine pumps and water turbines.

At the present time, the circumferential nonuniformity of the flow, produced by the trailing wakes has been studied. Such a nonuniformity may also be caused by technical errors in the manufacture of the blades, by the presence of rotary inlet or outlet nozzles, the edges, etc.

Several problems arise which are of interest for purposes of mill rolling.

The first problem is that circumferential nonuniformity leads to the appearance of nonstationary forces and moments producing dynamic stresses in the blades. It is essential to be able to evaluate the dynamic stresses from the given nonuniformity.

The second problem is that the nonstationary flow around the cascade produces a supplemental dispersion of the energy in comparison with that found in a uniform flow.

The third problem is that operation of the cascade under the conditions of a periodically varying angle of attack may cause the earlier appearance of cavitation in the hydraulic machines than would follow from computation according to the mean velocity.

Let us look first at the characteristics of the trailing wake and the possible ways of simplifying the problem.

In cascades in which a viscous liquid flows, turbulent trailing wakes are propagated behind the blades; this is shown schematically on Figure 9.1. The wake may be divided into three zones: 1) a zone which is directly adjacent to the trailing edge, where a large nonuniformity is observed in the velocity and static pressure fields. Significant surges are observed here; 2) a basic zone where the static pressure is practically constant and the wake has the characteristic properties of a turbulent jet; 3) a zone following joining of the

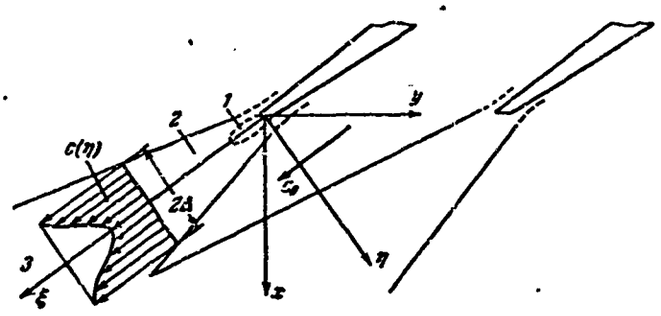


Figure 9.1. Trailing wake behind the cascade.

wakes, which is characterized by a periodicity in the velocity distribution and a relatively small degree of nonuniformity in the flow. The next cascade is usually located in the second zone, which is therefore of the greatest interest. For details we cite the books of L. G. Loytsyanskiy [42] and G. N. Abramovich [2] where the general questions are discussed and also the books of G. Yu. Stepanov [78], M. Ye. Deych and G. S. Samoylovich [30] where a more detailed discussion is given relative to the theory of cascades.

Here we shall cite the essential qualitative characteristics by examining the flow only in the second zone. We know that in this zone we can use the methods employed in the theory of turbulent jets for studying a wake.

Let us arrange the coordinate axes as shown on Figure 9.1 and denote them by: c_0 is the maximum velocity in the center of the flow (outside the zone of the trailing wake); $c = c(\eta)$ is the instantaneous velocity in the trailing wake with the fixed coordinate ξ, 2Δ is the width of the wake for measurements along the η axis. Figure 9.1 shows the velocity profile in the wake on the base segment.

Let us introduce the concept of a supplemental velocity in the wake $v^0(\eta) = c_0 - c(\eta)$, which is used in the theory of turbulent jets.

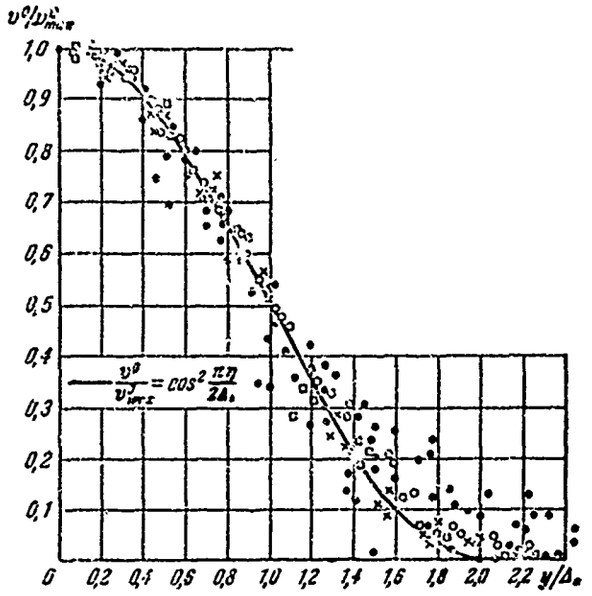


Figure 9.2. Dimensionless universal profile of the supplemental velocity in the trailing wake.

- ● Turbine cascades at various distances, M up to 0.9 (Experimental data of G. Yu. Stepanov [78].
- O Rods of circular cross section at various distances, M = 0.3 - 0.8, Re ~ 10^4.
- □ Plate with rectangular trailing edge, relative width $\delta/2b = 0.12$, relative spacing $t/2b = 1.5 - 1.8$, when M = 0.3 - 0.75 and various distances; Re ~ $2 \cdot 10^4$ (in thickness).
- x Compression blades (including symmetrical and strongly bent)

  M = 0.4 - 0.8; Re ≈ $6 \cdot 10^5$.

The dimensionless profile of the supplemental velocity in the wake is given on Figure 9.2. The ratio of the supplemental velocity to the maximal supplemental velocity $v^0_{max} = c_0 - c_{min}(\eta)$ is plotted along the ordinate axis; here $c_{min}(\eta)$ is the magnitude of the supplemental velocity on the ξ axis. The ratio η/Δ_0 is plotted along the ordinate axis; $2\Delta_0$ is the width of the wake at a supplemental velocity equal to half the maximal value. For comparison we have chosen the quantity $2\Delta_0$ rather than the physical width of the wake 2Δ, in order to

eliminate the error which arises in an experimental determination of the diffused wake boundary.

Experimental points are plotted on Figure 9.2 that were obtained in numerous measurements conducted in the wakes of turbulent and compressor cascades. The graph also shows the points which correspond to the turbulent wakes behind circular rods and flat plates, obtained in the experiments of N. Neruda [50]. The importance of these latter measurements will be discussed below. It is obvious from Figure 9.2 that the experimental points are grouped sufficiently close together and agree well with the familiar law from the theory of turbulent jets

$$\frac{v^0}{v^0_{max}} = \cos^2 \frac{\pi\eta}{2\Delta_*}. \tag{9.1}$$

Since we must have $v^0/v^0_{max} = 1/2$ when $\eta = \Delta_*$, then in using this expression we must assume $2\Delta_* = \Delta$, i.e., Δ_* is equal to one fourth of the wake width.

We know from the theory of turbulent jets that in a two-dimensional flow the coefficient of nonuniformity $x = v^0_{max}/c_0$ is inversely proportional to $\sqrt{\xi}$. For turbine cascades G. Yu. Stepanov cites the semi-empirical formula (a coefficient 0.66 was experimentally determined)

$$x = 0{,}66 \sqrt{\frac{t_1 \zeta_{pr} \sin \alpha_1}{\xi}}. \tag{9.2}$$

Here t_1 is the cascade stage, ζ_{pr} is the coefficient of profile losses, α_1 is the angle of departure of the flow from the cascade.

The width of the wake can be established using the equation of continuity and for the assumed conditions is equal to

$$2\Delta = \frac{t_1 \zeta_{pr} \sin \alpha_1}{0{,}9x}. \tag{9.3}$$

The formulas obtained fully describe the base segment of the trailing wake; experimental proof has been made and they may be

assumed to be reliable. A similar type of expression must be valid for cascades of any type because of the universal nature. There may be some slight difference only in the numerical coefficients that depend on the turbulent mixing.

In the selected coordinates the trailing wake is symmetrical in the base zone in the cross sections ξ = const. The coordinates which have been used in the past are convenient for describing a single wake, but not for a system of wakes for the entire cascade; therefore, let us proceed to new coordinates xy and set the axes parallel and normal to the axis of the cascade (see Figure 9.1). The blades of the second cascade intersect the trailing wakes along the line x = const and for this case the flow is not symmetrical. The velocity distribution function is periodic, and therefore the nonuniformity in the velocity distribution may be characterized by the relative magnitude of the coefficients of the Fourier series a_n/a_0 (a_n is the coefficient of the n^{th} harmonic).

In the past we have been speaking about the velocity distribution and the degree of nonuniformity in the absolute flow of a liquid, i.e., a liquid described in an absolute coordinate system associated with a moving cascade. In a nonuniform flow we will find that the moving cascade and the characteristics of the nonuniformity for it will be different, since the variation in velocities in the basic flow and wake will not be proportional. Only the modulus of the velocity varies in the absolute motion, but the direction remains constant. Let us associate the coordinate system x_1y_1 with the moving blades. In this moving coordinate system (in relative motion) the nonuniformity of the flow is characterized by nonuniformity of the normal w_n and tangential w_s velocity components which are supplemental to the constant relative velocity of the flow w_1^0, approaching the operating blades.

The physical problem could be postulated by examining the picture of the flow of a viscous liquid, the formation of wakes and the overflowing of the nonuniform nonstationary flow onto the moving operating

cascade. However, it is so complicated that before mathematical formulation is possible we must suggest a simpler model that would retain the basic characteristics of the phenomenon.

First of all let us look at a schematization of the edge wakes. A vortex flow of viscous liquid is observed in real wakes. The flow outside the wakes is a potential flow. This will already be a simplification based on boundary layer theory. Let us introduce a further simplification, i.e., we shall assume the liquid to be ideal. In other words we assume linear viscosity. The wakes can be replaced by a free vorticity, transported by the basic flow. We can select the distribution of free vorticity such that the velocity distribution in a fixed control cross section will be the same for a real or an idealized wake. As a result of such substitution we do not have to allow for diffusion of the vortex as a result of turbulent exchange. Consequently, in a free flow (in the absence of a second cascade) the trailing wake will have a constant width of a linear formulation. This scheme retains the basic characteristics of the real process and must not strongly distort the final result, since the process of interaction between the nonuniform flow and the second cascade takes place over a short path segment. We can of course never expect to describe the flow inside the channels of a strongly curved cascade in this way. We must emphasize that the overall scheme of the vortex wake in an ideal liquid and the conversion to relative motion are admissible for arbitrary cascades. This is complicated, since it is difficult to describe the motion of an eddying liquid in a strongly curved channel.

Furthermore, let us look for determinancy at the cascade of thin profiles and arrange the coordinate system $\xi\eta$ such that the ξ axis, as previously, is parallel to the vector of the absolute velocity of the unperturbed flow c and consequently is directed along the vortex wake (Figure 9.3). In this coordinate system the vorticity is a periodic function only of the coordinate η. The period of this function is equal to $t_1 \sin \alpha$, i.e., the least distance between axes of neighboring wakes (t_1 is the stage of the stationary cascade,

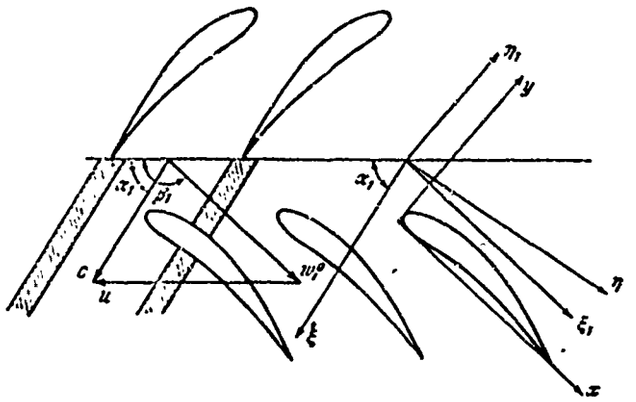


Figure 9.3. Movement of the cascade in vortex wakes, excited by the previous cascade.

α_1 is the angle between the axis of the cascade and the vector of the absolute velocity). The law of vorticity distribution may be represented by a Fourier series. Since in the coordinates $\xi\eta$ the vorticity is connected with the supplemental velocity in the wakes by the trivial equation $\omega = 1/2\, \partial v^0/\partial\eta$, then $v^0(\eta)$ is expressed by the analogous series

$$v^0(\eta) = v^0 \sum_n a_n \exp\left(i \frac{2\pi n}{t_1 \sin \alpha_1} \eta\right). \tag{9.4}$$

In order to study the flow around a moving cascade by a nonuniform vortex flow, let us transfer to a movable system of coordinates. The system xy is connected to one of the profiles of the second cascade; the abscissa axis is parallel to the relative unperturbed velocity of the inlet flow onto the second cascade w_1^0.

Let us make the transition to the new coordinate system by first rotating by the angle $\beta_1 - \alpha_1$ (the angle between the absolute and the relative velocities):

$$\xi = \xi_1 \cos(\beta_1 - \alpha_1) - \eta_1 \sin(\beta_1 - \alpha_1),$$
$$\eta = \xi_1 \sin(\beta_1 - \alpha_1) + \eta_1 \cos(\beta_1 - \alpha_1).$$

Thus, let us first convert to a stationary system of coordinates $\xi_1\eta_1$, whose axes are parallel to the movable system xy; then let us make the Galilean transformation

$$\xi_1 = x + u\tau\cos\beta_1, \quad \eta_1 = y - u\tau\sin\beta_1.$$

Here β_1 is the angle between the transport velocity of the second cascade u and the axis ξ_1; τ is the time. The final relationship between the movable and the stationary systems of coordinates is given by the formulas

$$\left.\begin{aligned}\xi &= x\cos(\beta_1-\alpha_1) - y\sin(\beta_1-\alpha_1) + u\tau\cos\alpha_1,\\ \eta &= x\sin(\beta_1-\alpha_1) + y\cos(\beta_1-\alpha_1) - u\tau\sin\alpha_1.\end{aligned}\right\} \qquad (9.5)$$

In the final transformation we can drop the nonessential constant which is connected with the parallel shift of the coordinates. From (9.4) and (9.5) it follows that the field of supplemental velocities in the movable system may be represented by the expression (let us further write only the value proportional to the first harmonic)

$$v^0(x, y, \tau) = v^0\exp\left\{2\pi j\frac{u}{t_1}\left[\tau - \frac{x\sin(\beta_1-\alpha_1) + y\cos(\beta_1-\alpha_1)}{u\sin\alpha_1}\right]\right\}.$$

The expression $2\pi u/t_1 = \nu$ is a circular frequency of the advance of the wakes to the operating cascade. We can use the equation $u\sin\alpha_1 = w_1^0\sin(\beta_1 - \alpha_1)$ which is obvious from the velocity triangles, and find

$$v^0(x, y, \tau) = v^0\exp\left\{j\nu\left[\tau - \frac{x + y\operatorname{ctg}(\beta_1-\alpha_1)}{w_1^0}\right]\right\}. \qquad (9.6)$$

The final scheme of flow around the second cascade in the coordinate system xy is given on Figure 9.4. The flow at the basic velocity w^0 approaches the cascade and brings the waves of the free vorticity. The arrow inside the vortex wakes shows the direction of the supplemental velocity. The vortex wakes which arise with periodic variation in the circulation are shown schematically behind the profiles.

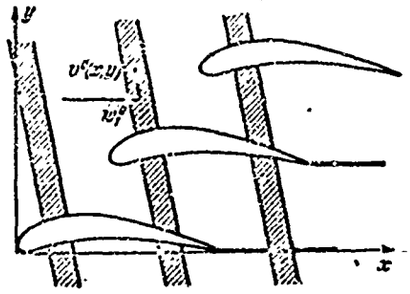


Figure 9.4. Operating cascade in a nonstationary vortex flow.

The front of the advancing waves is described by the equation

$$w_1^0 \tau - x - y \operatorname{ctg}(\beta_1 - \alpha_1) = 0. \tag{9.7}$$

The process of flow around each blade of the cascade is the same; however, in the general case it is shifted in time by the phase angle α. For flow around a moving cascade each subsequent blade encounters a fixed trailing wake with a shift in time $T = t/u$ (t is the stage of the second cascade). The phase shift is determined from the known period of the flow process, equal to $T_0 = t_1/u$, and consequently,

$$\alpha = 2\pi \frac{T}{T_0} = 2\pi \frac{t}{t_1}. \tag{9.8}$$

Thus, the problem is reduced to the problem of flow around the cascade in the system of periodic vortex waves, advancing to the neighboring profiles with the phase shift. This problem was studied in § 4.5 in a linear formulation.

Before we look at the total characteristics, the force and the moment which are necessary in computing blades for dynamic stability, let us turn our attention to the distribution of pressure on the blades. In the specific case (angle of departure $\gamma_b = 0$, phase shift

$\alpha = 0$) the distribution of pressure along the profile of the cascade may be expressed by the formula

$$p = \rho^0 v^0 \omega_1^0 R(k, q) e^{jv\tau} \sqrt{\frac{\operatorname{sh}[q(1-x)]}{\operatorname{sh}[q(1+x)]}}.$$

This solution was found for one wave $v^0(x, \tau) = v^0 \exp jv(\tau - x/\omega_1^0)$. For the profile of the supplemental velocities in the wake given arbitrarily, the solution is found by summation. We must only take into account the change R(k, q) due to change in the Strouhal number k. In particular, for the cascade with extremely low density ($q \to 0$) the graph of a typical dimensionless perturbed velocity and dimensionless nonstationary force is given on Figure 9.5. The dependence is shown as a function of harmonic number. It is obvious that with an increase in the number of the harmonics the force is diminished more strongly than the perturbing velocity.

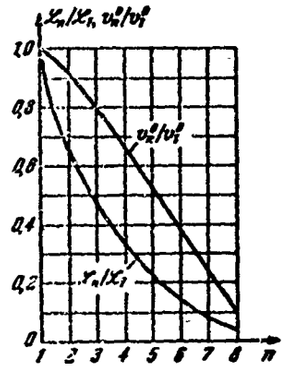


Figure 9.5. Dependence of v_n^0/v_1^0 and $\mathcal{P}_n/\mathcal{P}_1$ on the number of the harmonic (v_n^0 is the modulus of the n^{th} harmonic of the supplemental velocity in the wake, $\mathcal{P}_n$ is the modulus of the n^{th} harmonic of the lift power) for a very thin cascade.

Since in a compressor-type cascade the supplemental velocities in the wake are directed to the curved side of the blades, the lift power will be increased. The opposite picture is observed in turbine cascades. Let us remember that the velocity distribution in vortex wakes is described by a universal function.

Let us expand the perturbed velocities normal to the blade chord produced by the trailing wakes into a Fourier series of the variable x. This is equivalent to the Expansion (9.1) into a Fourier series for the variable n and multiplication of the result by sin γ, where $\gamma = \beta_1 - \alpha_1$ is the inclination angle of the wakes with respect to the chord. In the expansion we must bear in mind that the Function (9.1)

gives the value of the perturbed velocity over the segment 2Δ, and on the segment $t_1 - 2\Delta$ the velocity is equal to zero.

Let us write the Fourier coefficient of the n^{th} harmonic of the series

$$v_n^0 = v^0 \frac{\sin\gamma}{\pi}\left[\frac{1}{n} + \frac{\Delta^2}{t_1^2 \sin^2\alpha_1} \frac{4n}{1 - 4n^2\Delta^2/t_1^2 \sin^2\alpha_1}\right] \sin\frac{2\pi n\Delta}{t_1 \sin\alpha}.$$

Here all symbols correspond to those used above.

In view of the linearity of the problem each harmonic in the velocity distribution corresponds to the harmonic of the nonstationary force expansion into a Fourier series.

In axial flow compressors the practical danger involves resonance with the first harmonic from the trailing wakes. Usually torsional vibrations occur, since the natural frequencies for bending vibrations are too low. If, in addition, the wakes are sufficiently narrow $(2\Delta/t_1 \ll 1)$, then we can ignore the terms of higher order of smallness, and we find

$$v_1^0 = \frac{2\Delta \cdot v^0 \sin\gamma}{t_1 \sin\alpha_1}. \qquad (9.9)$$

After using Formula (9.9) under the condition $\varkappa = v^0/c$, we obtain

$$v_1^0 = 1{,}1\zeta_{a_2} \sin(\beta_1 - \alpha_1).$$

This value is proportional to the nonstationary force. This means that the influence of distance between cascades on the nonstationary force in this case will be expressed only by higher order terms. This comment refers to the basic zone of the boundary wake and is valid of course when the problem is linearized.

Let us look at the motion of trailing wakes through an aerodynamic cascade in greater detail. In § 3.5 we discussed the problem of rotation of trailing wakes with passage through the cascade where

the static circulation was not equal to zero; however we assume that the pitch of the blades is infinitely small. If we examine the cascade of the final stage, it will then cause not only a rotation of the wakes, but also their breakup.

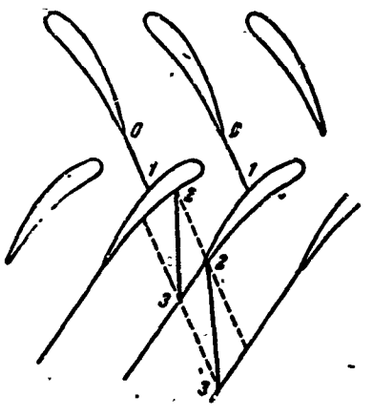


Figure 9.6. Schematic of intersection and revolution of the trailing wake in an aerodynamically loaded cascade.

Figure 9.6 shows the schematic of the breakup of the trailing wake in the stages of the axial flow compressor. The trailing wake (0 - 1) which emanates from the guide blade, is intersected by the operating blades. The particles of the liquid, belonging to the wake, move in the interblade channel at different velocities. The particles moving along the edge of the blades have a higher mean velocity than the particles of the liquid flowing along the concave sides. This results in the wake being broken down into individual segments (2 - 3), since the ends of the vortex sheet which intersect the blade are not connected. This phenomenon was noted by Smith [76] and other authors.

Thus, the trailing wake of one blade is located inside the band, whose boundaries are shown in Figure 9.6 by the broken lines. The width of this band may be estimated by determining the mean velocities on the edge and the concave side of the operating blade.

Above, in the theoretical examination of the problem on advance of the wakes to the aerodynamic cascade, we assumed that the velocity diagram in the traveling wave does not vary. In fact there are several reasons why the shape of the traveling wave is distorted. First of all, the blades do not intersect wakes of constant width, but those diffused along the path of the basic flow in absolute

motion. Thus, in proportion to the displacement of the wave in relative motion to the trailing edge the width of the wave is increased, and the values of the forced velocities are diminished.

The influence of distortion of the shape of the traveling wave on the variable lift should then be studied only for the occasional cascades where the aftereffect is high. In thick cascades the value of the variable force is determined basically by the shape of the wave intersected by the leading edges of the moving cascade. In general it is more correct to speak about the "transmissivity" relative to the traveling waves of a given orientation instead of the thickness of the cascade. To evaluate the transmissivity let us introduce the dimensionless quantity which has a simple geometric meaning

$$\bar{q} = \frac{t}{2b} \frac{\sin(\beta_1 + \gamma)}{\sin\gamma}.$$

The single profile has infinitely high transmissivity. The transmissivity of the cascade for any possible orientation of the wakes may be very small with a sufficiently large thickness. The rate of change of circulation around the profile with advance of the vortex wakes onto the cascade must depend on the transmission coefficient.

Let us examine the second cause for distortion of the traveling wave. When the vortex wake is intersected by the profile, the liquid begins to move in the direction shown by the arrows on the side (Figure 9.7). The appearance of these flows leads to a narrowing of the wake from one side (in this case over the profile) and to its expansion from the other side (in this case under the profile). The influence of these flows must be diminished in the cascades with a small transmissivity, since deceleration of the particles moving at the supplemental velocities inside the wake will take place very rapidly and only in the region of the leading edges.

The order of the time of the wake's passage along the profile is equal to $2b/w^0$. The wake is diffused at a velocity having the

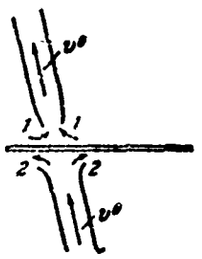


Figure 9.7. Distortion of the shape of the wake with movement along the profile. The arrows v^0 show the direction of the supplemental velocity in the wake. The arrows 1-1 and 2-2 show the direction of movement of the liquid with intersection of the wake.

order of the supplemental velocity in the wake. Then the ratio of change in wake width to its original width, as Mayer [119] noted, is on the order of $2bv^0/\Delta \cdot w^0$. For axial flow compressors $2bv^0/\Delta \cdot w^0 \sim 1$; hence, it follows that linear theory will give erroneous results for the pressure and velocity distribution near the traveling wake. If the wake were assumed narrow, then this effect would be analogous to the effect of a singular point, traveling along the leading edge of an absolutely thin profile. At some distance from the wake, linear theory will give the correct result; the total characteristics will also be determined with sufficient accuracy.

More precise computations using the nonlinear equation (given by Mayer who used a numerical method) for the wake which travels along a free blade will lead to the results shown on Figure 9.8. Computation is plotted on the schematic corresponding to the sudden intersection of the two-dimensional jet by the plate.

Figure 9.8 a shows distribution of the dimensionless pressure gradient $\bar{p}_x = (b/\rho^0 w_1^0 \bar{v}^0)(\partial p/\partial x)$ along the plate. Here $\bar{v}^0$ is the integral mean of the supplemental velocity in the wake:

$$\bar{v}^0 = \frac{1}{2\cdot\Delta}\int_0^{2\Delta} v(x)\,dx.$$

Figure 9.8 b shows distribution of the dimensionless perturbed tangential velocity $\bar{w}_t = w_t/\bar{v}^0$. The broken line shows the results of linear theory; the solid line that of the refined computation. We assumed in the computations that $\gamma = \pi/2$, $\Delta/b = 0{,}15$, $b\bar{v}^0/\Delta \cdot w^0 = 1{,}06$. The

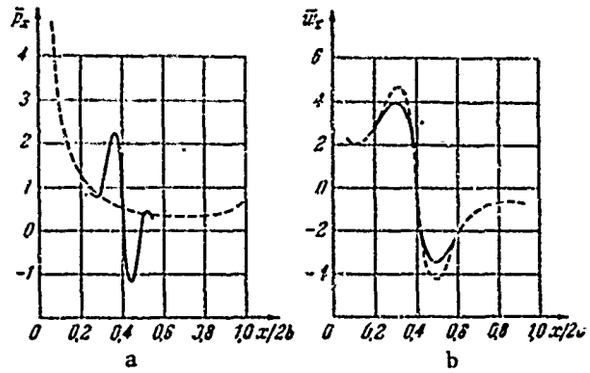


Figure 9.8. Comparison of the results of computations according to linear (broken line) and nonlinear (solid line) theories; (a)-distribution of the dimensionless pressure gradient; (b)-distribution of the dimensionless perturbed velocity.

schematics of the perturbed velocities agree well for both computations. As far as the pressure gradient is concerned, linear theory, as mentioned above, gives the same law for the change in pressure, irrespective of the shape of the wake and its frequencies.

Experimental research on the distribution of nonstationary pressure along the thin profile when the wake is intersected was conducted by Lefcort [115]. The research was carried out on a water trough. The pressure was recorded at several points along the profile.

Similar research on the nonstationary flow around a turbine cascade was conducted by I. I. Kirillov and A. S. Laskin [30]. The investigations were made on a radial inverted turbomachine, whose flowing part is shown on Figure 9.9, where the basic geometric characteristics of the cascade are depicted. The operating blades were drawn off in average cross section, and quick-response sensors were installed on them. The schematic of the drainage arrangement is shown on Figure 9.10. For technical reasons the sensors were not installed on one blade; however, the experimental data cited below were shifted in time so that the sensors would appear to be located on one blade.

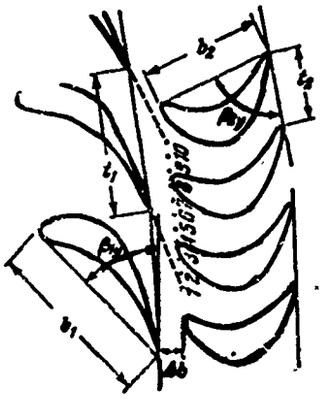


Figure 9.9. Flowing part of the inverted radial turbine. The guide cascade is composed of blades TN-2-40, $2b_1 = 59$ mm, $\bar{t}_1 = t_1/2b_1 = 0.8$; $\beta_1 = 46.5°$. The operating cascade is composed of blades T-3-40, $2b_2 = 41$ mm, $\beta_2 = 78°$.

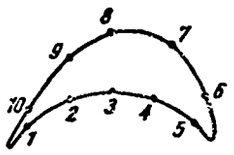


Figure 9.10. Location of ports on operating blades.

Figure 9.11 shows oscillograms with the recording of the static pressure on the surface of the blade located behind the rotating nozzle cascade. The numbers on the right-hand side of the oscillograms represent the location of the drainage on the surface of the blade according to Figure 9.10. A network of straight lines is plotted on the oscillograms and denoted by the numbers which determine the mutual arrangement of the cascades. The respective positions of the cascades are denoted on Figure 9.9 by the same numbers. The width of the band, occupied by the lines, corresponds to the time of shift of the guide cascade by one stage $\tau_0 = t_1/u$, where u is the circumferential velocity of the cascade, t_1 is its stage. The oscillograms also show the direction of the time axis τ, and the readings from the time marker (TM) are plotted from the top at intervals of 2 μsec. The investigations were made with an axial clearance of $\Delta b = 4$ mm.

The pressure surges have a periodic character with the basic frequency of nz_1 (n is the number of revolutions of the turbomachine; z_1 is the number of guide blades). Turbulent surges are simultaneously observed with a higher frequency. Especially turbulent surges are observed at points 8, 9 and 10, on the convex side behind the

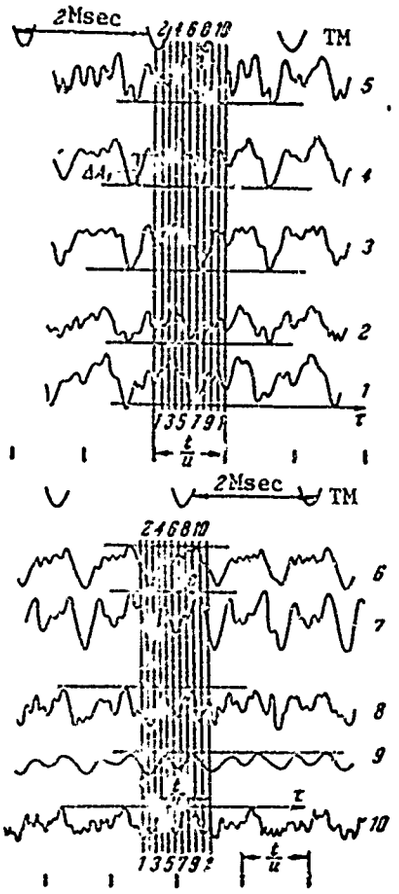


Figure 9.11. Surges in pressure at various points of the operating blade, found in the vortex wakes of the guide cascade.

minimum pressure point. With incidence of the wake onto the inlet edge of the blade at point six the pressure is increased and drops at point five. This is denoted on the oscillograms by the arrow c. Such a rule can be explained in that the supplemental velocity in the wake for a turbine stage is directed to the side of the convex surface of the blade. Consequently, intersection of the wake produces a local increase in the angle of attack of the second cascade.

The measurements show also that the perturbations produced by the trailing wake arise on the entire blade almost simultaneously, since the signal is propagated at a velocity on the order of the speed of sound.

We assumed above that all the trailing wakes are identical. In this case the lowest frequency of the perturbing force is equal to nz, where n is the number of revolutions of the turbomachine rotor, and z is the number of guide blades. We know that resonance vibrations of the blades are also observed in turbomachines at frequencies of $k_n n$, $k_n = 1, 2, 3 \ldots$. One of the reasons for onset of the low-frequency perturbing forces is the different intensity of the trailing wakes in the vicinity of the impeller. The reason for such an aerodynamic heterogeneity may be the structural heterogeneity of the cascade. Furthermore, the wakes

are turbulent jets for which random surges are characteristic and obey statistical laws. A zone of intermittence exists at the boundary of the jet where large-scale surges are observed. In view of the fact that the large-scale spectrum of turbulence may be very dense, it is possible that resonance oscillations will occur under the influence of random forces. Such oscillations of the blades have been observed in turbomachines.

In the work of I. N. Pis'min and the author [69], experimental investigations of the trailing wakes behind the rotating wheel of an axial flow compressor were carried out. The measurements were made in relative motion using quick-response strain gauges [70, 71]. The design of one such gauge is shown in Figure 9.12. The probe can measure both the constant and the variable component of the pressure. The thickness of the gauge head (Type B) is equal to 1.8 mm which permits using it for measurements in turbomachines.

The measurement installation is shown in Figure 9.13. A coordinate apparatus (2) which is actuated by a special electric motor (3) is placed behind the rotating wheel of the axial flow compressor (1), A strain gauge (4) is placed on the coordinate apparatus. The number of revolutions of the electric motor (3) may be regulated and kept equal to or almost equal to the number of revolutions of the compressor wheel. In measuring trailing wakes a system may be constructed such that the relative speed of rotation of the probe relative to the compressor wheel is, for example, 200 times less than the absolute speed of rotation. When the wheel revolves at 150 rev/sec. the probe makes 0.75 rev/sec relative to the wheel, which permits making reliable measurements. The signals emitted by the probe are transmitted through a contactless current collector (5) to the strain gauge amplifier (6) and to the cathode (7) or loop (8) oscillograph. The circuit has a system for self-adjustment of the rotation rate of the coordinate apparatus (9). To interpret the results of the observations we included in the circuit: inductive sensors for the number of revolutions of the coordinate apparatus (10), a compressor (11) and a tuning fork time marker (12).

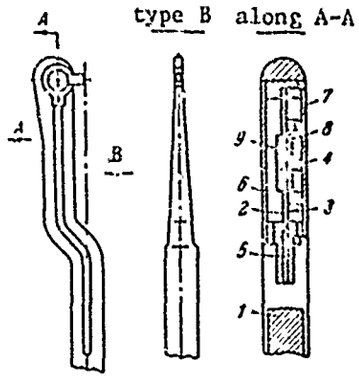


Figure 9.12. Quick-response strain gauge: 1- casing of the probe; 2- active membrane ; 3- compensation membrane; 4- membrane support; 5- barrier between membranes; 6,7- covers of the casing; 8,9- strain guage sensors.

In front of and behind the guide cascade (13) we set up the usual probes (14) and the stationary quick response strain guages (15). The circuit also contains a voltage stabilizer (16) and a resistance box (17).

The results of measuring the flow behind the rotating wheel of the axial flow compressor stage are given on Figure 9.14. The figure shows: (1) the recording of responses from the probe which registers the total pressure, (2) the recording of the marker of the number of revolutions of the compressor wheel, (3) the recording of the marker of the number of revolutions of the rotating probe.

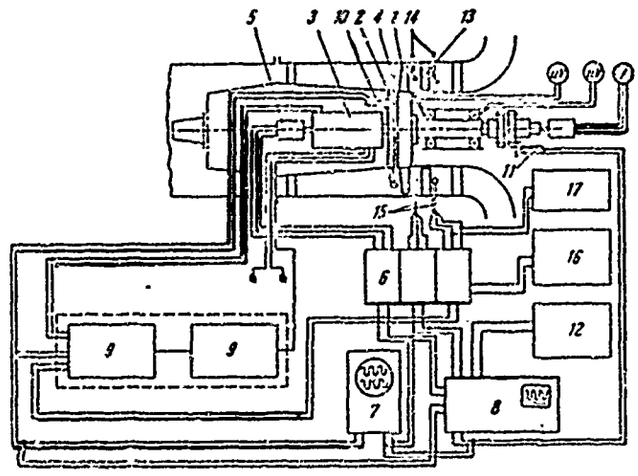


Figure 9.13. Schematic for measuring the flow in a turbomachine in relative motion.



Figure 9.14. Recording of the pressure of deceleration behind the revolving wheel of the axial-flow compressor in relative motion.

The dips in the curve for the total pressure correspond to the moment of passage of the trailing wakes. The experiment shows that all trailing wakes vary in width and shape. Two of the middle trailing wakes have a normal width agreeing with the static tests. The extreme right hand wake on the oscillogram is very wide and spikes and dips in the total pressure are observed in it, which obviously indicates a separation of the flow from the blade. Between the wakes we can see a large-scale surge in total pressure. The intensity of this surge varies according to the height of the blade and depends on the performance of the stage.

Let us also note the basic problem which is associated with the trailing wakes forming during the flow of wet steam in subsequent stages of the condensation steam turbines. It is obvious that the water which forms in the condensation of the steam is separated into curvilinear channels of the nozzle cascade and moves along the surface of the guide blades. It enters the trailing wake from the boundary layer. The rate of motion of the drops is less than the rate of motion of the steam, and therefore the drops strike the operating blade at a significant angle of attack. The forces which set in here may produce not only erosion of the blades but also vibrations. Since the operating blades have a low natural frequency of vibrations, for dangerous vibrations to set in it is necessary to have a circumferential nonuniformity of the wakes.

§ 9.2 Dynamic Stresses in Blades, Produced by Nonuniformity in the Flow.

Let us pose the problem of determining dynamic stresses in the blades of a turbomachine operating in a nonuniform flow.

We shall look at the stage of an axial flow turbomachine consisting of two ring cascades. The wakes are induced by the first cascade; the second rotates in a nonuniform flow. Nonstationary forces and moments producing the dynamic stresses influence the blades of the second cascade. Let us assume that the blades have a constant cross section profile and are not bound into packets. This assumption is made for simplicity of discussion.

Let us set the origin at the root cross section of the blade and combine it with the center of the bend. The absicissa axis is directed along the blade and the ordinate axis along the axis of minimum inertia. Let us represent the blade of the turbomachine as an elastic rod of constant profile fixed at the base and free at the top which may carry out small bending and torsional oscillations. The rigidity of the rod in the direction of the flow is quite high.

We can write the equations of the forced rod oscillations subjected to the moment M and the force $\mathscr{L}$, applied to the center of the bend. The deformations are determined by the shift in the centers of the bend $y(x, \tau)$ and the angles of rotation of the cross sections $\theta(x, \tau)$:

$$\left.\begin{aligned} EI\frac{\partial^4 y}{\partial x^4}+m\frac{\partial^2 y}{\partial \tau^2}+mx_0\frac{\partial^2\theta}{\partial \tau^2}+2hm\frac{\partial y}{\partial \tau}=\mathscr{L},\\ GJ\frac{\partial^2\theta}{\partial x^2}+I_\theta\frac{\partial^2\theta}{\partial \tau^2}+mx_0\frac{\partial^2 y}{\partial \tau^2}+2h_1 I_\theta\frac{\partial\theta}{\partial y}=M. \end{aligned}\right\} \qquad (9.10)$$

Here EI and GJ are the bending and torsional rigidities, m is the mass of the blade per unit length, I_θ is the mass moment of inertia around the elastic axis per unit of length, x_0 is the distance of the

bending center from the center of mass, and h represents the damping factors.

In the general case the blade oscillations are limited bending torsional vibrations. In this case, if the center of the masses coincides with the bending center, the differential Equations (9.10) are separated into two independent equations

$$\left.\begin{aligned} EI\frac{\partial^4 y}{\partial x^4}+m\frac{\partial^2 y}{\partial \tau^2}+2hm\frac{\partial y}{\partial \tau}=\mathscr{L},\\ GJ\frac{\partial^2 \theta}{\partial x^2}+I_\theta\frac{\partial^2 \theta}{\partial y^2}+2hI_\theta\frac{\partial \theta}{\partial \tau}=M. \end{aligned}\right\} \tag{9.11}$$

Consequently the bending and torsional vibrations become independent and may be considered separately. If the distance between the mass center and the bending center is not equal to zero, but is relatively small (which is often satisfied in the blades of turbomachines), then although we observe combined bending-torsional vibrations, they can be referred to the first two modes. One vibration mode will be primarily bending and the other torsional. Accordingly, the natural frequencies of such bound oscillations will not differ much from the natural frequencies of pure bending and pure torsional vibrations.

In certain problems of forced vibrations of turbomachine blades we can, with completely sufficient accuracy, ignore the relationship between bending and torsional vibrations and study them separately. In problems on classical flutter the coupling of the bending and torsional vibrations is important mainly, since in the absence of coupling, generally no flutter can take place. In this section, which is devoted to forced vibrations we shall ignore the influence of coupling.

Let us [41] further consider the bending vibrations. All arguments in analogy can be extended to purely torsional oscillations.

If the exciting force is absent, then Equation (9.11) is transformed into the equation of free damped vibrations

$$EI\frac{\partial^4 y}{\partial x^4}+2hm\frac{\partial y}{\partial \tau}+m\frac{\partial^2 y}{\partial \tau^2}=0. \tag{9.12}$$

We shall convert to the dimensionless coordinate $\xi=x/l$, where l is the length of the blade, and express the linear mass through the density of the blade material ρ_1 and the area F of the cross section $m = \rho_1 F$:

$$\frac{EI}{\rho_1 F l^4}\frac{\partial^4 y}{\partial \xi^4}+\frac{\partial^2 y}{\partial \tau^2}+2h\frac{\partial y}{\partial \tau}=0. \tag{9.13}$$

After using the method of separation of variables

$$y=X(\xi)T(\tau),\quad 0\leqslant\xi\leqslant 1, \tag{9.14}$$

we find two ordinary differential equations:

$$\left.\begin{aligned}&\frac{\partial^2 T}{\partial \tau^2}+2h\frac{\partial T}{\partial \tau}+\nu^2 T=0,\\&\frac{\partial^4 X}{\partial \xi^4}-\varkappa^4 X=0,\quad \varkappa^4=\frac{\rho_1 l^4 F\nu^2}{EI}.\end{aligned}\right\} \tag{9.15}$$

Here κ is a dimensionless parameter and ν^2 is a separation constant.

Solution to the first of these equations is known:

$$T=Ae^{-h\tau}\cos(\bar{\nu}\tau+\varepsilon),\quad \bar{\nu}=\sqrt{\nu^2-h^2}, \tag{9.16}$$

where $\bar{\nu}$ is the circular frequency of the blade oscillations with damping.

In problems of turbomachine blade vibrations (as, by the way, in the vibration of other engineering designs with no special dampers) the value of $h^2 << \nu^2$, so that in the future we can ignore the influence of damping on the natural frequency and set $\bar{\nu}=\nu$ with a high degree of accuracy.

The second of the equations in (9.15) must be solved for the boundary conditions at the clamping point (there is no bending or rotation of the rod) and at the free end (the bending moment and the intersection force are absent):

$$\left.\begin{aligned} X(0)=0, \quad \frac{\partial X(0)}{\partial \xi}=0, \\ \frac{\partial^2 X(1)}{\partial \xi^2}=0, \quad \frac{\partial^3 X(1)}{\partial \xi^3}=0. \end{aligned}\right\} \tag{9.17}$$

The general solution to this equation will be:

$$X=B_1 \operatorname{ch} \varkappa\xi+B_2 \operatorname{sh} \varkappa\xi+B_3 \cos \varkappa\xi+B_4 \sin \varkappa\xi.$$

Here B_1, B_2, B_3, B_4 are constants which are determined with the aid of the boundary conditions (9.17).

The obtained system of four equations is a homogeneous one. After equating the determinant of the system to zero, we find the equation for the natural frequencies of the blade (see, for example, [41]):

$$\operatorname{ch} \varkappa \cos \varkappa=-1.$$

This equation has an infinite set of roots, the first six of which are equal to

$$\varkappa=1{,}875;\ 4{,}694;\ 7{,}855;\ 10{,}966;\ 14{,}137;\ 17{,}289.$$

The natural frequencies of the blade vibration are determined by the formula

$$\nu_n=\frac{\varkappa_1}{l^2}\sqrt{\frac{EI}{\rho_1 F}}. \tag{9.18}$$

The general solution to Equation (9.15) is the sum of the partial solutions and represents the damping vibration

$$y=\sum_{n=1}^{\infty} A_n X_n e^{-kt} \cos(\nu\tau+e_n). \tag{9.19}$$

Here X_n represents the so-called major forms of the vibrations and satisfies the orthogonality condition

$$\int_0^1 X_n(\xi) X_m(\xi) d\xi = 0, \quad (n \neq m), \tag{9.20}$$

which physically denotes the energy independence of the oscillation modes, i.e., the impossibility of transmitting energy from one mode to another.

Since the functions $X_n(\xi)$ may be determined only with an accuracy up to a constant factor, we can subject them to the condition of normalization

$$\int_0^1 X_n^2(\xi) d\xi = 1. \tag{9.21}$$

Now let us look at the forced blade oscillations acted on by the perturbing forces. Let us write the vibration equation in the form

$$EI \frac{\partial^4 y}{\partial x^4} + \rho_1 F \frac{\partial^2 y}{\partial \tau^2} = \mathscr{Q}(x, \tau), \tag{9.22}$$

where by $\mathscr{Q}$ we mean all forces which may act on the blade. If $\mathscr{Q}=0$ then (9.22) is converted into the equation of free vibrations without damping.

Let us write the system of forces in the following manner:

$$\mathscr{Q}(x, \tau) = \mathscr{Q}_1(x) e^{i\Omega\tau} - \mathscr{Q}_2 \frac{1}{jl} \frac{\partial y}{\partial \tau} - 2hF\rho_1 \frac{\partial y}{\partial \tau}. \tag{9.23}$$

Here the first term represents the distributed force which excites the blade oscillations. In the future we shall bear in mind that this force is produced by the nonuniformity of the flow. The law governing its distribution along the blade is now assumed to be arbitrary and is given by the dimesionless function $\mathscr{Q}_1(x)$. We look at only one

harmonic of the force with frequency f. The second term is the aerodynamic damping force of the vibrations due to the transfer of energy to the flow. Here we have taken the fact that the force of damping is proportional to the velocity of the vibrations into account. The quantity $\mathcal{P}_2$=const has the dimensionality of force; the factor $1/l$ is introduced in order to satisfy the dimensionality. The latter term was encountered above and represents the force of the mechanical damping (due to the energy dissipation in the blade material and at the site of the closing). A minus sign is placed before the forces of damping since they damp the vibrations. Let us convert to dimensionless coordinates and time

$$\xi=\frac{x}{l}, \quad \eta=\frac{y}{l}, \quad \lambda=\tau f. \tag{9.24}$$

After combining (9.22), (9.23) and (9.24) we find

$$\frac{EI}{\rho_1 F l^4 f^2}\frac{\partial^4\eta}{\partial\xi^4}+\frac{\partial^2\eta}{\partial\lambda^2}=\frac{\mathcal{P}_1(\xi)}{\rho_1 F l f^2}e^{i\lambda}-\frac{\mathcal{P}_2}{\rho F l f^2}\frac{\partial\eta}{\partial\lambda}-\frac{2h}{f}\frac{\partial\eta}{\partial\lambda}. \tag{9.25}$$

On the basis of the Gilbert-Schmidt theorem, solution to this equation can be sought in the form of a series

$$\eta=\sum_{n=1}^{\infty}T_n X_n. \tag{9.26}$$

Here $X_n(\xi)$ represents the free blade vibration modes, $T_n(\lambda)$ represents the unknown functions which depend only on dimensionless time. After substituting the Series (9.26) in Equation (9.25) and substituting the derivative of fourth order with the aid of (9.15) we obtain

$$\sum_{n=1}^{\infty}\left[\frac{\partial^2 T_n}{\partial\tau^2}+\frac{1}{\pi}(\delta_2+\delta_3)\frac{\partial T_n}{\partial\tau}+\frac{\nu_n^2}{f^2}T_n\right]X_n=\frac{\mathcal{P}_1(\xi)}{\rho_1 F l f^2}e^{i\lambda}. \tag{9.27}$$

Here we have introduced the symbols δ_2, the aerodynamic and δ_3, the mechanical logarithmic decrements of the vibrations.

$$\delta_2 = \frac{\pi \mathscr{P}_0}{\rho_1 F l j^2}, \quad \delta_3 = \frac{2hn}{\nu}; \tag{9.28}$$

ν_n is the frequency of the natural vibrations for the mode X_n.

To determine the function T, we multiply the left-hand and the right-hand sides of (9.28) by $X_m(\xi)$ and integrate with respect to ξ in the limits 0 to 1. Then on the basis of the condition of orthogonality (9.20) only the term with the index m remains on the left-hand side. On the basis of the condition of normalization (9.21) the integral of $X_n^2(\xi)$ is equal to 1. Then to determine the time function we find the equation

$$\frac{\partial^2 T_m}{\partial \tau^2} + \frac{1}{\pi}(\delta_2 + \delta_3 j)\frac{\partial T_m}{\partial \tau} + \frac{\nu_m^2}{l^2} T_m = \frac{1}{\pi}\delta_1 e^{j\lambda}. \tag{9.29}$$

Here we have introduced the concept of the coefficient of excitation

$$\delta_1 = \int_0^1 \frac{\pi \mathscr{P}(\xi) X_m(\xi)\, d\xi}{\rho_1 F l^2}. \tag{9.30}$$

Equation (9.29) describes the process of forced vibrations and its solution consists of a sum of two functions, one of which damps out with time and the other is a periodic function. In studying the stationary forced vibrations we are interested only in the periodic solution

$$T_m = \frac{\delta_1 e^{j\lambda}}{\pi\left(\frac{\nu_m^2}{l^2} - 1\right) + j(\delta_2 + \delta_3)}. \tag{9.31}$$

We shall confine ourselves only to one harmonic and shall not examine the sum of series, since it is of practical interest to study the resonance or near-resonance systems. In this case all the harmonics are negligibly small in comparison with the harmonic having the frequency of the perturbing force. In this expression the coefficient of excitation δ_1 may be assumed to have a real (for j) value, since for stationary vibrations, the phase shift of the perturbing force has no significance. The coefficient of mechanical damping δ_3 is also a real value (for j) since we took

into account that the mechanical resistance is in phase with the velocity of the vibrations. The coefficient of aerodynamic damping may be a complex quantity since the aerodynamic dampting force has a phase shift with respect to the velocity of the vibrations.

However, in view of the smallness of δ_2 and δ_3 the maximum amplitude will be observed in practice when $f = \nu$ and will be equal to

$$|T_{max}| \approx \frac{\delta_1}{\delta_2 + \delta_3}. \tag{9.32}$$

Here by δ_2 we mean its real part.

Now let us determine the maximum stress in the base section of the blade. Using (9.26) and (9.32) we can find the bending moment at the base of the blade at resonance

$$M(0) = EI\left(\frac{\partial^2 y}{\partial x^2}\right)_{x=0} \approx \frac{\delta_1}{\delta_2 + \delta_3} \frac{EI}{l}\left(\frac{\partial^2 X}{\partial \xi^2}\right)_{\xi=0}.$$

The maximum dynamic stress in the base section at resonance is equal to

$$\sigma(0) = \frac{M}{W} \approx \frac{\delta_1}{\delta_2 + \delta_3} \frac{EI}{lW} X''(0). \tag{9.33}$$

Here, W is the minimum moment of resistance of the blade section.

The energy of the coefficients of excitation and damping was studied in the section devoted to modeling and experimental research.

Analogous formulas may be found for the torsional vibrations. We shall assume that we can study the purely torsional vibrations of blades subject to the equation

$$GJ\frac{\partial^2 \theta}{\partial x^2} + I_\theta \frac{\partial^2 \theta}{\partial \tau^2} = M(x, \tau). \tag{9.34}$$

The moment which acts on the blade can be determined in the following manner:

$$M(x, \tau) = M_1(x) e^{i\Omega\tau} - M_2 \frac{1}{f} \frac{\partial\theta}{\partial\tau} - 2h_1 I_\theta \frac{\partial\theta}{\partial\tau}. \qquad (9.35)$$

Here, the first term is a distributed moment which excites the blade vibrations. The second (M_2 = const) and the third terms take into account the aerodynamic and mechanical damping during torsional vibrations. Let us convert (9.34) and (9.35) to dimensionless coordinates and time using (9.24):

$$-\frac{GI}{I_\theta l^2 f^2} \frac{\partial^2\theta}{\partial\xi^2} + \frac{\partial^2\theta}{\partial\lambda^2} = \frac{M_1(\xi)}{I_\theta f^2} - \frac{M_2}{I_\theta \nu^2} \frac{\partial\theta}{\partial\tau} - \frac{2h_1}{f} \frac{\partial\theta}{\partial\lambda}. \qquad (9.36)$$

To solve this equation, we must first find the vibration modes. Let us set the right hand side of (9.36) equal to zero and proceed to an examination of the free vibrations by substituting ν for f (the natural frequency of the torsional vibrations. After denoting $\theta = X(\xi)T(\lambda)$, we can separate the variables

$$\frac{\partial^2 X_n}{\partial\xi^2} + \varkappa^2 X_n = 0, \quad \frac{\partial^2 T_n}{\partial\tau^2} + \nu^2 T_n = 0, \quad \varkappa^2 = \frac{I_\theta l^2 \nu^2}{GI}. \qquad (9.37)$$

After writing the solutions

$$X_n = A_n \cos \varkappa_n \xi + B_n \sin \varkappa_n \xi, \quad T_n = C_n \cos p_n \theta + D_n \sin p_n \theta,$$

and using the boundary conditions in the blade vibration, which is strictly restrained at the base and free at the top

$$X_n(0) = 0, \quad \frac{\partial X(1)}{\partial\xi} = 0,$$

we find

$$A_n = 0, \quad \varkappa_n = \frac{\pi}{2} + k\pi.$$

The natural frequencies are determined by the formula

$$\nu_n = \frac{\varkappa_n}{l} \sqrt{\frac{GI}{I}}. \qquad (9.38)$$

The constant B_n can be determined from the condition of normalization

$$B_n^2 \int_0^1 \sin^2 \varkappa_n \xi \, d\xi = 1, \quad B_n = \sqrt{2}$$

Equation (9.36) for the forced vibration is solved in the usual manner and is reduced to Formula (9.31).

The coefficient of excitation of the torsional vibrations is equal to

$$\delta_1 = \frac{\pi \sqrt{2}}{\nu^2 I_0} \int_0^1 M_1(\xi) \sin \varkappa \xi \, d\xi. \tag{9.39}$$

The coefficients of the aerodynamic and mechanical damping with torsional vibrations are respectively equal to

$$\delta_2 = \frac{\pi M_\xi}{I_0 \nu^2}, \quad \delta_3 = \frac{2\pi h_1}{\nu}. \tag{9.40}$$

The maximum torsion of the blade occurs at resonance and then by using (9.31) we find

$$\theta = \frac{\sqrt{2}\delta_1}{\delta_2 + \delta_3} \sin \varkappa \xi.$$

The maximum moment in the base section of the blade is equal to

$$M(0) = GI \left(\frac{\partial \theta}{\partial x}\right)_{x=0} = \frac{GI}{l} \left(\frac{\partial \theta}{\partial \xi}\right)_{\xi=0} = \frac{\sqrt{2}\delta_1}{\delta_2 + \delta_3} \frac{\varkappa GI}{l}. \tag{9.41}$$

As follows from Formulas (9.33) and (9.41), the dynamic stresses at resonance are proportional to the coefficient of excitation and inversely proportional to the total coefficient of damping. If the coefficient of aerodynamic damping is small, then the stresses are proportional to the ratio δ_1/δ_3. Since δ_1 is proportional to the density of the liquid, in this case then the dynamic stresses are proportional to the density of the liquid also. Consequently, under this condition ($\delta_2 = \text{const}$) a proportionality will exist between the dynamic and the static stresses in the blades. In the other limiting case, when the aerodynamic coefficient of damping is substantially greater than the mechanical one ($\delta_2 \gg \delta_3$), the dynamic stresses are proportional to the

ratio δ_1/δ_2 . Since δ_1 and δ_2 are proportional to the density of the liquid, then in this case the dynamic stresses will not depend on the density of the liquid, i.e., they are not proportional to the static stress. In fact, the mechanical decrement of the vibrations is also not a constant value but depends on the stress.

These comments have practical application, for example, in converting the dynamic stresses in the blades, measured in static tests at reduced pressure, into real operating conditions.

From these same formulas there follows still one other important conclusion.

The coefficient of excitation (i.e., essentially the nonstationary aerodynamic force) depends on the value of the phase shift when the vortex wakes act on the blades. This is explained by the fact that there is a reciprocal influence of the blades through the flowing gas or liquid. The circulation induced by the wake to some blade creates forced circulations (and this means forces as well) on the neighboring blades. In turn, the vortex wakes induce circulation also on the neighboring blades. Thus, the nonstationary aerodynamic forces depend both directly on the effect of the wake on the given blade and on a certain supplemental force produced on the given blade (due to interference in the cascade) by the effect of wakes on the neighboring blades. It is obvious that the total nonstationary force depends on the phase shift of the component forces.

The coefficient of aerodynamic damping also depends on the phase shift of the blade vibrations. In a uniform cascade, when all blades are under identical conditions, the phase shift of the blade vibrations is equal to the phase shift of the neighboring exciting forces. In a nonuniform cascade, the phase shift of the blade vibrations depends also on the scatter of the natural partial frequencies of the blades.

Thus, ultimately the dynamic stresses in the blades must depend on the phase shift of the influence from the vortex wakes.

§ 9.3. Dynamic stresses in Blades With Partial Input

In several stages of steam turbines it is necessary to use the so-called partial input of steam, i.e., an input over only a part of the wheel rather than the entire circumference. The ratio of the length of the arc on which the input of the working medium is carried out, to the length of the circumference is called the degree of partiality, e. Thus, in the operation of such a stage, the operating blades are periodically subjected with a full load and then are completely unloaded. When the blades are struck by a steam jet flowing at a high (often supersonic) velocity, and the jet then leaves, complicated nonstationary phenomena take place. The lifting on a quite small segment reaches the maximum value, is maintained constant on some segment and then with no jet drops to zero. The precess of change in the lefting must be accompanied by the formation of intense vortex wakes on which the actual loading rate of the blades depends. At supersonic velocities the picture is complicated by the formation of nonstationary schock waves and expansion waves. The physical picture is so complicated that at the present time no methods can be suggested for solving such a problem.

For practical purposes, it is first of all necessary to evaluate the maximal dynamic stresses which occur in the blades. This problem was studied by U. Ye. Rivosh, A. Z. Shemtov, A. V. Levin [41] et al. At the present time, it is possible only to give an upper estimate for these stresses for the most unfavorable operating conditions, and also to conduct experimental proof of this evaluation. The most unfavorable load will be the sudden application of the total power at the blade inlet by a jet and then also the sudden removal of the force on the blade at the exhaust.

Before we solve the problem, let us mention several characteristics of the conditions of blade oscillations of stages with partial input of steam. The blades of these stages have a very high rigidity and low height, such that their natural vibration frequency is equal to several kilohertz (up to 3000 - 4000 Hz). Therefore, at a standard

50 Hz frequency of rotation of the turbine rotor the resonance frequencies differ by 1 — 2%. Along with this, the scatter in natural frequencies of the blades on the wheel is no less than 10% as measurements show. Therefore, in evaluating the incipient stresses it is necessary, as we know, to assume that some blades are always in resonance. From the above, it is clear that it is impossible to get rid of the resonance by building up the blades.

Let us write the equation for blade vibrations for a system with one degree of freedom, ignoring the relationship with other blades:

$$\ddot{y}+\nu\frac{\delta}{2\pi}\dot{y}+\nu^2 y=\frac{1}{m}\mathscr{P}(\tau). \tag{9.42}$$

Here, ν is the natural frequency of the blade vibrations, δ is the logarithmic decrement of the vibrations, m is the mass of the blade, $\mathscr{P}(\tau)$ is the force which acts on the blade; the force is chosen in the form of a rectangular load.

In general, since the problem is a linear one, it may be solved by ordinary methods, since any periodic load may be represented by a Fourier series. However, it is simpler to represent it in another form which permits making several simplifications in the course of the conclusion and confirming the characteristics of the problem.

First, instead of the periodically repeating rectangular surge, let us look at the simple gradual change in the load $\mathscr{P}(\tau)=\mathscr{P}_0\sigma(\tau)$,

$$\text{where}\begin{cases}\sigma(\tau)=0 \text{ when } \tau<0,\\ \sigma(\tau)=1 \text{ when } \tau>0.\end{cases}$$

Here, $\sigma(\tau)$ is the unit function. Let us assume that we know the initial conditions: $y(0)$ is the bend and $\dot{y}(0)$ is the rate of the blade vibration just before the load is applied.

After applying the Laplace transform to Equation (9.42) under the given initial conditions, we find

$$s^2Y + Y(0)s - \dot{Y}(0) + \nu\frac{\delta}{2\pi}[sY - Y(0)] + \nu^2 Y = \frac{\mathcal{P}_0}{m}\frac{1}{s}.$$

After solving this algebraic equation relative to the Laplace transform, from the unknown function we find

$$Y(s) = \frac{\mathcal{P}_0}{m}\frac{1}{s\left(s^2 + \frac{s\nu\delta}{2\pi} + \nu^2\right)} + Y(0)\frac{s + \frac{\nu\delta}{2\pi}}{s^2 + \frac{s\nu\delta}{2\pi} + \nu^2} + \dot{Y}(0)\frac{1}{s^2 + \frac{s\nu\delta}{2\pi} + \nu^2}.$$

If we expand the denominator into factors, we can ignore the quantity $(\delta/2\pi)^2$ in comparison with unity, since in these problems the logarithmic coefficient of damping is equal to 0.01 — 0.03, i.e., we can set

$$s_{1,2} = -\frac{\delta}{2\pi}\nu \pm \nu\sqrt{(\delta/2\pi)^2 - 1} \approx \delta\nu/2\pi \pm j\nu.$$

Then after taking the inverse Laplace transform, we find, with an accuracy up to the first power of δ:

$$y(\tau) = \frac{\mathcal{P}_0}{\nu^2 m} + \frac{\mathcal{P}_0}{\nu^2 m}e^{-\frac{\delta}{2\pi}\nu\tau}\left(-\frac{\delta}{2\pi}\sin\nu\tau - \cos\nu\tau\right) + \\ + y(0)e^{-\frac{\delta}{2\pi}\nu\tau}\left(\frac{\delta}{2\pi}\sin\nu\tau + \cos\nu\tau\right) + \dot{y}(0)e^{-\frac{\delta}{2\pi}\nu\tau}\frac{1}{\nu}\sin\nu\tau. \qquad (9.43)$$

This expression is valid on the segment following the jump in the load ($\tau > 0$). As we would expect after the jump in the load, the amplitudes change and furthermore the vibrations damp out according to an exponential law. It is also obvious that the vibration amplitude directly after the jump slightly depends on the oscillation decrement ($\delta/2\pi \ll 1$).

Let us assume temporarily that the vibration decrement is equal to zero and we find

$$y(\tau) = y_0 + [y(0) - y_0]\cos\nu\tau + \frac{1}{\nu}\dot{y}(0)\sin\nu\tau. \qquad (9.44)$$

To obtain this dependence we must also take into account that the first term in Expression (9.43) is a static deflection in the

blade subjected to the force $\mathscr{P}_0$

$$y_0 = \frac{\mathscr{P}_0}{\nu^2 m}.$$

Since the blade also oscillated prior to change in load according to a sinusoidal law

$$y(\tau) = y_1 \cos(\nu\tau + \varphi), \tag{9.45}$$

then at zero time we have

$$y(0) = y_1 \cos\varphi, \quad \dot{y}(0) = -\nu y_1 \sin\varphi. \tag{9.46}$$

Expression (9.44) is reduced to the form using (9.46)

$$y(\tau) = y_0 + (y_1 \cos\varphi - y_0)\cos\nu\tau - y_1 \sin\varphi \sin\nu\tau. \tag{9.47}$$

Thus, the vibration amplitude after the jump in the load depends on the phase angle

$$\sqrt{(y_1\cos\varphi - y_0)^2 + y_1^2\sin^2\varphi} = \sqrt{y_1^2 - 2y_1y_0\cos\varphi + y_0^2}, \tag{9.48}$$

and will be greater when $\varphi = \pi$, i.e., in the case when the blade encounters the load at zero velocity and with a deviation to the side opposite to the force. This condition is obvious, since in this case the greatest energy will be introduced into the vibrating system. The energy is introduced at half the vibration period. The force then remains constant and consequently does not introduce energy into the vibrating system.

If the load is removed suddenly, then the arguments remain the same, since the jump takes place in the opposite direction. Thus, it is obvious that the blade receives the greatest energy if a whole number of cycles and a half is stacked up on the segment where the forces are acting. This case leads to a maximum vibration amplitude; therefore, it will be the worst and consequently we must take it into account.

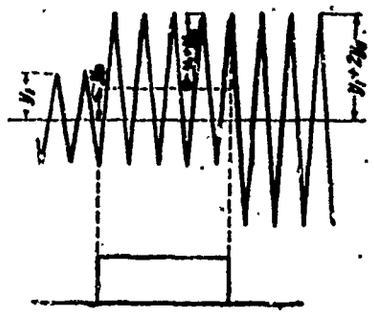


Figure 9.15. Blade vibrations without damping with the single effect of a gradual load (the sine curve is conventionally shown by the broken line); y_1 is the amplitude of the vibrations before effect of the load; y_0 is the static deflection.

The graph of the vibration (without damping and the simple effect of the load) is shown on Figure 9.15. The amplitude of the vibrations on the initial segment is equal to y_1; on the active segment according to (9.48) it is equal to $y_1 + y_0$ and after the load is removed is equal to $y_1 + 2y_0$.

If the action of the force is repeated periodically, then the amplitude of the vibrations will increase infinitely. However, this does not take place if we take into account the dissipation of energy during the vibrations. In this case, vibrations occur for which the removal of energy over one revolution of the wheel will be equal to the input.

If we return to Formula (9.43) and ignore the terms where the factor is a small quantity δ, we find the vibration law over the active segment (for the most dangerous case)

$$y(\tau) = y_0 - e^{-\frac{\delta}{2\pi}\nu\tau}(y_1 + y_0)\cos\nu\tau - y_1 e^{-\frac{\delta}{2\pi}\nu\tau}\sin\nu\tau. \qquad (9.49)$$

Let the blade, being in resonance, make k_n complete vibrations per one revolution of the wheel. We can find the vibration amplitude at the end of the active segment, whose relative length is equal to the degree of partiality

$$(y_1 + y_0)e^{-\varepsilon\delta k_n}. \qquad (9.50)$$

This expression is found ing Formula (9.49) by taking into account the fact that on the active arc, εk_n vibrations occur.

εk_n is equal to the integral and one half. Consequently, the time of passage of this arc is equal to $2\pi\varepsilon k_n/\nu$ and $\cos \nu\tau=-1$, and $\sin \nu\tau=0$.

After removal of the load the vibration amplitude is increased due to the potential energy of the static deformation and will be equal to

$$y_0+(y_1+y_0)e^{-\varepsilon\delta k_n}. \tag{9.51}$$

Furthermore, on the arc, equal to $1-\varepsilon$, the free damped vibrations continue. On this arc $(1-\varepsilon)k_n$ vibrations take place and, consequently, the amplitude at the end of the free arc is found by multiplying the initial amplitude (9.51) by the exponential factor $\exp\left[-(1-\varepsilon)\delta k_n\right]$. The obtained expression in view of the periodicity of the process $y(\tau)=y(\tau+k_n 2\pi/\nu)$, must be equal to the amplitude of the vibrations directly before the load is applied to the blade, i.e.,

$$\left[(y_1+y_0)e^{-\delta\varepsilon k_n}+y_0\right]e^{-\delta(1-\varepsilon)k_n}=y_1.$$

Hence, we find

$$\frac{y_1}{y_0}=\frac{e^{-\delta k_n}+e^{-\delta(1-\varepsilon)k_n}}{1-e^{-\delta k_n}}. \tag{9.52}$$

The danger of the vibration process may be evaluated as the ratio of the maximum deflection to the known static deflection

$$\lambda=\frac{y_1+2y_0}{y_0}=2+\frac{y_1}{y_0}=2+\frac{e^{-\delta k_n}+e^{-\delta(1-\varepsilon)k_n}}{1-e^{-\delta k_n}}. \tag{9.53}$$

From (9.53) it follows that the influence of the degree of partiality for small δk_n on the dynamic coefficient λ is small, and the worst case corresponds to the maximally possible ε (theoretically):

$$\varepsilon=\frac{\left(k_n-\frac{1}{2}\right)}{k_n}=1-\frac{1}{2k_n}\approx 1, \text{ since } k_n\gg 1.$$

If we assume $\varepsilon = 1$ and assume that δk_n also has a sufficiently small value, then from (9.53) we find the approximate dependence

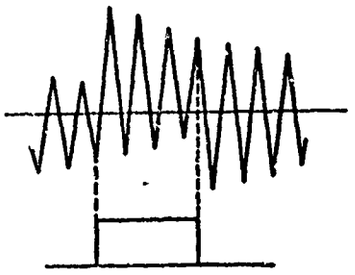


Figure 9.16. Blade vibration with damping with a gradual load.

ordinarily used in the theory of turbine strength [41],

$$\lambda = 1 + \frac{2}{\delta k_n}. \tag{9.54}$$

Figure 9.16 shows a graph of the blade vibrations with transmission of a rectangular load allowing for damping. The maximum amplitude of the oscillations takes place at the inlet with the load $y_1 + y_0$ or at the output $y_0 + (y_1 + y_0)\exp(-\varepsilon\delta k_n)$. Using (9.52) it is easy to show that the first case is realized when $\varepsilon > 0{,}5$, and the second when $\varepsilon < 0{,}5$.

Analogously, we can find the dependences for other types of loads.

It is also interesting to compute the general case when we have several input arcs of the working body.

From the characteristics of the turbine operation [72] we know that the static deflections on all active arcs are identical, with the exception possibly of one arc whose valve is partially open. However, if several input arcs are open, then it is of considerable interest to determine the dynamic stresses with complete input of the working medium, i.e., under identical static deflections. From turbine theory we also know that the maximal static stresses set in with one completely open valve, supplying one input arc. When the number of input arcs is increased, the static stresses drop; however, the dynamic stresses may increase, since the number of segments is increased on which the energy is introduced into the oscillating system. Usually, the maximal dynamic stresses set in with two fully open valves, feeding two input arcs. The value of the static pressures depends on the turbine characteristics; the method of determining them for any process has been developed, and therefore they may be

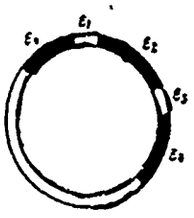


Figure 9.17. Distribution of the input arcs.

assumed to be known. Therefore, we are concerned only with the problem of evaluating the maximal dynamic coefficient.

Let the circumference of the wheel be divided into an even number of arcs equal to n. Let the input arcs be all the odd arcs (Figure 9 17). We can denote the the relative length of the arcs $\varepsilon_1, \varepsilon_2, \ldots, \varepsilon_n$, and obviously $\varepsilon_1 + \varepsilon_2 + \ldots + \varepsilon_n = 1$. Let us denote the amplitude of the oscillations at the beginning of each active odd arc by y_m. We assume that on each arc the most dangerous case is realized on each arc, and the numbers $\varepsilon_m k_n$ are whole numbers plus one half, where k_n is a whole number of blade oscillations with passage around the entire circumference.

From these conditions, on the basis of the previous computations it follows that first of all at the site of the transition from one arc to another the amplitude of the oscillations increases by the value of the static deflection y_0, which the blade had with passage of the active arc. Secondly, with passage of the blade along any arc, either even or odd, damping oscillations are observed. This latter comment permits us to relate the amplitude of the blade oscillations at the end of the arc with the amplitude of the oscillations at the beginning of the arc.

In view of the linearity of the problem, we can use the principles of superposition. Thus, at the beginning of the first arc let the maximum amplitude of the blade oscillations be equal to y_1. For one revolution of the wheel the blade completes k_n oscillations and the amplitude is lowered, due to damping, to a value of $y_1 \exp(-\delta k_n)$. At the end of the first arc the blade receives a supplemental surge; its amplitude increases by the quantity y_0. If we look separately at the blade oscillations with this supplemental amplitude, we find that the

blade completes, up to the moment of entry into the first arc, a number of oscillations equal to $(\varepsilon_2 + \varepsilon_3 + \ldots + \varepsilon_n)k_n$. Consequently, the respective amplitude is reduced to a magnitude $y_0 \exp[-\delta(\varepsilon_2+\varepsilon_3+\ldots+\varepsilon_n)]$. Analogous increases in the blade amplitude will be obtained at the ends of the arcs ε_2, ε_3, ..., ε_n. Each of these vibration amplitudes, initially equal to y_0, will be lowered due to damping at frequencites equal respectively to the lengths of the arcs $(\varepsilon_3 + \varepsilon_4 + \ldots \varepsilon_n)$, $(\varepsilon_4 + \varepsilon_5 + \ldots + \varepsilon_n)$, ..., 0. In view of the fact that we are looking at the worst case, each of these oscillations takes place in the same phase. Consequently, the full amplitude at the beginning of the first arc must be equal to the sum of all the computed amplitudes. And this sum, in view of the periodicity of the process, must be equal to the initially selected amplitude at the beginning of the first arc.

Consequently, we find

$$y_1 = y_1 e^{-\delta k_n} + y_0 e^{-\delta(\varepsilon_2+\varepsilon_3+\cdots+\varepsilon_n)k_n} + y_0 e^{-\delta(\varepsilon_3+\varepsilon_4+\cdots+\varepsilon_n)k_n} + y_0.$$

Hence we find

$$\frac{y_1}{y_0} = \frac{e^{-\delta(\varepsilon_2+\varepsilon_3+\cdots+\varepsilon_n)k_n} + e^{-\delta(\varepsilon_3+\varepsilon_4+\cdots+\varepsilon_n)k_n} + \ldots + 1}{1 - e^{-\delta k_n}}. \tag{9.55}$$

For the cyclical permutation we may find the amplitudes of blade vibrations at the beginning of each segment. Usually, it is of practical interest to know only the maximum amplitude. Since the blades receive surges only at the ends of the arcs, then the position of the maximum amplitude is determined by the distance between arc ends. Let the numeration of the segments be selected such that the amplitude y_1 is a maximum.

Then the dynamic coefficient, allowing for the fact that on the active segment there is also a static bend y_0, will be equal to

$$\lambda = \frac{y_1 + y_0}{y_0} = 1 + \frac{e^{-\delta(\varepsilon_2+\varepsilon_3+\cdots+\varepsilon_n)k_n} + \ldots + e^{-\delta\varepsilon_2 k_n} + 1}{1 - e^{-\delta k_n}}. \tag{9.56}$$

If δk_n is such a small value that in the expansion it is sufficient to retain only the first power, then we find the approximate

formula

$$\lambda = 1 + \frac{n - [\varepsilon_1 + 2\varepsilon_2 + \ldots + (n-1)\varepsilon_n]\delta k_a}{\delta k_a}. \qquad (9.57)$$

The maximum dynamic coefficient will be for that arc for which the expression in brackets has a minimal value. Therefore, the proof is easily carried out by computing this sum with the origin on the arc being examine. Here we look at the worst case, which may also not be realized. The comments on this input are given in Chapter 11, where we shall look at the experimental results.

To determine the dynamic forces and also to study the operation of the cascade with partial input of the working medium, it is of interest to measure nonstationary pressures on the surface of the blade. Several experimental investigations in this direction were made by V. T. Yurinskiy and I. Ya. Shestachenko. The experimental turbine had six nozzles with barriers between them that are unequal in thickness. Chang[illegible] the nonstationary pressures on the surface of the rotating blades was carried out using piezoelectric sensors with the signal transmitted through a mercury current collector. The schematic of the measurements and the measuring equipment are described in [91, 92].

Let us look at several experimental results (1). Figure 9.18 shows the operating cascade with the locations indicated where measurements of the nonstationary pressure were made. Figure 9.19 gives typical oscillograms with the recording of pressure at points 1, 3, 6, 7, 9 and 10 (at the remaining measuring points an analogous picture is observed). On all oscillograms we can see six pressure peaks corresponding to the moment of passage of the blades past the nozzles. The pressure peaks are grouped in pairs, since the nozzles are also thus arranged. The barriers between the nozzles in each pair are not the same (the thinnest barrier is in the second pair of nozzles), which determines the value of the trough in the pressure curve between the two peaks.

Footnote (1) appears on page 391

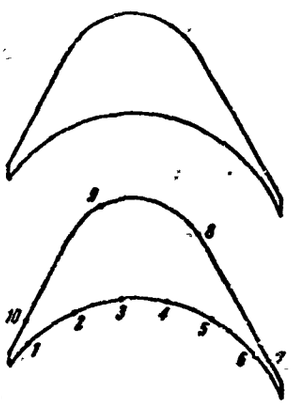


Figure 9.18. Aerodynamic cascade with measuring points of the nonstationary pressure shown.

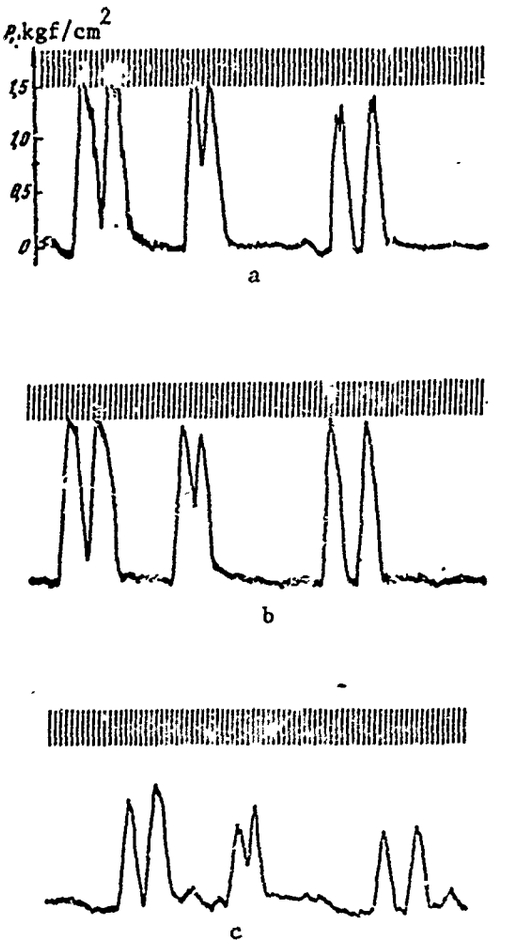
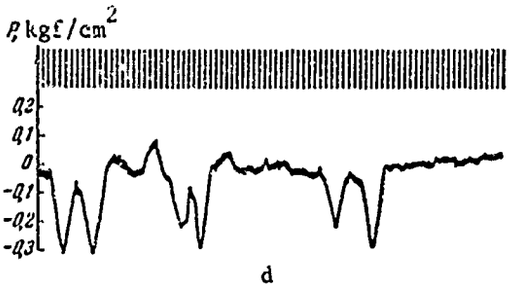
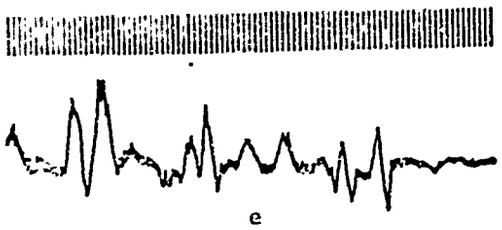


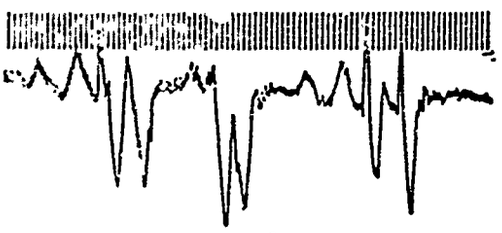
Figure 9.19a,b,c. Oscillograms with recording of pressure on the blade of the rotating cascade with partial in input: a, b, c correspond to points 1, 3, 6 on Figure 9.18. The scale is shown on Figure a.



d



e



f

Figure 9.19d,e,f. Oscillograms with recording of pressure on the blade of the rotating cascade with partial input: d, e, f correspond to points 7, 9, 10 on Figure 9.18. The scale is shown on Figure d.

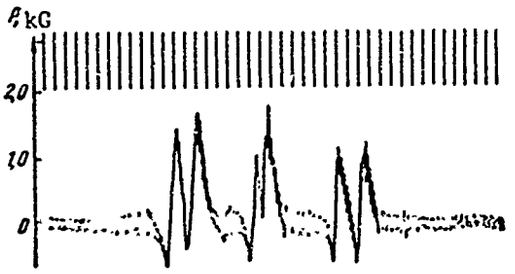


Figure 9.20.

On Oscillograms 9.19a, b and c, corresponding to the concave side of the blade, with entry into the jet coming from the nozzles, we observe an increase in the pressure. At measurement points 10 and 7 (Oscillograms 9.19 and f) the pressure is lowered. At point 9 (Oscillogram 9.19e) we observe more random oscillations in pressure, which obviously is produced by the appearance of jumps in density since a supersonic flow approaches the operating blades (the ratio of pressures in the state is 0.2). Let us note that on the convex side of the blade with entry into the nozzle, up to the appearance of vacuum, the pressure after passage of the wide barriers is

increased (especially at points 9 and 10). This is explained by the deviation of the gas jets, coming from the nozzle cascade, to the side opposite the rotation of the wheel, i.e., by the appearance of a negative angle of attack.

The observed process influences the efficiency of operation of the cascade and also is of interest from the viewpoint of dynamic strength of the blades. The direct experiment on weighing the force acting on the rotating blade confirms this phenomenon. Figure 9.20 (where the force which acts on the blade in this stage is described) clearly shows that until a positive force directed to the side of the rotation of the wheel occurs, a negative force is observed. An analogous picture is also observed in the partial stages with subsonic velocities of the flow.

The appearance of a negative force with the given relationships of loading time and period of natural oscillation of the blades may lead to an increase in the dynamic stresses. However, we must mention that these preliminary investigations have primarily a qualitative character.

FOOTNOTE

1. on page 387 Analogous investigations on a large stage were made in the Moscow Power Institute (MPI) using strain gauge measurements.

CHAPTER 10

OSCILLATION OF A COUPLED SYSTEM OF BLADES

§ 10.1. The Blade Ring as a Coupled System of Blades

In the preceding sections, each blade was regarded as a separate elastic system, not coupled with the other blades. Account was taken of the aerodynamic interference of the blade in a cascade; however, no consideration was given as to how this affects the oscillation of the entire system. In actuality, in many cases it is necessary to regard the blade ring as a single elastic system. In the general case, coupling between the blades is effected through the elastic disk, through elastic couplings (tape bindings and wires) and through a fluid flow.

Consideration of the oscillation of a set of blades as a single system shows that new phenomena can originate in it, which are not manifested in a single blade. It turns out that under specific conditions, dynamic instability of the blade can appear, and self-oscillations can originate. Interesting problems, which are of practical importance, arise during a study of the oscillations of a

cascade consisting of nonuniform blades[1]. The basic feature of the oscillation of a blade ring in comparison to the oscillation of an individual blade consists in the exchange of energy among the blades themselves and between the flow and the blades.

Practical interest is afforded by two problems. The first concerns the forced oscillations of blades situated in an unsteady stream, and the second one concerns the stability loss of an elastic system in a uniform flow.

Let us consider a system of uniform blades fixed on an elastic disk. A stream of gas flows around the blade system.

For the analysis of specific problems, we introduce some simplifying assumptions. We shall replace a blade which is an elastic blade with an infinite number of degrees of freedom by an oscillator having only one degree of freedom. The possibility of such a replacement is explained by the fact that the greatest interest is afforded by the study of near-resonance regimes, while loss of blade stability in a cascade takes place considerably more easily in the case of purely bending or purely torsional oscillations. Velocities usually unattainable in turbomachines are required for inducing bending-torsional flutter. In most cases it is also possible to consider these oscillations separately when studying forced oscillation.

We shall take account of the interaction among the blades through the elastic disk, as well as through the flow, by means of influence coefficients. We assume that the profiles in the cascade have an arbitrary shape, but that their shift in the course of the oscillation process is small in comparison to the cascade step, and that the oscillation velocity is small in comparison to the velocity of the main stream. Thus, we assume that the effect of unsteady interference may be linearized, i.e., the unsteady part of the mutual influence

---

Footnote (1) appears on page 438.

may be linearized, i.e., the unsteady part of the mutual influence may be represented by a sum of two terms, one of which is proportional to the shift, and the other is proportional to the oscillation velocity. We emphasize that the value of steady profile interaction, determined by the cascade geometry and by the main stream, may be arbitrary.

Questions connected with replacement of the blades by an equivalent oscillator, as well as the choice of influence coefficients, have in a sense been touched upon above, and at present we shall devote our attention to the problem of stability on the whole.

We write the equation of the oscillation of an arbitrary n^{th} blade:

$$m\ddot{y} + K_n y_n = F_n. \qquad (10.1)$$

Here m is the mass of the oscillator, K_n is the rigidity of the oscillator spring, F_n is the external force acting upon the blade. The dot signifies differentiation in time.

In the case at hand the damping coefficient takes account of that part of the damping which originates for oscillation of only the blade under consideration, while the others are motionless. The influence of the remaining blades upon the damping (or, on the contrary, upon excitation) of oscillations of the blade under consideration is taken into account by the external load.

With the assumptions made above, the external load may be expressed in terms of the influence coefficients

$$F_n = \sum_{k=1}^{z} K_n^{(k)} y_k + \sum_{k=1}^{z} \mathcal{L}_n^{(k)} \dot{y}_k. \qquad (10.2)$$

Here z is the number of blades on the wheel, $K_n^{(k)}$ is the force acting upon blade n with a unit shift of blade k, $\mathcal{L}_n^{(k)}$ is the force acting

upon the blade n with a single instantaneous oscillation velocity of blade k.

The propagation velocities of a signal are not infinitely great either in a gas or in the material of the disk. This must be taken into account when determining the influence coefficients. However, in practice this pertains only to aerodynamic influence coefficients, since the propagation velocities of a displacement wave $a = \sqrt{\mu/\rho_1}$ and a longitudinal wave $a = \sqrt{E/\rho_1}$ in metal are very great (μ is the shear modulus, E is the modulus of elasticity, ρ_1 is the density of the metal). Since only the influence of adjacent blades is significant, and the ratio of the perturbation wavelengths to the blade spacing $2\pi a/\nu t$ (even with an oscillation frequency of several kilohertz) is very great, the problem of elastic influence coefficients may be regarded as a quasi-steady one.

In the general case influence coefficients are complex numbers, since the acting forces, generally speaking, are not in phase with the causes that have induced them: displacement and displacement velocity. For aerodynamic influence coefficients, this is explained by the origination of a vortex wake in case of a change of circulation brought about both by displacement and by displacement velocity. The influence coefficients include the coefficients of elastic and aerodynamic coupling of the cascade. Let us note the basic difference between these coefficients.

The coefficients of elastic coupling are subject to the reciprocity theorem

$$K_n^{(k)} = K_k^{(n)},$$

and constitute the force with which blade k with a unit displacement acts upon blade n (or conversely). These influence coefficients are real numbers.

The aerodynamic influence coefficients do not constitute the force of action by one plate upon another. For example, a displacement of blade k produces a change in the aerodynamic force acting upon blade n. What is changed is a force acting from a third body — the stream. Therefore, a displacement of blade n need not necessarily induce an equal and opposite force on blade k. A similar remark is valid with respect to coefficients $\mathcal{D}_n^{(k)}$. Aerodynamic influence coefficients, as has already been said, are complex numbers, since during vibration of blades, forces with a phase shift are induced. The aerodynamic component of coefficients $K_n^{(k)}$ is significant only in the case where there is static circulation of velocity about the blades of the cascade, i.e., the cascade deflects the stream (external cascade). In this case the field about the cascade is nonuniform, and the shift of the blade during the oscillation process brings about the appearance of a supplemental unstable force. In case of the oscillation of a single wing or a plate cascade with a zero angle of attack of the main stream, this supplemental force is absent (or is a value of the second order of smallness, since the nonuniformity of the stream is of the first order of smallness and a small displacement induces aerodynamic forces of the second order of smallness).

The relationship between the values of the aerodynamic forces proportional to the displacement and the oscillation velocity depends upon the oscillation frequency and the static circulation. In case of oscillations of low-frequency heavily loaded blades, a relatively greater influence is exerted by displacement. Conversely, in the case of oscillations of high-frequency blades in a lightly loaded cascade, the aerodynamic interference is determined mainly by the oscillation velocity.

The aerodynamic velocity coefficients can be computed by means of the methods set forth in the preceding sections. It should only be kept in mind that in practical calculations, cascades with a finite number of blades are considered (annular cascades or packets consisting of a finite number of blades).

In the study of blade vibration, interest is usually expressed only in harmonic oscillations, and therefore with a specific frequency it is possible, instead of Series (10.2), to consider also the series

$$F_n = \sum_{k=1}^{z} M_{nk}^{(\omega)} y_k, \quad M_{nk}^{(\omega)} = K_{nk}^{(\omega)} + j\omega Q_{nk}^{(\omega)}. \tag{10.3}$$

§ 10.2. Quasi-steady Influence Coefficients

Aerodynamic influence coefficients may be computed by means of the methods set forth in Chapters 5 and 7. To determine the influence coefficients for displacement, it is necessary to find the aerodynamic forces acting upon the profiles after displacement. In a strict formulation, this problem presents considerable calculation difficulties. Since we are dealing only with computation of the integral forces, and since details of pressure distribution are of no interest in the problem under consideration, use may be made of an approximate procedure based upon an estimate of the average values. In determining the influence coefficients of a displacement, the main difficulty consists in separate determination of the forces acting upon the convex side and the concave side of the blade. Here we shall use only the quasi-steady approach.

The integral forces acting upon the concave side and the convex side of a blade are brought about by rotation of the stream in the cascade. Therefore, we shall utilize the determination of some average velocities and pressures that are characteristic of the indicated sides of a blade. For an approximate solution we shall use the method of determining average velocities proposed by G. Yu. Stepanov [78] which is applicable, in rough calculations, to cascades with a constant spacing (without displacement).

Let us first consider an aerodynamic cascade of arbitrary profiles distributed with the identical spacing t (Figure 10.1). We designate by w_1^0 and w_2^0 the velocities of the stream, respectively,

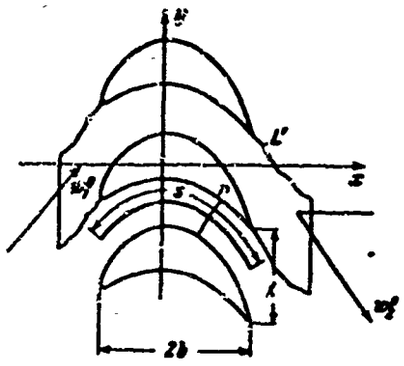


Figure 10.1. An aerodynamic cascade with constant spacing.

far in front and far behind the cascade, and by β_1 and β_2 we designate the angles formed by these velocities with the cascade axis. Instead of true variable velocities on the cascade profiles, we shall introduce some constant average values on the back edge w_A and on the concave side w_B. We shall introduce these velocities in such a manner as to satisfy the integral equation of momentum and the condition of the absence of vortices.

We express the force acting upon an arbitrary profile of the cascade in the direction of the cascade axis in terms of the introduced average velocities

$$Y = \oint_L p^0(s)\,dx = \oint_L \left(p_0 - \frac{\rho}{2}\rho^0 w^2\right)dx = \rho^0\left(w_A^2 - w_B^2\right)b. \qquad (10.4)$$

Here p^0 and ρ^0 are the pressure and density of the fluid, p_0 is the braking pressure, 2b is the width of the cascade. Integration proceeds counterclockwise.

The same force may be computed by means of the equations of the change of momentum, and then by means of (10.4) we obtain

$$\rho^0\left(w_A^2 - w_B^2\right)b = t\rho^0 w_1^0 \sin\beta_1\left(w_1^0\cos\beta_1 + w_2^0\cos\beta_2\right). \qquad (10.5)$$

We write the condition stating that the velocity circulation along contour L_1 is zero. L_1 does not encompass a single blade (the cascade is considered in a potential stream)

$$\oint_{L'} w^0(s)\,ds = w_A s_A - w_B s_B - tw_2^0\cos\beta_2 - tw_1^0\cos\beta_1 = 0. \qquad (10.6)$$

Here s_A, s_B are the arc lengths of the back edge and the concave side of the blade. Henceforth, we shall assume that these arcs are equal $s_A = s_B = s$.

Simultaneously solving (10.5) and (10.6), we find the average velocities on the back edge and on the concave side of a blade:

$$w_A = \frac{s}{2b}\omega_1^0 \sin\beta_1 + \frac{t}{2s}(\omega_1^0 \cos\beta_1 + \omega_2^0 \cos\beta_2),$$
$$w_B = \frac{s}{2b}\omega_1^0 \sin\beta_1 - \frac{t}{2s}(\omega_1^0 \cos\beta_1 + \omega_2^0 \cos\beta_2).$$

We utilize the continuity equation for an incompressible fluid $\omega_1^0 \sin\beta_1 = \omega_2^0 \sin\beta_2$ and find the final form of the preceding formulas:

$$\left.\begin{aligned} w_A &= \omega_1^0\left[\frac{s}{2b}\sin\beta_1 + \frac{t}{2s}\frac{\sin(\beta_1+\beta_2)}{\sin\beta_1}\right], \\ w_B &= \omega_1^0\left[\frac{s}{2b}\sin\beta_1 - \frac{t}{2s}\frac{\sin(\beta_1+\beta_2)}{\sin\beta_1}\right]. \end{aligned}\right\} \qquad (10.7)$$

Before passing on to a solution of the problem concerning the influence of a displacement, let us consider a somewhat different approach to the problem and obtain another rough formula.

We shall again consider a cascade with a constant spacing in a potential stream of incompressible fluid. Since potential flow is being considered, the equation for the absence of vortices

$$\frac{\partial v}{\partial x} - \frac{\partial u}{\partial y} = 0.$$

must be satisfied.

We pass from the Cartesian system of coordinates to a natural system, designating by s and n, respectively, the arc length of the streamlines and their orthogonal trajectories. At a point A, selected on a streamline, we identify directions x and y with directions s and n (Figure 10.2). Then the equation for the absence of vortices will assume the form

$$\frac{\partial w_1}{\partial s} - \frac{\partial w^0}{\partial n} = 0.$$

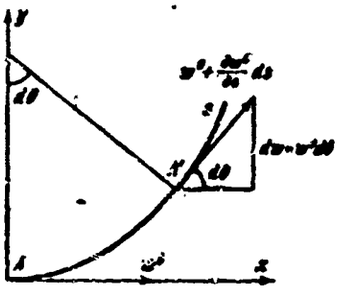


Figure 10.2. Derivation of an equation in a natural system of coordinates.

Here w^0 is the total velocity of the stream at the selected point, w_n is its normal component (at point A, naturally, equal to zero). We designate by $d\theta$ the angle between the velocity at point A', situated along the arc at the distance ds, and the fixed direction of the x-axis. Then (see Figure 10.2) the increment of normal velocity will be equal to $dw_n = w^0 d\theta$, and we obtain $\partial w_n/\partial s = w^0 \partial\theta/\partial s$. Finally, we obtain the equation for the absence of vortices in a natural system of coordinates

$$\frac{\partial w^0}{\partial n} - w^0 \frac{\partial \theta}{\partial s} = 0 \quad \text{или} \quad \frac{\partial w^0}{\partial n} - w^0 K = 0. \tag{10.8}$$

Here K = K(s) is the curvature of the streamline.

Let us first consider an aerodynamic cascade with a constant spacing t (see Figure 10.1). In the channel between the blades we pass an average streamline s and a normal trajectory n, which in accordance with the condition is equipotential.

Integrating the first equation of (10.8) in the direction of the normal, we obtain the law governing the change of velocities across the channel between blades

$$w^0 = w^0_m \exp\left(\int \frac{\partial \theta}{\partial s} dn\right). \tag{10.9}$$

Here w^0_m is the value of the velocity on an average line.

Henceforth, we could use Expression (10.9), but for the sake of simplifying the following calculations we shall expand the exponent in a series and shall retain only two terms:

$$w^0 = w_m^0\left(1 + \int \frac{\partial \theta}{\partial s}\, dn\right). \qquad (10.10)$$

It can be easily shown that this will not introduce any substantial error, since the second term estimates the velocity change of the stream at a distance equal to half the channel width. Such a simplification is all the more permissible, since average values are being estimated, while subsequently only small variations of average values will be considered.

By means of Equation (10.9) or (10.10) it is possible in principle to find a law governing velocity change at any section of the channel, including one for the velocity at the blade contours [78]. However, we are now dealing only with average values, and therefore, shall introduce into the considerations the average channel curvature, for which it is natural to assume

$$K_m = \left(\frac{\partial \theta}{\partial s}\right)_m = \frac{\pi - \beta_1 - \beta_2}{s}. \qquad (10.11)$$

Here $\pi - \beta_1 - \beta_2$ is the angle of turn of the stream in the cascade (i.e., the angle increment), s is the length of the average streamline within the channel (i.e., the length over which the angle increment occurs).

Substituting Condition (10.11) into Equation (10.10) and integrating in the direction of the convex blade surface and the concave blade surface, we obtain the values of the characteristic velocity

$$w_A = w_m^0 + \frac{\pi - \beta_1 - \beta_2}{2s} h w_m^0, \quad w_B = w_m^0 - \frac{\pi - \beta_1 - \beta_2}{2s} h w_m^0. \qquad (10.12)$$

Here h is the channel width (the length of the equipotential between the convex side and the concave side of adjacent blades).

It follows from Formula (10.12) that the velocity w_m^0 is an average one with respect to rate in the channel cross section, and

therefore the product hw_m^0 may be replaced, on the basis of the continuity equation, by the values $hw_m^0 = tw_1^0 \sin\beta_1$, which are known on the basis of the condition of the problem. Then from (10.12) we obtain

$$w_A = w_m^0 + \frac{\pi-\beta_1-\beta_2}{2s} tw_1^0 \sin\beta_1, \quad w_B = w_m^0 - \frac{\pi-\beta_1-\beta_2}{2s} tw_1^0 \sin\beta_1. \tag{10.13}$$

Such a substitution is valid for any cross section of the channel. Thus, there remains a freedom of choice of the location of the characteristic cross section of the channel. This choice is equivalent to a choice of the value of velocity w_m^0. We select w_m^0 in such a manner as to satisfy the integral condition upon which the value of the acting forces depends: the given change of momentum.

Let us first of all note that w_A and w_B are related by Condition (10.5), which proceeds from the equation of momentum.

Substituting w_A and w_B from (10.5) into (10.13), we find the value of the average velocity at which the equation of momentum is satisfied:

$$w_m^0 = \frac{w_1^0}{\pi-\beta_1-\beta_2} \frac{\sin(\beta_1+\beta_2)}{\sin\beta_2} \frac{s}{2b}. \tag{10.14}$$

Substituting (10.14) into (10.13), we find the final formulas for the average velocities on the back edge and concave side

$$\left.\begin{aligned} w_A &= w_1^0\left[\frac{\sin(\beta_1+\beta_2)}{(\pi-\beta_1-\beta_2)\sin\beta_2}\frac{s}{2b} + \frac{(\pi-\beta_1-\beta_2)\sin\beta_1}{2}\frac{t}{s}\right], \\ w_B &= w_1^0\left[\frac{\sin(\beta_1+\beta_2)}{(\pi-\beta_1-\beta_2)\sin\beta_2}\frac{s}{2b} - \frac{(\pi-\beta_1-\beta_2)\sin\beta_1}{2}\frac{t}{s}\right]. \end{aligned}\right\} \tag{10.15}$$

Formulas (10.7) and (10.15) have the same structure and the difference consists only in the coefficients in front of s/2b and t/s. In the limiting case for a cascade of plates that are in a flow without angle of attack, we have $\beta_1=\beta_2=\pi/2$, $s=2b$. Then from (10.7) we obtain $w_A = w_B = w_1^0$, which corresponds to the exact value. The same result follows from Formula (10.15) after expansion of the indeterminacies in the first term.

When estimating the velocities on thick and strongly bent profiles, more exact results are found by Formula (10.15). This is evidently connected with the fact that $s_A = s_B$ was assumed in the derivation of (10.7), whereas for thick profiles the indicated relationship may assume the form $s_A \approx 1{,}5 s_B$.

As an example we shall determine the average velocities on a blade in a cascade which is characterized by the following values:

$$\beta_1 = 39°,\ \beta_2 = 25°,\ s = 63\ мм,\ 2b = 52\ мм,\ t = 40\ мм.$$

Computations according to Formulas (10.15) yield $w_A/w_1^0 = 1{,}44$, $w_B/w_1^0 = 0{,}74$. In Figure 10.3 these values are compared with an exact calculation of the velocity distribution on the profile; for the sake of a clear comparison, a cascade was selected with approximately equal velocities on the back edge and on the concave part.

Let us determine the influence coefficients. Let us assume that one profile (m = 0) in the cascade has been displaced in the positive direction of the ordinate by the value $\zeta \ll t$, while the others have remained at their former places (Figure 10.4). With a displacement of profile m = 0, the greatest change will take place in the conditions of flow about the displaced profile, as well as about profiles m = +1 and m = -1. The method considered above will make it possible to carry out the calculation for the channels and therefore will permit an estimate to be made of change of the pressures only on the concave side of profile m = +1, both sides of profile m = 0, and the convex side of profile[2] m = -1.

We utilize the Bernoulli equation for an incompressible fluid

$$\frac{p_A}{\rho} + \frac{w_A^2}{2} = \frac{p_B}{\rho^0} + \frac{w_B^2}{2}$$

Footnote (2) appears on page 438.

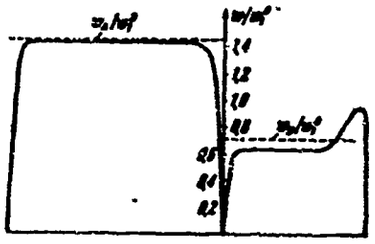


Figure 10.3. Comparison of average velocities with precise calculation.

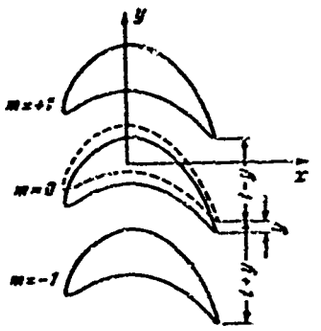


Figure 10.4. Displacement of a profile in a cascade.

and we represent the pressure increment on the convex side of the profile, taking into account the smallness of the perturbations

$$\Delta p_A = p'_A - p_A = \frac{1}{2}\rho^0\left(w_A^2 - w_A'^2\right) = \rho^0 w_A\left(w_A - w'_A\right). \qquad (10.16)$$

Here the prime denotes the pressure and velocity of the fluid on the convex side after displacement.

We designate $t' = t + y$, where $y>0$, if the channel width increases, and $t' = t - y$ if the channel width decreases.

Then the pressure change on the convex side is determined according to (10.15) and (10.16):

$$\Delta p_A = -\rho^0 w_1^0 w_A \frac{(\pi-\beta_1-\beta_2)}{2}\frac{y}{s}\sin\beta_1. \qquad (10.17)$$

Here it is assumed that the channel width increases; if the channel narrows, a minus sign should be placed in front of the formula.

In an analogous manner we find the formula for determining the pressure change on the concave side (the channel width increases)

$$\Delta p_B = \rho^0 w_1^0 w_B \frac{(\pi-\beta_1-\beta_2)}{2}\frac{y}{s}\sin\beta_1. \qquad (10.18)$$

The increment of a force acting upon the concave side of blade m = +1 is found according to (10.18) under the condition that the channel has narrowed:

$$\Delta Y_{+1} = \Delta p_B \cdot 2b = -\rho^0 \omega_1^2 \omega_B \frac{(\pi - \beta_1 - \beta_2)\sin\beta_1}{2} \frac{2b}{s} y. \tag{10.19}$$

Then the corresponding influence coefficient, defined as the force acting with a unit shift, will according to (10.19) and (10.15) be equal to

$$K_{+1}^{(0)} = -\rho^0 (\omega_1^0)^2 \frac{b(\pi - \beta_1 - \beta_2)\sin\beta_1}{s} \left[\frac{\sin(\beta_1 + \beta_2)}{(\pi - \beta_1 - \beta_2)\sin\beta_2} \frac{s}{2b} - \frac{(\pi - \beta_1 - \beta_2)\sin\beta_1}{2} \frac{t}{s} \right]. \tag{10.20}$$

Analogously, according to (10.17) and (10.15) the influence coefficient for blade m = -1 will be determined (it should only be taken into account that the force acting in a positive direction along the ordinate is considered positive)

$$K_{-1}^{(0)} = \rho^0 (\omega_1^0)^2 \frac{b(\pi - \beta_1 - \beta_2)\sin\beta_1}{s} \left[\frac{\sin(\beta_1 + \beta_2)}{(\pi - \beta_1 - \beta_2)\sin\beta_2} \frac{s}{2b} + \frac{(\pi - \beta_1 - \beta_2)\sin\beta_1}{2} \frac{t}{s} \right]. \tag{10.21}$$

In computing the influence coefficient for blade m = 0, account should be taken of the fact that from one direction the channel narrows, and from the other direction it widens, and account should also be taken of the signs of the resultant forces.

Then from (10.17), (10.18), and (10.15) we obtain

$$K_0^{(0)} = -\rho^0 \omega_1^0 \omega_A \frac{(\pi - \beta_1 - \beta_2)\sin\beta_1}{2} \frac{2b}{s} + \rho^0 \omega_1^0 \omega_B \frac{(\pi - \beta_1 - \beta_2)\sin\beta_1}{2} \frac{2b}{s} = -\rho^0 (\omega_1^0)^2 (\pi - \beta_1 - \beta_2)^2 \sin^2\beta_1 \frac{b}{s} \frac{t}{s}. \tag{10.22}$$

Let us note some singularities of the obtained influence coefficients that have practical significance and determine the oscillation singularities of the blade rings.

First of all, since an arbitrary three blades were selected, it is possible to write

$$K_{+1}^{(n)} = K_n^{(n-1)},\ K_{-1}^{(n)} = K_n^{(n+1)},\ K_0^{(n)} = K_n^{(n)}. \qquad (10.23)$$

From (10.20) and (10.21) it follows that the influence of the displaced blade upon the neighboring blades is not identical, i.e., the influence coefficients may be imagined as having symmetrical and asymmetrical parts.

From (10.20), (10.21) and (10.23) it follows that the influence of the displaced blade upon its neighboring blades is greater from its concave side than from the convex side:

$$K_n^{(n+1)} > |K_n^{(n-1)}| \qquad (10.24)$$

This is explained by the fact that (for the same displacement) the pressure on the neighboring blades changes more on the convex side and less on the concave side.

From (10.22) and (10.23) it follows that the displaced blade is acted upon by a supplemental aerodynamic restoring force $K_n^{(n)} < 0$. The following should hold true for the formulation under consideration:

$$K_n^{(n)} = -K_n^{(n+1)} - K_n^{(n-1)}.$$

It is furthermore necessary to note that the influence coefficients are proportional to the kinetic energy of the main stream. Since the problem has been considered in a quasi-steady formulation, the obtained influence coefficients are real numbers. With account taken of the vortex wake, the influence coefficients will be complex numbers, but for the oscillation of low-frequency blades, i.e., in the case of low Strouhal numbers, the real parts will be much greater than the imaginary parts.

We determine the influence coefficients for the numerical values:

$$\beta_1 = 30°,\ \beta_1 = 25°,\ s = 63\ мм,\ 2b = 52\ мм,\ l = 40\ мм,$$

which are typical for an active cascade. According to Formula (10.20) - (10.22), taking (10.23) into account we obtain

$$K_n^{(n+1)} = 1{,}29\rho^2(\omega_1^2)^2, \quad K_n^{(n-1)} = -0{,}66\rho^2(\omega_1^2)^2. \quad K_n^{(n)} = -0{,}63\rho^2(\omega_1^2)^2.$$

§ 10.3. Energy Exchange During the Oscillation of a Blade System

When a cascade oscillates as a connected system, energy exchange is possible both directly among the blades and between the blades and the fluid.

We write the equation for the oscillation of a blade in a cascade, assuming that interaction exists only between neighboring blades

$$m\ddot{y}_n + K_n y_n = K_n^{(n-1)} y_{n-1} + K_n^{(n)} y_n + K_n^{(n+1)} y_{n+1} + \\ + \mathcal{L}_n^{(n-1)} \dot{y}_{n-1} + \mathcal{L}_n^{(n)} \dot{y}_n + \mathcal{L}_n^{(n+1)} \dot{y}_{n+1}. \qquad (10.25)$$

Here the characteristics of the blade under consideration (the oscillator), namely the attenuation coefficient and the stiffness of the spring, are written in the form of influence coefficients $\mathcal{L}_n^{(n)}$ and K_n. Influence coefficients $\mathcal{L}_n^{(n)}$ include both mechanical and aerodynamic damping. Coefficients $\mathcal{L}_n^{(n)}$ describe only the aerodynamic effect; $K_n^{(n)}$ determine the aerodynamic and the elastic relationship.

We shall assume that steady harmonic oscillations are possible in the system, and after analysis of the energy exchange we shall establish the cases in which this is possible. Since the system is a connected one, the oscillation of all the blades takes place with the same frequency, but, generally speaking, with different amplitudes and phases.

Let an arbitrary n^{th} blade oscillate according to the law

$$y_n = y_n^0 e^{i(\nu t + \varphi_n)}. \qquad (10.26)$$

Here y_n^0 is the oscillation amplitude, φ_n is the phase shift.

In view of the fact that steady oscillation is being considered, the total energy change of each blade is equal to zero. However, when investigating resonance phenomena and flutter it is of interest to study the balance of energy supply and removal, as well as the directions of the energy flows across the cascade.

Let us first of all compute only that part of the energy which is dissipated by the n^{th} oscillating blade and does not depend upon the oscillation law of the neighboring blades. This energy dissipation is brought about by a resistance force proportional (in a linear formulation) to the oscillation velocity $\mathcal{Z}_n^{(\omega)}\dot{y}_n$.

The amount of energy dissipated per oscillation cycle is obviously equal (the sign Re designates the real part) to

$$A_{n2}^{(\omega)} = \int_0^T \mathrm{Re}\left[\mathcal{Z}_n^{(\omega)}\dot{y}_n\right]\mathrm{Re}\left[\dot{y}_n\right]d\tau, \quad T = \frac{2\pi}{\nu}. \tag{10.27}$$

When determining the average energy it is necessary to compute an average of two periodic functions that are in complex form, over a period. In order to avoid cumbersome transformations, it is desirable to use a general formula.

Let there first be two periodic functions, given in real form:

$$F_1 = F_{01}\cos(\nu\tau + \varphi_1), \quad F_2 = F_{02}\cos(\nu\tau + \varphi_2).$$

We compute the average of their product for a period (T is the total period):

$$[F_1F_2] = \frac{1}{T}\int_0^T F_1F_2\,d\tau = \frac{F_{01}F_{02}}{T}\int_0^T \cos(\nu\tau + \varphi_1)\cos(\nu\tau + \varphi_2)\,d\tau = \frac{F_{01}F_{02}}{2}\cos(\varphi_1 - \varphi_2). \tag{10.28}$$

Let the periodic functions now be given in complex form

$$F_1 = F_{01}e^{i(\nu\tau + \varphi_1)}, \quad F_2 = F_{02}e^{i(\nu\tau + \varphi_2)}.$$

Let us consider the product of the first function and the function which is conjugate to the second function:

$$F_1 \cdot \bar{F}_2 = F_{01} F_{02} e^{i(\varphi_1 - \varphi_2)}.$$

If the real part of this expression is divided by two, the result coincides with (10.28). Thus we arrive at the final form for the average for the period:

$$[F_1 F_2] = \frac{1}{2} \operatorname{Re}(F_1 \bar{F}_2). \tag{10.29}$$

Here the complex conjugate value is designated by a bar.

By means of Formulas (10.26), (10.27), and (10.29) we find that part of the energy which is dissipated by the oscillating blade per oscillation cycle (per unit of time)

$$A_{n1}^{(n)} = \frac{1}{2} v^2 \left[(\dot{y}_n^0)^2 \operatorname{Re} \mathcal{Z}_n^{(n)}\right], \quad A_{n1}^{(n)} = \frac{1}{2} v (\dot{y}_n^0)^2 \operatorname{Re}\left[-jK_n^{(n)}\right]. \tag{10.30}$$

The real part of $\mathcal{Z}_n^{(n)}$ is negative, since it is a damping coefficient.

The energy supplied to the n^{th} cascade due to displacement of the $(n-1)^{th}$ blade is equal to

$$A_{n1}^{(n-1)} = \int_0^T \operatorname{Re}\left[K_n^{(n-1)} y_{n-1}\right] \operatorname{Re}\left[\dot{y}_n\right] d\tau. \tag{10.31}$$

Computations by means of (10.26), (10.29), and (10.31) yield

$$A_{n1}^{(n-1)} = \frac{v}{2} \dot{y}_n^0 \dot{y}_{n-1}^0 \operatorname{Re}\left[-jK_n^{(n-1)} e^{-i(\varphi_n - \varphi_{n-1})}\right]. \tag{10.32}$$

In an analogous manner we compute the work supplied to the n^{th} blade due to the influence of the displacement rate of the $(n-1)^{th}$ blade:

$$A_{n2}^{(n-1)} = \int_0^T \operatorname{Re}\left[\mathcal{Z}_n^{(n-1)} \dot{y}_{n-1}\right] \operatorname{Re}\left[\dot{y}_n\right] d\tau, \tag{10.33}$$

$$A_{n2}^{(n-1)} = \frac{1}{2}\nu^2 y_n^0 y_{n-1}^0 \operatorname{Re}\left[\mathcal{L}_n^{(n-1)} e^{-i(\varphi_n - \varphi_{n-1})}\right]. \tag{10.34}$$

Computation of the work that depends respectively upon the displacement and the displacement rate of the $(n + 1)^{st}$ blade yields

$$\left.\begin{aligned} A_{n1}^{(n+1)} &= \int_0^T \operatorname{Re}\left[K_n^{(n+1)} y_{n+1}\right] \operatorname{Re}\left[\dot{y}_n\right] d\tau, \\ A_{n1}^{(n+1)} &= \frac{\nu}{2} y_n^0 y_{n+1}^0 \operatorname{Re}\left[-jK_n^{(n+1)} e^{-i(\varphi_n - \varphi_{n+1})}\right], \end{aligned}\right\} \tag{10.35}$$

$$\left.\begin{aligned} A_{n2}^{(n+1)} &= \int_0^T \operatorname{Re}\left[\mathcal{L}_n^{(n+1)} \dot{y}_{n+1}\right] \operatorname{Re}\left[\dot{y}_n\right] d\tau, \\ A_{n2}^{(n+1)} &= \frac{1}{2}\nu^2 y_n^0 y_{n+1}^0 \operatorname{Re}\left[\mathcal{L}_n^{(n+1)} e^{-i(\varphi_n - \varphi_{n+1})}\right]. \end{aligned}\right\} \tag{10.36}$$

Note that the influence coefficients in the form that has been adopted for them in Equation (10.25) have real parts that are considerably larger than the imaginary parts. This is explained by the fact that the lift force components induced on blade number n must be approximately in phase with the corresponding displacements and velocities which induce them. Analyzing the solution in order to contract the notation, we shall assume that these coefficients are real (numbers M and k are small).

Then the expressions for the work performed are transformed into the following form:

$$\left.\begin{aligned} A_n^{(n)} &= \frac{1}{2}\nu^2 (y_n^0)^2 \mathcal{L}_n^{(n)}, \\ A_{n1}^{(n-1)} &= -\frac{\nu}{2} y_n^0 y_{n-1}^0 \sin(\varphi_n - \varphi_{n-1}) K_n^{(n-1)}, \\ A_{n2}^{(n-1)} &= \frac{1}{2}\nu^2 y_n^0 y_{n-1}^0 \cos(\varphi_n - \varphi_{n-1}) \mathcal{L}_n^{(n-1)}, \\ A_{n1}^{(n+1)} &= -\frac{\nu}{2} y_n^0 y_{n+1}^0 \sin(\varphi_n - \varphi_{n+1}) K_n^{(n+1)}, \\ A_{n2}^{(n+1)} &= \frac{1}{2}\nu^2 y_n^0 y_{n+1}^0 \cos(\varphi_n - \varphi_{n+1}) \mathcal{L}_n^{(n+1)}. \end{aligned}\right\} \tag{10.37}$$

Let us first consider flow by a uniform stream about a cascade, all the profiles of which have identical aerodynamic and mechanical characteristics. We shall call such a cascade a homogeneous cascade. Let the cascade be infinite or let it be situated on a wheel, i.e., let it be closed. Then in view of the symmetry of the problem all

the profiles are under identical conditions and can oscillate with the same amplitude and with a constant phase shift between adjacent profiles. If the cascade is an annular one, the phase shift cannot be arbitrary, since a whole number of waves must be situated on the circumference. The latter condition requires satisfaction of the relationship $\alpha z = 2\pi k$, where z is the number of blades on the wheel, k = 1, 2, 3, ..., z.

Thus, for a homogeneous cascade in the case of a symmetrical problem, it is possible to set:

$$\left.\begin{gathered} y_{n-1}^0 = y_{n+1}^0 = y_n^0 = y^0, \quad \varphi_n - \varphi_{n-1} = -(\varphi_n - \varphi_{n+1}) = \alpha, \\ K_n^{(n+1)} = K^+, \; K_n^{(n-1)} = K^-, \; \mathcal{Z}_n^{(n+1)} = \mathcal{Z}^+, \; \mathcal{Z}_n^{(n-1)} = \mathcal{Z}^-, \\ \mathcal{Z}_n^n = \mathcal{Z}^0. \end{gathered}\right\} \tag{10.38}$$

In order that non-attenuating harmonic oscillations be possible in the system, the energy supplied and removed must be equal for all the blades.

By means of (10.37) and (10.38) we obtain the condition for a non-attenuating oscillation:

$$\frac{1}{2}(y_n^0)^2\left[\nu^2\mathcal{Z}^0 + \nu^2(\mathcal{Z}^- + \mathcal{Z}^+)\cos\alpha - \nu(K^- - K^+)\sin\alpha\right] = 0. \tag{10.39}$$

We break down the influence coefficients into terms which depend upon the mechanical properties of the system, and terms which depend upon the aerodynamic properties of the system:

$$\left.\begin{gathered} K^+ = K_M + K_a^+, \quad K^- = K_M + K_a^-, \\ \mathcal{Z}^0 = \mathcal{Z}_M^0 + \mathcal{Z}_a^0, \quad \mathcal{Z}^+ = \mathcal{Z}_a^+, \quad \mathcal{Z}^- = \mathcal{Z}_a^-. \end{gathered}\right\} \tag{10.40}$$

Here, $K_M > 0$ is the mechanical influence coefficient, which on the basis of the reciprocity theorem does not depend upon the direction of action of the force; K_a^+ and K_a^- are the respective coefficients of aerodynamic influence, and furthermore (as has been noted in § 10.2):

$$K_a^+ > 0, \; K_a^- < 0; \; \mathcal{Z}_M^0 < 0 \text{ and } \mathcal{Z}_a^0 < 0 -$$

are respectively influence coefficients which take into account the mechanical and aerodynamic damping of the blade under consideration.

Thus, the first two terms in (10.39) express the energy dissipated with the mechanical and aerodynamic damping of each blade:

$$\frac{1}{2}(\gamma^0)^2\nu^2\mathscr{L}_n^0+\frac{1}{2}(\gamma^0)^2\nu^2[\mathscr{L}_n^0+(\mathscr{L}_n^1+\mathscr{L}_n)\cos\alpha], \tag{10.41}$$

the value of the aerodynamic damping naturally depending upon the phase shift of the neighboring blades, but always remaining a positive value.

The last term in (10.39) constitutes the energy supplied to (or let off from) the oscillating blade from the stream

$$-\frac{1}{2}\nu(\gamma^0)^2(K_n^-K_n^+)\sin\alpha. \tag{10.42}$$

Since $(K_n^--K_n^+)<0$, energy is supplied when $0<\alpha<\pi$ and is dissipated when $\pi<\alpha<2\pi$.

Thus, with a certain relationship among the coefficients Condition (10.39) may be satisfied, and then non-attenuating oscillation exists. We emphasize that the energy for maintaining this oscillation is derived from the uniform stream, while the oscillations of the neighboring blades serve only as a sort of regulator, which delivers this energy in definite portions. Such a process is called self-oscillating, and in application to blades it is called flutter. The possibility of flutter of this kind has been pointed out by Shioiry [136].

The case under consideration deals with flutter with one degree of freedom, since blades can carry out only purely flexural (or purely torsional) oscillations. It should not, however, be forgotten that the entire elastic system has $z>1$ degrees of freedom. When z = 1 (one oscillating blade in the cascade or a single wing), flutter of this type is impossible, as can be readily seen from Expression (10.37) when $\gamma_{n-1}^0=\gamma_{n+1}^0=0$. Therefore, it is more correct to call flutter of

this type cascade flutter. We shall also emphasize that such flutter is possible only in loaded cascades where there is static circulation of a definite value, since the coefficients K_a^+ and K_a^- depend on it.

Above, we have considered the conditions at the stability boundary. The necessary values of the aerodynamic coefficients were established from (10.39) and (10.40). Since the influence coefficients are proportional to the kinetic energy of the main stream (§ 10.2), the critical energy at which the cascade will lose stability can be established on the basis of the difference $K_a^+ - K_a^-$.

$$K_a^+ - K_a^- = \frac{-v\mathcal{L}^0 - v(\mathcal{L}^- + \mathcal{L}^+)\cos\alpha}{\sin\alpha} = \text{const} \cdot \frac{\rho^0 (w_1^0)^2}{2}. \qquad (10.43)$$

Here, ρ^0 and w_1^0 are respectively the density of the gas and the velocity of the main stream. Obviously, the smaller the left-hand part of (10.43), the more will a stability loss be observed at lower velocities.

If aerodynamic damping is small in comparison to mechanical damping, loss of stability will occur earliest of all with a phase shift $\alpha = \pi/2$. Since the input of the second term in the numerator of (10.43) is small, flutter of this kind is usually observed in cascades of axial compressors with a phase shift of about $\pi/2$. Under the influence of compressibility, α will change.

Let us note that in the linear formulation it is possible to determine only the boundary of the instability region, but it is impossible to determine the oscillation amplitude of the blades in the case of flutter, since Condition (10.39) is satisfied at any value of y^0.

Let us now consider the possibility of energy transmission from blade to blade. For this, we shall represent the influence coefficients for blade displacement, not in the manner employed in (10.40), but in the form of a sum of the symmetric and antisymmetric terms of (10.20), (10.21):

$$K^+ = K_1 + K_2, \quad K^- = K_1 - K_2. \tag{10.44}$$

We determine the energy supplied to the $(n-1)^{-th}$ and the n^{-th} blades only due to the forces originating in the space between these blades. We shall find the energy supplied per oscillation cycle to the n^{-th} blade from the side facing the $(n-1)^{-th}$ blade according to the second formula of (10.37):

$$A_{n1}^{(n-1)} = -\pi (y^0)^2 K_1 \sin\alpha + \pi (y^0)^2 K_2 \sin\alpha. \tag{10.45}$$

The energy supplied per oscillation cycle to the $(n-1)^{-th}$ blade from the side facing the n^{-th} blade is found according to the fourth formula of (10.37) by making use of the symmetry of the problem and replacing n + 1 by n and n by n - 1:

$$A_{(n-1)1}^{(n)} = \pi (y^0)^2 K_1 \sin\alpha + \pi (y^0)^2 K_2 \sin\alpha. \tag{10.46}$$

The second terms of Expressions (10.45) and (10.46) are equal and constitute the energy delivered from the fluid stream. Thus, the energy from the stream is supplied due to the antisymmetric components of the influence coefficients; this can also be established from the second term of Formula (10.39) by using Designation (10.44). Since the mechanical influence coefficient K_N enters according to (10.44) only into the symmetrical part, it can naturally also not induce energy from outside. The first terms of (10.45) and (10.46) are equal in value but are opposite in sign and, consequently, constitute the quantity of energy transmitted from one blade to the other. The direction of the transmission depends upon the value of the phase shift. Negative energy is considered to be removed from a given object, and positive energy is considered to be supplied.

In the specific problem at hand, flutter, as has been ascertained above, can originate only when $0 < \alpha < \pi$; consequently, due to the symmetrical component, energy will be transmitted from the n^{-th} blade to the $(n-1)^{-th}$ during oscillation.

In the problem at hand, due to symmetry, this energy circulates in the system and need not be taken into account, since each blade obtains just as much from the preceding one as it passes on to the succeeding one.

§ 10.4. Free Oscillation of a Blade Ring

Before taking up the general case, let us pause for consideration of the free oscillation of the system in order to ascertain the basic governing laws. Let us assume that the cascade is in a vacuum and, consequently, that aerodynamic coupling is absent. Let us also assume that mechanical damping is equal to zero. Thus, we shall consider that only elastic coupling exists between the blades. Such a problem pertains to the area of physics wherein the propagation of waves in periodic structures [9] is studied. In application to turbomachine cascades, a problem of this kind was solved by G. G. Abezgauz and I. I. Rusakov [1] by means of a frequency equation, and also by I. K. Chernyshevskiy [88], who used the method of differential equations.

A diagram of part of the oscillatory system is shown in Figure 10.5, where K_0 is the rigidity of the main spring. K_1 is the rigidity of the spring effecting the elastic coupling, the circles represent concentrated masses m (the springs have no mass). We write the equation of free oscillation of such a system, taking into account the fact that elastic interaction exists only between neighboring blades and that the reciprocity forces are proportional to the distance between them

$$m\ddot{y}_n + K_1(y_n - y_{n+1}) + K_1(y_n - y_{n-1}) + K_0 y_n = 0 \quad (n = 1, 2, 3, \ldots, z). \tag{10.47}$$

In the case at hand, blades will refer to their models.

We group the terms and represent the equation in the following form:

$$m\ddot{y}_n + K_1(2y_n - y_{n+1} - y_{n-1}) + K_0 y_n = 0. \tag{10.48}$$

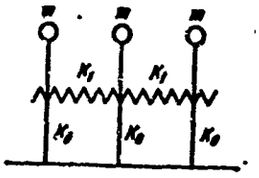


Figure 10.5. Diagram of a blade ring.

Since the system is homogeneous, the the solution is naturally to be sought in the form of a traveling wave

$$y_n = y^0 e^{i(\nu\tau - 2\pi\varepsilon\xi)}.$$

Here, y^0 is the oscillation amplitude, identical for all blades, ν is the frequency of the process, τ is time, ε is the wave number (the reciprocal of the wave lengtn), ξ is a coordinate measured along the cascade axis. Since the cascade is regarded as a discrete system, it is sufficient to fix only the position of the material points.

In view of this, we represent the traveling wave in the following form:

$$y_n = y^0 e^{i(\nu\tau - n\alpha)}, \tag{10.49}$$

where α is the constant phase-shift angle between adjacent blades.

We substitute Expression (10.49) into Expression (10.47):

$$y^0 e^{-in\alpha}[-\nu^2 m + K_1(2 - e^{-i\alpha} - e^{i\alpha}) + K_0] = 0,$$

and from this, after elementary transformations, we find

$$4\frac{K_1}{m}\sin^2\frac{\alpha}{2} + \frac{K_0}{m} - \nu^2 = 0. \tag{10.50}$$

Since the system is closed in a ring, the phase shift cannot be arbitrary, but must satisfy the condition of the location of a whole number of waves on the circumference

$$\alpha = \frac{2\pi k}{z}, \quad k = 1, 2, 3, \ldots, z. \tag{10.51}$$

Jointly with (10.50), Condition (10.51) determines the natural frequency of the system. From these conditions it follows that an annular system has 1 + z/2 different natural frequencies when z is even and (z + 1)/2 different natural frequencies when z is odd.

The least natural frequency is less than the partial frequency of the blade

$$\nu_{min} = \sqrt{\frac{K_0}{m}} < \sqrt{\frac{K_0 + 2K_1}{m}}. \qquad (10.52)$$

and corresponds to cophasal oscillation when the rigidity of a connecting spring is zero.

The greatest natural frequency corresponds to the phase shift $\alpha = \pi$, when the effect of the connecting spring will be greatest

$$\nu_{max} = \sqrt{\frac{K_0 + 4K_1}{m}} > \sqrt{\frac{K_0 + 2K_1}{m}}. \qquad (10.53)$$

The remaining natural frequencies lie within this range, which is called the pass band or the transparency band of the cascade. The least frequency corresponds to the length of a wave of infinite extent, and the greatest frequency corresponds to the shortest possible wavelength in a discrete system, which is equal to twice the spacing. Consequently, in the cascade under consideration, waves with frequencies lying within the transmission range can propagate. Waves with smaller or greater frequencies must attenuate.

This is of great significance in the study of resonance and aeroelastic phenomena,. Therefore, let us become acquainted with the behavior of a cascade when it is acted upon by a force with a frequency that lies outside the transmission range. In the cascade itself, free oscillation can be maintained only with natural frequencies which satisfy Equations (10.50) and (10.51). For studying the oscillation of a given arbitrary frequency, it is necessary to apply an induced force.

To blade number zero let there be applied the harmonic force

$$X = X_0 e^{j\Omega t}.$$

Then the equations of motion of the system have the form

$$m\ddot{y}_n + K_1(2y_n - y_{n+1} - y_{n-1}) + K_0 y_n = \delta_{n0} X_0 e^{j\Omega t}. \tag{10.54}$$

Here, δ_{0n} is the Kronecker symbol:

$$\left.\begin{aligned} \delta_{0n} &= 1 \text{ for } n = 0, \\ \delta_{0n} &= 0 \text{ for } n \neq 0. \end{aligned}\right\}$$

As before, we seek the solution in the form of (10.49), but we assume that α may assume complex values. For $n \neq 0$ the solutions correspond in form to Condition (10.50), but now the frequency ν is considered as given, since it is equal to the frequency of the perturbing force f.

From Condition (10.50) we define the value α:

$$\sin\frac{\alpha}{2} = \frac{1}{2}\sqrt{\frac{f^2 m - K_0}{K_1}}. \tag{10.55}$$

If the inequality

$$0 \leqslant \frac{mf^2 - K_0}{4K_1} \leqslant 1, \tag{10.56}$$

is valid, the frequency f lies within the pass band. If Condition (10.56) is not maintained, two cases are possible.

a) the frequency of the coercive force is lower than the minimum pass frequency $f < \nu_{min} = \sqrt{K_0/m}$. In such a case, the right-hand part of Expression (10.55) will be a purely imaginary value

$$\sin\frac{\alpha}{2} = \pm\frac{1}{2} j \sqrt{\frac{K_0 - f^2 m}{K_1}}. \tag{10.57}$$

Assuming $\alpha = \alpha_1 + j\alpha_2$, we find

$$\sin\frac{\alpha}{2}=\sin\frac{\alpha_1}{2}\operatorname{ch}\frac{\alpha_2}{2}+j\cos\frac{\alpha_1}{2}\operatorname{sh}\frac{\alpha_2}{2}. \qquad (10.58)$$

Since this expression must be a purely imaginary one, we obtain $\alpha_1 = 0$ and, consequently, the blades oscillate in phase. From (10.58) it also follows that

$$\operatorname{sh}\frac{\alpha_2}{2}=\pm\frac{1}{2}\sqrt{\frac{K_0-f^2m}{K_1}}. \qquad (10.59)$$

The constant $\alpha=\alpha_1+j\alpha_2$ now determines not only the phase shift, but also the decrease of the amplitudes of the oscillating blades as their distance from the zero blades increases. This amplitude decrease takes place according to the exponential law

$$y_n^0=y^0e^{-(\alpha_1+j\alpha_2)n}. \qquad (10.60)$$

In view of the symmetry of the problem, the distribution pattern of amplitudes should also be symmetrical with respect to the diameter passing through the zeroth blade. Therefore, in this case, it is convenient to count the blades in the left-hand half and right-hand half of the disk, starting with the zeroth blade.

b) The frequency of the coercive force is greater than the maximum pass frequency $f>\nu_{max}$, where ν_{max} is defined by Formula (10.53). In this case, the value of the right-hand part is real and greater than one. Consequently, from (10.58) we obtain the result that the blade oscillation must take place in counterphase $\alpha_1=\pi$.

The attenuation coefficient is defined by the formula

$$\operatorname{ch}\frac{\alpha_2}{2}=\pm\frac{1}{2}\sqrt{\frac{f^2m-K_0}{K_1}}. \qquad (10.61)$$

Consequently, in this case a decrease of the oscillation amplitudes as the distance from the excited blade increases also takes place.

To find the amplitude of the excited blade we substitute Condition (10.49) into (10.54) when n = 0 and, taking into account the

conditions of symmetry for y_{n-1} and y_{n+1}, we obtain

$$y^2(-\nu^2 m - 2K_1 e^{-\alpha_1} + K_2) = X_0. \qquad (10.62)$$

As the frequency of the perturbing force moves farther away from the transparency zone into the subresonance region, α_2 increases, which follows from Formula (10.59). The second term in (10.62) tends toward zero, and the formula passes into the conventional relationship for the dynamic coefficient for the oscillation of an isolated blade (it should be kept in mind that in practical cases, when dealing with influences through an elastic disk, $K_1 \ll K_0$). An analogous transition, as follows from Formulas (10.61) and (10.62), is observed with increasing distance from the transparency zone into the super resonance region. Consequently, far from the transparency zone, the cascade does not appear to be coupled, and the oscillation of isolated blades may be considered.

The transparency zone is of special interest when investigating resonance phenomena, particularly when studying aeroelastic processes, since their origination depends in principle upon the coherence of the cascade, and the oscillation takes place in the principal modes. The oscillation of systems without damping has been considered above; therefore, within the pass zone there will be infinite resonance peaks. In the presence of energy dispersion, the peaks will be smoothed out, and in the case of weak coupling will merge into a single resonance band.

Up to now we have been dealing with the oscillation of an annular closed cascade. Practical interest is also afforded by the problem of the oscillation of packets consisting of a limited number of blades as models of packets used in turbomachines and during stand tests of aeroelastic processes.

We shall adopt a packet design such as the one shown in Figure 10.6. Such a version of a packet may be realized, for example, on a turbomachine wheel if the boundary blades have much more rigidity

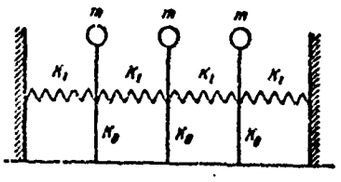


Figure 10.6. Diagram of a blade packet.

than do z blades side by side. The packet consists of z elastic blades with identical properties.

We write the differential equations of the packet:

$$\left.\begin{aligned} &m\ddot{y}_1 + K_1(2y_1 - y_2) + K_0 y_1 = 0, \\ &\dots\dots\dots\dots\dots\dots\dots\dots \\ &m\ddot{y}_n + K_1(-y_{n-1} + 2y_n - y_{n+1}) + K_0 y_n = 0, \\ &\dots\dots\dots\dots\dots\dots\dots\dots \\ &m\ddot{y}_z + K_1(-y_{z-1} + 2y_z) + K_0 y_z = 0, \quad n = 1, 2, 3, \dots, z. \end{aligned}\right\} \tag{10.63}$$

These equations, essentially, are reduced to the differential equations which describe the transverse oscillation of an elastic string with concentrated masses; therefore, it is natural to seek the solution in the form of a harmonic wave

$$y_n = y_n^0 e^{i\nu t}. \tag{10.64}$$

Substituting (10.64) into (10.63), we obtain the system of algebraic equations:

$$\left.\begin{aligned} &(K_0 + 2K_1 - m\nu^2) y_1^0 - K_1 y_2^0 = 0, \\ &\dots\dots\dots\dots\dots\dots\dots\dots \\ &-K_1 y_{n-1}^0 + (K_0 + 2K_1 - m\nu^2) y_n^0 - K_1 y_{n+1}^0 = 0, \\ &\dots\dots\dots\dots\dots\dots\dots\dots \\ &-K_1 y_{z-1}^0 + (K_0 + 2K_1 - m\nu^2) y_z^0 = 0. \end{aligned}\right\} \tag{10.65}$$

The condition for solving System (10.65) requires that the determinant be equal to zero

$$\begin{vmatrix} x & 1 & 0 & \dots & 0 \\ 1 & x & 1 & \dots & 0 \\ \dots & \dots & \dots & \dots & \dots \\ 0 & 0 & 0 & \dots & x \end{vmatrix} = 0. \tag{10.66}$$

Here we have introduced the designation

$$x = \frac{K_0 + 2K_1 - mv^2}{-K_1} = \frac{mv^2 - K_0}{K_1} - 2. \tag{10.67}$$

Determinant (10.66) is expressed in terms of a second-order Chebyshev function

$$(\sqrt{ab})^z U_z\left(\frac{x}{2\sqrt{ab}}\right) = \begin{vmatrix} x & b & 0 & \dots & 0 \\ a & x & b & \dots & 0 \\ \cdot & \cdot & \cdot & \cdot & \cdot \\ 0 & 0 & 0 & \dots & x \end{vmatrix}. \tag{10.68}$$

By definition, the expression

$$U_z(x) = \frac{\sin[(z+1)\arccos x]}{\sqrt{1-x^2}}. \tag{10.69}$$

is called a Chebyshev polynomial of the second kind. This polynomial satisfies the recurrence formula

$$U_{z+1}(x) - 2xU_z(x) + U_{z-1}(x) = 0. \tag{10.70}$$

The degree of the polynomial is equal to its order, the polynomials are orthogonal and have only real, simple zeros which lie in the interval -1, +1.

When $|x|<1$, assuming $x = \cos\theta$, from (10.69) we obtain

$$U_z(\cos\theta) = \frac{\sin[(z+1)\theta]}{\sin\theta}. \tag{10.71}$$

When $|x|>1$, assuming $x = \operatorname{ch}\theta$, we obtain

$$U_z(\operatorname{ch}\theta) = \frac{\operatorname{sh}[(z+1)\theta]}{\operatorname{sh}\theta}. \tag{10.72}$$

The indicated properties explain the extensive application of Chebyshev polynomials in various problems with catenary systems. Comparing (10.66), (10.68), and (10.69), we obtain the solution

$$U_z\left(\frac{x}{2}\right) = 0, \quad \sin\left[(z+1)\arccos\frac{x}{2}\right] = 0. \tag{10.73}$$

From (10.73) and (10.67) we find the formula for the natural frequencies of the system

$$\nu_k = \sqrt{\frac{1}{m}\left[4K_1\cos^2\frac{k\pi}{2(z+1)} + K_0\right]} \quad k = 1, 2, \ldots, z. \tag{10.74}$$

Substituting (10.74) into (10.65), we obtain

$$\left.\begin{aligned} -2y_1^0\cos\frac{k\pi}{z+1} + y_2^0 &= 0,\\ \cdots\cdots\cdots\cdots\cdots\cdots\\ y_{n-1}^0 - 2y_n^0\cos\frac{k\pi}{z+1} + y_{n+1}^0 &= 0,\\ \cdots\cdots\cdots\cdots\cdots\cdots\\ y_{z-1}^0 - 2y_z^0\cos\frac{k\pi}{z+1} &= 0. \end{aligned}\right\}$$

From this, we find the distribution of the oscillation amplitudes

$$y_n^0 = y^0\sin\frac{nk\pi}{z+1}, \quad k = 1, 2, 3, \ldots, . \tag{10.75}$$

§ 10.5. Forced Oscillation of a Connected Blade System

Let us first consider the resonance in a homogeneous cascade under the action of a harmonic force. The equation for the oscillation of the n^{th} blade is written in the conventional manner, but with a supplement to the right-hand part (the coefficient K_1 takes into account only the elastic coupling between the blades)

$$m\ddot{y}_n + \nu_0\mathcal{L}\dot{y}_n + K_0y_n + K_1(2y_n - y_{n-1} - y_{n+1}) = Fe^{i(\nu t+\alpha n)}. \tag{10.76}$$

Here it is assumed that force F acts upon the blade of the cascade with a constant phase shift α, as is the case in turbomachines.

The oscillation of the blades of a rotating cascade is induced by aerodynamic forces brought about by the circumferential nonuniformity of the stream which passes through the stationary cascade. Let the circumferential nonuniformity contain K_n waves; then, obviously, when

the force acts upon the adjacent blades the phase shift will have a constant value, equal to

$$\alpha = \frac{2\pi k_n}{z}, \tag{10.77}$$

where z is the number of the rotating cascade blades.

In view of the symmetry of the oscillation pattern, the solution of equations (10.76) may be sought in the form of a traveling wave with a phase shift β with respect to the acting force, constant for all blades:

$$y_n = y^0 \exp j(\nu\tau + n\alpha - \beta). \tag{10.78}$$

All the blades should oscillate with the same amplitude y^0.

Substituting (10.78) into (10.76) and separating the real part and the imaginary part, we obtain

$$\left.\begin{aligned} y^0\left(-\nu^2 m + 4K_1 \sin^2\frac{\alpha}{2} + K_0\right) &= A\cos\beta, \\ y^0 \nu\nu_0 &= A\sin\beta. \end{aligned}\right\} \tag{10.79}$$

The sum of the second and third terms in the parentheses may be replaced in accordance with (10.50) by $m\nu_0^2$, where ν_0 is the natural oscillation frequency of the blade system with a fixed phase shift α. Making the indicated substitution, squaring Equality (10.79) and adding the left-hand and the right-hand parts, we obtain the expression for the oscillation amplitude

$$y^0 = \frac{A\exp j\nu\tau}{\sqrt{m^2(\nu_0^2 - \nu^2) + \nu^2\nu_0^2\Sigma^2}}. \tag{10.80}$$

Obtaining the ratio of the left-hand parts and the right-hand parts of equations (10.79), we find the value of the phase shift between the force acting upon the n^{th} blade and its displacement:

$$\operatorname{tg}\beta = \frac{1}{1-(\nu/\nu_0)^2}\,\frac{\nu}{\nu_0}\,\frac{\Sigma}{m}. \tag{10.81}$$

If the force is represented by only a single harmonic, the solutions of (10.80) and (10.81) do not differ from the corresponding solutions for an oscillatory system with one degree of freedom. It is only necessary, in place of the natural frequency of an isolated blade, to use the natural frequency of the system, which depends upon the elastic coupling between the blades. If only weak elastic coupling is considered (for example, through an elastic disk in which the blades are fastened), this introduces no basic changes into the nature of the oscillation. However, if the rigidity of the coupling is very large (for example, the blades are connected by bands), the natural frequency of the system, equal to

$$\nu_0 = \sqrt{\frac{K_0 + 4K_1 \sin^2 \frac{\alpha}{2}}{m}},$$

will become so great that resonance will be practically unobtainable at any phase shift α, except for the case $\alpha = 0$, when the system oscillates as a single whole, and its natural frequency becomes equal to the minimum frequency of the system. Since the phase shift (or the number of waves of the perturbing force that fit onto the wheel circumference) depends only upon the design of the turbomachine, such a system can have no vibrations. This is also obvious from the fact that when forces act upon blades with a phase shift, and the blades are connected in a rigid system, the total force is equal to zero (except for the case $\alpha = 0$).

In order to decrease the dynamic stresses, it is not necessary to connect all the blades into a single packet. Let us consider a packet consisting of z_1 blades linked by a rigid coupling. Let it be possible for the packet to oscillate only as a single whole. The total perturbing force acting upon the entire packet is equal to

$$F \sum_{n=0}^{z_1-1} \cos(\nu\tau + \alpha n) = \frac{\sin \frac{z_1 \alpha}{2}}{\sin \frac{\alpha}{2}} \cos\left(\nu\tau + \frac{z_1 - 1}{2}\alpha\right).$$

In the case of rigid coupling, this force is distributed uniformly on all the blades of the packet. Therefore, the value of the

relative force for each blade of the packet is equal to

$$\mu = \left| \frac{\sin \frac{z_1 \alpha}{2}}{z_1 \sin \frac{\alpha}{2}} \right| = \left| \frac{\sin \frac{\pi k_n z_1}{z}}{z_1 \sin \frac{\pi k_n}{z}} \right|. \qquad (10.82)$$

This value takes into account the load decrease per blade in the packet in comparison to an isolated blade and is called the packet multiplier [41]. If $k_n z_1 = z$, then $\mu = 0$, and the average force is also equal to zero. For a given case of k_n and z, an optimum number of blades z_1 in the packet can be selected in such a manner that the packet multiplier would assume a minimal value.

From what has been said above, it is obvious that the connection of blades into a packet will not always bring about the desired effect. The packet multiplier tends toward unity if $\pi k_n/z \to 0$ (the number of blades of the wheel is much greater than the number of perturbation waves) or if $k_n/z \to 1$ (the number of perturbation waves approximately coincides with the number of blades).

A typical graph of the change of the packet multiplier as a function of the ratio of the number of perturbation waves to the number of blades upon the wheel, for a fixed number of blades in the packet $z_1 = 10$, is given in Figure 10.7. Such a method of connecting blades into packets (where this is possible) is used in turbomachines for the reduction of dynamic stresses. However, it does not provide absolute protection against vibration damage, since each blade is an elastic one with an infinite number of degrees of freedom, and therefore, oscillation of the blades within the packet is possible. This question cannot be considered by means of an idealized diagram of a blade as an oscillator. This purely vibrational problem is studied in special literature [41].

Let us pass on to the oscillation of a circle of inhomogeneous blades.

In § 10.3, it was shown that in case of the vibration of a connected system of blades, energy exchange between them is possible.

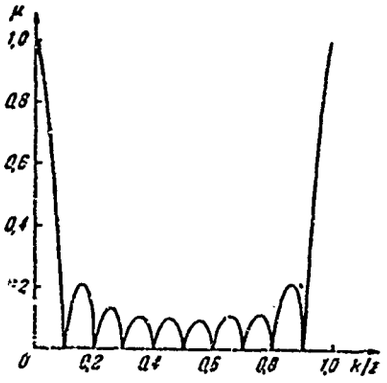


Figure 10.7. Values of the packet multiplier.

This energy exchange originates if the blades in the oscillating system are inhomogeneous. Such inhomogeneity is always present in a real blade circle. This is explained by technological inaccuracies when a set of blades is produced on the basis of the same drawings. In the general case, the blades can have different partial frequencies of natural oscillations, different masses, and different oscillation decrements. However, scatter with respect to natural frequencies represents the greatest significance in this problem.

The problem of the oscillation of an inhomogeneous blade circle was studied by Whitehead [147], V. O. Bauer and B. F. Shorr [4], R. A. Shipov [94], V. B. Kurzin, and others. In the general case, with arbitrary distribution of inhomogeneity, the problem involves much computation work, the result depending strongly not only upon the level of inhomogeneity, but also upon the distribution law. In view of the fact that the assemblage of a given set of blades can take place in random sequence, the problem, generally speaking, is of a probabilistic nature. When the problem is solved in such a formulation, an answer can be given concerning the probable scatter of dynamic stresses in the blades in the case of resonance. On the other hand, since we are dealing with design reliability, it is of interest to investigate some unfavorable limit cases of distribution of the inhomogeneities. In this case, the solution makes it possible to approach the selection of permissible stresses with the necessary safety factor.

Let us consider the singularities of the forced resonance oscillation of an inhomogeneous ring on the basis of a particular problem

in which the basic laws can be ascertained [94]. Let us assume that the cascade is made up of alternating blades of two types, which in the general case differ with respect to rigidity, mass, and coefficient of mechanical attenuation. The aerodynamic characteristics of the blades are considered to be identical. We shall also assume that the coefficients of aerodynmaic and mechanical influence decrease with distance so rapidly that it is possible to take account only of the interaction of adjacent blades. In the general case, as has been noted above, influence coefficients can be complex numbers. However, in the case under consideration we shall assume that the imaginary component may be disregarded in comparison to the real components; this is valid in analysis of the oscillation of cascades that are subjected to a large load.

R. A. Shipov has carried out calculations of maximum dynamic stresses on the blades of an inhomogeneous ring of an axial compressor by means of an electronic digital computer.

The number of blades on the wheel is z = 24. During the calculation, it was taken into account that resonances of equal multiplicity occur at different compressor rpm numbers, i.e., at different air densities. The influence of a change of any parameter on the maximum dynamic stresses was analyzed; the remaining parameters characterizing frequency difference were held constant.

Figure 10.8 shows the relationship of the relative increment (with respect to a homogeneous cascade) of the maximum stresses in blades in the case of resonance due to blade-thickness inhomogeneity. The blade thicknesses were measured in such a manner that the average thickness remained constant, and the mass of the blades did not change. The relative value $\psi = (h_1 - h_0)/h_0$, characterizing the relative change of blade thickness, was plotted along the abscissa. Relative stress increments

$$\Delta\sigma = \frac{\sigma_{max}(\psi) - \sigma_{max}(0)}{\sigma_{max}(0)},$$

were plotted along the ordinate.

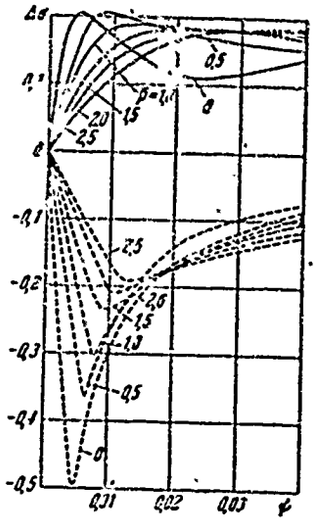


Figure 10.8. Increment of maximum dynamic stresses in an inhomogeneous cascade as a function of the blade thickness scatter.

The solid lines refer to thick blades, and the dotted lines refer to thin blades. The curves show a relative pressure in the compressor which changed in proportion to the square of the rpm number.

It can be seen that in the case of frequency differences with respect to thicknesses (and, consequently, also with respect to natural oscillation frequency), the maximum stresses in the blades increase. In the example at hand, the stress increment comprises more than 20%. A stress increase is observed in the more rigid blades, i.e., in blades which resonate at high frequency. Simultaneously with an increase of the maximum stresses in the thicker blades, a decrease of the maximum stresses is observed in thin blades. In the example under consideration, the maximum stresses of the thin blades decrease by 50% in comparison to the case of a homogeneous cascade.

Thus, the stress scatter comprises $\sigma_{max}/\sigma_{max} = 1.2/0.5 = 2.4$, i.e, is very great. These calculations explain the reason for the appearance of the scatter of dynamic stresses in a real blade ring that is known to occur in the practice of turbomachine testing. We emphasize that the blade-thickness scatter can here comprise but 1%.

The appearance of such a strong scatter is explained by energy exchange between the oscillating blades in an inhomogeneous cascade, some blades building up oscillation, and others attenuating. With an increase in the thickness scatter (or with an increase in the natural

partial oscillation frequencies), the scatter of dynamic stress decreases, since the blades begin to oscillate as practically uncoupled systems. For example, in the construction under consideration only the thin blades or only the thick blades will oscillate, and this cannot bring about an energy exchange, since the motion of adjacent blades is necessary for such an exchange.

An analogous pattern is observed when other parameters of inhomogeneity are varied, for example, the blade masses, since change of the masses brings about a change in the natural oscillation frequencies. If the methods are changed simultaneously with the blade rigidity in such a manner that the natural frequencies remain constant, the scatter of dynamic stresses will be small. This is also explained by the fact that strong interference in the system can be observed only with a definite frequency scatter.

Obviously, a small scatter of the damping coefficients also cannot bring about a large effect, since the resonance frequencies change in an approximately inverse proportion to the oscillation decrements.

§ 10.6. The Self-Oscillations of a Connected System of Blades

Let us consider a system of blades situated in a homogeneous stream. We shall assume that the oscillation velocities of the blades and the value of their displacement are so small that a linear approximation may be used. As before, we shall take account of interaction only between adjacent blades.

Then the equation system describing the oscillation of the blades has the form (n = 1, 2, 3, ..., z)

$$m_n\ddot{y}_n + K_n y_n = \mathcal{L}_n^{(n-1)}\dot{y}_{n-1} + \mathcal{L}_n^{(n+1)}\dot{y}_{n+1} + \mathcal{L}_n^{(n)}\dot{y}_n + \\ + K_n^{(n)}y_n + K_n^{(n-1)}y_{n-1} + K_n^{(n+1)}y_{n+1}. \qquad (10.83)$$

Here $\mathcal{L}_n^{(k)}$ and $K_n^{(k)}$ are influence coefficients. $K_n^{(k)}$ takes into account the force acting upon the n^{th} blade when the k^{th} blade is displaced,

$\mathcal{Z}_n^{(k)}$ determines the force originating on the n^{th} blade if the k^{th} blade is moving. The first term of the equation expresses the inertial force; the second term expresses the elasticity force. The fifth term expresses the resistance force induced by the scatter on energy in a blade. The remaining five terms take into account the forces which depend upon the velocity and position of two adjacent blades.

In an analysis of the energy exchange between the blades of a cascade and the stream, it was shown above in § 10.3 that the origination of dynamic instability is possible in principle. In other words, under certain conditions the energy extracted by the blades from the stream may surpass the energy dissipated by damping. In this case, non-attenuating oscillations of the blades will originate.

Such self-oscillations are called blade flutter. This phenomenon differs essentially from forced blade oscillation by the fact that the blades absorb energy from a uniform stream; the energy input is regulated by the blade system itself. The problem of blade flutter was analyzed by Shioiry [136] and Lane [116]. A similar problem dealing with the influence of blade interaction in a cascade in the case of separation flutter was examined by L. Ye. Ol'shteyn and R. A. Shipov [51].

To determine the stability boundary, it is sufficient to consider harmonic oscillation. This can determine the conditions under which flutter originates. However, the oscillation amplitude cannot be found by considering the linear problem. In a real system, a definite oscillation amplitude will become established which is determined by the balance of supplied and dissipated energy, which is determined by nonlinear relationships present in any real system.

For determination of the boundary of flutter initiation, we employ the substitution

$$y_n = y_n^0 e^{i\nu\tau}, \tag{10.84}$$

which reduces System (10.83) to a system of algebraic equations:

$$\left[K_n - K_n^{(n)} - j\nu\mathcal{L}_n^{(n)} - m_n\nu^2\right] y_n^0 = \left[K_n^{(n-1)} + j\nu\mathcal{L}_n^{(n-1)}\right] y_{n-1}^0 + \\ + \left[K_n^{(n+1)} + j\nu\mathcal{L}_n^{(n+1)}\right] y_{n+1}^0 = 0, \quad n = 1, 2, 3, \ldots, z. \tag{10.85}$$

Here, y_n^0 is the complex amplitude of oscillations of the n^{th} blade.

We consider first the problem of the oscillation of a homogeneous cascade. Then the influence coefficients will be the same for all blades and therefore, designating

$$K_n - K_n^{(n)} = K^0, \quad K_n^{(n-1)} = K^-, \quad K_n^{(n+1)} = K^+, \\ \mathcal{L}_n^{(n)} = \mathcal{L}^0, \quad \mathcal{L}_n^{(n-1)} = \mathcal{L}^-, \quad \mathcal{L}_n^{(n+1)} = \mathcal{L}^+,$$

we reduce System (10.85) to the form

$$y_n^0\left[K^0 - j\nu\mathcal{L}^0 - m\nu^2\right] - \left[K^- + j\nu\mathcal{L}^-\right] y_{n-1}^0 - \left[K^+ + j\nu\mathcal{L}^+\right] y_{n+1}^0 = 0. \tag{10.86}$$

It should be emphasized that the influence coefficients for all blades forward K^- and $\mathcal{L}^-$ (from n - 1 to n) and backwards K^+ and $\mathcal{L}^+$ (from n + 1 to n) are assumed constant, but, generally speaking, $K^+ \neq K^-$ and $\mathcal{L}^+ \neq \mathcal{L}^-$.

Equation (10.86) must be solved with definite boundary conditions, which depend upon whether an infinite cascade, an annular cascade, or a blade packet is being considered.

In order to abbreviate the notation, we introduce the designations:

$$K^- + j\nu\mathcal{L}^- = -a_1, \quad K^0 - j\nu\mathcal{L}^0 - m\nu^2 = a_2, \quad K^+ + j\nu\mathcal{L}^+ = -a_3. \tag{10.87}$$

Then Equation (10.86) assumes the form

$$a_1 y_{n-1}^0 + a_2 y_n^0 + a_3 y_{n+1}^0 = 0. \tag{10.88}$$

Let us first consider the problem of an annular cascade of uniform blades. Such a problem was investigated by L. Ye. Ol'shteyn and R. A. Shipov [51]. When solving Equations (10.88) it could be

possible to seek the solution in wave form. However, in the present instance we shall proceed somewhat differently.

We compile the determinant of System (10.88) and set it equal to zero, in order to find the condition for a neutral solution:

$$D_z = \begin{vmatrix} a_1 & a_2 & a_3 & 0 & \dots & 0 \\ 0 & a_1 & a_2 & a_3 & \dots & 0 \\ \dots & \dots & \dots & \dots & \dots & \dots \\ a_2 & a_3 & 0 & 0 & \dots & a_1 \end{vmatrix} = 0. \tag{10.89}$$

When compiling the determinant, we consider the condition that the system is a closed one: $y^0_{n+z} = y^0_n$. This determinant is a particular case of a cyclical determinant and is equal to

$$D_z = \prod_{k=0}^{z-1} (a_1 + a_2\varepsilon_k + a_3\varepsilon_k^2), \quad \varepsilon_k = e^{j\frac{2\pi k}{z}}, \quad k = 0, 1, 2, \dots, (z-1). \tag{10.90}$$

Here ε_k are all z-index roots of unity.

From Formulas (10.89) and (10.90) we obtain the condition that must hold at the boundary of the stability region and the instability region

$$a_1 + a_2\varepsilon_k + a_3\varepsilon_k^2 = 0.$$

After substituting $\varepsilon_k = \exp(2\pi jk/z) = \exp(j\alpha)$, where α is the value of the phase shift between adjacent blades, we obtain this condition in the following form

$$a_2 = -(a_1 e^{-j\alpha} + a_3 e^{j\alpha}). \tag{10.91}$$

Substituting (10.91) into (10.88), we find the distribution of complex amplitudes

$$y^0_{n+1} = y^0_n e^{j\alpha}.$$

Thus, just as should have been expected, all blades oscillate with the same amplitude and with a constant phase shift between adjacent blades.

Substituting into (10.91) the designation from (10.87) and separating the real and imaginary parts, we find two equations:

$$\left.\begin{aligned} K^0 - m\nu^2 &= (K^- + K^+)\cos\alpha + \nu(\mathcal{L}^- - \mathcal{L}^+)\sin\alpha, \\ -\nu\mathcal{L}^0 &= (K^+ - K^-)\sin\alpha + \nu(\mathcal{L}^- + \mathcal{L}^+)\cos\alpha. \end{aligned}\right\} \qquad (10.92)$$

From the first equation we determine the oscillation frequency of the blades in the case of flutter:

$$\nu^2 = \frac{K^0 - (K^- + K^+)\cos\alpha}{m + \nu(\mathcal{L}^- + \mathcal{L}^+)\sin\alpha} \approx \frac{K^0}{m}. \qquad (10.93)$$

Since under actual conditions the influence coefficients are very small, the computed frequency practically coincides with the natural frequency of an individual blade.

The second equation of (10.92) makes it possible (for the spectrum of permissible phase-shift values $\alpha = 2\pi k/z$) to find the values of the coefficients of aerodynamic damping and, consequently, the value of the kinetic energy of the main stream at which loss of stability will occur. If the influence of adjacent blades upon aerodynamic damping is disregarded in (10.93) (which is possible at low oscillation frequencies), stability will be most easily lost with a phase shift of $\alpha = \pi/2$. The energy interpretation of this relationship was brought out above.

Let us emphasize some essential singularities of cascade flutter in actual blade rings.

It can be seen from an analysis of the preceding problem that the possibility of the origination of flutter is substantially affected by the presence of many degrees of freedom, i.e., the properties of the system as a whole. Thus, for example, if all the blades of the ring were absolutely rigid, and only one were elastic (or, in real terms, its rigidity were substantially less than that of the others), cascade flutter could not originate at all. This is explained by the fact that one oscillating blade cannot absorb energy from a unifrom potential stream. This was e. lained in § 10.3 in the analysis of

the conditions of energy exchange. The blade can extract energy from the stream only if the influence coefficients are inhomogeneous and if the neighboring blades oscillate. From these considerations, it is obvious that when, for instance on a turbomachine ring, rigid and elastic blades alternate, cascade flutter practically does not originate. Since, for technological reasons, real turbomachine rings have blades of different rigidity, the problem of blade flutter of an inhomogeneous cascade appears, which is formulated in [63].

Another problem of practical importance is the problem of flutter in a bounded cascade or blade packet. Such a packet may be regarded as a system of uniform blades, bounded by rigid end blades. Generally, this problem is a particular case of the preceding one. However, this particular case deserves special study, since experimental research on flutter is frequently conducted under static conditions on packets, and it is therefore necessary that the possibility of transfer of the results to an annular cascade be clear.

Let us consider the problem of the flutter of a packet of uniform blades [51]. Let the packet contain $z=2k+1$ elastic blades. The basic equation of motion (10.88) remains the same. It must be solved with the boundary conditions $y^0_{n+1} = y^0_{-(n+1)} = 0$.

We seek a solution in the form

$$y^0_n = e^{\lambda n}\cos \mu n$$

From the boundary conditions, it follows that $\mu(n+1)=0$, whence we obtain

$$\mu(n+1) = \frac{\pi}{2} + k\pi, \quad \mu = \frac{\pi}{2}\frac{2k+1}{n+1}.$$

Substituting the solution into Equation (10.88), we find

$$a_1 e^{\lambda(n-1)}\cos\mu(n-1) + a_2 e^{\lambda n}\cos\mu n + a_3 e^{\lambda(n+1)}\cos\mu(n+1) = 0$$

or

$$(a_1e^{-\lambda}\cos\mu + a_2 + a_3e^{\lambda}\cos\mu)\cos\mu n + (-a_1e^{-\lambda} + a_3e^{\lambda})\sin\mu n\sin\mu = 0.$$

Since this equation must be satisfied for all values of n, we obtain

$$\left.\begin{aligned} a_1e^{-\lambda}\cos\mu + a_2 + a_3e^{\lambda}\cos\mu &= 0,\\ -a_1e^{-\lambda} + a_3e^{\lambda} &= 0. \end{aligned}\right\} \tag{10.94}$$

From the second condition of (10.94) it follows that

$$e^{\lambda} = \sqrt{\frac{a_1}{a_3}}. \tag{10.95}$$

Then from the first condition of (10.94) we find

$$a_2 = 2\sqrt{a_1a_3}\cos\left(\frac{\pi}{2}\,\frac{2k+1}{n+1}\right).$$

To each value of k corresponds its own form of excitation. In the case at hand, the phase shift between adjacent blades may be equal to either zero or to $\pi/2$. To each form of oscillation corresponds a specific law of amplitude distribution, which is determined by the number of blades in the packet and by the relationship between the symmetric and the asymmetric part of the influence coefficients. The maximum amplitude is established at one of the ends of the blade packet, since the conditions are asymmetric due to the asymmetry (in the general case) of the influence coefficients. The pattern asymmetry of the excited oscillation is explained by the fact that energy transmission between the blades takes place in one direction.

It should be noted that the stability of the packet is higher than the stability of a homogeneous annular cascade. In view of this fact, as has been noted by R. A. Shipov, care must be exercised in transferring the experimental results obtained on the basis of a packet with a small number of blades to an annular cascade.

The problem of the flutter of an inhomogeneous circle of blades has been considered in Reference [85]. The basic conclusions consist

in the fact that an inhomogeneous circle is more stable than a homogeneous one. In connection with this, a practical conclusion is drawn concerning the possibility of protection against flutter by the introduction of inhomogeneity, i.e., by a decreased maladjustment of the blades on the ring on the basis of natural frequencies.

FOOTNOTES

1. on page 393 — The importance of studying this type of problems was first noted in [63].

2. on page 403 — Thus, the circulation values are not related.

CHAPTER 11

INVESTIGATION OF THE AERODYNAMIC DAMPING AND AERODYNAMIC EXCITATION OF TURBOMACHINE BLADES

§ 11.1. A Device for the Investigation of Aeroelastic Processes in Turbomachines

Let us consider some singularities in the experimental investigation of dynamic stresses in turbomachine blades.

The investigation of dynamic stresses in the blades of full-scale turbomachines is of considerable interest, and is at present being extensively carried out in factories. However, it is to be understood that just as in any investigation of a full-scale machine, test data, in addition to a number of advantages, also have disadvantages.

In the first place, the experimental investigation of blade vibration in a number of stages of full-scale machines represents considerable difficulties (for example, the vibration of the first stages of superhigh-pressure steam turbines).

In the second place, when testing full-scale machines it is not possible to investigate separate factors in detail; thus it is impossible to go deeply into a complex pattern of phenomena which may themselves be overshadowed by a number of subsidiary processes.

In model tests it is in many cases possible to retain the determining singularities of a phenomenon, and at the same time to create the possibility of carrying out sufficiently precise and fine measurements. Variation of the basic parameters which determine a phenomenon makes possible an investigation of their separate influence. All this makes model tests particularly necessary in the process of creating theoretical calculation methods, which at present are still far from being completely developed.

In order to emphasize only the basic singularities, let us consider a cascade of elastic blades that are oscillating in a stream of nonviscous incompressible fluid. We assume that the stream carries a system of periodically repeating vortex wakes, from which energy is extracted for maintenance of the oscillation. The cascade is defined by the characteristic dimension l. The blades are defined by the density of the materials ρ_1, modulus of elasticity E, and the mechanical oscillation decrement δ_3. The stream is characterized by a basic velocity of w^0, a fluid density of ρ^0, a typical velocity of v^0 in the wake, and a wake spacing of t.

Thus, the cascade-stream system is defined by eight parameters:

$$l,\ \rho_1,\ E,\ \delta_3,\ w^0,\ \rho^0,\ v^0,\ t. \tag{11.1}$$

Seven of these parameters are dimensional, and four dimensionless parameters can be compiled from them:

$$\frac{\rho^0}{\rho_1},\quad \frac{E}{\rho_1 (w^0)^2},\quad \frac{v^0}{w^0},\quad \frac{l}{t}. \tag{11.2}$$

Then according to similitude theory the dimensionless dynamic stresses in the blades are a function of five dimensionless criteria:

$$\frac{\sigma}{E} = f\left(\frac{\rho^*}{\rho_1},\ \frac{E}{\rho_1 [\omega^* l]^2},\ \frac{v^*}{\omega^* l},\ \frac{l}{l},\ \delta_3\right). \tag{11.3}$$

Considering the real problem and the turbomachine stage as a whole, to the number of determining criteria the Reynolds number must be added the Mach number and the Strouhal number, which characterize the operating conditions of the stage (the criteria: isentropy index, the degree of turbulence, and the degree of roughness will be secondary for this problem, and for the sake of simplification we shall not discuss them).

The obtained relationships indicate that the consideration of full similitude when modeling the aeroelastic oscillation of blades is scarcely of practical interest, since such similitude is difficult to obtain because of technical considerations.

Let us dwell upon questions of partial modeling of aeroelastic phenomena in aerodynamic cascades of turbomachines.

For the sake of definiteness we shall again consider the problem of the investigation of resonance dynamic stresses in working blades, the oscillation of which is induced by edge wakes of the directing cascade. The oscillation of an elastic system in resonance or close to resonance under the action of relatively small perturbing forces takes place in one of the main forms of free oscillation. The dynamic stresses in an elastic system in the case of stabilized oscillation are determined by the balance of the supplied energy and the dissipated energy.

For a cascade with blades of finite length, the shape of the vortex wakes which induce the oscillation is practically constant along the entire blade. Only in narrow zones, situated at the ends of the directing blades, is a sharp increase in the thickness of the boundary layer observed, brought about by secondary transverse leaks.

Thus, the oscillation of a working blade is induced by a distributed force, and by a concentrated force applied to the blade vortex

(the second concentrated force at the blade root cannot induce oscillation). In the case of oscillation in resonance, the deflection curve of the blade may be given by the principal oscillation mode

$$y = y^0 X(\xi) \sin \nu\tau, \quad \xi = \frac{x}{l}. \tag{11.4}$$

Here account is taken of the fact that between the excitation force, which is in phase with $\cos \nu\tau$, and the deflection there is a phase shift of $\pi/2$. We shall employ the energy method. The work of the distributed excitation force applied to the blade per oscillation cycle is equal (l is the blade length, $2b$ is the chord)

$$A_1 = \int_0^l \int_0^{2\pi/\nu} \mathcal{P}_1 \dot{y}\, d\tau\, dx = 4\pi^2 \omega^0 v^0 b l y^0 R I_1, \quad I_1 = \int_0^1 X(\xi)\, d\xi. \tag{11.5}$$

Function R must now depend also upon $l/2b$.

The work per oscillation cycle of the excitation force induced by tip phenomena is equal to

$$A_{1a}' = 4\pi^2 \rho^0 v_n^0 b \cdot \Delta \cdot y^0 R_0. \tag{11.6}$$

Here v_n^0 is the coefficient of the n^{th} harmonic of the Fourier series when the supplemental velocities in the wake at the ends of the directing cascade are expanded, Δ is the thickness of the tip loss zone.

The work of the aerodynamic damping forces per cycle is equal to

$$A_2 = \int_0^l \int_0^{2\pi/\nu} \mathcal{P}_2 \dot{y}\, d\tau\, dx = -4\pi^2 \rho^0 \omega^0 \nu b l (y^0)^2 T I_2. \tag{11.7}$$

Function T must now depend also upon the blade length $l/2b$.

The work of the mechanical damping forces per cycle is equal to

$$A_3 = \int_0^l \int_0^{2\pi/\nu} \mathcal{P}_3 \dot{y}\, d\tau\, dx = -2\pi h m \nu l (y^0)^2 I_2, \quad I_2 = \int_0^1 X^2(\xi)\, d\xi. \tag{11.8}$$

We shall consider in the first approximation that functions R(k, q, α) and T(k, q, α) do not depend upon the blade span $l/2b$.

This assumption is equivalent to the hypotheses of two-dimensional sections that is employed in steady-state aerodynamics.

In view of the smallness of the work of the aerodynamic damping forces in comparison to the energy of the oscillating blades, the aerodynamic damping coefficient may be represented as a ratio of A_2 to twice the maximum kinetic energy of the blade

$$\delta_2 = \frac{A_2}{2A_k} = 4\pi^2 \frac{\rho^*}{\rho_1} \frac{w^* b}{vF} T.$$

Here v is the circular velocity of the oscillation, F is the area of the blade section.

Defining the excitation coefficient in such a manner that it does not depend upon the blade deflection, we analogously find

$$\delta_1 = \frac{A_1}{2A_k} = 2\pi^2 \frac{\rho^*}{\rho_1} \frac{w^* v^*}{v^2 F} R.$$

Thus, δ_1 and δ_2 are expressed in terms of functions R and T. The coefficients of excitation in aerodynamic damping can also be determined experimentally.

The basic value of modeling consists in the fact that it becomes possible to conduct tests on a cascade that is operating at very high (or low) pressures on the basis of air with normal parameters.

However, if a conventional blade design is used in the model, it is impossible to decrease substantially the density of the working medium. Considerable gain may be obtained by making the blade rigid and hollow in the form of a shell or of foam material, and to effect elastic suspension. In this case a certain amount of freedom appears in the selection of the oscillation frequency of the blade and of the

model and, what is significant, it becomes possible to alter the mechanical damping coefficient within wide limits.

For such a problem, it is expedient to formulate the similitude criteria in a somewhat different form from above.

We define the cascade — stream system by the following parameters:

$$l,\ m,\ \nu,\ \delta_3,\ w^0,\ \rho^0,\ f,\ v^0. \tag{11.9}$$

Here new designations have been introduced: m is the linear mass of the blade, ν is the natural circular frequency of the blade oscillation, f is the natural circular frequency of action of the perturbing wakes.

Five dimensionless criteria are formed from these parameters.

$$\frac{\rho^0 l^2}{m},\ \frac{\nu l}{w^0},\ \frac{v^0}{w^0},\ \frac{f}{\nu},\ \delta_3. \tag{11.10}$$

The dimensionless dynamic stress depends on them

$$\frac{\sigma}{w^2 m} = f\left(\frac{\rho^0 l^2}{m},\ \frac{\nu l}{w^0},\ \frac{v^0}{w^0},\ \frac{f}{\nu},\ \delta_3\right). \tag{11.11}$$

However, in this problem a direct conversion of the dynamic stresses from the model to full scale cannot be effected, since their constructions are unlike. In the tests, only a similitude (approximate form) of the unstabilized processes is observed.

The model tests serve for determination of the coefficients of aerodynamic damping and excitation, and on the basis of these coefficients the dynamic stresses in full-scale blades are determined.

The following tests must be made on the models.

First the mechanical damping coefficient δ_3' (for $w^0 = 0$) is determined, then the total damping coefficient $(\delta_3' + \delta_2')$ for a given

dimensionless stream velocity w^*/vl and in the absence of wakes ($v^0 = 0$). Both of these tests may be based either upon measurement of the attenuation of free oscillation, or upon measurement of the power necessary for the maintenance of stabilized harmonic oscillation.

Then the model is tested at a given stream velocity and a given wake system. The maximum dimensionless deflection y/l is measured. Then the coefficient of aerodynamic excitation for the model is found from the expression, obtained from the energy balance:

$$\delta_1' = (\delta_2' + \delta_3') \frac{y/l}{2b/l}. \tag{11.12}$$

The coefficients of aerodynamic damping δ_2' and oscillation excitation δ_1', found experimentally in the model, may be transferred to full scale, if use is made of the hypotheses of two-dimensional cross sections.

Then we obtain the following values of the energy supplied from the stream and dispersed into the stream for an element the length of the full-scale blade

$$dA_1 = 4\delta_1' \frac{b}{y} dA_k, \quad dA_2 = 2\delta_2' dA_k. \tag{11.13}$$

Here and henceforth the values without a prime refer to full-scale conditions.

Integrating (11.13) through, taking (11.4 - 11.8) into account, we obtain the values of the coefficients of excitation and aerodynamic damping for a full-scale blade as a whole, expressed in terms of the obtained model values (we simplify, disregarding shifting)

$$\delta_1 = \frac{l_1}{l_0} \delta_1', \quad \delta_2 = \delta_2'. \tag{11.14}$$

Then the dynamic stresses in the root of the full-scale blade (in the case of purely flexural oscillation) are found according to the formula

$$\sigma = -\frac{2bEIX''(0)}{l^2W}\frac{\delta_1}{\delta_2+\delta_3}. \qquad (11.15)$$

Here the coefficient of mechanical damping δ_3 may be considered as known.

The influence of viscosity in the problems under consideration will be manifested in at least three directions: (a) the edge wakes will change due to diffusion of the vortices; (b) the presence of a boundary layer will bring about a change of the circulation and a delay in its establishment; (c) unstabilized phenomena in the boundary layer will bring about a change in the losses.

In experimental study of these problems, the determining criteria will include the Reynolds number. The indicated systematic research is of great interest, but its formulation involves considerable difficulties.

Experimental study of the influence of gas compressibility upon the characteristics of unstabilized flow about cascades is simpler than study of the influence of viscosity.

It is of interest for practical purposes to study the characteristics for all typical cases: subsonic, transonic, and supersonic.

Let us consider the design of an installation developed for investigating unstabilized aerodynamic and aeroelastic phenomena in turbomachines[1] (Figures 11.1, 11.2). The installation is intended for the study of dynamic stresses evoked by edge wakes, partial supply, or some other circular nonuniformity of the stream. On the installation, flow about cascades in a periodically unsteady and strongly turbulized stream can be studied. The installation is also suitable for studying flutter, rotating separation, and aerodynamic damping.

Footnote (1) appears on page 504.

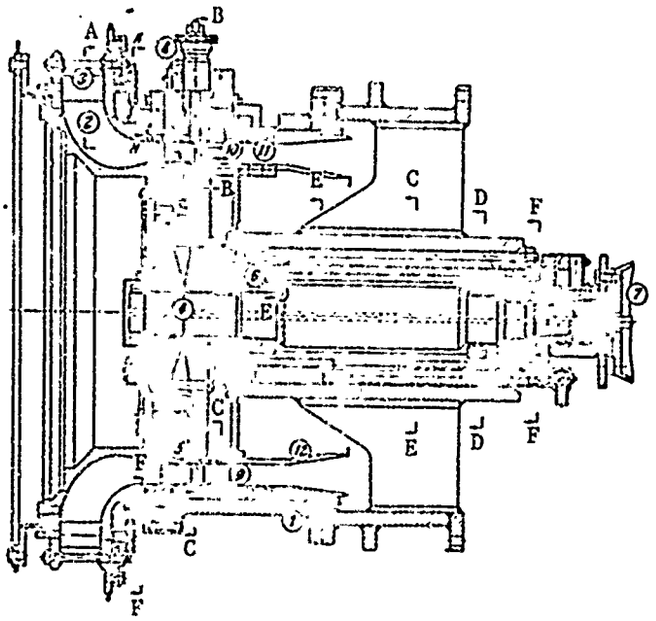


Figure 11.1. Longitudinal section through the experimental installation.

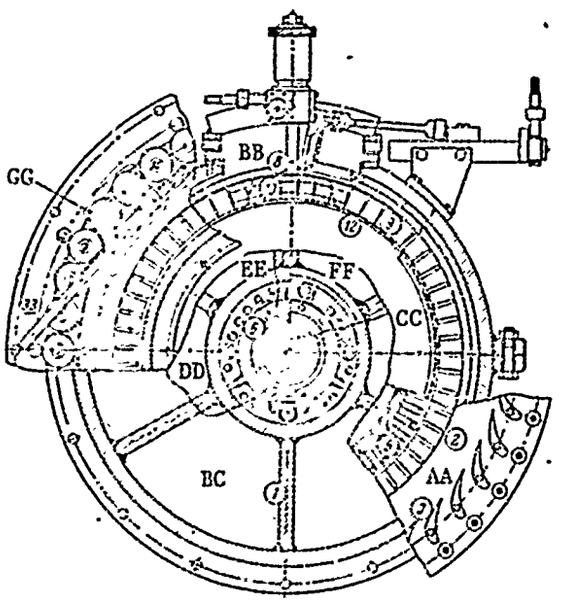


Figure 11.2. Cross section of the experimental installation.

The design of the installation is based upon considerations dealing with modeling of the basic singularities of unsteady aerodynamic phenomena.

For convenience in making the measurements, the aerodynamic cascade under investigation is made stationary, and the cascade preceding it is a rotating one. The installation possesses great flexibility because various problems and regimes can be taken into consideration, since its rotor can either be driven by an electric motor or, on the contrary, energy can be removed from the rotor by means of a hydraulic brake. Air flow through the installation at a rate of up to 4 m^3/sec is provided by a multistage compressor with a rotor speed of up to 9000 rpm.

The basic subassemblies of the installation include the frame (1), the annular intake fitting (2), the directing device (3), a shaft with a disk (4), rotor blades with a turn mechanism (5), a yoke with bearings (6), an electric motor (7), (a hydraulic brake may be installed instead of the electric motor), a coordinate device with movable rings (8), stator blades (9), a segment with the investigated blades in a special suspension (10), distance rings (11), a fairing (12).

The yoke with bearings, in assembly with the rotor of the installation, is fastened at the rear part of the frame. A circle of stator blades, the movable rings of the coordinate devices, and the distance rings are located in the front part of the frame, which has a horizontal joint. The segment with specially suspended blades, made of light material, and the coordinate devices with measuring probes is located across a window in the upper part half of the front part. An effuser with a directional prerotation unit is attached to the end flange of the front part of the frame. The attitude is changed simultaneously for all blades of the directional unit by means of a turn mechanism.

A conception of the investigation methods is given by the measurement diagram (Figure 11.3) used in studying the unsteady aerodynamic forces which excite and damp blade oscillation.

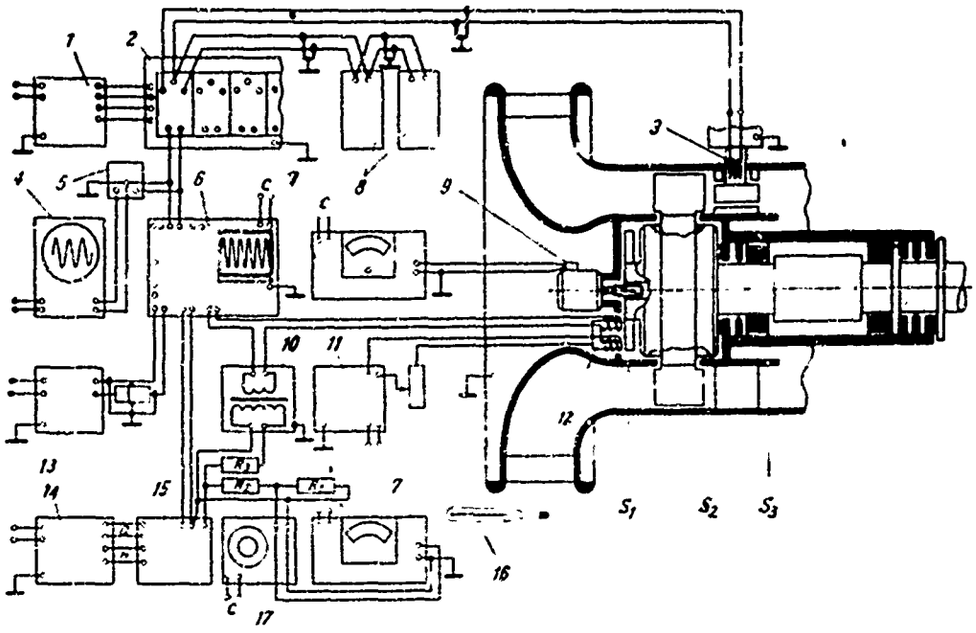


Figure 11.3. Measurement layout for the experimental installation (see Figure 11.1).

(1)-tensometer station power supply, (2)-tensometer station, (3)-tensometric sensor, (4)-cathode oscillograph, (5)-filter, (6)-loop oscillograph, (7)-frequency meter, (8)-resistance magazine, (9)-tachogenerator, (10)-output transformer, (11)-stabilized rectifier, (12)-turn-marker pickup, (13)-time marker, (14)-amplifier power supply, (15)-amplifier, (16)-thermometer, (17)-audio-frequency generator.

Measurement of the aerodynamic parameters (total and static pressure, and the stream angle) is conducted at three control cross sections: before the perturbed cascade S_1, after it S_2, and after the cascade under investigation S_3. The coordinate units which shift the probes have an electric drive with remote control. The probes may be moved in three directions: circumferential, radial, and axial, and can also turn.

Rough measurement of the rpm number is performed by means of a tachogenerator and a frequency meter. For precise measurement of the rpm number, an rpm marker with an induction type pickup is incorporated in the scheme. The induction coil works in conjunction with an oscillograph loop. For precise measurement, oscillation beats are produced by means of a sonic generator. For decoding on film, in addition to the beats and the signal of the rpm marker, the signal of the time marker is registered at a frequency of 1000 Hz.

Tensometric sensors, adhesively attached to the blades, register their displacement. The signal is delivered to a multichannel tensometric amplifier which functions without distortion up to a frequency of 7000 Hz. A loop oscillograph and a cathode oscillograph are connected at the amplifier output.

The sonic generator may be connected at the cathode oscillograph directly to the scanning unit in order to produce light marks on the curve of the process under investigation.

Let us consider the design of the blades.

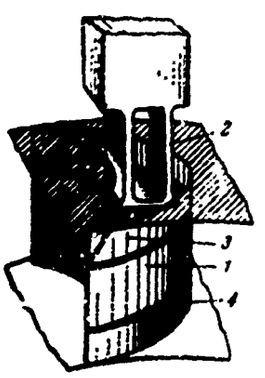


Figure 11.4. Design of suspended blade: (1)-suspended part of blade, (2)-elastic suspension, (3, 4)-profile fairings.

The blade under investigation (1) (Figure 11.4) is fastened on an elastic suspension (2) which consists of two plates; this provides for almost two-dimensional oscillation of the blade. Stationary profile parts (3) and (4) are situated at the ends. Their purpose is to decrease the influence of steady secondary leakages, originating at the ends of the curvilinear channel, upon the blade part under investigation. The investigated oscillating part of the blade may be made of materials of various density, so

that tests may be carried out on the basis of air with normal parameters with concurrent maintenance of the necessary relationships between the stream density and the blade density. Such a system makes it possible in practice to span the necessary range of natural frequencies of tangential, axial, and torsional oscillation of the blades from dozens of Hertz to 3000 - 4000 Hz. Thus, for example, an investigation was made of the blades of steam-turbine first stages, having natural frequencies of 2000 - 3500 Hz. In this case steel blades in turbines operate in steam of very high density, so that for maintenance of the mass criteria they were made of foam plastic in the air models. The profile part of the blade must be sufficiently rigid so that it does not participate in the oscillation. In the cited example the profile part had natural frequencies of tangential, axial, and torsional oscillation of 7000 to 17000 Hz.

The suspension of the blade part under investigation is designed in the form of two springs. The shape and the pickup adhesion points are shown in Figure 11.5. Cases (a), (b), and (c) of Figure 11.5 correspond to deformation in the case of tangential, axial, and torsional vibration of the blades. The dimensions of springs P and R, as well as angles α_1 and α_2 are selected on the basis of assigned natural-oscillation frequencies, as well as according to the condition of the locating the center of gravity and axis of torsion of the simulated blades.

Figure 11.6 shows a diagram of the adhesion of the tensometric sensors, used in investigating the vibration of active-profile blades and which provides for independent measurement of deformations in the axial direction X, the tangential direction Y, and the rotational direction M.

Senosrs 3 and 6 are so situated that when the blade is loaded in the direction Y it will undergo a corresponding deformation of the opposite sign. The action of a force along X will not bring about deformation of these sensors, since the plane passing through axis V of the elastic element will be neutral. The stress brought about

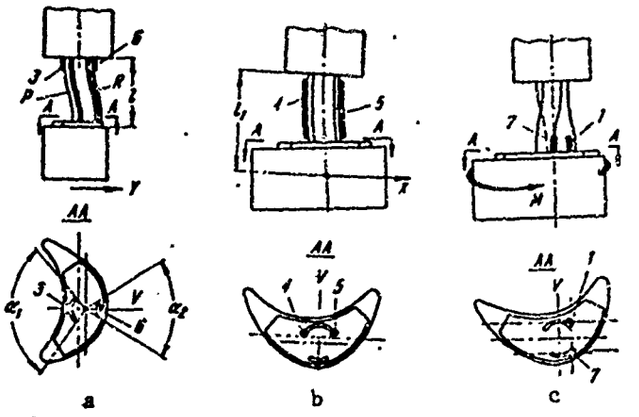


Figure 11.5. Deformation of blade suspension for three basic kinds of load. The tensometric sensors corresponding to the numbers serve to measure the following deformations:
(1, 3)-in the direction of the X-axis;
(4, 5)-in the direction of the Y-axis;
(1, 7)-torsional.

by the torque applied to the blade will also not be received by these sensors, since they are situated in neutral axes.

Sensors 4 and 5 are cemented on the side edges of spring P and are intended for measuring deformations of the opposite sign, originating with the action of a force along X.

Sensors 1 and 7 receive stresses brought about by torque. Sensors 4, 5, 1, and 7 are situated in such a manner that they react only to a specific form of load.

A bridge circuit for the connection of the sensors is shown in Figure 11.6. Sensor 2 is cemented onto the blade and is used for tuning the circuit (the necessity for tuning is brought about by inaccuracy in selection of the adhesion points, as well as by scattering of the resistances).

Small tensometric sensors (not more than 2 mm wide) of constantan wire 0.032 mm in diameter, with a resistance of not less than 100 ohms,

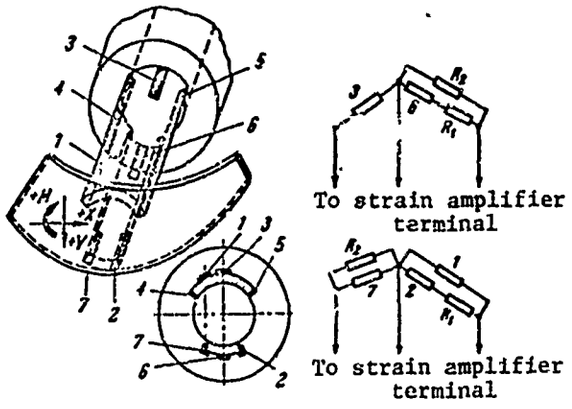


Figure 11.6. Displacement of tensometric sensors on a blade.

are used in the circuits.

Let us first devote some time to the determination of aerodynamic damping and mechanical damping in oscillating blades. This question is important by itself, since the level of the resonance stresses, depends upon the value of the damping as does the possibility of the origination of flutter. Proper determination of damping in research on models is also important because dispersed energy is determined from it. Consequently, in research on stabilized oscillation, the energy makes it possible to perform conversions and to find the dynamic stresses in systems with other characteristics.

§ 11.2. Determination of Aerodynamic Damping

We shall consider methods of experimental determination of serodynamic damping of the blades in a cascade, and some experimental results.

Direct experimental determination of the value of aerodynamic damping of the blades in a cascade is a difficult problem. The basic difficulty consists in the fact that aerodynamic damping depends essentially upon the phase shift of the blade oscillation. Maintenance of oscillation of the entire blade system with an arbitrary

assigned phase shift is impossible in practice. Therefore, it is usually necessary to be restricted to measurements of the value of aerodynamic damping for some accessible special cases.

A second difficulty is the necessity for sufficiently precise measurements, since the value of aerodynamic damping is relatively small, and it is necessary to measure aerodynamic damping in systems which inevitably have mechanical damping (damping in the most elastic structure and attachment points).

Two basic methods are employed for studying aerodynamic damping: the method of free attenuating oscillation and the method of forced oscillation. In the first method the oscillating system is brought out of the state of equilibrium and the attenuation rate of the oscillation is measured. This method has a drawback when applied to the study of aerodynamic damping in a cascade, since it can be employed only in the case of oscillation of the blade under consideration, and with the others stationary (with the excitation of several blades simultaneously the necessary phase shift will not be maintained, and the oscillation amplitudes will not be identical).

In the second method the stabilized harmonic oscillation of the system is maintained, and the energy dispersed by the system is measured in one way or another.

It is expedient to conduct the measurement of aerodynamic damping on special installations in which it is possible to change the air density and the blade material, the Mach number, the Reynolds number, and the angle of attack. The research must usually be carried out on blade models which oscillate two-dimensionally. This has definite advantages, since flow abut two-dimensional cascades has been studied most of all. However, in this case it is necessary to act on the basis of the hypotheses of two-dimensional sections; this hypothesis is generally justified in the study of steady-state phenomena. In this case, however, the experiments are not entirely representative,

since the tip effects are also unavoidably taken into account. A check on the share of the end effects can be made only by changing the length of the investigated part of the blade.

In a case where the aerodynamic damping of one oscillating blade is determined (the others are stationary), the method of free oscillation may be used.

The process of attenuation of the blade oscillation without a stream and in a stream is recorded by means of an oscillograph.

In the first case, attenuation of the oscillation is brought about only by mechanical damping, and in the second case — by mechanical damping and aerodynamic damping. By definition, the logarithmic coefficient of oscillation is equal to

$$\delta = \frac{1}{n} \ln \frac{y_0^0}{y_n^0}.$$

Here y_0^0 and y_n^0 are respectively the initial and the final (n periods later) oscillation amplitudes.

The aerodynamic damping coefficient is found as the difference between the total coefficient and the mechanical coefficient.

For studying the influence of the oscillation of the remaining blades upon the aerodynamic damping of the blade under consideration, it is necessary to consider an annular cascade of elastic blades. In many cases it is sufficient to consider the oscillation of a packet of blades, since the most significant influence is exerted by the adjacent blades. Excitation of the blade oscillation must be effected with an assigned phase shift, which must be controllable. Such excitation may be effected by the preceding rotating cascade, which creates vortex wakes. In a case where the excited cascade is completely homogeneous, the phase shift between the oscillations of the blades depends only upon the ratio of the spacing of the exciting

cascade and that of the excited cascade. The blade performs nz_1 oscillations per unit of time, where n is the number of revolutions, $z_1 = \pi d/t_1$ is the number of blades of the excited cascade, d is its diameter, and t_1 is the blade spacing. Then the oscillation period is equal to $t_1/\pi nd$. The adjacent blades obtain momentum with a time shift equal to $t_2/\pi nd$, where t_2 is the spacing of the excited cascade. Consequently, the phase shift of the oscillation of the adjacent blades is equal to

$$\alpha = 2\pi \frac{\pi n\, dt_2}{\pi n\, dt_1} = 2\pi \frac{t_2}{t_1}. \tag{11.16}$$

A resonance peak can be constructed by tensometric measurement of the oscillating blades. The total damping coefficient is obtained on the basis of the sharpness of the peak.

The dynamic coefficient (the ratio of the oscillation amplitude to the static deflection under the action of the same force), as is known, is equal to

$$\lambda = \frac{y}{y_0} = \left\{\left[1 - \left(\frac{f}{\nu}\right)^2\right]^2 + \left(\frac{\delta}{\pi}\right)^2 \left(\frac{f}{\nu}\right)^2\right\}^{-1/2}. \tag{11.17}$$

Here f and ν are respectively the frequencies of the forced oscillation and the natural oscillation. We designate $\Delta\nu = f/\nu - 1$ and $\lambda = \lambda_m \lambda_1$, where $\lambda_m = \pi/\delta$ is the maximum value of the dynamic coefficient. Considering a sufficiently narrow area in the vicinity of resonance, it may be considered that $\Delta\nu \ll 1$. In all actual cases the damping coefficient is also very small, $\delta \ll 1$. Discarding terms of the second order of smallness, from (11.17) we obtain, after transformations,

$$\delta = \frac{2\pi |\Delta\nu|}{\sqrt{\lambda^2 - 1}}. \tag{11.18}$$

Constructing a resonance peak on the basis of experimental data, by means of (11.18) we find the total damping coefficient. Subtracting from it the mechanical damping coefficient, obtained, for example, on the basis of attenuation of the system without a stream,

we determine the aerodynamic damping coefficient. It is obvious that in order to increase the accuracy, it is necessary to create an oscillating system with the smallest possible coefficient of mechanical damping.

It must be noted that determination of the damping coefficient on the basis of results of measurements conducted in turbomachines is inevitably made with relatively low accuracy. Therefore, in cases where this is possible, it is better to determine the damping coefficient on a special stand.

Let us compare the resonance amplitudes of the oscillation of the same blade without a stream y_1^0 and in a stream y_2^0. If this blade is excited by the same force, which can be accomplished on a stand, the amplitudes must be inversely proportional to the corresponding oscillation decrements

$$\frac{y_1^0}{y_2^0} = \frac{\delta_2 + \delta_3'}{\delta_3}.$$

Here δ_2 is the coefficient of aerodynamic damping, δ_3 and δ_3' are respectively the coefficients of mechanical damping for amplitudes y_1^0 and y_2^0.

The coefficient of aerodynamic damping is found according to the formula

$$\delta_2 = \frac{y_1^0}{y_2^0}\delta_3 - \delta_3'. \qquad (11.19)$$

However, the application of this method is restricted, since when studying the damping of a blade system it is a complex matter to provide for forced vibration of the blades with assigned amplitudes and phase shifts. The advantage of this method is greater accuracy.

One additional difficulty must be overcome when conducting research. The point of the matter is that it is in practice impossible to make the cascade absolutely homogeneous. Since the blades always

have an unavoidable scattering of the natural partial frequencies, at oscillation close to resonance there will originate a phase shift, different for different blades, between the acting force and the deflection. Consequently, the oscillation phase shift of adjacent blades will not be equal to the phase shift of the forces acting upon these blades. Let us note that Formula (11.16) expresses precisely this force phase shift, and only in the case of a homogeneous cascade does it simultaneiously yield the oscillation phase shift.

Let us assume that there is an unconnected system of blades[2] with a certain scatter of the natural frequencies: ν_1, ν_2, ...

Let this system be acted upon by a perturbing force with the frequency f. The phase shift between the force acting upon the blade and the side of the blade is expressed by the well-known formula

$$\psi_n = \operatorname{arctg} \frac{\frac{\delta}{\pi}\frac{f}{\nu}}{1-\left(\frac{f}{\nu_n}\right)^2}.$$

Let us consider a case where the scattering of the natural frequencies is small and oscillations close to resonance are being studied. Designating $f/\nu_n - 1 = \Delta\bar{\nu} \ll 1$, we obtain

$$\psi_n = \operatorname{arctg} \frac{\delta}{2\pi(\Delta\bar{\nu})}. \tag{11.20}$$

We express the phase-shift difference $\Delta\psi = \psi_1 - \psi_2$ of adjacent blades, for example, the first and the second, by the formula

$$\Delta\psi = \operatorname{arctg} \frac{\delta}{2\pi(\Delta\bar{\nu}_1)} - \operatorname{arctg} \frac{\delta}{2\pi(\Delta\bar{\nu}_2)}.$$

In this case, if the first blade is in resonance, we obtain

$$\Delta\psi = \frac{\pi}{2} - \operatorname{arctg} \frac{\delta}{2\pi\Delta\bar{\nu}_2}.$$

In order that $\Delta\psi$ be a small value, it is necessary to have a very small frequency difference with respect to the natural frequencies. Thus, for example, when $\delta = 0.03$ and with the condition $\Delta\psi < 10°$,

Footnote (2) appears on page 504.

it is necessary to maintain $|\Delta\bar{\nu}_2| < 8{,}5 \cdot 10^{-4}$. Thus, for the selected conditions the natural frequencies should not differ by more than 0.085%.

With such a frequency scatter, the dynamic coefficient will in practice be equal to the maximum value, and the blades will oscillate with equal amplitudes.

For adjusting high-frequency blades with such precision, a special method of monitoring is necessary. For precise control, I. Neruda proposed the marker method. In this method a cathode oscillograph is used, the circuit of which makes it possible to superimpose, on the image of the oscillatory process, luminescence markers the frequency of which may be controlled by means of an external source. The oscillatory tube must have an afterglow. The marker frequency is selected an integer greater than the natural frequency of the blade. Then, as is shown in Figure 11.7 a, the disposition of the markers is the same on all waves of the attenuating-oscillation curve. If a scanning scale of the image with respect to time is so selected that the individual waves will merge, converging continuous bands formed by the markers on the attenuation curve can be observed on the stream. In a case where the ratio of the marker frequency to the natural oscillation frequency of the blades is a fraction, the bands will intersect in the manner shown in Figure 11.7 b. From the slope of the bands the deviation of the frequency of one blade from the frequency of another can be computed, for which the markers generate nonintersecting strips

$$\Delta\nu = \frac{\nu}{nk_n}. \qquad (11.21)$$

Here k_n is the multiplicity, n is the number of blade oscillations in the interval $\Delta\tau$ between the points of intersection of two adjacent bands with the abscissa. For the example under consideration (k_n = 12, n = 6) the relative frequency change equals $\Delta\nu/\nu \approx 0.014$. With the use of this monitoring method it was possible to adjust the high-frequency blade (ν = 3000 Hz) with an accuracy to within 0.1%.

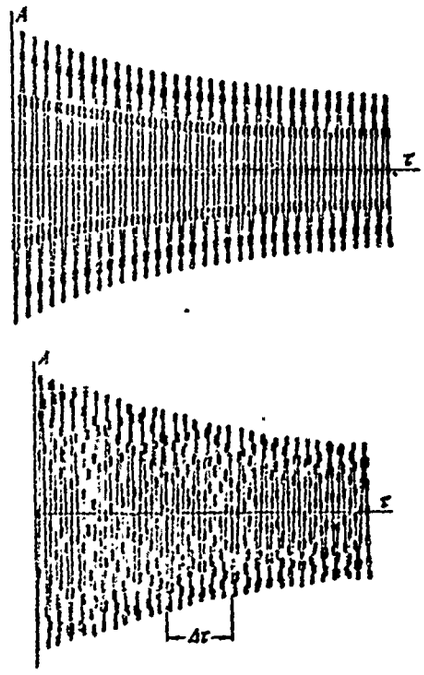


Figure 11.7. Marker method for precise determination of oscillation frequency.

The scatter of the natural frequencies of the blades in a cascade of a real turbomachine may reach 10% for technological reasons. Therefore, it must be emphasized that in laboratory research, an idealized system is created for the purpose of obtaining in pure form the influence coefficients which may then be converted to an arbitrary oscillating cascade.

At present it would be difficult to point out a method that did not have some drawbacks. Therefore, it is important to compare damping coefficients obtained by various methods.

Let us consider the method of determining the damping coefficient employed by F. Ruben. The method is based upon the excitation of synchronized forced oscillation by means of electromagnets, and makes possible smooth adjustment of the phase angle. The method becomes complex if the oscillation of more than three adjacent blades is studied.

The idea is understandable from the measurement diagram (Figure 11.8). The blade under investigation (1) is fastened on an elastic suspension (2), as has been described above. Adjacent blades (1a) and (1b) have their own suspensions, and there is no mechanical connection with blade (1). Let us consider the special case where the last blades have a common tuning-fork suspension and may oscillate only in phase. The overall system looks the same, but requires a third electromagnet and separate suspension. The oscillation of

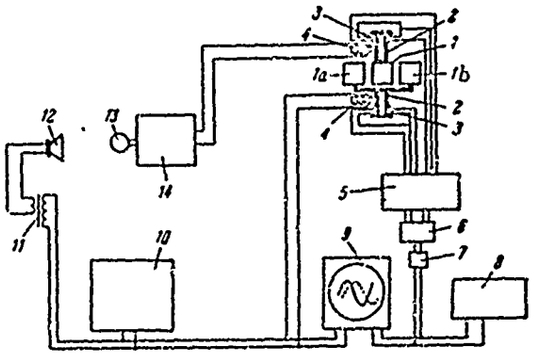


Figure 11.8. Measurement layout for the determination of aerodynamic damping.

blades (1a) and (1b) is maintained by an electromagnet (4) connected to the audio-frequency generator (10). The signal is delivered with the same frequency from the generator (10) through a transformer (11) to a dynamic loudspeaker (12), at a definite distance from which a microphone (13) is installed. The signal is received with a time lag which may be controlled by changing the distance between the dynamic speaker and the microphone. It is this device that creates the necessary phase shift. Then the signal passes through the amplifier (14) and arrives at the electromagnetic (4) which oscillates the central blade.

Strain gauges (3) are located on the suspensions connected with the strain-gauge data unit (5). The pulses from the strain gauge data unit pass one by one through the commutator (6) and the filter (7) to the cathode oscillograph (9), which is synchronized with the audio-frequency generator. Here a measurement of the blade-oscillation phase shift can be made. In the measurement of amplitudes, the signal from the strain guage data units on the suspension is fed to the millivoltammeter (8).

Let us consider some experimental results with regard to the determination of aerodynamic damping for a cascade of turbine blades.

An active cascade with TR-1A profiles had an incidence of $\beta_y = 80°$ (the calculated entry angle is $\beta_1 = 25°$). In most of the experiments the relative spacing was equal to $\bar{t} = t/2b = 0.6$, except for specifically stipulated cases. The natural frequency of the cascade was varied from 112 to 1520 Hz. The stream velocity ranges from 10 to 200 m/sec.

Figure 11.9 shows resonance peaks recorded when the blade under investigation oscillated outside a stream, in order to determine mechanical damping (these losses include losses for friction in air, and for acoustic radiation). The frequency of the perturbing oscillation is plotted along the abscissa, and along the ordinate are plotted the readings of the millivoltammeter, which are porportional to the deformations of the blade. In Figure 11.10 the same peaks are plotted in terms of relative coordinates. From a comparison of the peak sharpness it follows that the mechanical damping of the system is weak, but nevertheless increases with an increase of the oscillation amplitude. This is also in agreement with the fact that in Figure 11.9 the resonance conditions at the smallest amplitudes correspond to high frequencies (in terms of relative values this change is negatively small), as follows from the theoretical considerations. Within the investigated load limits, the mechanical damping coefficient changed from 0.0045 to 0.0065. The values obtained by the two methods generally coincide. The oscillating system was designed on purpose to have such a small mechanical damping coefficient, in order to increase the accuracy of the determination of aerodynamic damping.

An experimental investigation was made of the influence of the oscillation amplitude on the aerodynamic damping coefficient. Figure 11.11 shows, as a function of the relative blade oscillation amplitude 2A/t (where t is the cascade spacing), the value $K_A = \delta_a/\delta_{am}$, the ratio of the aerodynamic damping coefficient to that at maximum amplitude. The experimental points refer to various oscillation frequencies and main stream velocities, which are indicated in the graph. In each series of

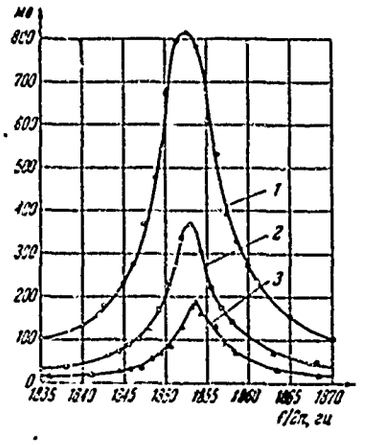


Figure 11.9. Resonance peaks for various load values.

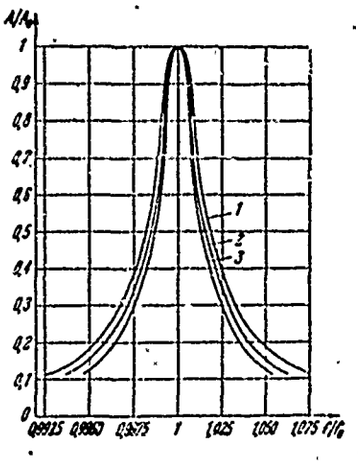


Figure 11.10. Resonance peaks in dimensionless coordinates.

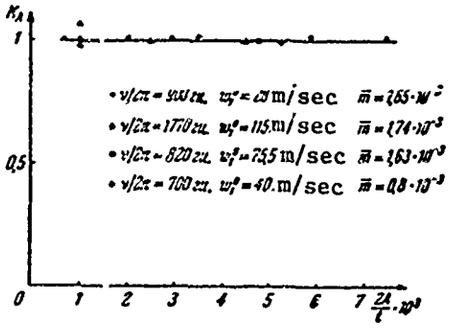


Figure 11.11. Relationship of relative aerodynamic damping coefficient to the oscillation amplitude (one blade is oscillating).

experiments the Strouhal number and the mass criteria $\bar{m}=\rho^0(2b)^2/m$. were held constant. From the obtained relationship it follows that the aerodynamic damping coefficient does not change when the oscillation amplitude is changed by a factor of seven. It should be kept in mind that these experiments are carried out with a single oscillating blade and, consequently, shifting cannot yield a force which performs work.

In Figure 11.12 are shown the results of a series of tests, the purpose of which is to establish the relationship of aerodynamic damping to the main stream velocity. Along the ordinate is plotted the relative damping, damping at maximum velocity being taken as the unit. It follows from the graph that the relationship obtained in a wide range of velocity variation remains linear, which coincides

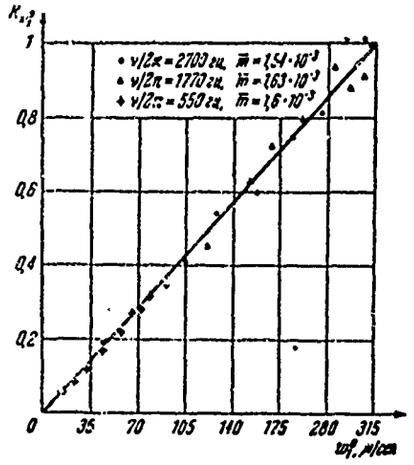


Figure 11.12. Relationship of the relative value of aerodynamic damping to the flow velocity.

with the theoretical considerations. Some scattering of points is observed at high stream velocities; this is evidently connected with the influence of compressibility. Somewhat unexpected is the fact that this influence is in this case insignificant. In each series of these experiments, the natural oscillation frequency and the mass criterion $\bar{m}$ were kept constant.

Since during the experiment the gas density was varied together with the velocity, a conversion was made to constant density (the same mass criteria). The justification for the possibility of such a conversion is obvious from theoretical and experimental considerations. In this experiment the Reynolds number changed as a function of gas velocity and gas density. Special research on determination of the influence of the Reynolds number was not conducted; however, the indirect conclusion may be arrived at that this influence cannot be significant in the range under consideration.

In Figure 11.13 is presented a graph of the absolute value of aerodynamic damping as a function of a combination of the mass criterion and the Strouhal number. The calculations were made with respect to the ratio of the resonance amplitudes. Let us first consider the justification for the selection of such a combination as a criterion upon which the aerodynamic damping coefficient depends.

The pressure distribution along the profile during oscillation is determined by the Lagrange integral

$$\tilde{p} = -\rho^0 \frac{\partial \Phi}{\partial \tau} - \frac{1}{2}\rho^0 \tilde{w}^2 + \text{const.} \qquad (11.22)$$

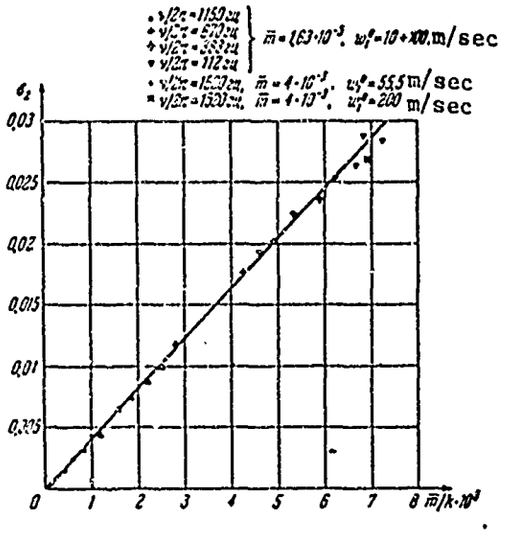


Figure 11.13. Relationship of aerodynamic damping to the dimensionless complex $\bar{m}/k$.

Here ρ^0, $\bar{p}$ are respectively the density of the fluid and the pressure, $\bar{w}$ is the absolute velocity of the stream flowing about the profile, φ is the velocity potential.

The distribution of pressures along the profile determines the force acting on the profile. Since aerodynamic damping depends upon the energy exchange between the oscillating blade and the stream, in the case at hand only that part of the force is of interest, which is in phase with the oscillation velocity and can perform work. Obviously, in this case account need not be taken of the first term in the Lagrange equation, since it is in phase with the acceleration (recollect that in this experiment the oscillation of only one profile in the cascade is being considered and, consequently, the velocity potential changes within time in phase with velocity, and its derivative changes in phase with acceleration). We shall also take into account the fact that high-frequency oscillation is being considered and, as has been noted above, shifting of the blade does not affect the energy exchange.

Thus the variable part of the pressure, which is in phase with velocity, is determined only by the second term of the Lagrange equation.

The square of the absolute stream velocity may be represented in the following manner:

$$\bar{w}^2 = (w^0 + w_x)^2 + w_n^2. \qquad (11.23)$$

Here w^0 is the distribution of velocity along the profile in stabilized stream, $w_s << w^0$ and $w_n << w^0$ are respectively the tangential velocity and the normal velocity of the perturbed movement of the fluid brought about by small oscillations of the profile.

Comparing (11.22) and (11.23) and discarding terms of the second order of smallness, we find that the variable part of the pressure, which is in phase with the oscillation velocity, is proportional to the product of velocities $p \sim \rho^0 w^0 w_s$. The perturbed velocity of the fluid must be proportional to the oscillation velocity of the blade, equal to $v_0 \cos \nu\tau$ (v_0 is the modulus of the oscillation velocity, ν is the oscillation frequency). Then we obtain

$$p \sim \rho^0 w^0 v_0 \cos \nu\tau.$$

The variable aerodynamic force is obtained by integrating this expression along the entire surface of the blade, and consequently will be proportional to the semichord b and the height l of the blade

$$Y \sim \rho^0 b l w^0 v_0 \cos \nu\tau.$$

The power released to the stream by the blade is proportional to the product of the force and the oscillation velocity

$$N \sim \rho^0 b l w^0 v_0^2 \cos^2 \nu\tau.$$

The energy released by the blade during one oscillation period equal to $2\pi/\nu$ is found by integration of the preceding expression over time and, consequently, will be proportional to

$$E \sim \frac{1}{\nu} \rho^0 b l w^0 v_0^2. \qquad (11.24)$$

We now find the expression for the aerodynamic damping coefficient in terms of the dispersed energy.

By definition, the logarithmic decrement of oscillation is equal to the logarithm of the ratio of two adjacent attenuating-oscillation amplitudes

$$\delta = \ln \frac{A_1}{A_2} = \ln \frac{v_{10}}{v_{20}}. \tag{11.25}$$

The latter replacement was made on the basis of the fact that the ratio of the oscillation amplitudes is equal to the ratio of the oscillation-velocity moduli. Multiplying the sublogarithmic expression by ml, where m is the linear mass and l is the height of the oscillating part of the blade, we obtain the expression for the oscillation decrement in terms of the ratio of kinetic energies taken one oscillation period apart:

$$\delta = \frac{1}{2} \ln \frac{ml v_{10}^2}{ml v_{20}^2}.$$

Further, by elementary transformations, we obtain

$$\delta = -\frac{1}{2} \ln \left[1 - \frac{ml\left(v_{10}^2 - v_{20}^2\right)}{ml v_{10}^2} \right] \approx \frac{ml\left(v_{10}^2 - v_{20}^2\right)}{2ml v_{10}^2}. \tag{11.26}$$

The latter simplifications were made on the basis of the fact that $\delta << 1$, and consequently, $(v_{10}^2 - v_{20}^2)/v_{10}^2 \ll 1$.

Expression (11.26) constitutes the ratio of the kinetic energy lost by the system per cycle during an attenuated oscillation, to twice the initial kinetic energy $2E_k = mlv_0^2$. The kinetic energy lost, on the basis of the law of conservation, must be equal to the energy dispersed in the oscillation process and, consequently,

$$\delta = \frac{E}{2E_k}. \tag{11.27}$$

From (11.24) and (11.27) we finally obtain the result that the damping coefficient must be proportional to the mass number and inversely proportion to the Strouhal number:

$$\delta \sim \frac{\rho^0 blw^0 v_0^2}{vmlv_0^2} \approx \frac{\rho b^2}{m} \frac{\omega^0}{v^0} = \frac{\bar{m}}{k}, \quad \bar{m} = \frac{\rho^0 b^2}{m}, \quad k = \frac{vb}{w^0}. \tag{11.28}$$

The above considerations are based upon a quasi-steady approach, since the influence of the vortex wake was not taken into account. All the considerations may be repeated also for the general case and the difference will lie in the fact that the obtained expression will be preceded by a correction multiplier which depends only upon the Strouhal number (this result is obtained from the consideration of similitude)

$$\delta = K(h)\frac{\rho}{\rho}. \qquad (11.29)$$

We now turn to an experiment (Figure 11.13) which, with the aim of confirming the criterial relationship, was conducted with broad and independent variation of the dimensional values. The stream velocity was varied from 10 to 200 m/sec, the natural blade frequency was varied from 112 to 1520 Hz, the mass of the blade was varied approximately threefold. During the entire experiment, the geometrical characteristics of the cascade and the angle of stream incidence remained constant.

From Figure 11.13 it follows that the Relationship (11.28) is confirmed very well and, thus the coefficient in Formula (11.29) is constant within the range of these experiments.

From these experiments an influence coefficient can be obtained directly: the velocity coefficient of the influence of the profile upon itself α_{nn}. The remaining influence coefficients may be obtained by studying the oscillation of the adjacent profiles.

All the described tests were carried out on an aerodynamic cascade with a relative spacing of $\bar{t} = t/2b = 0.6$ (2b is the chord of the profile). It was noted that with this spacing, self-similarity with respect to the Strouhal number was detected. Experiments with cascades of large spacing permit this pattern to be clarified. Investigations have shown that in cascades with a large spacing, (Figure 11.14) a relationship of aerodynamic damping to the Strouhal

number is observed, namely, just as in a single wing, aerodynamic damping increases with a decrease of $k = vb/\omega_1$. It has been shown experimentally that the smaller the cascade spacing, the less is the influence of the Strouhal number. When $k > 1$, self-similarity is observed for all investigated cascades. Along the ordinate the ratio of the aerodynamic damping coefficient with an arbitrary $\bar{t}$ to the same value when $\bar{t}$ equals 0.6 is plotted. These tests also pertain to the case where one blade is oscillating in the cascade.

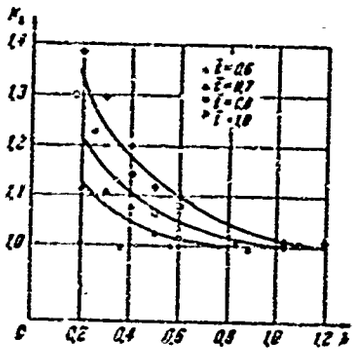


Figure 11.14. Relationship of relative aerodynamic damping to the relative cascade spacing.

For dense cascades with cophasal oscillation, the cause of self-similarity was explained earlier.

Research conducted with the aim of ascertaining the influence of the spacing upon aerodynamic damping shows (Figure 11.15) that in the range which is of practical interest, the relationship of aerodynamic damping to the spacing is monotonic.

This comparison was made with self-similar Strouhal numbers. The coefficient of aerodynamic damping at a relative spacing of $\bar{t}$ = 0.6 was taken as the unit of comparison. With a decrease of the spacing the aerodynamic damping increases, since the induced velocities increase. This increase (which agrees with the theory) is brought about by an increase in the rate of displacement of the fluid, during oscillation, from the narrower interblade channel. The corresponding precise calculations of the cascades were carried in Chapter 7. Here, for clarification of this phenomenon, we shall carry out an elementary calculation based upon a crude hypotheses. In a sufficiently dense aerodynamic cascade, the origination of induced velocities w_s may be imagined as a process of displacement of the fluid from the inter-

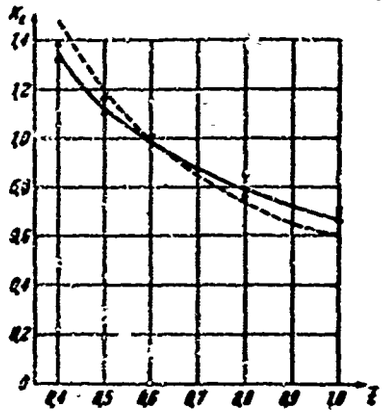


Figure 11.15. Relationship of relative aerodynamic damping to the relative cascade spacing.

blade channel as the profiles come closer together and, conversely, as an inflow of the fluid when the profiles move farther apart. During oscillation of the blades, these two processes in adjacent interblade channels take place simultaneously. In the relatively narrow interblade channel the perturbed velocities will be inversely proportional to the distance between the profiles and directly proportional to the length of the contour arc. Since the geometry of the profile remains constant, the induced velocities are inversely proportional to the ratio of the spacings of the two compared cascades $w_2^{(2)}/w_2 = l/l^{(2)}$. On the basis of previous considerations it is obvious that the coefficients of aerodynamic damping $\delta^{(2)}/\delta = l/l^{(2)}$ must be in the same proportion. From Figure 11.15 it follows that this elementary calculation (dotted curve) yields satisfactory results.

Figure 11.16 shows the relationship of the relative aerodynamic damping coefficient to the angle of attack. It has been experimentally shown that relative aerodynamic damping has the greatest value in calculated streamline flow.

Up to now we have been dealing with the determination of aerodynamic damping in the case of flexural blade oscillation. Now we present experimental values of aerodynamic damping in the case of torsional oscillation (Figure 11.17). Along the abscissa the dimensionless quantity $\rho^0(2b)^4/Jk$ is plotted which is analogous to the quantity $\bar{m}/k$ used above when studying flexural oscillation. Here $\rho^0(2b)^4/J$ is the dimensionless moment of inertia, ρ^0 is the density of the gas, 2b is the blade chord, J is the physical moment of blade inertia

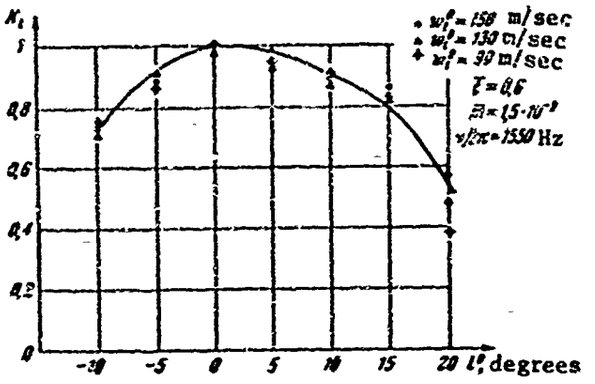


Figure 11.16. Relationship of relative aerodynamic damping to the angle of attack.

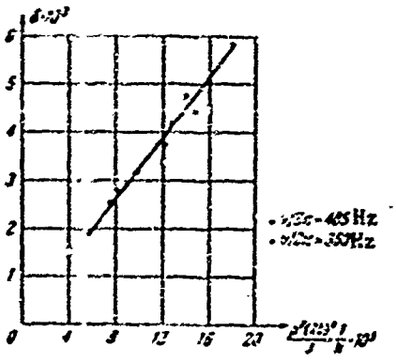


Figure 11.17. Relationship of aerodynamic damping in case of the torsional oscillation of profile TR-1A to the value $\rho^2(2b)^4 f/k$.

about the center of torsion, k is the Strouhal number.

Experiments have proven (in case of the oscillation of a single blade) the presence of a proportional relationship between the coefficient of aerodynamic damping and the above-mentioned quantity. During the experiment the velocity of the main stream and the natural frequency of the torsional oscillation of the blade were varied.

§ 11.3. Investigation of Forced Oscillation

The investigation of forced blade oscillation, and study of the exciting and damping forces in cascades, were conducted on the inverted turbomachine described in § 11.1.

Let us first consider the selection of the type of exciting cascade which generates vortex wakes. In turbines (or compressors), cascades may vary very greatly with respect to geometrical and aerodynamic characteristics. However, in the case of subsonic streamline flow at some distance from the cascades, the dimensionless characteristics of the edge wakes should be identical. This property follows from the theory of turbulent jets or vortex wakes propagating behind bodies of arbitrary shape.

The characteristics of a turbulent edge wake behind cascades were discussed in § 9.1, where the basic dimensionless relationships are also presented. For regimes where the cascades are well streamlined systems, the edge wakes are subject to a universal relationship at a relatively small distance from the outlet edges. This research concerns the study of vortex wakes behind the central part of the blades, i.e., in that part of them where the influence of tip effects brought by finite blade length has no effect.

In the vicinity of the end walls bounding an annular directing cascade, complex secondary flows originate, which change the shape of the edge wakes.

In order to clarify the basic governing laws, it is desirable to conduct the research (in any case, the initial research) for wakes that are constant with respect to blade height. Therefore, as has been shown above, the oscillating part of the blade is constructed in such a manner as to cut off the peripheral part of the wakes, which impinge on the peripheral profile fairings.

The standard TS-2A nozzle cascade (Figure 11.18) was adopted as the perturbing cascade. The distribution of the relative supplemental velocities in the edge wakes of this cascade at a differing relative axial distance $\Delta b/t$ is shown in Figure 11.19. Tests were conducted with a Reynolds number of 7×10^5 (the profile chord was taken as the characteristic dimension) and the dimensionless velocity $\lambda = c/a_* = 0.64$ (a is the absolute stream velocity, a_* is the critical velocity).

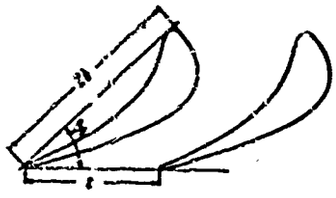


Figure 11.18. The TS-2A nozzle cascade.

The characteristic decrease of the velocity dip and the increase of the wake with increasing distance from the cascade can be seen in Figure 11.19.

On the circumference of the wheel z = 48 nozzle blades were located, which corresponded to a relative spacing of $\bar{t} = t/2b = 0.51$.

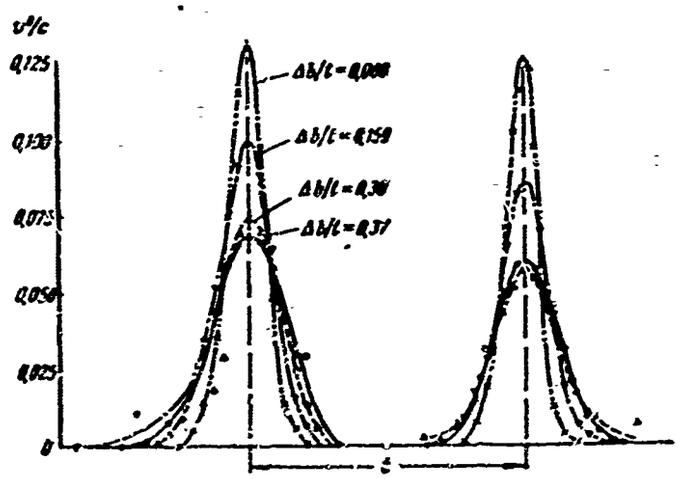


Figure 11.19. Graph of relative supplemental velocities in wakes behind the TS-2A nozzle cascade.

All research on edge wakes at cascades is conducted under static conditions and in the absence of a working cascade. In a real working stage the structure of the wakes naturally changes, since they are intercepted by working cascades; in addition, a downstream influence of the cascade is observed. However, in order to find the general governing rules in the value of the exciting force, it is desirable to try to find the connection between the characteristics of the static edge wakes and the dynamic stresses.

During an investigation of a turbomachine stage consisting of a directing cascade and a working cascade, the dynamic forces in the working blades are excited not only due to edge wakes, but also due to the immediate mutual influence of the cascades. This influence is brought about by nonuniformity of the velocity field in the vicinity of the cascades, and essentially can be manifested also in a potential stream. The nonuniformity of a velocity field of this type decreases rapidly as the axial distance between the cascades is increased. The corresponding theoretical questions and the calculation method were considered in Chapter 8. In a detailed experimental study of excitation, it is desirable to separate these two different forms of cascase interference in a stream. This can be accomplished to a certain extent if advantage is taken of the fact that at a certain distance from the perturbing bodies, wakes are universal and do not depend upon the specific shape of the bodies.

In this case it is convenient to take a cascade of round rods as the exciting cascade.

Figure 9.2 shows the results of a number of experiments in regard to the investigation of vortex wakes behind turbine and compressor cascades, rods with a round cross section, and plates with a rectangular outlet edge. When working with the characteristics in terms of the dimensionless coordinates of turbulent-jet theory, satisfactory agreement is observed with the universal theoretical curve. Here y/Δ_* is the ratio of the coordinate measured across the wake to the halfwidth of the wake, taken when $v^0 = \frac{1}{2} v^0_{max}$, where v^0_{max} is the maximum velocity dip in the center of the wake. The greatest scatter of points is observed near the boundary of the jet. This is connected with the known intermittence effect and a decrease in the accuracy of the measurements. Let us also note that some points correspond to measurements carried out in planes situated closer to the perturbing bodies than is permitted by classical jet theory.

It must be emphasized that when a rod cascade is used, attention must be paid to the value of the Reynolds number. This is due to the

fact that the rods are poorly streamlined bodies, and at critical values of the Reynolds number a critical resistance will be observed. Rods are most convenient of all to use if the Reynolds number lies between 10^3 and 10^5, since within this range the resistance coefficient does not change (Figure 11.20).



Figure 11.20. Relationship of the resistance coefficient for a round rod to the Reynolds number.

The rod diameters must be selected with the condition that wakes of the required intensity be stimulated. It is known from the theory of turbulent vortex wakes that at a certain distance from the body, in the case of two-dimensional streamline flow the halfwidth of the wake and the supplemental velocity may be expressed by the formulas

$$\Delta = \sqrt{10\varepsilon}\sqrt{xc_x d}, \quad v^0 = \frac{\sqrt{10}}{10\varepsilon}\sqrt{\frac{c_x d}{x}}\cos^2\frac{\pi y}{2\Delta}.$$

Here d is the diameter of the cylinder, c_x is the resistance coefficient, x and y are coordinates measured respectively along and across the wake, ε is an experimental constant.

The relationships among the rod (or thread) diameter, the stream velocities, and the air viscosity in such experiments are such that the desired range may be expressed in terms of Reynolds numbers.

When using rods as the perturbing cascade, it is necessary to effect a pre-rotation analogously to the manner in which this takes place in the nozzle equipment (such pre-rotation must also be effected when using a nozzle cascade, since the installation is constructed in an inverse way). For this purpose a blade device is provided in

the inlet fitting in the experimental turbomachine. The use of a rod cascade provides definite advantages, since it makes it possible to vary the velocity direction and the angle between the vortex wakes and the main stream velocity. Here it is essential that the characteristic of the wake itself, in a section normal to its axis, will practically not change, since a round rod reacts in the same way to any angle of attack.

A drawback in the use of a rod cascade is the fact that for the excitation of vortex wakes which correspond to small losses, in modern aerodynamic cascades it is in many cases necessary to select such small diameters that the rods can oscillate in the stream. In this connection, some experience is available with regard to the use of stretched nylon threads.

Figure 11.21 presents the distribution of dimensionless velocities with respect to the spacing behind a rod cascade, taken at various axial velocities $\Delta b/t$. The rods were immersed in a flow under static conditions at an angle of incidence of the stream in relation to the cascade axis of 16.5° and the relative rod diameter is $d/t = 0.035$. The Reynolds number is 7×10^3. Similar tests were conducted at other angles of incidence. These experiments were carried out in the zone where the wakes join. Therefore, there is no potential stream core in Figure 11.21.

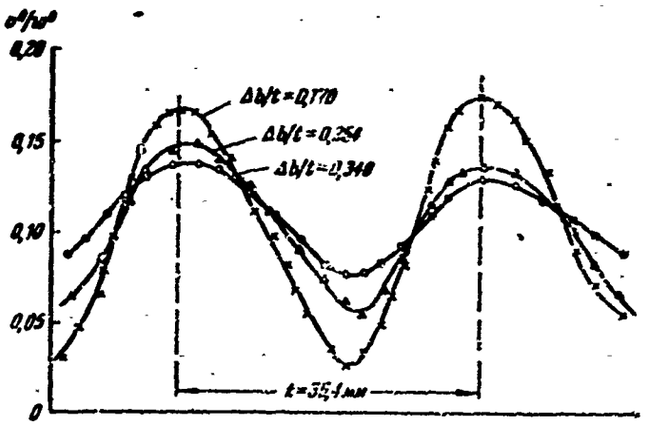


Figure 11.21. The velocity field behind a rod cascade in a zone of wake connection.

Obviously, in this region the wakes will not satisfy the universal relationship of the sppplemental-velocity field. The obtained characteristics are necessary for investigation of the vibration of cascades in a zone of connected wakes. Such research is necessary, as has already been mentioned, because the apex of a blade may be working in a zone where the wakes have become connected. The distribution of the velocity field beyond the rods in this case is asymmetric, since the plane of the measurements was parallel to the axis of the rod cascade.

In some experiments use was also made of an exciting cascade consisting of symmetrical wing profiles. Its drawback is sensitivity to the angle of attack; this can bring about separation of the stream and an uncontrollable form of wakes.

Let us consider some results of experiments devoted mainly to determination of the excitation coefficient or the relative dynamic force. This research was carried out by I. Neruda, B. E. Kapelovich, and F. Ruben.

Two cascade types, which simulated real aerodynamic cascades of high-parameters steam turbines, were subjected to experimental investigation.

Model cascade No. 1 (Figure 11.22) is characterized by the following values: profile TR-3A, relative spacing $\bar{t} = 0.59$, profile attitude $\beta_y = 78°$, calculated entry angle $\beta_1 = 26°$, blade chord $2b = 37.5$ mm, the natural frequencies of the tangential, axial, and torsional oscillations are respectively equal to 1850, 1500, and 3220 Hz. In the calculated operating regime the Strouhal number (determined on the basis of the angular frequency) is equal to $k = va/\omega_1^2 = 1.42$, while the mass number is $m = \rho^0(2b)^2/m = 0.44 \times 10^{-2}$.

Aerodynamic cascade No. 2 is also composed of profiles TR-3A: the relative spacing is $\bar{t} = 0.62$, the profile attitude is $\beta_y = 76°$, the natural frequency of the tangential oscillations is $\nu = 2465$ Hz.

Let us consider the results of experiments conducted for determination of the basic rules governing the behavior of the excitation coefficient.

The experiments were conducted with cascade No. 1. The mechanical oscillation decrement is equal to 0.027. The blades were tuned at the natural oscillation frequency by the method described above. Vortex wakes were generated by a rod cascade with a spacing of $t_1 = 1.5\ t_2$.

Figure 11.23 shows resonance curves recorded at a fixed incidence angle of $\beta_1 = 30°$ and for different values of velocity w_1^0. Since resonance originates at a definite constant rotational velocity of the excited cascade, it is obvious that angle α_1, formed by the velocity vector c_1 with the front of the rod cascade, must change during this time. The mass number will also change somewhat, since the air density changes during change of the incoming velocity.

In the figure are given: the Mach numbers $M = w_1^0/a$ computed on the basis of the entrance velocity w_1^0 of the stream to the working cascade, the Strouhal numbers $k = \omega b/w_1^0$, determined on the basis of the natural blade-oscillation frequency, v_{max}^0/w_1^0 — the relative value of the perturbation velocity in the wake (v_{max}^0 is the maximum supplemental velocity in the wake), the mass number $\bar{m} = \rho^0 (2b)^2/m$, where m is the linear reduced mass of the oscillating blade, the angle of flow direction α_1.

Analogous resonance curves were obtained at constant values of the angle of entry to the working blades, equal to $\beta_1 = 25°$ and $\beta_2 = 40°$.

Let us consider the velocity diagram (see Figure 1.3). Here, w_1^0 and β_1 are respectively the velocity and angle of entry of the stream onto the excited cascade, w_2^0 and β_2 are the velocity and exit angle of the stream from the cascade, u is the circular velocity of rotation of the exciting cascade, c_1 and α_1 are the velocity and angle of direction of the stream with respect to the rotating cascade.

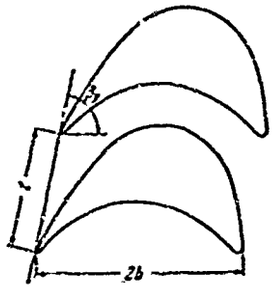


Figure 11.22. The TR-3A working cascade.

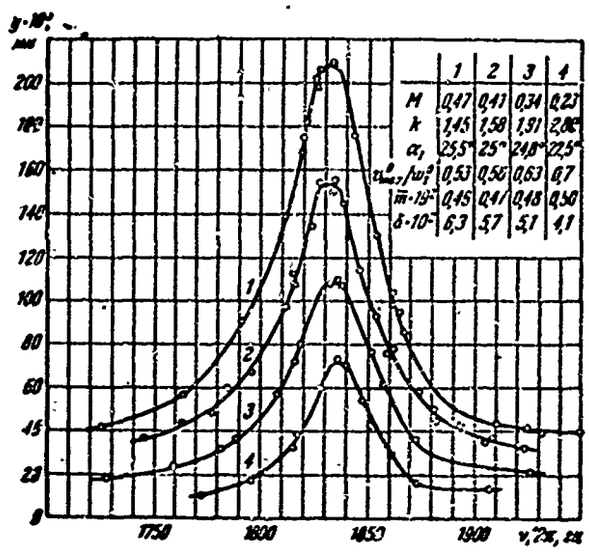
Let us assume that these velocities correspond to a uniform stream that carries no vortex wakes. Vortex wakes are in fact observed behind the exciting cascade; they may be characterized by the supplemental velocity v (and also by the width of the wake and by its shape). The velocity diagram corresponding to a particle of liquid belonging to the wake is marked with primed letters. Thus, with passage of the wakes the value and direction of the incident velocity onto the working cascade periodically change. This brings about a change of the force acting upon the blades, and induces their oscillation.

The velocity diagram that has been depicted is typical for the stages of a steam or gas turbine. The difference consists only in the fact that the experimental installation is inverse, and, therefore, the absolute and relative velocities have changed places.

The unsteady process taking place in a cascade of strongly bent, thick profiles is very complex, and at present there are no methods for calculating it. However, a rather crude assumption makes it possible to explain the basic outlines of the phenomenon and to obtain formulas for estimating the integral effect, which agrees satisfactorily with experimental results.

Let us determine the force acting upon a blade in a aerodynamic cascade in a uniform stream.

The value of a projection of the force (acting upon a unit of blade length) upon the cascade axis is found according to the momentum equation



	1	2	3	4
M	0,47	0,41	0,34	0,23
k	1,45	1,58	1,91	2,08
α_1	25,5°	25°	24,8°	22,5°
w_{max}^0/w_1^0	0,53	0,56	0,63	0,7
$\bar{m}\cdot 10^2$	0,45	0,41	0,48	0,50
$\delta\cdot 10^2$	6,3	5,7	5,1	4,1

Figure 11.23. Resonance peaks at a constant angle of entry of the stream onto the working cascade $\beta_1 = 30°$.

$$Y = \rho^0 l \left(w_1^0 \cos\beta_1 + w_2^0 \cos\beta_2\right) w_1^0 \sin\beta_1. \tag{11.30}$$

We shall consider a cascade with a small reactivity ratio, and shall therefore assume that the density of the fluid at the input and at the output is approximately the same. Then, by means of the continuity equation $w_1^0 \sin\beta_1 = w_2^0 \sin\beta_2$, we obtain from the preceding formula

$$Y = \rho^0 l \left[w_1^0\right]^2 \sin^2\beta_1 (\operatorname{ctg}\beta_1 + \operatorname{ctg}\beta_2). \tag{11.31}$$

We now obtain the value of the force for the diagram of the velocity designated by primes $(\alpha_1' = \alpha,\ \beta_2' = \beta_2,\ c_1' = c_1 = v^0)$. From trigonometric considerations, it follows that

$$w_1^0 \sin\beta_1' = \left(1 - \frac{v^0}{c_1}\right) w_1^0 \sin\beta_1, \quad w_1^0 \cos\beta_1' = w_1^0 \cos\beta_1 - v^0 \cos\alpha_1. \tag{11.32}$$

By means of (11.30), (11.32), and the continuity equation, we express the new value of the force in terms of the previous values of the velocities and angles and the value of the supplemental velocity v^0.

$$Y' = \rho^0 l \left[\omega_1^0\right]^2 \sin^2\beta_1 \left(1 - \frac{v^0}{c_1}\right)\left[\operatorname{ctg}\beta_1 + \operatorname{ctg}\beta_2 - \frac{v^0}{c_1}\left(\operatorname{ctg}\alpha_1 + \operatorname{ctg}\beta_2\right)\right]. \qquad (11.33)$$

By means of (11.31) and (11.33) we find the force increment

$$\Delta Y = Y - Y' = \frac{v^0}{c_1}\rho^0 l \left[\omega_1^0\right]^2 \sin^2\beta_1 \left(\operatorname{ctg}\alpha_1 + \operatorname{ctg}\beta_1 + 2\operatorname{ctg}\beta_2\right).$$

This expression constitutes the increment of the static force when c_1 is replaced by $c_1' = c_1 - v^0$ and under the condition that $\alpha_1' = \alpha_1$ and u = const. If it is considered that the cascade has a very small spacing (much less than the length of the perturbation wave), and $v^0 = v^0(\tau)$ constitutes a supplemental velocity in the wakes, it follows that $\Delta Y = \Delta Y(\tau)$ yields the change of the perturbing force in time. This force is found in a quasi-steady formulation.

In the more general case, when the assumption concerning quasi-steadiness and the small cascade spacing is not satisfied, it may nevertheless be assumed that ΔY is a value that is proportional to the modulus of the perturbing force. In this case, v^0 refers to a constant which has the sense of a characteristic supplemental velocity in the wake.

In principle, refinements may be made if the given stream is considered nonuniform and if the conservation equations are employed for two sections at the input and output for each channel between the blades. However, we are now dealing with the general character of the relationship, and therefore shall restrict ourselves to the selected assumption.

We shall show the degree to which the assumptions are confirmed experimentally.

Let two resonance blade-oscillation regimes in a cascade be compared. The ratio of the dynamic deflections must be directly

proportional to the ratio of the perturbing forces and inversely proportional to the ratio of the total logarithmic oscillation decrements.

$$\frac{p'}{p} = \frac{\Delta\gamma'}{\Delta\gamma}\frac{\delta}{\delta'}. \qquad (11.34)$$

Since the same perturbing cascade is used in the experiments under consideration, it should be considered that v^0/c_1 = const, since according to jet theory the value of the supplemental velocity in a wake is proportional to the mainstream velocity.

In the experiments under consideration, the velocity of flow about the blades w_1^0 and its direction, determined by the angle β_1, change independently, and the angle α_1 formed by velocity c_1 with the front of the rod cascade is also constrained. The change of the angle is brought about by the fact that due to the resonance condition it is necessary to maintain constant circumferential velocity of the exciting cascade.

By means of Formula (11.34) we find the ratio of the exciting forces for any two comparable regimes

$$\frac{\Delta\gamma'}{\Delta\gamma} = \frac{\rho''}{\rho'}\left(\frac{\lambda_1''}{\lambda_1'}\right)^2 \frac{\sin^2\beta_1'}{\sin^2\beta_1''}\frac{\operatorname{ctg}\alpha_1' + \operatorname{ctg}\beta_1' + 2\operatorname{ctg}\beta_2}{\operatorname{ctg}\alpha_1'' + \operatorname{ctg}\beta_1'' + 2\operatorname{ctg}\beta_2}. \qquad (11.35)$$

Here, $\lambda_1 = w_1^0/a_*$. a_* is the critical velocity, β_2 = const, since in dense cascades the exit angle does not depend upon the entry angle and at subsonic velocities practically does not depend upon λ_1.

Out of geometric considerations, it is easy to obtain

$$\operatorname{ctg}\alpha_1 = \operatorname{ctg}\beta_2 + \frac{a}{w_1^0 \sin\beta_1}. \qquad (11.36)$$

From (11.35) and (11.36), it follows that the ratio of the forces depends only upon λ_1 and β_1 for two comparable relations, since $\frac{\rho''}{\rho'}$ depends only upon λ_1 and λ_1.

Selecting for comparison Figure 11.23 and taking advantage of the fact that in this case $\beta_1' = \beta_1'' = 30°$, a graph of the calculated ratio

of the perturbing forces can be plotted and compared with the graph of the ratio of forces found experimentally via dynamic deflections and oscillation decrements $y'\delta'/y\delta$.

Figure 11.24 shows plotted points corresponding to an experiment conducted when $\beta_1 = 25°$ and $\beta_1 = 30°$. The calculation curve (the calculation curves for $\beta = 25°$ and $\beta = 30°$ coincide) agrees with the experimental relationship. In the calculations, the experimental values of the perturbing force have been reduced to a single fluid density (to an identical mass number).

Comparison of the calculated relationship for the case of $\beta_1 = 40°$ (Figure 11.25) is presented separately, since the experiment was conducted with a different maximum velocity value.

In the preceding graphs, a comparison was essentially made between experiments conducted at different stream velocities w_1^0 but with a constant angle β_1.

Let us now ascertain the influence of angle β_1 upon the value of the dynamic force; for this, we shall compare the resonance deflections taken at equal flow velocities from three different experiment series conducted for different angles β_1. The experimental points are shown in Figure 11.26, the maximum value of the force for each of the velocities being taken as the unit. Also plotted there is the curve of the relative force, computed by means of Formulas (11.35) and (11.36).

From graphs (Figure 11.24 — 11.25) it follows that a rather crude assumption nevertheless makes it possible to represent the basic features of the relationships.

For studying the influence of the relationship of the dynamic stresses to the nonuniformity of the main stream field, a special experiment was conducted. In order to exclude the influence of all extraneous factors, the experiment was conducted at a constant stream velocity of $M = 0.29$, a constant axial gap of $\Delta b = 6$ mm and angles

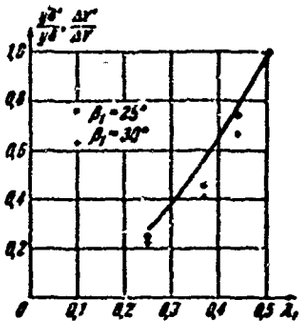


Figure 11.24. Relationship of the relative perturbing force to the stream velocity for $\beta_1 = 25°$ and $\beta_1 = 30°$.

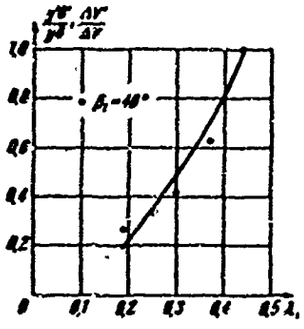


Figure 11.25. Relationship of the relative perturbing force to the stream velocity for $\beta_1 = 40°$.

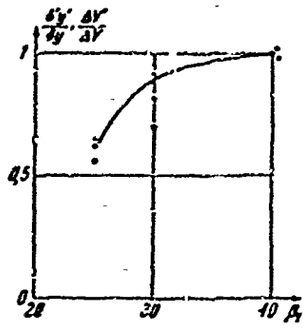


Figure 11.26. Relationship of the relative preturbing force to the stream angle of incidence.

$\alpha_1 = 18°$ and $\beta_1 = 28°$. The circumferential velocity and the rod spacing of the excited cascade were also constant, as is required by the condition of resonance. In the process of the experiment only the rod diameters of the exciting cascade were varied, which changed the nonuniformity of the velocity field.

Figure 11.27 presents a graph of the change of the relative dynamic oscillation amplitudes with resonance as a function of the rod diameter (1). As can be seen from the graph, the maximum dynamic stresses are obtained at a rod diameter of 1.5 mm. The course of the curve becomes clear if consideration is given to the distribution curves of supplemental velocities in the wakes behind cascades of rods of various diameters. In the course of experimental investigation of the velocity field behind cascades of rods 1, 1.5, 2 and 3 mm in diameter (at a fixed angle of incidence and at an axial distance) it was found that the nonuniformity will be the greatest when d = 1.5 mm.

Estimation Formula (11.34) indicates a linear relationship between the nonuniformity of the velocity field and the value of the perturbing force.

If it is assumed that this relationship is correct, it is expedient to understand by the characteristic velocity v^0 the Fourier coefficient when the supplemental velocity field is expanded into series. Further, by relative nonuniformity of the field, we mean the ratio v^0/c_1. In Figure 11.27, curve (2) represents the change of the coefficient of the first harmonic (the first harmonic is taken, since resonance of the first multiplicity is being studied) when the supplemental velocities of the wake are expanded into a Fourier series. This curve clarifies the reason for the drop of the dynamic deflections when the rod diameter is increased above 1.5 mm (or is decreased below 1.5 mm). Let us note that the position of the maximum depends, of course, upon the angle of incidence of the stream upon the perturbing cascade. In the case under consideration ($\alpha_1 = 18°$), the decrease of the nonuniformity is brought about by the wakes joining. This can be confirmed by considering an experiment with the same exciting cascades, but which are flowed about at the angle of attack $\alpha_1 = 32°$. Here, joining of the wakes is not observed, and the stream nonuniformity increases with an increase of the rod diameter. In accordance with this is observed an increase of the relative resonance dynamic deflections of the blades (see Figure 11.27, curve [3]). Curve (4) represents the dimensionless nonuniformity of the stream for the given flow conditions.

In turbomachines, an important characteristic of a stage is the value of the axial gap, upon which the efficiency of the stage and the level of dynamic stresses depend. Figure 11.28 presents the relationship of the relative resonance amplitude to the relative distance between cascades (1). Curve (2) is also shown, which is a plot of the relative value of the first harmonics obtained when the supplemental velocities of the wake are expanded into a Fourier series. Let us note that the tests were conducted in a zone of wake linkage. During the experiment, the angles α_1 and β_1 and, consequently, also the angle $\alpha_1 - \beta_1$ between the wake axis and the stream velocity, were

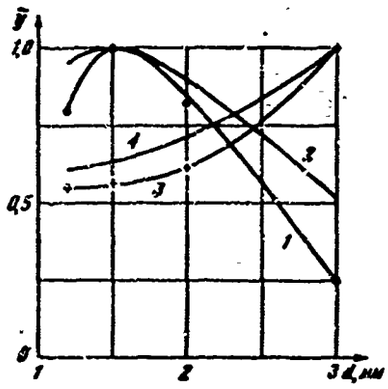


Figure 11.27. Relationship of the relative dynamic deflection during oscillation to stream nonuniformity.

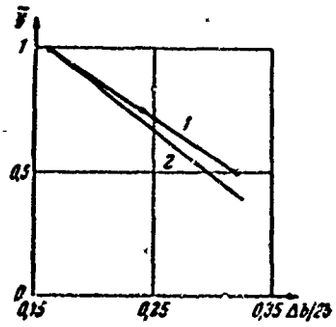


Figure 11.28. Relationship of the relative dynamic deflection to the axial distance between cascades.

maintained constant.

Let us now determine the relationship of the unsteady force to the nonuniformity of the stream.

In experiments conducted with different axial distances, the absolute stream velocity c_1 and the relative stream velocity w_1^0, the flow angles α_1, β_1 and the circumferential velocity remained constant. In this case, the unsteady force ΔY must depend only upon the relative flow nonuniformity v^0/c_1. Figure 11.29 shows the relationship of the relative now-stationary force $\Delta Y/\bar{Y}$ ($\bar{Y}$ is a stationary force which was constant under the conditions of the experiment) to the relative nonuniformity of the stream (the experimental points of this series are designated by circles).

In the next phase of experiments, the same values were maintained constant, while the stream nonuniformity was varied by varying the diameter of the rods (the experimental points of this series are marked by crosses).

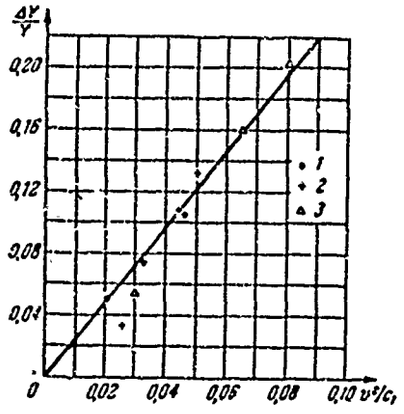


Figure 11.29. Relationship of the relative perturbing force ΔY/Y (ΔY is the perturbing force, Y is the steady force) to stream nonuniformity. The conditions of the experiment: $\beta_1 = 26°$, $a_1 = 17,3°$, $M = \omega_1^0/a = 0,29$, the axial distance between the cascades was varied, $\beta_1 = 26°$, $a_1 = 17,3°$, $M = 0,29$, $\Delta b/2b = 0.16$, the diameter of the rods of the exciting cascade was varied, 3) $\beta_1 = 26°$, $\Delta b/2b = 0.16$, the rod spacing of the exciting cascade was varied.

Finally, in the third series of experiments the rod spacing was varied. The circumferential velocity was changed in inverse proportion to the spacing, in order to retain the resonance frequency of excitation. In these experiments, angle β_1 was also maintained constant, but in view of this, it was necessary to change angle α_1.

The experimental points of all three series fit satisfactorily on a straight line passing through the origin of the coordinates, i.e., they confirm the proportional relationship between ΔY/Y and v^0/c_1. In the case of perturbations, the wavelength of which is much greater than the cascade spacing, this relationship follows from Formulas (11.31) and (11.34).

No mention was made here of the values of the gas density and the flow velocity under the conditions of the experiment, since ΔY and Y are proportional to the same value $\rho^0[w_1^0]^2$.

In the presently described results of experiments conducted at various spacings of the exciting cascade, it turned out that ΔY/Y depends only upon the nonuniformity of the stream. This question deserves more detailed investigation in the future.

When the relationship of the cascade spacings changes in the process of the experiment, comparison of the results becomes much

more difficult. This is explained by the fact that a change takes place in the aerodynamic damping, which depends upon the phase shift of the oscillation. In addition, and this should be emphasized, the value of the exciting force depends upon the phase shift when the vortex wakes act upon the blades. This factor is not taken into account when blade oscillation is studied from the point of view of solid-state mechanics. The influence of the phase shift due to wake action is brought about by the fact that the change of pressure on any blade which has been acted upon by a vortex wake brings about a pressure change on the adjacent blades. The interactions are cumulative, and this brings about a decrease or an increase of the aerodynamic exciting force.

It should be expected that aerodynamic damping will be the greatest with a phase shift of the oscillation of the adjacent blades equal to $\alpha = \pi$. However, in the same case aerodynamic excitation can have reached its maximum point. Then the final result depends upon the relationship of the aerodynamic damping to the mechanical damping, as well as upon the value of the aerodynamic excitation force. Therefore, the question of the optimal relationship of the cascade spacings from the point of view of dynamic strength requires special research.

Let us consider the results of an investigation of the axial resonance oscillation of blades. Figure 11.30 presents resonance curves obtained for four values of the Mach number $M = w^0/a$, which are indicated in the figure together with the other characteristic values. The experiments were conducted with TR-3A blades. The natural frequencies of tangential and axial oscillation are equal respectively to 1830 and 1440 Hz.

Figure 11.31 shows the relationship between the excitation coefficient for axial oscillation (1) and the Mach number. Presented for comparison in the figure are analogous relationships for the tangential oscillation of the same blades (2 and 3). Relationship (2) was obtained in experiments with a constant $\beta_1 = 26°$ and a variable a_1,

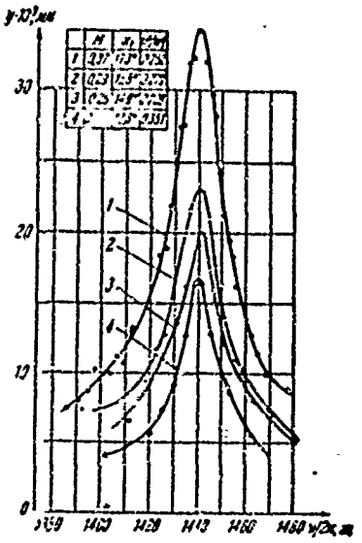


Figure 11.30 Resonance curves of blade axial oscillation (profile TR-3A, $\bar{t} = 0.59$, $\Delta b/2b = 0.16$).

Relationship (3) was obtained at a constant value of $\alpha_1 = 16°$ and a variable β_1. The excitation coefficient for axial oscillation (under comparable conditions) is approximately 2 — 3 times less than for tangential blade oscillation.

The experiments for which the results have been presented above pertain mainly to the excition of oscillation in a nonuniform stream brought about by a cascade with comparatively large losses. In a case where the exciting cascade has small losses, sharper peaks of the supplemental velocities in the wakes will correspond to the same average degree of nonuniformity (if the nonuniformity is characterized by the corresponding coefficients of a Fourier series). Since the connection between the nonuniformity of the stream and the unsteady force exciting it may be nonlinear, research on wakes of various shapes is necessary.

Figure 11.32 shows the distribution of supplemental velocities in a wake behind an exciting rod cascade for three angles of incidence. The x coordinate is measured along the cascade axis; the tests were carried out with rods having a diameter of d = 0.75 mm at a relative distance from the cascade axis equal to $\Delta b/d = 7$.

On the basis of the results of these and analogous measurement series, in which the rod diameter, the cascade spacing, the angle of incidence, and the axial distance were varied, a nonuniformity characteristic of the velocity field can be constructed. For such a

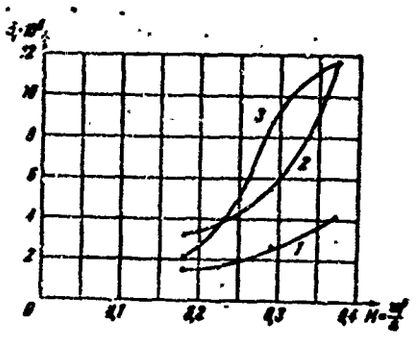


Figure 11.31. Relationship of the excitation coefficient to stream velocity: 1) axial oscillation — β_1 = const; 2) tangential oscillation — β_1 = const; 3) tangential oscillation α_1 = const.

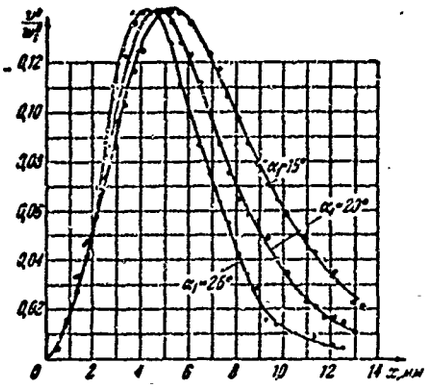


Figure 11.32. Distribution of supplemental velocities in the wakes behind an exciting cascade ($d = 0{,}75$ мм, $\Delta b/d = 7$).

characteristic, as has been ascertained above, it is expedient to adopt Fourier series coefficients when expanding the supplemental velocity fields.

As an example, Figure 11.33 whows the relationship of the relative nonuniformity v^0/w^0 (v^0 is the coefficient of a Fourier series, w^0 is the mainstream velocity) to the relative cascade spacing for the first two harmonics. In these experiments, both the spacing and the rod diameter of the cascade which caused the nonuniformity in the stream were varied.

Figure 11.34 shows the dependence of the relative nonuniformity upon the axial distance from the measurement plane.

Figure 11.35a shows the relationship of the average value of the unsteady force (1) to the relative distance between cascades. In the range under investigation, this relationship is linear. The

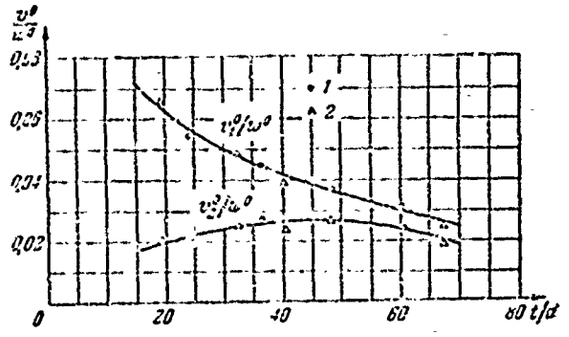


Figure 11.33. Dependence of the coefficients of a Fourier series which characterize stream nonuniformity upon the ratio of the spacing to the rod diameter. ($\Delta b/d = 7$, $\alpha = 25°$) at t = const, d = var; 2) d = const, t = var.

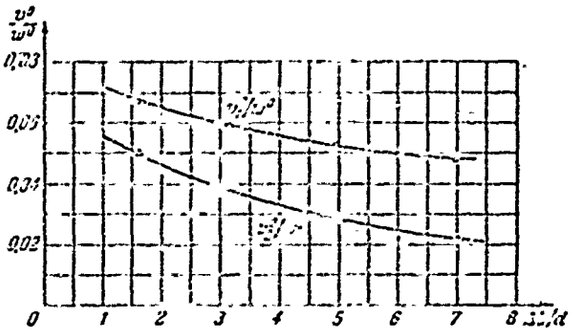


Figure 11.34 Dependence of the coefficients of a Fourier series which characterize flow nonuniformity upon the ratio of the axial distance to the rod diameter ($t/d = 21$, $\alpha_1 = 25°$).

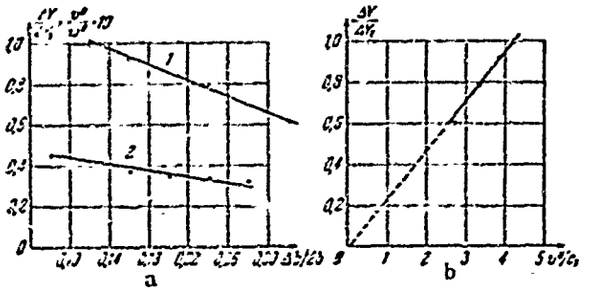


Figure 11.35. Relationship of the relative exciting force to stream nonuniformity.

same figure shows the relative stream nonuniformity (2), determined on the basis of results of the statistical tests described above.

Figure 11.35b shows the relationship of the relative nonstationary force $\Delta Y/\Delta Y_1$ (ΔY_1 is the nonstationary force at an axial distance between the cascades of $\Delta b/2b=0{,}12$) to the stream inhomogeneity). The experiments also confirm the direct proportionality between the stream inhomogeneity and an unsteady exciting force.

Let us dwell upon one more question, the investigation of which is of practical interest. In real turbomachines, for technological reasons the cascade spacing and, consequently, the spacing of the perturbing wakes, cannot be maintained absolutely identical. Stream nonuniformity may, as before, be characterized by Fourier coefficients when the supplemental velocity system in the wakes is expanded. In the general case of inequality of the directing-cascade spacing, the pattern must possess a periodicity with a spacing equal to the wheel circumference $2l = zt_{av}$ (z is the number of blades of the directing cascade, t_{av} is the average spacing in this cascade).

In addition, the vortex wakes are not strictly identical. This is due both to scatter of the spacings, and to scatter of the profile attitudes in the cascade, and to some difference in the geometry of the profiles (in the first place, due to scatter of the outlet-edge thickness), also due to technological reasons. From this, it follows that in a real stage, the perturbing forces possess a line spectrum. The emergence of the spectrum brings about oscillation of the low-frequency blades with the perturbing frequency k_n, where n is the rotation frequency of the wheel, and $k_n = 1, 2, 3, \ldots$. In the high-frequency region, the presence of a spectrum can bring about the excitation of oscillation with frequencies of $(z \pm k_n)\, n$, where $k_n = 0, 1, 2, \ldots$.

It is obvious that the most dangerous oscillation will be oscillation in the case of coincidence of the natural blade frequency with the frequency zn, since the greatest stream inhomogeneity is

observed here, and consequently, the exciting aerodynamic forces have the greatest value.

The spectrum of the perturbing forces in the region of high frequencies will be particularly dense, since 100/z = 1.5 - 2%.

As an example, we cite the frequency spectrum of diaphragm PS-1A$_{II}$, which has z = 47 nozzles. The average spacing, according to the measurement results, turned out equal to t_{av} = 44.77 mm. The maximum deviations from the average value comprised + 5.3% and -6.4%. Computations carried under the assumption that the pulse values of each edge wake are identical yield the spectrum presented in Figure 11.36. Due to scatter of the spacings, the modulus of the main harmonic decreases to 0.925; however, secondary harmonics originate. In this case, the relative value of the secondary harmonics is not great (the second harmonics are equal to approximately 0.25).

We have been speaking above concerning the technologically unavoidable scatter of the spacings of a directing cascade. However, it is generally possible to use a directing cascade which is intentionally made with nonidentical spacings. The problem concerning optimal selection of the spacings can be formulated with the aim of decreasing the value of certain harmonics. However, two consequences must be kept in mind: in the first place, the appearance of secondary harmonics, and in the second place, decrease of the aerodynamic efficiency of the cascade.

Let us consider experimental determination of the influence of scatter of the spacings of a perturbing cascade upon the stress level in case of the resonance of a high-frequency blade. We emphasize that this experiment was formulated not for seeking out optimal scattering of the spacings, but for ascertaining the possibilities of an estimate calculation upon which it will be possible to rely when analyzing the problem.

The influence of three variants of spacing scatter was studied. Alternation of the relative spacings was determined by the



Figure 11.36. Frequency spectrum of the exciting force in the case of imprecise manufacture of the nozzle cascade.

relationship: 1) -- (0,9; 1,1; 0,9; ...) t_{av}; 2) -- (0,8; 1,2; 0,8; ...) t_{av} and 3) -- (0,8; 1,0; 1,2; 0,9; 1,0; 1,1; 0,8, ...) t_{av}.

The experiment was conducted on the above-described cascade with TR-3A profiles with a flow velocity with respect to the blades of M = 0.37, an angle of incidence β_1 - 26°, a relative axial gap of $\Delta b/2b = 0.16$, and a ratio of the average spacings equal to 1.6. The experiment determined the ratios of the oscillation amplitudes in the resonance case to the corresponding amplitude in the case of oscillation excited in a cascade with a constant spacing. For the enumerated cases, the relative values are equal respectively to 0.96, 0.79, and 0.80. These values agree satisfactorily with the relative nonuniformity of the supplemental-velocity field.

In all the described experiments, very precise tuning of the vibrating blades was carried out at the natural oscillation frequency. Thus, the question of the mutual influence of oscillating blades having different, but similar natural frequencies was not investigated here.

This problem is of important practical significance; however, its study is tied to certain difficulties.

§ 11.4. Investigation of Dynamic Stresses in the Case of Partial Supply

Tests on investigation of the dynamic stresses in the case of partial supply were conducted on an experimental installation with a hydraulic brake that removes power developed by the rotating nozzle unit (Figure 11.37).

Figure 11.37. Experimental installation with a hydraulic brake for the investigation of dynamic stresses:
1) nozzle cascade with partial air admission;
2) blade under investigation;
3) hydraulic brake.

Used as the directing cascade was an aerodynamic cascade with TS-2A (S — 9015A) profiles, shown in Figure 11.18. The research was conducted on working cascade No. 2 consisting of profiles TR-3A (R3525A), represented in Figure 11.22.

Blades of modern steam turbines, operating with a partial steam supply, have very high natural frequencies. The tested model was designed on the basis of similitude theory and has the following characteristics: a natural frequency of tangential oscillation in the fundamental tone is 3560 Hz, frequency scatter of adjacent blades is ±7 Hz, material of elastic suspension — steel EI612, material of the profile part — foam rubber, material of stationary profile parts — Silumin. The dimensions of the strain gauges are 2 X 4 mm; the resistance is 120 ohms.

The measurement diagram is in its general features similar to the one described above, and provides for all the necessary aerodynamic measurements which monitor the aerodynamic regime during testing.

The diagram and the measuring equipment make it possible to traverse the stream.

A multiplicity indicator is used in the layout which consists of a small metal cantilever beam with a shifting load. The position of the load may be selected in such a manner that the frequency of the natural oscillation of the beam will correspond precisely to the rotation frequency of the rotor for resonance of a definite multiplicity. A three-phase tachogenerator is mounted on the rotor of the installation which generates alternating current with a frequency equal to twice the rotation frequency of the rotor. This current feeds an electromagnet which rocks the beam. The resonance stresses of the beam are noted by a strain gauge connected at the input of the strain gauge unit. After amplification, the signal is delivered to the cathode oscillograph and to the loop oscillograph. The beam has a very small oscillation decrement, which makes the resonance peak narrow and increases the measurement precision. The large time constant of the

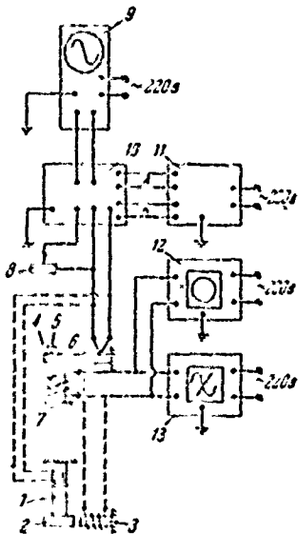


Figure 11.38. Measurement layout for the investigation of dynamic stresses in blades in the case of partial supply.

beam in comparison to that of the blade under investigation makes it possible to select the necessary velocity when the resonance has ceased. This layout facilitates work in investigating resonances of high multiplicity (k_n = 60 - 80), when adjacent resonances with respect to the rotation frequency of the rotor do not excede 1 Hz.

Very precise determination of the natural oscillation frequency of the investigated blade and the multiplicity-indicator beam is required for the investigation. The appropriate measurements were carried out according to the layout presented in Figure 11.38. The investigated blade (2) and the beam (4) are rocked by electromagnets (3 and 7) fed from the audio-frequency generator (13). Pulses are also delivered to the pulse counter (12). Resonance oscillations are observed on the oscillograph screen (9) after amplification by the strain gauge unit (10). Frequency measurements are made by means of a pulse counter.

The investigated blade also undergoes static calibration, which is subsequently necessary in decoding the results of the experiments. The blade is loaded by a control static force, and its deflection is registered by an indicator; electric measurements are simultaneously made by means of strain gauges.

Let us consider the results of experiments dealing with determination of the dynamic coefficient with partial supply. Some results in connection with this operation are described in an article [67].

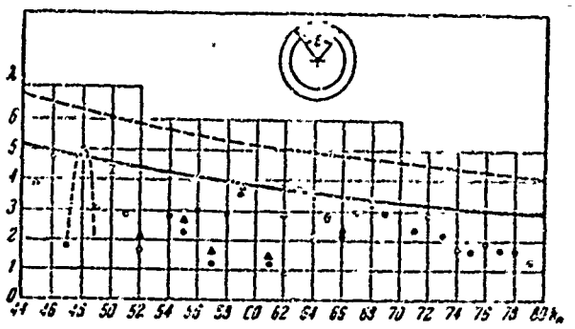


Figure 11.39. Dynamic coefficient for one supply arc.

The relationship of the dynamic coefficient to the resonance multiplicity k_n for the degree of partiality $\varepsilon = 0.229$ and one supply arc is represented in Figure 11:39.

Each point on the graph represents an apex of a resonance peak at the corresponding multiplicity.

The tests were conducted at a ratio of the circumferential velocity to the velocity of the emergence of the stream from the narrow cascade of $u/c = 0.40$ in the Mach number range $M = 0.28 - 0.51$ and at a constant relative axial gap $\Delta b/2b = 0.046$ (2b is the chord of the nozzle blade).

The apparent randomness of the location of the points in Figure 11.39 is explained by the fact that the oscillating blade is not under the heaviest operating condtions, which depend upon the nature of the load change and the number of oscillation cycles in the supply arc, at every multiplicity. It was noted above that, for example in the case of idealized rectangular loading, the maximum stresses will originate when there are one-and-a-half times the number of cycles at the supply arc. Obviously, in this case all deviations from these conditions

will bring about a considerable change in the oscillation amplitude. In addition, the time of one blade-oscillation cycle is equal to 4×10^{-4} sec. The jet at the ends of the supply arc is turbulent, and small changes of its width in the so-called intermittence zone determine the value of the oscillation phase when the blade is loaded and when it is unloaded. Thus, the final result is also affected by probabilistic phenomena.

An envelope passed through the apexes of the maximum peaks (the solid line) remains below the theoretical limit curve constructed for a rectangular load

$$\lambda = 1 + \frac{2}{k_n \delta},$$

at the experimental value of the damping coefficient $\delta = 0.008$.

A special case corresponds to a point with a multiplicity of $k_n = 48$. Here, the resonance of the 48^{th} multiplicity with partial supply coincides with the resonance from the edge wakes of the nozzle cascade, where $z = 48$ is the fictitious number of nozzles which would fit on the entire circumference of the wheel. As can be seen from the graph, the maximum dynamic deflection under these conditions of operation originates at the end of the supply arc and somewhat exceeds all the other values of the resonance deflections under other conditions.

From theoretical considerations, it is known that the maximum deflections depend little upon the degree of partiality. Experimental verification confirms this conclusion.

The resonance of the 48^{th} multiplicity is an exception. In this case, the stresses in the blades must be increased as the supply arc is increased, since the length of the arc at which attenuation of the oscillation takes place will decrease. Figure 11.40 shows the relationship of the dynamic coefficients for special cases of resonance for the multiplicities $k_n = 48$ and $k_n = 96$. The scatter of the points

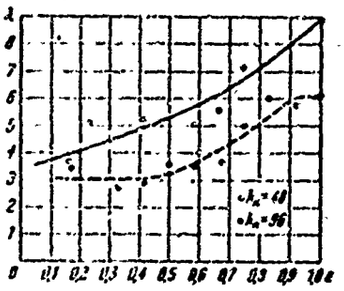


Figure 11.40. Dynamic coefficient in the case of oscillations of the first and second multiplicity of the edge wakes.

with respect to the resultant curve is explained by the influence of the unsteady and random phenomena when the load is applied and removed.

For determining the character of loading and unloading of the blade, aerodynamic measurements of the velocity profile were made at the boundaries of the supply segment. Figure 11.41 presents the results of measurements at the relative distances $\Delta b/t = 0.15$, and $\Delta b/t = 0.088$ (Δb is the axial gap between cascades, t is the spacing of the nozzle cascade) from the front of the nozzle cascade. The distance along the cascade axis is plotted. The numbers correspond to positions noted in the measurement plane along the abscissa.

The Mach number is plotted along the ordinate. A velocity dip corresponding to the edge wake behind nozzle blade No. 1 can be seen opposite point 1. The supply arc contains 11 nozzles (the degree of partiality is 11/48 = 0.239). A gap has been made in the graph, but between points 1 and 10 the velocity-distribution pattern repeats periodically. It follows from the graph that loading and unloading of the blade does not take place simultaneously. The slope of the side branches decreases as the distance from the cascade increases. The time necessary for the blades to get into the stream nucleus comprises from 1/4 to 1/3 of a blade oscillation period, equal to 4×10^{-4} sec. Furthermore, since the time required for the blade to become loaded is greater than the time required to become unloaded, in some cases maximum stresses originate in experiments during unloading.

In the operation of steam turbines, the most dangerous conditions from the point of view of dynamic blade strength of the controlling

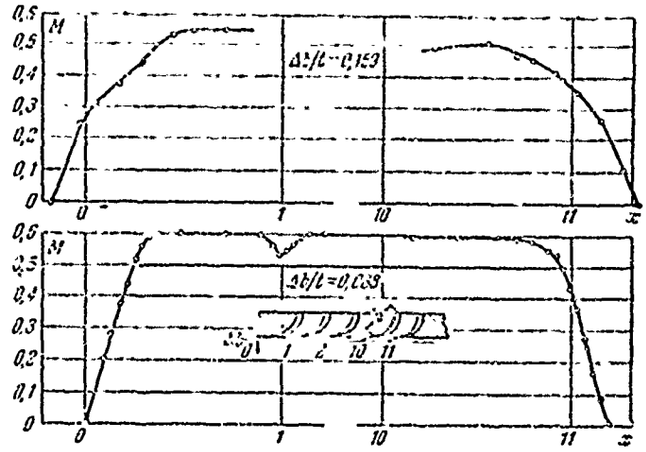


Figure 11.41. Distribution of stream velocity behind a nozzle cascade in the case of partial supply.

stage can originate when two supply segments are fed by completely open regulating valves. The experimental values corresponding to this investigation are given in Figure 11.42. The supply arcs have 11 nozzles each, which corresponds to a total degree of partiality of 2 X 11/48 = 0.458. The length of the crosspiece is equal to two nozzle spacings, which corresponds to a relative arc value of 2/48 = = 0,042. Here, an increase of the dynamic coefficient occurs in comparison to the case of one open valve. However, as is known, the increase of absolute stresses in the blades of the controlling system may be determined only by a comparison of the static loads determined by the steam consumption and the thermal gradient of the stage [11,67]. It must be noted that variation of the length of the connecting piece between the supply segments may bring about a considerable change in the stresses, since they depend upon the number of blade-oscillation cycles that fit on this arc. Just as before, the 48th multiplicity is specially marked.

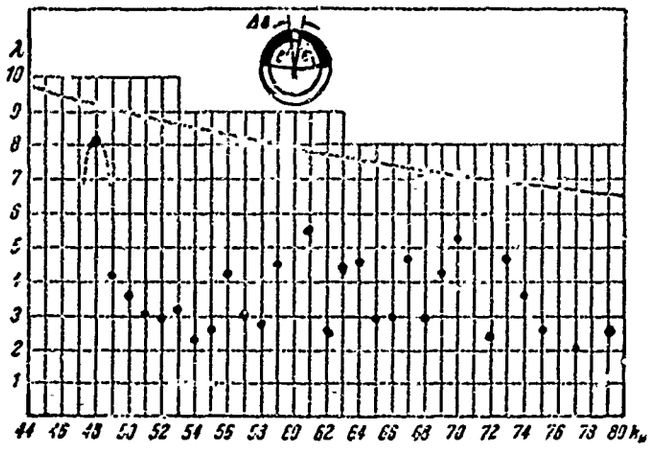


Figure 11.42. Dynamic coefficient with two supply arcs.

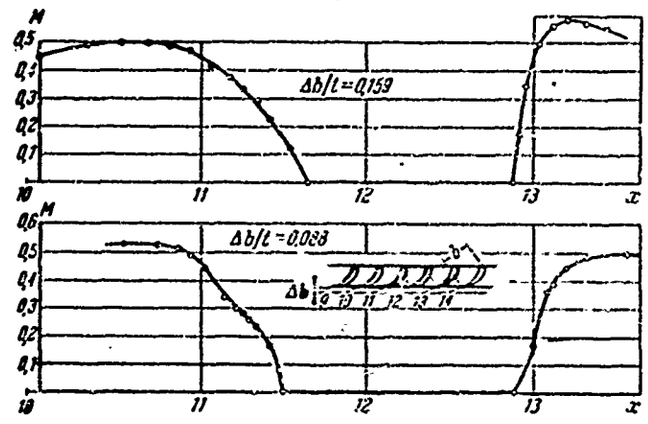


Figure 11.43. Distribution of stream velocity in the vicinity of the crosspiece between supply arcs.

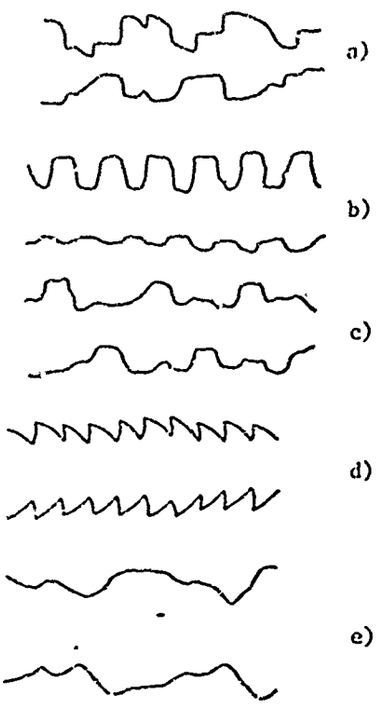


Figure 11.44. Envelopes of the oscillation processes of blades for various varients of partial supply.

Figure 11.43 presents a graph of the distribution of velocities along the edge of the crosspiece; this graph characterizes the slope of the load front.

The blade-oscillation pattern for two and more segments is very complex, since various combinations of blade load are possible with a change in the multiplicity.

Figure 11.44 shows the envelopes for several typical cases of oscillation. Case a) corresponds to three symmetrically situated segments and with a common degree of partiality $\varepsilon = 3 \times 0.229 = 0.687$. On the basis of the example of b) and c), one can observe the extent to which the character of the oscillation changes in a transition from a multiplicity of 67 to a multiplicity of 68 for two symmetrically situated segments with a partiality of $\varepsilon = 2 \times 0.229 = 0.458$. Case d) corresponds to a multiplicity of $k_n = 68$ and four symmetrically situated segments with $\varepsilon = 4 \times 0.229 = 0.916$. In case 3), the supply was effected along a single arc $\varepsilon = 0.229$ with a multiplicity of $k_n = 96$. Consequently, in this case resonance oscillation of the second multiplicity of the edge wakes was simultaneously observed.

All the figures show the basic period of the oscillation process, equal to the time of one turn of the wheel during which k_n oscillations of the blade occur. Small local dips and spikes of the amplitude,

brought about by random phenomena in the turbulent stream, can also be noticed.

In all the preceding graphs the values of the Mach number were not noted, since special experiments failed to detect its influence in the investigated range up to M = 0.55.

The study of partial supply at high supersonic velocities is of great interest, since in this case shock waves appear, which may bring about an increase of the dynamic stresses.

FOOTNOTES

1. on page 446 — The method of model tests was proposed by the author in 1958, the installation was constructed and adjusted by I. Neruda.

2. on page 458 — This has been assured for the sake of clarity.

SUPPLEMENTS AFTER PROOF READING

To § 4.6:

For a cascade without offset made of thin, slightly curved profiles oscillating with an arbitrary phase shift α, an effective solution can also be obtained by means of the method of singularity isolation [74].

We introduce the function

$$F(z)=w(z)\sqrt{\frac{\operatorname{sh}[\pi(z+b)/l]}{\operatorname{sh}[\pi(z-b)/l]}} \quad (2b-\text{chord})$$

On the vortex wakes we assume the value of the root to be positive.

Utilizing the relationships between the values of the velocities on the upper and lower sides of the sections, which replace profiles ($u_+=-u_-$, $v_+=v_-=v_0$), we obtain the connection between the values of F on the sections when approached from above and from below:

$$F_+=-\overline{F}_-=(v_0-iu_+)\sqrt{\frac{\operatorname{sh}[\pi(b+x)/l]}{\operatorname{sh}[\pi(b-x)/l]}}$$
$$(-b\leqslant x\leqslant b,\ y=int,\ n=\pm1,\ \pm2,\ \pm3,\ \ldots).$$

Here, the bar designates conjugate values. An analogous relationship that is valid on the wakes has the form

$$F_+=-\overline{F}_-=(u_++iv)\sqrt{\frac{\operatorname{sh}[\pi(x+b)/l]}{\operatorname{sh}[\pi(x-b)/l]}}$$
$$(x>b,\ y=int,\ n=\pm1,\ \pm2,\ \pm3,\ \ldots).$$

We use an integral representation of (4.3) for expressing function F (z) on the basis of its boundary values. After integrating along the contour of the main profile and its wake with account taken of F_+ and F_- we obtain [63]

$$w(z,\tau)=\frac{1}{t}\sqrt{\frac{\operatorname{sh}[\pi(z-b)/t]}{\operatorname{sh}[\pi(z+b)/t]}}\left[\int_{-b}^{+b}v_0(\xi,\tau)\sqrt{\frac{\operatorname{sh}[\pi(b+\xi)/t]}{\operatorname{sh}[\pi(b-\xi)/t]}}\times\right.$$

$$\left.\times K(\xi-z)\,d\xi+\int_{b}^{\infty}u_+(\xi,\tau)\sqrt{\frac{\operatorname{sh}[\pi(\xi+b)/t]}{\operatorname{sh}[\pi(\xi-b)/t]}}K(\xi-z)\,d\xi\right].$$

Here

$$K(\xi-z)=\frac{1}{t}\left\{\operatorname{ch}\frac{[(\pi-\alpha)z/t]}{\operatorname{sh}[\pi z/t]}-ij\frac{\operatorname{sh}[(\pi-\alpha)z/t]}{\operatorname{sh}[\pi z/t]}\right\}.$$

In the special case when $t\to\infty$ the expression becomes the well-known relationship for an isolated wing [74].

To § 9.2:

Let us consider the question of the possibility of the origination of parametric resonance in turbomachine cascades. Parametric resonance, i.e., resonance at fractional frequencies, may in principle originate if the blades comprising an aerodynamic cascade oscillate in a periodically changing stream. In practice, this condition is always satisfied, since the blades of a rotating working cascade are moving in an inhomogeneous field created by a stationary system. Considerations concerning the possibility of parametric resonance have been expressed in the work of Sabatiuk and Sisto [132], the corresponding problem has been investigated in Reference [60].

The velocity distribution in traveling vorticity waves can be expressed by an arbitrary function of the type of

$$v^0(x,y,\tau)=v^0\left(\tau-\frac{x-y\operatorname{ctg}\varepsilon}{\omega_1^0}\right).$$

Here, y is the blade shift, ε is the angle between the wake and the profile chord.

With a change in the oscillation of the blade (in view of the linearity of the problem) it is sufficient to introduce formulas for

the n^{th} harmonic of the velocity component normal to the blade

$$v_n^0(x, y, \tau) = v_n^0 \exp j\Omega_n\left(\tau - \frac{x - y\operatorname{ctg}\varepsilon}{\omega_1^0}\right).$$

Here, v_n^0 is the amplitude of the n^{th} harmonic. Then, taking into account the fact that the wake is usually close to symmetrical, for the sake of abbreviated notation we shall write only the component with respect to cosines

$$v_n^0 = \frac{4\sin\varepsilon}{t_1}\int_0^{t_1/2} v^0(x)\cos\left(\frac{2\pi n x}{t_1}\right)dx.$$

Here, t_1 is the spacing of the perturbation velocity curve. The circular frequency of the n^{th} harmonic may, obviously, be expressed in terms of t_1. The term $\frac{(x - y\operatorname{ctg}\varepsilon)}{\omega_1^0}$ is a phase shift of the passage of a vorticity wave through a given point of the plane. If the blade is stationary, the phase shift is constant for each fixed point on it. Let us consider a more general case, when the blade can oscillate under the action of the above-described nonstationary forces. In this case, if y denotes a shift of the blade, and taking into account the fact that it is small, we obtain

$$v_n^0(x, y, \tau) = v_n^0\left(1 + j\Omega_n\frac{y\operatorname{ctg}\varepsilon}{\omega_1^0}\right)\exp j\Omega_n\tau.$$

In this notation, the subsequently trivial phase shift, equal to $\nu_n x/\omega_1^0$, has been discarded. The appearance of a perturbation field brings about the appearance of a nonstationary force, the harmonic of which may be represented by:

$$\mathcal{P}_{1n} = 2\pi\omega_1^0 v_n^0 bR(k_n, q, \gamma_b, n);\ k_n = \frac{\Omega_n b}{\omega_1^0} = \frac{n\Omega_1 b}{\omega_1^0},\ q = \frac{\pi b}{t}.$$

The aerodynamic damping force, which is proportional to the oscillation velocity, may be expressed in this manner:

$$\mathcal{P}_2 = -2\pi\rho b\omega_1^0\frac{dy}{d\tau}T(k, q, \gamma_b, n).$$

Mechanical damping will also appear in blades; it is induced by the force

$$\mathcal{P}_3 = -2hm\frac{dy}{d\tau}.$$

The equation of the oscillation of a blade has the form

$$m\left(\frac{d^2y}{d\tau^2}+\nu^2y\right)=2\pi\rho\omega_1^2b\left[v_n^2e^{j\beta_n\tau}R\left(1+j\bar{l}_n\right)\frac{\eta\operatorname{ctg}\varepsilon}{\omega_1^2}-T\frac{dy}{d\tau}\right]-2hm\frac{dy}{d\tau}.$$

Here, ν is the natural frequency of the blade oscillation. We reduce the preceding equation to dimensionless form, introducing the dimensionless deflection $\eta = y/b$ and the dimensionless time $\theta=\tau f_n$:

$$\frac{d^2\eta}{d\theta^2}+(\delta_2+\delta)\frac{d\eta}{d\theta}+(p^2+j\delta_4e^{j\theta})\eta=\delta_1v^2.$$

Here, δ_1 is the coefficient of oscillation excitation, δ_4 is the coefficient of parametric excitation, δ_2 is the coefficient of aerodynamic damping, δ_3 is the coefficient of mechanical damping.

$$\delta_1=2\pi\frac{\rho}{\rho_1}\cdot\frac{\omega_1^2v_n^2}{f_n^2F}R,\quad \delta_4=2\pi\frac{\rho}{\rho_1}\cdot\frac{v_n^2b\operatorname{ctg}\varepsilon}{f_nF}R,$$

$$\delta_2=2\pi\frac{\rho}{\rho_1}\frac{\omega_1^2b}{f_n^2F}\Gamma,\quad \delta_3=\frac{2h}{f_n}.$$

The presence of the term $\delta_4\exp(j\theta)$ indicates the essential possibility of of the appearance of parametric resonance with a frequency equal to a fraction of the frequency of the perturbing force.

We discard the term $\delta_4\exp(j\theta)$ and study the demultiplication resonance. By replacement of the variables

$$\eta=z(\theta)\exp\left[-{}^1/_2(\delta_2+\delta_3)\right],$$
$$\theta=2\varphi-\alpha_0+\pi/2$$

the equation of oscillation of the variables is reduced to the Mathieu function in canonical form

$$\frac{d^2z}{d\varphi^2}+4\left[p^2+\frac{3}{4}(\delta_3+\delta_2)^2-|\delta_4|\cos 2\varphi\right]z=0.$$

The value of the phase shift α_0 is so selected here that in place of the complex value δ_4 it would be possible to consider its modulus; this is accomplished by selection of the origin of dimensionless time. In real problems the term $(\delta_2+\delta_3)^2$ is negligibly small in comparison to p^2 and may be discarded.

It is known that the Mathieu equation possesses regions of unstable solutions, where the amplitude of the functions increases without limit. In our case the solution will be unstable if (we consider δ to be real):

$$\delta_3+\delta_2<\mu.$$

Here μ is the characteristic coefficient of the Mathieu equation; it is a function of δ_4 and p. In the plane of p, δ_4 there is an infinitely great number of instability regions, which have their origin near the points $4p^2 = n^2$. Since μ decreases greatly with an increase of n, the greatest practical danger is presented by resonance at the half-frequency of the perturbing force $\nu=1/2$. The characteristic coefficient for this case ($\nu=1/2$, $|\delta_4|\ll\rho$) is determined with great accuracy by the approximate formula $\mu=|\delta_4|$. Then the origination of dynamic instability is determined by the inequality

$$\delta_3+\delta_2<|\delta_4|,\ \delta_3+2\pi\frac{\rho}{\rho_a}\frac{w_1^0\delta}{vb}T<2\pi\frac{\rho}{\rho_a}\cdot\frac{v_n^0\delta\operatorname{ctg}\varepsilon}{v_1b}R.$$

From this it follows that in the case of purely translational oscillations, parametric resonance cannot originate in two-dimensional cascades, since ($|R/T|\approx 1$)

$$\frac{v_n^0\operatorname{ctg}\varepsilon}{w_1^0}\cdot\frac{R}{T}=\frac{v\cos\varepsilon}{w_1^0}\cdot\frac{R}{T}<1.$$

Consequently, parametric resonance cannot originate in two-dimensional cascades due to the presence of aerodynamic damping (even if $\delta_3 = 0$).

If there were only mechanical damping (T = 0), parametric resonance could have originated with sufficiently great air density and a sufficiently great stream velocity.

It should be emphasized that these calculations pertained only to flexural oscillation. The problem deserves further study for torsional oscillations, a different perturbation form, and a different cascade shape.

References

1. Abezgauz, V.G. and I.G. Rusakov. Concerning Turbine Blade Resonances. Zhurnal Tekhnicheskoy Fiziki, Vol. 5, No. 10, 1935.

2. Abramovich, G.N. Teoriya Turbulentnykh Struy (The Theory of Turbulent Jets). Fizmatgiz, 1960.

3. Aerodynamics, edited by B.F. Durend, translated from English, Oborongiz, 1939.

4. Bauer, V.O. and B.F. Shorr. Resonance Oscillation of a Blade Ring in the Presence of Blade Maladjustment. In: Lopatochnyye Mashiny i Struynye Apparty (Blade Machines and Jet Mechanisms), No. 4, 1967.

5. Armstrong, Ye.K. Modern Methods of Research on Blade Vibration. Energeticheskiye Mashiny i Ustranovki (Power Machines and Installations). Translated from English, No. 3, 1957.

6. Belotserkovskiy, S.M., A.S. Ginevskiy and Ya.Ye. Polonskiy. Aerodynamic Forces Acting Upon a Cascade of Profiles in the Case of Unsteady Streamline Flow. In: Promyshlennaya Aerodinamika (Industrial Aerodynamics), Oborongiz, 1961.

7. Bisplingkhoff, R.L., H. Ashley and R.L. Halfman. Aeroelasticity. Translated from English, Foreign Language Publishing House (IL), 1958.

8. Bolotin, V.V. Nekonservativnyye Zadachi Teorii Uprugoy Ustoychivosti (Nonconservative Problems of Elastic Stability Theory). Fizmatgiz, 1961.

9. Brillouin, L. and M. Parodi. Wave Distribution in Periodic Structures. Translated from French, 1959.

10. Van-de-Vuren, A.I. Theory of Unsteady Motion of a Wing. In: Problemy Mekhaniki, No. III. Translated from English, IL, 1961.

11. Vakhomchik, V.P. Determination of Unsteady Forces in a Cascade of Profiles. Inzhenernyy Zhurnal, No. 1, 1965.

12. Vakhomchik, V.P. Analytic Solution of the Oscillation of Thin Profiles in a Cascade. Inzhenernyy Zhurnal, No. 2 1965.

13. Vidyakin, Yu.A. The Oscillation of Steam-Turbine Blade Packets With the Partial Inlet of Steam. Sudostroyeniye, No. 7, 1957.

14. Garrik, I.E. Unsteady Characteristics of the Wing. Aerodynamics of Aircraft Parts at High Speeds, translation from English, 1959.

15. Gorelov, D.N. Three-Dimensional Flow About a Blade Circle of an Axial Turbomachine in a Subsonic Unsteady Gas Stream. Izvestiya Akademii Nauk, SSSR, Otdeleniye Tekhnicheskikh Nauk, Mekhanika i Mashinostroyeniye, No. 6, 1963.

16. Gorelov, D.N. and L.V. Dominas. Calculation of the Aerodynamic Forces and Moments Acting Upon a Cascade of Plates that Oscillate in a Two-Dimensional Flow of Incompressible Fluid. Izvestiya Akademii Nauk SSR, Mekhanika, No. 3, 1965.

17. Gorelov, D.N. and L.V. Dominas. Determination of Unsteady Aerodynamic Forces for a Three-Dimensional Cascade of Plates in a Two-Dimensional Gas Stream. Mekhanika Zhidkosti i Gaza, No. 6, 1967.

18. Gorelov, D.N. and L.V. Dominas. A Cascade of Plates in a Subsonic Unsteady Gas Stream. Mekhanika Zhidkosti i Gaza, No. 6, 1966.

19. Gradshteyn, N.S. and I.M. Ryzhik. Tables of Integrals, Sums, Series, and Products, Fizmatgiz, 1963.

20. Deych, M. Ye and G.S. Samoylovich. Osnovy Aerodinamiki Osevykh Turbomashin (Principles of the Aerodynamics of Axial Turbomachines). Mashgiz, 1959.

21. Deutsch, G.D. Handbcook for the Practical Application of Laplace Transforms, translated from German, 2nd edition. Fizmatgiz, 1960.

22. Ditkin, V.A. and A.P. Prudnikov. Spravochnik po Operatsionnomu ischisleniyu (Handbook on Operational Calculus). Vysshaya Shkola, 1965.

23. Yershov, V.N. Neustoychivyye Rezhimy Turbomashin (Unsteady Regimes of Turbomachines). Mashgiz, 1966.

24. Zhukovskiy, M.I. Raschet Obtekaniya Reshetok Profiley Turbomashin (Calculation of Flow About Profile Cascades of Turbomachines), Mashgiz, 1960.

25. Seidel, R. Asymmetric Currents at the Inlet Into Axial Turbomachines. Power Machines and Installations, translated from English, No. 1, 1964.

26. Zaslavskiy, A.G. Analysis of the Conditions of the Origination of Self-Oscillations of a System with one Degree of Freedom. In: Prochnost' i Dinamika Aviatsionnykh Dvigateley (The Strength and Dynamics of Aircraft Engines), No. 1, Mashinostroyeniye, 1964.

27. Kazakevich, V.V. Avtokolebaniya (pompazh) v Ventilyatorakh i Kompressorakh (Self-Oscillation [Surges] in Fans and Compressors), Oborongiz, 1959.

28. Kapelovich, B.E. Issledovaniye aerodinamicheskikh vozbuzhdayushchikh sil v turbomashinakh (An Investigation of Aerodynamic Exciting Forces in Turbomachines). Candidate's Dissertation, Moscow Power Engineering Institute, 1966.

29. Kara, F.A. Flutter Instability of the Blade - Disk - Connecting Member in Turbojet Engine Rotors. Power Machines and Installations, translated from English, No. 3, 1967.

30. Kirillov, I.I. and A.S. Laskin. Investigation of the Variable Aerodynamic Forces in a Turbine Cascade in an Unsteady Streamline Flow. Energomashinostroyeniye, No. 12, 1966.

31. Kochin, N.Ye. Gidrodinamicheskaya Teoriya Reshetok (Hydrodynamic Theory of Cascades). Gostekhizdat, 1949.

31a. Kovalenko, V.I. Issledovaniye Dinamicheskikh Napryazheniy v Lopatkakh Stupeney s Partsial'nym Podvodom Para (Study of the Dynamic Stresses in the Blades of Stages With Partial Steam Supply). Candidate's Dissertation, Moscow, Power Engineering Institute, 1967.

32. Krol', A.P. Concerning Flutter Phenomena of Turbomachine Blades. In: Prochnost' Elementov Parovykh Turbin (The Strength of Steam Turbine Components). ONTI, 1951.

33. Kurzin, V.B. The Oscillation of a Cascade of Thin Profiles in a Compressible Subsonic Stream. Prikladnaya Mekhanika i Tekhnicheskaya Fizika, No. 1, 1962.

34. Kurzin, V.B. Calculation of Unsteady Flow About a Cascade of Thin Profiles by a Subsonic Stream of Gas by the Method of Integral Equations. Prikladnaya Mekhanika i Tekhnicheskaya Fizika, No. 2, 1964.

35. Kurzin, V.B. Concerning the Calculation of Forces in the Case of Arbitrary Small Oscillations of Profiles in a Cascade. Izvestiya Akademii Nauk SSSR, Ser. Mekh. Mash., No. 2, 1964.

36. Kurzin, V.B. Concerning the Aerodynamic Interference of Profiles in a Subsonic Unsteady Stream. Mekhanika Zhidkosti i Gaza, No. 1, 1966.

37. Kurzin, V.B. Concerning the Dynamic Stability of Turbomachine Blades in a Stream, the Natural Frequencies of Which Have a Small Frequency Difference. Mekhanika Zhidkosti i Gaza, No. 5, 1966.

38. Lavrent'yev, M.A. and B.M. Shabat. Metody Teorii Funktsiy Kompleksnogo Peremennogo (Methods of the Theory of Functions of a Complex Variable), Nauka, 1955.

39. Lamb, G. Hydrodynamics. Translated from English, Gostekhizdat, 1947.

40. Laskin, A.S. Investigation of Unsteady Phenomena in a Turbine Stage. Scientific Notes of Graduate Students and Researchers of the Leningrad Polytechnical Institute, Power Machinery Construction, 1964.

41. Levin, A.V. Rabochiye Lopatki i Diski Parovykh Turbin (Working Blades and Disks of Steam Turbines). State Scientific and Technical Power Engineering Publishing House, 1953.

42. Loytsyanskiy, L.G. Mekhanika Zhidkosti i Gaza (Fluid and Gas Mechanics). Gostekhizdat, 1957.

43. Lyakhovitskiy, I.D. Stream Turbulence in a Turbine Stage and the Profile Losses of Active Blades. Izvestiya VTI, No. 5, 1950.

44. Miles, G.U. Potential Theory of Unsteady Supersonic Streams. Translated from English, Fizmatgiz, 1963.

45. Maclaurin, N.V. The Theory and Applications of Mathieu Functions. Translated from English, IL, 1953.

46. Markov, N.M. Teoriy i Raschet Lopatochnogo Apparata Osevykh Turbomachin (Theory and Calculation of the Blades of Axial Turbomachines). Mashinostroyeniye, 1966.

47. Movshovich, I.M. Concerning the Self-Oscillations of Axial-Compressor Blades. Izvestiya Vysshikh Uchebnykh Zavedeniy, Seriya Aviatsionnaya Tekhnika, No. 3, 1964.

48. Musatov, V.V. Concerning the Calculation of Unsteady Flow About a Cascade of Profiles in an Incompressible Fluid. Izvestiya Akademii Nauk, SSSR, Ser. Mekh. Mash., No. 3, 1963.

49. Nekrasov, A.I. Teoriya Kryla v Nestatsionarnom Potoke (The Theory of the Wing in an Unsteady Stream). USSR Academy of Sciences, Publishers, 1947.

50. Neruda, I. Issledovaniye Vozbuzhdeniya i Dempfirovaniya Kolebaniy Lopatok Turbomashin (Investigation of the Excitation and Damping of Turbomachine Blade Oscillations). Candidate's Dissertation, Moscow Power Engineering Institute, 1964.

51. Ol'shteyn, L.Ye and R.A. Shipov The Influence of Aerodynamic Coupling Upon the Separation Flutter of a Profile Cascade. In: Promyshlennaya Aerodinamika, No. 24, 1962.

52. Polyakhov, N.N. Teoriya Nestatsionarnykh Dvizheniy Nesushchey poverkhnosti (Theory of Unsteady Motion of a Lifting Surface). Published by the Leningrad State University, 1960.

53. Rusanova, Ye.I. Investigation of Dynamics Stresses in the Blades of an Axial Compressor With a Wide Range of Control. In: Kolebaniya v Turbomashinakh (Oscillation in Turbomachines). Academy of Sciences, USSR, Publishers, 1953.

54. Rusanova, Ye.I. and S.V. Korovkin. Investigation of the Vibration Stresses in the Blades of an Axial Compressor. Energomashinostroyeniye, No. 1, 1958.

55. Ryzhkova, L.S. Investigation of the Blade Vibrations of a Full-Scale Axial Compressor. Sbornik Trudov LMZ, No. 6, Mashgiz, 1959.

56. Samylovich, G.S. Calculation of Hydrodynamic Profiles. Prikladnaya Matematika i Mekhanika, No. 2, 1950.

57. Samylovich, G.S. Concerning the Calculation of an Unsteady Stream About a Cascade of Arbitrary Profiles Oscillating With an Arbitrary Phase Shift. Prikladnaya Matematika i Mekhanika, No. 1, 1962.

57a. Samoylovich, G.S., V.V. Nitusov and Z.B. Kazimierski. Calculation of the Flow About a Cascade of Arbitrary Profiles, Vibrating With an Arbitrary Phase Shift in a Two-Dimensional Stream of Incompressible Fluid. Mekhanika Zhidkosti i Gaza, No. 5, 1968.

58. Samoylovich, G.S. A Nonstationary Vortex Stream About a Cascade of Thin Vibrating Profiles. Prikladnaya Matematika i Mekhanika, No. 5, 1961.

59. Samoylovich, G.S. Flow About an Aerodynamic Cascade of Thin Vibrating Profiles. Prikladnaya Matematika i Mekhanika, No. 4, 1961.

60. Samoylovich, G.S. Concerning the Unstabilized Aerodynamic Forces and Dynamic Stresses in Blades in the Case of Resonance Oscillation Brought About by Vortex Wakes. Izvestiya Akademii Nauk SSR, Ser. Mekh. Mash., No. 4, 1962.

61. Samoylovich, G.S. An Investigation of Unstabilized Aerodynamic Phenomena in Axial Compressors. Izvestiya Vysshikh Uchebnykh Zavedenii, Ser. Mash., No. 2, 1959.

62. Samoylovich, G.S. Resonance Phenomena in Cascades in a Subsonic and a Supersonic Streamline Flow of Gas. Mekhanika Zhidkosti i Gaza, No. 3, 1967.

63. Samoylovich, G.S. Flexural-Torsional Flutter of Blades in a Dense Aerodynamic Cascade. Izvestiya Akademii Nauk SSSR, Ser. Mekh. Mash., No. 6, 1962.

64. Samoylovich, G.S. and I.N. Pis'min. Measurement of Pressure Pulsations and Dynamic Stresses on the Rotating Blade of an Axial Compressor. Teploenergetika, No. 8, 1962.

65. Samoylovich, G.S. and G.A. Kharin. Investigation of Unstabilized Aerodynamic Phenomena in a Model and a Full-Scale Multistage Axial Compressor. In: Issledovaniya Elementov Parovykh i Gazovykh Turbin i Osevykh Kompressorov (Research on Elements of Steam and Gas Turbines and Axial Compressors). Mashgiz, 1960.

66. Samoylovich, G.S. and B.E. Kapelovich. Overall Characteristics of Quasi-Steady Flow Above Cascades of Arbitrary Profiles, Oscillating With an Arbitrary Phase Shift. Mekhanika Zhidkosti i Gaza, No. 1, 1967.

66a. Samoylovich, G.S. and V.V. Nitusov. Obtaining Unsteady Characteristics of Aerodynamic Cascades by the Electrohydrodynamic Analog Method. Teploenergetika, No. 4, 1968.

67. Samoylovich, G.S., V.I. Kovalenko, and F. Ruben. Experimental Investigation of Dynamic Stresses in the Blade of a Turbine Stage With Partial Steam Supply. Izvestiya Vysshikh Uchebnikh Zavedeniye, No. 4, 1967.

68. Samoylovich, G.S. A Dense Aerodynamic Cascade With an Arbitrary Turn Angle of the Stream in an Unsteady Vortex Field. Reports of a Scientific and Technical Conference, Published by the Moscow Power Engineering Institute, 1967.

69. Samoylovich, G.S. and I.N. Pis'min. Investigation of the Flow in a Turbomachine in Relative Motion by Means of Quick-Response Probes. Reports of a Scientific and Technical Conference, Published by the Moscow Power Engineering Institute, 1967.

70. Samoylovich, G.S. and I.N. Pis'min. Author's Certificate (patent) No. 201743, Strain-Gauge Elements. Bulletin No. 18, 1967.

71. Samoylovich, G.S., Pis'min and V.V. Nitusov. Author Certificate No. 182374, Device for the Installation of Sensor Units Which Monitor the Stream Parameters of Relative Motion Behind a Turbomachine Wheel. Bulletin No. 11, 1966.

72. Samoylovich, G.S. and B.M. Troyanovskiy. Peremennyy Rezhim Raboty Parovykh Turbin (Variable Operating Conditions of Steam Turbines). State Scientific and Technical Power Engineering Publishing House, 1955.

73. Saren, V.E. Flow About a Cascade of Thin Curvilinear Profiles by an Unsteady Stream of Incompressible Fluid. Mehanika Zhidkosti i Gaza, No. 1, 1966.

74. Sedov, L.I. Ploskiye Zadachi Gidrodinamiki i Aerodinamiki (Two-Dimensional Problems in Hydrodynamics and Aerodynamics). Fizmatgiz, 1966.

74a. Sedov, L.I. Metody Podobiya i Razmernosti v Mekhaike (Similitude and Dimensionality Methods in Mechanics). Nauka, 1967.

75. Sirazetdinov, T.K. Concerning Flow About Oscillating Cascades. Transactions of the Kuybyshev Aviation Institute, Vol. 38, 1958.

76. Smith, L.N. Weight Dispersion in Turbomachines. Theoretical Foundations of Engineering Calculations, translated from English, No. 3, 1966.

77. Stepanov, G.Yu. The Use of Electrical Simulation for Determining a Conformal Transform in the Solution of Two-Dimensional Boundary Problems (Survey). Inzhenernyy Zhurnal, No. 3, 1965.

78. Stepanov, G.Yu. Gidrodinamika Reshetok Turbomashin (The Hydrodynamics of Turbomachine Cascades). Fizmatgiz, 1962.

79. Stepanov, G.Yu. Vvedeniye v Teoriyu Kolebaniy (Introduction to Oscillation Theory). Nauka, publishers, 1964.

80. Sukharveskiy, I.V. Efficient Computation of the Velocity and Circulation of the Stream in the Case of Potential Flow About a Cascade, Trudy KhPI, Ser. Inzh. Fiz., Vol. V., No. 1, 1965.

81. Fyn, Ya. Ts. Introduction to the Theory of Aeroelasticity. Translated from English, Fizmatgiz, 1959.

82. Kharkevich, A.A. Spektry i Analiz (Spectra and Analysis) Fizmatgiz, 1962.

83. Khaskind, M.D. The Acoustic Radiation of Oscillating Bodies in a Compressible Fluid. Zhurnal Eksperimental'noy i Teoreticheskoy Fiziki, No. 7, 1946.

84. Khaskind, M.D. The Oscillation of a Wing in a Subsonic Gas Stream. Prikladnaya Matematika i Mekhanika, No. 1, 1947.

85. Khaskind, M.D. The Oscillation of a Cascade of Thin Profiles in an Incompressible Stream. Prikladnaya Matematika i Mekhanika, No. 2, 1958.

86. Hoenl, H., A. Maue, and K. Westphal. Theory of Diffraction. Translated from German, Mir, 1964.

87. Khin, G.K. and R.V. Man. Hydraulic Analogy Applied to an Unsteady Two-Dimensional Stream in a Partial Turbine. Transactions of the American Society of Mechanical Engineers. Translated from English, No. 3, 1961.

88. Chernyshevskiy, I.K. The Blade-Circle of Steam Turbines as a Mechanical Filter. Collection: Prochnost' elementov parovykh turbin (The Strength of Steam Turbine Components). Mashgiz, 1951.

89. Schwart, L. Mathematical Methods for Physical Sciences. Translated from the French, Mir, 1965.

90. Shemtov, A.Z. Measurement of Dynamic Stresses in Working Blades and Other Turbine Parts Under Operating Conditions. Sbornik Trudov LMZ, No. 6, Mashgiz, 1959.

91. Shestachenko, I.Ya. Procedure for Measurement of the Variable Forces Acting Upon the Plates of Rotating Turbomachine by Piezoelectric Sensor Units. Izvestiya Vysshikh Uchebnykh Zavedeniy, Seriya Elektromekhanika, No. 9, 1967.

92. Shestachenko, I.Ya. Elimination of Distortion in Piezoelectric Measurements of Variable Pressures on the Blade of a Turbomachine. Promyshlennaya Aerodinamika, Vol. 171. Published by the Novocherkassky Polytechnical Institute, 1967.

93. Shipov, R.A. Concerning the Theory of the Flutter of Dynamically Inhomogeneous Profile Cascades. Collection: Lopatochnyye Mashiny i Struynyye Apparaty, No. 4, 1967.

94. Shipov, R.S. Concerning a Problem of the Resonance Excitation of A Dynamically Inhomogeneous Blade Circle. Collection: Lopatochnyye Mashiny i Struynyye Apparaty, No. 4, Mashinostroyeniye, 1967.

95. Erdelin, A. Asymptotic Expansions. Translated from English, Fizmatgiz, 1962.

96. Armstrong, E.K. and R.E. Stevenson. Some Practical Aspects of Compressor Blade Vibration. J. Roy. Aeron. Soc., No. 591, 1960.

97. Bellenot, C. and J.L. d'Epinay. Selbsterregte Schaufelschwingungen in Turbomaschinen (Self-Excited Blade Oscillations in Turbomachines). Brown Boveri Mitt, No. 10. 1950.

98. Bilek J. Turbulency v lopatkovych strojech (Turbulence in Blade Machines). Sb. ustavu pro vyznum stroju, No. 1, 1955.

99. Carter, A.D.S. A Theoretical Investigation of the Factors Affecting Stalling Flutter of Compressor Blades. ARC, CP, No. 265, 1956.

100. Carter, A.D.S. and D.A. Kilpatrick, Self-Excited Vibration of Axial-Flow Compressor Blades. Proc. Instn. Mech. Engrs. No. 7, 1957.

101. Chang, C.C. and W.H. Chu. Aerodynamic Interference of Cascade Blades in Synchronized Oscillation. J. of Appl. Mech., No. 4, 1959.

102. Carter, A.D.S., D.A. Kilpatrick, C.E. Moss, and J. Ritchie. An Experimental Investigation of the Blade Vibratory Stresses in Single Stage Compressor. ARC, CP, No. 226, 1956.

103. Chi-ten Wang, F. Lane and R.J. Vaccaro. An Investigation of the Flutter Characteristics of Compressor and Turbine Blade Systems. JAS, No. 4, 1956.

104. Feindt, E.G. Berechnung der Strömung des instationären vielstufigen Plattengitters (Flow Calculation of a Nonstationary Multistage Plate Cascade). Ing. Archiv., Vol. 30, No. 5, 1962.

105. Feindt, E.G. Berechnung der instationären Strömung des vielstufigen gestaffelten Plattengitters (Flow Calculation of a Nonstationary, Multistage, Staggered Plate Cascade). Ing. Archiv., Vol. 31, No. 5, 1962.

106. Feindt, E.G. Berechnung der Strömung des Tendemgitters mit bewegter zweiter Schaufelreihe (Flow Calculation of a Tandem Cascade With a Second Moving Blade Row). Ing. Archiv., Vol. 30, No. 2, 1961.

107. Forshow, J.R. A Survey of the Alternating Pressures Exciting High Frequency Vibrations in Gas Turbines. ARC R. a. M., No. 2989, 1957.

108. Forshow, J.R., H. Tylor, and R. Chaplin. Alternating Pressures and Blade Stresses in an Axial-Flow Compressor. ARC R. A. M., No. 2846, 1956.

109. Isay, W.H. Die Strömung durch ein schwingendes und rotierendes radiales Schaufelgitter (Flow Through an Oscillating and Rotating Radial Blade Cascade). Z. Flugwiss, No. 11, 1958.

110. Kazimierski, Z. Plaski przeplyw przez osiowy stopien maszyny przeplywowey o dowolnich parametrach geometryczych (Plane Flow Through an Axial Stage of Flow Machines Having Arbitrary Geometry). Archiwun budowy maszyn, No. 2, 1966.

111. Kemp, N.H. and W.R. Sears. Aerodynamic Interference Between Moving Blade Rows. JAS, No. 9, 1953.

112. Kemp, N.H. and W.R. Sears. On the Wake Energy of Moving Cascade. J. Appl. Mech., No. 2, 1956.

113. Kemp, N.H. and W.R. Sears. The Unsteady Forces to Viscous Wakes in Turbomachines. JAS, No. 7, 1955.

114. Kraft, H. Nonsteady Flow Through a Turbine. IX Intern Congr. Appl. Mech., Vol. II, 1957.

115. Lefcort, M.D. An Investigation Into Unsteady Blade Forces in Turbomachinery. J. of Engng for Power, No. 5, 1965.

116. Lane, F. System Mode Shapes in the Flutter of Compressor Blade Rows. JAS, No. 1, 1956.

117. Legendre, R. Premiers éléments d'un calcul del'amortissement aérodynamique des vibrations d'aubes de compressor (First Calculations of the Aerodynamic Damping of Compressor Blade Oscillations). La rech. aeronaut, No. 37, 1954.

118. Lotz, M. Erregung von Schaufelschwingungen in axialen Turbomaschinen durch benachbarte Schaufelgitter(Excitation of Blade Oscillations in Axial Turbomachines by Adjacent Blade Cascades). Wärme, No. 2, 1966.

119. Mayer, R.X. The Effect of Wake on the Transit Pressure and Velocity Distributions in Turbomachinery. Trans. ASME, No. 7, 1958.

120. Meister, E. Über ein Randwertrproblem aus der Aerodynamik eines Gitters (A Boundary Value Problem in Aerodynamics of a Cascade). ZAMM, No. 9 - 11, 1959.

121. Meister, E. Flow of an Incompressible Fluid Through an Oscillating Staggered Cascade. Arch. for rat. Mech. and Anal., No. 3, 1960.

122. Meister, L. Beitrag zur Aerodynamik eines schwingenden Gitters (Unterschallströmung) (Contribution to the Aerodynamics of an Oscillating Cascade [Subsonic Flow]). ZAMM, No. 1/2, 1962.

123. Meister, E. Beitrag zur Aerodynamik eines schwingenden Gitters (Unterschallstromung) (Contribution to the Aerodynamics of an Oscillating Cascade [Subsonic Flow]). ZAMM, No. 6, 1962.

124. Mendelson, A. Aerodynamic Hysteresis as a Factor in Critical Flutter Speed of Compressor Blades at Stalling Conditions. JAS, No. 11, 1949.

125. Meller, A.G. Etude schématique des forces aérodynamiques pulsées dues aux passages des aubes mobiles dans le sillage des aubes du distributeur d'une turbomachine (Schematic Study of Pulsed Aerodynamic Forces Due to the Passage of Moving Blades Through the Wake of Distributing Blades in a Turbomachine). La Rech. aéron, No. 44, 1955.

126. Nickel, K. Über Tragflugelsysteme in ebener Stromung bei beliebegen instationaren Bewegungen (Lifting Wing Systems in Plane Flow for Arbitrary Unsteady Flow). Ing. Archiv., Vol. 24, No. 3, 1955.

127. Oellers, H.J. Die inkompressible Potentialstromung in der ebenen Gitterstufe,(Incompressible Potential Flow in a Plane Cascade Stage). Sonderdruck aus dem Jahrbuch der WGLR, 1962.

128. Owczarek, J.A. On a Wave Phenomenon in Turbines. Trans. ASME, ser. A, No. 3, 1966.

129. Pearson, H. and A.B. Mckenzie. Wakes in Axial Compressors. J. Roy. aeron. soc., No. 588, 1959.

130. Popescu, I.L. Asupra miscarii nepermanente a unui fluid intr-o refea de profile (Nonsteady Fluid Flow Through a Profile Network). Nota I, Bul. stiint, Acad. RPR, sec. mat. fiz., No. 1, 1957.

131. Popescu, I.L. Asupra miscarii nepermanente a unuii fluid intr-o refea de profile (Nonsteady Fluid Flow Through a Profile Network). Nota II, Communic. Acad. RPR, No. 10, 1958.

132. Rabatuik, A. and F. Sisto. A Survey of Aerodynamic Excitation Problems in Turbomachines. Trans. ASME, No. 3, 1956.

133. Schnittger, J.R. Blade Flutter in Axial Flow Turbomachines. Appl. Mech. Rev., No. 4, 1958.

134. Schnittger, J.R. Single Degree of Freedom Flutter of Compressor Blades in Separated Flow. JAS, No. 1, 1954.

135. Schnittger, J.R. The Stress Problem of Vibrating Compressor Blades. J. Appl. Mech., No. 1, 1955.

136. Shioiry, J. Non stall normal mode flutter annular cascade. Trans. JSAE, No. 1, 1956.

137. Sisto, F. Unsteady Aerodynamic Reactions on Airfoil in Cascade. JAS, No. 5, 1955.

138. Sisto, F. Stall Flutter in Cascade. JAS, No. 9, 1953.

139. Sohngen, H. Luftkrafte an einmm schwingenden Schaufelkranz kleiner Teilung (Air Forces Acting on an Oscillating Blade Ring With a Small Division). ZAMP, No. 4, 1953.

140. Sohngen, H. and E. Meister. Beitrag zur Aerodynamik eines schwingenden Gitters (Contribution to Aerodynamics of an Oscillating Cascade). ZAMM, No. 11/12, 1958.

141 Sohngen, H. and A.W. Quick. Schwingungen in Axialverdichtern (Oscillations in Axial Compressors). Deutsche Versuchsanstalt für Luftfahrt, No. 105, 1960.

142. Tanida, Y., K. Hatta and T. Asanuma. Experimental Study on Flutter in Cascading Blades. Bulletin of JSME, Vol. 6, No. 24, 1963.

143. Timman, R. The Aerodynamic Forces on an Oscillating Airfoil Between Two Parallel Walls. Appl. Sci. Res., No. 31, 1954.

144. Whitehead, D.S. Vibration of Cascade Blades Treated by Actuator Disk Methods. Proc. Instn. Mech. Engnrs., No. 21, 1959.

145. Whitehead, D.S. Force and Moment Coefficients for Vibrating Aerofoils in Cascade. ARCR. a M., No. 3454, 1960.

146. Whitehead, D.S. Bending Flutter of Unstalled Cascade Blades at Finite Deflection. ARC R. a. M., No. 3386, 1962.

147. Whitehead, D.S. Effect of Mistuning on the Vibration of Turbomachine Blades Induced by Wakes. J. Mach. Engng. Sci., No. 1, 1966.

148. Whitehead, D.S. The Analysis of Blade Vibration Due to Random Excitation. ARC R. a. M., No. 3253, 1962.

149. Woolston, D.S. and H.L. Runyan. Some Considerations on the Air Forces on a Wing Oscillating Between Two Walls for Subsonic Compressible Flow. JAS, No. 1, 1955.

150. Woods, L.C. On Unsteady Flow Through a Cascade of Airfoils. Proc. Roy. Soc., ser. A, No. 1172, 1955.

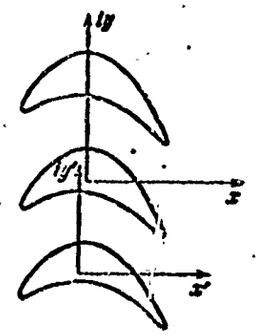
151. Yeh, H. and J.J. Eisenhuth. The Unsteady Wake Interaction in Turbomachinery and its Effect on Cavitation. Trans. ASME, ser. D., No. 2, 1959.

152. Yeh, H. Sears Functions in Unsteady Flows. JAS, No. 7, 1957.

NOTATION

For convenience in using this monograph, in this section we have collected the most important designations adopted for the entire book.

The adopted position of the coordinate axes is shown below.



Two-dimensional system of coordinates xOy — the coordinate system is stationary with respect to the fluid at infinity, x'O'y' is a mobile system of coordinates, connected with the body.

$z = x + iy$ — a complex variable.

$c(z)$, c — the absolute velocity and the modulus of the absolute velocity of the stream in the coordinate system xOy.

$\tilde{w}(z)$ — the absolute velocity of nonsteady flow through a cascade in the coordinate system $x'O'y'$ $(\tilde{w}(z) = w^0(z) + w(z))$.

$w^0(z)$, w^0 — the absolute velocity and the modulus of the absolute velocity of steady flow in the coordinate system x'O'y'.

$w(z)$ — absolutely perturbed velocity in the coordinate system x'O'y'.

$\tilde{p}(z)$ — pressure in the case of unsteady flow through a cascade $(\tilde{p}(z) = p^0(z) + p(z))$.

$p^0(z)$ — pressure in the case of steady flow through a cascade.

$p(z)$ — pressure perturbation in the case of unsteady flow.

ρ^0, ρ — density and density perturbation in the case of steady and unsteady flow.

$\vec{v}(z)$, $v(s)$ — velocity and modulus of velocity of perturbed motion of fluid on the contour of a cascade in the coordinate system x'O'y'.

$v_0(z, \tau)$ — oscillation velocity of point z of a profile.

v_0 — modulus of oscillation velocity of point z of a profile.

v_{0x}, v_{0y} — components of the modulus of oscillation velocity along the coordinate axes.

c^0, w^0 — corresponding velocities in wakes behind a stationary cascade.

$v^0(x, y, \tau)$ — supplementary velocity in a wake.

v^0 — modulus of supplemental velocity in a wake.

v_n^0 — modulus of the n^{th} harmonic of a Fourier series of supplemental velocity in the wake.

U, V — velocity components of the mainstream along the coordinate axes.

u, v — velocity components of a particle of fluid along the coordinate axes.

$\theta(x, y, \tau)$ — angular shift of a profile.

θ_0 — modulus of the amplitude of an angular profile shift.

$y = y^0 e^{i\nu\tau}$ — oscillation amplitude.

y^0 — modulus of the oscillation amplitude.

L — integration contour, blade contour, etc.

h — displacement during the oscillation of a profile.

t — cascade spacing.

$\bar{y} = y^0/t$ — dimensionless oscillation amplitude.

y_0 — static deflection of blades.

$2b$ — profile chords.

ν — circular frequency of natural blade oscillation (gas).

ω — circular frequency of perturbing forces.

$k = \frac{vb}{w}$ — Strouhal number for velocity w.

k_1 — multiplicity with respect to number of revolutions.

M — moment acting upon a profile.

$\mathscr{L}$ — force acting upon a profile.

τ — time.

ω — vorticity.

γ — intensity of vortex sheet.

Γ — velocity circulation.

M — Mach number.

a_0 — velocity of sound in an unperturbed stream.

ρ_1 — density of blade material.

c_N, c_y, c_x — coefficients of normal force, lift force, and drag force.

γ_0 — angle of cascade offset.

β_y — profile attitude.

$\alpha_1, \alpha_2, \beta_1, \beta_2$ — angles corresponding to velocity c and w of the velocity triangles in the stage of a turbomachine.

α — phase shift during the oscillation of adjacent profiles.

$\tau = \frac{\pi b}{t}$ — relative cascade density.

Δb — gap between a stationary cascade and a mobile cascade.

l — blade length.

EI — flexural rigidity.

GJ — torsional rigidity.

W — moment of resistance of a blade section.

δ_1 — coefficient of aerodynamic excitation.

δ_2 — coefficient of aerodynamic dampings.

δ_3 — mechanical oscillation detriment.

The imaginary unit j is used for recording time processes in complex form; imaginary unit i, which does not interact with j, is used, as usual, for the com[illegible] coordinate.

SYMBOL LIST

RUSSIAN CHARACTER	MEANING	TYPED AS
Ц.М	center of mass	cm
Ц.К	center of torsion	ct
ГРАД	degree	deg
ГЦ	Hertz	Hz
СР	average	av
СЕК	second	sec
В	volt	V

UNCLASSIFIED
Security Classification

DOCUMENT CONTROL DATA - R & D

(Security classification of title, body of abstract and indexing annotation must be entered when the overall report is classified)

1. ORIGINATING ACTIVITY (Corporate author) Foreign Technology Division Air Force Systems Command U. S. Air Force	2a. REPORT SECURITY CLASSIFICATION UNCLASSIFIED 2b. GROUP

3. REPORT TITLE

UNSTEADY FLOW AROUND AND AEROELASTIC VIBRATION IN TURBOMACHINE CASCADES

4. DESCRIPTIVE NOTES (Type of report and inclusive dates)

Translation

5. AUTHOR(S) (First name, middle initial, last name)

Samoylovich, G. S.

6. REPORT DATE 1969	7a. TOTAL NO. OF PAGES 526	7b. NO. OF REFS 152
8a. CONTRACT OR GRANT NO. F33657-70-D-0607-P004 b. PROJECT NO. 6040104 c. d. DIA Task Nos. T65-04-19A;18A	9a. ORIGINATOR'S REPORT NUMBER(S) FTD-HC-23-242-70 9b. OTHER REPORT NO(S) (Any other numbers that may be assigned this report)	

10. DISTRIBUTION STATEMENT

Distribution of this document is unlimited. It may be released to the Clearinghouse, Department of Commerce, for sale to the general public.

11. SUPPLEMENTARY NOTES	12. SPONSORING MILITARY ACTIVITY Foreign Technology Division Wright-Patterson AFB, Ohio

13. ABSTRACT

Methods of calculating, and experimental results of research on, unsteady flow in aerodynamic cascades of turbomachines are set forth. The conditions of excitation and damping of blade vibration in compressible and incompressible fluid flow are considered. The theoretical methods are based upon a model of an ideal fluid. The incoming stream may be inhomogeneous and have vortices due to the influence of a preceding cascade. The experimantel results pertain to determination of the dynamic stresses brought about by stream inhomogeneity in the turbomachine, as well as to determination of the unsteady aerodynamic forces which excite and damp blade vibrations. Consideration is given to the origination of cascade flutter and the effect of inhomogeneity of an aerodynamic cascade. The experimental research methods are described. Orig. art. has: 32 tables, 72 illustrations.

DD FORM 1 NOV 68 1473

UNCLASSIFIED
Security Classification

UNCLASSIFIED
Security Classification

14. KEY WORDS	LINK A		LINK B		LINK C	
	ROLE	WT	ROLE	WT	ROLE	WT
Aerodynamic Force						
Aeroelasticity						
Turbine Cascade						
Turbomachine						
Cascade						
Subsonic Flow						
Supersonic Flow						

UNCLASSIFIED
Security Classification